

Dissertation zur Erlangung des Doktorgrades
der Fakultät für Chemie und Pharmazie
der Ludwig-Maximilians-Universität München

**Novel Energetic Materials based on
1,5-Diaminotetrazole and 3,5-Diamino-1*H*-
1,2,4-triazole**

Franz Albert Martin

aus

Würzburg

2011

Erklärung:

Diese Dissertation wurde im Sinne von § 13 Abs. 3 bzw. 4 der Promotionsordnung vom 29. Januar 1998 (in der Fassung der sechsten Änderungssatzung vom 16. August 2010) von Herrn Professor Dr. Thomas M. Klapötke betreut.

Ehrenwörtliche Versicherung:

Diese Dissertation wurde selbstständig, ohne unerlaubte Hilfe erarbeitet.

München, den 07. Juli 2011

(Franz Albert Martin)

Dissertation eingereicht am: 08. Juli 2011

1. Gutachter: Prof. Dr. Thomas M. Klapötke

2. Gutachter: Prof. Dr. Konstantin Karaghiosoff

Mündliche Prüfung am: 03. August 2011

„Go ahead, make my day!“

(Clint Eastwood in, ‘Dirty Harry’)

Dedicated to my parents

Acknowledgements:

First and foremost I would like to express my thanks to Professor Dr. Thomas M. Klapötke, not only for giving me the opportunity to work on my PhD thesis within his group or for paying my bills for three years, but also and mostly for believing in me, for many fruitful discussions, for extended stays in foreign countries, for being a patient mentor and for his love for cigars and whiskey. Thank you very much for every opportunity I was able to take over these years!

I am indebted to Professor Dr. Konstantin “Conny” Karaghiosoff for being available as the co-referee of this thesis. I’m very thankful for numerous evenings we shared in either NMR or X-ray rooms and for the discussion of the results, which sometimes took even longer than the measurement itself! Thank you for your enthusiasm and for every minute you carved out of your very busy work schedule and for your ability to brighten up the dullest days!

I’m also indebted to Professor Dr. Christina Scheu, Professor Dr. Ingo-Peter Lorenz, Professor Dr. Wolfgang Beck and PD Dr. Hans- Christian Böttcher for being available as examiners in my Rigorosum.

I would also like to thank Ms. Irene S. Scheckenbach for being the best secretary in the world, for her help with every kind of forms and bureaucracy and for arranging perfect journeys in many parts of the world.

In detail I would like to express my thanks to:

- Dr. Jan Welch who remained a close friend over the years and who, besides all, was able to excel my abilities in the English language to new heights.
- Dr. Burkhard Krumm and Alexander Penger for their enthusiasm and joy for cars and technique and also for sharing their soccer knowledge.
- Dr. Jörg Stierstorfer for his help in the early days of my PhD thesis and his support over the years.
- Dr. Karin Lux for spending numerous hours on work days, evenings and weekends with our beloved X-ray diffractometer and in -20 °C cold rooms for crystal picking. It wouldn’t have been half the fun without you!

- Dr. Hendrik Radies, Dr. Karin Lux, Anian Nieder, Franziska Betzler, Alexander Dippold and Alexander Penger for the exhilarating coffee breaks.
- Dr. Stefan Sproll (“Ich will heim!”), Dr. Hendrik Radies („Geht doch alles den Bach runter...“) and Anian Nieder (“Fraaaaanz, sag mal...”) for their humor, the numerous conversations we had and for becoming close friends during the course of my studies.
- Anian Nieder for many fruitful discussions about chemistry, talking gossip, staying in the lab much longer than necessary and for countless “Werner” sessions.
- “dem Zentrum des Wahnsinns” aka Can-Carlo Dörtbudak for his never ending humor and support in every aspect of university and private life.
- my Master student Alexander Dippold (“Nein! Doch! Ohhhh!”) for his working attitude, the perfect results, his humor and support and for becoming a great friend.
- Franziska Betzler (“Soooooooo flauschig!!!”) who was always able to lighten up my days, even if nothing really worked, with her fantastic sense of humor.
- our neighbor lab D3.110 for the supply of glass ware and their endurance of the wonderful sound generated by the ultra sonic bath.
- my lab D3.107, Anian, Magda, Marcos, Michi and Vera for the best (and also very creative) working atmosphere in the world aided by the immense pool of heavy metal, hard rock and sometimes electric and trance music.
- my F-students and Bachelor students Isabelle König, Christine Hieke, Frank Tambornino and Sandra Wiedbrauk for their enthusiasm, interest, many great results, much fun and an overall great time.
- Camilla Evangelisti for all her help with theoretical calculations and just for her Italian temperament.
- Dr. Karina Tarantik for the shared supervision of practical trainings and her perfect “Schwarzwälderkirchtorte”.
- Mr. Stefan Huber for measuring sensitivity values of countless samples.
- the whole work group and all the close friends and colleagues in the inorganic chemistry department. Thank you for a perfect time!

Above all, I would like to express my thanks to my parents, my family and especially my wife Marianne who never stopped encouraging and believing in me and for their continuous support in every aspect of my life. Words are not enough to describe how grateful I am!

Table of contents

1. Introduction	1
1.1 History, Background and Definitions	1
1.2 Requirements for Modern Explosives	3
1.3 Motivation and Objective	6
1.4 References	7
2. Synthesis and characterization of 4,5-dicyano-1,2,3-triazole and its sodium, ammonium and guanidinium salts	8
2.1 Introduction	8
2.2 Experimental Section	9
2.3 Results and Discussion	15
2.3.1 Synthesis and Characterization of 1 – 3	15
2.3.2 Synthesis and Characterization of 4 – 8	17
2.3.3 Molecular Structures	19
2.3.4 Energetic Properties of 1 and 5 – 8	32
2.4 Conclusion	36
2.5 References	37
3. <i>N</i> -bound primary nitramines based on 1,5-diaminotetrazole	41
3.1 Introduction	41
3.2 Results and Discussion	43
3.2.1 Synthesis	43
3.2.2 Molecular Structures	45
3.2.3 Spectroscopic Data	58
3.2.4 Mass Spectrometry	64
3.2.5 Theoretical Calculations and Stabilities	64
3.3 Conclusion	68
3.4 Experimental Part	69
3.5 References	76
4. C ₂ N ₁₄ : A new energetic and highly sensitive binary azidotetrazole	80
4.1 Introduction	80
4.2 Results and Discussion	81
4.3 References	86
5. Novel azidotetrazoles – structurally interesting and extremely sensitive	88
5.1 Introduction	88
5.2 Results and Discussion	89
5.2.1 Synthesis	89
5.2.2 Spectroscopic Data	92
5.2.3 Molecular Structures	96
5.2.4 Sensitivities and Thermal Stabilities	104
5.3 Conclusion	105
5.4 Experimental Part	106

5.5	References	110
6.	Synthesis and characterization of 3,5-diamino-1,2,4-triazolium dinitramide	113
6.1	Introduction	113
6.2	Results and Discussion	114
6.2.1	Synthesis	114
6.2.2	NMR Spectroscopy	115
6.2.3	Molecular Structures	115
6.2.4	Theoretical Calculations	123
6.2.5	Detonation Parameters	125
6.3	Conclusions	128
6.4	Experimental Part	128
6.5	References	132
7.	Nitraminoazoles based on ANTA – A comprehensive study of structural and energetic properties	136
7.1	Introduction	136
7.2	Results and Discussion	137
7.2.1	Synthesis	137
7.2.2	Molecular Structures	140
7.2.3	Spectroscopic Data	159
7.2.4	Mass Spectrometry	166
7.2.5	Theoretical Calculations, Performance Characteristics and Stabilities.....	166
7.3	Conclusion	172
7.4	Experimental Part	174
7.5	References	188
8.	5-Nitramino-3-tetrazol-1-yl-1 <i>H</i> -1,2,4-triazole – Synthesis and complete characteriza-tion of a novel energetic material	191
8.1	Introduction	191
8.2	Results and Discussion	192
8.2.1	Synthesis	192
8.2.2	Spectroscopic Data	194
8.2.3	Crystal Structures	198
8.2.4	Sensitivities and Thermal Stabilities	205
8.3	Conclusion	207
8.4	Experimental Part	208
8.5	References	216
9.	Synthesis and characterization of bis(triaminoguanidinium) 5,5'-dinitrimino-3,3'-azo-1 <i>H</i> -1,2,4-triazole – A novel insensitive energetic material	218
9.1	Introduction	218
9.2	Results and Discussion	220
9.2.1	Synthesis	220
9.2.2	NMR Spectroscopy	222
9.2.3	Vibrational Spectroscopy	223
9.2.4	Structural Characterization	224

9.2.5	Theoretical Calculations	234
9.2.6	Detonation Parameters and Thermal Properties	236
9.3	Conclusions	240
9.4	Experimental Part	241
9.5	References	246
10.	Nitrated derivatives of 1,3-bis(5-amino-1,2,4-triazol-3-yl)-triazene	249
10.1	Introduction	249
10.2	Results and Discussion	250
10.2.1	Synthesis	250
10.2.2	Vibrational and NMR Spectroscopy	254
10.2.3	Molecular Structures	257
10.2.4	Physical Properties	266
10.3	Conclusion	267
10.4	Experimental Part	267
10.5	References	274
11.	Summary	277
12.	Appendix	282
12.1	Supplementary Material for Chapter 2	282
12.2	Supplementary Material for Chapter 3	284
12.3	Supplementary Material for Chapter 4	288
12.4	Supplementary Material for Chapter 5	298
12.5	Supplementary Material for Chapter 6	301
12.6	Supplementary Material for Chapter 7	303
12.7	Supplementary Material for Chapter 8	310
12.8	Supplementary Material for Chapter 9	311
12.9	Supplementary Material for Chapter 10	312
12.10	List of Abbreviations	313
13.	Curriculum vitae and bibliography	315

1. Introduction

1.1 History, Background and Definitions

The chemistry of explosives, their development and application are as old as 220 years BC, when blackpowder was discovered by the Chinese accidentally. Even though this discovery remained unused till the middle age in Europe, the development and investigation of these materials drew much more attention over the following centuries. Although the history of energetic materials is well chronicled in literature, a small look on milestone developments should be given.^[1] Blackpowder and other early energetic material were mostly used for fireworks, but their potential use as propellants for small and middle caliber weapons was also recognized quickly. Later on, nitroglycerine (NG) was invented in the 19th century, first as medication for heart disease by Ascanio Sobrero, but its sensitivity and blasting properties led to the first industrial process development for high explosives, by Alfred Nobel in the 1860s and 1870s. Sensitivity was always an issue with the production of nitroglycerine and many accidents occurred during its preparation. Hence we see one very important property of high explosives, the ability to explode while certain outer stimuli are applied. The much less sensitive trinitrotoluene (TNT) was also invented in the 19th century and replaced the common picric acid in most weapon systems. TNT was used as the standard explosive in one of the worlds biggest armed conflicts, the 1st world war, while the later invented hexogen (RDX) fared as the standard explosive in the 2nd world war. In our modern times, not only the application for warfare is studied, but the utilization of energetic materials for civilian use in mining, construction, demolition and safety equipment such as airbags, signal flares and fire extinguishing systems is extensively studied. One of the biggest steps for mankind would have been impossible without the development of energetic materials and no one would be able to remember the words of Neil Armstrong on July 20st 1969 “That’s one small step for man, but...one giant leap for mankind”.^[1-2]

As one may have recognized, many different applications have drawn attention and can be reached by the use of energetic materials. A definition of energetic materials and their subsequent classification is hence necessary in order to understand and clarify the wide area of application and development. The entirety of energetic materials is defined by the American Society for Testing and Material as “...a compound or mixture of substances

which contains both the fuel and the oxidizer and reacts readily with the release of energy and gas...”^[3] Energetic materials themselves are then divided into three unique classes: explosives, propellants and pyrotechnics. Since this work focuses on chemistry of energetic materials, these compounds have to derive their energy from chemical reactions, not from physical or nuclear reactions, which will therefore be omitted. Explosives can be defined as chemical substances which are capable of propagating a chemical reaction within the material that releases gas, pressure and high temperature at certain speeds, capable of causing damage to the surroundings.^[1c, 1d] The class of explosives can be divided further into primary and secondary explosives. Primary explosives like lead azide, which is commonly used in blasting caps, are highly sensitive materials that can be ignited by small physical stimuli of mechanical, electrostatic or thermal nature. They usually don't exhibit very high performance values but undergo a rapid transition from deflagration to detonation (DDT, explained in detail below). Secondary explosives on the other hand cannot be ignited by the same stimuli as primary explosives since they are not only much more stable in terms of friction, impact and electrostatic discharge but also kinetically stable (metastable) compounds and hence they have to be ignited by much larger stimuli. Normally the energy needed for the initiation of secondary explosives is generated by the detonation shockwave of primary explosives. Although they need a much higher impetus to be detonated, secondary explosives exhibit much higher performances (release more energy per time) than primary explosives. Propellants on the other hand are energetic materials consisting of one compound carrying both, oxidizer and fuel, or a mixture of these. They combust or deflagrate very fast, releasing a high amount of gas and energy (heat, combustion temperature), sufficient enough to increase the temperature and the pressure applied to the surroundings and finally providing propulsive force (specific impulse) in order to lift defined payloads into their destined orbits. Pyrotechnic compositions are not known primarily for the transfer of stored chemical energy into kinetic energy to the surroundings, but use the stored chemical energy for the purpose of generating “pyrotechnical” effects, either of visual or acoustic nature.^[1a, 1c, 1d] The discussion of pyrotechnic systems is omitted, since the primary objective of this thesis is the synthesis and characterization of secondary explosives and, to a certain extent, propellant systems.

The chemical reaction of the energetic materials defines their application. Propellants are usually combusted to deliver high amounts of gaseous reaction products at high temperatures in order to deliver high pressure and subsequently a high velocity of the

detonation products. Combustions or burning reactions are the slowest reactions that occur in energetic materials, and are defined as self propagating oxidation reactions, either performed on air or by an oxidizing function.^[1a, 1b] Two different chemical processes are known for secondary as well as for primary explosives, both of them being much faster than normal combustions. Secondary explosives on the one hand can undergo a deflagration if they are not used in confined spaces. This means, that the reaction proceeds on the surface of the material at slightly subsonic linear velocities, mostly propagated by heat transfer, and moves from there through the unreacted material. A detonation on the other hand is not propagated by heat transfer, but by a supersonic shockwave travelling through the unreacted material, hence representing the fastest release of chemical energy known. The reaction is always sustained by the rapid release of energy behind the wavefront and is normally observed under strong confinement of energetic materials or if initiated by the shockwave from a primary explosive. A transition from deflagration to detonation can occur, while the other direction is impossible. This transition is known as the “Deflagration to Detonation Transition (DDT)” and a material, able to undergo these transition is defined as an explosive, while the corresponding self sustained reaction is called the detonation.^[1a, 1b] As we refer to explosives as compounds being able to undergo the before mentioned transition and have the ability to detonate, we characterize and discuss the compounds within this work mainly by the use of their detonation properties.

1.2 Requirements for Modern Explosives

Before we discuss the requirements necessary for novel explosives, we have to discuss the most common physical as well as chemical properties of these materials and the disadvantages of the classical explosives. Chemical substances are described at first by chemical composition and molecular structure together with their decomposition point (T_{dec}). From the chemical composition, we are able to determine the oxygen balance of a material (Ω)^[4] or the nitrogen content while the molecular structure determines the connectivity, density (ρ) and hence the energy of formation (ΔU_f^0 (s)) of the material. The energy of formation together with the density of the material are the key values which affect the detonation parameters of energetic compounds. The detonation parameters can either be measured (detonation velocity and pressure) or calculated by certain programs

like EXPLO5 or Cheetah, delivering very good estimated values for comparison and discussion. The detonation parameters eminent for discussion are the detonation velocity (V_{det}) describing the rate of propagation through the material, the detonation pressure at the front of the shockwave (P_{det}), the heat of explosion (ΔU_{ex}), the temperature of the explosion (T_{ex}) and the volume of the gaseous decomposition products (V_0). In addition to these values, the reaction of the explosive material towards outer stimuli has to be determined. These measurements include the sensitivity against friction, impact, electrostatic discharge and thermal shock.

Classical secondary explosives like 2,4,6-trinitrotoluene (TNT), nitroglycerine (NG) and 1,3,5-trinitro-1,3,5-triazacyclohexane (RDX) show different performance characteristics and reaction pathways for decomposition. TNT and NG derive all their energy from the oxidation of the carbon backbone, which works very well in the case of nitroglycerine, while TNT has a negative oxygen balance and hence much material remains unreacted. Both compounds exhibit negative heats of formation and hence much lower performance rates than RDX. RDX itself obtains its energy from the oxidation of the carbon backbone but as well from the formation of dinitrogen due to the N–N bonds in the nitramine moieties. Due to the presence of N–N bonds within the nitramine moieties, a positive heat of formation is generated, which results, together with the higher density, in significantly higher performance values. The performance values and structures of TNT, NG and RDX are compiled in Figure 1.

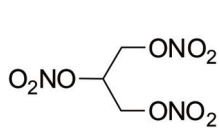
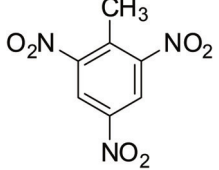
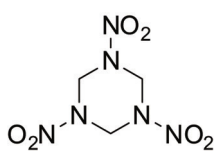
			
Name systematic	1,2,3-Propanetrioltrinitrate (NG)	2,4,6-Trinitrotoluene (TNT)	1,3,5-Trinitro-1,3,5-triazinane (RDX)
T_m (°C)	13	80	204
T_{dec} (°C)	200	300	--
N (%)	18.5	18.5	37.8
Ω (%)	3.5	-73.9	-21.6
ρ (g cm ⁻³)	1.591	1.654	1.82
ΔH_f^0 (kJ mol ⁻¹)	-349.7	-49.7	89.2
Impact sensitivity (J)	0.2	15	7.5
Friction Sensitivity (N)	> 360	353	120
V_{det} (m s ⁻¹)	7600	6900	8750

Figure 1: Classical explosives and their performance characteristics. Values are taken from Ref.^[5]

At the examples of TNT and RDX, we are able to recognize the features necessary for modern explosives. They should have high positive heats of formation, paired with high densities and more balanced oxygen balances. Since the density of materials is hardly to be predicted and influenced, the introduction of nitrogen either catenated, like in heterocyclic ring systems or in the form of nitramine groups is a good starting point for the development of novel materials. Another very important point is the cage strain eminent in heterocyclic ring systems and structures. Much more energy can be derived by the combination of the oxidation of carbon together with the energy delivered from the cage strain introduced to the backbone, increasing the energy of formation. These concepts led to new materials over the last decade. Strained cage and ring systems have been developed like TEX (4,10-dinitro-2,6,8,12-tetraoxa-4,10-diazaisowurtzitane), CL-20 (2,4,6,8,10,12-hexanitro-hexaazaisowurtzitane), ONC (octa nitrocubane) and TNAZ (1,3,3-trinitroazetine), while catenated nitrogen systems are also well under investigation like DNAT (5,5'-Dinitro-3,3'-azo-1,2,4-1*H*-triazole). (Figure 2)

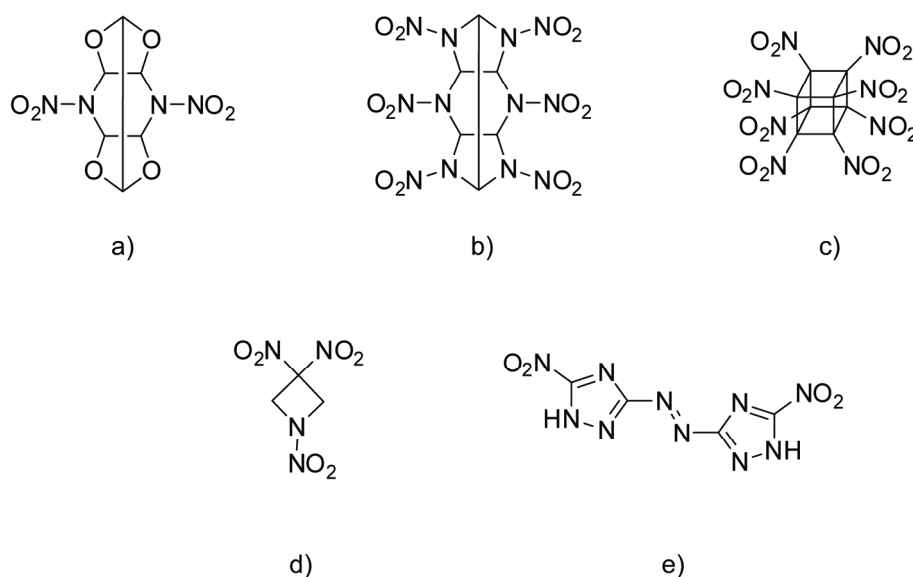


Figure 2: Modern explosives: a) TEX (4,10-dinitro-2,6,8,12-tetraoxa-4,10-diazaisowurtzitane), b) CL-20 (2,4,6,8,10,12-hexanitro-hexaazaisowurtzitane), c) ONC (octa nitrocubane), d) TNAZ (1,3,3-trinitroazetine) and e) DNAT (5,5'-Dinitro-3,3'-azo-1,2,4-1*H*-triazole).

Another very important point when talking about the synthesis of new energetic materials is the environmental aspect. RDX as well as TNT show a high aqua toxicity and due to the overall release of HEMs to the environment, they are increasingly becoming a soil and ground water contaminant.^[6] Hence the development of environmentally friendly compounds, which are completely consumed within the process of detonation should be

avored. The detonation products of these compounds, build up from e.g. nitrogen rich heterocyclic systems are mainly dinitrogen, carbon dioxide and water which would be the overall goal for a well performing novel explosive.^[7]

1.3 Motivation and Objectives

The general area of this thesis is the synthesis and complete characterization of novel secondary explosives and, to a certain extent, propellants. The concept of new green energetic compounds as explained above is thereby the main topic of this work. The benefits of the development of new high energetic density materials with a high nitrogen content paired with high positive heats of formation are improved performance and also environmental compatibility. With all respect to environmentally friendly compounds and high performance values to be realized, the compounds must exhibit also high thermal stabilities and, for better and safer handling, low sensitivities against impact, friction and electrostatic discharge.

In this context, three classes of heterocyclic systems have been intensively studied, 4,5-dicyano-1,2,3-triazole, 3,5-diamino-1*H*-triazole and its nitrated derivatives as well as compounds based on 1,5-diaminotetrazole. While the 1,2,3-triazoles exhibit much higher heats of formation, the 1,2,4-triazoles show a higher thermal stability, always dependent on the substituents. Hence the substituents in 3 and 5 position of 3,5-diamino-1*H*-1,2,4-triazole have been varied, introducing nitro, nitramine and azo functionalities and their stabilities against outer stimuli as well as the decomposition temperatures have been studied. The effect of the formation of energetic salts on the thermo chemical and physical properties as well as the detonation parameters has also been extensively studied and compared to known secondary explosives.

Even though, many energetic nitrogen rich ionic compounds share the 1,5-diamino-1*H*-tetrazolium cation or its 4-methylated derivative, no nitrated compounds using the nitramine functionality are known. Reaction pathways of these compounds have been investigated thoroughly and new examples for *N*-bound nitramines have been synthesized, completely characterized and evaluated. Ionic compounds with even increased nitrogen contents have been synthesized and investigated regarding their potential use as secondary explosives for special applications. Finally, our efforts in increasing the nitrogen content and heats of formation for the tetrazole backbone peaked in the synthesis and investigation of novel azidotetrazole systems.

1.4 References

- [1] a) T. M. Klapötke, in *High Energy Density Materials* (Ed.: T. M. Klapötke), Springer, Heidelberg, **2007**, pp. 84-122; b) T. M. Klapötke, *Chemie der hochenergetischen Materialien*, 1 ed., Walter de Gruyter, Berlin, New York, **2009**; c) J. Akhavan, *The chemistry of explosives*, Royal Society of Chemistry, Cambridge, UK, **1998**; d) *Chimia* **2004**, 58, 351-429.
- [2] http://www.nasa.gov/mission_pages/apollo/apollo11_40th.html.
- [3] www.astm.org.
- [4] *Calculation of oxygen balance: Ω (%) = $(wO - 2xC - 1/2yH - 2zS)1600/M$.* (*w*: number of oxygen atoms, *x*: number of carbon atoms, *y*: number of hydrogen atoms, *z*: number of sulfur atoms, *M*: molecular weight).
- [5] J. Köhler, R. Meyer, *Explosivstoffe*, Vol. 9th edition, Wiley-VCH, Weinheim, **1998**.
- [6] M. B. Talawar, R. Sivabalan, T. Mukundan, H. Muthurajan, A. K. Sikder, B. R. Gandhe, A. S. Rao, *J. Hazard. Mater.* **2009**, 161, 589-607.
- [7] A. K. Sikder, N. Sikder, *J. Hazard. Mater.* **2004**, A112, 1-15.

2. Synthesis and characterization of 4,5-Dicyano-2H-1,2,3-triazole and its sodium, ammonium and guanidinium salts

Margaret-Jane Crawford, Konstantin Karaghiosoff, Thomas M. Klapötke and Franz A. Martin

As published in: Inorganic Chemistry, 2009, 48(4), 1731-1743.

2.1 Introduction

Energetic materials that derive their energy from a positive heat of formation rather than oxidation of the carbon backbone have recently attracted attention as gas generators or propellants.^[1-21] High-nitrogen compounds which contain only the elements C, H and N and which are free of both oxygen and metals are potentially useful either as gas generators or energetic materials which have a low flame temperature, in order to increase the impulse in gun or rocket propellants.^[15]

Nitrogen-containing five-membered heterocycles are traditional sources of energetic materials, since the N-N bonds in the ring are stabilized by pseudoaromatic electron delocalization and therefore relatively insensitive. Therefore, stable nitrogen-rich salts can be formed when employing such rings. A result of this is that considerable attention is currently focused on azoles as new, future energetic materials, and in particular the tetrazole series.^[20-26] Whereas the chemistry and application of nitrogen-rich tetrazole compounds as energetic materials has been extensively studied by us^[1-11] and others,^[12-19,27] the corresponding chemistry of the related triazole ring has only recently been the subject of systematic investigations.^[28-36] Both 1,2,4-triazole and 1,2,3-triazole have been reported previously in the literature and both have positive heats of formation of 109 kJ mol⁻¹ and 272 kJ mol⁻¹, respectively.^[37,38] Therefore, 1,2,3-triazole based compounds are energetically of greater interest than 1,2,4-triazole derivatives. Energetic materials that are salts are often advantageous over non-ionic molecules since the salts tend to exhibit lower vapor pressures (essentially eliminating the risk of exposure through inhalation)^[29,39] and higher densities than their atomically similar neutral and non-ionic analogues.^[28] The synthesis of 4,5-dicyano-1,2,3-triazole, was reported as early as 1921 by E. Gryszkiewicz-Trochimowski^[40a; 40d] by the diazotation of aminomalononitrile with

“HNO₂”. In the same work E. Gryszkiewicz-Trochimowski published some ionic species of the 4,5-dicyano-1,2,3-triazole, namely the silver, potassium, ammonium, copper and barium 4,5-dicyano-1,2,3-triazolate, characterized mainly by solubility and melting point. The publication of the calcium salt followed in 1924.^[40e] The lithium salt was quite recently investigated by *P. Johansson et al.*^[40b] and characterized using Raman spectroscopy. However no experimentally determined structural data were presented, although the structure of the 4,5-dicyano-1,2,3-triazolate anion was computed for the gas phase.^[40b] These authors were interested however, in a different aspect of the chemistry of this species, namely the relatively non-coordinating behaviour of this anion for use in polymer electrolytes. To the best of our knowledge there is no report in the literature concerning a structurally characterized salt containing the 4,5-dicyano-1,2,3-triazolate anion, and little has been reported on this anion. Furthermore, only very few structurally characterized compounds containing the 4,5-dicyano-1,2,3-triazole ring can be found. Therefore, this prompted us to determine the molecular structure of the neutral compound **1** and to investigate its potential as possible precursor for the synthesis of ionic nitrogen-rich 4,5-dicyano-1,2,3-triazolate salts. Consequently, a report on the preparation of the corresponding ammonium (**4**), guanidinium (**5**), aminoguanidinium (**6**), diaminoguanidinium (**7**) and triaminoguanidinium salts (**8**) of the 4,5-dicyano-1,2,3-triazolate anion is given in this paper.

2.2 Experimental Section

Materials. All chemical reagents and solvents of analytical grade were obtained from Sigma-Aldrich Fine chemicals Inc. and used as supplied. Solvents were dried according to known procedures, freshly distilled and stored under a nitrogen atmosphere.

General Procedure. The ¹H, ¹³C and ¹⁴N/¹⁵N NMR spectra were recorded using Multinuclear NMR. Spectra were recorded using a Jeol EX 400 FT-NMR spectrometer operating at 399.782 MHz (¹H), 100.525 MHz (¹³C) and 28.889 MHz (¹⁴N), a Jeol 400 eclipse FT-NMR spectrometer operating at 400.182 MHz (¹H), 100.626 MHz (¹³C), 28.918 MHz (¹⁴N) or a Jeol 270 FT-NMR spectrometer operating at 270.166 MHz (¹H), 67.933 MHz (¹³C) and 27.376 MHz (¹⁵N). Chemical shifts are given with respect to TMS (¹H, ¹³C) and MeNO₂ (¹⁴N) as external standards. Coupling constants are given in Hz. Infrared (IR) spectra were recorded on a Perkin-Elmer Spectrum One FT-IR instrument between KBr plates at 25°C. Raman spectra were recorded on a Perkin Elmer Spectrum

2000R NIR FT-Raman instrument equipped with a Nd:YAG laser (1064 nm). The intensities are reported relative to the most intense peak and given in parenthesis. Elemental analyses were performed with a Netsch Simultaneous Thermal Analyser STA 429. Melting points were determined by differential scanning calorimetry (Perkin-Elmer Pyris 6 DSC, calibrated by standard pure Indium and Zinc). Measurements were performed at a heating rate of $\beta = 5^\circ\text{C}$ in closed Al-containers with a hole (1 μm) on the top for gas release and a 0.003*3/16-in. disk was used to optimize good thermal contact between the sample and the container with a nitrogen flow of 20 mL/min. The reference sample was an Al-container with air.

Synthesis of 4,5-dicyano-2*H*-1,2,3-triazole (**1**)

The synthesis of **1** was undertaken according to the literature procedure^[40b] using the following scale: Diaminomaleodinitrile (10.81 g, 100.0 mmol) was dissolved in 125 mL water and acidified with hydrochloric acid (1M, 100 mL). At 0°C sodium nitrite (6.89 g, 100.0 mmol) was added portion wise, while maintaining the reaction temperature below 4°C. The reaction mixture was then allowed to warm up to room temperature and stirred for one hour. After filtration the brownish solution was extracted five times with a total of 600 mL of diethylether. After removal of the solvent of the combined ether extracts under reduced pressure, a pale light brown solid was obtained. Yield of crude product = 10.6 g (89 %). Analytically pure **1** was obtained by subliming the crude product at 90°C under vacuum to yield white crystals suitable for single crystal X-ray diffraction. The white solid was used for the reported characterization.

$T_{\text{melt}} = 148.8^\circ\text{C}$. $T_{\text{dec}} = 221.1^\circ\text{C}$. IR (KBr, 25 °C, cm^{-1}) $\nu = 3258$ (vs), 2839vw, 2263 (s), 1554 (vw), 1478 (m), 1382 (s), 1250 (w), 1228 (w), 1185 (w), 1131 (vs), 1090 (w), 999 (m), 792 (s) 627 (m), 521 (m), 465 (m). Raman (200 mW, 25 °C, cm^{-1}) $\nu = 3258$ (6), 2263 (100), 2209 (2), 1486 (48), 1400 (3), 1381 (32), 1351 (2), 1299 (15), 1208 (24), 992 (9), 727 (3), 660 (19), 539 (6), 524 (12), 459 (12), 230 (2), 202 (2), 183 (3), 154 (6). ^1H NMR, δ (ppm): 7.63 (s, 1H, NH). ^{13}C NMR, δ (ppm): 111.7 (s, $\text{C}_2\text{N}_3(\text{CN})_2$), 123.8 (s, -CN). ^{15}N NMR, δ (ppm): -108.6 (N2), -76.9 (N4, N5), -39.2 (N1, N3). MS (DEI+) C_4HN_5 , calcd. 119.10, found 119.1. C/H/N analysis: calcd. (found) C 40.34 (40.34), H 0.85 (1.05), N 58.81 (59.10) %.

Synthesis of sodium 4,5-dicyano-1,2,3-triazolate monohydrate (**2**)

The synthesis of **2** was undertaken according to modification of the literature procedure for the lithium salt^[40b] using the following scale: To a solution of **1** (10.5 g, 89.0 mmol) in acetonitrile (100 mL) a slight excess of sodium carbonate (12.4 g, 116.0 mmol) was added. The mixture was stirred for 1 hour and placed for 10 minutes into an ultrasonic bath. The solution was then centrifuged for 20 minutes (5000 rpm) and the resulting clear supernatant decanted and evaporated to dryness. The white solid obtained was dried under vacuum to yield **2** (11.5, 81%). Single crystals suitable for X-ray diffraction were obtained by allowing isohexane to slowly diffuse into a methanol solution of **2**.

IR (KBr, 25 °C, cm^{-1}) $\nu = 3757$ (w), 3615 (w), 3381 (m), 2729 (w), 2573 (w), 2431 (w), 2251 (vs), 2114 (m), 1696 (w), 1512 (m), 1370 (s), 1290 (m), 1247 (m), 1178 (m), 1013 (w), 641 (m), 534 (m), 479 (m). Raman (200 mW, 25 °C, cm^{-1}) $\nu = 2260$ (100), 1506 (44), 1382 (21), 1292 (16), 1183 (10), 1099 (31), 1086 (6), 1013 (11), 711 (8), 622 (15), 533 (24), 472 (14), 170 (11), 146 (21). ^{13}C NMR, δ (ppm) 114.5 (s, C_4N_5^-), 121.6 (s, C_4N_5^-). ^{14}N NMR, δ (ppm) 24 (s, $\nu_{1/2} = 760$ Hz, N2), -19 (s, $\nu_{1/2} = 806$ Hz, N1, N3), -116 (s, $\nu_{1/2} = 656$ Hz, N4, N5). ^{15}N NMR, δ (ppm): -113.0 (N4, N5), -20.0 (N1, N3), 21.3 (N2). C/H/N analysis: calcd. (found) C 30.18 (30.30), H 1.27 (1.33), N 44.03 (44.25)%.

Synthesis of silver 4,5-dicyano-1,2,3-triazolate (**3**)

Compound **2** (0.795 g, 5.0 mmol) was dissolved in water (15 mL) and reacted under stirring with a solution of silver nitrate (0.850 g, 5.0 mmol) in 10 mL water. After 2 hours stirring, the precipitated product was filtered off, washed with water, dried under vacuum and finally in the oven overnight at 50°C to yield a pale beige solid.

$T_{\text{melt}} = 305$ °C. $T_{\text{dec.}} = 386$ °C. IR (KBr, 25 °C, cm^{-1}): $\nu = 2247$ (s), 2159 (vw), 2131 (vw), 1520 (vw), 1503 (vw), 1421 (vw), 1408 (vw), 1377 (s), 1293 (w), 1283 (vw), 1242 (vw), 1234 (vw), 1190 (m), 1178 (m), 1113 (vw), 1097 (vw), 1086 (vw), 1029 (m), 710 (vw), 661 (vw), 649 (m), 635 (w), 528 (m), 516 (s), 470 (m). Raman (200 mW, 25 °C, cm^{-1}) $\nu = 2245$ (100), 2194(5), 1522 (63), 1380 (25), 1292 (36), 1175 (17), 1095 (31), 1052 (15), 1030 (15), 708 (17), 662 (24), 518 (18), 475 (21), 166 (23). C/H/N analysis: calcd. (found) C 21.26 (21.36), N 31.00 (31.32)%.

Synthesis of ammonium 4,5-dicyano-1,2,3-triazolate (**4**)

A solution of ammonium bromide (0.196 g, 2.0 mmol) in methanol (5 mL) was reacted with 0.452 g (2.0 mmol) **3** and stirred for 1 hr at room temperature. The yellowish solid precipitate (AgBr) was filtered off and the remaining solution evaporated to dryness. Recrystallization from methanol/isohexane yielded crystalline material of **4** which was suitable for X-ray diffraction.

Melting with decomposition 194.8 °C. IR (KBr, 25 °C, cm^{-1}) ν = 3292 (m), 3167 (m), 3133 (m), 3014 (s), 2904 (w) 2881 (w), 2814 (w), 2484 (vw), 2393 (vw), 2248 (s), 2194 (vw), 2170 (vw), 1949 (vw), 1780 (vw), 1687 (m), 1473 (s), 1456 (s), 1421 (m), 1388 (m), 1296 (m), 1238 (w), 1189 (w), 1177 (m), 1118 (vw), 1095 (w), 988 (vw), 708 (vw), 658 (w), 640 (m), 522 (m), 480 (w). Raman (200 mW, 25°C, cm^{-1}) ν = 2245 (100), 2198 (7), 1701 (6), 1509 (73), 1492 (13), 1417 (8), 1390 (40), 1297 (26), 1178 (20), 1095 (47), 1015 (20), 715 (13), 659 (20), 523 (33), 481 (14), 470 (12), 223 (14), 163 (21). ^1H NMR, δ (ppm) 7.05 (4H, NH_4^+); ^{13}C NMR, δ (ppm) 114.4 (s, C_4N_5^-), 121.5 (s, C_4N_5^-). ^{14}N NMR, δ (ppm) 21 (s, $\nu_{1/2}$ = 676 Hz, N2), -12 (s, $\nu_{1/2}$ = 806 Hz, N1, N3), -112 (s, $\nu_{1/2}$ = 736 Hz, N4, N5), -359 (s, NH_4^+). C/H/N analysis: calcd. (found) C 35.30 (35.03), H 2.96 (3.12), N 61.74 (61.11)%. MS (FAB+) NH_4^+ , calcd. 18.0, found 18.3. MS (FAB-) C_4N_5^- , calcd. 118.1, found 118.0.

Synthesis of guanidinium 4,5-dicyano-1,2,3-triazolate (**5**)

A solution of guanidinium chloride (0.192 g, 2.0 mmol) in methanol (5 mL) was reacted with solid **3** (0.452 g, 2.0 mmol) and the reaction mixture was stirred for 1.5 hours at room temperature. The white/grey precipitate (AgCl) was filtered off and the remaining clear solution was evaporated to dryness yielding a light off-white product (**5**). Recrystallisation from methanol/isohexane yielded crystalline material of **5** which was suitable for X-ray diffraction.

T_{melt} = 135 °C. $T_{\text{dec.}}$ = 241 °C. IR (KBr, 25 °C, cm^{-1}) ν = 3494 (s), 3423 (s), 3349 (m), 3250 (m), 3180 (m), 3100 (m), 2478 (vw), 2235 (s), 2182 (w), 2158 (w), 1670 (vs), 1658 (vs), 1386 (s), 1295 (m), 1233 (w), 1184 (m), 1169 (m), 1123 (w), 1092 (w), 1004 (vw), 986 (vw), 765 (w), 717 (w), 655 (vw), 643 (m), 618 (m), 563 (vw), 539 (m), 521 (m) 482 (w), 465 (w). Raman (200 mW, 25 °C, cm^{-1}) ν = 3264 (3), 2238 (100), 2185 (3), 1652

(4), 1563 (6), 1502 (35), 1488 (16), 1416 (3), 1388 (19), 1297 (11), 1170 (8), 1093 (27), 1011 (38), 814 (3), 711 (8), 656 (14), 538 (14) 523 (19), 484 (8), 466 (9), 229 (5), 183 (6), 142 (9). ^1H NMR, δ (ppm) 6.87 (s, 6H, $\text{C}(\text{NH}_2)_3^+$). ^{13}C NMR, δ (ppm) 114.4 (s, C_4N_5^-), 121.5 (s, C_4N_5^-), 158.4 (s, $\text{C}(\text{NH}_2)_3^+$). ^{14}N NMR, δ (ppm) 23 (s, $\nu_{1/2} = 601$ Hz, N2, C_4N_5^-), -19 (s, $\nu_{1/2} = 818$ Hz, N1, N3 C_4N_5^-), -112 (s, $\nu_{1/2} = 825$ Hz, N4, N5 C_4N_5^-). C/H/N analysis: calcd. (found): C 33.71 (33.62), H 3.39 (3.37), N 62.90 (62.59)%. MS (FAB+) CH_6N_3^+ , calcd. 60.08, found 60.1. MS (FAB-) C_4N_5^- , calcd. 118.1, found 118.0.

Synthesis of aminoguanidinium 4,5-dicyano-1,2,3-triazolate (**6**)

The reaction was carried out using the same general procedure as described above for the preparation of **5**. Aminoguanidinium bromide (0.31 g, 2.0 mmol) was used instead of guanidinium chloride.

Alternative synthesis of aminoguanidinium 4,5-dicyano-1,2,3-triazolate (**6**)

Analytically pure **6** could be prepared by the portion-wise addition of 0.357 g (3.0 mmol) of **1** to a stirred suspension of aminoguanidinium hydrogencarbonate (0.408 g, 3.0 mmol) in approximately 10 mL CH_3CN at room temperature. To this, 10 mL distilled H_2O were then added and the reaction mixture warmed up to 60°C until no further evolution of gas was observed. After the evolution of gas had stopped, the solvent was removed from the reaction mixture under reduced pressure at 40°C and the residue dried overnight at 60°C in a crystallizing dish in the oven yielding an off-white crystalline solid, which was used for characterization.

Melting point = 108°C . $T_{\text{dec}} = 219^\circ\text{C}$. IR (KBr, 25°C , cm^{-1}) $\nu = 3389$ (s), 3337 (s), 3268 (s), 3159 (m), 3122 (m), 2923 (w), 2255 (s), 2234 (s), 1681 (s), 1661 (s), 1589 (m), 1387 (m), 1300 (m), 1186 (w), 1171 (w), 1103 (w), 1081 (w), 914 (s), 667 (m), 641 (m), 624 (w), 565 (w), 531 (m), 484 (w). Raman (200 mW, 25°C , cm^{-1}) $\nu = 3367$ (6), 3343 (7), 3280 (6), 2257 (100), 2237 (82), 1665 (6), 1500 (35), 1486 (18), 1390 (23), 1302 (12), 1204 (6), 1172 (9), 1084 (36), 1006 (12), 963 (11), 710 (6), 663 (12), 533 (18), 530 (18), 486 (6), 470 (6), 207 (7), 195 (7), 148 (12). ^1H NMR, δ (ppm) 4.67 (s, (2H), H1, H2), 6.72 (s, (2H), H5, H6), 7.24 (s, (2H), H3, H4), 8.54 (s, (1H), H7). ^{13}C NMR, δ (ppm) 113.9 (s, C_4N_5^-), 121.0 (s, C_4N_5^-), 158.8 (s, $\text{C}(\text{NHNH}_2)(\text{NH}_2)_2^+$). ^{14}N NMR, δ (ppm) 25 (s, $\nu_{1/2} = 688$ Hz, N2 in C_4N_5^-), -18 (s, $\nu_{1/2} = 636$ Hz, N1, N3 in C_4N_5^-), -106 (s, $\nu_{1/2} = 606$

Hz, N4, N5 in $C_4N_5^-$), -322 (s, br, $\nu_{1/2} = 1515$ Hz, $C(NHNH_2)(NH_2)_2^+$). C/H/N analysis: calcd. (found) C 31.09 (31.34), H 3.65 (3.95), N 65.26 (65.89)%. MS (FAB+) $CH_7N_4^+$, calcd. 75.09, found 75.1. MS (FAB-) $C_4N_5^-$, calcd. 118.1, found 118.0.

Synthesis of diaminoguanidinium 4,5-dicyano-1,2,3-triazolate (**7**)

The reaction was carried out using the same general procedure as described above for the preparation of **5**. Diaminoguanidinium iodide (0.434 g, 2.0 mmol) was used instead of guanidinium chloride.

$T_{melt} = 124$ °C. $T_{dec.} = 228$ °C. IR (KBr, 25 °C, cm^{-1}) $\nu = 3460$ (s), 3374 (m), 3355 (m), 3241 (s), 3090 (s), 2240 (s), 1672 (s), 1501 (w), 1380 (m), 1362 (m), 1322 (w), 1288 (m), 1188 (w), 1171 (s), 1086 (w), 1055 (w), 961 (s), 946 (s), 762 (m), 707 (w), 680 (m), 651 (m), 639 (w), 524 (m), 477(w). Raman (200 mW, 25°C, cm^{-1}) $\nu = 3358$ (5), 3295 (7), 2242 (100), 1636 (4), 1503 (17), 1483 (5), 1383 (11), 1290 (6), 1165 (5), 1088 (10), 1009 (5), 922 (7), 711 (3), 654 (6), 550 (5), 525 (8), 478 (4), 465 (5), 375 (2), 268 (4), 199 (2). 1H NMR, δ (ppm) 4.55 (s, (4H), H1, H4), 7.10 (s, (2H), H5, H6), 8.51 (s, (2H), H7, H8). ^{13}C NMR, δ (ppm) 114.5 (s, $C_4N_5^-$), 121.5 (s, $C_4N_5^-$), 160.2 (s, $C(NHNH_2)_2(NH_2)^+$). ^{14}N NMR, δ (ppm) 19 (s, $\nu_{1/2} = 739$ Hz, N2 in $C_4N_5^-$), -19 (s, $\nu_{1/2} = 681$ Hz, N1, N3 in $C_4N_5^-$), -111 (s, $\nu_{1/2} = 622$ Hz, N4, N5 in $C_4N_5^-$). C/H/N analysis: calcd. (found) C 28.85 (28.36), H 3.87 (3.93), N 67.28 (66.65)%. MS (FAB+) $CH_8N_5^+$, calcd. 90.1, found 90.1. MS (FAB-) $C_4N_5^-$, calcd. 118.1, found 118.0.

Synthesis of triaminoguanidinium 4,5-dicyano-1,2,3-triazolate (**8**)

A clear solution of triaminoguanidinium bromide (0.370 g, 2.0 mmol) in water/methanol (5/1, 10 mL) was reacted with 0.452 g (2.0 mmol) of solid **3**. The reaction mixture was left stirred for 1 ½ hrs and the yellowish precipitate (AgBr) was filtered off. The remaining clear solution was evaporated to dryness and the product dried under vacuum yielding a cream coloured solid (**8**). Recrystallization from methanol/isohehexane yielded crystals of compound **8** which were suitable for X-ray diffraction.

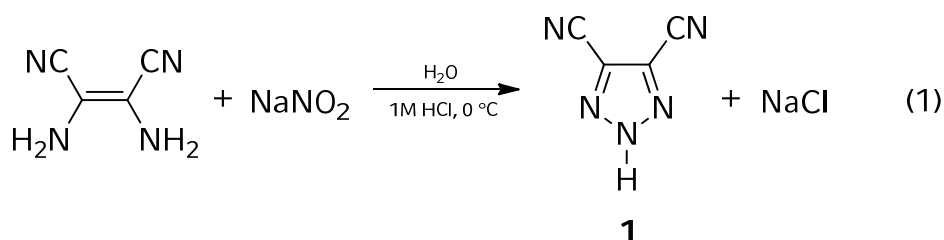
$T_{melt} = 169$ °C. $T_{dec.} = 227$ °C. IR (KBr, cm^{-1}) $\nu = 3355$ (m), 3291 (s), 3209 (s), 3164 (m), 3107 (m), 3027 (m), 2246 (s), 2236 (s), 2121 (vw), 1681 (vs), 1612 (vw), 1566 (vw), 1503 (w), 1447 (vw), 1370 (m), 1349 (s), 1281 (m), 1184 (w), 1158 (w), 1135 (s), 1069

(w), 962 (s), 752 (w), 706 (w), 638 (m), 615 (m), 527 (w), 479 (w). Raman (200 mW, 25°C, cm⁻¹) $\nu = 3355$ (5), 3348 (5), 3294 (6), 2247 (100), 2235 (80), 1681 (3), 1643 (2), 1504 (40), 1484 (4), 1373 (14), 1314 (1), 1283 (12), 1159 (6), 1072 (35), 1007 (6), 885 (6), 709 (5), 650 (8), 629 (4), 529 (8), 523 (6), 479 (6), 474 (6), 408 (4), 245 (3), 230 (3), 152 (5). ¹H NMR, δ (ppm) 4.48 (s, (6H), H1 - H6), 8.58 (s, (3H), H7 - H9). ¹³C NMR, δ (ppm) 114.5 (s, C₄N₅⁻), 121.5 (s, C₄N₅⁻), 159.6 (s, C(NHNH₂)₃⁺). ¹⁴N NMR, δ (ppm) 20 (s, $\nu_{1/2} = 543$ Hz, N2 in C₄N₅⁻), -20 (s, $\nu_{1/2} = 526$ Hz, N1, N3 in C₄N₅⁻), -119 (s, $\nu_{1/2} = 730$ Hz, N4, N5 in C₄N₅⁻). C/H/N analysis: calcd. (found) C 26.91 (25.72), H 4.06 (4.15), N 69.03 (68.19) %. MS (FAB+) CH₉N₆⁺, calcd. 105.1, found 105.1. MS (FAB-) C₄N₅⁻, calcd. 118.1, found 118.0.

2.3 Results and Discussion

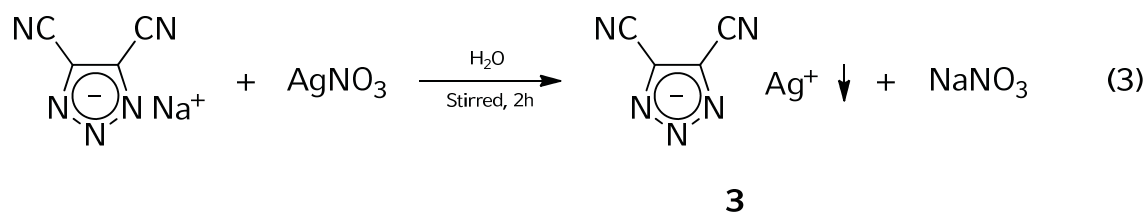
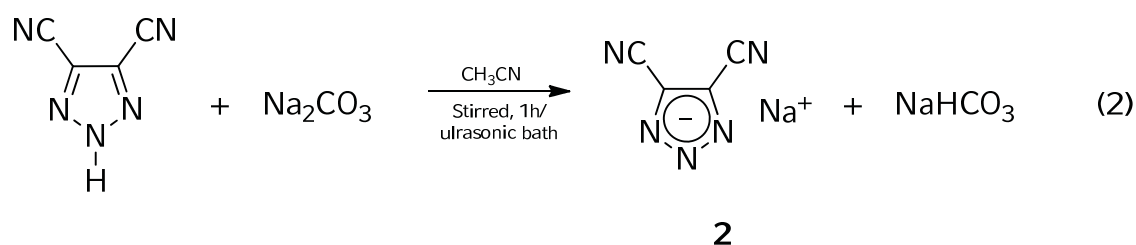
2.3.1 Synthesis and Characterization 1 – 3

Compound **1**, 4,5-dicyano-2H-1,2,3-triazole was synthesized by the reaction of diaminomaleodinitrile in water with hydrochloric acid (1M) and sodium nitrite at 0 °C following the literature procedure (equation 1).^[40b] After sublimation of the crude product, analytically pure **1** was obtained as a white crystalline powder.



Compound **1** is air stable, under ambient conditions and shows no sensitivity towards friction (> 360 N) or impact (> 30 J). The vibrational spectra (IR, Raman) of **1** show the presence of the N-H (3258 cm⁻¹ (IR), 3258 cm⁻¹ (Raman)) and C≡N (2263 cm⁻¹ (IR), 2263 cm⁻¹ (Raman)) groups. Other vibrations are difficult to unambiguously assign but suggest the presence of the triazole ring. In the ¹H NMR spectra compound **1** showed resonance at 7.63 ppm, which is in the expected N-H range. The ¹³C NMR spectrum of **1** shows two signals with chemical shifts of 112.6 and 123.1 ppm which correspond to the

triazole ring carbon atoms and the exocyclic carbon atoms of the nitrile groups. However, since the chemical shifts of both are very similar, an assignment has not been made. Attempts to obtain a ^{14}N NMR spectrum of **1** in d^6 -dmsO showed only very broad peaks, and therefore a ^{15}N NMR spectrum of a highly concentrated solution of **1** in d^6 -dmsO was measured. In the ^{15}N NMR spectrum three signals are observed which correspond to the central ring N-H nitrogen atom (-108.6 ppm), the two equivalent ring nitrogen atoms (-39.2 ppm) and the two equivalent nitrile nitrogen atoms (-76.9 ppm). Compound **1** could be sublimed at relatively low temperature (90°C) under vacuum with cooling of the cold finger using dry-ice to yield white, crystalline **1** in good yields. The mass spectrum (DEI+) of **1** was readily obtained showing a peak corresponding to the molecular peak of **1**. Since **1** could be prepared on a multigram scale and also purified using the above mentioned method in significant quantities, salts of the 4,5-dicyano-1,2,3-triazolate anion could be conveniently prepared by deprotonating compound **1** with Na_2CO_3 to form sodium 4,5-dicyano-1,2,3-triazolate monohydrate (**2**) in good yields (equation 2), which could then be easily converted into the corresponding silver salt (**3**) (equation 3), which was suitable for metathesis reactions with metal-free salts containing nitrogen-rich cations.

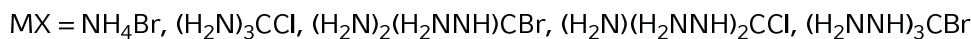
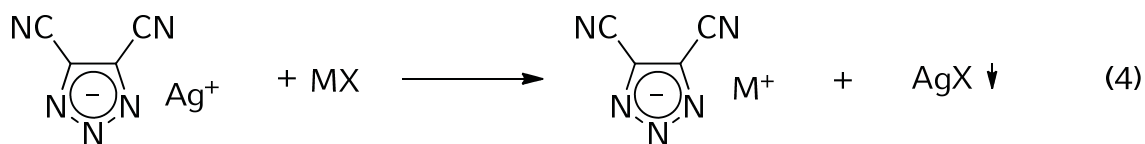


Compounds **2** and **3** were also useful starting materials since neither was shown to be friction ($> 360 \text{ N}$) or impact ($> 30 \text{ J}$) sensitive. Due to the low solubility of **3** in the organic solvents used, it was only characterized using IR and Raman spectroscopy, as well as elemental analysis and Differential Scanning Calorimetry. Compound **2** however, was characterized using various techniques. The IR and Raman spectra of **2** and **3** show

similar features such as the strong nitrile vibration in the Raman spectrum and a similar pattern of peaks in the ring vibration region between 450 – 1550 cm^{-1} . This characteristic pattern of ring vibrations is also observed for the nitrogen-rich salts **4** – **8**. However, the nitrile stretching vibration appears at slightly different wavenumbers (2263 cm^{-1} (**1**); 2260, 2253 cm^{-1} (**2**) and 2245 cm^{-1} (**3**)) and IR (2263 cm^{-1} (**1**); 2251 cm^{-1} (**2**) and 2247 cm^{-1} (**3**)) in the vibrational spectra of compounds **1** – **3**. Notably absent from the IR and Raman spectra of **2** and **3** are the vibrations observed in **1** which were assigned to the N-H group (3258 cm^{-1}), suggesting that deprotonation has occurred. A comparison of the ^{13}C NMR of **1** and **2** shows little change in the positions of signals corresponding to the ring and nitrile carbon atoms following deprotonation. The ^{14}N NMR spectrum of **2** shows the presence of three resonances at 24, -19 and -116 ppm which correspond to the central ring nitrogen atom (N2), the two equivalent ring nitrogen atoms (N1, N3) and the nitrile group nitrogen atoms (N4, N5) respectively. Due to the high solubility of compound **2** in d^6 -dmsO, it was possible to obtain a ^{15}N NMR spectrum of this compound which showed much sharper resonances than the ^{14}N NMR at 21.3 (N2), -20.0 (N1, N3) and -113.0 ppm. These values show very good agreement with the calculated ^{14}N NMR chemical shifts for the DCT anion in the gas phase at the MPW1PW91/aug-cc-pVDZ level of theory (+21, -20 and -113). A comparison of the ^{15}N NMR spectra of compounds **1** and **2** shows that on deprotonation, the N1, N3 and N4, N5 signals (-20.0, -113.0 ppm in **2**; -39.2, -76.9 ppm in **1**) differ less than the values for the signals corresponding to the N2 nitrogen atom which is considerably shifted from -108.6 ppm in **1** to 21.3 ppm in **2**. A comparison of the experimentally obtained (d^6 -dmsO solution) ^{15}N NMR chemical shifts for **1** (-39.2, -108.6, -76.9 ppm) with the calculated (gas-phase) ^{14}N NMR chemical shifts (-36, -136, -76) at the MPW1PW91/aug-cc-pVDZ level of theory shows satisfactory agreement.

2.3.2 Synthesis and Characterization of **4** – **8**

The synthesis of compounds **4** – **8** can be achieved in a convenient and straightforward route, by the simple metathesis reactions of a halide salt of the corresponding nitrogen-rich cation with **3** in organic solvents at room temperature (equation 4). The reactions were carried out in methanol except for the preparation of **8**, where a methanol/water mixture was used due to the poor solubility of triaminoguanidinium bromide in methanol.



The sensitivity tests performed on compounds **4** – **8** showed that they are neither friction (> 360 N) or impact (> 30 J) sensitive, and were insensitive towards electric discharge. On substituting the sodium cation in the dmonohydrate **2**, for the metal-free cations in **4** – **8**, a large jump in the % nitrogen content (by weight) is observed. The theoretical percent nitrogen values increase from 61.7 % in **4** to 62.9 % in **5**, 65.3 % in **6**, 67.3 % in **7** and 69.0 % in **8**, which contains the triaminoguanidinium cation.

In the vibrational (IR, Raman) spectra of **4** – **8**, the absorptions and peaks corresponding to the C≡N triple bond were clearly observed, with little variation in the values observed in changing the countercation, but a slight shift from the values observed for the neutral **1** ($\nu(\text{C}\equiv\text{N}) = 2263$ (IR), 2263 (Ra) cm^{-1} in **1**; 2248 (IR), 2249 (Ra) cm^{-1} in **4**; 2235 (IR), 2238 (Ra) cm^{-1} in **5**; 2255, 2234 (IR), 2257, 2237 (Ra) cm^{-1} in **6**; 2240 (IR), 2242 (Ra) cm^{-1} in **7**; 2246, 2236 (IR), 2247, 2235 (Ra) cm^{-1} in **8**). In addition, the characteristic peak pattern in the Raman spectrum corresponding to vibrations of the 4,5-dicyano-1,2,3-triazolate ring are observed in the spectra for all of the salts of the 4,5-dicyano-1,2,3-triazolate anion reported in this work (**2** – **8**).

For compounds **4** – **8** the ^1H NMR spectra were recorded which showed signals corresponding only to the different cations present. Whereas the ammonium salt **4** showed one resonance at 7.05 ppm corresponding to the NH_4^+ group, and **5** one resonance at 6.87 ppm corresponding to the $\text{C}(\text{NH}_2)_3^+$ cation, the ^1H NMR spectra of compounds **6** – **8** were more complicated, as a result of the presence of both NH and NH_2 groups in the nitrogen-rich cations. The ^1H NMR spectrum of **6** showed four signals which were assigned as follows (atom numbering scheme used is given in Figure 4): $\delta = 4.67$ (H1, H2), $\delta = 6.72$ (H3, H4), $\delta = 7.24$ (H5, H6) and $\delta = 8.54$ (H7) ppm. In the ^1H NMR spectrum of **7** three resonances corresponding to the eight hydrogen atoms in the diaminoguanidinium cation were observed and the resonances can be assigned as follows: $\delta = 4.58$ (H1, H2, H3, H4), $\delta = 7.14$ (H5, H6) and $\delta = 8.55$ (H7, H8) ppm. Finally, the ^1H NMR spectrum of **8** showed only two resonances at 4.48 and 8.58 ppm, corresponding to the three equivalent NH_2 and three equivalent NH groups (H7 – N9) respectively.

In contrast to the ^1H NMR spectra, the ^{13}C NMR spectra of **4** - **8** are all very similar and show relatively little difference in the chemical shifts corresponding to the ring and nitrile groups of the C_4N_5^- anion on swapping the cations. For compounds **4** - **8**, in the ^{13}C NMR spectra a signal was observed at 114 ± 1 ppm, and a second at 121 ± 1 ppm. In addition, **5** - **8** showed one additional signal in each ^{13}C NMR spectrum which corresponded to the central carbon atom of the guanidinium cations. The ^{14}N NMR spectra were recorded of **4** - **8** and showed three broad resonances corresponding to the 4,5-dicyano-1,2,3-triazolate anion at 20 ± 5 ppm, -15 ± 5 ppm and -108 ± 5 ppm. Assignment of these signals was made by calculating the chemical shifts of the 4,5-dicyano-1,2,3-triazolate anion in the gas-phase at the MPW1PW91/aug-cc-pVDZ level of theory. A comparison of the average chemical shifts for **4** - **8** (22, -16 and -110 ppm) which were experimentally obtained in d^6 -dmsO solution, with the calculated (gas-phase) ^{14}N NMR chemical shifts (21, -20, -113) at MPW1PW91/aug-cc-pVDZ level of theory shows very good agreement and were therefore assigned to the N2, N1/N3 and N4/N5 atoms respectively (for labelling scheme see Figure 1). It is worth pointing out that a satisfactory agreement of the experimentally obtained and calculated ^{15}N NMR chemical shifts for the neutral compound **1** was also obtained using this method.

2.3.3 Molecular Structures

The X-ray crystallographic data for compounds **1**, **2** and **4** - **8** were collected on a XCalibur3 CCD diffractometer using graphite-monochromated MoK_α radiation ($\lambda = 0.71073 \text{ \AA}$). The structures were solved with SHELXS-97 and were refined by means of full-matrix least-square procedures using SHELXL-97^[59] implemented in the program package WINGX^[60] and finally checked using PLATON.^[61] Crystallographic data are summarized in Table 1. Selected bond length and angles are available in Table 2, the labeling of the 4,5-dicyano-1,2,3-triazole frame is given in Figure 1. All non-hydrogen atoms were refined anisotropically. Further information on the crystal-structure determinations has been deposited with the Cambridge Crystallographic Data Centre^[62] as supplementary publication no. 702141 (**1**), 702142 (**2**), 702143 (**4**), 702144 (**5**), 702145 (**6**), 702146 (**7**) and 702147 (**8**). Copies of the data can be obtained free of charge on application to CCDC, 12 Union Road, Cambridge CB2 1EZ, UK (fax: (+44) 1223-336-033; e-mail: deposit@ccdc.cam.ac.uk).

Table 1: Crystal data and details of the structure determination for **1**, **2** and **4 - 8**.

Parameter	HC ₄ N ₅ (1)	NaC ₄ N ₅ ·H ₂ O (2)	NH ₄ C ₄ N ₅ (4)	C(NH ₂) ₃ C ₄ N ₅ (5)	C(NHNH ₂)(NH ₂) ₂ C ₄ N ₅ (6)	C(NHNH ₂) ₂ (NH ₂)C ₄ N ₅ (7)	C(NHNH ₂) ₃ C ₄ N ₅ (8)
Formula	C ₄ H N ₅	C ₄ H ₂ N ₅ Na ₁ O ₁	C ₄ N ₆ H ₄	C ₅ H ₆ N ₈	C ₅ H ₇ N ₉	C ₅ H ₈ N ₁₀	C ₅ H ₉ N ₁₁
F. Wt. (g/mol)	119.10	159.10	136.12	178.18	193.20	208.21	223.23
Crystal system	monoclinic	monoclinic	orthorhombic	monoclinic	monoclinic	monoclinic	monoclinic
Space group	<i>P2₁/c</i>	<i>P2₁/c</i>	<i>Pnma</i>	<i>Cc</i>	<i>Pa</i>	<i>P2₁</i>	<i>C2/c</i>
Size	0.06x0.05x0.06	0.08x0.06x0.01	0.05x0.04x0.05	0.06x0.05x0.03	0.06x0.05x0.02	0.07x0.06x0.04	0.05x0.04x0.04
<i>a</i> / Å	6.0162(6)	3.6767(6)	6.5646(13)	12.6000(11)	7.0921(9)	3.7727(4)	14.0789(14)
<i>b</i> / Å	11.2171(10)	20.469(4)	7.5707(16)	17.1138(15)	7.2893(9)	15.6832(17)	11.5790(11)
<i>c</i> / Å	7.5625(7)	9.6223(13)	13.303(3)	12.0952(9)	8.8671(11)	8.3416(10)	13.5840(14)
α / °	90.00	90.00	90.0	90.0	90.0	90.0	90.0
β / °	94.21(1)	97.355(13)	90.0	106.098(7)	105.141(1)	101.797(10)	115.239(10)
γ / °	90.00	90.00	90.0	90.0	90.0	90.0	90.0
<i>V</i> / Å ³	508.97(8)	718.2(2)	661.1(2)	2505.9(4)	442.48(10)	483.13(9)	2003.1(3)
<i>Z</i>	4	4	4	12	2	2	8
$\rho_{\text{calc.}}$ / g/cm ³	1.554	1.470	1.368	1.417	1.450	1.431	1.480
μ / mm ⁻¹	0.114	0.181	0.107	0.104	0.108	0.107	0.111
$\lambda_{\text{MoK}\alpha}$ / Å	0.71073	0.71073	0.71073	0.71073	0.71073	0.71073	0.71073
<i>T</i> / °K	200	200	200	200	200	200	200
<i>F</i> (000)	240	350	304	1104	200	216	928
GooF	1.003	1.019	1.133	1.009	1.055	0.975	0.909
<i>R</i> ₁ ^a (obs)	0.0373	0.0376	0.0527	0.0487	0.0342	0.0459	0.0551
w <i>R</i> ₂ ^b (all data)	0.0957	0.1080	0.1420	0.1236	0.0879	0.1025	0.1174

$$^a R_1 = \sum |F_o| - |F_c| / \sum |F_o|, \quad ^b wR_2 = \left[\frac{\sum [w(F_o^2 - F_c^2)]}{\sum [w(F_o^2)]} \right]^{1/2}, \quad \text{where } w = \left[\sigma_c^2(F_o^2) + (xP)^2 + yP \right]^{-1}, \quad P = (F_o^2 - 2F_c^2) / 3$$

Table 2: Comparison of selected bond lengths (Å) and angles (°) in 4,5-dicyano-2*H*-1,2,3-triazole (**1**), with the 4,5-dicyano-1,2,3-triazolate anions in **2** and **4 – 8** compared with the previously calculated structural parameters of the C₄N₅⁻ optimized in C_{2v} symmetry at the MPW1PW91/aug-cc-pVDZ level of theory. The numbering scheme used is illustrated in Figure 1.

Parameter (<i>d</i> / Å; ∠ / °)	(1)	(2)	(4)	(5)	(6)	(7)	(8)	calculated
N1 – N2	1.319(1)	1.329(1)	1.336(1)	1.340(4)	1.340(5)	1.336(3)	1.342(4)	1.325
N2 – N3	1.320(4)	1.329(2)	1.336(1)	1.340(6)	1.334(2)	1.346(6)	1.339(3)	1.325
N3 – C2	1.338(5)	1.353(4)	1.349(2)	1.348(4)	1.350(9)	1.359(6)	1.351(4)	1.351
N1 – C1	1.341(3)	1.349(2)	1.349(2)	1.340(6)	1.344(7)	1.380(8)	1.350(3)	1.351
C1 – C3	1.433(4)	1.423(2)	1.421(2)	1.425(5)	1.421(8)	1.434(4)	1.424(4)	1.417
C2 – C4	1.429(2)	1.423(3)	1.421(2)	1.428(7)	1.421(5)	1.450(8)	1.417(3)	1.417
C1 – C2	1.402(4)	1.385(4)	1.386(2)	1.380(5)	1.391(2)	1.379(4)	1.383(4)	1.404
C3 – N4	1.143(3)	1.140(2)	1.148(2)	1.149(5)	1.139(7)	1.146(4)	1.145(4)	1.164
C4 – N5	1.145(2)	1.141(3)	1.148(2)	1.133(6)	1.144(4)	1.163(7)	1.147(3)	1.164
N2 – H2	0.986(15)	--	--	--	--	--	--	--
N1–N2–N3	116.92(8)	111.77(9)	111.62(7)	110.80(22)	112.18(14)	110.85(20)	111.06(21)	112.17
N2–N3–C2	103.07(8)	106.35(10)	106.4(1)	106.24(15)	105.99(14)	107.71(22)	106.59(18)	106.80
N2–N1–C1	103.13(8)	106.70(9)	106.4(1)	106.73(25)	106.01(14)	106.21(19)	106.73(20)	106.80
N3–C2–C1	108.59(8)	107.72(10)	107.79(11)	107.67(27)	107.78(14)	107.03(21)	107.95(23)	107.12
N1–C1–C2	108.28(8)	107.47(10)	107.79(11)	108.15(24)	108.04(13)	108.20(21)	107.68(20)	107.12
C3–C1–C2	131.05(9)	129.36(11)	128.03(12)	126.51(27)	126.94(15)	128.77(32)	128.77(25)	129.76
C4–C2–C1	130.58(9)	129.98(11)	128.03(12)	128.00(31)	127.02(14)	129.64(23)	129.43(21)	129.76
C1–C3–N4	179.24(11)	179.36(14)	176.66(15)	177.02(41)	176.06(20)	177.72(29)	177.73(29)	
C2–C4–N5	179.67(11)	178.79(13)	176.66(15)	176.19(39)	174.86(18)	178.46(27)	178.29(25)	

Crystal structures of of 4,5-dicyano-2H-1,2,3-triazole (1) and sodium 4,5-dicyano-1,2,3-triazolate hydrate (2)

4,5-Dicyano-2H-1,2,3-triazole (**1**) crystallizes in the monoclinic space group $P2_1/c$ with four molecular moieties in the unit cell and a calculated density of 1.554 g cm^{-3} , which is low to be considered as being a possible useful energetic material, and a cell volume of $V = 508.97(8) \text{ \AA}^3$. In the neutral compound **1**, the C1-N1 and C2-N3 bond lengths were found to be much shorter ($1.340(3)$ and $1.338(6) \text{ \AA}$) than the average value for a C-N single bond (1.47 \AA),^[41] but significantly longer than a C=N double bond (1.22 \AA), suggesting that some multiple bond character is present.^[41] A similar trend is observed for the C1-C2 bond in **1** ($1.402(6) \text{ \AA}$), which is significantly shorter than a C-C single (1.54 \AA), but longer than a C=C double bond (1.33 \AA)^[41] and the N1-N2 and N2-N3 bonds ($1.318(5)$ and $1.321(4) \text{ \AA}$ respectively) which are also significantly shorter than a N-N single bond (1.48 \AA) but considerably longer than a N=N double bond (1.20 \AA).^[41] These findings support the presence of a delocalized π – system in the five-membered ring of compound **1**. The triazole ring is completely planar with the cyanogen groups and the hydrogen atom lying in one plane with the ring (Figure 1). The angles and bond length are therefore in good agreement with the expected values and values calculated by Johansson.^[40b]

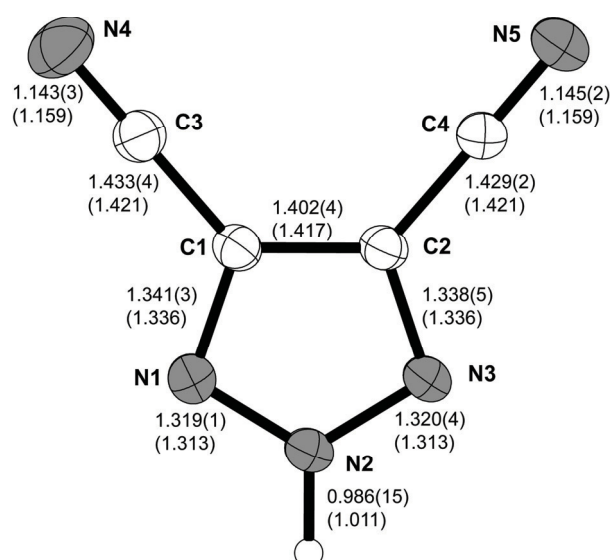


Figure 1: ORTEP representation of the molecular structure of **1** in the solid state determined using single crystal X-ray diffraction. Thermal ellipsoids are shown with 50 % probability. Bond lengths given in parenthesis (\AA) are the calculated (MPW1PW91/aug-cc-pVDZ level of theory) gas-phase values for comparison with the experimentally determined values for the crystalline state.

The packing of the structure of **1** is characterized by two significant hydrogen bonds which were found located between the N2 and N3 (donor and acceptor) and the N2 and N5 nitrogen atoms. Since we have only one donor center, we see a bifurcated hydrogen bonding scheme starting from N2 as the donor atom. The two hydrogen bonds show a distance of less than 3 Å (2.997(2) and 2.91(1) Å) from the donor to the acceptor atom. Both hydrogen bonds are within the sum of van der Waals radii for two nitrogen atoms ($r_{A(N)} + r_{D(N)} = 3.20$ Å) but are more of an electrostatic rather than a strongly directed nature due to the bond angles of 135.2(1) and 122.3(1)° respectively (Table 3, Figure 2). The hydrogen bonding forms ordered rows in the structure formed by opposite lying HDCT moieties (Figure 2).

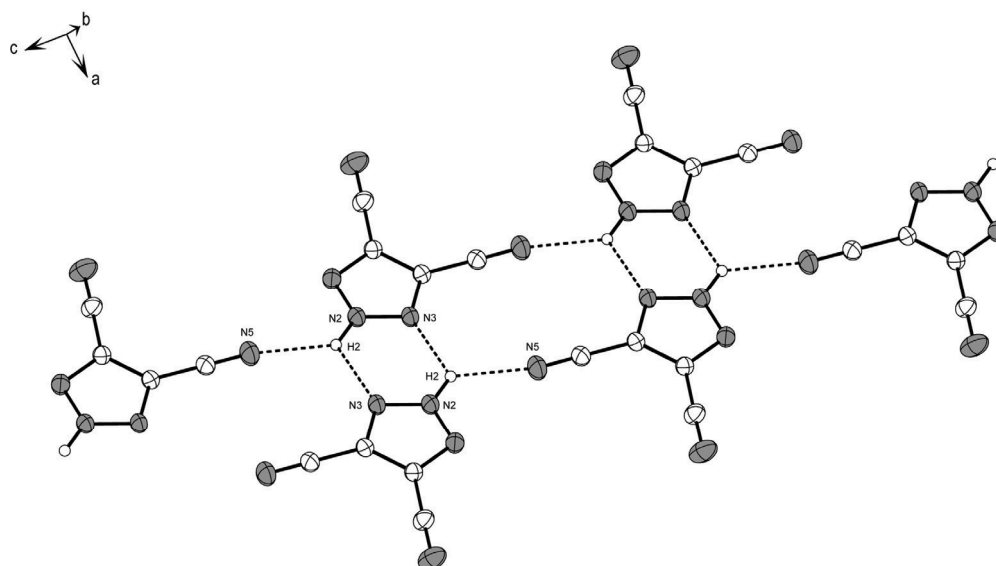


Figure 2: ORTEP representation showing selected intermolecular hydrogen bonds in **1** as determined using single crystal X-ray diffraction. Thermal ellipsoids are shown with 50 % probability.

The sodium 4,5-dicyano-1,2,3-triazolate hydrate (**2**) crystallizes in the monoclinic space group $P2_1/c$ with four molecular moieties in the unit cell and a calculated density of 1.470 g cm⁻³ and a cell volume of $V = 718.2(2)$ Å³. The 4,5-dicyano-1,2,3-triazolate anion in **2** shows a similar structure to that observed for the neutral compound **1**, the predominate difference being the absence of a N-H bond in **2** as a result of deprotonation. The C1-C2 bond length in **2** (1.38(1) Å) is shorter than the corresponding C1-C2 bond in **1** (1.399(6) Å), whereas the N1-N2 and N2-N3 bonds in the C₄N₅⁻ anion in **2** are found to be essentially the same (1.325(4), 1.328(8) Å) as those observed in **1** (1.318(5), 1.321(4) Å). The C1-N1 and C2-N3 bonds in **2** (1.354(9) and 1.357(8) Å respectively) are slightly longer than the corresponding bond lengths in **1** (1.340(3) and 1.338(6) Å respectively).

There is some variation between the angles observed in **1** and **2**, namely the N1-N2-N3 angle is larger in **1** ($116.87(9)^\circ$) than in **2** ($111.5(1)^\circ$), whereas the N2-N3-C2 and N2-N1-C1 angles are smaller in **1** ($103.02(9)^\circ$, $103.26(9)^\circ$), than in **2** ($106.6(1)$ and $106.9(1)^\circ$). The angles and bond lengths observed show no unexpected values and are in good agreement with the calculated values published by Johansson.^[40b] The density of **2** is still very low (1.470 g cm^{-3}), and is therefore lower than the density of the neutral compound **1**.

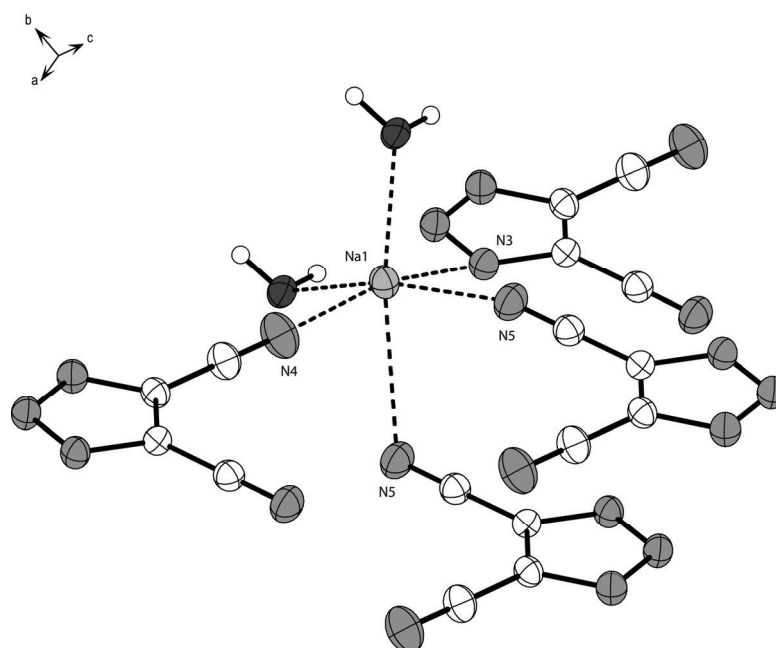


Figure 3: ORTEP representation showing the coordination environment of the sodium cations in **2** as determined using single crystal X-ray diffraction. Thermal ellipsoids are shown with 50 % probability.

The sodium cation shows a distorted octahedral environment, which is made up of the coordination of four C_4N_5^- anions and two water molecules. Surprisingly, the interactions between the sodium cation and triazolate anion involve predominantly the nitrile nitrogen atoms (three contacts) and not the ring nitrogen atoms (one contact). The coordination sphere of the sodium cation in **2** is shown in Figure 3. Since this report is primarily concerned with metal-free C/H/N compounds and **2** was primarily of interest as a starting material for the preparation of **3**, the structure of **2** will not be discussed here in more detail.

Molecular structures of ammonium (4), guanidinium (5), aminoguanidinium (6), diaminoguanidinium (7) and triaminoguanidinium (8) 4,5-dicyano-1,2,3-triazolate

The structures of compounds **4** – **8** in the crystalline state showed the presence of the 4,5-dicyano-1,2,3-triazolate anion in addition to the metal-free cation. A comparison of the structural parameters of the metal-free cations observed in **5** – **8** with those of other guanidinium and related aminoguanidinium salts previously described in the literature^[42] showed that no significant differences were observed in salts **5** – **8**.^[42] A summary of selected structural parameters of the cations in **5** – **8** is given in Table 4. In addition, the structural parameters of the 4,5-dicyano-1,2,3-triazolate anion are summarised in Table 3 and show no significant differences in comparison with the structural parameters of the $C_4N_5^-$ anion described in **2**. Therefore, the structures of the $C_4N_5^-$ anions in **4** – **8** are not discussed here in more detail.

The calculated densities of the compounds are all in the same range, with the density for **4** being the lowest at 1.368 g cm^{-3} and 1.480 g cm^{-3} being the highest for **8**. If we only compare the guanidinium salts, we see less variation with the density of **5** being the lowest at 1.417 g cm^{-3} of the four guanidinium compounds and **8** being the highest at 1.480 g cm^{-3} . Unfortunately, the densities are all low, in contrast to required high densities for energetic materials.

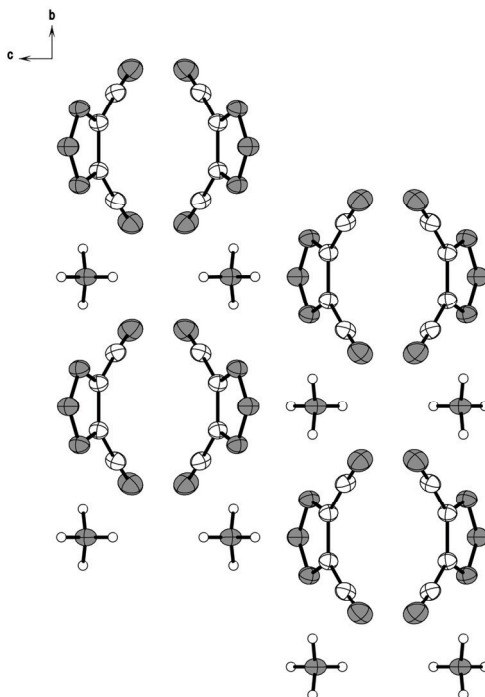
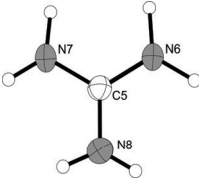
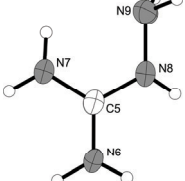
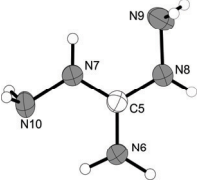
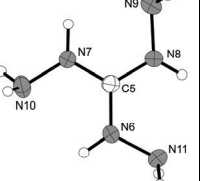


Figure 5: ORTEP representation showing the unit cell of **4** along the a-axis, as determined using single crystal X-ray diffraction. Thermal ellipsoids are shown with 50 % probability.

Table 3: Comparison of selected hydrogen bond length (Å) and angles (°) between 4,5-dicyano-2*H*-1,2,3-triazole (**1**), and the 4,5-dicyano-1,2,3-triazolate anions in salts **4 – 8** containing the nitrogen-rich cations. The numbering scheme used is illustrated in Figure 1 (for the anion without the hydrogen atom H2 located at N2) (D = hydrogen bond donor atom; A = hydrogen bond acceptor atom).

(1)		(4)		(5)		(6)		(7)		(8)	
Atoms	$d(\text{D-A})/\text{Å}$	Atoms	$d(\text{D-A})/\text{Å}$	Atoms	$d(\text{D-A})/\text{Å}$	Atoms	$d(\text{D-A})/\text{Å}$	Atoms	$d(\text{D-A})/\text{Å}$	Atoms	$d(\text{D-A})/\text{Å}$
N2-N5	2.997(2)	N6-N5	3.02(3)	N7-N4	3.24(7)	N8-N5	3.14(2)	N6-N3	2.88(3)	N8-N1	2.91(7)
N2-N3	2.91(1)	N6-N4	3.02(3)	N7-N2	3.05(5)	N6-N4	3.00(2)			N6-N3	2.88(9)
		N6-N1	2.99(2)	N6-N3	2.91(5)	N7-N1	3.02(2)				
		N6-N3	2.99(2)			N6-N2	2.91(2)				
		N6-N2	2.91(2)			N7-N3	3.04(2)				
Atoms	$\angle(\text{D-H-A})/\text{°}$	Atoms	$\angle(\text{D-H-A})/\text{°}$	Atoms	$\angle(\text{D-H-A})/\text{°}$	Atoms	$\angle(\text{D-H-A})/\text{°}$	Atoms	$\angle(\text{D-H-A})/\text{°}$	Atoms	$\angle(\text{D-H-A})/\text{°}$
N2H2N5	135.3(1)	N6H1N4	123.7(6)	N7H7bN4	158.7(3)	N8H8N5	137.1(2)	N6H6aN3	166.1(2)	N8H8N1	149.8(2)
N2H2N3	122.3(1)	N6H1N5	123.7(6)	N7H7aN2	163.0(3)	N6H6aN4	166.7(2)			N6N6N3	156.0(2)
		N6H3N6	170.2(2)	N6H6bN3	158.4(3)	N7H7aN1	162.7(2)				
		N6H4N1	170.2(2)			N6H6bN2	170.0(2)				
		N6H2N2	172.5(2)			N7H7bN3	153.1(2)				

Table 4: Comparison of selected bond length (Å) and angles (°) of the nitrogen-rich guanidinium cations in the 4,5-dicyano-1,2,3-triazolate salts **5** – **8**.

Compound	(5)	(6)	(7)	(8)
				
$d(\text{C5-N8}) / \text{Å}$	1.34(5)	1.34(1)	1.35(4)	1.38(8)
$d(\text{C5-N7}) / \text{Å}$	1.31(6)	1.32(1)	1.33(3)	1.30(7)
$d(\text{C5-N6}) / \text{Å}$	1.33(6)	1.32(4)	1.34(8)	1.34(6)
$d(\text{N8-N9}) / \text{Å}$	--	1.41(4)	1.44(9)	1.38(8)
$d(\text{N7-N10}) / \text{Å}$	--	--	1.41(4)	1.41(8)
$d(\text{N6-N11}) / \text{Å}$	--	--	--	1.41(6)
$\angle(\text{N7-C5-N8}) / ^\circ$	119.7(3)	118.8(1)	120.1(2)	115.4(5)
$\angle(\text{N6-C5-N7}) / ^\circ$	120.7(3)	121.3(1)	121.0(2)	124.3(4)
$\angle(\text{N8-C5-N6}) / ^\circ$	119.6(3)	120.0(1)	118.9(2)	120.3(5)
$\angle(\text{C5-N8-N9}) / ^\circ$	--	118.6(1)	118.0(2)	115.5(5)
$\angle(\text{C5-N7-N10}) / ^\circ$	--	--	117.5(2)	113.1(4)
$\angle(\text{C5-N6-N11}) / ^\circ$	--	--	--	121.5(4)
$\angle(\text{N9-N8-C5-N7}) / ^\circ$	--	4.8(2)	0.4(3)	2.9(8)
$\angle(\text{N10-N7-C5-N6}) / ^\circ$	--	--	0.4(3)	5.2(8)
$\angle(\text{N11-N6-C5-N8}) / ^\circ$	--	--	--	5.2(8)
$\angle(\text{C5-N8-N7-N6}) / ^\circ$	0.0(3)	1.1(1)	0.4(2)	1.3(4)

Compound **4** crystallizes in the orthorhombic space group $Pnma$ with four molecular moieties in the unit cell, a density of 1.417 g cm^{-3} and a unit cell volume of $V = 661.1(2) \text{ Å}^3$. Due to the relatively high symmetry of the orthorhombic space group, we observe a very ordered structure. In the unit cell of **5**, the NH_4^+ cations are located between columns of 4,5-dicyano-1,2,3-triazolate anions, which are located as pairs with the nitrile groups pointing towards each other. In addition, the five-membered rings of the 4,5-dicyano-1,2,3-triazolate anions do not lie in one plane, but are staggered with respect to one another. Furthermore, each row of the C_4N_5^- anions present in the columns is comprised of a stack of C_4N_5^- anions from different layers. (Figure 5)

Each ammonium cation in **4** forms five significant hydrogen bonds with both the ring and nitrile nitrogen atoms of the surrounding 4,5-dicyano-1,2,3-triazolate anions (Figure 6). Three of the hydrogen bonds observed involve the triazole ring nitrogen atoms (N1, N2 and N3), whereas the other occur with the two nitrogen atoms in the exocyclic nitrile groups (N4 and N5). However, the donor-acceptor distances are essentially the same. The donor-acceptor distances in the stronger hydrogen bonds involving the ring nitrogen atoms are just under 3.0 Å ($2.99(2) \text{ Å}$, $2.91(2) \text{ Å}$) and are directed with $\text{D} - \text{H} \cdots \text{A}$

angles of $170.2(2)^\circ$ and $172.5(2)^\circ$. The slightly longer ($3.02(3) \text{ \AA}$) donor-acceptor distances in the hydrogen bonds between the ammonium cation and the nitrogen atoms of the exocyclic nitrile group of the C_4N_5^- anion are more of an electrostatic nature with a bent $\text{D} - \text{H} \cdots \text{A}$ angle of $123.7(6)^\circ$. The hydrogen bonding towards the nitrile group shows a bifurcated character, which explains the electrostatic nature of the bonding, as well as the comparably small $\text{D} - \text{H} \cdots \text{A}$ angle of $123.7(6)^\circ$. The hydrogen bonds formed involve the ammonium cation and form a three dimensional network. The selected important hydrogen bonds discussed above are illustrated in Figure 6 and summarized in Table 3.

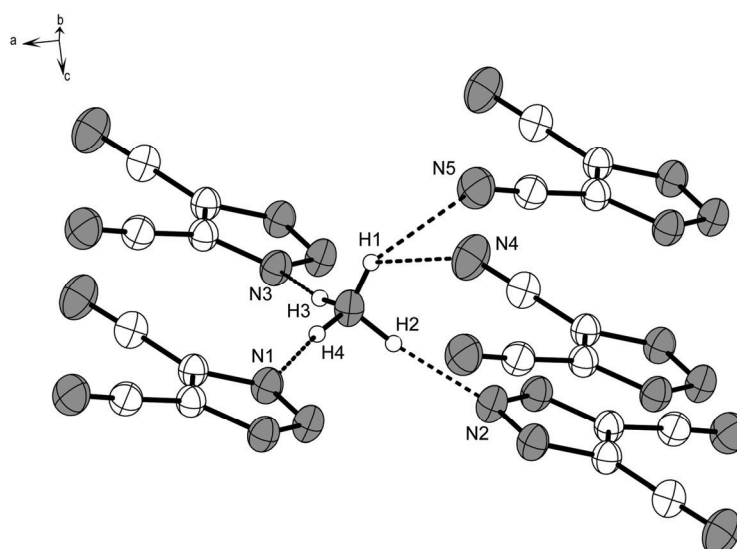


Figure 6: ORTEP representation showing selected hydrogen bonds between the NH_4^+ cation and C_4N_5^- anion in **4**, as determined using X-ray diffraction. Thermal ellipsoids are shown with 50 % probability.

The cation used in the C_4N_5^- salts was then changed from the tetrahedral NH_4^+ to the planar guanidinium cation. Guanidinium 4,5-dicyano-1,2,3-triazolate (**5**) crystallizes in the monoclinic space group Cc with 12 molecular moieties per unit cell, a calculated density of 1.417 g cm^{-3} and a unit cell volume of $V = 2505.9(4) \text{ \AA}^3$. The structure of **5** is strongly influenced by the formation of the hydrogen bonds between the guanidinium cation and the C_4N_5^- anion. Three different hydrogen bonds form infinite rows which are packed in a co-planar manner. In **5**, one guanidinium cation forms three hydrogen bonds to two 4,5-dicyano-1,2,3-triazolate anions which are at either side of the guanidinium cation within a row. However, only two of these bonds are below the sum of van der Waals radii for N-N donor-acceptor hydrogen bonds at $2.913(5)$ and $3.049(5) \text{ \AA}$, respectively. The third hydrogen bond shows a donor acceptor distance of $3.237(7) \text{ \AA}$

which is longer than the sum of van der Waals radii ($r_{A(N)} + r_{D(N)} = 3.20 \text{ \AA}$).^[43] All of these bonds are of a rather directed than only an electrostatic nature with $D - H \cdots A$ angles between 158° and 166° (Figure 7). No unexpected structural parameters were observed for the guanidinium cation (Table 4).

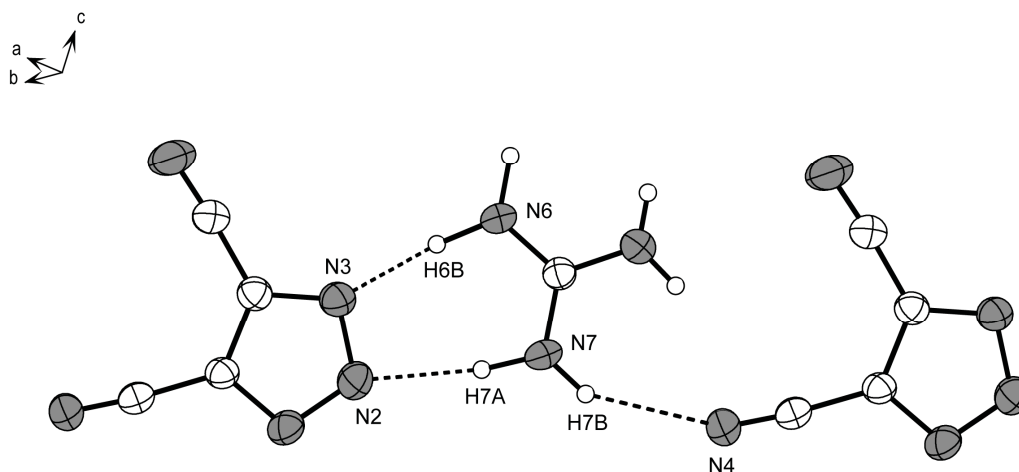


Figure 7: ORTEP representation showing selected hydrogen bonds between the guanidinium cation and $C_4N_5^-$ anion in **5**, as determined using X-ray diffraction. Thermal ellipsoids are shown with 50 % probability.

On introducing the aminoguanidinium cation instead of the guanidinium cation, the percentage nitrogen content by weight of **6** was increased relative to **5**, however, the density of **6** remained low (1.450 g cm^{-3}). Aminoguanidinium 4,5-dicyano-1,2,3-triazolate (**6**) crystallizes in the monoclinic space group Pa with 2 molecular moieties per unit cell, a calculated density of 1.450 g cm^{-3} and a unit cell volume of $V = 442.48(10) \text{ \AA}^3$. The structure of **6** is relatively simple and consists of layers. Within these co-planar layers, four aminoguanidinium cations surround one 4,5-dicyano-1,2,3-triazolate anion and form five hydrogen bonds to each anion. Four of the hydrogen bonds shown in Figure 8 are within the range of the sum of the van der Waals radii ($r_{A(N)} + r_{D(N)} = 3.20 \text{ \AA}$),^[43] and the $D - H \cdots A$ angles between are found in the range $152 - 170^\circ$. They are therefore again more of a directed rather than only of an electrostatic nature. However, the $N8 - H4 \cdots N7$ hydrogen bond is relatively long ($3.14(2) \text{ \AA}$) and has an angle of only $137.1(2)^\circ$, which suggests that it should only be considered a very weak hydrogen bond. A list of selected hydrogen bonds found in **6**, is given in Table 3. Again, in **6**, the structural parameters for both the aminoguanidinium cation and 4,5-dicyano-1,2,3-triazolate anion are in good agreement with previously published structures,^[40c, 40b] and the structures of

compounds **2**, **4**, **5**, **7** and **8** given in this work respectively (Table 2), and therefore are not discussed here in more detail.

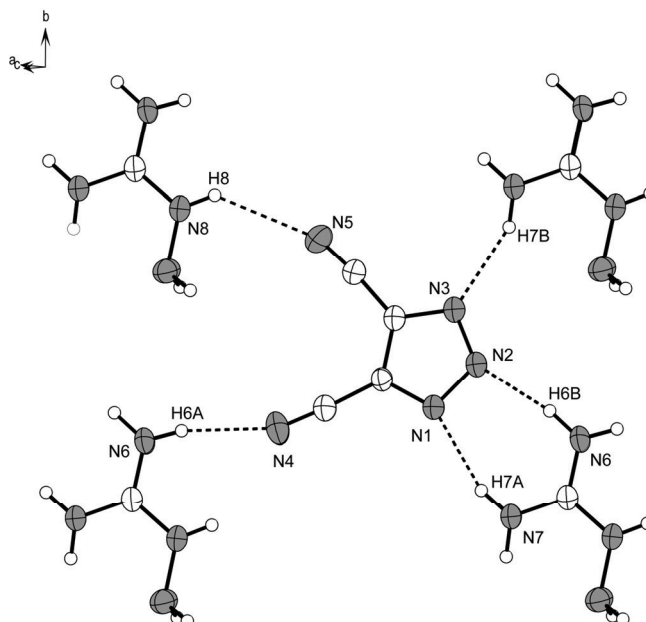


Figure 8: ORTEP representation showing selected hydrogen bonds between the aminoguanidinium cation and $C_4N_5^-$ anion in **6**, as determined using X-ray diffraction. Thermal ellipsoids are shown with 50 % probability.

On addition of a further amino group to the cation, the diaminoguanidinium salt of the 4,5-dicyano-1,2,3-triazolate anion (**7**) could be prepared. Diaminoguanidinium 4,5-dicyano-1,2,3-triazolate (**7**) crystallizes in the monoclinic space group $P2_1$ with 2 molecular moieties per unit cell, a calculated density of 1.431 g cm^{-3} and a unit cell volume of $483.13(9) \text{ \AA}^3$. The calculated density of **7** (1.431 g cm^{-3}) is lower than that found for **6** (1.450 g cm^{-3}), but higher than that found for **5** (1.417 g cm^{-3}). As was observed in the structure of **6**, the structure of **7** is also built up of layers containing the diaminoguanidinium cations and 4,5-dicyano-1,2,3-triazolate anions. (Figure 9) In contrast to **6**, however, only one significant hydrogen bond was observed between the NH_2 group of the diaminoguanidinium cation and one ring nitrogen atom of a neighbouring $C_4N_5^-$ anion (Table 3). This hydrogen bond is relatively strong with a donor-acceptor distance of $2.88(3) \text{ \AA}$ and a $N-H \cdots N$ angle of $166.1(2)^\circ$.

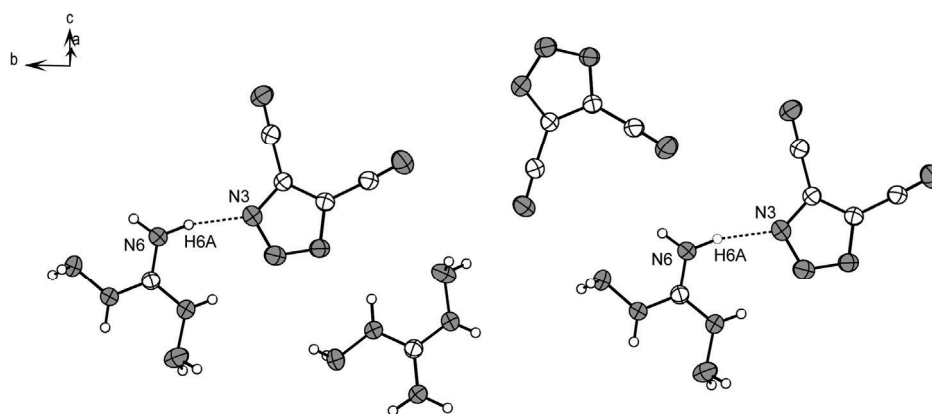


Figure 9: ORTEP representation showing selected hydrogen bonds between the diaminoguanidinium cation and $C_4N_5^-$ anion in **7**, as determined using X-ray diffraction. Thermal ellipsoids are shown with 50 % probability.

The highest calculated density for the metal-free salts containing the 4,5-dicyano-1,2,3-triazolate anion discussed in this work was observed for compound **8**, which has a calculated density of 1.480 g cm^{-3} . Triaminoguanidinium 4,5-dicyano-1,2,3-triazolate (**8**) crystallizes in the monoclinic space group $C2/c$ with 8 molecular moieties per unit cell, a calculated density of 1.480 g cm^{-3} and a unit cell volume of $V = 2003.1(3) \text{ \AA}^3$. As was observed for **6** and **7**, compound **8** also features a layer structure in the unit cell. The layers are again ordered in a co-planar fashion. Two strong hydrogen bonds are observed in the structure of **8** between the NH group of the triaminoguanidinium cation and the N1 and N3 atoms of the nitrogen ring of one of the 4,5-dicyano-1,2,3-triazolate anions. Both hydrogen bonds show similar distances with $2.91(7)$ and $2.88(9) \text{ \AA}$ and non-linear angles of $149.8(3)^\circ$ and $156.0(6)^\circ$ (Table 3). One monolayer with the corresponding hydrogen bonds is shown in Figure 10.

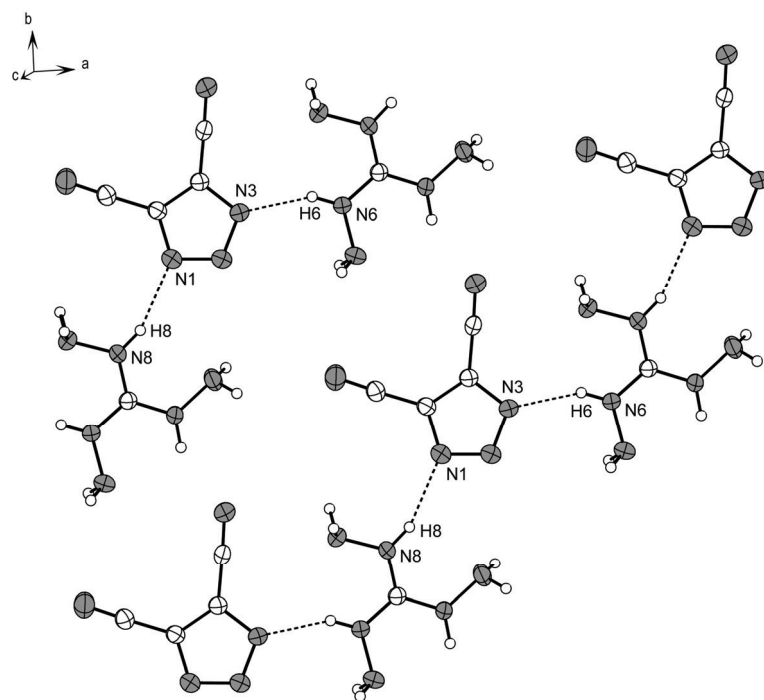


Figure 10: ORTEP representation showing selected hydrogen bonds between the triaminoguanidinium cation and C₄N₅⁻ anion in **8**, as determined using X-ray diffraction. Thermal ellipsoids are shown with 50 % probability.

2.3.4 Energetic Properties of **1** and **5 – 8**

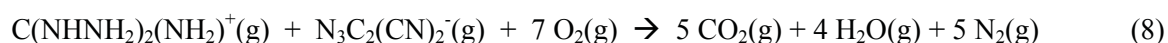
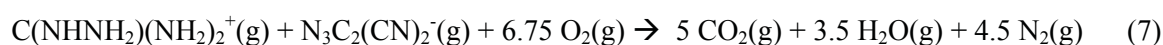
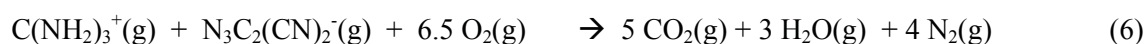
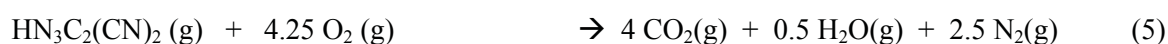
All calculations were carried out using the program package G03W.^[44] The structure and frequency calculations were performed at the electron correlated Møller-Plesset (MP) level of theory, truncated at second order (MP2).^[45] For all atoms H, C, N and O an augmented correlation consistent polarized double-zeta basis set was used (aug-cc-pVDZ).^[46] The calculation of the detonation parameters was performed with the program package EXPLO5 (version 5.02).^[47] The computational results are summarized in Table 5.

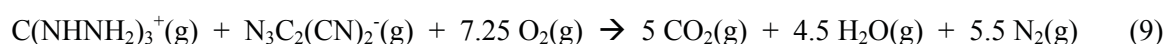
Table 5: Computational results (MP2/aug-cc-pVDZ).

Compound	Formula	p.g	$-E / \text{a.u.}$	$zpe / \text{kcal mol}^{-1}$	<i>NIMAG</i>
ammonium	NH_4^+	T_d	56.739780	31.2	0
guanidinium	$\text{C}(\text{NH}_2)_3^+$	D_{3h}	205.218050	55.3	0
amino-guanidinium	$\text{C}(\text{NH}-\text{NH}_2)(\text{NH}_2)_2^+$	C_1	260.403398	66.2	0
diamino-guanidinium	$\text{C}(\text{NH}-\text{NH}_2)_2(\text{NH}_2)^+$	C_1	315.588401	77.5	0
triamino-guanidinium	$\text{C}(\text{NH}-\text{NH}_2)_3^+$	C_3	370.773187	100.8	0
dicyanotriazolate	$\text{N}_3\text{C}_2(\text{CN})_2^-$	C_{2v}	425.137114	26.9	0
4,5-dicyano-2 <i>H</i> -triazole	$\text{HN}_3\text{C}_2(\text{CN})_2$	C_{2v}	425.633873	36.6	0
carbonmonoxide	CO	$C_{\infty v}$	113.054970	3.0	0
water	H_2O	C_{2v}	76.260910	13.4	0
dihydrogen	H_2	$D_{\infty h}$	1.156216	6.4	0
dinitrogen	N_2	$D_{\infty h}$	109.280650	3.1	0
carbondioxide	CO_2	$D_{\infty h}$	188.169700	7.1	0
dioxygen	O_2	$D_{\infty h}$	150.004290	2.0	0

For compounds **5** – **8** the lattice energies and lattice enthalpies were calculated according the Jenkins equations and are summarized in Table 6.^[48-51] For compound **1** the enthalpy of sublimation was estimated according to the formula: $\Delta H_{\text{sub}} [\text{J mol}^{-1}] = 188 [\text{J mol}^{-1} \text{K}^{-1}] T_m [\text{K}]$.

With the values given in Table 5 the ΔE^{el} for equations 5 – 9 were calculated and are summarized in Table 6.





The ΔE^{el} values for equations 5 – 9 (Table 6) were converted into the gas phase reaction enthalpy ($\Delta_{\text{rxn}}H$) after correction for the work term ($p\Delta V = \sum v_i RT$), the vibrational correction ($\Delta_{\text{vib}}U = \sum v_i (zpe)_i$), the translational ($\Delta_{\text{trans}}U = \sum v_i (1.5) RT$) and rotational term ($\Delta_{\text{rot}}U = \sum v_i (F_i^{\text{rot}} / 2) RT$).^[52] With the help of the calculated lattice enthalpies (Table 6) the $\Delta_{\text{rxn}}H$ values were now converted into combustion enthalpies $\Delta_{\text{comb}}H$ (Table 6).

Table 6: Calculated reaction energies and enthalpies for equations (5) – (9)

	$\Delta E^{\text{el}} / \text{kJ mol}^{-1}$	$\Delta_{\text{rxn}}H / \text{kJ mol}^{-1}$	$\Delta_{\text{comb}}H / \text{kJ mol}^{-1}$
equation (5)	-2253.2	-2248.1	-2168.8
equation (6)	-3596.6	-3596.3	-3092.2
equation (7)	-3817.9	-3822.0	-3325.2
equation (8)	-4040.2	-4052.1	-3566.8
equation (9)	-4263.0	-4332.8	-3851.6

With the known enthalpies of formation of carbon dioxide ($\Delta_f H^\circ_{298}(\text{CO}_2(\text{g})) = -393.7 \text{ kJ mol}^{-1}$)^[53] and water ($\Delta_f H^\circ_{298}(\text{H}_2\text{O}(\text{g})) = -241.8 \text{ kJ mol}^{-1}$)^[53] the enthalpy of formation of solid compounds **1** and **5 – 8** can now be calculated (Table 7). The energies of formation ($\Delta_f U^\circ_{298}$) can easily be obtained from the above calculated enthalpies of formation according to the following equation with Δn being the change of moles of the gaseous components.^[54]

$$\Delta_f U^\circ_{298} = \Delta_f H^\circ_{298} - \Delta n RT$$

The detonation parameters of compounds **1** and **5 – 8** were calculated using the EXPLO5 computer program.^[47] The program is based on the chemical equilibrium, steady-state model of detonation. It uses the Becker-Kistiakowsky-Wilson's equation of state (BKW EOS) for gaseous detonation products and Cowan-Fickett's equation of state for solid carbon.^[55-58] The calculation of the equilibrium composition of the detonation products is

done by applying modified White, Johnson and Dantzig's free energy minimization technique. The program is designed to enable the calculation of detonation parameters at the CJ point. The BKW equation in the following form was used with the BKWN set of parameters (α , β , κ , θ) as stated below the equations and X_i being the mol fraction of i -th gaseous product, k_i is the molar co-volume of the i -th gaseous product:^[55-58]

$$pV / RT = 1 + xe^{\beta x} \qquad x = (\kappa \sum X_i k_i) / [V(T + \theta)]^\alpha$$

$$\alpha = 0.5, \beta = 0.176, \kappa = 14.71, \theta = 6620.$$

The detonation parameters of compounds **1** and **5 - 8** calculated with the EXPLO5 program using the experimentally determined densities (see Table 1) are summarized in Table 7.

The velocities of detonation and also the detonation pressures and detonation temperatures for compounds **1** and **5 - 7** are low compared to nitrogen rich salts of tetrazoles and triazoles (e.g. TAG AtNO₂ or TAG DN). Compound **8** shows, despite its low density, the best detonation values of the prepared compounds with an VOD of over 8000 m s⁻¹, a detonation temperature of close to 3000 °K and a detonation pressure of 210 kbar. These values are not as high as the ones from known secondary explosives like TNT or RDX, but lie within the range of other triaminoguanidinium salts. This makes compound **8** the only potentially interesting compound for the further investigation regarding the use as an energetic material or additive in energetic compositions functioning as burn rate modifiers.

Table 7: Lattice energies, lattice enthalpies, detonation parameters, energies and enthalpies of formation for compounds **1** and **5 – 8**.

	(1)	(5)	(6)	(7)	(8)
V_M (nm ³)	0.127	0.209	0.221	0.242	0.250
U_L (kJ mol ⁻¹)		499.1	491.8	480.3	476.2
ΔH_L (kJ mol ⁻¹)	79.3 (ΔH_{sub})	504.1	496.8	485.3	481.2
$\Delta_f H^\circ_{298}(s)$ (kJ mol ⁻¹)	+473.1	+398.3	+518.4	+631.1	+795.0
$\Delta_f U^\circ_{298}$ (kJ mol ⁻¹)	+480.3	+415.6	+530.2	+653.4	+819.8
M (g mol ⁻¹)	119.1	178.2	193.2	208.2	223.2
$\Delta_f U^\circ_{298}$ (J g ⁻¹)	+4032.7	+2332.2	+2744.3	+3138.3	+3672.9
Oxygen balance Ω (%)	-114.2	-116.8	-111.8	-107.6	-103.9
Heat of detonation Q_v (kJ kg ⁻¹)	-4154.0	-2877.5	-3330.2	-3756.7	-4321.8
Explosion Temperature T_{ex} (K)	3318	2292	2514	2710	2958
Detonation pressure P_{C-J} (kbar)	143	130	159	171	210
Detonation velocity V_{det} (m s ⁻¹)	6377	6466	7054	7307	7919
Volume of detonation gases V_0 (L kg ⁻¹)	519	680	710	738	759

2.4 Conclusions

From the experimental and theoretical study presented in this contribution the following conclusions can be drawn:

- (i) 4,5-Dicyano-2*H*-1,2,3-triazole was prepared according to the literature in good yield and converted into various salts containing the 4,5-dicyano-1,2,3-triazolate anion.
- (ii) Various salts containing the 4,5-dicyano-1,2,3-triazolate anion (Na⁺, Ag⁺, NH₄⁺, guanidinium, amionoguanidinium, diaminoguanidinium, triaminoguanidinium) were synthesized for the first time and spectroscopically characterized.
- (iii) The solid state structures of free 4,5-dicyano-2*H*-1,2,3-triazole, and six salts containing the 4,5-dicyano-1,2,3-triazolate anion (Na⁺, NH₄⁺, guanidinium, amionoguanidinium, diaminoguanidinium, triaminoguanidinium) were determined using single crystal X-ray diffraction.

- (iv) The detonation parameters of the energetically most promising guanidinium salts (guanidinium, amionoguanidinium, diaminoguanidinium, triaminoguanidinium) were calculated and the performance predicted to increase from the guanidinium to the triaminoguanidinium salt.
- (v) Due to the limited detonation abilities of compounds 1, 5, 6 and 7, relating the slow velocity of detonation and the low detonation pressure, the only compound for a potential use as energetic material is compound 8 with a comparable VOD and detonation temperature to other triaminoguanidinium compounds.
- (vi) To the best of our knowledge, compounds 2 and 4 – 8 are the first structurally characterized salts containing the binary $C_4N_5^-$ anion to be reported.

2.5 References

- [1] Hammerl, A.; Klapötke, T. M.; Nöth, H.; Warchhold, M.; Holl, G.; Kaiser, M. *Inorg. Chem.*, **2001**, *40*, 3570.
- [2] Hammerl, A.; Holl, G.; Kaiser, M.; Klapötke, T. M.; Mayer, P.; Nöth, H.; Piotrowski, H.; Warchhold, M. *Eur. J. Inorg. Chem.*, **2002**, 834.
- [3] Hammerl, A.; Holl, G.; Kaiser, M.; Klapötke, T. M.; Piotrowski, H. *Z. Anorg. Allg. Chem.*, **2003**, *629*, 2117.
- [4] Geith, J.; Klapötke, T. M.; Weigand, J.; Holl, G. *Propellants Explosives and Pyrotechnics*, **2004**, *29*, 3.
- [5] v. Denffer, M.; Klapötke, T. M.; Kramer, G.; Spieß, G.; Welch, J. M.; Heeb, G. *Propellants Explosives and Pyrotechnics*, **2005**, *30*, 191.
- [6] Hammerl, A.; Klapötke, T. M.; Mayer, P.; Weigand, J. J.; Holl, G. *Propellants Explosives and Pyrotechnics*, **2005**, *30*, 17.
- [7] Klapötke, T. M.; Mayer, P.; Schulz, A.; Weigand, J. J. *J. Am. Chem. Soc.*, **2005**, *127*, 2032.
- [8] Gálvez-Ruiz, J. C.; Holl, G.; Karaghiosoff, K.; Klapötke, T. M.; Löhnwitz, K.; Mayer, P.; Nöth, H.; Polborn, K.; Rohbogner, Ch. J.; Suter, M.; Weigand, J. J. *Inorg. Chem.*, **2005**, *44*, 4237.
- [9] Hiskey, M. A.; Hammerl, A.; Holl, G.; Klapötke, T. M.; Polborn, K.; Stiersdorfer, J.; Weigand, J. J. *Chemistry of Materials*, **2005**, *17*, 3784.
- [10] Berger, S.; Karaghiosoff, K.; Klapötke, T. M.; Mayer, P.; Piotrowski, H.; Polborn, K.; Willer, R. L.; Weigand, J. J. *J. Org. Chem.*, **2006**, *7*, 1295.
- [11] Klapötke, T. M.; Karaghiosoff, K.; Mayer, P.; Penger, A.; Welch, J. M. *Propellants, Explosives and Pyrotechnics*, **2006**, *31*, 188.
- [12] Tremblay, M. *Can. J. Chem.*, **1965**, *43*, 1230.
- [13] Hiskey, M. A.; Goldman, N.; Stine, J. R. *J. Energ. Mater.*, **1998**, *16*, 119.
- [14] Ali, A. N.; Son, S. F.; Hiskey, M. A.; Naud, D. L. *J. Prop. Power*, **2004**, *20*, 120.

- [15] Tappan, B. C.; Ali, A. N.; Son, S. F.; Brill, T. B. *Propellants, Explosives and Pyrotechnics*, **2006**, *31*, 163.
- [16] Singh, R. P.; Verma, R. D.; Meshri, D. T.; Shreeve, J. M. *Angew. Chem., Int. Ed.*, **2006**, *45*, 3584.
- [17] Jin, C.-M.; Ye, C.; Piekarski, C.; Twamley, B.; Shreeve, J. M. *Europ. J. Inorg. Chem.*, **2005**, 3760.
- [18] Xue, H.; Gao, Y.; Twamley, B.; Shreeve, J. M. *Inorg. Chem.*, **2005**, *44*, 5068.
- [19] Ye, C.; Xiao, J.-C.; Twamley, B.; Shreeve, J. M. *Chem. Commun.*, **2005**, 2750.
- [20] Hammerl, A.; Holl, G.; Kaiser, M.; Klapötke, T. M.; Mayer, P.; Piotrowsky, H.; Vogt, M. *Z. Naturforsch.*, **2001**, *56b*, 847.
- [21] Klapötke, T. M., New Nitrogen-Rich High Explosives, in: *Structure and Bonding*, Vol. 125/2007: High Energy Density Compounds, T. M. Klapötke (vol. editor), D. M. P. Mingos (series editor), Springer, Berlin/Heidelberg, **2007**.
- [22] Ang, H.-G.; Fraenk, W.; Karaghiosoff, K.; Klapötke, T. M.; Nöth, H.; Sprott, J.; Suter, M.; Vogt, M.; Warchhold, M. *Z. Anorg. Allg. Chem.*, **2002**, *628*, 2901.
- [23] Fischer, G.; Holl, G.; Klapötke, T. M.; Weigand, J. J. *Thermochim Acta*, **2005**, *437*, 168.
- [24] Hammerl, A.; Klapötke, T. M.; Rocha, R. *Eur. J. Inorg. Chem.*, **2006**, 2210.
- [25] Klapötke, T. M.; Karaghiosoff, K.; Mayer, P.; Penger, A.; Welch, J. M. *Propellants, Explosives and Pyrotechnics*, **2006**, *31*, 188.
- [26] Boese, R.; Klapötke, T. M.; Mayer, P.; Verma, V. *Propellants, Explosives and Pyrotechnics*, **2006**, *31*, 263.
- [27] Xue, H.; Gao, Y.; Twamley, B.; Shreeve, J. M. *Chem. Mater.*, **2005**, *17*, 191.
- [28] Xue, H.; Shreeve, J. M. *Adv. Mater.*, **2005**, *17*, 2142.
- [29] Xue, H.; Twamley, B.; Shreeve, J. M. *Inorg. Chem.*, **2005**, *44*, 7009.
- [30] Xue, H.; Twamley, B.; Shreeve, J. M. *J. Mater. Chem.*, **2005**, *15*, 3459.
- [31] Xue, H.; Gao, H.; Twamley, B.; Shreeve, J. M. *Chem. Mater.*, **2007**, *19*, 1731.
- [32] Huang, Y.; Gao, H.; Twamley, B.; Shreeve, J. M. *Eur. J. Inorg. Chem.*, **2007**, 2025.
- [33] Gao, Y.; Ye, C.; Twamley, B.; Shreeve, J. M. *Chem. Eur. J.*, **2006**, *12*, 9010.
- [34] Wang, R.; Gao, H.; Ye, C.; Shreeve, J. M. *Chem. Mater.*, **2007**, *19*, 144.
- [35] Xue, H.; Arritt, S. W.; Twamley, B.; Shreeve, J. M. *Inorg. Chem.*, **2004**, *43*, 7972.
- [36] Xue, H.; Gao, H.; Twamley, B.; Shreeve, J. M. *Eur. J. Inorg. Chem.*, **2006**, 2959.
- [37] Jimenez, P.; Roux, M. V.; Turrion, C. *J. Chem. Thermodyn.*, **1989**, *21*(7), 759.
- [38] Pedley, J. B. *Thermochemical Data and Structure of Organic Compounds*, Vol. I, Thermodynamic Research Center, College Station, **1994**.
- [39] Sikder, A. K.; Sikder, N. *J. Haz. Mater.* **2004**, *A112*, 1.
- [40] (a) Gryszkiewicz-Trochimowski, E. *Chem. Zent. bl.*, **1923**, *94*, 1366. (b) Johansson, P.; Beranger, S.; Armand, M.; Nilsson, H.; Jacobsson, P. *Solid State Ionics* **2003**, *156*, 129. (c) Hammerl, A.; Hiskey, M. A.; Holl, G.; Klapötke, T. M.; Pollborn, K.; Stierstorfer, J.; Weigand, J. J. *Chem. Mater.*, **2005**, *17*, 3784. (d) Gryszkiewicz-Trochimowski, E. *Roczniki Chemji*, **1921**, *1*, 468. (e) Gryszkiewicz-Trochimowski, E. *J. Russ. Phys. Chem. Soc.*, **1924**, *55*, 548.

- [41] Holleman, A. F.; Wiberg, E.; Wiberg, N. *Lehrbuch der Anorganischen Chemie*, 102nd edn., Walter de Gruyter, Berlin, New York, **2007**, appendix V, p. 2006.
- [42] Göbel, M.; Klapötke, T. M. *Z. Anorg. Allg. Chem.* **2007**, *633*, 1006.
- [43] Holleman, A. F.; Wiberg, E.; Wiberg, N. *Lehrbuch der Anorganischen Chemie*, 102nd edn., Walter de Gruyter, Berlin, New York, **2007**, appendix IV, p. 2002.
- [44] Gaussian 03, Revision A.1, M. J. Frisch, G. W. Trucks, H. B. Schlegel, G. E. Scuseria, M. A. Robb, J. R. Cheeseman, J. A. Montgomery, Jr., T. Vreven, K. N. Kudin, J. C. Burant, J. M. Millam, S. S. Iyengar, J. Tomasi, V. Barone, B. Mennucci, M. Cossi, G. Scalmani, N. Rega, G. A. Petersson, H. Nakatsuji, M. Hada, M. Ehara, K. Toyota, R. Fukuda, J. Hasegawa, M. Ishida, T. Nakajima, Y. Honda, O. Kitao, H. Nakai, M. Klene, X. Li, J. E. Knox, H. P. Hratchian, J. B. Cross, C. Adamo, J. Jaramillo, R. Gomperts, R. E. Stratmann, O. Yazyev, A. J. Austin, R. Cammi, C. Pomelli, J. W. Ochterski, P. Y. Ayala, K. Morokuma, G. A. Voth, P. Salvador, J. J. Dannenberg, V. G. Zakrzewski, S. Dapprich, A. D. Daniels, M. C. Strain, O. Farkas, D. K. Malick, A. D. Rabuck, K. Raghavachari, J. B. Foresman, J. V. Ortiz, Q. Cui, A. G. Baboul, S. Clifford, J. Cioslowski, B. B. Stefanov, G. Liu, A. Liashenko, P. Piskorz, I. Komaromi, R. L. Martin, D. J. Fox, T. Keith, M. A. Al-Laham, C. Y. Peng, A. Nanayakkara, M. Challacombe, P. M. W. Gill, B. Johnson, W. Chen, M. W. Wong, C. Gonzalez, and J. A. Pople, Gaussian, Inc., Pittsburgh PA, **2003**.
- [45] Møller, C.; Plesset, M. S. *Phys. Rev.* **1934**, *46*, 618.
- [46] (a) Woon, D. E.; Dunning Jr., T. H. *J. Chem. Phys.*, **1993**, *98*, 1358. (b) Kendall, R. A.; Dunning Jr., T. H.; Harrison, R. J. *J. Chem. Phys.*, **1992**, *96*, 6796. (c) Dunning Jr., T. H. *J. Chem. Phys.*, **1989**, *90*, 1007. (d) Peterson, K. A.; Woon, D. E.; Dunning Jr., T. H. *J. Chem. Phys.*, **1994**, *100*, 7410. (e) Wilson, A.; van Mourik, T.; Dunning Jr., T. H. *J. Mol. Struct. (Theochem)*, **1997**, *388*, 339.
- [47] Sućeska, M. EXPL05 program, Zagreb, Croatia, **2005**.
- [48] Jenkins, H. D. B.; Rootbottom, H. K.; Passmore, J.; Glasser, L. *Inorg. Chem.* **1999**, *38*, 3609.
- [49] Glasser, K.; Jenkins, H. D. B. *J. Am. Chem. Soc.* **2000**, *122*, 632.
- [50] Jenkins, H. D. B.; Tudela, D.; Glasser, L. *Inorg. Chem.* **2002**, *41*, 2364.
- [51] Rootbottom, H. K.; Jenkins, H. D. B.; Passmore, J.; Glasser, L. *J. Chem. Educ.* **1999**, *76*, 1570.
- [52] Klapötke, T. M.; Schulz, A. *Quantum Chemical Methods in Main-Group Chemistry*, Wiley, Chichester, **1996**, 89.
- [53] *NIST Chemistry WebBook*, NIST Standard Reference Database Number 69, June **2005** Release: <http://webbook.nist.gov/chemistry/>.
- [54] Köhler, J.; Meyer, R. *Explosivstoffe*, 9th edn., Wiley-VCH, Weinheim, **1998**, 46.
- [55] Sućeska, M. *Materials Science Forum*, **2004**, *465-466*, 325.
- [56] Sućeska, M. *Propellants, Explos., Pyrotech.* **1991**, *16*, 197.
- [57] Sućeska, M. *Propellants, Explos., Pyrotech.* **1999**, *24*, 280.
- [58] Hobbs, M. L.; Baer, M. R. *Proc. of the 10th Symp. (International) on Detonation*, ONR 33395-12, Boston, MA, July 12 – 16, **1993**, p. 409.
- [59] Sheldrick, G. M. *Shelxl-97*, University of Göttingen, Germany, 1994.

- [60] Farrugia, L. J. WinGX, *J. Appl. Crystallogr.*, **1999**, 32, 837-838.
- [61] Speck, A. L. *Platon*, Utrecht University, Utrecht, The Netherlands, 1999.
- [62] Crystallographic data for the Structures have been deposited with the Cambridge Crystallographic Data Center. Copies of the data can be obtained free of charge on application to The Director, CCDC, 12 Union Road, Cambridge CB2 1EZ, UK (Fax: int.code (1223)336-033; E-mail for inquiry: filesrv@ccdc.cam.ac.uk; E-mail for deposition: deposit@ccdc.cam.ac.uk).

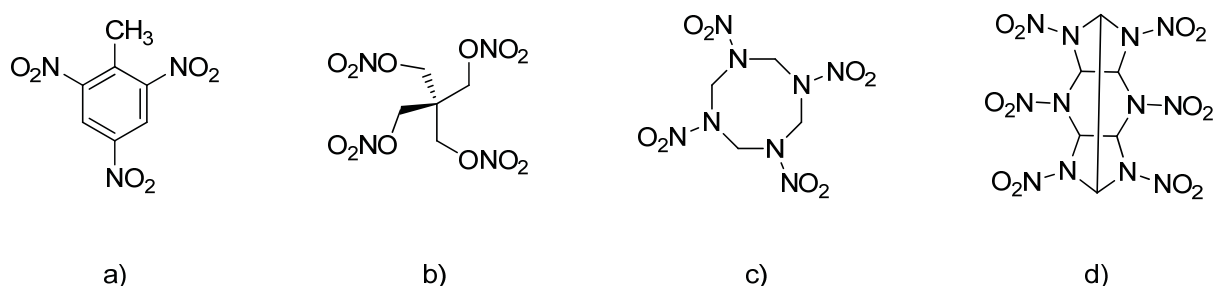
3. *N*-bound primary nitramines based on 1,5-diaminotetrazole

Thomas M. Klapötke, Franz A. Martin and Jörg Stierstorfer

As submitted to: Chemistry – A European Journal 2011

3.1 Introduction

The synthesis of new energetic materials has attracted research groups worldwide over the last centuries. Since the discovery of trinitrotoluene (TNT) in 1863 by J. Wilbrand,^[1] or pentaerythritol tetranitrate (PETN) in 1894,^[2] much effort has been put into the development of more powerful, stable and non toxic secondary explosives. Hexahydro-1,3,5-trinitro-1,3,4-triazine (RDX) and octahydro-1,3,5,7-tetranitro-1,3,5,7-tetracozine (HMX) which have been discovered between 1920 and 1943^[3] are till today the most widely used explosive compounds for both, civil and military applications. These classical polynitro compounds derive their energy primarily from the oxidation of their carbon backbones using the nitrogen provided by the carried nitro groups.^[4] Modern nitro compounds derive their energy not only from the oxidation of their carbon backbone but additionally from ring or cage strain and therefore from their high positive heats of formation. Examples for these new class of compounds are CL-20^[5] and hepta- or octanitrocubane^[6] possessing very high densities and very good performance characteristics.^[7]



Scheme 1: Classical and modern explosives: a) 1,3,5-trinitrotoluene (TNT), b) pentaerythritol tetranitrate (PETN), c) octogen (HMX), d) hexanitrahexaazaisowurtzitane (CL-20).

Other possibilities for the generation of ring strain and high positive heats of formation are the use of heterocyclic ring systems. Within the five membered nitrogen containing

heterocycles, tetrazole possesses a high positive heat of formation with $\Delta H_f^0 = +237.2 \text{ kJ mol}^{-1}$, for example compared to 1,2,4-triazole providing only $\Delta H_f^0 = +109.0 \text{ kJ mol}^{-1}$.^[8] These high positive heats of formation are achieved due to the high number of N–N and C–N bonds, yielding dinitrogen as the major decomposition product. Notable benefits from these circumstances are the production of more moles of gaseous products per gram of energetic material, paired with a higher detonation pressure and the inherently cooler temperature of explosion due to the formation of N_2 .^[9] Moreover, a good oxygen balance is easier to achieve due to the small number of carbon atoms, which leads to the avoidance of environmental pollution as it is known for aromatic polynitrocompounds.^[10] The good characteristics of the tetrazole backbone and the “green” approach to energetic materials, made tetrazoles a widely studied system in the research of energetic materials. The formation of 5-nitraminotetrazole, first synthesized in 1949 by O’Connor et al.^[11] and further investigated between 1951 and 1953 by Lieber and Herbst,^[12] has been utilized as starting material for numerous derivatives, e.g. 1- and 2-methyl-5-nitraminotetrazole, or 1- and 2- ethyl-5-nitraminotetrazole.^[13] Chemistry with derivatives of 5-nitraminotetrazoles has also been a very large research topic in our group, resulting in new high performing secondary explosives as well as pyrotechnical compositions.^[3, 14] In contrast to this overwhelming collection of compounds, close to no *N*-bound nitraminotetrazoles are known in literature. *N*-bound nitramines are well known for 1,2,4-triazoles and also 1,2,3-triazoles, for example 4-nitramino-1,2,4-triazole^[15] and its alkyl or amine derivatives or 1-nitramino-1,2,3-triazole.^[15-16] The same class of compounds is reported for imidazole systems, e.g. 1-nitramino-2,5-dinitroimidazole.^[17] Taking this big variety of *N*-bound heterocyclic nitramine compounds into consideration, it is surprising, that only ammonium and silver salts of 1- and 2-nitraminotetrazole have been described in literature so far but without providing structural and NMR data.^[18] Although theoretical calculations regarding the neutral 1- and 2-nitraminotetrazoles are found in literature,^[19] to the best of our knowledge, no neutral *N*-bound nitraminotetrazole is yet reported.

Herein we will present the first complete study of two novel *N*-bound nitramines, namely 5-amino-1-nitrimino-4*H*-tetrazole and 5-amino-4-methyl-1-nitriminotetrazole based on 1,5-diaminotetrazole. The focus of this study is the full structural as well as spectroscopic characterization of these compounds and the formation and complete characterization of high nitrogen containing salts of 5-amino-1-nitrimino-4*H*-tetrazole using ammonium, hydrazinium, guanidinium, aminoguanidinium and triaminoguanidinium as counter ions.

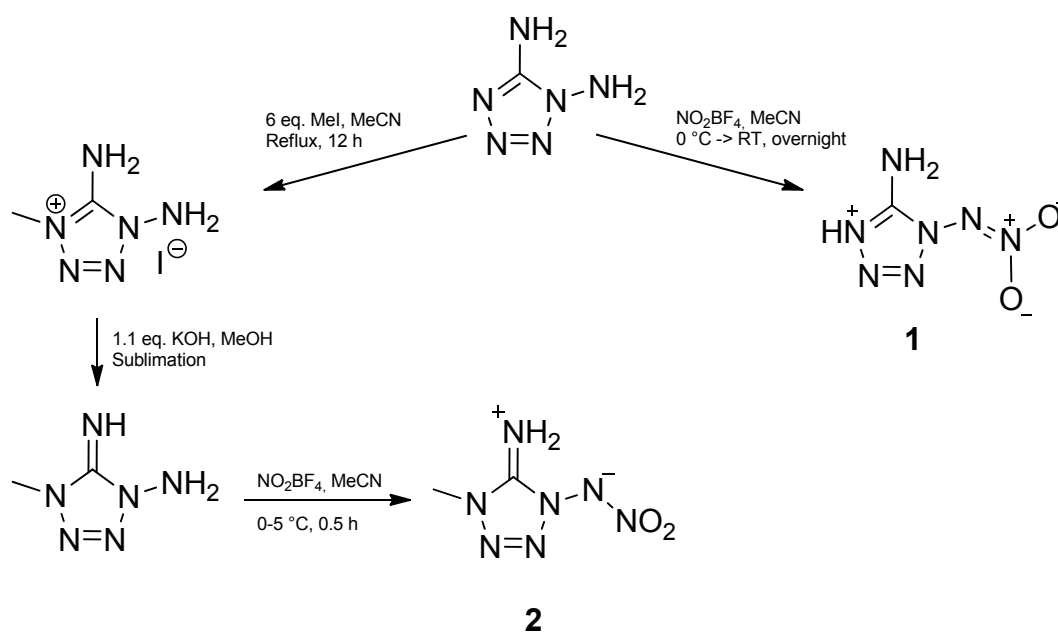
The potential application of the synthesized compounds as energetic materials will be studied and evaluated using the experimentally obtained values for thermal decomposition as well as sensitivity data together with calculated performance characteristics.

3.2 Results and Discussion

3.2.1 Synthesis

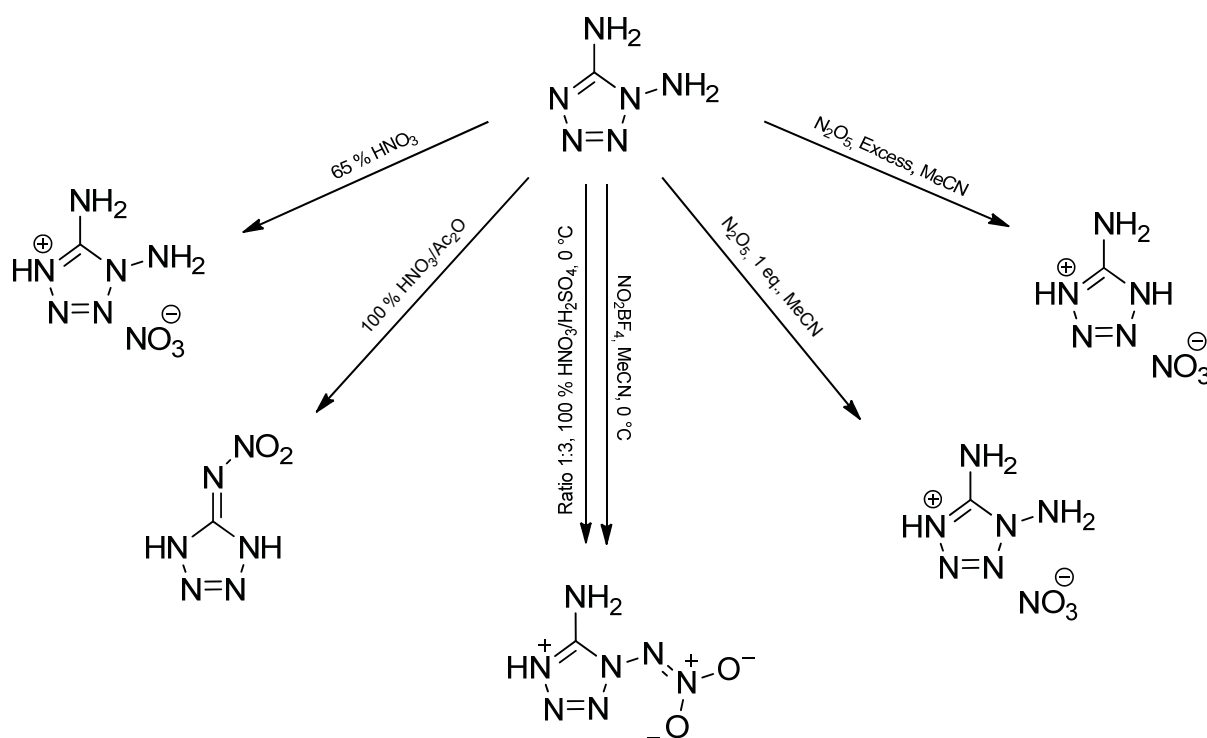
1,5-Diaminotetrazole (DAT) was synthesized according to the literature by the reaction of thiosemicarbazide with two equivalents of sodium azide, ammonium chloride and lead(II)oxide each.^[20] The methylated derivative, 1,5-diamino-4-methyltetrazole (MeDAT) was synthesized according to the literature, starting with the methylation of DAT with six equivalents of methyl iodide in acetonitrile forming 1,5-diamino-4-methyl-tetrazolium iodide selectively, followed by deprotonation with potassium hydroxide in methanol and subsequent sublimation to obtain pure MeDAT.^[21]

The nitration of DAT and MeDAT forming 5-amino-1-nitrimino-4*H*-tetrazole (**1**) and 5-amino-4-methyl-1-nitriminotetrazole (**2**) was performed using one equivalent of nitronium tetrafluoroborate in dry acetonitrile at 0 °C (Scheme 2).



Scheme 2: Reaction pathway towards the formation of 5-amino-1-nitrimino-4*H*-tetrazole (**1**) and 5-amino-4-methyl-1-nitriminotetrazole (**2**).

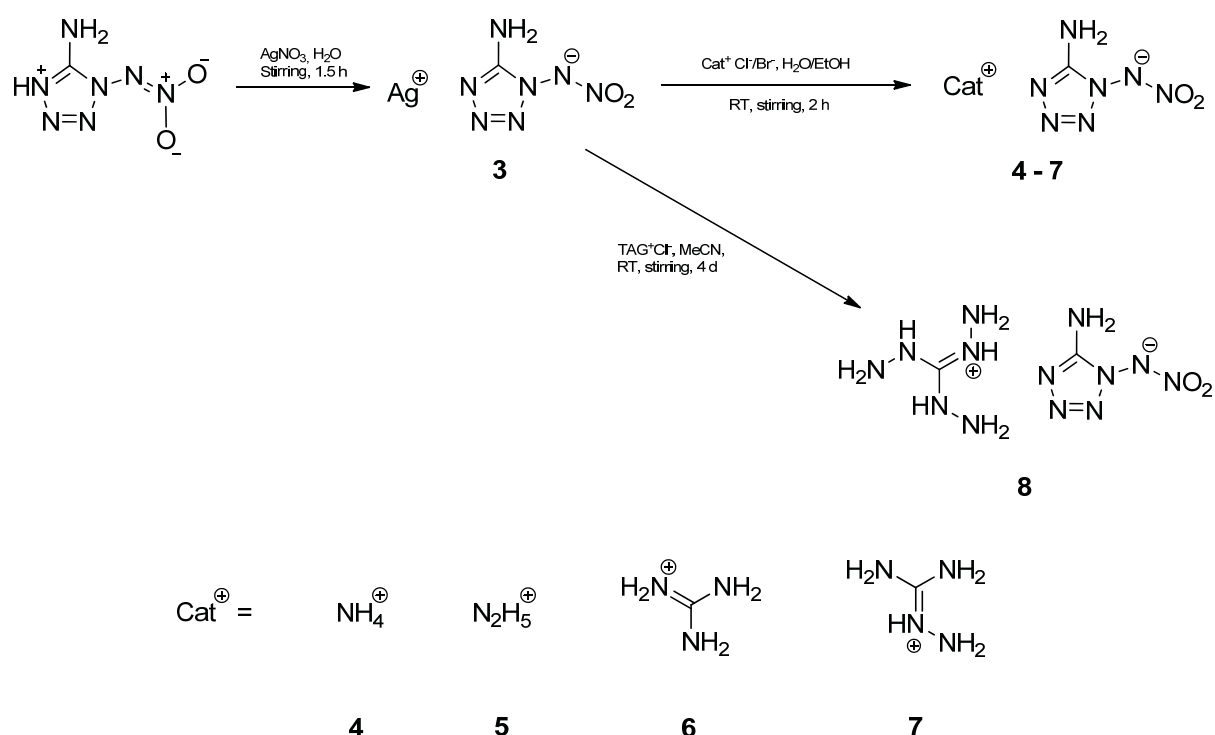
Even though attempts were undertaken to eliminate the very expensive nitration reagent nitronium tetrafluoroborate, none of these attempts resulted in reasonable yield, often not even in the desired compound. Compound **1** was obtained only in 3 % yield by the usage of a nitration mixture consisting of concentrated sulfuric acid and 100 % nitric acid in a 3:1 ratio after various attempts. The mixture had to be extracted with diethyl ether immediately after quenching with ice-water, otherwise **1** was destroyed by acidic hydrolysis. The different reaction routes are summarized in Scheme 3.



Scheme 3: Reaction routes using different nitration reagents starting from 1,5-diaminotetrazole.

The formation of the nitrogen rich salts was accomplished straightforward by metathesis reactions using silver 5-amino-1-nitriminotetrazolate (**3**) in water/ethanol mixtures or acetonitrile in the case of the triaminoguanidinium salt. Silver 5-amino-1-nitriminotetrazolate was synthesized by the addition of a small excess of silver nitrate to a solution of **1** in water. The reaction pathways are presented in Scheme 4. Since **2** has a very high decomposition temperature (150 °C) for a neutral nitraminotetrazole, the corresponding salts should exhibit an even higher thermal stability together with a decrease in sensitivity, when compared with the nitrogen rich salts of **1**. However, all attempts to deprotonate **2** failed, always recovering the neutral compound again. The

same reason for the high thermal stability of **2** also prohibits the compound from donating a proton to guanidine bases. Compound **2** is a zwitter ionic compound, with the amine group carrying the positive charge, while the negative charge is located on the nitrimine and gains its high stability from this circumstance together with the +I effect of the methyl group donating electron density towards the tetrazole ring. Compound **1** is also a zwitter ionic compound, but the hydrogen atom in 4 position is too acidic to stabilize the system and is therefore being easily donated to bases.



Scheme 4: Reaction pathways via metathesis reaction of silver 5-amino-1-nitriminotetrazolate (**3**) with nitrogen rich cations.

3.2.2 Molecular Structures

Single crystal X-ray diffraction studies have been undertaken for compounds **1**, **2** and **4 – 8**. While **1** has been recrystallized from diethyl ether, yielding colorless blocks, **2** and **8** have been recrystallized from acetonitrile as colorless plates and rods, respectively. The nitrogen rich salts **4 – 7** have been recrystallized without crystal water from ethanolic solutions using an ethanol/water ratio of 9:1. Selected crystallographic data for all compounds have been compiled in Table S1 (Appendix 12.2). A discussion of the geometric parameters of all compounds regarding the DATNO_2 moieties is performed

first, evaluating the effects of methylation and deprotonation on the DATNO₂ moiety. A compilation of selected bond lengths, bond angles and torsion angles of compounds **1**, **2** and **4 – 8** is presented in Table 1. Additionally, the structures of the two neutral compounds, 5-amino-1-nitrimino-4*H*-tetrazole (**1**) and 5-amino-4-methyl-1-nitriminotetrazole (**2**) are discussed in detail. Since all ionic structures are composed of strong hydrogen bonded networks, only one compound, the ammonium 5-amino-1-nitrimino-tetrazolate (**4**), presenting the most interesting structure, is discussed exemplarily. The hydrogen bonds present in compounds **5 – 8**, not discussed in detail, are compiled in Tables S2 – S5 (Appendix 12.2).

Table 1: Selected bond lengths [Å], bond angles [°] and torsion angles [°], presenting the geometries of the DATNO₂ moieties.

	HDATNO ₂ (1)	NH ₄ ⁺ , 1 st (4)	NH ₄ ⁺ , 2 nd (4)	N ₂ H ₅ ⁺ (5)	G ⁺ (6)	AG ⁺ (7)	TAG ⁺ (8)	MeDATNO ₂ (2)
N1–N2	1.370(3)	1.364(2)	1.367(2)	1.364(2)	1.360(3)	1.371(2)	1.361(3)	1.365(2)
N2–N3	1.279(3)	1.279(2)	1.290(2)	1.284(2)	1.287(3)	1.290(2)	1.299(3)	1.273(2)
N3–N4	1.362(3)	1.362(2)	1.373(2)	1.369(2)	1.361(3)	1.372(2)	1.370(3)	1.371(2)
N4–C1	1.333(3)	1.329(2)	1.333(2)	1.327(2)	1.336(3)	1.321(2)	1.325(3)	1.332(2)
C1–N1	1.346(3)	1.345(2)	1.351(2)	1.346(2)	1.341(3)	1.347(2)	1.346(3)	1.341(2)
N1–N5	1.383(3)	1.392(2)	1.400(2)	1.386(2)	1.391(3)	1.393(2)	1.401(3)	1.390(2)
N5–N6	1.352(3)	1.340(2)	1.323(2)	1.333(2)	1.335(3)	1.328(2)	1.318(3)	1.336(2)
N6–O1	1.229(3)	1.248(1)	1.249(2)	1.246(2)	1.242(3)	1.250(2)	1.261(3)	1.227(2)
N6–O2	1.244(2)	1.249(1)	1.260(2)	1.259(2)	1.252(2)	1.258(2)	1.257(2)	1.258(2)
C1–N7	1.311(3)	1.340(2)	1.333(2)	1.336(2)	1.327(3)	1.342(2)	1.344(4)	1.302(2)
N7–H7a	0.89(3)	0.92(2)	0.81(2)	0.95(2)	0.94(3)	0.85(2)	0.85(3)	0.87(2)
N7–H7b	0.82(3)	0.88(2)	0.84(2)	0.87(2)	0.84(3)	0.92(2)	0.86(2)	0.90(2)
N4–H1 (CH ₃)	0.96(3)	--	--	--	--	--	--	1.448(2)
N1–N2–N3	107.1(2)	105.6(1)	105.6(1)	105.5(1)	105.1(2)	105.3(1)	105.6(2)	107.7(1)
N2–N3–N4	108.7(2)	112.2(1)	112.0(1)	112.0(1)	112.4(2)	111.9(1)	111.0(2)	108.2(1)
N3–N4–C1	109.7(2)	105.5(1)	105.5(1)	105.6(1)	105.2(2)	105.6(1)	106.4(2)	109.7(1)
N4–C1–N1	104.6(2)	107.9(1)	108.0(1)	107.9(2)	107.7(2)	108.4(2)	107.6(2)	104.6(1)
C1–N1–N2	109.8(2)	108.9(1)	109.0(1)	109.0(2)	109.5(2)	108.8(1)	109.4(2)	110.0(1)
N1–C1–N7	126.5(2)	124.9(1)	124.5(1)	123.7(2)	124.1(2)	122.8(2)	124.0(2)	126.2(2)
C1–N1–N5	127.0(2)	130.6(1)	121.8(1)	127.2(2)	126.7(2)	125.1(1)	129.9(2)	126.0(1)
N1–N5–N6	109.4(2)	109.4(1)	111.5(1)	109.8(2)	109.9(2)	110.0(1)	110.0(2)	108.7(1)
N5–N6–O1	122.6(2)	123.1(1)	123.3(1)	124.3(1)	124.4(2)	123.2(1)	123.8(2)	124.1(1)
N5–N6–O2	114.3(2)	115.2(1)	115.3(1)	115.1(1)	114.7(2)	115.6(1)	115.5(2)	113.3(1)
O1–N6–O2	123.1(2)	121.7(1)	121.3(1)	120.6(2)	120.9(2)	121.2(2)	120.7(2)	122.5(1)
N2–N1–N5–N6	97.5(2)	-109.2(1)	69.3(2)	91.3(2)	-89.8(3)	-80.3(2)	-114.2(2)	98.0(2)
N1–N5–N6–O1	-1.6(3)	-2.7(2)	-10.2(2)	-1.0(2)	-1.1(3)	-0.7(2)	-2.1(3)	-0.5(2)

The discussion of the structure displayed by the guanidinium cations is omitted, because they do not differ by much from the already performed studies, known in literature.^[22] As observed for tetrazoles in general, the bond lengths of the C–N and N–N bonds within the tetrazole moiety of **1** are located between the lengths of formal single and double bonds (C–N: 1.47 Å, 1.22 Å; N–N: 1.48 Å, 1.20 Å),^[23] displaying the aromatic character of the compounds. The N–N bonds show distances between 1.279(3) Å (N₂–N₃) and 1.370(3) Å, while the two C–N bonds show distances of 1.333(3) Å (C₁–N₄) and 1.346(3) Å (C₁–N₁). The amine group in 5 position shows a bond length of only 1.311(3) Å and is hence closer to a formal double bond, resulting in a sp² hybridized nitrogen atom N₇, forcing the amine group into a nearly planar geometry setting. The bond is shortened by 0.03 Å when compared to the educt (DAT, 1.3422(3) Å). The positive charge must therefore be distributed between N₄ and N₇, while the negative charge is more narrowly located on the N₅ bridging atom of the nitramine group. The N₁–N₅ bond is longer than the N₅–N₆ bond, displaying 1.383(3) Å and 1.353(3) Å, respectively. Both bonds are in between formal single and double bonds, and together with the short N–O distances of the nitro group, 1.229(3) Å (N₆–O₁) and 1.244(2) Å (N₆–O₂), present a delocalized π electron system, with partial charges located on O₁ and O₂ (negative) and on the N₆ atom (positive). The zwitter ionic character of the compound is obvious, since the hydrogen atom H₄ is located on the ring atom site, not on the nitramine substituent, as far apart as possible.

Only very small deviations are observed for the molecular structure of **2**, basically displaying the same pattern as observed for **1**. The C₁–N₇ bond (1.302(2) Å) is shortened by 0.01 Å compared to **1**. This is even closer to a formal double bond (1.22 Å), again resulting in the planar geometry of the amine group N₇. The same distribution of the partial charges can be stated for **2**, compared to **1**. Even though a positive charge is located on the amine group, no deprotonation was possible at this position, stating a very stable zwitter ionic configuration, aided also by the +I effect of the methyl group in 4 position, donating electron density towards the heterocyclic ring system. The bond and torsion angles are basically the same for **1** and **2** with only slight deviations < 1.5°. Even the nitramine moiety is twisted out of the tetrazole plane at nearly the same value (97.5(2)° (**1**), 98.0(2)° (**2**)).

The bonds lengths also differ only slightly for the anions of **1** in compounds **4** – **8**. The N₄–H₄ bond is missing due to deprotonation, hence the C₁–N₇ bond is elongated for all ionic compounds between +0.016 Å (**6**) and +0.033 Å (**8**) and the positive partial charge

is diminished slightly. The second difference is observed for the N₁–N₅ and N₅–N₆ bonds. While the N₁–N₅ bond is elongated slightly (mean value: 0.011 Å), the N₅–N₆ bond is shortened much more (mean value: 0.23 Å), while the two N–O bonds of the nitro group are elongated at the same time. The elongations are in the range between 0.011 Å (N₆–O₂, mean value) and 0.20 Å (N₆–O₁, mean value).

The biggest difference between **1** and the anions presented in **4** – **8** are the bond angles within the tetrazole moieties, differing up to 3.7°. The deprotonation at the 4 position changes all three bond angles the N₄ atom is participating in: N₂–N₃–N₄, N₃–N₄–C₁ and N₄–C₁–N₁. While N₂–N₃–N₄ and N₄–C₁–N₁ are both widened by 3.2° and 3.3° (mean values), respectively, N₃–N₄–C₁ is reduced by -4.0° (mean value, Table 1). The O–N–O angle at the nitro group is also reduced, approaching the standard bond angle of 120° for the planar geometry of the nitro group. The N₂–N₁–N₅–N₆ torsion angle is widely varying, showing angles between -114.2° and +91.3°, forced by the packing scheme within the crystal structure aided by free rotation around the N₁–N₅ bond.

5-Amino-1-nitrimino-4*H*-tetrazole (**1**) crystallizes in the orthorhombic space group *Pna*2₁ with a cell volume of 525.03(4) Å³ and four molecular moieties in the unit cell. The calculated density at 200 K is 1.835 g cm⁻³ and hence in the range of other nitriminotetrazoles, e.g. 5-nitramino-1*H*-tetrazole at 1.867 g cm⁻³.^[14d] The asymmetric unit of **1** together with the atom labeling is presented in Figure 1.

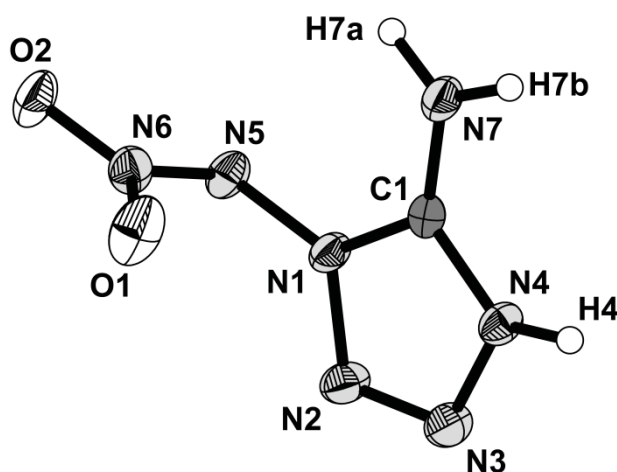


Figure 1: Asymmetric unit of **1**. Thermal ellipsoids are set to 50 % probability.

The crystal structure of **1** is built up by six hydrogen bonds, which use only the amine group and the N₄ hydrogen as donor atoms. All three donor sites N₄–H₄, N₇–H_{7a} and N₇–H_{7b} form bifurcated hydrogen bonds. Three hydrogen bonds can be considered

moderately strong hydrogen bonds, with H \cdots A distances of 1.80(3) Å, 2.15(3) Å and 2.20(3) Å, respectively, for N₄–H₄ \cdots N₅(i), N₇–H_{7a} \cdots N₃(ii) and N₇–H_{7b} \cdots O₂(i). They are also not only of electrostatic nature but directed with D–H \cdots A angles of 171(2)°, 166(2)° and 157(3)°, respectively. The other three hydrogen bonds, representing always the second hydrogen bond formed by every donor atom, N₄–H₄ \cdots O₂(i), N₇–H_{7a} \cdots O₁(iii) and N₇–H_{7b} \cdots O₁(iii), are much weaker with H \cdots A distances of 2.67(2) Å, 2.42(3) Å and 2.67(3) Å, respectively. They are mostly of electrostatic nature with D–H \cdots A angles of only 121(2)°, 111(2)° and 91(2)°.

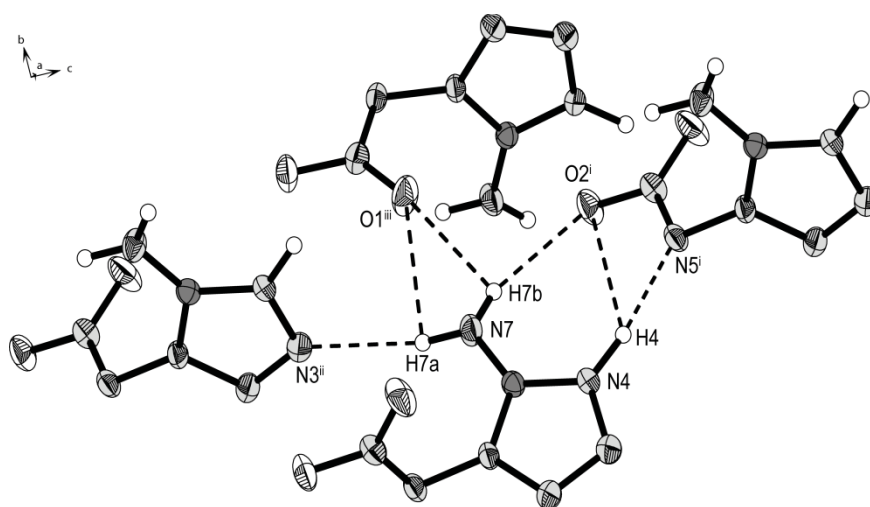


Figure 2: Hydrogen bonding scheme in the structure of **1**, displayed for the asymmetric unit only for reasons of clarity. Thermal ellipsoids are set at 50 % probability. Symmetry Operators: (i) $-x+1/2, y+1/2, z+1/2$; (ii) $-x+1/2, y+1/2, z-1/2$; (iii) $x+1/2, -y+5/2, z$.

Table 2: Hydrogen bonds present in **1**.

D–H \cdots A	d (D–H) [Å]	d (H \cdots A) [Å]	d (D–H \cdots A) [Å]	\angle (D–H \cdots A) [°]
N ₄ –H ₄ \cdots N ₅ ⁱ	0.96(3)	1.80(3)	2.760(2)	171(2)
N ₄ –H ₄ \cdots O ₂ ⁱ	0.96(3)	2.67(2)	3.278(2)	121(2)
N ₇ –H _{7a} \cdots N ₃ ⁱⁱ	0.89(3)	2.15(3)	3.019(3)	166(2)
N ₇ –H _{7a} \cdots O ₁ ⁱⁱⁱ	0.89(3)	2.67(3)	2.826(3)	91(2)
N ₇ –H _{7b} \cdots O ₂ ⁱ	0.82(3)	2.20(3)	2.968(3)	157(3)
N ₇ –H _{7b} \cdots O ₁ ⁱⁱⁱ	0.82(3)	2.42(3)	2.826(3)	111(2)

Symmetry Operators: (i) $-x+1/2, y+1/2, z+1/2$; (ii) $-x+1/2, y+1/2, z-1/2$; (iii) $x+1/2, -y+5/2, z$.

The hydrogen bonds discussed build up a very dense 3D network as presented in Figure 3. The 3D network consists of condensed “rhombic prisms” build by the HDATNO₂ molecules with an angle of 67.44° enclosed. The prisms of HDATNO₂ molecules are

stacked along the *c*-axis, while the representation in Figure 3 displays a view coplanar to the *ab* plane. The formation of this structure is aided by the torsion angle between the tetrazole ring and the nitramine group, mentioned before.

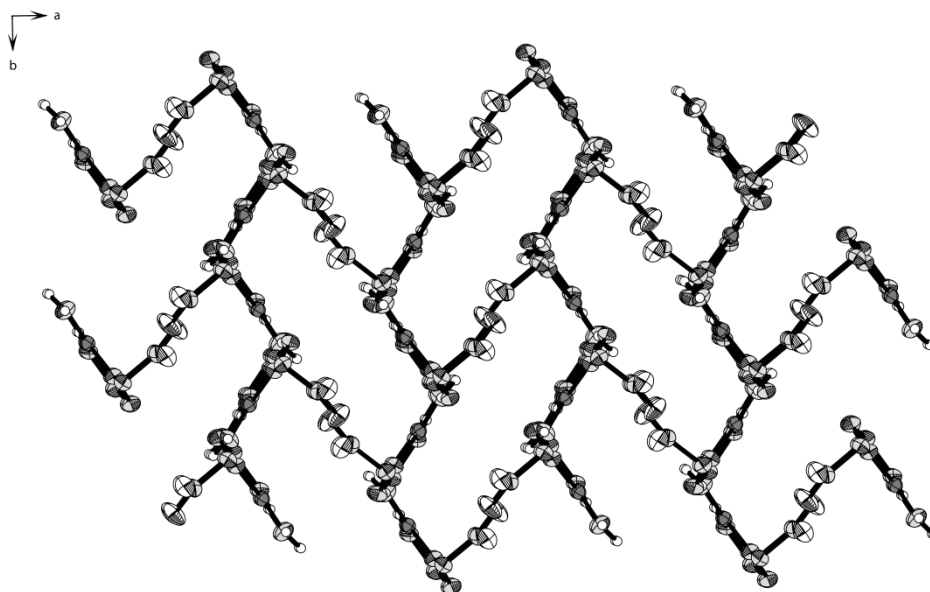


Figure 3: Packing scheme of the crystal structure along the *c*-axis in **1**, displayed coplanar to the *ab* plane. Thermal ellipsoids are set to 50 % probability.

5-Amino-4-methyl-1-nitriminotetrazole (**2**) crystallizes in the monoclinic space group $P2_1/n$ with a cell volume of $643.2(2) \text{ \AA}^3$ and four molecular moieties in the unit cell. The calculated density at 173 K is 1.643 g cm^{-3} and hence 0.1 g cm^{-3} lower than compared to 1-methyl-5-nitramino-1*H*-tetrazole displaying a density of 1.755 g cm^{-3} .^[14d] The asymmetric unit of **2** together with atom labels is presented in Figure 4.

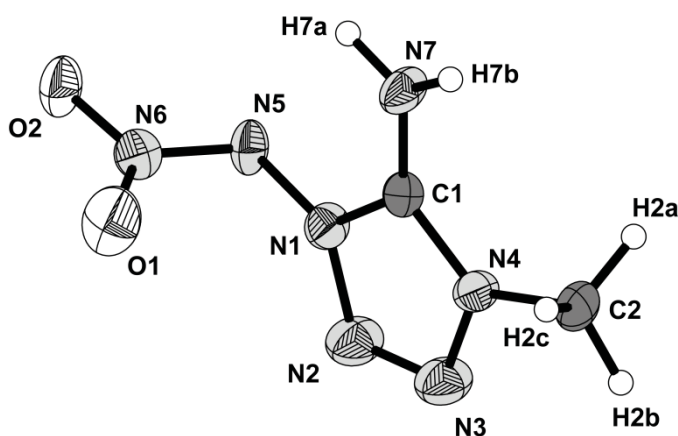


Figure 4: Asymmetric unit of **2**. Thermal ellipsoids are set to 50 % probability.

The crystal structure of **3** is built up pretty simple by mainly three hydrogen bonds. Only the $N_7-H_{7a}\cdots O_2(ii)$ hydrogen bond is again only of electrostatic nature and rather weak with a $H\cdots A$ distance of $2.63(2)$ Å, again being the second bond from a bifurcated hydrogen bonding scheme with N_7 as the donor atom as observed for **1**. The $D\cdots A$ distances of the other two hydrogen bonds, $N_7-H_{7a}\cdots N_5(ii)$ and $N_7-H_{7b}\cdots O_2(i)$ are well below the sum of van der Waals radii at $2.935(2)$ Å and $2.815(2)$ Å, respectively ($r_w(N) + r_w(N) = 3.10$ Å; $r_w(N) + r_w(O) = 3.07$ Å).^[23] These hydrogen bonds build up a planar, either twelve or eight membered ring system, depending on the considered bifurcated hydrogen bonds. These ring motive connects four MeDATNO₂ molecules each lying opposite to one another. Due to the different position of the nitramine moiety, these pattern is repeated, always twisted by the torsion angle of the nitramine group toward the tetrazole ring (98.0°) and therefore an extended three dimensional network is formed. The presentation of the unit cell is omitted because it does not offer additional information. The fourth hydrogen bond connects the methyl group towards the $O_1(iii)$ atom of the nitro group over C_2-H_{2b} . The hydrogen bond is moderately strong, showing a $D\cdots A$ distance of $3.159(2)$ Å, shorter than the sum of van der Waals radii ($r_w(C) + r_w(O) = 3.21$ Å).^[23]

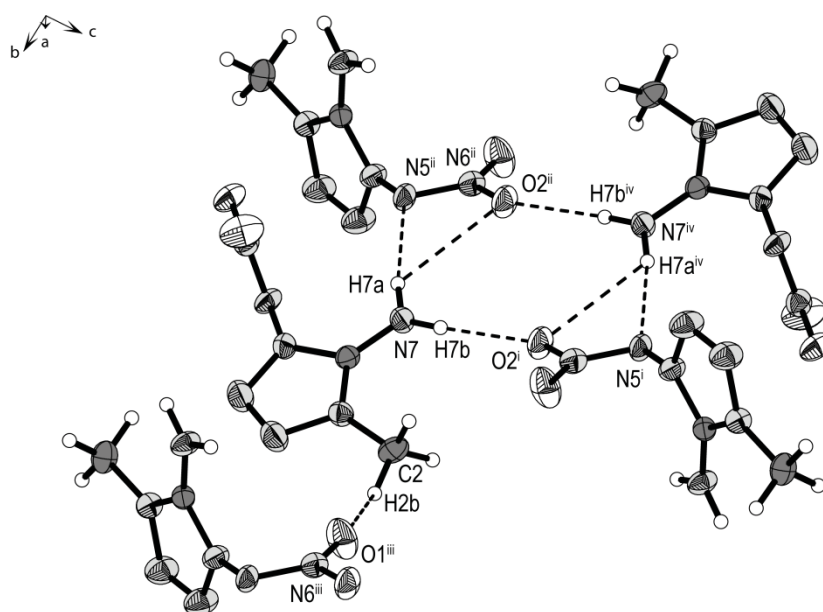


Figure 5: Hydrogen bonding pattern within the structure of **3**, displaying the motive for the formation of the 3D network. Thermal ellipsoids are set at 50 % probability. Symmetry Operators: (i) $x+1/2, -y-1/2, z+1/2$; (ii) $-x+1/2, y-1/2, -z+1/2$; (iii) $-x+3/2, y+1/2, -z+1/2$.

Table 3: Hydrogen bonds present in **2**. The C–H hydrogen atom of the methyl group is set restraint, therefore no standard deviations are given.

D–H⋯A	d (D–H) [Å]	d (H⋯A) [Å]	d (D–H⋯A) [Å]	< (D–H⋯A) [°]
N7–H7b⋯O2 ⁱ	0.87(2)	1.99(2)	2.815(2)	157.9(16)
N7–H7a⋯N5 ⁱⁱ	0.90(2)	2.04(2)	2.935(2)	170.5(18)
N7–H7a⋯O2 ⁱⁱ	0.90(2)	2.63(2)	3.141(2)	117.0(15)
C2–H2b⋯O1 ⁱⁱⁱ	0.98	2.37	3.159(2)	137

Symmetry Operators: (i) $x+1/2, -y-1/2, z+1/2$; (ii) $-x+1/2, y-1/2, -z+1/2$; (iii) $-x+3/2, y+1/2, -z+1/2$.

Ammonium 5-amino-1-nitriminotetrazolate (**4**) crystallizes in the monoclinic space group $C2/c$ with a cell volume of 2451.1(2) Å³ and 16 molecular moieties in the unit cell. The calculated density at 173 K is 1.757 g cm⁻³. The asymmetric unit of **4**, consisting of two independent ammonium 5-amino-1-nitriminotetrazolate moieties, together with the atom labels is presented in Figure 6.

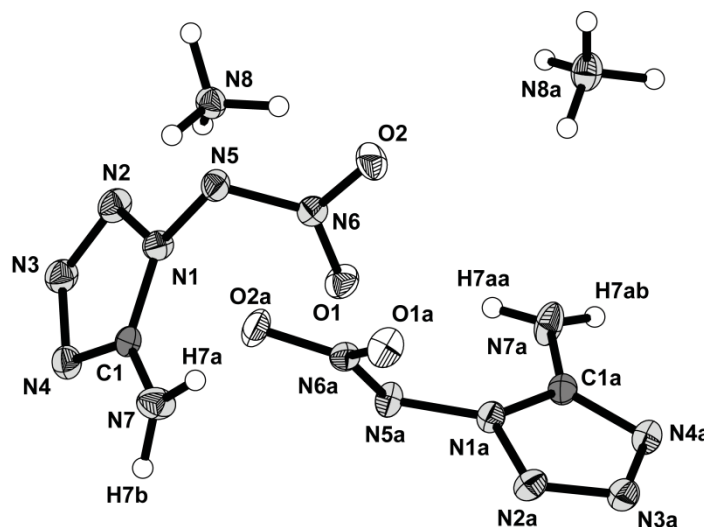


Figure 6: Asymmetric unit of **4**. Thermal ellipsoids are set to 50 % probability.

All hydrogen bonds observed in the structure of **4** can be considered moderately strong with D⋯A distances all below, or within the standard deviations of the sum of van der Waals radii (Table 4). Hydrogen bonds showing strong, mostly electrostatic interactions are formed only with oxygen atoms as acceptor molecules (N_{7a}–H_{7aa}⋯O₂, N₈–H_{8a}⋯O₁(iii) and N₈–H_{8b}⋯O₂ with D–H⋯A angles of 139(2)°, 128(2)° and 114(2)°. Since the asymmetric unit of **4** consists of two independent sets of cations and anions, two sets of hydrogen bonds are formed for each pair, the sets being connected over two hydrogen bonds, N₈–H_{8d}⋯N_{3a}(vi) and N_{8a}–H_{8aa}⋯N_{2a}(vi). The hydrogen bonding motives

for the surrounding of each ammonium ion are presented in Figure 7. It is observed, that the ammonium cations mostly form hydrogen bonds towards the DATNO₂⁻ anion of their sets.

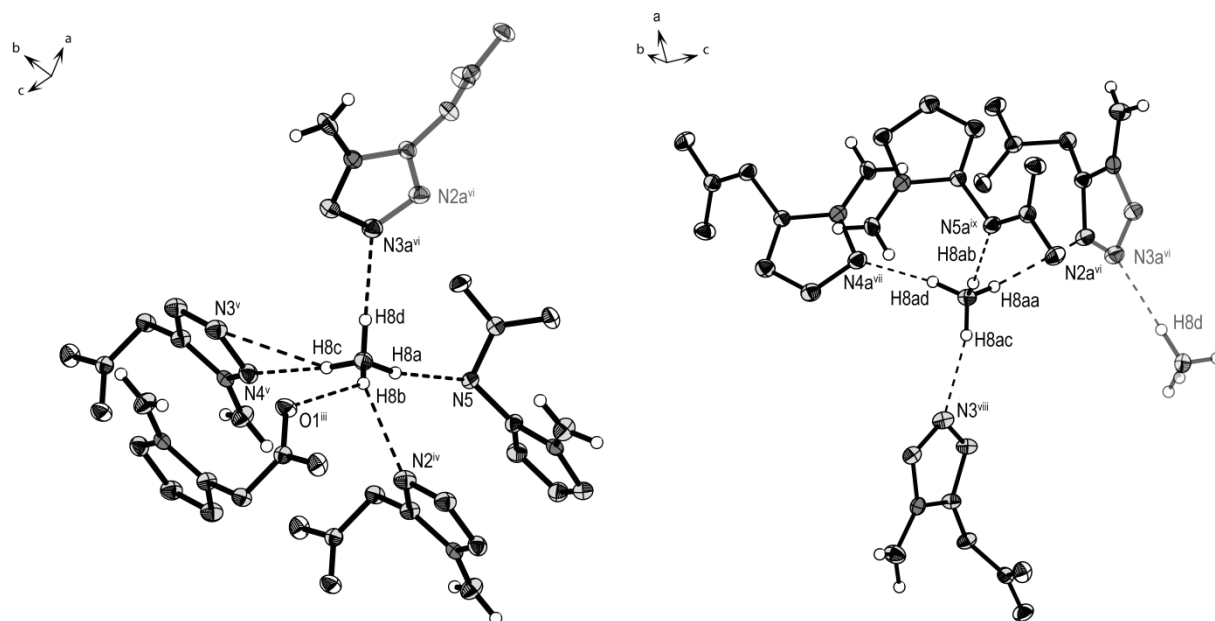


Figure 7: Surrounding of the two independent ammonium cations formed by hydrogen bonds in 4. Surrounding for N8 is shown on the left side, while surrounding for N8a is shown on the right side. The connection site between the two motives is set transparent. Thermal ellipsoids represent the 50 % probability level. Symmetry operators: (i) $x, y-1, z$; (ii) $x, -y+1, z-1/2$; (iii) $x, -y+1, z+1/2$; (iv) $-x, y, -z+1/2$; (v) $-x, y+1, -z+1/2$; (vi) $-x+1/2, y+1/2, -z+1/2$; (vii) $-x+1/2, -y+3/2, -z$; (viii) $-x, -y+1, -z$; (ix) $x, y+1, z$.

Table 4: Hydrogen bonds present in 4.

D-H...A	d (D-H) [Å]	d (H...A) [Å]	d (D-H...A) [Å]	< (D-H...A) [°]
N7-N7a...O2a	0.92(2)	2.12(2)	3.030(2)	167(1)
N7-H7b...O2 ⁱ	0.88(2)	2.16(2)	3.002(2)	161(2)
N7a-H7ab...O1a ⁱⁱ	0.84(2)	2.10(2)	2.919(2)	165(2)
N7a-H7aa...O1	0.81(2)	2.27(2)	3.057(2)	166(2)
N7a-H7aa...O2	0.81(2)	2.56(2)	3.213(2)	139(2)
N8-H8a...O1 ⁱⁱⁱ	0.83(2)	2.24(2)	2.832(2)	128(1)
N8-H8a...N2 ^{iv}	0.83(2)	2.38(2)	3.003(2)	132(1)
N8-H8b...N5	0.96(2)	2.00(2)	2.941(2)	166(1)
N8-H8b...O2	0.96(2)	2.61(2)	3.128(2)	114(1)
N8-H8c...N4 ^v	0.97(2)	1.95(2)	2.915(2)	174(1)
N8-H8c...N3 ^v	0.97(2)	2.62(2)	3.447(2)	144(1)
N8-H8d...N3a ^{vi}	0.94(2)	2.11(2)	3.053(2)	178(1)
N8a-H8ad...N4a ^{vii}	0.95(2)	1.94(2)	2.888(2)	171(1)
N8a-H8ac...N3 ^{viii}	0.90(2)	2.10(2)	2.975(2)	166(2)
N8a-H8ab...N5a ^{ix}	0.93(2)	2.21(2)	3.103(2)	161(1)
N8a-H8aa...N2a ^{vi}	0.87(2)	2.49(2)	3.161(2)	135(1)

Symmetry Operators: (i) $x, y-1, z$; (ii) $x, -y+1, z-1/2$; (iii) $x, -y+1, z+1/2$; (iv) $-x, y, -z+1/2$; (v) $-x, y+1, -z+1/2$; (vi) $-x+1/2, y+1/2, -z+1/2$; (vii) $-x+1/2, -y+3/2, -z$; (viii) $-x, -y+1, -z$; (ix) $x, y+1, z$.

If a look is taken at the connection between the DATNO_2^- anion themselves, two independent sets of rows can be identified (Figure 8). One row consists of the first independent set of DATNO_2^- anions, connected by the $\text{N}_7\text{-H}_{7b}\cdots\text{O}_2(\text{i})$ hydrogen bond, while the second row, lying nearly perpendicular to the first one, enclosing an angle of 86.02° , is formed by the second set of DATNO_2^- anions, connected by $\text{N}_{7a}\text{-H}_{7ab}\cdots\text{O}_{1a}(\text{ii})$. The rows are connected to one another by three hydrogen bonds, $\text{N}_7\text{H}_{7a}\cdots\text{O}_{2a}$, $\text{N}_{7a}\text{-H}_{7aa}\cdots\text{O}_1$ and $\text{N}_{7a}\text{-H}_{7aa}\cdots\text{O}_2$. Hence the rows lie always coplanar to one another, while the ammonium cations build up connections between the rows.

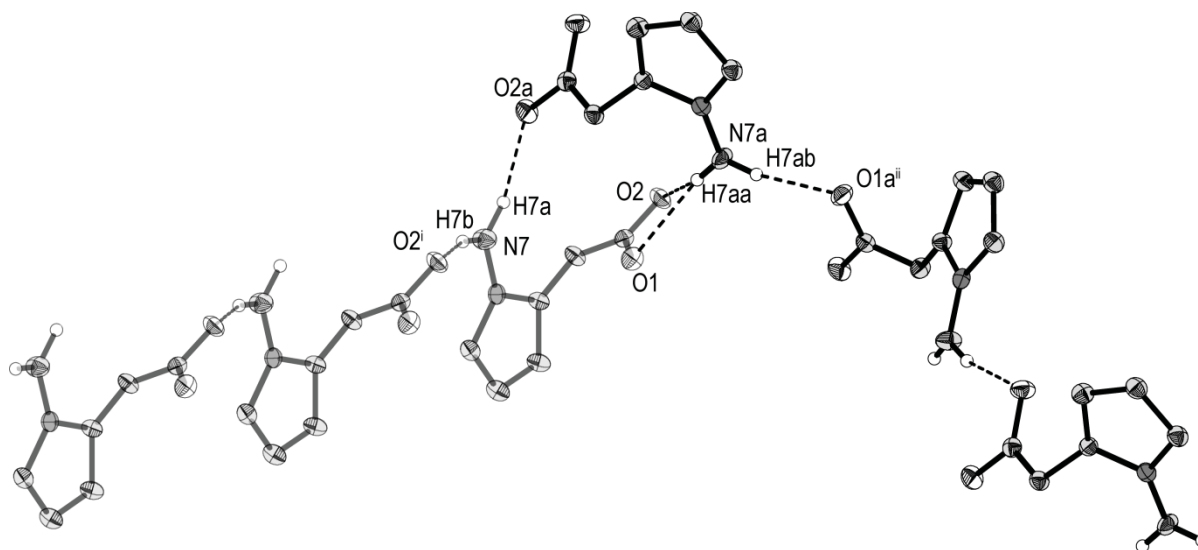


Figure 8: Rows of DATNO_2^- anions formed in **4** by the two independent moieties. Ammonium cations are omitted for clarity. Thermal ellipsoids are set to 50 % probability.

Hydrazinium 5-amino-1-nitriminotetrazolate (**5**) crystallizes in the monoclinic space group $P2_1/c$ with a cell volume of $701.3(2) \text{ \AA}^3$ and four molecular moieties in the unit cell. The calculated density at 173 K is 1.678 g cm^{-3} . The asymmetric unit of **5** is presented in Figure 9. Hydrogen bonds present in **5** are compiled in Table S2 (Appendix 12.2).

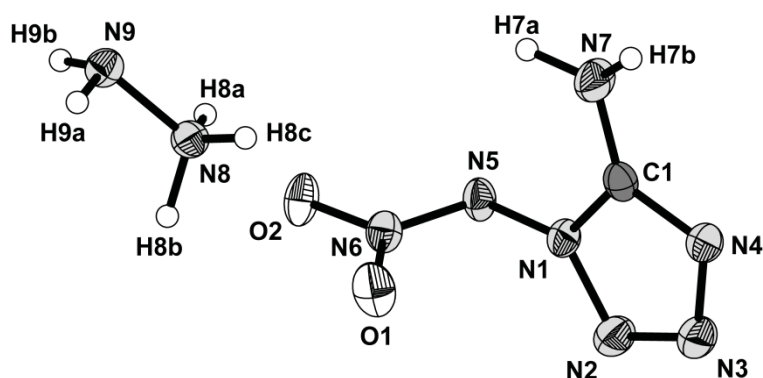


Figure 9: Asymmetric unit of **5**. Thermal ellipsoids are set to 50 % probability.

Guanidinium 5-amino-1-nitriminotetrazolate (**6**) crystallizes in the orthorhombic space group $Pca2_1$ with a cell volume of $837.52(8) \text{ \AA}^3$ and four molecular moieties in the unit cell. The calculated density at 200 K is lower than the values of the hydrazinium and ammonium salts at 1.619 g cm^{-3} , and hence in the normal range observed for guanidinium compounds. The asymmetric unit of **6** is presented in Figure 10. Hydrogen bonds present in **6** are compiled in Table S3 (Appendix 12.2).

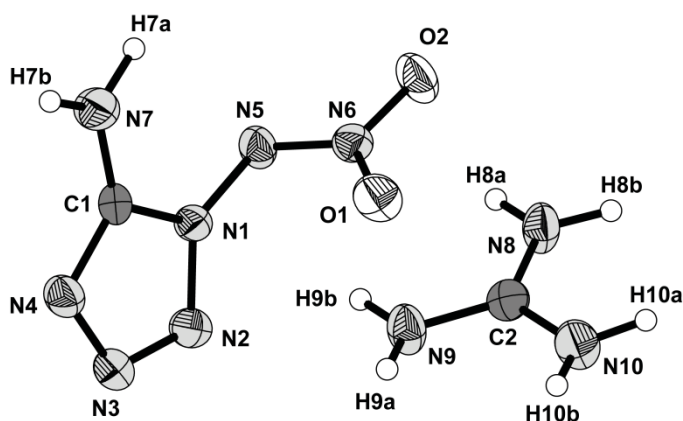


Figure 10: Asymmetric unit of **6**. Thermal ellipsoids are set to 50 % probability.

Aminoguanidinium 5-amino-1-nitriminotetrazolate (**7**) crystallizes in the monoclinic space group $P2_1/c$ with a cell volume of $882.36(8) \text{ \AA}^3$ and four molecular moieties in the unit cell. The calculated density at 200 K is 1.650 g cm^{-3} . The asymmetric unit of **7** is presented in Figure 11. Hydrogen bonds present in **7** are compiled in Table S4 (Appendix 12.2).

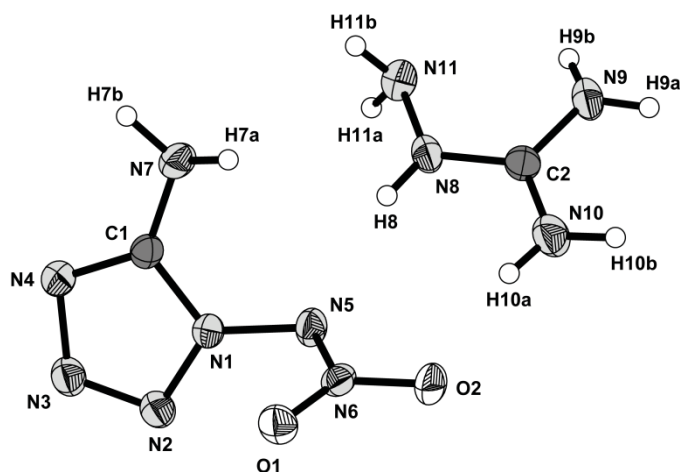


Figure 11: Asymmetric unit of **7**. Thermal ellipsoids are set to 50 % probability.

Triaminoguanidinium 5-amino-1-nitriminotetrazolate (**8**) crystallizes in the orthorhombic space group $Pna2_1$ with a cell volume of $1009.9(2) \text{ \AA}^3$ and four molecular moieties in the unit cell. The calculated density at 173 K is 1.639 g cm^{-3} . The asymmetric unit of **8** is presented in Figure 12.

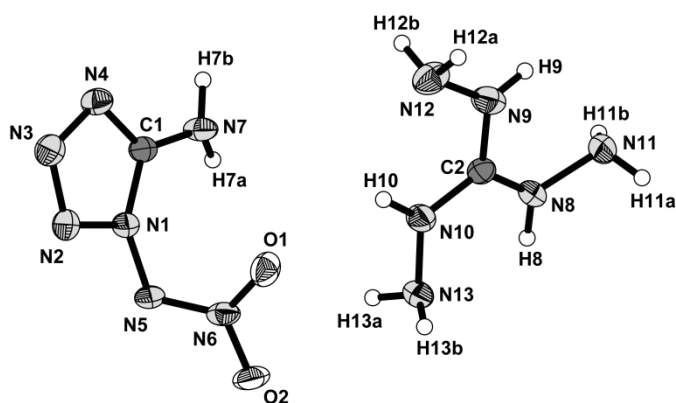


Figure 12: Asymmetric unit of **7**. Thermal ellipsoids are set to 50 % probability.

The structure of **8** consists of ten independent hydrogen bonds, eight of which use the nitrogen atoms of the triaminoguanidinium cation as donor atoms, connecting to seven independent DATNO_2^- moieties. Hence the structure presents a very dense 3D hydrogen bonded network. The presentation of the hydrogen bonding pattern is displayed Figure S1 while the hydrogen bonds are compiled in Table S5 (Appendix 12.2).

3.2.3 Spectroscopic Data

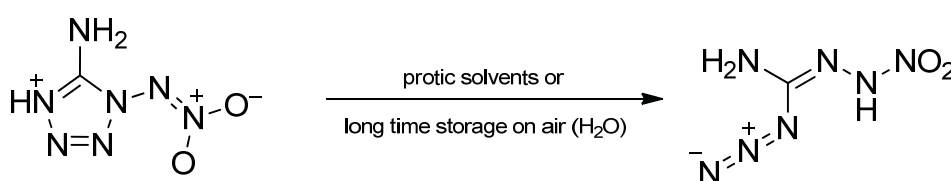
Vibrational Spectroscopy

IR and Raman spectra of all compounds have been recorded and the frequencies have been assigned based on literature^[24] and also based on quantum mechanical calculations at the B3LYP/cc-pVDZ^[25] level of theory as implemented in the Gaussian 09W program package.^[26] The calculated frequencies have been fitted according to Witek et al.^[27] with a scaling factor of 0.9704.

The two neutral compounds 5-amino-1-nitrimino-4*H*-tetrazole (**1**) and 5-amino-4-methyl-1-nitriminotetrazole (**2**) show ν_s and ν_{as} stretch modes of the C-bound amine groups in the region of 3440 – 3380 cm^{-1} in both IR and Raman spectra. Additionally, the bending deformation mode of the amine groups is observed at 1512 cm^{-1} (**1**) and 1515 cm^{-1} (**2**) in the IR spectra and at 1480 cm^{-1} (**1**) and 1517 cm^{-1} (**2**) in the corresponding Raman spectra. Compound **2** shows three stretching modes (ν C–H, ν_s CH₃ and ν_{as} CH₃) of the methyl group in the region of 3050 – 2963 cm^{-1} . All three modes were identified in the Raman spectra, while only ν_{as} is observed in the IR spectra. While the C_{Tet}–N₅ stretching mode is not observed for **1**, it is clearly observed at 1690 cm^{-1} (IR) and 1703 cm^{-1} (Raman) for compound **2**. The energy necessary to activate the stretching mode is in the range normally known for the excitation of C=N double bonds, also accentuating the sp² character of the amine groups nitrogen atom. ν_s and ν_{as} stretching modes of the nitramine groups in **1** and **2** are observed in both, IR and Raman spectra. Compound **1** shows ν_{as} (NO₂) at 1646 cm^{-1} (IR), while **2** shows the stretching mode at 1665 cm^{-1} (IR). As expected, the asymmetric stretching mode is not observed in the Raman spectra. The ν_s (NO₂) is observed at 1302 cm^{-1} (IR) and 1307 cm^{-1} (Raman) for **1** and at 1275 cm^{-1} (IR) and 1293 cm^{-1} (Raman) for **2**, respectively. The ν_{as} of N₁–C₁–N₄ is observed at 1448 cm^{-1} in the IR spectra of **1**, while **2** shows this stretching mode in both, IR and Raman spectra at 1460 cm^{-1} and 1459 cm^{-1} , respectively. The N₂=N₃ stretching mode of the double bond is observed at 1400 cm^{-1} (IR) and 1413 (Raman) for **1** and at 1424 cm^{-1} (IR) and 1427 cm^{-1} (Raman) for **2**. While many out of plane and in plane as well as combined stretching and deformation modes of the tetrazole ring and its substituents are observed in the fingerprint region below 1100 cm^{-1} , one unique stretching mode can be assigned at 891 cm^{-1} (IR) and

917 (Raman) for **1** and at 898 cm^{-1} (IR) and 902 cm^{-1} (Raman) for **2**, representing the $\nu_{\text{N}_5\text{-NO}_2}$ stretching vibration.

If **1** is stored at ambient temperature on humid air, two additional stretching modes are observed in the IR spectra at 2157 cm^{-1} and 1701 cm^{-1} , together with a broadening of the ν_{as} (NO_2) band. These two bands represent the stretching mode of a covalent bound azide (ν_{as}) at 2157 cm^{-1} , while the stretching mode of a $\text{C}=\text{N}$ double bond is represented at 1701 cm^{-1} (comparison with **2**). Compound **1** is therefore not stable on air, since humidity can decompose the compound, forming nitraminoguanylazide as a decomposition product or an intermediate within the decomposition process of **1**. (Scheme 5)



Scheme 5: Decomposition reaction forming nitraminoguanylazide from 5-amino-1-nitrimino-4*H*-tetrazole (**1**).

This decomposition tendency is also observed in protic solvents and therefore no clean NMR spectra of compound **1** could be recorded, since the decomposition (intermediate) product is always observed. No NMR spectra could be recorded in aprotic solvents like deuterated acetonitrile.

The salts of **1** with nitrogen rich cations as counter ions showed very broad bands of high intensity for ν N-H , ν_{s} NH_2 and ν_{as} NH_2 in the IR spectra in the region of 3400 – 3040 cm^{-1} . Peaks with smaller intensity are observed in the Raman spectra in the same region. Around 1500 cm^{-1} the deformation modes of the amine group are also observed. The ν_{as} stretching modes of the NO_2 groups are observed at 1635 cm^{-1} (**4**), 1643 cm^{-1} (**5**), 1645 cm^{-1} (**6**), 1658 cm^{-1} (**7**) and 1647 cm^{-1} (**8**) in the IR spectra and at frequencies of 1637 cm^{-1} (**4**), 1643 cm^{-1} (**5**), 1643 cm^{-1} (**6**) and 1651 cm^{-1} (**7**) in the Raman spectra. Compound **8** showed a too high amount of fluorescence in this region and the signal was therefore not observable. The ν_{s} stretching modes of the NO_2 groups are observed at 1296 cm^{-1} (**4**), 1301 cm^{-1} (**5**), 1308 cm^{-1} (**6**), 1298 cm^{-1} (**7**) and 1328 cm^{-1} (**8**) in the IR spectra and at frequencies of 1305 cm^{-1} (**4**), 1302 cm^{-1} (**5**), 1302 cm^{-1} (**6**), 1304 cm^{-1} (**7**) and 1324 cm^{-1} (**8**) in the Raman spectra. As observed for the neutral compounds, many combined

stretching and deformation vibrations of the tetrazole ring and its substituents are observed in the fingerprint region below 1100 cm^{-1} .

Multinuclear NMR spectroscopy

As observed in the vibrational spectra, **1** has a tendency to open the tetrazole ring in protic media or with longer exposure to humidity (Scheme 5). In the NMR spectra of **1** both compounds can be identified, but no NMR spectra without decomposition of **1** could be recorded after numerous attempts in different solvents. The amine groups of both compounds are present in the ^1H NMR spectra at a chemical shift of 5.39 ppm showing a very broad signal. The carbon atom of **1** is observed in the ^{13}C NMR spectra at a chemical shift of 152.7 ppm, while the carbon atom of the decomposition product is shifted to lower field and observed at a chemical shift of 164.8 ppm. The intensities of the decomposition product are much smaller than **1** close to a 1:5 ratio. Therefore the azide group of the decomposition product is observed only in the ^{14}N NMR spectra at -143 ppm (N_γ , br), -146 ppm (N_β) and -300 ppm as a very broad signal, indicating the N_α nitrogen atom. The NO_2 group of the decomposition product is observed at a chemical shift of -21 ppm, while the NO_2 group of **1** is observed at -18 ppm. The amine group(s) are observed at a chemical shift of -330 ppm. The coupled and decoupled ^{15}N NMR spectra of a 1 M solution of **1** in CD_3OD presented no signals of the azide group due to the low concentration of the decomposition product, but revealed the signal of the NO_2 group in the coupled spectra at a chemical shift of -18.3 ppm and the resonance of the amine group at a chemical shift of -334.1 ppm in the decoupled ^{15}N NMR spectra. According to the ^{15}N NMR spectra of the educt, 1,5-diaminotetrazole,^[21b] and with calculations performed at the MPW1PW91/cc-pVDZ level of theory, we were able to correctly assign the signals. Signals are observed at chemical shifts of -18.0 ppm, -26.1 ppm, -28.0 ppm, -161.5 ppm, -176.7 ppm and -331.4 ppm presenting the N_6 (NO_2), N_2 , N_3 , N_5 , N_1 and N_7 (NH_2) nitrogen atoms in the coupled ^{15}N NMR spectra. Additionally, the N_4 nitrogen atom is present in the decoupled ^{15}N NMR spectra at a chemical shift of -56.4 ppm. The signal of the N_5 atom is not observed, while the signal corresponding to the N_1 nitrogen atom is evident at 177.7 ppm in the decoupled spectra. The signals of the N_6 (NO_2), N_2 , N_3 and N_7 (NH_2) atoms are observed at chemical shifts of 17.5 ppm, -26.0 ppm, -28.1 and -331.5 ppm, respectively.

The resonances of the amine groups in **4** – **8** are observed in the ^1H NMR spectra at chemical shifts between 6.10 – 6.14 ppm. Additionally, signals are observed for the hydrogen atoms located on the cations at chemical shifts of 7.14 ppm for the ammonium cation (**4**), 7.05 ppm for the hydrazinium cation (**5**), 6.94 ppm for the guanidinium cation (**6**), 8.88 ppm ($-\text{NH}-\text{NH}_2$), 7.24 ppm ($-\text{NH}_2$), 6.83 ppm ($-\text{NH}_2$) and 4.68 ppm ($-\text{NH}_2$) for the aminoguanidinium cation (**7**) and 8.58 ppm ($-\text{NH}-\text{NH}_2$) and 4.48 ppm ($-\text{NH}_2$) for the triaminoguanidinium cation (**8**), respectively.

The signal of the carbon atom of the DATNO_2^- anion is observed at a chemical shift of 152.6 ppm for all ionic compounds **4** – **8** in the ^{13}C NMR spectra. Signals for the carbon containing cations are additionally observed in the ^{13}C NMR spectra at chemical shifts of 157.9 ppm for the guanidinium cation (**6**), 158.8 ppm for the aminoguanidinium cation (**7**) and 159.0 ppm for the triaminoguanidinium cation (**8**).

The N_6 nitrogen atom ($-\text{NO}_2$) of the DATNO_2^- anion is observed at a chemical shift of -4 ppm for all ionic compounds **4** – **8**. Compound **4** shows another signal at a chemical shift of -359 ppm, representing the ammonium cation, while at a chemical shift of -359 ppm the hydrazinium cation is observed in **5**. The NH_2 group nitrogen atom of DATNO_2^- is only observed in the ^{14}N NMR spectra of **5** at a chemical shift of -334 ppm.

Additionally, ^{15}N NMR spectra have been recorded of triaminoguanidinium 5-amino-1-nitriminotetrazolate as an example for the ionic compounds of **1**. All nitrogen atoms have been assigned using the combination of both coupled and decoupled ^{15}N NMR spectra. The N_6 nitrogen atom (NO_2) is observed at a chemical shift of -2.9 ppm in both ^{15}N and $^{15}\text{N}\{^1\text{H}\}$ NMR spectra. The nitrogen atoms of the tetrazole ring N_1 , N_2 , N_3 and N_4 showed signals at chemical shifts of -174.3 ppm, -5.9 ppm, -23.6 ppm and -96.7 ppm in the decoupled spectra. The signal of the N_1 nitrogen atom is not observed in the coupled ^{15}N NMR while N_2 , N_3 and N_4 are clearly observed at chemical shifts of -5.9 ppm, -23.6 ppm and -95.7 ppm. The amine group bound to the C_1 atom is observed at chemical shifts of -338.8 ppm in both ^{15}N NMR spectra. The nitrogen atoms of the triaminoguanidinium cation showed two signals in both ^{15}N NMR spectra at chemical shifts of -289.1 ppm ($-\text{NH}-$) and -329.5 ppm ($-\text{NH}_2$). The signals represent a doublet and a triplet for the $-\text{NH}-$ and $-\text{NH}_2$, respectively in the coupled ^{15}N NMR spectra showing 1J coupling constants of $^1J_{\text{NH}} = 102.5$ Hz for the doublet and $^1J_{\text{NH}} = 69.8$ Hz for the triplet (Figure 13). Both coupling constants are in the region normally observed for $^1J_{\text{NH}}$ coupling constants.^[24]

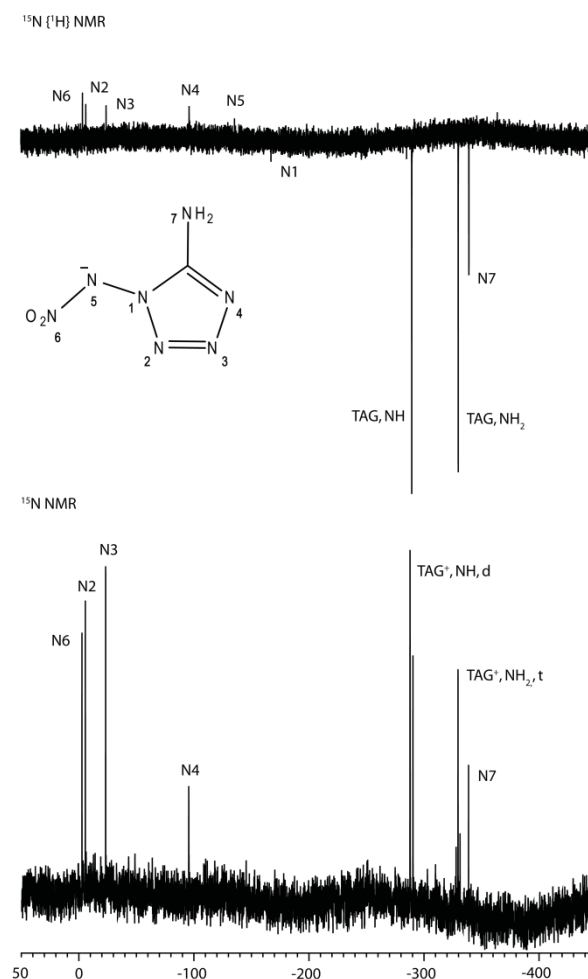


Figure 13: ^{15}N and $^{15}\text{N}\{^1\text{H}\}$ NMR spectra of triaminoguanidinium 5-amino-1-nitriminotetrazolate (**8**), recorded in DMSO-d_6 at 25°C . The x-axis represents the chemical shift δ in ppm.

The methyl and amine group in **2** are observed in the ^1H NMR spectra at chemical shifts of 8.88 ppm (NH_2) and at 3.84 ppm (CH_3). The shift towards lower field for the amine group is owed to the positive charge located on the nitrogen atom resulting in a deshielding of the attached hydrogen atoms. Two signals are observed in the ^{13}C NMR spectra of **2** for the tetrazole carbon at a chemical shift of 145.6 ppm and the methyl group at 34.4 ppm. The tetrazole carbon atom is shifted to higher field compared to the neutral compound (MeDAT) at 148.5 ppm. Only the signal for the nitramine (NO_2) nitrogen atom is observed in the ^{14}N NMR spectra at -3 ppm.

The signals of all nitrogen atoms contained in **2** have been assigned using coupled and decoupled ^{15}N NMR spectroscopy together with calculations of the nitrogen NMR spectra on the MPW1PW91/cc-pVDZ level of theory. The proton coupled ^{15}N NMR spectra showed, as expected, seven well resolved resonances at higher (negative) field. N_6 (NO_2) is observed at -2.3 ppm. The N_2 and N_3 nitrogen atoms are observed as a singlet and a

quadruplet, respectively, at chemical shifts of -26.1 ppm and -36.2 ppm. The quadruplet is observed due to the 3J coupling of the nitrogen atom with the methyl group attached to N_4 with a coupling constant of $^3J_{NH} = 1.86$ Hz. The N_5 nitrogen atom is observed at a chemical shift of -126.9 ppm, while the N_1 nitrogen atom is observed at -147.1 ppm. N_4 showed no coupling towards the attached methyl group and is found at a chemical shift of -185.5 ppm. The amine group showed a triplet in the proton coupled ^{15}N NMR spectra at -320.0 ppm displaying a coupling constant of $^1J_{NH} = 91.29$ Hz, as expected. All seven resonances are also observed in the proton decoupled ^{15}N NMR spectra at chemical shifts of -2.2 ppm (N_6), -26.0 ppm (N_2), -36.2 ppm (N_3), -126.9 ppm (N_5), -147.3 ppm (N_1), -185.5 ppm (N_4) and -320.5 ppm (N_7). The spectra are compiled in Figure 14 below.

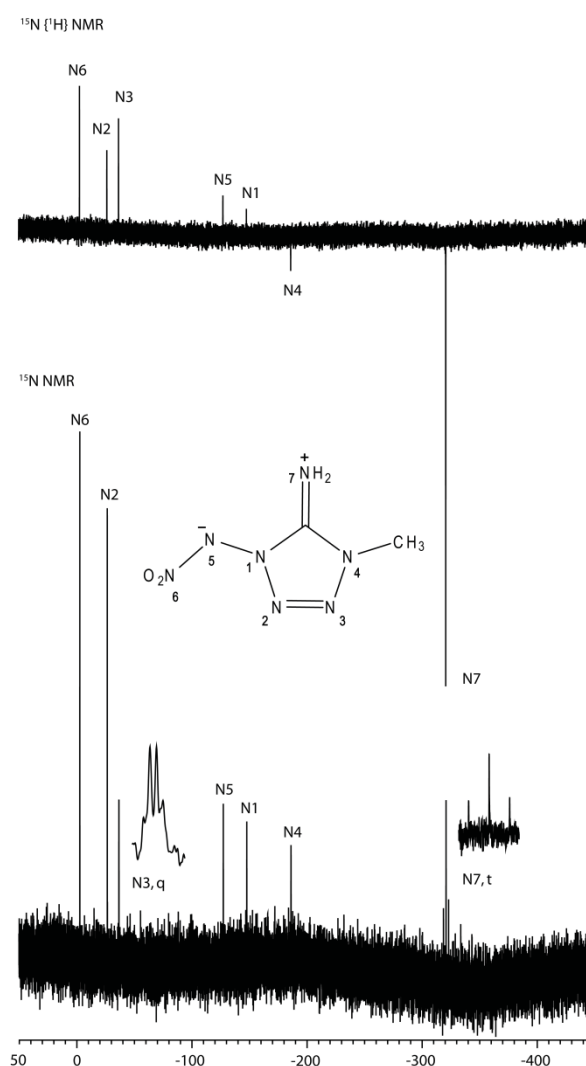


Figure 14: ^{15}N and $^{15}\text{N}\{^1\text{H}\}$ NMR spectra of 5-amino-4-methyl-1-nitriminotetrazole (2), recorded in DMSO-d_6 at 25°C . The x-axis represents the chemical shift δ in ppm.

3.2.4 Mass Spectrometry

Mass spectra were recorded using the FAB+ and FAB- techniques for all ionic compounds, as well as **2**, in glycerin matrix. The anion of **1** (DATNO_2^-) was always observed at m/z 144.0 in the FAB- spectra, while the cations are observed at m/z 18.0 (**4**), m/z 33.0 (**5**), m/z 60.1 (**6**), m/z 75.1 (**7**) and m/z 105.13 (**8**). Compound **2** is observed in both, FAB+ and FAB- spectra, at m/z 160.1 $[\text{M}+\text{H}]^+$ and at m/z 158.0 $[\text{M}-\text{H}]^-$. Additionally, **1** is observed using the DCI+ technique at m/z 146.03 $[\text{M}+\text{H}]^+$. During the investigation and characterization of **1** with DEI+ methods, an explosion took place due to the high heating rates used for the measurements, therefore no additional informations about the fragmentation pattern were gathered from DEI+ measurements.

3.2.5 Theoretical Calculations and Stabilities

All calculations regarding energies of formation were carried out using the Gaussian G09W Version 7.0 program package.^[26] Since very detailed descriptions of the calculation process have been published earlier^[28] and can be found in specialized books,^[3] only a short summary of computational methods will be given. The enthalpies (H) and Gibbs free energies (G) were calculated using the complete basis set method (CBS) of Petersson *et al.* in order to obtain very accurate energies. In this contribution, we used the modified CBS-4M method with M referring to the use of minimal population localization, which is a re-parameterized version of the original CBS-4 computational method and also includes additional empirical calculations.^[29]

The enthalpies of formation for the gas phase species were computed according to the atomization energy method, using NIST^[30] values as standardized values for the atoms standard heats of formation ($\Delta_f H^0$) according to equation 1.^[31]

$$\Delta_f H^0_{(\text{g, Molecule, 298})} = H_{(\text{Molecule})} - \sum H^0_{(\text{Atoms})} + \sum \Delta_f H^0_{(\text{Atoms, NIST})} \quad (1)$$

The solid state enthalpy of formation for neutral compounds is estimated from the computational results using TROUTONS rule,^[32] where T_m was taken equal to the decomposition temperatures.

$$\Delta H_m = \Delta_f H^0_{(\text{g, Molecule, 298})} - \Delta H_{\text{sub}} = \Delta_f H^0_{(\text{g, Molecule, 298})} - (188 \text{ J mol}^{-1} \text{ K}^{-1} \cdot T_m)$$

The solid state enthalpies of formation for the ionic compounds are derived from the calculation of the corresponding lattice energies (U_L) and lattice enthalpies (H_L), calculated from the corresponding molecular volumes,^[33] by the equations provided by Jenkins et al.^[34]

The derived molar standard enthalpies of formation for the solid state (ΔH_m) were used to calculate the solid state energies of formation (ΔU_m) according to equation three, with Δn being the change of moles of gaseous components.^[3]

$$\Delta U_m = \Delta H_m - \Delta nRT \quad (3)$$

The calculated standard energies of formation were used to perform predictions of the detonation parameters with the program package EXPLO5, Version 5.04.^[35] The program is based on the chemical equilibrium, steady state model of detonation. It uses Becker-Kistiakowsky-Wilsons equation of state (BKW EOS) for gaseous detonation products together with Cowan-Ficketts equation of state for solid carbon.^[36] The calculation of the equilibrium composition of the detonation products is performed by applying modified White, Johnson and Dantzigs free energy minimization technique. The program was designed to enable calculations of detonation parameter at the Chapman-Jouguet point. The BKW equation as implemented in the EXPLO5 program was used with the BKW-G set of parameters (α , β , κ , θ) as stated below the equation, with X_i being the mol fraction of the i -th gaseous detonation product while k_i is the molar co-volume of the i -th gaseous detonation product.^[35-36]

$$pV / RT = 1 + xe^{\beta x} \quad \text{with} \quad x = (\kappa \sum X_i k_i) / [V(T + \theta)]^\alpha$$

$$\alpha = 0.5, \beta = 0.096, \kappa = 17.56, \theta = 4950$$

The results of the detonation runs, together with the calculated energies of formation, the corresponding sensitivities and decomposition temperatures are compiled in Table 5.

HDATNO₂ (**1**) shows a very low decomposition temperature of only 85 °C as a neutral compound, due to the very high acidity of the hydrogen located in 4 position. Upon

deprotonation of **1**, the decomposition temperatures are increased, depending on the cation. Ammonium 5-amino-1-nitriminotetrazolate (**4**) shows the lowest decomposition temperature at only 107 °C, while triaminoguanidinium 5-amino-1-nitriminotetrazolate (**8**) exhibits the highest decomposition temperature at 160 °C. The decomposition temperatures for compounds **5**, **6** and **7** are 134 °C, 148 °C and 142 °C, respectively. Even though 5-amino-4-methyl-1-nitriminotetrazole (**2**) is a neutral nitrimino compound, it displays a very high thermal stability with decomposition starting at 150 °C while the Onset value is 160 °C. Compound **2** derives its stability towards heat from its zwitter ionic character and the +I effect of the methyl group, donating electron density towards the electron deficient tetrazole ring. The DSC plots of selected compounds are shown in Figure 15.

The friction and impact sensitivities of all compounds have been determined for the anhydrous materials and show a very wide spread. While both neutral compounds, **1** and **2** are extremely sensitive (IS/FS: < 0.25 J/ < 5 N (**1**); < 1 J/ < 5 N (**2**)), hence more sensitive than lead azide, the salts show no real trend. While **4** and **5** (ammonium and hydrazinium as cations) are extremely sensitive towards friction (3 J (**4**), < 1J (**5**)) and very sensitive towards friction (52 N (**4**), 48 N (**5**)), the guanidinium and aminoguanidinium 5-amino-1-nitriminotetrazolates point in the other direction. **6** and **7** are both less sensitive towards impact (40 J (**6**), 20 J (**7**)) and also show much lower sensitivity towards friction (240 N (**6**), 192 (**7**)). The result for the testing of the triaminoguanidinium salt (**8**) was not really as expected: it is again very sensitive towards friction at 32 N and extremely sensitive towards impact at only 2 J. Since **8** shows the highest thermal stability we had hoped for a better value. It seems that the hydrazine moieties in the triaminoguanidinium cation excels the decomposition process and therefore affects the stability as observed also for **5**.

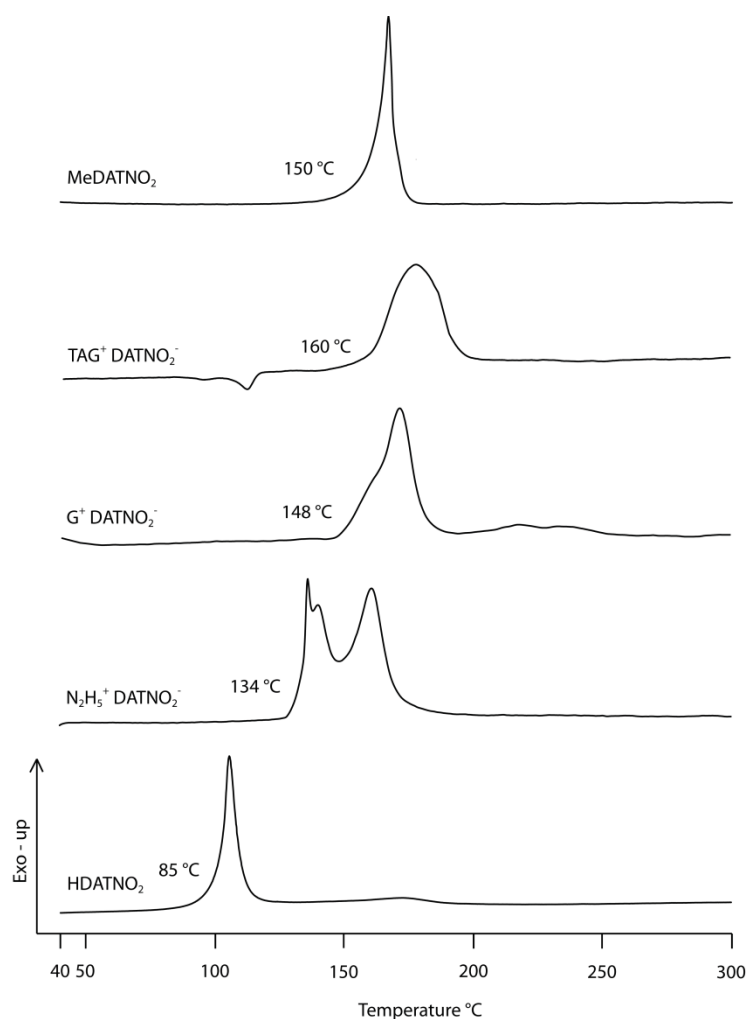


Figure 15: DSC plots of MeDATNO₂ (**2**), HDATNO₂ (**1**), N₂H₅⁺ DATNO₂⁻ (**5**), G⁺ DATNO₂⁻ (**6**) and TAG⁺ DATNO₂⁻ (**8**), recorded at a heating rate of 5 °C min⁻¹.

From the calculation of the detonation parameter we observe the well expected picture. **1** is, as a result of the high density and high heat of formation, extremely powerful, exceeding the performance characteristics of RDX by far ($V_{\text{det.}}$ 9460 m s⁻¹ (**1**), 8748 m s⁻¹ (RDX)). The same is observed for **4** and **5** displaying detonation velocities of 9110 m s⁻¹ and 9102 m s⁻¹ paired with an enormous amount of gas release (875 L kg⁻¹ (**4**); 886 L kg⁻¹ (**5**)) and detonation pressures of 344 kbar and 334 kbar, respectively. These values as well as the ones for **8** ($v_{\text{det.}}$ 8731 m s⁻¹; $p_{\text{C-J}}$: 295 kbar; 871 L kg⁻¹) are in the range of RDX values or even exceed them. The drawback is, that all these compounds are, as described above, very sensitive towards both, impact and friction, and despite a reasonable good thermal stability for **8** are not very safe in use and handling. Compounds **6** and **7** display very high sensitivity values and are therefore easy to handle, but show only reasonable performance characteristics, well below the benchmark values of RDX.

Table 5: Physico-chemical properties of compounds **1**, **2** and **4** – **8** in comparison to hexogen (RDX)

	1	2	4	5	6	7	8	RDX*
Formula	CH ₃ N ₇ O ₂	C ₂ H ₅ N ₇ O ₂	CH ₆ N ₈ O ₂	CH ₇ N ₉ O ₂	C ₂ H ₈ N ₁₀ O ₂	C ₂ H ₉ N ₁₁ O ₂	C ₂ H ₁₁ N ₁₃ O ₂	C ₃ H ₆ N ₆ O ₆
Molecular Mass [g mol ⁻¹]	145.09	159.12	162.12	177.14	204.16	219.18	249.21	222.12
Impact sensitivity [J] ^a	< 0.25	< 1	3	< 1	40	20	2	7
Friction sensitivity [N] ^b	< 5	< 5	52	48	240	192	32	120
ESD–test [J]	0.025	0.211	0.20	0.10	0.26	0.20	0.065	--
<i>N</i> [%] ^c	67.6	61.6	69.1	71.1	68.6	70.3	73.1	37.8
<i>O</i> [%] ^d	-16.5	-45.2	-29.6	-31.6	-47.0	-47.5	-48.1	-21.6
<i>T</i> _{dec.} [°C] ^e	85	150	107	134	148	142	160	204
<i>ρ</i> [g cm ⁻³] ^f	1.835	1.643	1.757	1.678	1.619	1.649	1.639	1.80
$\Delta_f H_m^\circ$ [kJ mol ⁻¹] ^g	496	453	356	516	343	451	676	70
$\Delta_f U^\circ$ [kJ kg ⁻¹] ^h	3419	2847	2195	2911	1678	2059	2711	417
EXPLO5 values:								
V5.04								
$-\Delta_E U^\circ$ [kJ kg ⁻¹] ⁱ	6498	5913	5326	5856	4299	4564	5023	6125
<i>T</i> _E [K] ^j	4642	3969	3613	3806	3072	3116	3297	4236
<i>p</i> _{C-J} [kbar] ^k	403	292	344	334	255	276	295	349
<i>V</i> _{Det.} [m s ⁻¹] ^l	9460	8561	9111	9102	8168	8465	8731	8748
Gas vol. [L kg ⁻¹] ^m	805	798	875	886	843	854	871	739

[^a] BAM drop hammer, grain size (75–150 μm); [^b] BAM friction tester, grain size (75–150 μm); [^c] Nitrogen content; [^d] Oxygen balance^[40]; [^e] Temperature of decomposition by DSC ($\beta = 5$ °C, Onset values); [^f] density calculated from X-ray measurements; [^g] Molar enthalpy of formation; [^h] Energy of formation; [ⁱ] Energy of Explosion; [^j] Explosion temperature; [^k] Detonation pressure; [^l] Detonation velocity; [^m] Assuming only gaseous products; * values based on Ref.^[37] and the EXPLO5 database; n.d.: not determined.

3.3 Conclusion

Two novel *N*-bound primary nitramines have been synthesized by the reaction of 1,5-diaminotetrazole and 1-amino-5-imino-4-methyltetrazole with the mild nitrating reagent nitronium tetrafluoroborate in good yields. Both compounds **1** and **2** exhibit very high sensitivities against friction, impact and electrostatic discharge, but have been fully characterized by means of vibrational and multinuclear NMR spectroscopy and also by mass spectrometry. The decomposition reaction of **1** in protic solvents has also been investigated by means of vibrational and ¹⁵N/¹H/¹³C NMR spectroscopy. Compounds **1** (85 °C) and **2** (150 °C) differ very much in decomposition temperature (65 °C), a result of

the introduction of the methyl group in 4 position. Both neutral compounds have also been investigated by single crystal X-ray diffraction measurements.

The energetic ionic compounds composed of the anion of **1** and the corresponding nitrogen rich cations have been synthesized by metathesis reactions from different solvents. All ionic compounds, **4** – **8** have been crystallized as anhydrous compounds from various solvents and single crystal X-ray diffraction measurements of all compounds have been performed. The characterization of **4** – **8** using vibrational and multinuclear NMR spectroscopy as well as mass spectrometry has been undertaken. Additionally, quantum mechanical calculations have been performed in order to obtain reasonable heats of formations for all compounds, since the highly energetic character of the salts prohibits the use of combustion experiments by bomb calorimetry. The densities derived from single crystal X-ray measurements have been used together with the calculated heats of formation to derive detonation parameters for all compounds (**1**, **2**, **4** – **8**) with the Explo5.04 program package. While **4** and **5** show very good performance data for v_{det} (9111 m s⁻¹ (**4**) and 9102 m s⁻¹ (**5**)) and the detonation pressure (344 kbar (**4**), 334 kbar (**5**)), they are on the other hand much too sensitive against friction and impact and decompose at low temperatures of only 107 °C (**4**) and 134 °C (**5**). Compounds **6** and **7** exhibit low sensitivities against friction and impact, but show much lower values for detonation velocities and detonation pressure. The best performing compound in terms of thermal stability is triaminoguanidinium 5-amino-1-nitriminotetrazolate (**8**). It exhibits a decomposition temperature of 160 °C and also shows promising values derived from the performance calculations (v_{det} : 8731 m s⁻¹; $P_{\text{C-J}}$: 295 kbar; V_0 : 871 L kg⁻¹) but unfortunately also exhibits very high sensitivities against friction and impact with 32 N and 2 J, respectively. Some compounds (**1**, **4**, **5** and **8**) show performance characteristics well above the values of RDX, but are too sensitive for use and handling and do not exhibit very high thermal stabilities.

3.4 Experimental Part

General. All chemical reagents and solvents were obtained from Sigma-Aldrich Inc. or Acros Organics (analytical grade) and were used as supplied without further purification. ¹H, ¹³C{¹H}, ¹⁴N{¹H}, ¹⁵N{¹H} and ¹⁵N NMR spectra were recorded on a JEOL Eclipse 400 instrument in DMSO-*d*₆ or CD₃OD at or near 25 °C. The chemical shifts are given relative to tetramethylsilane (¹H, ¹³C) or nitromethane (¹⁴N, ¹⁵N) as external standards and

coupling constants are given in Hertz (Hz). Infrared (IR) spectra were recorded on a Perkin-Elmer Spectrum BX FT-IR instrument equipped with an ATR unit at 25 °C. Transmittance values are qualitatively described as “very strong” (vs), “strong” (s), “medium” (m), “weak” (w) and “very weak” (vw). RAMAN spectra were recorded on a Bruker RAM II spectrometer equipped with a Nd:YAG laser operating at 1064 nm and a reflection angle of 180°. The intensities are reported as percentages of the most intense peak and are given in parentheses. Elemental analyses (CHNO) were performed with a Netzsch Simultaneous Thermal Analyzer STA 429. Melting and decomposition points were determined by differential scanning calorimetry (Linseis PT 10 DSC, calibrated with standard pure indium and zinc). Measurements were performed at a heating rate of 5 °C min⁻¹ in closed aluminum sample pans with a 1 µm hole in the top for gas release to avoid an unsafe increase in pressure under a nitrogen flow of 20 mL min⁻¹ with an empty identical aluminum sample pan as a reference. The mass spectra were recorded with DEI, DCI and FAB methods on a JEOL MStation JMS 700 mass spectrometer.

For initial safety testing, the impact and friction sensitivities as well as the electrostatic sensitivities were determined. The impact sensitivity tests were carried out according to STANAG 4489,^[38] modified according to WIWEB instruction 4-5.1.02^[39] using a BAM^[40] drop hammer. The friction sensitivity tests were carried out according to STANAG 4487^[41] and modified according to WIWEB instruction 4-5.1.03^[42] using the BAM friction tester. The electrostatic sensitivity tests were accomplished according to STANAG 4490^[43] using an electric spark testing device ESD 2010EN (OZM Research) operating with the “Winspark 1.15 software package”.^[44]

Crystallographic measurements. The single crystal X-ray diffraction data of **1**, **2** and **4** – **8** were collected using an Oxford Xcalibur3 diffractometer equipped with a Spellman generator (voltage 50 kV, current 40 mA) and a KappaCCD detector. The data collection was undertaken using the CRYVALIS CCD software^[45] while the data reduction was performed with the CRYVALIS RED software.^[46] The structures were solved with SIR-92^[47] or SHELXS-97^[48] and refined with SHELXL-97^[49] implemented in the program package WinGX^[50] and finally checked using PLATON.^[51] Further information regarding the crystal-structure determination have been deposited with the Cambridge Crystallographic Data Centre^[52] as supplementary publication Nos. 824129 (**1**), 824135 (**2**), 824133 (**4**), 824134 (**5**), 824131 (**6**), 824130 (**7**) and 824132 (**8**).

5-Amino-1-nitriminotetrazole (HDATNO₂, **1**)

1,5-Diaminotetrazole (2 g, 20 mmol) was dissolved in 50 mL of dry acetonitrile. The solution was held at 0°C (ice bath cooling) and nitronium tetrafluoroborate (2.65 g, 20 mmol) was added under stirring to the solution which turned slightly yellow. The reaction mixture was allowed to stir over night at room temperature. Acetonitrile was then evaporated under vacuum resulting in a yellowish solid. The solid was re-dissolved in a small amount of 5 mL ethanol and 20 mL ethanolic solution of potassium hydroxide (1.12 g, 20 mmol) was added, resulting in the precipitation of potassium tetrafluoroborate, which was filtered off. The ethanolic solution was then reduced until dryness leaving a crude yellow product of HDATNO₂ (1.7 g, 59 %). The crude product was recrystallized from ethanol and ether, yielding 1.6 g (55 %) of pure HDATNO₂.

T_{dec.}: 85 °C (DSC, Onset, 5 °C min⁻¹); ¹H NMR (CD₃OD, 25 °C) δ (ppm) = 5.39 (s, 2H, -NH₂); ¹³C {¹H} NMR (CD₃OD, 25 °C) δ (ppm) = 152.7; ¹⁴N NMR (CD₃OD, 25 °C) δ (ppm) = -18 (-N-NO₂, N₆), -21 (-N-NO₂, dec. product), -143 (N_γ, dec. product), -146 (N_β, dec. product), -176 (N₁), -300 (br, N_α, dec. product), -330 (NH₂, N₇); ¹⁵N NMR (CD₃OD, 25 °C) δ (ppm) = -18.0 (N₆), -18.3 (N-NO₂, dec. product), -26.1 (N₂), -28.0 (N₃), -161.5 (N₅), -176.7 (N₁), -331 (NH₂, N₇); ¹⁵N {¹H} NMR (CD₃OD, 25 °C) δ (ppm) = -17.5 (-N-NO₂, N₆), -26.0 (N₂), -28.1 (N₃), -56.4 (N₄), -177.7 (N₁), -331.5 (NH₂, N₇), -334.1 (NH₂, dec. product); IR (ATR, 25 °C, cm⁻¹) ν 3424 (m), 3335 (m), 3262 (m), 1705 (m), 1645 (m), 1495 (w), 1445 (mw), 1384 (vs), 1302 (m), 1259 (w), 1102 (w), 1050 (w), 1039 (w), 976 (vw), 838 (vw), 727 (vw), 710 (vw); RAMAN (Nd:YAG, 1064 nm, cm⁻¹) ν 3304 (2), 3250 (8), 3150 (1), 1710 (3), 1697 (3), 1583 (7), 1481 (38), 1413 (5), 1373 (15), 1307 (55), 1267 (15), 1130 (21), 1084 (8), 971 (68), 917 (9), 771 (100), 716 (12), 664 (1), 829 (8), 452 (20), 415 (13), 325 (13), 275 (5); m/z: (DCI+): 146.03 [M+H]⁺; Sensitivities (anhydrous) (grain size: 100-500 μm): IS: < 0.25 J; FS: < 1 N; ESD: 25 mJ.

Silver 5-amino-1-nitriminotetrazolate (Ag⁺ DATNO₂⁻, **3**)

5-Amino-1-nitriminotetrazole (0.725 g, 5 mmol) was dissolved in 50 mL water and a solution of silver nitrate (0.934 g, 5.5 mmol) in 25 mL water was added slowly, forming a grey precipitate immediately. The suspension was stirred for an additional hour under the

exclusion of light. The precipitate was filtrated off, washed silver free with 500 mL water and dried at 50 °C overnight to yield 1.22 g (97 %) $\text{Ag}^+ \text{DATNO}_2^-$.

T_{dec} : 158 °C (DSC, Onset, 5 °C min^{-1}); IR (ATR, 25 °C, cm^{-1}) ν = 3431 (m), 3332 (m), 3203 (w), 3140 (w), 1655 (vs), 1647 (vs), 1546 (w), 1462 (m), 1436 (m), 1351 (w), 1300 (s), 1255 (s), 1139 (w), 1061 (w), 903 (w), 816 (w), 768 (w), 727 (w); RAMAN (Nd:YAG, 1064 nm, cm^{-1}) ν = 3329 (9), 3216(9), 1645 (35), 1575 (12), 1547 (21), 1491 (20), 1457 (30), 1354 (35), 1334 (31), 1293 (58), 1267 (22), 1243 (22), 1137 (43), 1101 (38), 1041 (48), 1012 (42), 993 (94), 902 (28), 778 (100), 728 (9), 713 (9), 547 (14), 463 (25), 422 (20), 327 (16), 296 (16); Sensitivities (grain size: 100-500 μm): IS: < 1J ; FS: < 5 N.

Ammonium 5-amino-1-nitriminotetrazolate ($\text{NH}_4^+ \text{DATNO}_2^-$, **4**)

$\text{Ag}^+ \text{DATNO}_2^-$ (1.02 g, 4 mmol) was suspended in 5 mL water and a solution of ammonium chloride (0.171 g, 3.2 mmol) in 5 mL water was added slowly. The suspension was left stirring for 2 hours under the exclusion of light and the resulting silver chloride was filtered off by vacuum filtration. 90 mL ethanol was added to the filtrate and the volume of the resulting solution was reduced in vacuum to 1/20 of its original volume and left standing for crystallization. Colorless crystals deposited overnight, were filtered off and washed with diethyl ether to yield 0.432 g (83.5 %) pure $\text{NH}_4^+ \text{DATNO}_2^-$.

T_{dec} : 107 °C (DSC, Onset, 5 °C min^{-1}); ^1H NMR (DMSO- d_6 , 25 °C) δ (ppm) 7.13 (s, 4H, NH_4^+), 6.14 (s, 2H, $-\text{NH}_2$); ^{13}C $\{^1\text{H}\}$ NMR (DMSO- d_6 , 25 °C) δ (ppm) 152.6; ^{14}N NMR (DMSO- d_6 , 25 °C) δ (ppm) -4 ($-\text{N}-\text{NO}_2$), -138, -359 (NH_4^+); IR (ATR, 25 °C, cm^{-1}) ν 3359 (m), 3235 (s), 3182 (s), 3039 (s), 2857 (m), 1635 (m), 1578 (w), 1418 (m), 1378 (m), 1296 (m), 1261 (m), 1121 (w), 1070 (w), 1000 (w), 901 (w), 871 (w), 825 (w), 736 (w); RAMAN (Nd:YAG, 1064 nm, cm^{-1}) ν 3241 (7), 3186 (9), 3059 (4), 1678 (3), 1637 (18), 1577 (12), 1470 (28), 1451 (25), 1322 (18), 1305 (41), 1264 (39), 1132 (25), 1082 (9), 1044 (17), 1023 (100), 1011 (83), 989 (30), 903 (10), 875 (13), 769 (64), 757 (39), 721 (21), 680 (3), 532 (17), 466 (7), 447 (9), 419 (8), 392 (28), 339 (18), 320 (13); m/z : (FAB+): 18.0 [NH_4^+]; m/z : (FAB-): 144.0 [DATNO_2^-]; EA ($\text{CH}_6\text{N}_8\text{O}_2 \cdot 1\text{H}_2\text{O}$) calcd.: C, 6.67; H, 4.48; N, 62.21; found: C, 6.67; H, 4.33; N, 60.23; Sensitivities (monohydrate) (grain size: 100-500 μm): IS: 3 J ; FS: 52 N ; ESD: 200 mJ.

Hydrazinium 5-amino-1-nitriminotetrazolate ($\text{N}_2\text{H}_5^+ \text{DATNO}_2^-$, **5**)

$\text{Ag}^+ \text{DATNO}_2^-$ (1.02 g, 4 mmol) was suspended in 5 mL water and a solution of hydrazinium chloride (0.219 g, 3.2 mmol) in 5 mL water was added slowly. The suspension was left stirring for 2 hours under the exclusion of light and the resulting silver chloride was separated by vacuum filtration. 90 mL ethanol was added to the filtrate and the volume of the resulting solution was reduced in vacuum to 1/4 of its original volume and left standing for crystallization. Light yellow crystals deposited immediately, were filtered off and washed with diethyl ether to yield 0.403 g (71 %) pure $\text{N}_2\text{H}_5^+ \text{DATNO}_2^-$.

T_{dec} : 134 °C (DSC, 5 °C min⁻¹), 151 °C (DSC, Onset, 5 °C min⁻¹); ¹H NMR (DMSO-*d*₆, 25 °C) δ (ppm) 7.03 (s, 5H, N_2H_5^+), 6.12 (s, 2H, -NH₂); ¹³C {¹H} NMR (DMSO-*d*₆, 25 °C) δ (ppm) 152.6; ¹⁴N NMR (DMSO-*d*₆, 25 °C) δ (ppm) -4 (N-NO₂), -138, -334, -359 (N_2H_5^+); IR (ATR, 25 °C, cm⁻¹) ν 3430 (s), 3317 (s), 3284 (vs), 3260(s), 3196 (s), 3160 (s), 1643 (s), 1574 (m), 1548 (m), 1467 (m), 1386 (s), 1301 (s), 1248 (s), 1143 (w), 1110 (m), 1094 (m), 1053 (m), 1012 (vw), 982 (m), 893 (m), 826 (w), 779 (w), 758 (w), 730 (w), 676 (w); RAMAN (Nd:YAG, 1064 nm, cm⁻¹) ν 3287 (4), 3265 (4), 3211 (6), 3179 (4), 1643 (5), 1629 (5), 1572 (8), 1455 (15), 1412 (3), 1357 (3)1324 (21), 1302 (20), 1263 (7), 1155 (6), 1127 (13), 1056 (6), 1012 (100), 986 (42), 896 (10), 761 (50), 725 (8), 537 (7), 455 (9), 403 (6), 327 (10), 296 (6); *m/z*: (FAB+): 33.0 [N_2H_5^+]; *m/z*: (FAB-): 144.0 [DATNO_2^-]; EA (CH₇N₉O₂) calcd.: C, 6.78; H, 3.98; N, 71.17; found: C, 6.51; H, 3.71; N, 70.47; Sensitivities (anhydrous) (grain size: 100-500 μm): IS: < 1 J; FS: 48 N; ESD: 100 mJ.

Guanidinium 5-amino-1-nitriminotetrazolate ($\text{G}^+ \text{DATNO}_2^-$, **6**)

$\text{Ag}^+ \text{DATNO}_2^-$ (1.02 g, 4 mmol) was suspended in 5 mL water and a solution of guanidinium bromide (0.445 g, 3.2 mmol) in 5 mL water was added slowly. The suspension was left stirring for 2 hours under the exclusion of light and the resulting silver bromide was separated by vacuum filtration. 90 mL ethanol was added to the filtrate and the volume of the resulting solution was reduced in vacuum to 1/4 of its original volume and left standing for crystallization. Colorless crystals deposited

overnight, were filtered off and washed with diethyl ether to yield 0.485 g (74 %) pure G^+ $DATNO_2^-$.

$T_{dec.}$: 148 °C (DSC, 5 °C min^{-1}), 159 °C (DSC, Onset, 5 °C min^{-1}); 1H NMR (DMSO- d_6 , 25 °C) δ (ppm) 6.94 (s, 6H, $C(NH_2)_3^+$), 6.10 (s, 2H, $-NH_2$); ^{13}C $\{^1H\}$ NMR (DMSO- d_6 , 25 °C) δ (ppm) 157.9 ($C(NH_2)_3^+$), 152.6 ($DATNO_2^-$); ^{14}N NMR (DMSO- d_6 , 25 °C) δ (ppm) -4 (N- NO_2), -137 ; IR (ATR, 25 °C, cm^{-1}) ν 3416 (s), 3314 (s), 3254 (s), 3183 (s), 1645 (s), 1579 (m), 1512 (w), 1466 (w), 1453 (w), 1383 (m), 1308 (m), 1264 (m), 1113 (w), 1052 (w), 1013 (vw), 980 (vw), 900 (w), 774 (w), 620 (vw); RAMAN (Nd:YAG, 1064 nm, cm^{-1}) ν 3338 (4), 3254 (5), 3198 (5), 2152 (2), 1643 (7), 1571 (5), 1466 (10), 1451 (16), 1326 (11), 1301 (14), 1265 (10), 1139 (5), 1115 (11), 1055 (30), 1014 (100), 902 (7), 768 (28), 724 (5), 538 (15), 525 (13), 459 (5), 417 (5), 332 (4); m/z : (FAB+): 60.1 [$C(NH_2)_3^+$]; m/z : (FAB-): 144.0 [$DATNO_2^-$]; EA ($C_2H_8N_{10}O_2 \cdot H_2O$) calcd.: C, 10.80; H, 4.68; N, 62.95; found: C, 11.58; H, 4.71; N, 62.82; Sensitivities (anhydrous) (grain size: 500 - 1000 μm): IS: 40 J ; FS: 240 N; ESD: 260 mJ.

Aminoguanidinium 5-amino-1-nitriminotetrazolate (AG^+ $DATNO_2^-$, 7)

Ag^+ $DATNO_2^-$ (1.02 g, 4 mmol) was suspended in 5 mL water and a solution of aminoguanidinium bromide (0.493 g, 3.2 mmol) in 5 mL water was added slowly. The suspension was left stirring for 2 hours under the exclusion of light and the resulting silver bromide was separated by vacuum filtration. 90 mL ethanol was added to the filtrate and the volume of the resulting solution was reduced in vacuum to 1/4 of its original volume and left standing for crystallization. Light yellow crystals deposited overnight, were filtered off and washed with diethyl ether to yield 0.532 g (76 %) pure AG^+ $DATNO_2^-$.

$T_{dec.}$: 142 °C (DSC, Onset, 5 °C min^{-1}); 1H NMR (DMSO- d_6 , 25 °C) δ (ppm) 8.58 (s, 1H, $-NH-NH_2$), 7.24 (s, 2H, $-NH_2$), 6.83 (s, 2H, $-NH_2$), 6.12 (s, 2H, $-NH_2$, $DATNO_2^-$), 4.68 (s, 2H, $-NH-NH_2$); ^{13}C $\{^1H\}$ NMR (DMSO- d_6 , 25 °C) δ (ppm) 158.8 ($CH_7N_4^+$), 152.6 ($DATNO_2^-$); ^{14}N NMR (DMSO- d_6 , 25 °C) δ (ppm) -4 (N- NO_2), -138 ; IR (ATR, 25 °C, cm^{-1}) ν 2448 (m), 3331 (s), 3254 (s), 3192 (s), 1658 (s), 1575 (m), 1517 (w), 1464 (m), 1405 (m), 1299 (m), 1264 (m), 1204 (w), 1069 (w), 981 (w), 891 (vw), 822 (vw), 772 (vw), 734 (vw); RAMAN (Nd:YAG, 1064 nm, cm^{-1}) ν 3350 (8), 3335 (10), 3256 (10), 3227 (11), 1675 (9), 1651 (5), 1633 (5), 1589 (6), 1535 (4), 1463 (16), 1400 (2), 1304

(32), 1273 (21), 1206 (5), 1119, (12), 1074 (8), 1050 (12), 1016 (100), 992 (25), 966 (35), 893 (8), 757 (28), 722 (7), 620 (9), 534 (5), 507 (13), 466 (13), 400 (7), 341 (7), 306 (4); m/z : (FAB+): 75.1 [CH_7N_4^+]; m/z : (FAB-): 144.0 [DATNO_2^-]; EA ($\text{C}_2\text{H}_9\text{N}_{11}\text{O}_2 \cdot 1/2 \text{H}_2\text{O}$) calcd.: C, 10.53; H, 4.42; N, 67.52; found: C, 11.01; H, 4.24; N, 66.60; Sensitivities (anhydrous) (grain size: 100-500 μm): IS: 20 J; FS: 192 N; ESD: 200 mJ.

Triaminoguanidinium 5-amino-1-nitriminotetrazolate ($\text{TAG}^+ \text{DATNO}_2^-$, **8**)

$\text{Ag}^+ \text{DATNO}_2^-$ (1.02 g, 4 mmol) was suspended in 50 mL of dry MeCN. Triaminoguanidinium chloride (0.374 g, 2.6 mmol) was added in one portion afterwards and the reaction mixture was stirred for 4 days under the exclusion of light. The suspension was then filtrated and the residue was washed with 10 mL of MeCN. The solvent was completely evaporated to leave analytically pure $\text{TAG}^+ \text{DATNO}_2^-$ (Yield 0.58 g = 89.5%). Crystals suitable for X-ray diffraction measurements were obtained after recrystallization from dry MeCN as colorless rods.

T_{melt} : 107 °C (DSC, Onset, 5 °C min^{-1}); $T_{\text{dec.}}$: 160 °C (DSC, Onset, 5 °C min^{-1}); ^1H NMR (DMSO- d_6 , 25 °C) δ (ppm) 8.58 (s, 3H, -NH-NH₂), 6.07 (s, 2H, -NH₂, DATNO_2^-), 4.48 (s, 6H, -NH-NH₂); $^{13}\text{C}\{^1\text{H}\}$ NMR (DMSO- d_6 , 25 °C) δ (ppm) 159.0 (CH_9N_6^+), 152.6 (DATNO_2^-); ^{14}N NMR (DMSO- d_6 , 25 °C) δ (ppm) -4 (-N-NO₂); $^{15}\text{N}\{^1\text{H}\}$ NMR (DMSO- d_6 , 25 °C) δ (ppm) = -2.9 (-N-NO₂, N₆), -5.9 (N₂), -23.5 (N₃), -96.7 (N₄), -166.7 (N₅), -174.3 (N₁), -289.2 (CH_9N_6^+), -329.6 (CH_9N_6^+), -338.8 (-NH₂, N₇); ^{15}N NMR (DMSO- d_6 , 25 °C) δ (ppm) = -2.9 (-N-NO₂, N₆), -5.9 (N₂), -23.6 (N₃), -95.7 (N₄), -289.1 (d, $^1J_{\text{NH}} = 102.5$ Hz, CH_9N_6^+), -329.5 (t, $^1J_{\text{NH}} = 69.8$ Hz, CH_9N_6^+), -338.8 (-NH₂, DATNO_2^-); IR (ATR, 25 °C, cm^{-1}) ν 3360 (s), 3318 (vs), 3209 (vs), 1685 (s), 1647(s), 1614(m), 1581 (m), 1466 (w), 1401 (s), 1328 (vs), 1275 (m), 1127 (m), 1061 (w), 1022 (w), 990 (w), 951 (m), 877 (w), 766 (w), 737 (w), 672 (vw), 638 w), 603 (m), 455 (vw); RAMAN (Nd:YAG, 1064 nm, cm^{-1}) ν 3256 (74), 3233 (77), 3124 (74), 1517 (94), 1459 (98), 1325 (90), 1267 (89), 1298 (98), 1133 (82), 1086 (80), 1013 (100), 991 (90), 893 (80), 764 (79), 418 (61); m/z : (FAB+): 105.13 [CH_9N_6^+]; m/z : (FAB-): 144.01 [DATNO_2^-]; EA ($\text{C}_2\text{H}_{11}\text{N}_{13}\text{O}_2$) calcd.: C, 9.64; H, 4.45; N, 73.07; found: C, 10.03; H, 4.64; N, 73.00; Sensitivities (anhydrous) (grain size: 100-500 μm): IS: 2 J ; FS: 32 N ; ESD: 65 mJ.

5-Amino-4-methyl-1-nitiminotetrazole (MeDATNO₂, **2**)

1-Amino-5-imino-4-methyl-tetrazole (0.342 g, 3 mmol) was dissolved in 15 mL MeCN and the solution was cooled down to 0 °C. NO₂BF₄ (0.397 g, 3 mmol) was added to the solution in one portion, resulting in a slightly yellow solution. The reaction mixture was stirred at 0 °C for an additional 30 minutes, removed from the ice bath afterwards and left stirring at room temperature for 1 hour. The solution was left standing overnight, letting MeCN evaporate slowly. On complete evaporation of the solvent, MeDATNO₂ deposited as colorless crystals. The crystals were washed with a small amount of water and ether afterwards to yield 0.255 g (53 %) elemental analysis clean MeDATNO₂.

T_{dec.}: 150 °C (DSC, 5 °C min⁻¹), 163 °C (DSC, Onset, 5 °C min⁻¹); ¹H NMR (DMSO-*d*₆, 25 °C) δ (ppm) 8.88 (s, 2H, =NH₂⁺), 3.84 (s, 3H, -CH₃); ¹³C{¹H} NMR (DMSO-*d*₆, 25 °C) δ (ppm) 145.6, 34.4 (-CH₃); ¹⁴N NMR (DMSO-*d*₆, 25 °C) δ (ppm) -3 (-N-NO₂); ¹⁵N NMR (DMSO-*d*₆, 25 °C) δ (ppm) -2.3 (-N-NO₂, N₆), -26.1 (N₂), -36.2 (q, ³J_{N-H} = 1.86 Hz, N₃), -126.9 (N₅), -147.3 (N₁), -185.5 (N₄), -320.4 (t, ¹J_{N-H} = 91.29 Hz, N₇); ¹⁵N{¹H} NMR (DMSO-*d*₆, 25 °C) δ (ppm) -2.2 (-N-NO₂, N₆), -26.0 (N₂), -36.2 (N₃), -126.9 (N₅), -147.3 (N₁), -185.8 (N₄), -320.5 (=NH₂, N₇); IR (ATR, 25 °C, cm⁻¹) ν 3241 (m), 3198 (w), 3068 (m), 1690 (vs), 1615 (w), 1560 (vw), 1515 (w), 1424 (m), 1392 (m), 1344 (w), 1275 (vs), 1232 (s), 1113 (w), 1036 (m), 1015 (m), 982 (m), 898 (m), 791 (w), 781 (m), 737 (w), 711 (w), 682 (w); RAMAN (Nd:YAG, 1064 nm, cm⁻¹) ν 3246 (3), 3047 (9), 3020 (7), 2964 (60), 2891 (2), 2831 (7), 1703 (9), 1621 (3), 1565 (4), 1518 (18), 1459 (16), 1427 (4), 1394 (28), 1345 (57), 1294 (3), 1237 (5), 1114 (19), 1039 (11), 1017 (34), 983 (66), 903 (11), 792 (100), 742 (18), 681 (4), 543 (5), 455 (16), 405 (17), 342 (8), 300 (25); *m/z*: (FAB+): 160.1 [M+H⁺]; *m/z*: (FAB-): 158.0 [M-H⁻]; EA (C₂H₅N₇O₂) calcd.: C, 15.10; H, 3.17; N, 61.62; found: C, 15.70; H, 2.91; N, 60.40; Sensitivities (anhydrous) (grain size: 100-500 μm): IS: < 1 J ; FS: < 5 N ; ESD: 211 mJ.

3.5 References

- [1] J. Wilbrand, *Liebigs Ann. Chem.* **1863**, 128, 178-179.
- [2] a) R. Meyer, J. Köhler, A. Homburg, *Explosives*, Sixth ed., Wiley-VCH Verlag GmbH & Co. KGaA, Weinheim, **2007**; b) J. A. Zukas, W. P. Walters, *Explosive effects and applications*, Springer, Heidelberg, New York, **1998**.
- [3] T. M. Klapötke, *Chemie der hochenergetischen Materialien*, 1 ed., Walter de Gruyter, Berlin, New York, **2009**.

- [4] a) H. Feuer, A. T. Nielsen, *Nitro compounds*, Wiley-VCH, Weinheim, **1990**; b) A. T. Nielsen, *Nitrocarbons*, Wiley-VCH, Weinheim, **1995**.
- [5] a) N. V. Latypov, U. Wellmar, P. Goede, A. J. Bellamy, *Org. Process Res. Dev.* **2000**, *4*, 156-158; b) A. T. Nielsen, US 5,693,794, **1997**.
- [6] M.-X. Zhang, P. E. Eaton, R. Gilardi, *Angew. Chem.* **2000**, *112*, 422-426; *Angew. Chem. Int. Ed.* **2000**, *39*, 401-404.
- [7] R. L. Simpson, P. A. Urtiew, D. L. Ornellas, G. L. Moody, K. J. Scribner, D. M. Hoffman, *Propell. Explos. Pyrot.* **1997**, *22*, 249-255.
- [8] V. A. Ostrovskii, M. S. Pevzner, T. P. Kofman, I. V. Tselinskii, *Targets Heterocyclic System* **1999**, *3*, 467-526.
- [9] M. B. Talawar, R. Sivabalan, T. Mukundan, H. Muthurajan, A. K. Sikder, B. R. Gandhe, A. S. Rao, *J. Hazard. Mater.* **2009**, *161*, 589-607.
- [10] W. D. Won, L. H. DiSalvo, J. Ng, *Appl. Environ. Microb.* **1976**, *31*, 576-580.
- [11] T. E. O'Connor, G. Flemming, J. Reilly, *J. Soc. Chem. Ind. L.* **1949**, *68*, 309-310.
- [12] a) E. Lieber, E. Sherman, S. H. Sherman, *J. Am. Chem. Soc.* **1951**, *73*, 2329-2331; b) E. Lieber, E. Sherman, R. A. Henry, J. Cohen, *1951* **1951**, *73*; c) R. M. Herbst, J. Garrison, *J. Org. Chem.* **1953**, *18*, 941-945.
- [13] J. A. Garrison, R. M. Herbst, *J. Org. Chem.* **1957**, *22*, 278-283.
- [14] a) R. Damavarapu, T. M. Klapötke, J. Stierstorfer, K. R. Tarantik, *Propell. Explos. Pyrot.* **2010**, *35*, 395-406; b) T. M. Klapoetke, J. Stierstorfer, A. U. Wallek, *Chem. Mater.* **2008**, *20*, 4519-4530; c) T. M. Klapötke, in *High Energy Density Materials* (Ed.: T. M. Klapötke), Springer, Heidelberg, **2007**, pp. 84-122; d) J. Stierstorfer, T. M. Klapötke, *Helvetica Chimica Acta* **2007**, *90*, 2132; e) J. Stierstorfer, K. R. Tarantik, T. M. Klapötke, *Chem. Eur. J.* **2009**, *15*, 5775-5792.
- [15] T. P. Kofman, G. Y. Kartseva, M. B. Shcherbinin, *Russ. J. Org. Chem.* **2002**, *38*, 1343-1350.
- [16] a) A. I. Glushkov, O. P. Shitov, V. A. Tartakovsky, *Russ. Chem. Bull.* **2003**, *52*, 467-470; b) Y. Huang, H. Gao, B. Twamley, J. Shreeve, *Eur. J. Inorg. Chem.* **2008**, *2008*, 2560-2568; c) A. R. Katrizky, G. L. Sommen, A. V. Grovoma, R. M. Witek, P. J. Steel, R. Damavarapu, *Chem. Het. Comp.* **2005**, *41*, 111-118; d) O. Shitov, V. Korolev, V. Tartakovsky, *Russ. Chem. Bull.* **2009**, *58*, 2347-2355; e) O. P. Shitov, V. L. Korolev, V. S. Bogdanov, V. A. Tartakovsky, *Russ. Chem. Bull.* **2003**, *52*, 695-699; f) C.-R. Zhang, Y.-L. Wang, *Synthetic Communications* **2003**, *33*, 4205-4208.
- [17] a) R. Damavarapu, in *37th ICT - Energetic Materials*, **2006**, pp. 17/11-17/15; b) R. Duddu, P. R. Dave, R. Damavarapu, N. Gelber, D. Parrish, *Tetrahedron Lett.* **2010**, *51*, 399-401.
- [18] M. A. Ilyushin, A. N. Terpigorev, I. V. Tselinskii, *Russ. J. Gen. Chem.* **1999**, *69*, 1654-1657.
- [19] a) Z. X. Chen, J. M. Xiao, H. M. Xiao, Y. N. Chiu, *J. Phys. Chem. A* **1999**, *103*, 8062-8066; b) Z.-X. Chen, H.-M. Xiao, *Huaxue Xuebao* **1998**, *56*, 1198-1206.
- [20] P. N. Gaponik, V. P. Karavai, *Chem. Heterocyc. Comp.* **1984**, 1683-1686.
- [21] a) T. M. Klapötke, C. M. Sabate, J. M. Welch, *Z. Anorg. Allg. Chem.* **2008**, *634*, 857-866; b) J. C. Galvez-Ruiz, G. Holl, K. Karaghiosoff, T. M. Klapötke, K.

- Löhnwitz, P. Mayer, H. Nöth, K. Polborn, C. J. Rohbogner, M. Suter, J. J. Weigand, *Inorg. Chem.* **2005**, *44*, 4237-4253.
- [22] M.-J. Crawford, K. Karaghiosoff, T. M. Klapötke, F. A. Martin, *Inorg. Chem.* **2009**, *48*, 1731-1743.
- [23] A. F. Holleman, E. Wiberg, *Lehrbuch der anorganischen Chemie*, 101st Ed., de Gruyter, New York, **1995**.
- [24] M. Hesse, Herbert, Meier, B. Zeh, *Spektroskopische Methoden in der Organischen Chemie*, 6 ed., Georg Thieme Verlag, Stuttgart, New York, **2002**.
- [25] a) T. H. Dunning, *J. Chem. Phys.* **1989**, *90*, 1007; b) C. Lee, W. Yang, R. G. Parr, *Phys. Rev. B* **1988**, *7*, 785; c) A. D. Becke, *J. Chem. Phys.* **1993**, *98*, 5648.
- [26] *Gaussian 09W, Version 7.0*, M. J. Frisch, G. W. Trucks, H. B. Schlegel, G. E. Scuseria, M. A. Robb, J. R. Cheeseman, G. Scalmani, V. Barone, B. Mennucci, G. A. Petersson, H. Nakatsuji, M. Caricato, X. Li, H. P. Hratchian, A. F. Izmaylov, J. Bloino, G. Zheng, J. L. Sonnenberg, M. Hada, M. Ehara, K. Toyota, R. Fukuda, J. Hasegawa, M. Ishida, T. Nakajima, Y. Honda, O. Kitao, H. Nakai, T. Vreven, J. A. Montgomery, Jr., J. E. Peralta, F. Ogliaro, M. Bearpark, J. J. Heyd, E. Brothers, K. N. Kudin, V. N. Staroverov, R. Kobayashi, J. Normand, K. Raghavachari, A. Rendell, J. C. Burant, S. S. Iyengar, J. Tomasi, M. Cossi, N. Rega, J. M. Millam, M. Klene, J. E. Knox, J. B. Cross, V. Bakken, C. Adamo, J. Jaramillo, R. Gomperts, R. E. Stratmann, O. Yazyev, A. J. Austin, R. Cammi, C. Pomelli, J. W. Ochterski, R. L. Martin, K. Morokuma, V. G. Zakrzewski, G. A. Voth, P. Salvador, J. J. Dannenberg, S. Dapprich, A. D. Daniels, Ö. Farkas, J. B. Foresman, J. V. Ortiz, J. Cioslowski, and D. J. Fox, *Gaussian, Inc., Wallingford CT*, 2009.
- [27] H. A. Witek, M. Keiji, *J. Comp. Chem. THEOCHEM* **2004**, *25*, 1858-1864.
- [28] a) A. Dippold, Thomas M. Klapötke, Franz A. Martin, *Z. Anorg. Allg. Chem.* **2011**, *637*, in press; b) T. Altenburg, T. M. Klapötke, A. Penger, J. Stierstorfer, *Z. Anorg. Allg. Chem.* **2010**, *636*, 463-471.
- [29] a) J. W. Ochterski, G. A. Petersson, J. A. M. Jr., *J. Chem. Phys.* **1996**, *104*, 2598; b) J. A. Montgomery, M. J. Frisch, J. W. Ochterski, G. A. Petersson, *J. Chem. Phys.* **2000**, *112*, 6532.
- [30] P. J. Lindstrom, W. G. Mallard, *NIST Chemistry Webbook, NIST Standard Reference 69, June 2005, National Institute of Standards and Technology, Gaithersburg MD, 20899* (<http://webbook.nist.gov>).
- [31] a) E. F. C. Byrd, B. M. Rice, *J. Phys. Chem. A* **2006**, *110*, 1005-1013; b) L. A. Curtiss, K. Raghavachari, P. C. Redfern, J. A. Pople, *J. Chem. Phys.* **1997**, *106*, 1063-1079; c) B. M. Rice, S. V. Pai, J. Hare, *Combust. Flame* **1999**, *118*, 445-458.
- [32] a) F. Trouton, *Philos. Mag.* **1884**, *18*, 54-57; b) M. S. Westwell, M. S. Searle, D. J. Wales, D. H. Williams, *J. Am. Chem. Soc.* **1995**, *117*, 5013-5015.
- [33] *Back-calculated from $V(\text{TAG}^+\text{Cl}^-)$ and the molecular volume of the chloride anion taken from Ref (Jenkins, *Inorg. Chem.*); Volume of the energetic anion has been derived from the TAG^+ structure; all other volumes have been backcalculated using the corresponding volume of the energetic anion from single crystal measurements.*

- [34] a) H. D. B. Jenkins, H. K. Roobottom, J. Passmore, L. Glasser, *Inorg. Chem.* **1999**, *38*, 3609-3620; b) H. D. B. Jenkins, D. Tudela, L. Glasser, *Inorg. Chem.* **2002**, *41*, 2364-2367.
- [35] M. Sućeska, *EXPLO5.4 program, Zagreb, Croatia, 2010*.
- [36] a) M. Suceška, *Propell. Explos. Pyrot.* **1991**, *16*, 197-202; b) M. Suceška, *Propell. Explos. Pyrot.* **1999**, *24*, 280-285; c) M. Sućeska, *Materials Science Forum* **2004**, 465-466, 325-330.
- [37] J. Köhler, R. Meyer, *Explosivstoffe, Vol. 9th edition*, Wiley-VCH, Weinheim, **1998**.
- [38] *NATO standardization agreement (STANAG) on explosives, no. 4489, 1st ed., Sept. 17, 1999*.
- [39] *WIWEB-Standardarbeitsanweisung 4-5.1.02, Ermittlung der Explosionsgefährlichkeit, hier: der Schlagempfindlichkeit mit dem Fallhammer, Nov. 08, 2002*.
- [40] <http://www.bam.de>.
- [41] *NATO standardization agreement (STANAG) on explosives, friction tests, no.4487, 1st ed., Aug. 22, 2002*.
- [42] *WIWEB-Standardarbeitsanweisung 4-5.1.03, Ermittlung der Explosionsgefährlichkeit, hier: der Reibempfindlichkeit mit dem Reibeapparat, Nov. 08, 2002*.
- [43] *NATO standardization agreement (STANAG) on explosives, electrostatic discharge sensitivity tests, no.4490, 1st ed., Feb. 19, 2001*.
- [44] <http://www.ozm.cz/en/sensitivity-tests/esd-2008a-small-scale-electrostatic-spark-sensitivity-test/>.
- [45] *CrysAlis CCD, Oxford Diffraction Ltd., Version 1.171.27p5 beta (release 01-04-2005 CrysAlis171.NET)*.
- [46] *CrysAlis RED, Oxford Diffraction Ltd., Version 1.171.27p5 beta (release 01-04-2005 CrysAlis171.NET)*.
- [47] A. Altomare, G. Cascarano, C. Giacovazzo, A. Guagliardi, *J. Appl. Cryst.* **1993**, *26*, 343-350.
- [48] G. M. Sheldrick, *SHELXS-97, Crystal Structure Solution, Version 97-1; Institut Anorg. Chemie, University of Göttingen, Germany, 1990*.
- [49] G. M. Sheldrick, *SHELXL-97, Program for the Refinement of Crystal Structures. University of Göttingen, Germany, 1997*.
- [50] L. Farrugia, *J. Appl. Cryst.* **1999**, *32*, 837-838.
- [51] A. L. Spek, *Platon, A Multipurpose Crystallographic Tool, Utrecht University, Utrecht, The Netherlands, 1999*.
- [52] *Crystallographic data for the structure(s) have been deposited with the Cambridge Crystallographic Data Centre. Copies of the data can be obtained free of charge on application to The Director, CCDC, 12 Union Road, Cambridge CB2 1EZ, UK (Fax: int.code (1223)336-033; e-mail for inquiry: fileserv@ccdc.cam.ac.uk; e-mail for deposition: deposit-@ccdc.cam.ac.uk).*

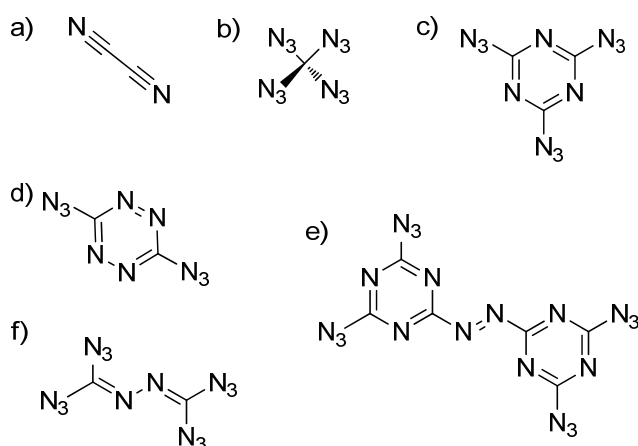
4. C₂N₁₄ – A new energetic and highly sensitive binary CN azidotetrazole

Thomas M. Klapötke, *Franz A. Martin, and Jörg Stierstorfer

As published in: Angewandte Chemie, 2011, 123, 4313 – 4316.

4.1. Introduction

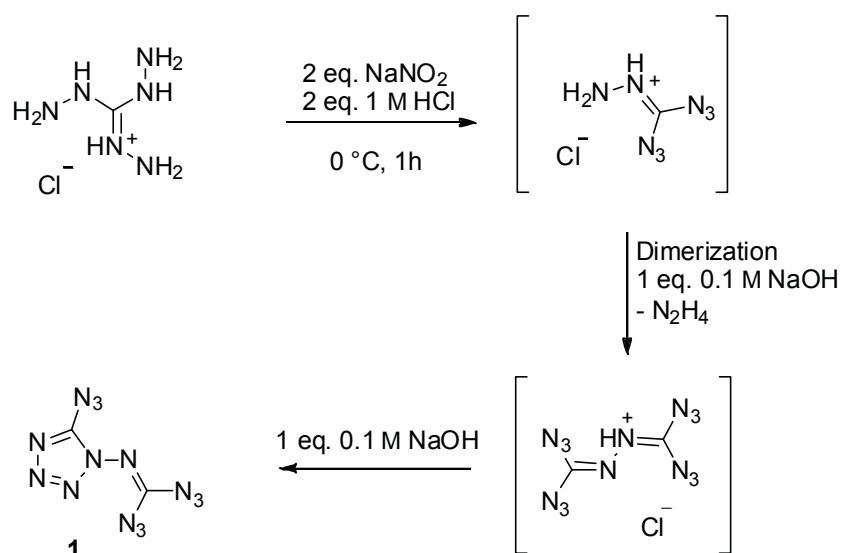
Although binary CN compounds are of great interest, only a few examples are known in literature, mostly due to the fact that their chemistry is very challenging. Binary CN compounds exhibit a large variety of characteristics. On the one hand they can be very harmful due to their toxicity like dicyanogen,^[1] on the other hand they are thought to be super hard as calculated for β -C₃N₄^[2] or show graphite-like nanostructures with good electric and catalytic properties as mpg-C₃N₄.^[3] Furthermore, binary CN compounds composed of azides show very high sensitivities towards shock, friction and electrostatic discharge. Investigations on these compounds started already in the beginning of the 20th century, when Ott presented C₃N₁₂ (Scheme 1) as the first binary azido-heterocyclic system.^[4] Research on heterocyclic azides was recently intensified,^[5] since they present very good systems to study highly energetic materials enabled by high positive heats of formation.^[5c,6] The high heats of formation are gathered by the energy input of the azide substituents (70 kJ/mol)^[7] and from the large number of energetic N–N and C–N bonds combined in the heterocyclic ring systems. Non heterocyclic binary CN systems also gathered a lot of interest like tetraazidomethane,^[8,5e] showing an extreme sensitivity towards shock and friction or the open form of the title compound C₂N₁₄, isocyanogentetraazide,^[9] presenting somewhat lower sensitivities than the title compound.^[10]



Scheme 1: Selected binary CN compounds: a) dicyanogen, b) tetraazidomethane, c) triazidotriazine, d) diazidotetrazine, e) tetraazidoazotriazine (TAAT) and f) C_2N_{14} (open form).

4.2. Results and Discussion

Up to now, only the open form of C_2N_{14} was known, which can be synthesized by a metathesis reaction of isocyanogen tetrabromide with sodium azide.^[9] In this paper, the synthesis of the closed form of C_2N_{14} , 1-diazidocarbamoyl-5-azidotetrazole, (**1**) is presented for the first time, being synthesized by diazotation of triaminoguanidinium chloride in water with two equivalents of sodium nitrite. A suggested mechanism of this reaction is presented in Scheme 2.



Scheme 2: Possible reaction pathway leading to the formation of C_2N_{14} (**1**).

Various attempts with different reaction conditions yielded always **1** as the kinetically stable product in different yields. To initiate the dimerization reaction and the following

ring closure reaction,^[11] respectively, the acidic reaction solution is brought to pH 8 slowly with sodium hydroxide solution. Basic reaction conditions are very important in this reaction step, otherwise residual sodium nitrite can decompose the azide groups partially, forming amines as byproducts. **1** can easily be isolated by extraction of the reaction solution with diethyl ether followed by a purification step using short column chromatography with CHCl₃ as solvent to get rid of above mentioned decomposition products.^[12] **1** is obtained as a colorless crystalline solid after recrystallization from diethyl ether showing a melting point at 78 °C and decomposition starting at 110 °C.

Single crystals of **1** suitable for X-ray diffraction measurements were obtained by recrystallization from diethyl ether. **1** crystallizes in the orthorhombic space group *Pbcn* with a cell volume of 1697.6(2) Å³ and eight molecules in the unit cell.^[13] The bond lengths and angles within the tetrazole rings are as expected in the normal range for an azidotetrazole.^[14] The N1–N8 bond is with 1.403(4) Å only a little bit shorter than a formal N–N single bond, while the N8–C2 bond is in the range of a C–N double bond with a bond length of 1.288(5) Å. As shown for 5-azido-1*H*-tetrazole, the azide group located on the 5 position lies perfectly within the plane of the tetrazole ring.^[5d] The asymmetric unit of **1** is presented in Figure 1.

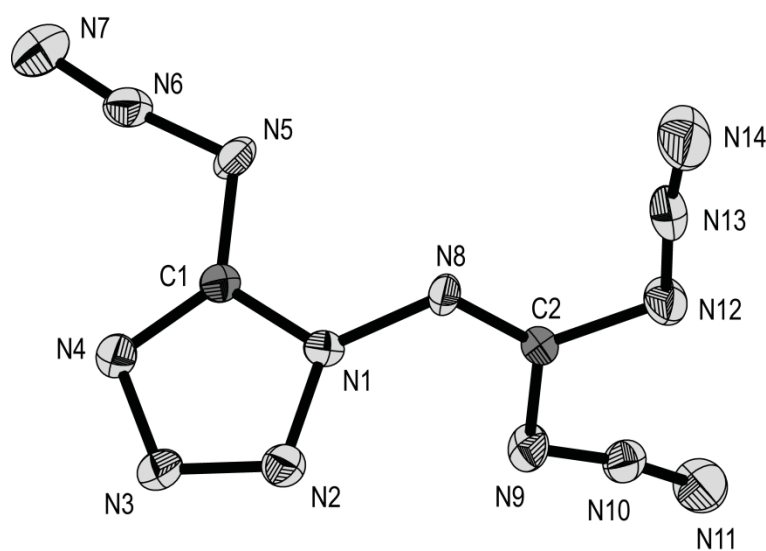


Figure 1: Ortep representation of **1**. Thermal ellipsoids are shown at the 50 % probability level. Selected crystallographic data: orthorhombic, *Pbcn*; *Z* = 8, *a* = 18.1289(1) Å, *b* = 8.2128(7) Å, *c* = 11.4021(9) Å, $\alpha=\beta=\gamma=90^\circ$, *V* = 1697.6(2) Å³.

The carbamoyl diazide group in **1** itself is twisted out of the plane of the tetrazole ring (N1 N2 N3 N4 C1) by 66.12° relative to the plane formed by N12, C2, N9 and N8. This twist within the molecule results in the buildup of 2D chains along the *c*-axis which show a zig-zag conformation representing an angle of 113.22° (Figure 4S). Calculations of the electrostatic potential on the B3LYP/cc-pVDZ level of theory^[15] in the gas phase show a clear charge distribution within **1**, which is reflected in the structure. The positive charge is located on the azide moieties, with N_β exhibiting the highest positive charge compared to N_α and N_γ . The negative charge is located on the N4, N3 and N2 nitrogen atoms of the tetrazole ring mainly, exhibiting a big inequality of the charge distribution (Figure 5S).

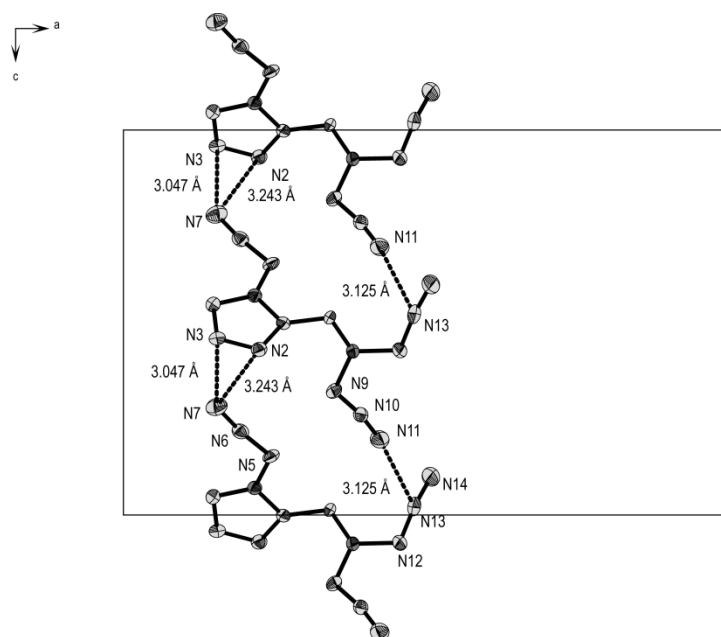


Figure 2: Scheme of short contacts representing electrostatic interactions. Thermal ellipsoids represent the 50 % probability level.

Therefore, short contacts are found between terminal nitrogen atoms N11 and N7 with N13 and N3 (N2), respectively, being much shorter than the sum of van der Waals radii for nitrogen atoms ($2 * r_w(\text{N}) = 3.2 \text{ \AA}$) at $3.125(6) \text{ \AA}$ and $3.047(5) \text{ \AA}$. The bonding situation is shown in Figure 2. It displays a very rare bonding situation where the structure is formed exclusively by interactions between partially charged nitrogen atoms.

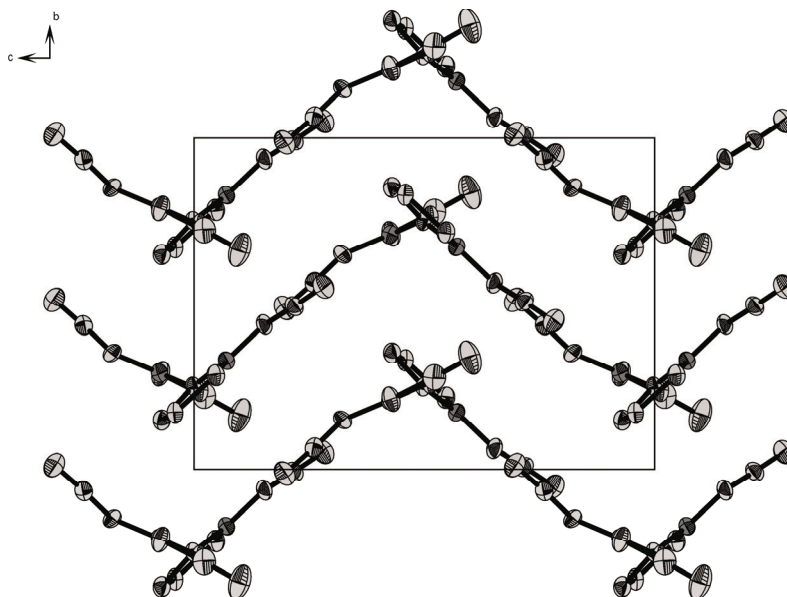


Figure 3: Stacking of the 2-D chains shown along the *a*-axis. Ortep representation shown along the *a*-axis with thermal ellipsoids representing the 50 % probability level.

The 2D chains are stacked along the *b*-axis with a distance of 5.993 Å between coplanar chains (every second chain, chains in between are turned by 180 °, Figure 3), exhibiting a very dense packing, represented by a high density of $\rho = 1.723 \text{ g cm}^{-3}$. The chains are connected through short N – N contacts, namely N9•••N3 at 3.051 Å and N9•••N2 at 3.001 Å, also showing very strong electrostatic interactions between negatively and positively charged nitrogen atoms.^[16]

IR and Raman spectra of **1** were recorded in the solid state. The IR frequencies have also been calculated using the B3LYP/cc-pVDZ level of theory and fitted according to Witek et al. with a scaling factor of 0.9704.^[17] They are in good agreement with the experimental data showing the stretching modes of the azide groups in the region between 2100 – 2200 cm^{-1} . In both, Raman and IR spectra, a splitting was observed. Stretching modes of the azide groups are observed at 2179 cm^{-1} , 2165 cm^{-1} and 2133 cm^{-1} (Raman) and 2175 cm^{-1} , 2155 cm^{-1} and 2133 cm^{-1} (IR) (Figure 4). Even though we performed computational calculations regarding the stretching modes, we cannot clearly distinguish between the stretching modes for each individual azide group because the difference in the wave numbers is too small. At the three above mentioned wave numbers in the IR spectra of **1**, stretching modes of all three azide groups are present, where the stretching mode for one individual azide group is clearly favored.

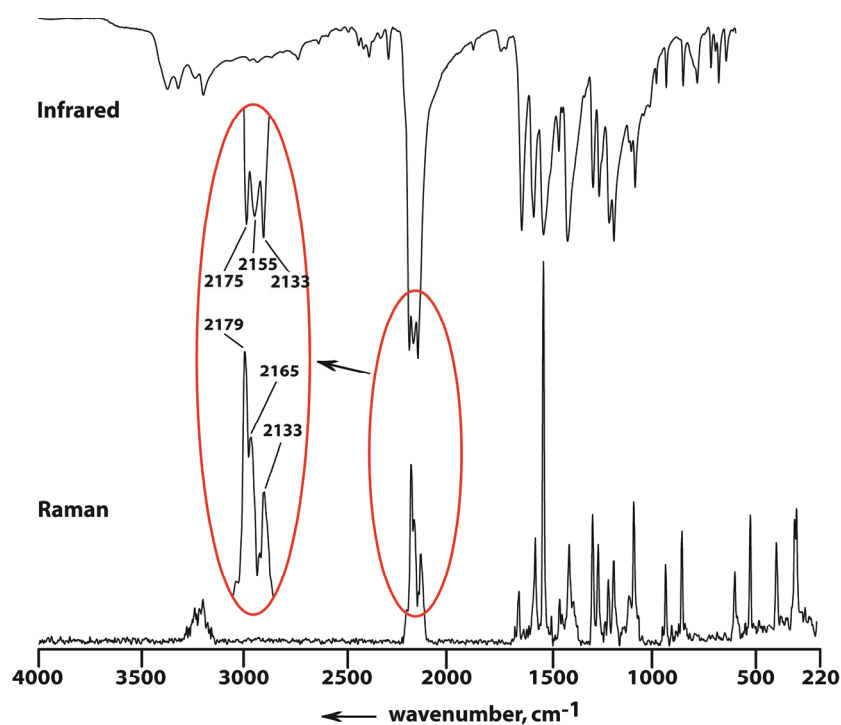


Figure 4: Comparison of IR (top) and Raman spectra (bottom) of **1**. The three individual stretching modes for each of the azide groups can be identified separately (ellipse).

NMR studies reveal clearly assignable peaks for the corresponding carbon or nitrogen atoms in ^{13}C as well as ^{14}N NMR spectra. Since the carbamoyl diazide group can rotate freely around the N1–N8 bond in solution, only two signals are observed in the ^{14}N spectra regarding the N_β nitrogen atoms of the three azide groups (N6, N10, N13). The N_α signals can be observed, but show a very broad signal. The N_γ signals were also observed as a very broad signal, but are overlapped by the two N_β peaks. If the solvent is changed from CDCl_3 to $[\text{d}_6]\text{-DMSO}$, only one broader peak can be observed for the three N_β atoms.

Concerning the sensitivities of C_2N_{14} it's beyond our capabilities of measuring. Therefore we have to state, that **1** is extremely sensitive towards shock and friction, exceeding 0.25 J in impact as well as 1 N in friction sensitivity (Table 1).

Table 1: Compiled sensitivities, calculated heat of formation and detonation parameters for **1**.

IS (J)	FS (N)	ρ (g cm^{-3})	ΔH_f^0 (s) (kJ mol^{-1})	Q_v (kJ kg^{-1})	P_{c-j} (kbar)	V_{det} (m s^{-1})
<0.25	<1	1.723	1495	-6855	339	8960

IS: Impact sensitivity; FS: Friction sensitivity; ΔH_f^0 : Heat of formation; Q_v : Heat of explosion; P_{c-j} : Detonation pressure at the Chapman-Jouguet point; V_{det} : Detonation velocity.

This is thought to be due to the enormous inequality in the charge distribution which is known to be responsible for an increase in sensitivity.^[18] Additionally, due to the extremely high heat of formation of 1495 kJ mol⁻¹, higher than most known heats of formation for CN systems,^[5c] and the very high nitrogen content of 89.08 %, it is a very powerful compound and has to be handled with extreme care!

4.3 References

- [1] W. Kesting, *Ber. Deut. Chem. Ges. B* **1924**, 57B, 1321–1324.
- [2] a) W. Schnick, *Angew. Chem.* **1993**, 105, 1649–1650; *Angew. Chem. Int. Ed.* **1993**, 32, 1580–1581; b) M. L. Cohen, *Phys. Rev. B* **1985**, 32, 7988; c) A. Y. Liu, M. L. Cohen, *Science* **1989**, 245, 841–842.
- [3] F. Goettmann, A. Fischer, M. Antonietti, A. Thomas, *Angew. Chem.* **2006**, 118, 4579–4583; *Angew. Chem. Int. Ed.* **2006**, 45, 4467–4471.
- [4] E. Ott, E. Ohse, *Berichte der Deutschen Chemischen Gesellschaft B: Abhandlungen* **1921**, 54B, 179–186.
- [5] a) M. H. V. Huynh, M. A. Hiskey, J. G. Archuleta, E. L. Roemer, R. Gilardi, *Angew. Chem.* **2004**, 116, 5776–5779; *Angew. Chem. Int. Ed.* **2004**, 43, 5658–5661; b) M. H. V. Huynh, M. A. Hiskey, D. E. Chavez, D. L. Naud, R. D. Gilardi, *J. Am. Chem. Soc.* **2005**, 127, 12537–12543; c) M. H. V. Huynh, M. A. Hiskey, E. L. Hartline, D. P. Montoya, R. Gilardi, *Angew. Chem.* **2004**, 116, 5032–5026; *Angew. Chem. Int. Ed.* **2004**, 43, 4924–4928; d) J. Stierstorfer, T. M. Klapötke, A. Hammerl, R. D. Chapman, *Z. Anorg. Allg. Chem.* **2008**, 634, 1051–1057. e) T. M. Klapötke, B. Krumm in *Organic Azides: Syntheses and Application* (Eds.: S. Bräse, K. Banert), John Wiley & Sons Ltd, **2010**, pp. 391–411.
- [6] J. Neutz, O. Grosshardt, S. Schäufele, H. Schuppler, W. Schweikert, *Propellants, Explos., Pyrotech.* **2003**, 28, 181–188.
- [7] C. Knapp, J. Passmore, *Angew. Chem.* **2004**, 116, 4938–4941; *Angew. Chem Int Ed.* **2004**, 43, 4834–4836.
- [8] K. Banert, Y. H. Joo, T. Rüffer, B. Walfort, H. Lang, *Angew. Chem.* **2007**, 119, 1187–1190; *Angew. Chem. Int. Ed.* **2007**, 46, 1168–1171.
- [9] C. J. Grundmann, W. J. Schnabel, *Vol. US 2290412* (Ed.: O. M. C. Corp.), United States of America, **1961**.
- [10] J. B. Ledgard, *The preparatory manual of explosives - a laboratory manual*, Paranoid Publications Group, **2003**, p 81-82.
- [11] J. C. Galvez-Ruiz, G. Holl, K. Karaghiosoff, T. M. Klapötke, K. Löhnwitz, P. Mayer, H. Nöth, K. Polborn, C. J. Rohbogner, M. Suter, J. J. Weigand, *Inorg. Chem.* **2005**, 44, 4237–4253.
- [12] Synthesis and experimental part as well as the complete compilation of all analytical data are included in Appendix 12.3.
- [13] Compilation of the crystallographic data can be found in Appendix 12.3.

- [14] Crystallographic data for the structure have been deposited with the Cambridge Crystallographic Data Centre filed under CCDC No. 693485. Copies of the data can be obtained free of charge on application to The Director, CCDC, 12 Union Road, Cambridge CB2 1EZ, UK (Fax: int. code (1223)336-033; e-mail for inquiry: fileserv@ccdc.cam.ac.uk; e-mail for deposition: deposit@ccdc.cam.ac.uk).
- [15] Gaussian 09 (Revision **A.1**): M. J. Frisch et al., see Supporting Information.
- [16] Additional illustrations of the packing scheme of the crystal structure along the *a*- and *b*-axis are supplied in Appendix 12.3.
- [17] H. A. Witek, M. Keiji, *J. Comp. Chem. THEOCHEM* **2004**, 25, 1858–1864.
- [18] a) B. M. Rice, J. J. Hare, *J. Phys. Chem.* **2002**, 106A, 1770; b) P. Politzer, J. S. Murray in *Theoretical and computational chemistry, Vol. 6*, (Eds.: Z. B. Maksic, W. J. Orville-Thomas), Elsevier, **1999**, pp. 347–363; c) P. Politzer, J. S. Murray, J. M. Seminario, P. Lane, M. E. Grice, M. C. Concha, *J. Mol. Struct.* **2001**, 573, 1; d) J. S. Murray, P. Lane, P. Politzer, *Mol. Phys.* **1998**, 93, 187.

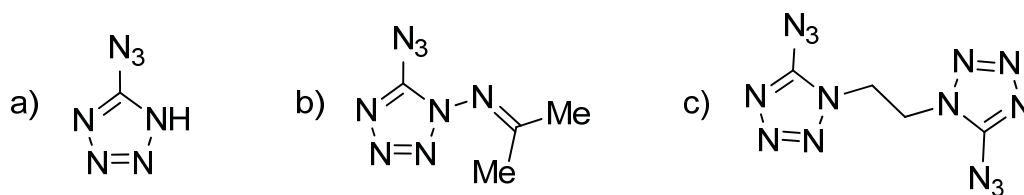
5. Novel azidotetrazoles – Structurally interesting and extremely sensitive

Thomas M. Klapötke, Franz A. Martin and Jörg Stierstorfer

As submitted to Chemistry – An Asian Journal 2011

5.1 Introduction

Tetrazoles possess, among the group of nitrogen containing heterocycles, the second highest amount of nitrogen at 80 % if pentazoles are also taken into consideration. Since pentazoles are only stable with large electron donating groups attached,^[1] tetrazoles are more often the compounds of choice for the synthesis of energetic nitrogen rich compounds.^[2] Together with their high thermal stability and the high heat of formation of + 237.2 kJ mol⁻¹ (without substituents),^[3] they offer a good backbone for the development of energetic compounds. In recent time, many examples of energetic compounds, containing the tetrazole moiety have been investigated and synthesized.^[4] An increase in nitrogen content is relevant for the formation of new HNC-HEMs with the goal to reduce CO in the decomposition products and to replace it with dinitrogen, N₂.^[5] The azido group as a highly energetic ligand, donating + 364 kJ mol⁻¹ to the enthalpy of formation,^[6] together with an increase in the nitrogen content is very well suited for these kind of compounds. Whereas tetrazole itself offers a nitrogen content of 80 %, azide substituents increase this ratio even more with 5-azidotetrazole showing a nitrogen content of 88.28 %, while the anion of the compound shows a content of 89.09 %. Both compounds have been synthesized more than 70 years ago^[7] and many publications have dealt with the synthesis and characterization of these compounds since then.^[8] Since azidotetrazoles are very sensitive towards shock and friction, attempts have been made to desensitize these materials through the introduction of aryl^[9] and alkyl groups^[4a, 10] or even the coupling of two azidotetrazole moieties with alkyl chains like ethyl or butyl groups.^[11]



Scheme 1: Known 5-azidotetrazole derivatives. a) 5-azidotetrazole, b) 1-(amino-propan-2-ylidene)-5-azidotetrazole c) 1,2-bis(5-azidotetrazol-1-yl)ethane.

The introduction of alkyl and aryl substituents is accompanied by a decrease in nitrogen content but also with slightly lower sensitivities against friction and impact. The approach to introduce electron donating substituents in either one or two position on the tetrazole ring to increase the overall electron density within the aromatic ring system led us to the conclusion that an amine substituent on either one or two position should also be capable of donating more electron density towards the ring system and at the same time will not decrease but increase the nitrogen content of the resulting compound. To the best of our knowledge only theoretical calculations on amino-azido-tetrazoles have been performed in the past,^[12] either with the azide group located on the C5, N1 or N2 position. Here we will present 1-amino-5-azidotetrazole (**1**) as the first tetrazole to carry only amino and azido functions as substituents, together with two very interesting 1-substituted 5-azidotetrazoles, namely 5-azido-1-(amino-azidocarbamoyl)-tetrazole (**3**) and 5-azido-1-diazidocarbamoyltetrazole (**2**), presented as a short communication earlier this year.^[13]

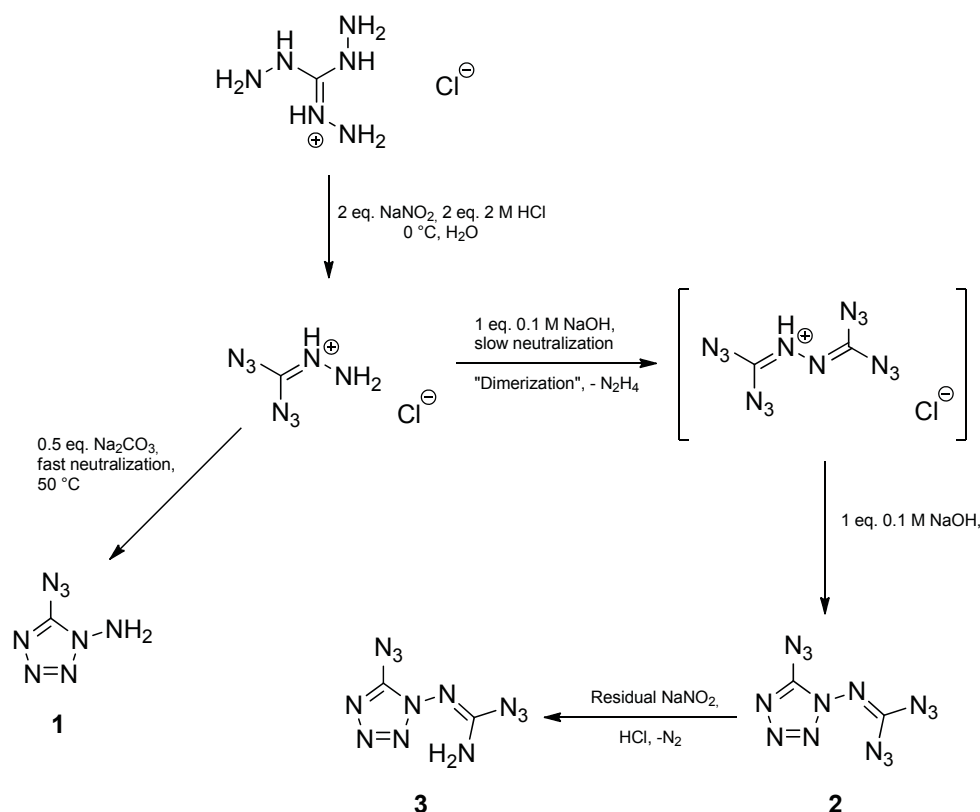
5.2 Results and Discussion

5.2.1 Synthesis

Initially, the direct formation of 1-amino-5-azido-tetrazole (**1**) from 1,5-diaminotetrazole (DAT), first synthesized by Gaponik *et al.*,^[14] was favored. A direct diazotation of the amino group in 5 position with sodium nitrite and hydrochloric acid was not possible since the attack took place at the amino group in one position, resulting in a ring opening and destruction of the heterocyclic ring system. Selective protection of the 1-substituted amino group followed by diazotation of the amino group in 5-position and displacement with an azide was omitted due to the harsh reaction conditions generally needed for deprotection of amine groups, which would have resulted in the destruction of the fragile azidotetrazole system. Therefore a different route was chosen. It is well known in the

recent literature, that tetrazole systems and especially DAT can be synthesized from diaminoguanidinium salts by diazotation of one hydrazine group and subsequent ring closure under basic conditions.^[15]

The reaction of triaminoguanidinium chloride with two equivalents of sodium nitrite instead of one, as used in the formation of DAT,^[15] and subsequent ring closure should therefore result in the formation of the desired product **1**. The diazotation of triaminoguanidinium chloride was performed with two equivalents of sodium nitrite and the subsequent ring closure reaction was initiated in two different ways afterwards. In one experiment the ring closure was performed slowly with two equivalents of 0.1 M sodium hydroxide solution while it was initiated quickly with one equivalent of solid sodium carbonate, added in one portion at elevated temperatures (50 °C), in a second experiment. The solutions were extracted with diethyl ether, dried with magnesium sulfate and left standing for evaporation. The raw products were examined by TLC and three different compounds were identified. While the reaction with 0.1 M sodium hydroxide solution yielded only two separable compounds, the neutralization with sodium carbonate showed three different reaction products, two of them having the same R_f values as the products from the neutralization reaction with 0.1 M sodium hydroxide solution. The compounds were found to be two dimerization products of the twice diazotized triaminoguanidinium species, namely 5-azido-1-diazidocarbamoyltetrazole (**2**) and 1-(amino-azidocarbamoyl)-5-azidotetrazole (**3**), extracted from both reaction mixtures, while the third product, the desired 1-amino-5-azido-tetrazole (**1**), was only isolated from the reaction neutralized with sodium carbonate. The reaction pathways and mechanisms are shown in Scheme 2.



Scheme 2: Reaction pathways and mechanism towards the formation of azidotetrazoles **1** – **3**.

Since **1** was only observed when the reaction was neutralized very fast at elevated temperature, it is obvious, that the “dimerization” products are favored over the single ring closure. Compound **1** could never be identified from reactions which have been slowly neutralized. Therefore it’s rather a kinetically and not a thermodynamically controlled reaction pathway for the formation of **1**. Compound **2** was found to be the direct dimerization product of two intermediate diazotation products under the cleavage of hydrazine, forming a binary carbon nitrogen compound with the sum formula C₂N₁₄, holding three azide groups as substituents.^[13] One azide group of the carbamoyldiazide group of **2** is then directly degraded with residual sodium nitrite under acidic conditions resulting in the formation of **3**. The formation of **3** can be forced to higher yields, if the reaction mixture is stirred at a pH value of 5-6 for a longer period of time during neutralization. Nevertheless, a complete degradation of **2** could not be observed. All three compounds are stable against hydrolysis in acidic media and can be easily isolated using short column flash chromatography with CHCl₃. Compounds **2** and **3** are recrystallized from diethyl ether in their anhydrous forms as colorless crystals with decomposition temperatures of 124 °C and 136 °C, respectively, while **1** can only be crystallized as the monohydrate as light yellow crystals, showing the highest decomposition temperature of

the three azidotetrazoles at 142 °C. **Caution:** All three azidotetrazoles tend to explode under nearly every kind of physical stress and therefore safety precautions have to be taken when handling or manipulating these materials, even if they are in solution.

5.2.2 Spectroscopic Data

Vibrational Spectroscopy

IR and Raman spectra of all three azidotetrazoles have been recorded with only very small amounts of material and the frequencies have been assigned based on literature^[16] and also based on quantum mechanical calculations at the B3LYP/cc-pVDZ^[17] level of theory as implemented in the Gaussian 09W program package.^[18] The calculated frequencies have been fitted according to Witek et al.^[19] with a scaling factor of 0.9704. The frequencies derived from Raman and IR measurements are compiled in the supplementary information Tables S1-S3 (Appendix 12.4) together with the calculated values and their possible assignment. Since all compounds could only be measured with traces of solvent (CHCl₃) left, bands in the C–H region are observed between 2800 cm⁻¹ and 3000 cm⁻¹ in the IR spectra of **2** and **3** and in the Raman spectra of **1** and **2**. **Caution:** Compound **2** detonated several times while Raman measurements were undertaken, laser energies not exceeding 150 mW! Measurements were therefore performed at 50 mW using a higher number of scans with a single crystal.

The ν_s stretching modes of the amine group of **1** are observed at 3332 cm⁻¹ and 3228 cm⁻¹ in the IR spectra and at 3205 cm⁻¹ in the Raman spectra, while the ν_{as} stretching mode is observed at 3152 cm⁻¹ for IR and at 3154 cm⁻¹ for the Raman spectra, respectively. While no stretching mode is observed for **2**, only the ν_s stretching mode of the amine group is observed for **3** in the IR spectra at 3278 cm⁻¹ as a very weak band. The stretching modes of interest for the characterization of the three compounds are the asymmetric stretching modes of the azide substituents, all of which lie in the region of 2200 – 2130 cm⁻¹ in both, IR and Raman spectra. Each single azide substituent can be assigned to one unique frequency. Hence **1** shows only one frequency ν_{as} at 2150 cm⁻¹ (IR) and 2156 cm⁻¹ (Raman) while **2** shows three frequency for its three chemically non equivalent azide substituents at 2175 cm⁻¹, 2155 cm⁻¹, and 2133 cm⁻¹ (IR) and at 2179 cm⁻¹, 2165 cm⁻¹, and 2133 cm⁻¹ (Raman). As expected from these findings two unique frequencies characterize

the two ν_{as} stretching modes at 2164 cm^{-1} and 2152 cm^{-1} in the IR spectra and at 2170 cm^{-1} and 2157 cm^{-1} in the Raman spectra of **3**, respectively. From the comparison of the IR and Raman spectra of the three compounds, the tetrazole bound azide substituents were identified at 2150 cm^{-1} (**1**), 2155 cm^{-1} (**2**) and 2152 cm^{-1} (**3**) (IR). The remaining stretching modes in the case of **2** and **3** are hence assigned to the remaining one (**3**) or two (**2**) azide substituents bound to the carbamoyl group. Although calculations of the Raman and IR spectra of these compounds were performed in order to assign the stretching modes correctly, they cannot be clearly distinguish from the results, because the difference in the wavenumber is too small and for all frequencies combined stretching modes of the azide substituents are observed. The comparison of the Raman as well as the IR spectra is presented in Figure 1 and Figure 2.

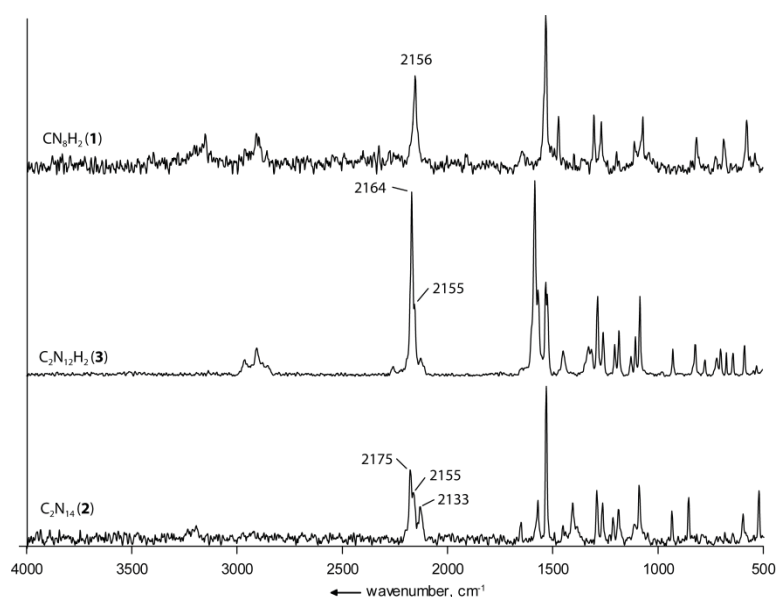


Figure 1: Direct comparison of the Raman spectra of CN_8H_2 (**1**), $\text{C}_2\text{N}_{12}\text{H}_2$ (**3**) and C_2N_{14} (**2**) presenting the unique frequencies of the azide substituents.

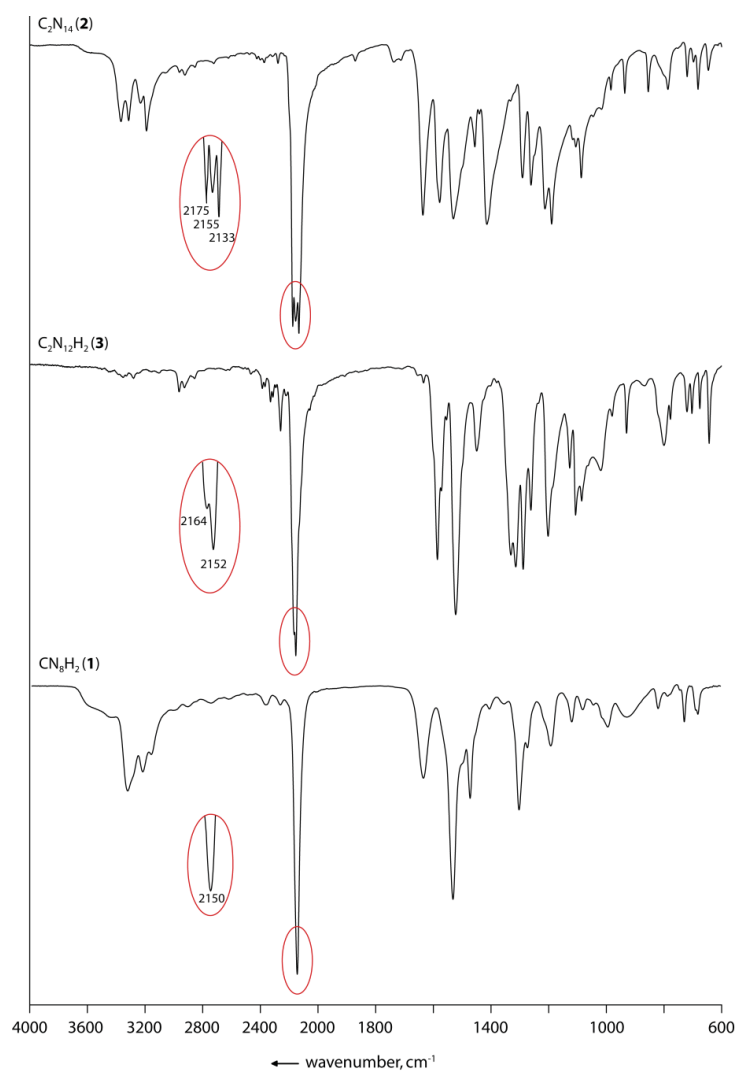


Figure 2: Direct comparison of the IR spectra of CN_8H_2 (**1**), $\text{C}_2\text{N}_{12}\text{H}_2$ (**3**) and C_2N_{14} (**2**) presenting the unique frequencies of the azide substituents.

Deformation stretching modes of the amine group are observed at 1639 cm^{-1} (IR) and 1648 cm^{-1} (Raman) for **1**, and at lower frequencies at 1526 cm^{-1} (Raman) for compound **3**. The difference in the wavenumber can be explained by the different chemical surrounding, the nitrogen atom in the amine group of **1** being rather sp^3 hybridized while the configuration of the amine group in **3** is planar and therefore the nitrogen atom is sp^2 hybridized. The “dimers” **2** and **3** both revealed stretching modes of the $\text{C}_2\text{-N}_8$ double bond at 1578 cm^{-1} (**2**) and 1584 cm^{-1} (**3**) in the IR spectra and at 1573 cm^{-1} (**2**) and 1586 cm^{-1} (**3**) in the Raman spectra. The stretching mode of $\text{C}_1\text{-N}_5$ bond is visible for all three compounds at 1532 cm^{-1} (**1**), 1530 cm^{-1} (**2**) and 1522 cm^{-1} (**3**) in the IR spectra and at 1536 cm^{-1} (**1**), 1534 cm^{-1} (**2**) and 1534 cm^{-1} (**3**) in the corresponding Raman spectra. The ν_{as} stretching mode $\text{N}_1\text{-C}_1\text{-N}_4$ of the tetrazole ring is observed for all three compounds in both, Raman and IR spectra. In the IR spectra the bands are observed at 1472 cm^{-1} (**1**),

1456 cm^{-1} (**2**) and 1448 cm^{-1} (**3**) while peaks are observed in the Raman spectra at 1476 cm^{-1} (**1**), 1454 cm^{-1} (**2**) and 1451 cm^{-1} (**3**). The stretching mode of the strongest double bond in the tetrazole rings $\text{N}_2=\text{N}_3$ is observed at 1302 cm^{-1} (**1**), 1291 cm^{-1} (**2**) and 1329 cm^{-1} (**3**) in the IR spectra and at 1308 cm^{-1} (**1**), 1293 cm^{-1} (**2**) and 1331 cm^{-1} (**3**) in the corresponding Raman spectra. Stretching modes of the $\text{N}_\alpha=\text{N}_\beta$ are observed for all three compounds, for **1** being a combination of $\nu_{\text{as}} \text{N}_8-\text{N}_1-\text{N}_2$ and $\nu \text{N}_5=\text{N}_6$ at 1191 cm^{-1} (IR) and 1200 cm^{-1} (Raman) while for **2** and **3** combinations of the stretching modes of the double bonds within the tetrazole ring ($\text{C}_1=\text{N}_4$ and $\text{N}_2=\text{N}_3$) and the corresponding $\text{N}_\alpha=\text{N}_\beta$ stretching modes are observed ($\text{N}_5=\text{N}_6$, $\text{N}_9=\text{N}_{10}$ and $\text{N}_{12}=\text{N}_{13}$ (**2**) and $\text{N}_5=\text{N}_6$ and $\text{N}_9=\text{N}_{10}$ (**3**)). The frequencies are observed at 1261 cm^{-1} (**2**) and 1287 cm^{-1} (**3**) in the IR spectra, while peaks are observed in the Raman spectra at 1266 cm^{-1} (**2**) and 1288 cm^{-1} (**3**). Asymmetric and symmetric stretching modes of the N_1-N_2 and N_3-N_4 bonds are observed for all compounds in the region of 1120 – 1080 cm^{-1} and are assigned in detail in the Tables S1, S2 and S3. Between 1000 cm^{-1} an 500 cm^{-1} , many combined stretch and deformations modes of the whole molecule and especially deformation (in plane and out of plane) and torsion stretching modes of the tetrazole ring are observed.

Multinuclear NMR spectroscopy

The ^1H NMR spectra of **1** showed, as expected, only one singlet at a chemical of 5.45 ppm representing the NH_2 group in 1 position. One resonance is also observed for compound **3** at a chemical shift of 5.35 ppm, assignable to the NH_2 group of the amino-azidocarbamoyl substituent.

^{13}C NMR studies revealed also clearly assignable peaks for each carbon atom. While only one signal for the tetrazole carbon is observed at a chemical shift of 151.4 ppm for **1**, both, **2** and **3**, showed, as expected, two signals. The peaks for **2** are observed at chemical shifts of 160.4 ppm representing the carbon atom of the diazidocarbamoyl moiety and at 148.4 ppm for the tetrazole carbon atom. The same order is observed for **3** at chemical shifts of 157.9 ppm and 148.2 ppm.

Although ^{15}N NMR studies could not be performed due to the amount of material needed of these highly energetic compounds, ^{14}N NMR studies in $\text{DMSO}-d_6$ and CDCl_3 revealed clearly assignable peaks for the nitrogen atoms of the azide groups. Compound **1** revealed only two signals in the NMR spectra. The signal of the N_β atom of the azide group is

observed at a chemical shift of -147 ppm as a very intense peak, while the N_γ atom showed a very broad singlet of low intensity, partially overlapped by the N_β peak at a chemical shift of -140 ppm. Two signals are observed for the N_β nitrogen atoms of the three azide groups in **2** at chemical shifts of -147 ppm and -149 ppm, representing the tetrazole bound azide group and the two azide groups of the diazidocarbamoyl moiety (N_6 , N_{10} , N_{13}). Since the diazidocarbamoyl moiety can rotate freely around the N_1 – N_8 bond, only one signal is observed for these two azide groups. As observed in **1**, the three N_γ atoms are observed as a very broad singlet at a chemical shift of -145, again partially overlapped by the very intense signals for the N_β atoms. The three N_α atoms are also observed as a very broad singlet at a chemical shift of -305 ppm. If the solvent is changed to DMSO- d_6 , only the N_β atoms are observed as one slightly broader singlet at -147 ppm, while N_α and N_γ atoms could not be observed at all. As observed for **2**, **3** exhibits two peaks for the chemically nonequivalent N_β nitrogen atoms (N_6 , N_{10}) of the azide substituents at chemical shifts of -148 ppm and -152 ppm. The N_γ nitrogen atoms are again observed as a very broad singlet at a chemical shift of -138 ppm, while the N_α nitrogen atoms are not observed.

5.2.3 Molecular Structures

Single crystals of 1-amino-5-azidotetrazole (**1**) have been prepared from chloroform at -18 °C as light yellow blocks, containing one molecule of crystal water. Single crystals of 5-azido-1-diazidocarbamoyltetrazole (**2**) and 1-(amino-azidocarbamoyl)-5-azidotetrazole (**3**) suitable for X-ray diffraction measurements have been obtained from diethyl ether and chloroform, respectively, as colorless blocks. Crystallographic data of compounds **1** – **3** are compiled in Table S4 (Appendix 12.4).

Compound **1** crystallizes in the monoclinic space group $P2_1$ with a cell volume of 293.72(3) Å³ and only two molecular moieties in the unit cell. The density calculated from the measurement at 173 K is 1.629 g cm⁻³, slightly lower as the densities calculated for **2** and **3** at 1.723 g cm⁻³ and 1.675 g cm⁻³. The asymmetric unit of **1** is displayed in Figure 3.

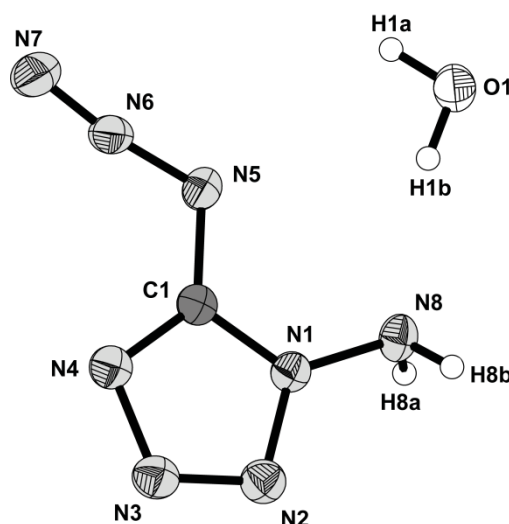


Figure 3: Asymmetric unit of **1**, thermal ellipsoids are set to 50 % probability. Selected bond lengths (Å): N1–C1 1.337(2), N1–N2 1.358(2), N1–N8 1.397(2), N2–N3 1.296(2), N3–N4 1.374(2), N4–C1 1.319(3), N8–H8A 0.91(2), N8–H8B 0.87(3), N5–N6 1.249(2), N5–C1 1.378(3), N6–N7 1.123(2), O1–H1A 0.86(3), O1–H1B 0.89(3); Selected bond angles (°): C1–N1–N2 108.30(2), C1–N1–N8 126.7(2), N2–N1–N8 125.0(2), N3–N2–N1 106.0(2), N2–N3–N4 111.3(2), C1–N4–N3 104.9(2), N6–N5–C1 113.4(2), N7–N6–N5 171.7(2), N4–C1–N1 109.6(2), N4–C1–N5 130.5(2), N1–C1–N5 120.0(2), H1a–O1–H1b 101(2); Selected torsion angles (°): C1–N1–N2–N3 -0.9(2), N8–N1–N2–N3 -178.77(18), N1–N2–N3–N4 0.8(2), N2–N3–N4–C1 -0.5(2), C1–N5–N6–N7 179.3(15), N3–N4–C1–N1 -0.1(2), N3–N4–C1–N5 -179.5(2), N2–N1–C1–N5 -179.89(17), N6–N5–C1–N4 3.6(3).

The bonds within the tetrazole ring are all, as expected for a heterocyclic ring system, between the bond length of single and double bonds, with the N₂–N₃ bond being the shortest with 1.296(2) Å and the N₃–N₄ bond being the longest of them at 1.374(2) Å. The bond length of the N₁–N₈ bond is slightly longer at 1.397(2) Å and more in the range of a formal N–N single bond (1.48 Å).^[20] Hence when we look at the structure of the amine group, we see a rather angled than a planar structure, indicating a sp³ hybridized nitrogen atom. The azide group lies nearly perfectly in the plane of the tetrazole ring, as expected for an azidotetrazole,^[8c] displaying a torsion angle of only 3.6(3)° (N₆–N₅–C1–N₄) and shows an angle N₅–N₆–N₇ of 171.7(2)°. The C₁–N₅ bond is shorter than the N₁–N₈ bond displaying a bond length of 1.378(3) Å but also closer to a formal C–N single than double bond (1.47 Å, 1.22 Å).^[20]

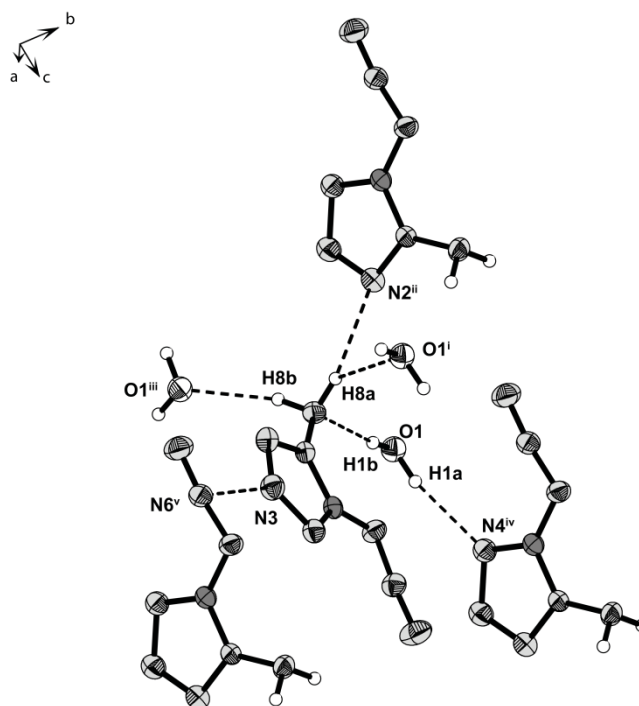


Figure 4: Hydrogen bonding scheme present in **1**, displayed for the asymmetric unit only, due to better clarity.

Table 1: Hydrogen bonds and short contacts present in **1**.

D–H···A	d (D–H) [Å]	d (H···A) [Å]	d (D–H···A) [Å]	< (D–H···A) [°]
N8–H8a···O1 ⁱ	0.91(2)	2.23(2)	2.981(2)	139(2)
N8–H8a···N2 ⁱⁱ	0.91(2)	2.57(2)	3.217(2)	128(2)
N8–H8b···O1 ⁱⁱⁱ	0.87(3)	2.10(3)	2.940(2)	161(2)
O1–H1a···N4 ^{iv}	0.86(3)	2.13(3)	2.979(2)	169(3)
O1–H1b···N8	0.89(3)	2.15(3)	3.025(2)	169(2)
N3···N6 ^v			2.998(3)	

Symmetry Operators: (i) $x-1, y, z$; (ii) $-x, y+1/2, -z$; (iii) $-x+1, y-1/2, -z$; (iv) $-x+1, y+1/2, -z+1$; (v) $-x, y-1/2, -z+1$.

Five hydrogen bonds are observed in the structure of **1**, one of them being bifurcated. Rows are formed with molecules of **1** being exactly opposite to one another. The rows are connected by the two hydrogen bonds N₈–H_{8a}···O₁ (D–H···A angle 139°) and O₁(i)–H_{1a}(i)···N₄(iv) (D–H···A angle 169°). Both bonds show D···A distances well below the sum of van der Waals radii ($r_w(\text{N}) + r_w(\text{O}) = 3.07 \text{ \AA}$)^[21] at 2.981(2) Å and 2.940(2) Å, respectively, representing moderately strong hydrogen bonds. A short contact between the N₃ nitrogen atom of the tetrazole ring and the partially positive charged N_β atom (N₆) of the azide group (2.998(3) Å) completes the connectivity pattern of the rows (symmetry operator: $-x, y-1/2, -z+1$). The remaining three hydrogen bonds connect the rows between

one another, building up a dense three dimensional network. $N_8-H_{8b}\cdots O_1(\text{iii})$ connects to one row below, while the $O_1-H_{1b}\cdots N_8$ and $N_8-H_{8a}\cdots N_2(\text{ii})$ connect to two independent rows above. The two hydrogen bonds involving an oxygen atom are very directed at an angle of 169° (both), while the $N_8-H_{8a}\cdots N_2(\text{ii})$ hydrogen bond exhibits a very small D–H \cdots A angle of 129° and also shows a longer D \cdots A distance than the sum of van der Waals radii ($r_w(\text{N}) + r_w(\text{N}) = 3.10 \text{ \AA}$)^[21] at $3.217(2) \text{ \AA}$. Hence this hydrogen bond is more of electrostatic nature and not as strong as the other four bonds observed. The bonding pattern within **1** is displayed in Figure 4 for the asymmetric unit while all hydrogen bonds are compiled in Table 1.

The rows show a zigzag motive, presenting an angle of 81.97° within the rows. The rows are stacked, as shown in Figure 5, displaying a distance of 3.118 \AA between the rows on top of each other.

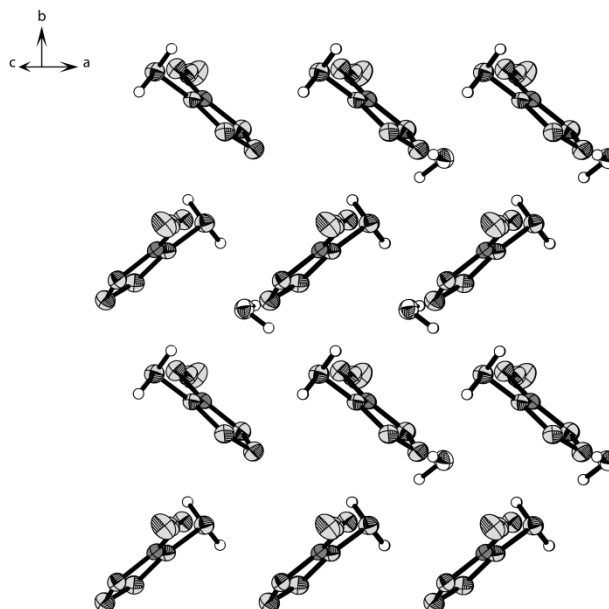


Figure 5: Presentation of the zigzag rows in **1**, including an angle of 81.97° , together with their stacked packing.

Compound **2** crystallizes in the orthorhombic space group *Pbcn* with a cell volume of $1697.6(2) \text{ \AA}^3$ and eight molecules in the unit cell. The asymmetric unit together with selected bond lengths and angles is presented in Figure 6. The structure will not be discussed in any detail, since a detailed description has been published earlier.^[13]

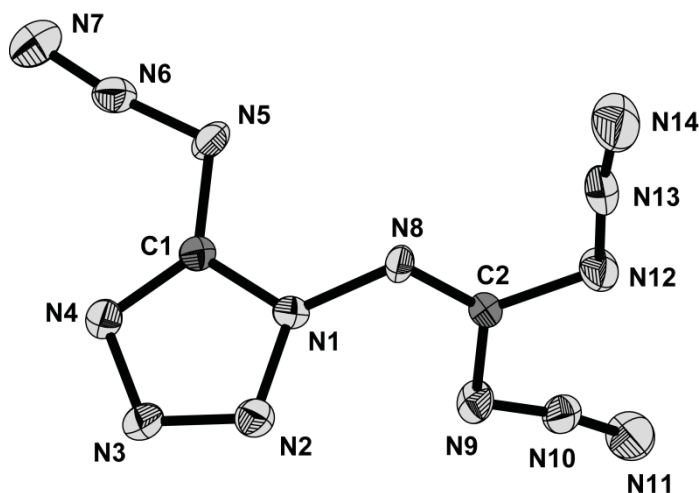


Figure 6: Asymmetric unit of **2**, thermal ellipsoids are set at 50 % probability. Selected bond lengths (Å): N1–C1 1.344(5), N1–N2 1.351(4), N1–N8 1.403(4), N4–C1 1.313(5), N4–N3 1.377(4), N10–N11 1.119(5), N10–N9 1.265(5), N8–C2 1.288(5), N9–C2 1.388(5), N2–N3 1.298(4), N6–N7 1.121(5), N6–N5 1.263(5), N12–N13 1.279(5), N12–C2 1.395(5), N5–C1 1.384(5), N14–N13 1.121(5); Selected bond angles (°): C1–N1–N2 108.0(3), C1–N1–N8 126.2(3), N2–N1–N8 123.3(3), C1–N4–N3 104.5(3), N11–N10–N9 171.0(4), C2–N8–N1 113.8(3), N10–N9–C2 114.5(3), N3–N2–N1 106.1(3), N7–N6–N5 172.4(5), N13–N12–C2 111.1(4), N6–N5–C1 112.0(4), N2–N3–N4 111.4(3), N14–N13–N12 173.2(4), N8–C2–N9 124.6(4), N8–C2–N12 120.4(4), N9–C2–N12 115.0(4), N4–C1–N1 109.9(4), N4–C1–N5 130.4(4), N1–C1–N5 119.7(4); Selected torsion angles (°): C1–N1–N8–C2 -123.8(5), C1–N1–N2–N3 2.1(5), N8–N1–N2–N3 165.1(3), N1–N8–C2–N9 -2.2(6), N1–N8–C2–N12 179.1(4), N13–N12–C2–N8 2.9(6), N3–N4–C1–N1 1.5(5), N8–N1–C1–N5 15.9(7), N6–N5–C1–N4 4.2(7).

Even though the compound has no ability to form hydrogen bonds, and is hence built up exclusively from nitrogen–nitrogen interactions, it displays a very high density of 1.732 g cm⁻³. That requires a very unequal charge distribution within the molecule, as it is observed from calculations of the electrostatic potential of **2** at the B3LYP/cc-pVDZ level of theory.^[17] (Figure 5S, Appendix 12.3) Short contacts are observed between the nearly uncharged N_γ atom (N₇) of the tetrazole bound azide group with the N₂ and N₃ atoms of the tetrazole ring, representing the region of the highest negative charge (N₇⋯N₃ = 3.047 Å, N₇⋯N₂ = 3.243 Å). A third contact is observed between N_γ (N₁₁, slightly negative charge) and N_β (N₁₃, most positive charge) at a distance of 3.125 Å.

The bond lengths and angles are in the normal range, expected for an azidotetrazole and close to the ones presented for **1**. The N₁–N₈ bond (1.403(4) Å) is close to a formal single bond (1.48 Å), as already seen in **1**, while the N₈–C₂ bond towards the diazidocarbamoyl moiety is much shorter at 1.288(5) Å and hence in the range of a formal C–N double bond (1.22 Å). As observed for **1**, the tetrazole bound azide moiety is nearly in the plane of the tetrazole, showing only slight deviations (N₄–C₁–N₅–N₆ 4.2(7)°). The diazido moiety is not in the plane of the tetrazole ring, but twisted out of the plane by 66.12°

regarding the plane formed by N₁₂, C₂, N₉ and N₈. The twist results in the formation of two dimensional chains along the *c*-axis, showing a zigzag conformation (113.22°). The rows are arranged next to one another, forming layer like structures, but every second row is oriented the opposite way (turned by 180°). The rows are stacked on top of each other along the *b*-axis. (Figure 7, only one set of rows is shown, the opposite rows are omitted for clarity)

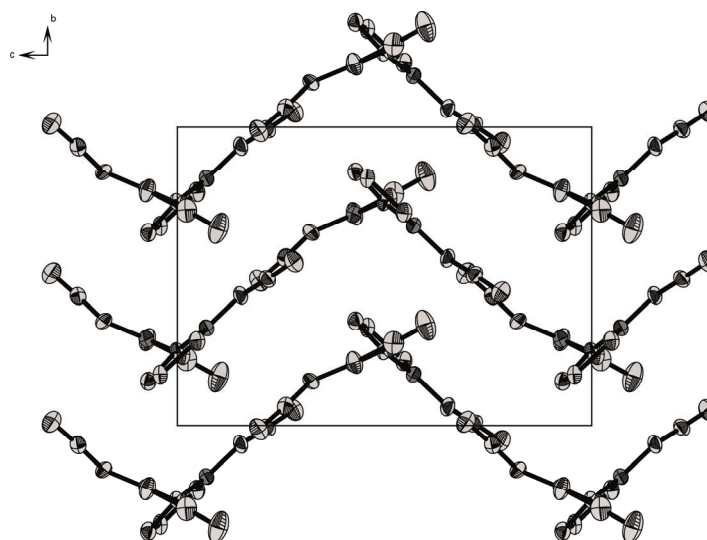


Figure 7: Stacking of the 2D chains along the *b*-axis in **2**. Thermal ellipsoids are set at 50 % probability.

Compound **3** crystallizes in the triclinic space group *P*-1 with a cell volume of 384.86(4) Å³ and two molecular moieties in the unit cell. The density is in between compounds **1** and **2** at 1.675 g cm⁻³. The asymmetric unit of **3** is displayed in Figure 8 together with selected bond lengths and angles.

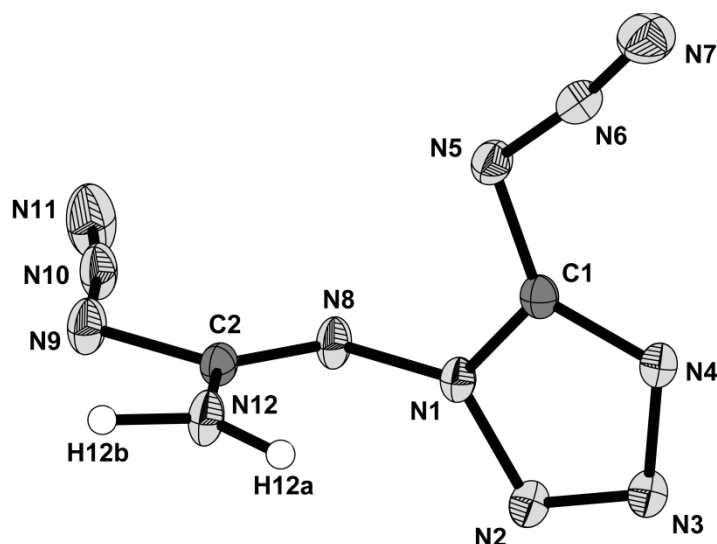


Figure 8: Asymmetric unit of **3**, thermal ellipsoids are set to 50 % probability. Selected bond lengths (Å): N1–C1 1.3390(1), N1–N2 1.356(1), N1–N8 1.397(1), N2–N3 1.296(1), N3–N4 1.367(1), N4–C1 1.322(1), N5–N6 1.265(1), N5–C1 1.383(1), N6–N7 1.116(1), N8–C2 1.312(1), N12–C2 1.324(1), N12–H12a 0.87(1), N12–H12b 0.88(1), N9–N10 1.259(1), N9–C2 1.403(1), N10–N11 1.117(1); Selected bond angles (°): C1–N1–N2 108.31(7), C1–N1–N8 128.27(8), N2–N1–N8 122.50(8), N3–N2–N1 105.75(8), N2–N3–N4 111.78(8), C1–N4–N3 104.72(7), N6–N5–C1 111.54(8), N7–N6–N5 172.8(1), C2–N8–N1 111.86(7), C2–N12–H12a 120.8(8), C2–N12–H12b 118.1(8), N10–N9–C2 113.09(8), N11–N10–N9 171.4(1), N4–C1–N1 109.41(8), N4–C1–N5 130.26(9), N1–C1–N5 120.31(8), N8–C2–N12 129.71(9), N8–C2–N9 117.49(8), N12–C2–N9 112.80(8); Selected torsion angles (°): C1–N1–N2–N3 1.5(1), N8–N1–N2–N3 171.36(7), C1–N5–N6–N7 -175.2(8), C1–N1–N8–C2 -90.3(1), N3–N4–C1–N5 179.37(9), N2–N1–C1–N4 -1.5(1), N8–N1–C1–N4 -170.66(8), N2–N1–C1–N5 179.85(8), N6–N5–C1–N1 176.86(8), N10–N9–C2–N8 -1.9(1), N10–N9–C2–N12 177.79(9).

As observed for **1** and **2**, the bond lengths of both, the C–N and N–N bonds in the tetrazole ring are right in between the formal bond lengths of single and double bonds, ranging between 1.296(1) Å (N₂–N₃) and 1.267(1) Å (N₃–N₄). The bond angles in the tetrazole ring range between 104.72(7)° (C₁–N₄–N₃) and 111.78(8)° (N₂–N₃–N₄). The N₁–N₈ bond, connecting the aminoazidocarbamoyl moiety to the tetrazole ring, again displays a bond length of 1.397(1) Å as observed for **1** and is hence close to a formal N–N single bond (1.48 Å),^[20] while the N₈–C₂ bond is again closer to a formal C–N double bond (1.22 Å)^[20] at 1.312(1) Å. The N₈ atom shows sp² hybridization as shows the C₂ atom with a close to planar surrounding. The C₂–N₈ bond is 0.3 Å longer than the corresponding bond in **2**, since the C₂–N₁₂ bond is also shortened to 1.324(1) Å in **3**. The double bonding character of the C₂–N₁₂ bond is also indicated by the planar amine group (H_{12a}–N₁₂–H_{12b}), showing sp² hybridization for N₁₂. The tetrazole bound azide lies nearly perfectly in the plane of the tetrazole ring, showing a torsion angle N₆–N₅–C₁–N₁ of 176.86(9)°. The aminoazidocarbamoyl moiety is twisted out of the plane of the tetrazole ring by 85.0°, regarding the plane formed by N₈, C₂, N₉ and N₁₂. The azide substituents

show bond lengths as expected and bond angles of $172.8(1)^\circ$ ($N_5-N_6-N_7$) and $171.4(1)^\circ$ ($N_9-N_{10}-N_{11}$).

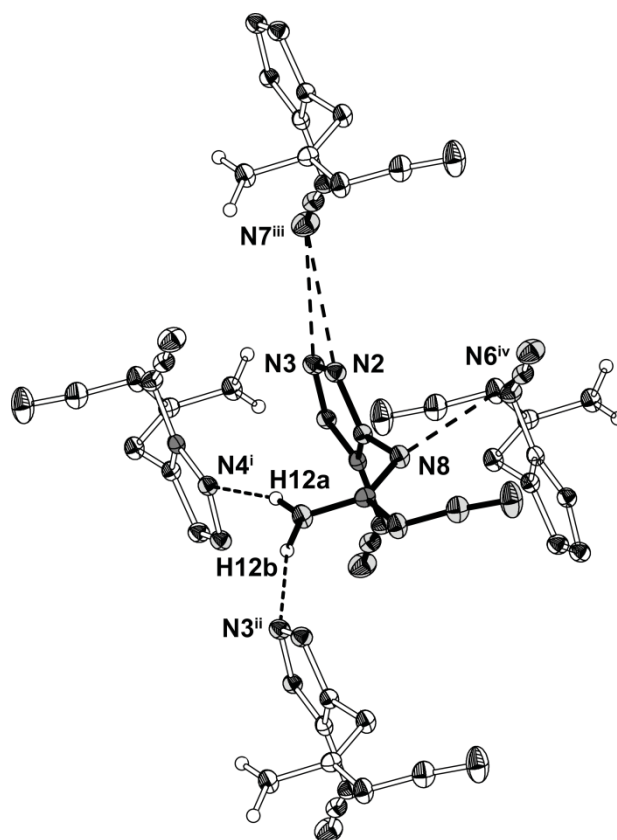


Figure 9: Hydrogen bonds and short contacts observed for **3**. Only the surrounding of the asymmetric unit is displayed, surrounding molecules are set transparent for clarity. Thermal ellipsoids set to 50 % probability. Symmetry operators: (i) $-x+1, -y+2, -z+1$; (ii) $x, y-1, z$; (iii) $x, y, z-1$; (iv) $-x, -y+2, -z+1$.

The structure of **3** is indeed built up pretty simple. The structure consists of rows along the c -axis connected through two short nitrogen nitrogen interactions favoring the N_7 atom of the tetrazole bound azide substituent and the N_2 and N_3 atoms of the tetrazole ring, presenting a planar arrangement. Both contacts, $N_3 \cdots N_7(\text{iii})$ and $N_2 \cdots N_7(\text{iii})$, are shorter than the sum of van der Waals radii ($r_w(\text{N}) + r_w(\text{N}) = 3.10 \text{ \AA}$) at $3.056(2) \text{ \AA}$ and $3.033(5) \text{ \AA}$, respectively. The third nitrogen–nitrogen contact, $N_8 \cdots N_6(\text{iv})$, is in the same range than the two before mentioned at $3.032(6) \text{ \AA}$. The interaction connects the rows to one another together with the two hydrogen bonds, $N_{12}-\text{H}_{12a} \cdots N_4(\text{i})$ and $N_{12}-\text{H}_{12b} \cdots N_3(\text{ii})$, being responsible for the formation of the three dimensional network. Both hydrogen bonds are shorter than the sum of van der Waals radii, displaying $D \cdots A$ distances of $3.032(1) \text{ \AA}$ and $3.026(1) \text{ \AA}$, respectively, and $D-H \cdots A$ angles of $164(1)^\circ$ and $157(1)^\circ$. The two bonds are hence not only of electrostatic nature, but also directed, as

can be seen in Figure 9, and, due to the also short $\text{H}\cdots\text{A}$ distances of $2.19(1)^\circ$ for both hydrogen bonds, can be assigned as moderately strong.^[22] The packing scheme within the unit cell is presented in Figure 10.

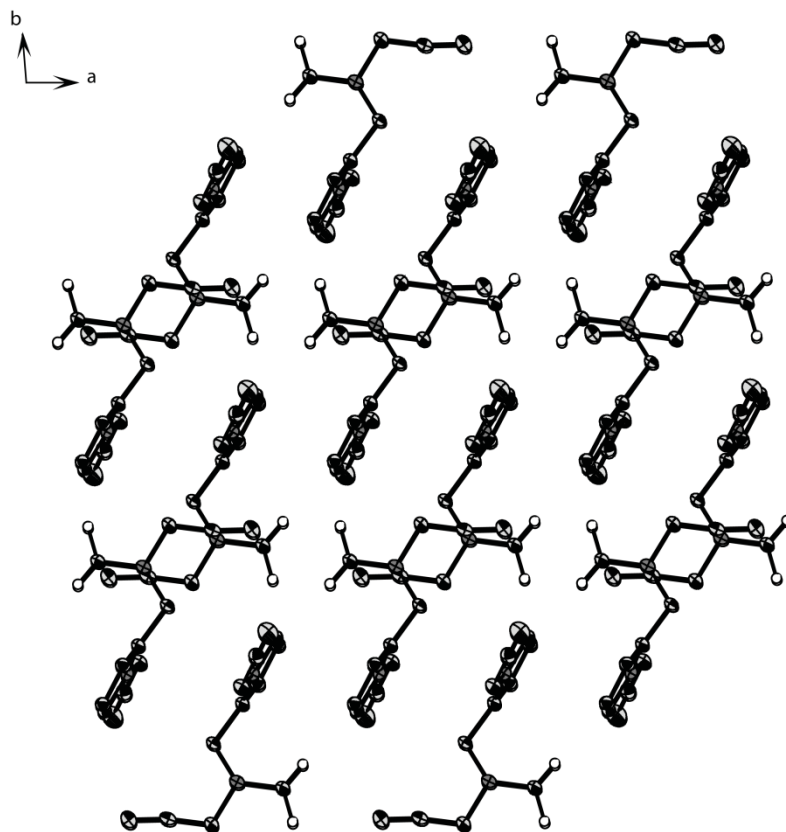


Figure 10: Presentation of the unit cell and the packing of **3** along the *c*-axis. The aminoazidocarbamoyl moieties are coplanar to the *ab* plane. Thermal ellipsoids are set to 50 % probability.

5.2.4 Sensitivities and Thermal Stabilities

All three azidotetrazoles **1** – **3** have been investigated towards their thermal stabilities and their sensitivities towards outer stimuli. Due to their behavior during the process of synthesis it was obvious, that the sensitivities will be not less than extreme, especially for compound **2**. The sensitivities have been measured using BAM techniques,^[23] as described in the experimental section, but the sensitivity values of **1** – **3** were too high to be measured and hence all smaller than 1 J in impact and smaller than 5 N in friction sensitivity (**1** and **3**). Compound **2** was initiated even by touching the material with a spatula without applying any force. Therefore we can state the impact and friction sensitivities to be lower than 0.25 J and 1 N, respectively. All three compounds have to be

considered extremely sensitive and proper safety precaution must be taken while handling them.

A “specialty” of **2** is the laser induced ignition we observed while recording RAMAN spectra of the compound. We had to measure the spectra at 50 mW at last, causing a very bad signal to noise ratio, because **2** detonated at a laser energy impact of 150 mW after the first scan. The decomposition temperatures of **1 – 3** rise with the loss of azide substituents: 124 °C for **2**, 136 °C for **3** and finally 142 °C for **1**.

Additionally, theoretical calculations have been performed at the CBS-4M^[24] level of theory to obtain heat of formation values of the compounds. These values have been used to calculate detonation parameter of **1 – 3** with the EXPLO5 (version 5.04) program package,^[25] just to get an idea of the power these compounds are able to generate. With detonation velocities well above the values known for commonly used secondary explosives like hexogen and very high energies of detonation, the respect for these materials and their handling increases even more. The calculated values together with the sensitivity values are compiled in Table 2. Compounds **1 – 3** have no realistic chance for use in any application, the detonation parameter should only illustrate their destructive potential.

Table 2: Compiled sensitivity data and detonation parameter of **1 – 3**.

Compound	IS (J)	FS (N)	ρ (g cm ⁻³)	ΔH_f^0 (s) (kJ mol ⁻¹)	Q_v (kJ kg ⁻¹)	P_{c-j} (kbar)	V_{det} (m s ⁻¹)
1	< 1	< 5	1.70 ^a	722	-5933	332	8983
2	< 0.25	<< 5	1.723	1495	-6855	339	8960
3	< 1	< 5	1.675	1100	-5794	305	8655

IS: Impact sensitivity; FS: Friction sensitivity; ΔH_f^0 : Heat of formation; Q_v : Heat of explosion; P_{c-j} : Detonation pressure at the Chapman-Jouguet point; V_{det} : Detonation velocity. [a] estimated density for the anhydrous compound.

5.3 Conclusion

Three novel azidotetrazole compounds (**1 – 3**) have been prepared by diazotation reactions of triaminoguanidinium chloride, followed by ring closure reactions with bases under various reaction conditions. All three compounds could only be synthesized in small yields but were successfully separated by short column chromatography with

chloroform. Not only single crystal X-ray structures of all three compounds were recorded, but they were also characterized by means of vibrational and multinuclear spectroscopy. A separation of the peaks and bands in Raman and IR measurements, respectively, was observed for the azide stretching modes in compounds **2** and **3**. While two unique stretching modes were observed for **3**, three stretching modes were observed for compound **2**, representing azide groups with different chemical surroundings in the solid state. The same phenomenon was also observed in the ^{14}N NMR spectra, where a separation into two signals was observed for compounds **2** and **3** due to the possible free rotation of the carbamoyl moieties around the $\text{N}_1\text{--N}_8$ bond. Finally, the sensitivities of all three compounds have been measured. They are all extremely sensitive against any form of physical outer stimuli like friction and impact. While **1** and **3** can be handled well with extreme care, compound **2** explodes under nearly any kind of conditions, which made the measurement of the vibrational data extremely difficult. Compound **2** exploded in solution as well as under radiation with a Nd:YAG laser (100 – 150 mW) while recording Raman spectra. The decomposition temperatures of **1** – **3** are in the range between 124 °C and 142 °C, which is not surprisingly when compared with the sensitivity values.

5.4 Experimental Part

Caution: All azidotetrazoles reported in this publication are unstable against outer stimuli like friction, impact and electrostatic discharge. Therefore proper safety precautions should be taken when handling these compounds. Laboratories and personnel should be properly grounded, and safety equipment such as Kevlar gloves, leather coats, face shields and ear plugs are recommended.

General. All chemical reagents and solvents were obtained from Sigma-Aldrich Inc. or Acros Organics (analytical grade) and were used as supplied without further purification. ^1H , $^{13}\text{C}\{^1\text{H}\}$, and $^{14}\text{N}\{^1\text{H}\}$ NMR spectra were recorded on a JEOL Eclipse 400 instrument in $\text{DMSO-}d_6$ or CDCl_3 at or near 25 °C. The chemical shifts are given relative to tetramethylsilane (^1H , ^{13}C) or nitro methane (^{14}N) as external standards and coupling constants are given in Hertz (Hz). Infrared (IR) spectra were recorded on a Perkin-Elmer Spectrum BX FT-IR instrument equipped with an ATR unit at 25 °C. Transmittance values are qualitatively described as “very strong” (vs), “strong” (s), “medium” (m), “weak” (w) and “very weak” (vw). RAMAN spectra were recorded on a Bruker RAM II

spectrometer equipped with a Nd:YAG laser operating at 1064 nm and a reflection angle of 180°. The intensities are reported as percentages of the most intense peak and are given in parentheses. Melting and decomposition points were determined by differential scanning calorimetry (Linseis PT 10 DSC, calibrated with standard pure indium and zinc). Measurements were performed at a heating rate of 5 °C min⁻¹ in closed aluminum sample pans with a 1 µm hole in the top for gas release to avoid an unsafe increase in pressure under a nitrogen flow of 20 mL min⁻¹ with an empty identical aluminum sample pan as a reference. Elemental analyses have not been performed due to the highly energetic nature of the synthesized compounds and to avoid possible damage of the measurement equipment. The mass spectra were recorded with DEI and DCI methods on a JEOL MStation JMS 700 mass spectrometer.

For initial safety testing, the impact and friction sensitivities as well as the electrostatic sensitivities were determined. The impact sensitivity tests were carried out according to STANAG 4489,^[26] modified according to WIWEB instruction 4-5.1.02^[27] using a BAM^[23] drop hammer. The friction sensitivity tests were carried out according to STANAG 4487^[28] and modified according to WIWEB instruction 4-5.1.03^[29] using the BAM friction tester. Electrostatic sensitivity test have not been performed due to the very high sensitivity and difficult handling of the compounds.

Crystallographic measurements. The single crystal X-ray diffraction data of **1**, **2** and **3** were collected using an Oxford Xcalibur3 diffractometer equipped with a Spellman generator (voltage 50 kV, current 40 mA) and a KappaCCD detector. The data collection was undertaken using the CRYCALIS CCD software^[30] while the data reduction was performed with the CRYCALIS RED software.^[31] The structures were solved with SIR-92^[32] or SHELXS-97^[33] and refined with SHELXL-97^[34] implemented in the program package WinGX^[35] and finally checked using PLATON.^[36] Further information regarding the crystal-structure determination have been deposited with the Cambridge Crystallographic Data Centre^[37] as supplementary publication Nos. 795273 (**1**), 693485 (**2**) and 693484 (**3**).

1-Amino-5-azidotetrazole (**1**)

Triaminoguanidinium chloride (2 mmol, 0.282 g) was dissolved in 30 mL of water and 2 mL 2 M hydrochloric acid was added. The reaction was carried out at 0 °C (ice bath cooling). A solution of sodium nitrite (4 mmol, 0.278 g) in 30mL water was added

dropwise over the course of 20 minutes. After complete addition, the mixture was allowed to warm up and stirred for an additional 30 minutes. The temperature was raised to 50 °C and half an equivalent of sodium carbonate was added fast in one portion (Caution, strong gas release!). The reaction mixture was stirred for an additional hour at ambient temperature and is afterwards extracted three times with 50 mL of diethyl ether and the combined organic extracts were allowed to evaporate till dryness to yield 51 mg of raw product. The raw material was cleaned by short column chromatography using chloroform as solvent yielding 32 mg of pure 1-amino-5-azidotetrazole monohydrate (11 % yield) with compounds **2** (app. 2.5 %) and **3** (app. 3 %) as side products.

R_f (CHCl₃) = 0.06; $T_{dec.}$: 142 °C (DSC, T_{onset} , 5 °C min⁻¹); ¹H NMR (CDCl₃, 25°C) δ (ppm) = 5.45 (s, 2H, -NH₂); ¹³C{¹H} NMR (CDCl₃, 25°C) δ (ppm) = 151.4; ¹⁴N NMR (CDCl₃, 25 °C) δ (ppm) = -140 (br, N_γ), -147 (N_β); IR (ATR, 25 °C, cm⁻¹) ν = 3332 (m), 3228 (m), 3162 (w), 2150 (vs), 1635 (m), 1531 (s), 1472 (m), 1404 (w), 1301 (m), 1272 (w), 1191 (m), 1118 (w), 1079 (w), 992 (w), 926 (w), 816 (w), 783 (w), 725 (w), 678 (m); RAMAN (Nd:YAG, 1064 nm, cm⁻¹) ν = 3205 (18), 3154 (26), 2156 (63), 1648 (14), 1535 (100), 1475 (37), 1307 (38), 1272 (34), 1200 (14), 1115 (21), 1075 (37), 1045 (14), 820 (2), 730 (11), 691 (22), 581 (34), 543 (14), 400 (11), 314 (37); m/z: (DEI+): 127.08 (2) [M+H⁺], 111.05 (2) [M-NH₂⁺], 77.13 (2), 69.02 (100), 55.01 (72), 41.05 (100), 31.07 (48), 30.04 (79), 29.06 (100), 28.05 (75); Sensitivities (anhydrous): IS: < 1 J; FS: < 5 N.

5-Azido-1-diazidocarbamoyltetrazole (**2**)

Triaminoguanidinium chloride (2 mmol, 0.282 g) was dissolved in 30 mL water and 2 mL 2 M hydrochloric acid was added. The reaction was carried out at 0 °C (ice bath cooling). A solution of sodium nitrite (4 mmol, 0.278 g) in 30mL water was added dropwise over the course of 20 minutes. After complete addition, the mixture was allowed to warm up and stirred for an additional 30 minutes. Exactly one equivalent of a 0.1 M sodium hydroxide solution was added slowly (slightly orange color). Immediately afterwards, the reaction mixture was extracted three times with 50 mL of diethyl ether. The combined organic fractions were allowed to evaporate till dryness to yield 0.058 g (26.3 %) as raw product. The raw material was cleaned by short column chromatography using chloroform as solvent yielding 0.036 g of pure 5-azido-1-diazidocarbamoyltetrazole (16.4 %).

R_f (CHCl₃) = 0.12; T_{melt} : 78 °C (DSC, Onset, 5 °C min⁻¹); T_{dec} : 124°C (DSC, Onset, 5 °C min⁻¹); ¹³C{¹H} NMR (DMSO-*d*₆, 25 °C) δ (ppm) = 160.4, 148.1; ¹⁴N NMR (DMSO-*d*₆, 25 °C) δ (ppm) = -148 (N _{β}); ¹⁴N NMR (CDCl₃, 25°C) δ (ppm) = -145 (br, N _{γ}), -147 (N _{β}), -149 (N _{β}), -305 (br, N _{α}); IR (ATR, 25 °C, cm⁻¹) ν = 3367 (m), 3314 (m), 3231 (m), 3190 (m), 2175 (vs), 2155 (vs), 2133 (vs), 1636 (s), 1578 (s), 1530 (s), 1456 (m), 1414 (s), 1290 (m), 1261 (m), 1213 (s), 1190 (s), 1106 (m), 1087 (m), 984 (w), 936 (w), 855 (w), 786 (w), 720 (w), 698 (w), 682 (w), 646 (w); RAMAN (Nd:YAG, 1064 nm, cm⁻¹) ν = 3196 (12), 2179 (48), 2165 (33), 2133 (25), 1653 (15), 1573 (28), 1534 (100), 1454 (13), 1408 (27), 1386 (12), 1293 (34), 1266 (27), 1216 (18), 1189 (23), 1115 (13), 1092 (38), 936 (22), 857 (30), 598 (29), 522 (35), 395 (27), 297 (37); m/z: (DCI+): 221.1 [M+H⁺]; Sensitivities (anhydrous): IS: < 0.25 J; FS: << 5 N.

1-(Amino-azidocarbamoyl)-5-azidotetrazole (**3**)

As in the preparation for C₂N₁₄, triaminoguanidinium chloride (2 mmol, 0.282 g) was dissolved in 30 mL water and 2 mL 2 M hydrochloric acid was added. The reaction was carried out at 0 °C (ice bath cooling). A solution of sodium nitrite (4 mmol, 0.278 g) in 30mL water was added dropwise over the course of 20 minutes. After complete addition, the mixture was allowed to warm up and stirred for an additional 30 minutes. Exactly one equivalent of a 0.1 M sodium hydroxide solution was added slowly (slightly orange color) within 1.5 hours and the reaction mixture was extracted three to four times with 50 mL of diethyl ether each afterwards. The combined organic extracts were allowed to evaporate till dryness to yield 0.04 g to 0.065 g as a raw product. Two products could be identified and separated by short column chromatography using chloroform. At an R_f value of 0.22, 1-(aminoazidocarbamoyl)-5-azidotetrazole was isolated with yields between 10 % (0.02 g) and 23 % (0.045 g) while at an R_f value of 0.12, 5-azido-1-diazidocarbamoyltetrazole was isolated in yields between 5 % (0.012 g) and 14 % (0.03 g). The exactly same ratio of products could not be prepared in successive attempts, yielding always different mixtures.

R_f (CHCl₃) = 0.22; T_{dec} : 136 °C (DSC, T_{onset} , 5 °C min⁻¹); ¹H NMR (CDCl₃, 25 °C) δ = 5.35 (-NH₂); ¹³C{¹H} NMR (CDCl₃, 25°C) δ = 157.9, 148.2; ¹⁴N NMR (CDCl₃, 25°C) δ = -138 (br, N _{γ}), -148 (N _{β}), -152 (N _{β}); IR (ATR, 25 °C, cm⁻¹) ν = 3278 (vw), 2327 (vw), 2257 (w), 2164 (vs), 2152 (vs), 1584 (s), 1573 (m), 1559 (w), 1521 (s), 1448 (w), 1330

(s), 1313 (s), 127 (s), 1260 (m), 1201 (m), 1126 (w), 1105 (m), 1084 (m), 1018 (w), 978 (w), 928 (w), 799 (w), 776 (w), 719 (w), 702 (w), 674 (w), 642 (w); RAMAN (Nd:YAG, 1064 nm, cm^{-1}) $\nu =$ 2170 (94), 2157 (37), 2128 (12), 1585 (100), 1580 (44), 1534 (48), 1526 (42), 1451 (13), 133 (15), 1317 (14), 1288 (41), 1261 (23), 1206 (16), 1186 (24), 1129 (10), 1108 (16), 1086 (41), 930 (14), 823 (17), 778 (8), 722 (9), 703 (14), 676 (12), 644 (12), 590 (16), 533 (5), 494 (13), 452 (22), 394 (13), 359 (18), 305 (26); m/z: (DCI+): 195.2 [M+H⁺]; Sensitivities (anhydrous): IS: < 1 J; FS: < 5 N.

5.5 References

- [1] P. Carlqvist, H. Östmark, T. Brinck, *J. Phys. Chem. A* **2004**, *108*, 7463-7467.
- [2] T. M. Klapötke, *Chemie der hochenergetischen Materialien*, 1 ed., Walter de Gruyter, Berlin, New York, **2009**.
- [3] V. A. Ostrovskii, M. S. Pevzner, T. P. Kofman, I. V. Tselinskii, *Targets Heterocyclic System* **1999**, *3*, 467-526.
- [4] a) T. Abe, G.-H. Tao, Y.-H. Joo, Y. Huang, B. Twamley, J. n. M. Shreeve, *Angew. Chem.* **2008**, *120*, 7195-7198; *Angew. Chem. Int. Ed.* **2008**, *47*, 7087-7090; b) M. A. Hiskey, N. Goldman, J. R. Stine, *J. Energ. Mater.* **1998**, *16*, 119-127; c) T. M. Klapötke, in *High Energy Density Materials* (Ed.: T. M. Klapötke), Springer, Heidelberg, **2007**, pp. 84-122; d) R. P. Singh, R. D. Verma, D. T. Meshri, J. n. M. Shreeve, *Angew. Chem.* **2006**, *118*, 3664-3682; *Angew. Chem. Int. Ed.* **2006**, *45*, 3584-3601; e) R. P. Singh, H. Gao, D. T. Meshri, J. M. Shreeve, in *High Energy Density Materials* (Ed.: T. M. Klapötke), Springer, Heidelberg, **2007**, pp. 35-83.
- [5] M. B. Talawar, R. Sivabalan, T. Mukundan, H. Muthurajan, A. K. Sikder, B. R. Gandhe, A. S. Rao, *J. Hazard. Mater.* **2009**, *161*, 589-607.
- [6] E. S. Domalski, E. D. Hearing, *J. Phys. Chem. Ref. Data.* **1993**, *22*, 805-1159.
- [7] F. Walter, K. Flick, US Patent 2179783, **1939**.
- [8] a) E. Lieber, D. R. Levering, *J. Am. Chem. Soc.* **1951**, *73*, 1313-1317; b) A. Hammerl, T. M. Klapötke, P. Mayer, J. J. Weigand, G. Holl, *Propell. Explos. Pyrot.* **2005**, *30(1)*, 17-26; c) J. Stierstorfer, T. M. Klapötke, A. Hammerl, R. D. Chapman, *Z. Anorg. Allg. Chem.* **2008**, *634*, 1051-1057; d) T. M. Klapötke, J. Stierstorfer, *J. Am. Chem. Soc.* **2009**, *131*, 1122-1134.
- [9] a) J. C. Kauer, W. A. Sheppard, *J. Org. Chem.* **1967**, *32*, 3580-3593; b) C. A. Maggiulli, R.E. Paine, BE 671402, **1966**.
- [10] T. M. Klapötke, F. A. Martin, S. M. Sproll, J. Stierstorfer, in *New Trends in Research of Energetic Materials, Proceedings of the 12th Seminar, Pt. 1*, Pardubice, Czech Republic, **2009**, pp. 327-340.
- [11] T. M. Klapötke, S. M. Sproll, *Eur. J. Org. Chem.* **2009**, *2009*, 4284-4289.

- [12] a) Xiao-Wei Zhang, Weihua Zhu, Tao Wei, Chenchen Zhang, H. M. Xiao, *J. Mol. Struct. Theochem* **2010**, *114*, 13142-13152; b) M. Goldberg, S. Hoz, H. Basch, *J. Mol. Struct. Theochem* **2003**, *663*, 135-143; c) Zhao Xu Chen, He Ming Xiao, H. Fan, *J. Mol. Struct. Theochem* **1999**, *458*, 249-256.
- [13] a) T. M. Klapötke, F. A. Martin, J. Stierstorfer, *Angew. Chem. Int. Ed.* **2011**, *50*, 4227-4229; *Angew. Chem.* **2011**, *123*, 4313-4316.
- [14] P. N. Gaponik, V. P. Karavai, *Chem. Heterocyc. Comp.* **1984**, 1683-1686.
- [15] J. C. Galvez-Ruiz, G. Holl, K. Karaghiosoff, T. M. Klapötke, K. Löhnwitz, P. Mayer, H. Nöth, K. Polborn, C. J. Rohbogner, M. Suter, J. J. Weigand, *Inorg. Chem.* **2005**, *44*, 4237-4253.
- [16] M. Hesse, Herbert, Meier, B. Zeh, *Spektroskopische Methoden in der Organischen Chemie*, 6 ed., Georg Thieme Verlag, Stuttgart, New York, **2002**.
- [17] a) T. H. Dunning, *J. Chem. Phys.* **1989**, *90*, 1007; b) C. Lee, W. Yang, R. G. Parr, *Phys. Rev. B* **1988**, *7*, 785; c) A. D. Becke, *J. Chem. Phys.* **1993**, *98*, 5648.
- [18] *Gaussian 09W, Version 7.0*, M. J. Frisch, G. W. Trucks, H. B. Schlegel, G. E. Scuseria, M. A. Robb, J. R. Cheeseman, G. Scalmani, V. Barone, B. Mennucci, G. A. Petersson, H. Nakatsuji, M. Caricato, X. Li, H. P. Hratchian, A. F. Izmaylov, J. Bloino, G. Zheng, J. L. Sonnenberg, M. Hada, M. Ehara, K. Toyota, R. Fukuda, J. Hasegawa, M. Ishida, T. Nakajima, Y. Honda, O. Kitao, H. Nakai, T. Vreven, J. A. Montgomery, Jr., J. E. Peralta, F. Ogliaro, M. Bearpark, J. J. Heyd, E. Brothers, K. N. Kudin, V. N. Staroverov, R. Kobayashi, J. Normand, K. Raghavachari, A. Rendell, J. C. Burant, S. S. Iyengar, J. Tomasi, M. Cossi, N. Rega, J. M. Millam, M. Klene, J. E. Knox, J. B. Cross, V. Bakken, C. Adamo, J. Jaramillo, R. Gomperts, R. E. Stratmann, O. Yazyev, A. J. Austin, R. Cammi, C. Pomelli, J. W. Ochterski, R. L. Martin, K. Morokuma, V. G. Zakrzewski, G. A. Voth, P. Salvador, J. J. Dannenberg, S. Dapprich, A. D. Daniels, Ö. Farkas, J. B. Foresman, J. V. Ortiz, J. Cioslowski, and D. J. Fox, *Gaussian, Inc., Wallingford CT*, 2009.
- [19] H. A. Witek, M. Keiji, *J. Comp. Chem. THEOCHEM* **2004**, *25*, 1858-1864.
- [20] A. F. Holleman, E. Wiberg, *Lehrbuch der anorganischen Chemie*, 101st Ed., de Gruyter, New York, **1995**.
- [21] A. Bondi, *J. Phys. Chem.* **1964**, *68*, 441-451.
- [22] G. A. Jeffrey, *An Introduction to Hydrogen Bonding*, Oxford University Press, Oxford, **1997**.
- [23] <http://www.bam.de>.
- [24] a) J. W. Ochterski, G. A. Petersson, J. A. Montgomery Jr., *J. Chem. Phys.* **1996**, *104*, 2598; b) J. W. Ochterski, G. A. Petersson, J. A. Montgomery Jr., *J. Chem. Phys.* **1996**, *104*, 2598-2619.
- [25] M. Sućeska, *EXPLO5.4 program, Zagreb, Croatia*, **2010**.
- [26] *NATO standardization agreement (STANAG) on explosives, no. 4489, 1st ed., Sept. 17*, **1999**.
- [27] *WIWEB-Standardarbeitsanweisung 4-5.1.02, Ermittlung der Explosionsgefährlichkeit, hier: der Schlagempfindlichkeit mit dem Fallhammer, Nov. 08*, **2002**.

- [28] *NATO standardization agreement (STANAG) on explosives, friction tests, no.4487, 1st ed., Aug. 22, 2002.*
- [29] *WIWEB-Standardarbeitsanweisung 4-5.1.03, Ermittlung der Explosionsgefährlichkeit, hier: der Reibempfindlichkeit mit dem Reibeapparat, Nov. 08, 2002.*
- [30] *CrysAlis CCD, Oxford Diffraction Ltd., Version 1.171.27p5 beta (release 01-04-2005 CrysAlis171.NET).*
- [31] *CrysAlis RED, Oxford Diffraction Ltd., Version 1.171.27p5 beta (release 01-04-2005 CrysAlis171.NET).*
- [32] A. Altomare, G. Cascarano, C. Giacovazzo, A. Guagliardi, *J. Appl. Cryst.* **1993**, 26, 343-350.
- [33] G. M. Sheldrick, *SHELXS-97, Crystal Structure Solution, Version 97-1; Institut Anorg. Chemie, University of Göttingen, Germany, 1990.*
- [34] G. M. Sheldrick, *SHELXL-97, Program for the Refinement of Crystal Structures. University of Göttingen, Germany, 1997.*
- [35] L. Farrugia, *J. Appl. Cryst.* **1999**, 32, 837-838.
- [36] A. L. Spek, *Platon, A Multipurpose Crystallographic Tool, Utrecht University, Utrecht, The Netherlands, 1999.*
- [37] *Crystallographic data for the structure(s) have been deposited with the Cambridge Crystallographic Data Centre. Copies of the data can be obtained free of charge on application to The Director, CCDC, 12 Union Road, Cambridge CB2 1EZ, UK (Fax: int.code (1223)336-033; e-mail for inquiry: fileserv@ccdc.cam.ac.uk; e-mail for deposition: deposit-@ccdc.cam.ac.uk).*

6. Synthesis and characterization of 3,5-diamino-1,2,4-triazolium dinitramide

Thomas M. Klapötke,* Franz A. Martin, Norbert T. Mayr and Jörg Stierstorfer

As published in: Zeitschrift für Anorganische und Allgemeine Chemie, 2010, 636(15), 2555-2564.

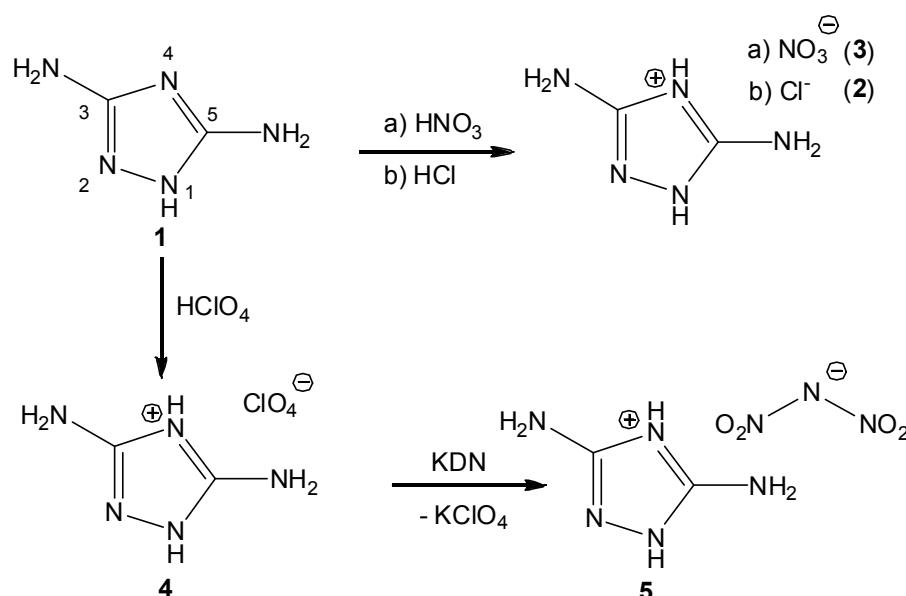
6.1 Introduction

The development of azole based new energetic materials^[1] for civil and military applications is of great interest in many research programs worldwide due to their unique properties: shock waves producing pressure up to 500,000 times that of Earth's atmosphere, detonation waves travelling at 10 kilometers per second, temperatures soaring to 5500 Kelvin, and power approaching 20 billion Watts per square centimetre. Advances in energetic materials, which include high explosives, propellants and pyrotechnics have been gained on nitrogen- and oxygen rich materials.^[2] Especially energetic ionic salts of tri- and tetrazoles have been utilized in energetic roles owing to their higher heats of formation, density and oxygen balance compared to those of their carbocyclic analogues. Azolium cations paired with nitrate, perchlorate, dinitramide, or picrate anions form highly energetic salts with mostly good thermal stabilities. With the exception of perchlorate they and their decomposition products are often environmentally benign. Probably most suitable as high explosives, gas generators or components in propellants or propellant charges^[3-6] are azolium salts containing the dinitramide anion, $\text{N}(\text{NO}_2)_2^-$ (DN).^[7] They often show excellent oxygen balances by combining both the fuel (tetrazole heterocycle) and the oxidizer (dinitramide). Many N-rich dinitramides like guanidinium dinitramide,^[8] aminoguanidinium dinitramide,^[9] bisguanidinium dinitramide,^[10] guanylurea dinitramide (FOX-12)^[11] and triaminoguanidinium dinitramide^[4, 12] were synthesized and characterized as energetic materials. Also tetrazolium derivatives, e.g. 5-aminotetrazolium dinitramide,^[13] 1,5-diaminotetrazolium dinitramide^[14] 1,4-dimethyl-5-aminotetrazolium dinitramide,^[15] 1,5-diamino-4-methyltetrazolium dinitramide^[16] are described as energetic materials in literature.^[17] In this work we present the synthesis and characterization of the new energetic compound 3,5-diamino-1,2,4-triazolium dinitramide (**5**) which is based on the commercially available guanazole (**1**).

6.2 Results and Discussion

6.2.1 Synthesis

3,5-Diamino-1,2,4-triazole (**1**) was protonated with diluted hydrochloric and nitric acid, forming the compounds 3,5-diamino-1,2,4-triazolium chloride hemihydrate (**2**) and 3,5-diamino-1,2,4-triazolium nitrate (**3**). **2** was then recrystallized from water and **3** from an ethanolic solution (water/ethanol: 1:1). The synthesis of 3,5-diamino-1,2,4-triazolium dinitramide (**5**) was performed according to Scheme 1. In the first step **1** was protonated with an equimolar amount of 1N perchloric acid. After removing the solvent, single crystals of 3,5-diamino-1,2,4-triazolium perchlorate (**4**) were obtained by recrystallization from hot ethanol. Compound **4** is well soluble in water, slightly soluble in MeOH, DMSO as well as DMF and low soluble in cold EtOH, acetone, diethyl ether or THF. In the second step, aqueous solutions of **4** and potassium dinitramide were combined forming **5** under precipitation of potassium perchlorate. The suspension was evaporated to dryness and extracted with ethanol yielding clean **5** after evaporation of the solvent. The solubility of **5** is comparable to that of **4**. Single crystals were obtained from a wet ethanolic solution.



Scheme 1: Protocol of the syntheses of 3,5-diamino-1,2,4-triazolium chloride (**2**), nitrate (**3**), perchlorate (**4**) and dinitramide (**5**).

6.2.2 NMR Spectroscopy

The formation of the 3,5-diamino-1,2,4-1*H*-triazolium ions can easily be monitored and observed due to the differences in the NMR spectra. The neutral compound **1** shows two unique peaks for each of the amine groups at chemical shifts of 5.56 ppm and 4.68 ppm and one broad peak at a chemical shift of 10.68 ppm for the nitrogen bonded hydrogen atom (N1, heterocyclic ring). This can be explained with the slow exchange of the N-H hydrogen atom between nitrogen atoms N1 and N2 in DMSO-*d*₆ which generates two different chemical surroundings for each amine group. The same is observed for the carbon atoms. In the ¹³C-{¹H} NMR spectra we observed two peaks at chemical shifts of 161.8 ppm and 156.4 ppm, respectively.

In contradiction to the neutral compound the triazolium ions always show a different pattern in the NMR spectra. When protonated, only one signal is observed for the two amine groups, shifted well to lower field, at a chemical shift of 7.07 ppm (**2**), 6.97 ppm (**3**), 6.94 ppm (**4**) and 6.94 ppm (**5**), respectively. The two hydrogen atoms located on the heterocyclic ring show only one broad singlet signal at chemical shifts of 12.03 ppm (**2**), 12.08 ppm (**3**), 11.93 ppm (**4**) and 12.13 ppm (**5**). The same is observed in the ¹³C{¹H} NMR spectra where we observe only one signal for the two equivalent carbon atoms of the heterocyclic ring at a chemical shift of 151.4 ppm (**2**), 151.8 ppm (**3**), 151.8 ppm (**4**) and 152.0 ppm (**5**), shifted to higher fields compared with **1**.

In addition unique peaks for the nitrate and dinitramide anions are observed in the ¹⁴N NMR spectra of compounds **3** and **5** at chemical shifts of – 4 ppm for compound **3** and – 10 ppm for compound **5**, respectively.

6.2.3 Molecular Structures

The single crystal X-ray diffraction data of **1–5** were collected using an Oxford Xcalibur3 diffractometer with a Spellman generator (voltage 50 kV, current 40 mA) and a KappaCCD detector. The data collection was undertaken using the CRYSA LIS CCD software^[18] and the data reduction was performed with the CRYSA LIS RED software.^[19] The structures were solved with SIR-92^[20] and refined with SHELXL-97^[21] implemented in the program package WinGX^[22] and finally checked using PLATON.^[23] Further information regarding the crystal-structure determination have been deposited with the

Cambridge Crystallographic Data Centre^[24] as supplementary publication Nos. 784960 (1), 784963 (2), 784962 (3), 784959 (4) and 784961 (5).

Table 1: Selected crystallographic data and parameters.

	1	2	3	4	5
Formula	C ₂ H ₅ N ₅	C ₄ H ₁₄ N ₁₀ Cl ₂ O	C ₂ H ₆ N ₆ O ₃	C ₂ H ₆ N ₅ ClO ₄	C ₂ H ₆ N ₈ O ₄
FW [g mol ⁻¹]	99.11	289.15	162.13	199.57	206.15
Crystal system	monoclinic	monoclinic	monoclinic	triclinic	monoclinic
Space Group	<i>P2₁/c</i> (No. 14)	<i>P2₁/n</i> (No. 14)	<i>P2₁/c</i> (No. 14)	<i>P</i> -1 (No. 2)	<i>P2₁/n</i> (No. 14)
Color / Habit	colorless rods	colorless plates	colorless rods	colorless prismn	colorless rods
Size [mm]	0.13x0.14x0.16	0.05x0.17x0.18	0.13x0.15x0.30	0.14x0.17x0.18	0.12x0.14x 0.20
<i>a</i> [Å]	10.6366(6)	6.0570(5)	9.5615(7)	5.3035(5)	13.0772(7)
<i>b</i> [Å]	4.3042(2)	24.662(2)	9.1082(6)	7.6267(7)	17.4883(5)
<i>c</i> [Å]	10.8114(6)	8.1341(6)	7.4390(6)	9.2813(8)	14.1722(5)
α [°]	90	90	90	74.399(8)	90
β [°]	118.784(7)	93.516(7)	96.362(8)	84.825(7)	107.678(4)
γ [°]	90	90	90	83.683(8)	90
<i>V</i> [Å ³]	433.81(5)	1212.78(16)	643.86(8)	358.67(6)	3088.1(2)
<i>Z</i>	4	4	4	2	16
ρ_{calc} [g cm ⁻³]	1.518	1.584	1.673	1.848	1.774
μ [mm ⁻¹]	0.114	0.541	0.150	0.520	0.162
<i>F</i> (000)	208	600	336	204	1696
$\lambda_{\text{MoK}\alpha}$ [Å]	0.71073	0.71073	0.71073	0.71073	0.71073
<i>T</i> [K]	200	200	200	200	200
<i>R</i> _{int}	0.019	0.038	0.033	0.023	0.026
<i>R</i> ₁ (obs)	0.0315	0.0350	0.0276	0.0327	0.0319
w <i>R</i> ₂ (all data)	0.0862	0.0623	0.0639	0.0885	0.0984
<i>S</i>	1.04	0.82	0.92	1.00	1.03
CCDC	784960	784963	784962	784959	784961

The structure of guanazole (1) was re-determined, since the solution published by G. L. Starova *et al.*^[25] (i) has been measured at room temperature and (ii) was published in the non standard space group *P2₁/b*. The asymmetric unit is shown in Figure 1. The bond distances, angles and torsion angles agree with the previously measured structure.

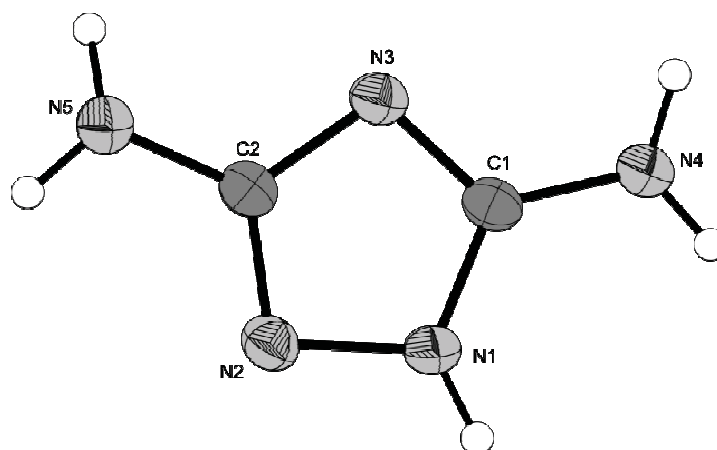


Figure 1: Molecular moiety of **1**. Thermal ellipsoids represent the 50% probability level. Selected bond lengths (Å): N5–C2 1.375(2), N3–C1 1.334(3), N3–C2 1.354(2), N2–C2 1.324(6), N4–C1 1.350(3), N2–N1 1.395(3), N1–C1 1.336(4); selected bond angles (°): N3–C1–N1 110.27(11), C2–N2–N1 101.28(11), N3–C1–N4 125.44(12), C1–N1–N2 109.67(12), N1–C1–N4 124.18(14), N2–C2–N3 115.76(13), N2–C2–N5 122.62(12), C1–N3–C2 103.02(11), N3–C2–N5 121.44(13).

Protonation of **1** using diluted hydrochloric acid yields 3,5-diamino-1,2,4-triazolium chloride as its semihydrate, which crystallizes in the monoclinic space group $P2_1/c$. The asymmetric unit, four times in a unit cell, includes two moieties of cations and anions resulting in a density of 1.584 g cm^{-3} . The chlorides participate in a strong hydrogen bond network interacting with all of the existing hydrogen atoms. The structure of the cation is influenced only very marginal by protonation at the nitrogen atom N3. With this, the angle C1–N3–C2 is slightly elongated to 106.6° (C3–N8–C4 106.4° ; **1**: C1–N3–C2 $103.02(11)^\circ$).

3,5-Diamino-1,2,4-triazolium chloride hemihydrate (**2**) crystallizes in the monoclinic space group $P2_1/n$ with eight molecular moieties in the unit cell. The asymmetric unit (Figure 2) consists of two anion/cation pairs and one crystal water. The density of 1.584 g cm^{-3} is in the range of other azole chlorides, e.g. 5-Azido-3-amino-1,2,4-triazolium hydrochloride mono-hydrate (1.572 g cm^{-3}).^[26] The two independent chloride ligands are coordinated by six (Cl1) as well as four (Cl2) hydrogen atoms forming no regular polyhedron.

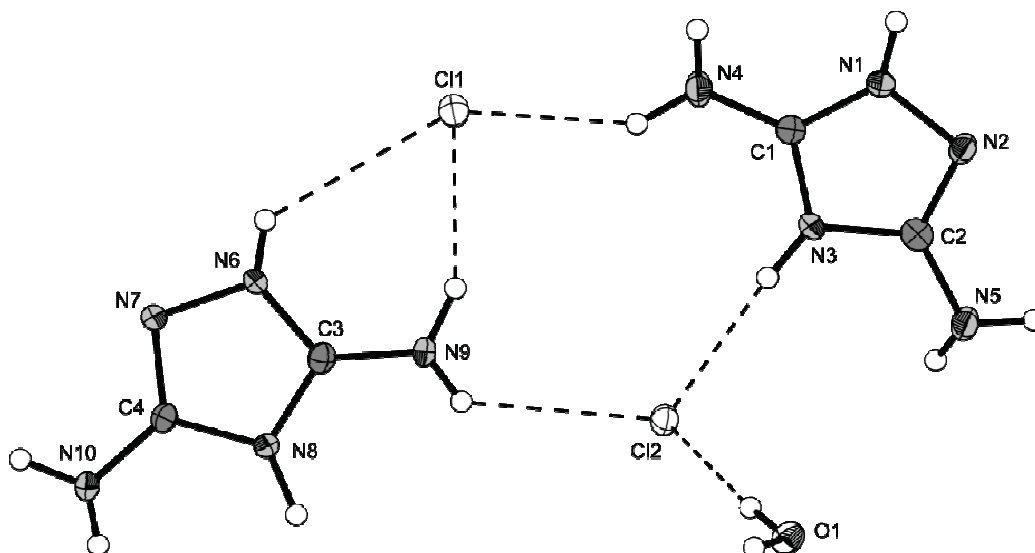


Figure 2: Molecular moiety of **2**. Thermal ellipsoids represent the 50% probability level. Selected bond lengths (Å): N1–C1 1.3173, N1–N2 1.3966, N2–C2 1.3074, N3–C1 1.3545, N3–C2 1.3725, N4–C1 1.3229, N5–C2 1.3532, N6–C3 1.3187, N6–N7 1.3948, N7–C4 1.3131, N8–C3 1.3445, N8–C4 1.3781, N9–C3 1.3326, N10–C4 1.3351.

3,5-Diamino-1,2,4-triazolium nitrate (**3**) crystallizes in the monoclinic space group $P2_1/c$ with four molecular moieties in the unit cell. The density of 1.672 g cm^{-3} is in the range of other azole nitrate derivatives, e.g. 5-aminotetrazolium nitrate.^[27]

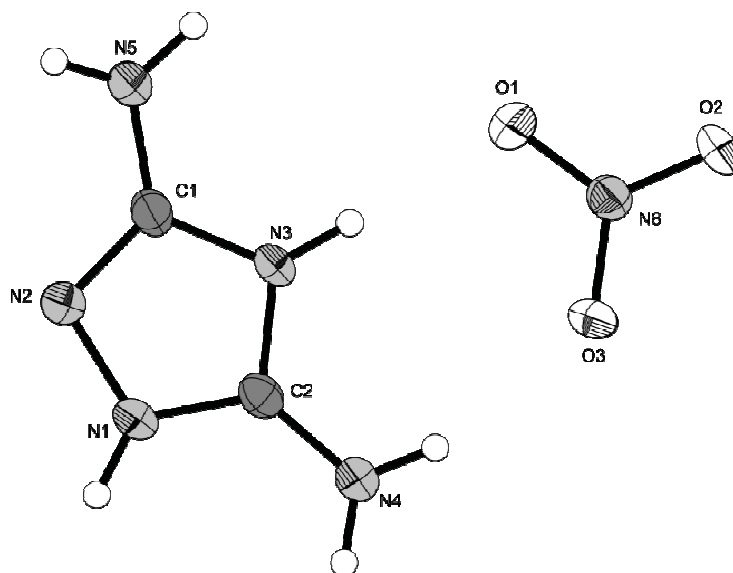


Figure 3: Molecular moiety of **3**. Thermal ellipsoids represent the 50% probability level. Selected bond lengths (Å): N1–C2 1.317(2), N1–N2 1.401(6), N5–C1 1.338(5), N2–C1 1.305(2), N3–C2 1.348(4), N3–C1 1.375(4), O1–N6 1.257(5), O2–N6 1.240(2), N4–C2 1.318(5), O3–N6 1.257(3); selected bond angles (°): C2–N1–N2 111.75(11), N2–C1–N5 125.99(13), C1–N2–N1 103.49(11), N2–C1–N3 111.23(12), N4–C2–N3 124.93(12), O2–N6–O1 120.92(11), O2–N6–O3 120.13(11), O1–N6–O3 118.95(10).

Compound **3** crystallizes layer-like, in which the layers are formed by a strong hydrogen-bond network. All of the oxygen atoms of the nitrate anions participate in strong hydrogen bonds listed in Table 2.

Table 2: Hydrogen bonds based on the nitrate anions in the structure of **3**.

Atoms D,H,A	Dist. D,H [Å]	Dist. H,A [Å]	Dist. D,A [Å]	Angle D,H,A [°]
N3–H3···O1 ⁱ	0.891(15)	1.945(16)	2.8362(15)	178.1(12)
N4–H4A···O3 ⁱ	0.869(18)	2.123(18)	2.9549(17)	159.9(14)
N5–H5B···O1 ⁱⁱⁱ	0.843(18)	2.094(19)	2.9350(18)	175.9(16)
N4–H4B···O3 ^{iv}	0.867(17)	2.057(17)	2.9038(17)	165.3(15)
N4–H4B···O2 ^{iv}	0.867(17)	2.643(16)	3.0789(16)	112.3(13)
N1–H1···O2 ^v	0.874(17)	2.048(17)	2.9190(16)	175.3(15)

Symmetry operators: (i) $x, 0.5-y, 0.5+z$; (ii) $-x, -0.5+y, 0.5-z$; (iii) $-x, 1-y, -z$; (iv) $1-x, 1-y, 1-z$; (v) $x, 1.5-y, 0.5+z$.

By analyzing the graph sets^[28] with the software RPLUTO^[29] several chain (**C1,1(6)**, **C1,1(4)** and **C2,2(5)**) and ring motifs (e.g. **R2,2(8)**) can be found within the layers, which are illustrated in Figure 4.

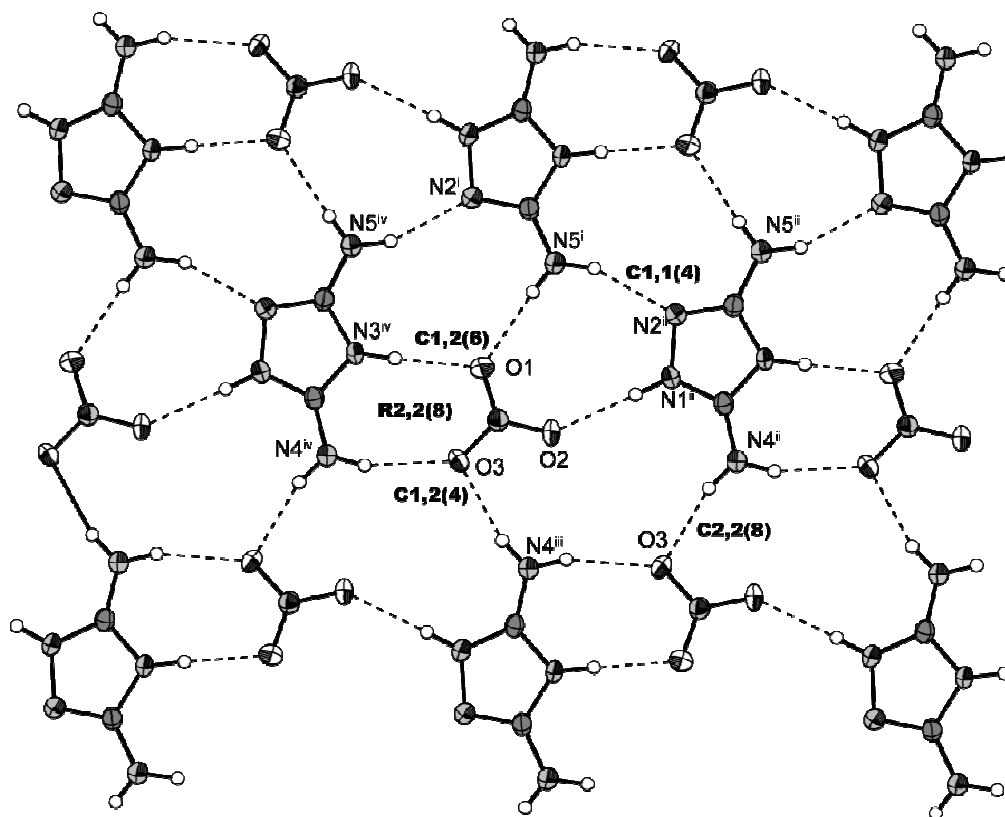


Figure 4: Hydrogen bonding within the layers in the structure of **3**. Thermal ellipsoids represent the 50 % probability level. Symmetry codes: (i) $-x, 1-y, -z$; (ii) $x, 1.5-y, -0.5+z$; (iii) $1-x, 1-y, 1-z$; (iv) $x, 0.5-y, -0.5+z$.

3,5-Diamino-1,2,4-triazolium perchlorate (**4**) crystallizes in the triclinic space group $P-1$ with two molecular moieties in the unit cell. The density of 1.848 g cm^{-3} is in the range of other azole perchlorate derivatives, e.g. 5-aminotetrazolium perchlorate.^[30] The molecular structure (Figure 5) of the cation is in accordance to that in **2** and **3**. The perchlorate anions show a regular tetrahedral structure (all O–Cl–O angles between 109° and 111°).

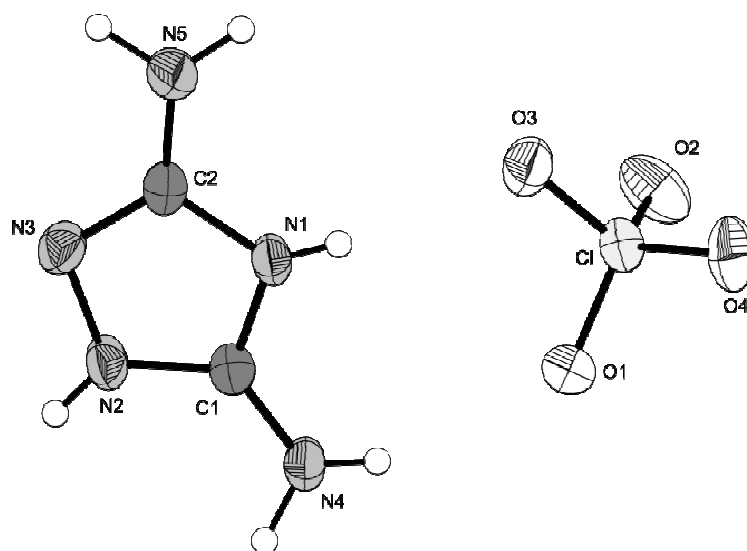


Figure 5: Molecular moiety of **4**. Thermal ellipsoids represent the 50% probability level. Selected bond lengths (Å): Cl–O4 1.431(6), N5–C2 1.354(8), Cl–O2 1.431(6), Cl–O3 1.440(5), Cl–O1 1.440(6), N2–C1 1.318(6), N3–C2 1.296(5), N3–N2 1.399(8), N4–C1 1.329(6), N1–C1 1.341(7), N1–C2 1.380(6); selected bond angles ($^\circ$): C1–N2–N3 111.81(18), C2–N3–N2 103.62(20), C1–N1–C2 107.48(19), N2–C1–N4 127.29(20), N2–C1–N1 105.98(20), N3–C2–N5 126.72(23), N3–C2–N1 111.10(21).

Again a layer-like structure is formed in which three of the oxygen atoms of the perchlorate anions participate in hydrogen bonds. The fourth oxygen atom is directed alternating to both the upper and lower layers. Analyzing the graph sets yields several chain and ring motives, some of them marked in Figure 6.

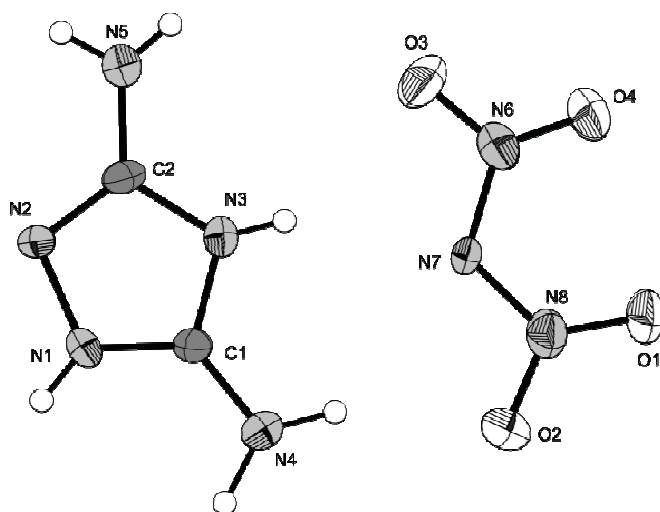


Figure 7: Molecular moiety of **5**. The ellipsoids represent the 50% probability level. Selected bond lengths (Å): O2–N8 1.240(4), O1–N8 1.251(4), N7–N8 1.354(4), N7–N6 1.368(4), O3–N6 1.238(4), O4–N6 1.218(4), N1–C1 1.317(4), N2–C2 1.308(5), N2–N1 1.403(4), N4–C1 1.313(5), C1–N3 1.358(5), N3–C2 1.367(5), C2–N5 1.343(5).

Compound **5** crystallizes in accordance to **3** and **4** forming a layer-like structure. Except for the outer nitrogen atoms in the dinitramide anions all atoms participate in hydrogen bonds, shown in Figure 8. Due to that fact, several remarkable also bifurcated ring graph sets are formed.

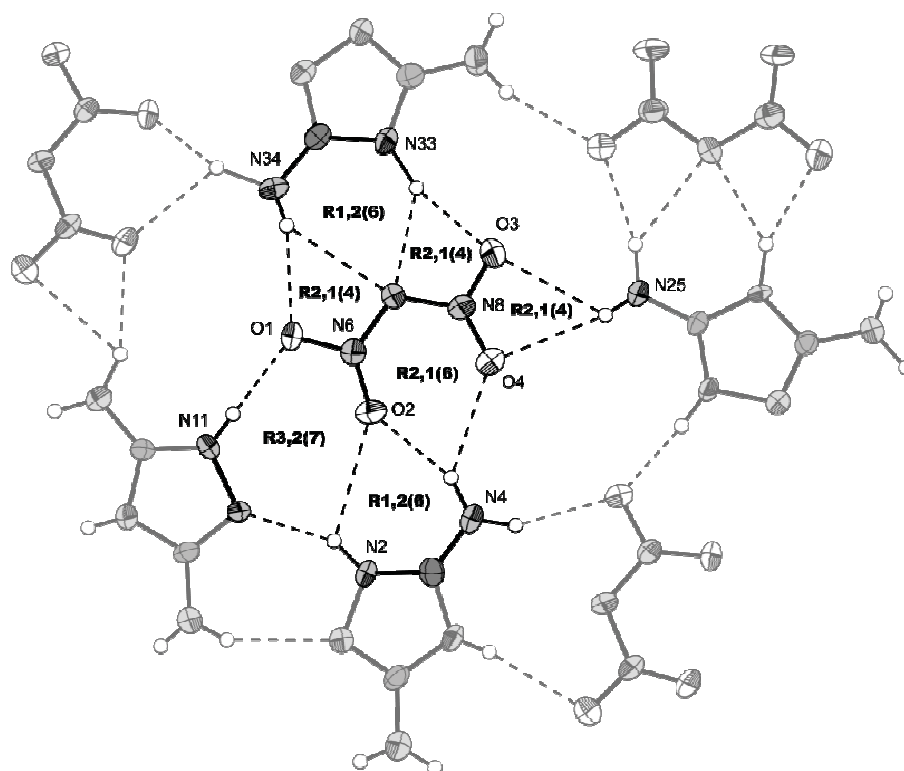


Figure 8: Hydrogen bonding of one dinitramide anion in the structure of **5**. Thermal ellipsoids represent the 50 % probability level.

6.2.4 Theoretical Calculations

Due to the highly energetic character of **3** and **5**, bomb calorimetric measurements could only be performed with small amounts, consequently doubtful combustion energies were obtained. Therefore an extensive computational study was accomplished for **1–5**, which is presented in the following. All calculations were carried out using the Gaussian G03W (revision B.03) program package.^[31] The enthalpies (H) and free energies (G) were calculated using the complete basis set (CBS) method of Petersson and coworkers in order to obtain very accurate energies. The CBS models use the known asymptotic convergence of pair natural orbital expressions to extrapolate from calculations using a finite basis set to the estimated complete basis set limit. CBS-4 begins with a HF/3-21G(d) geometry optimization; the zero point energy is computed at the same level. It then uses a large basis set SCF calculation as a base energy, and a MP2/6-31+G calculation with a CBS extrapolation to correct the energy through second order. A MP4(SDQ)/6-31+(d,p) calculation is used to approximate higher order contributions. In this study we applied the modified CBS-4M method (**M** referring to the use of Minimal Population localization) which is a re-parametrized version of the original CBS-4 method and also includes some additional empirical corrections.^[32] The enthalpies of the gas-phase species M were computed according to the atomization energy method (eq. 1) (Tables 3–5).^[33]

$$\Delta_f H^\circ_{(g, M, 298)} = H_{(Molecule, 298)} - \sum H^\circ_{(Atoms, 298)} + \sum \Delta_f H^\circ_{(Atoms, 298)} \quad (1)$$

Table 3: CBS-4M results

	point group	el. state	$-H^{298} / \text{a.u.}$	<i>NIMAG</i>
DATr (1)	C_s		352.484409	0
HDATr⁺	C_s	1A_1	352.839733	0
Cl⁻	K_h		459.809901	0
NO₃⁻	D_{3h}	1A	280.080446	0
ClO₄⁻	T_d		760.171182	0
DN⁻	C_2		464.499549	0
H		$^2A_{1g}$	0.500991	0
C			37.786156	0
N		$^4A_{1g}$	54.522462	0
O			74.991202	0
Cl			459.674576	0

Table 4: Literature values for atomic $\Delta H_f^{\circ 298}$ / kcal mol⁻¹

	NIST ^[34]
H	52.1
C	171.3
N	113.0
O	59.6
Cl	29.0

Table 5: Enthalpies of the gas-phase species M.

M	M	$\Delta_f H^\circ(\text{g,M})$ / kcal mol ⁻¹
DATr (1)	C ₂ H ₅ N ₅	41.8
HDATr⁺	C ₂ H ₆ N ₅ ⁺	185.3
Cl⁻	Cl ⁻	-55.9
NO₃⁻	NO ₃ ⁻	-74.9
ClO₄⁻	ClO ₄ ⁻	-66.1
DN⁻	N ₃ O ₄ ⁻	-29.6

The solid state energy of formation (Table 7) of **DATr** was calculated by subtracting the gas-phase enthalpy with the heat of sublimation (22.5 kcal mol⁻¹) obtained by the TROUTMAN rule ($\Delta H_{\text{sub}} = 188 \cdot T_m$) ($T_m=204$ °C).^[35] In the case of the salts, the lattice energy (U_L) and lattice enthalpy (ΔH_L) were calculated from the corresponding molecular volumes (Table 9) according to the equations provided by Jenkins *et al.*^[36] With the calculated lattice enthalpy (Table 6) the gas-phase enthalpy of formation (Table 5) was converted into the solid state (standard conditions) enthalpy of formation. These molar standard enthalpies of formation (ΔH_m) were used to calculate the molar solid state energies of formation (ΔU_m) according to equation 2 (Table 7).

$$\Delta U_m = \Delta H_m - \Delta n RT \quad (2)$$

(Δn being the change of moles of gaseous components)

Table 6: Lattice energies and lattice enthalpies.

	V_M / nm^3	$U_L / \text{kJ mol}^{-1}$	$\Delta H_L / \text{kJ mol}^{-1}$	$\Delta H_L / \text{kcal mol}^{-1}$
2	0.151	543.8	545.8	130.3
3	0.161	535.0	538.5	128.6
4	0.179	520.1	523.6	125.0
5	0.193	509.8	513.2	122.6

Table 7: Solid state energies of formation ($\Delta_f U^\circ$)

	$\Delta_f H^\circ(\text{s}) /$ kcal mol ⁻¹	$\Delta_f H^\circ(\text{s}) /$ kJ mol ⁻¹	Δn	$\Delta_f U^\circ(\text{s}) /$ kJ mol ⁻¹	M / g mol ⁻¹	$\Delta_f U^\circ(\text{s}) /$ kJ kg ⁻¹
1	19.4	81.1	5	93.4	99.12	942.8
2	-29.8	-124.7	6.5	-108.6	144.57	-751.0
3	-18.2	-76.1	7.5	-57.6	162.14	-354.9
4	-6.0	-25.2	8	-5.4	199.58	-26.8
5	33.1	138.7	9	161.0	206.16	781.1

6.2.5 Detonation Parameters

The calculation of the detonation parameters was performed with the program package EXPLO5 (version 5.03 and 5.04).^[37] The program is based on the chemical equilibrium, steady-state model of detonation. It uses the Becker-Kistiakowsky-Wilson's equation of state (BKW EOS) for gaseous detonation products and Cowan-Fickett's equation of state for solid carbon. The calculation of the equilibrium composition of the detonation products is done by applying modified White, Johnson and Dantzig's free energy minimization technique. The program is designed to enable the calculation of detonation parameters at the CJ point. The BKW equation in the following form was used with the BKWN set of parameters (α , β , κ , θ) as stated below the equations and X_i being the mol fraction of i -th gaseous product, k_i is the molar covolume of the i -th gaseous product:^[38]

$$pV / RT = 1 + xe^{\beta x} \qquad x = (\kappa \sum X_i k_i) / [V(T + \theta)]^\alpha$$

$$\alpha = 0.5, \beta = 0.176, \kappa = 14.71, \theta = 6620. \quad (5.03)$$

$$\alpha = 0.5, \beta = 0.096, \kappa = 17.56, \theta = 4950. \quad (5.04)$$

The detonation parameters calculated with the EXPLO5 versions V5.03 and V5.04 using the experimentally determined densities (X-ray) are summarized in Table 8. It is not possible to calculate detonation parameters of compounds containing chlorine; therefore, the corresponding cells have been abandoned.

Table 8: Physico-chemical properties of **1–5** in comparison with trinitrotoluene (**TNT**), nitropenta (**NP**) and hexogen (**RDX**).

	1	2	3	4	5	TNT*	NP*	RDX*
Formula	C ₂ H ₅ N ₅	C ₂ H ₇ N ₅ ClO _{1/2}	C ₂ H ₆ N ₆ O ₃	C ₂ H ₆ Cl N ₅ O ₄	C ₂ H ₆ N ₈ O ₄	C ₇ H ₅ N ₃ O ₆	C ₅ H ₈ N ₄ O ₁₂	C ₃ H ₆ N ₆ O ₇
Molecular Mass [g mol ⁻¹]	99.12	144.57	162.14	199.58	206.12	227.13	316.14	222.12
Impact sensitivity [J] ^a	> 40	> 40	40	25	> 3	15	3	7.5
Friction sensitivity [N] ^b	> 360	> 360	288	240	192	353	60	120
ESD–test [J]	> 5	> 10	0.3	0.8	0.3	n.d.	n.d.	0.1 - 0.2
<i>N</i> [%] ^c	70.67	48.44	51.84	35.10	54.36	18.50	17.72	37.8
<i>Q</i> [%] ^d	-104.9	-71.91	-39.48	-20.04	-23.28	-73.96	-10.1	-21.6
<i>T</i> _{dec.} [°C] ^e	204 (mp)	282	276	252	164	>160	202	210
<i>ρ</i> [g cm ⁻³] ^f	1.520	1.584	1.672	1.848	1.774	1.654	1.778	1.800
<i>Δ_fH_m</i> ^o [kJ mol ⁻¹] ^g	81.1	-124.7	-76.1	-25.2	138.7	-59.1	-539.0	70
<i>Δ_fU</i> ^o [kJ kg ⁻¹] ^h	942.8	-751.0	-354.9	-33.1	781.1	-184.9	-1611.7	417
EXPLO 5 values:								
V5.03 (V5.04)								
- <i>Δ_EU</i> ^o [kJ kg ⁻¹] ⁱ	1853 (1674)	---	4052 (4060)	---	5101 (5157)	5112 (5227)	5979 (6190)	6038 (6125)
<i>T_E</i> [K] ^j	1152 (1561)	---	3104 (2996)	---	3810 (3705)	3756 (3657)	4423 (4306)	4368 (4236)
<i>p_{C-J}</i> [kbar] ^k	113 (134)	---	233 (246)	---	302 (321)	205 (216)	321 (320)	341 (349)
<i>V</i> _{Det.} [m s ⁻¹] ^l	6058 (6516)	---	7789 (7927)	---	8624 (8681)	7178 (7253)	8665 (8320)	8906 (8748)
Gas vol. [L kg ⁻¹] ^m	847 (758)	---	833 (826)	---	833 (810)	617 (574)	765 (688)	793 (739)

[^a] BAM drophammer, grain size (75–150 μm); [^b] BAM friction tester, grain size (75–150 μm); [^c] Nitrogen content; [^d] Oxygen balance [³⁹]; [^e] Temperature of decomposition by DSC (*β* = 5 °C); [^f] X-ray structure; [^g] Molar enthalpy of formation; [^h] Energy of formation; [ⁱ] Energy of Explosion; [^j] Explosion temperature; [^k] Detonation pressure; [^l] Detonation velocity; [^m] Assuming only gaseous products; * values based on Ref. [⁴⁰] and the EXPLO5 database; n.d.: not determined.

Especially the detonation parameters of compound **5** show promising values, higher than those of trinitrotoluene (**TNT**) and in the range of those of pentaerythryl tetranitrate (**PETN**). Also compound **3** exceeds the values of TNT in addition to its great thermal stability of 276 °C and low sensitivities (Table 8). The most important criteria of high explosives are the detonation velocity ($v_{\text{det.}}$ = **3**: 7927, **5**: 8681, TNT: 7253, PETN: 8320, RDX: 8748 m s⁻¹), the detonation pressure ($p_{\text{det.}}$ = **3**: 246, **5**: 321, TNT: 216, PETN: 320, RDX: 349 kbar) and the energy of explosion ($\Delta_E U^\circ$ = **3**: -4060, **5**: -5157, TNT: 5227, PETN: 6190, RDX: 6125 kJ kg⁻¹).

For application of new energetic compounds important values for safety, handling and processing are the sensitivity data. All values were determined according to BAM standard methods described in the NATO STANAG 4487, 4489 and 4490 specifications for energetic materials.^[41-47]

Whereas the most promising compound **5** lacks the impact sensitivity (> 3 J) which is slightly below the commercial available PETN (3 J) and RDX (7.5 J), but is not as sensitive in terms of friction (**5**: > 192 N, RDX: > 120 N) and electrostatic discharge (**5**: > 0.3 J, RDX: > 0.1-0.2 J). The latter values are most important for handling and processing on an industrial scale and therefore compound **5** could be considered for application.

The most promising compound regarding to the sensitivity data is compound **3** which shows rather low sensitivity to friction (288 N), to impact (40 J) and to electrostatic discharge (0.3 J). According to the UN Recommendations on the Transport of Dangerous Goods compound **3** is regarded insensitive.^[48, 49]

Thermostability of energetic compounds is considered important especially in processing and storing the material. Because of the diverse use of energetic materials e.g. under extreme climatic conditions like in deserts, for oil drilling or military ammunition high temperature stability is desired. The introduced compounds **3** and **5** display good values for melting (**3**: 159 °C, **5**: 155 °C) and decomposition (**3**: 276 °C, **5**: 164 °C). Compound **5** melts at 155 °C and decomposes subsequently at 164 °C, whereas compound **3** shows a melting point at 159 °C followed by a wide liquid range of 110 °C and decomposes finally at 276 °C. The high difference between melting and decomposition point leaves compound **3** very suitable as melt cast explosive. Comparing compounds **3** and **5** to common explosives, they both exceed TNT (m.p. 80 °C, $T_{\text{dec.}}$ >160 °C) and compound **3** passes even RDX (m.p./ $T_{\text{dec.}}$ 210 °C) and PETN (m.p. 140 °C, $T_{\text{dec.}}$ 200 °C), regarding the thermal stability.

6.3 Conclusions

From this combined experimental and theoretical study the following conclusions have been drawn:

- 3,5-Diamino-1,2,4-triazole (**1**) can be protonated using diluted mineralic acids such as hydrochloric, nitric and perchloric acid. Its dinitramide salt can be synthesized by metathesis reaction of the perchlorate salt with potassium dinitramide. The obtained compounds 3,5-diamino-1,2,4-triazolium chloride hemihydrate (**2**), 3,5-diamino-1,2,4-triazolium nitrate (**3**) and 3,5-diamino-1,2,4-triazolium perchlorate (**4**), and 3,5-diamino-1,2,4-triazolium dinitramide (**5**) are air-stable, not hygroscopic colorless solids.
- All salts were be recrystallized from ethanol/water mixtures yielding single crystals, which were analyzed by X-ray diffraction. The salts crystallizes in common space groups (**2, 5**: $P2_1/n$, **3**: $P2_1/c$, **4**: $P-1$). All structures are dominated by a strong hydrogen-bond network.
- The energetic properties of **1–5** were determined and compared with trinitrotoluene (TNT), pentaerythrityl tetranitrate (PETN) and hexogen (RDX). The sensitivities towards impact, friction and electrostatic discharge were discovered. The sensitivities escalate from **1** to **5**. The dinitramide salt **5** is very sensitive towards impact (3 J) and moderately towards friction (192 N).
- The detonation parameters of **1, 3**, and **5** were calculated with the computer codes EXPLO5.03 and EXPLO5.04, respectively. The inputs were made based on calculated (CBS-4M) energies of formation and the X-ray densities.

6.4 Experimental Part

Caution: Although all 3,5-diamino-1,2,4-triazolium salts reported in this publication are rather stable against friction, impact and electric discharge, proper safety precautions should be taken when handling dinitramide salts. The derivatives are energetic materials and tend to explode under certain conditions, especially under physical stress. Laboratories and personnel should be properly grounded, and safety equipment such as Kevlar gloves, leather coats, face shields and ear plugs are recommended.

General. All chemical reagents, except 3,5-diamino-1,2,4-1*H*-triazole and ammonium dinitramide, and solvents were obtained from Sigma-Aldrich Inc. or Acros Organics (analytical grade) and were used as supplied. 3,5-diamino-1,2,4-1*H*-triazole was obtained from ABCR and ammonium dinitramide was supplied by EURENCO Bofors AB. Potassium dinitramide was prepared from ammonium dinitramide following known literature procedures.^[7a] ¹H, ¹³C{¹H}, and ¹⁴N NMR spectra were recorded on a JEOL Eclipse 400 instrument in DMSO-*d*₆ at or near 25 °C. The chemical shifts are given relative to tetramethylsilane (¹H, ¹³C) or nitromethane (¹⁴N) as external standards and coupling constants are given in Hertz (Hz). Infrared (IR) spectra were recorded on a Perkin-Elmer Spectrum BX FT-IR instrument equipped with an ATR unit at 25 °C. Transmittance values are qualitatively described as “very strong” (vs), “strong” (s), “medium” (m) and “weak” (w). Raman spectra were recorded on a Bruker RAM II spectrometer equipped with a Nd:YAG laser (1064 nm) and a reflection angle of 180°. The intensities are reported as percentages of the most intense peak and are given in parentheses. Elemental analyses were performed with a Netsch Simultaneous Thermal Analyzer STA 429. Melting points were determined by differential scanning calorimetry (Setaram DSC141 instrument, calibrated with standard pure indium and zinc). Measurements were performed at a heating rate of 5 °C/min in closed aluminum sample pans with a 1 μm hole in the top for gas release under a nitrogen flow of 20 mL/min with an empty identical aluminum sample pan as a reference. For initial safety testing, the impact and friction sensitivities as well as the electrostatic sensitivity were determined.^[48] The impact sensitivity tests were carried out according to STANAG 4489^[41] modified according to instruction^[44] using a BAM^[46] drophammer. The friction sensitivity tests were carried out according to STANAG 4487^[42] modified according to instruction^[45] using the BAM friction tester. The electrostatic sensitivity tests were carried according to STANAG 4490^[43] out using an electric spark testind device ESD 2010EN (OZM Research) operating with the “Winspark 1.15 software package”.^[48]

3,5-Diamino-1,2,4-triazole (**1**)

As obtained from ABCR.

DSC (5 °C min⁻¹): 205 °C (mp., onset); ¹H NMR: δ (ppm) = 10.68 (s, 1H, NH), 5.56 (s, 2H, NH₂), 4.68 (s, 2H, NH₂); ¹³C{¹H} NMR (D₆-DMSO): δ (ppm) = 161.8, 156.4; *m/z* (DEI) = 99.09 ([M]⁺); IS: > 40 J; FS: > 360 N; ESD: >1.5 J.

3,5-Diamino-1,2,4-triazolium chloride hemihydrate (**2**)

0.99 g (10 mmol) of 3,5-diamino-1,2,4-*H*-triazole was added with stirring to 10 mL (10 mmol) of 1 *M* hydrochloric acid solution. The resulting solution was heated slightly to 50 °C and was kept at this temperature for 10 minutes. After cooling to room temperature the solvent was evaporated completely and the white residue was recrystallized from water, yielding 1.34 g (99%) of pure **2** as white crystalline needles.

DSC (5 °C min⁻¹): 105 °C (mp., onset), 145 °C (-H₂O, onset), 282 °C (dec., onset); IR (ATR): 3328 (s), 3224 (s), 3157 (vs), 2899 (m), 2651 (m), 1690 (m), 1657 (s), 1651 (ms), 1646 (m), 1635 (m), 1352 (w), 1297 (w), 1160 (w), 1059 (w), 1011 (w), 794 (w), 711(w); Raman (1064 nm, 25 °C): 3322 (17), 3229 (24), 3181 (22), 1688 (75), 1657 (31), 1593 (15), 1568 (18), 1540 (12), 1455 (36), 1333 (26), 1305 (17), 1166 (28), 1071 (100), 1051 (65), 797 (50), 724 (16), 664 (74), 500 (33), 355 (42); ¹H NMR: δ (ppm) = 12.03 (s, br, 2H, NH), 7.07 (s, 4H, NH₂); ¹³C{¹H} NMR: δ (ppm) = 151.4; MS: FAB⁺ = 100.12 ([M]⁺), FAB⁻ = 34.95 ([Cl]⁻); EA:calcd.: C 16.62, H 4.88, N 48.45; found: C 16.74, H 4.58, N 48.21; IS: > 40 J; FS: 360 N; ESD: > 1.5 J.

3,5-Diamino-1,2,4-triazolium nitrate (**3**)

0.99 g (10 mmol) of 3,5-diamino-1,2,4-*H*-triazole was added with stirring to 5 mL (10 mmol) of 2 *M* nitric acid solution. The resulting solution was heated slightly to 50 °C and was kept at this temperature for 10 minutes. After cooling to room temperature the solvent was reduced to about one third of its original volume and the slightly yellow solution was left standing for crystallization. **3** separated from the solution over the course of one week, left standing on air, yielding 1.46 g (91%). Crystals of **3** suitable for X-ray diffraction measurements were obtained by recrystallization from a water/ethanol mixture (1:1).

DSC (5 °C min⁻¹): 159 °C (mp., onset), 276 °C (dec., onset); IR (ATR): 3792 (vw), 3423 (m), 3326 (m), 3282 (m), 3166 (m), 2936 (m), 2792 (m), 2688 (m), 1680 (s), 1662 (vs), 1612 (m), 1537 (w), 1425 (m), 1321 (s), 1297 (s), 1040 (w), 1010 (w), 812 (w), 794 (w), 716 (w), 657 (w); Raman (1064 nm, 25 °C): 3274 (7), 3175 (14), 1705 (20), 1689 (37), 1660 (22), 1601 (20), 1551 (7), 1468 (18), 1418 (11), 1354 (8), 1172 (16), 1076 (77), 1053 (100), 1042 (95), 1016 (51), 796 (32), 718 (26), 665 (65), 499 (15), 347 (26); ¹H NMR: δ (ppm) = 12.08 (s, br, 2H, NH), 6.97 (s, 4H, NH₂); ¹³C{¹H} NMR: δ (ppm) = 151.8; ¹⁴N NMR: δ (ppm) = -4 (NO₃⁻); MS: FAB⁺ = 100.09 ([M]⁺), FAB⁻ = 62.01 ([NO₃]⁻); EA: calcd.: C 14.82, H 3.73, N 51.84; found: C 15.07, H 3.57, N 51.64; IS: 40 J; FS: 288 N; ESD: 0.3 J.

3,5-Diamino-1,2,4-triazolium perchlorate (**4**)

0.99 g (10 mmol) of 3,5-diamino-1,2,4-*H*-triazole was added with stirring to 10 mL (10 mmol) of 1 M perchloric acid solution. After complete dissolution of **1**, the solvent was evaporated to dryness and the remaining white residue was recrystallized from hot ethanol, yielding 1.95 g (98%) of pure **4**. Crystals suitable for X-ray diffraction measurements were also obtained from hot ethanol.

DSC (5 °C min⁻¹): 185 °C (mp., onset), 252 °C, 294 °C, 335 °C (dec., onset); IR (ATR): 3561 (w), 3468 (m), 3455 (m), 3408 (s), 3366 (s), 3276 (m), 3216 (s), 3178 (s), 1672 (s), 1601 (m), 1541 (m), 1456 (m), 1344 (w), 1079 (s), 1050 (s), 1011 (m), 932 (w), 667 (w), 621 (w); Raman (1064 nm, 25 °C): 3460 (2), 3414 (4), 3369 (5), 3217 (6), 3176 (5), 1698 (18), 1664 (13), 1600 (14), 1458 (18), 1342 (7), 1170 (11), 1063 (26), 1016 (10), 935 (100), 797 (20), 667 (30), 630 (23), 491 (14), 470 (17), 453 (24), 343 (16); ¹H NMR: δ (ppm) = 11.93 (s, br, 2H, NH), 6.94 (s, 4H, NH₂); ¹³C{¹H} NMR: δ (ppm) = 151.8; MS: FAB⁺ = 100.10 ([M]⁺), FAB⁻ = 99.00 ([ClO₄]⁻); EA: calcd.: C 12.04, H 3.03, N 35.10; found: C 12.00, H 3.13, N 35.34; IS: 25 J; FS: 240 N; ESD: 0.8 J.

3,5-Diamino-1,2,4-triazolium dinitramide (**5**)

Aqueous solutions of 0.997 g (5 mmol) of **4** in 3 mL of water and 0.725 g (5 mmol) potassium dinitramide in 3 mL of water were combined under stirring, resulting in the formation of a yellow precipitate. The suspension was then stirred for an additional 15 minutes and the solvent was evaporated completely afterwards. The remaining yellow

(slightly wet) residue was extracted with 40 mL of ethanol. The ethanolic solution was concentrated to one fourth of its original volume and left for crystallization, yielding 0.86g (83%) of clean **5**. Crystals suitable for X-ray diffraction measurements were obtained from a wet ethanolic solution.

DSC (5 °C min⁻¹): 155 °C (mp., onset), 164 °C (dec., onset); IR (ATR): 3788 (vw), 3460 (w), 3425 (w), 3397 (m), 3319 (w), 3269 (m), 3180 (m), 3114 (m), 1707 (m), 1691 (m), 1652 (s), 1512 (s), 1469 (m), 1429 (m), 1342 (m), 1173 (vs), 1150 (s), 1054 (w), 1034 (m), 1004 (s), 960 (m), 815 (w), 799 (w), 761 (m), 723 (w), 688 (m), 673 (m); Raman (1064 nm, 25 °C): 3408 (3), 3346 (7), 3323 (6), 3284 (6), 3224 (5), 1699 (23), 1659 (19), 1607 (8), 1589 (9), 1544 (10), 1527 (9), 1470 (22), 1435 (13), 1326 (100), 1285 (20), 1213 (7), 1182 (17), 1151 (21), 1050 (51), 963 (27), 819 (53), 802 (22), 767 (7), 670 (30), 499 (35), 486 (18), 452 (10), 352 (25), 306 (23); ¹H NMR: δ (ppm) = 12.13 (s, br, 2H, NH), 6.94 (s, 4H, NH₂); ¹³C{¹H} NMR: δ (ppm) = 152.0; ¹⁴N NMR: δ (ppm) = -10 (N₃O₄⁻); MS: FAB⁺ = 100.10 ([M]⁺), FAB⁻ = 106.00 ([N₃O₄]⁻); EA:calcd.: C 11.65, H 2.93, N 54.36; found: C 11.46, H 2.80, N 53.93; IS: > 3 J; FS: 192 N; ESD: 0.3 J.

6.5 References

- [1] a) T. M. Klapötke, in *Moderne Anorganische Chemie*, E. Riedel (Hrsg.), 3. Aufl., Walter de Gruyter, Berlin, New York, **2007**, 99-104; b) R. P. Singh, R. D. Verma, D. T. Meshri, J. M. Shreeve, *Ang. Chem. Int. Ed.* **2006**, 45(22), 3584; c) T. M. Klapötke, in *High Energy Density Materials*, T. M. Klapötke (Hrsg.), Springer, Berlin, Heidelberg, **2007**, 85-122; d) R. D. Chapman, in *High Energy Density Materials*, T. M. Klapötke (Hrsg.), Springer, Berlin, Heidelberg, **2007**, 123-152.
- [2] a) Y.-H. Joo, J. M. Shreeve, *Angew. Chem. Int. Ed.* **2009**, 48, 564–567; (b) J. M. Veauthier, D. E. Chavez, B. C. Tappan, D. A. Parrish, *J. Energ. Mater.* **2010**, 28, 229–249; (c) T. M. Klapötke, M. Göbel, *Adv. Funct. Mater.* **2009**, 19, 347–365.
- [3] Y. N. Matyushin, T. S. Kon'kova, A. B. Vorob'ev, Y. A. Lebedev, *International Annual Conference of ICT* **2005**, 36th, 92/1-92/9.
- [4] a) T. M. Klapötke, J. Stierstorfer, *Dalton Transactions*, **2008**, 4, 643-653. (b) T. M. Klapötke, J. Stierstorfer, *New Trends in Research of Energetic Materials*, Proceedings of the Seminar, 11th, Pardubice, Czech Republic, **2008**, 2, 810-831.
- [5] N. Wingborg, N. V. Latypov, *Propellants, Explos., Pyrotech.* **2003**, 28(6), 314-318.
- [6] H. R. Blomquist, U.S. **1999**, 9 pp. US 6004410 A 19991221 CAN 132:24485 AN 1999:808506
- [7] a) K. O. Christe, W. W. Wilson, M. A. Petrie, H. H. Michels, J. C. Bottaro, R. Gilardi, *Inorg. Chem.* **1996**, 35, 5068-5071; b) V. A. Shlyapochnikov, M. A. Tafipolsky, I. V. Tokmakov, E. S. Baskir, O. V. Anikin, Yu.A. Strelenko, O. A.

- Luk'yanov, V. A. Tartakovsky, *J. Molec. Struct.* **2001**, 559, 147-166; c) J. C. Bottaro, P. E. Penwell, R. J. Schmitt, *Synth. Commun.* **1991**, 21, 945; d) O. A. Luk'yanov, V. P. Gorelik, V. A. Tartakovskii, *Russ. Chem. Bull.* **1994**, 43, 89.
- [8] R. Gilardi, R. J. Butcher *J. Chem. Cryst.* **2002**, 32(11), 477-484.
- [9] M. E. Sitzmann, R. Gilardi, R. J. Butcher, W. M. Koppes, A. G. Stern, J. S. Trasher, N. J. Trivedi, Z.-Y. Yang, *Inorg. Chem.* **2000**, 39, 843-850.
- [10] N. B. Bolotina, M. J. Hardie, A. A. Pinkerton, *J. Appl. Crystallogr.* **2003**, 36(6), 1334-1341.
- [11] a) H. Östmark, U. Bemm, H. Bergman, A. Langlet, *Thermochim. Acta* **2002**, 384, 253-259; b) P. B. Kempa, M. Herrmann, I. Fuhr, H. Östmark, International Annual Conference of ICT, 40th, **2009**, 40/1-40/11.
- [12] T. M. Klapötke, J. Stierstorfer, *Phys. Chem. Chem. Phys.* **2008**, 10, 4340-4346.
- [13] a) V. P. Sinditskii, A. I. Levshenkov, V. Y. Egoroshev, V. V. Serushkin, Proceedings of the Seminar, 7th, Pardubice, Czech Republic, **2004**, 2, 649-658. b) C. J. Hinshaw, R. B. Wardle, T. K. Highsmith, U.S. patent **1998**, US 5741998, A 19980421.
- [14] T. M. Klapötke, J. Stierstorfer, *Eur. J. Inorg. Chem.* **2008**, 26, 4055-4062.
- [15] K. Karaghiosoff, T. M. Klapötke, P. Mayer, C. M. Sabate, A. Penger, J. M. Welch, *Inorg. Chem.* **2008**, 47, 1007-1019.
- [16] a) T. M. Klapötke, P. Mayer, A. Schulz, J. J. Weigand, *J. Am. Chem. Soc.* **2005**, 127(7), 2032-2033; b) G. Fischer, G. Holl, T. M. Klapötke, P. Mayer, J. J. Weigand, New Trends in Research of Energetic Materials, Proceedings of the Seminar, 8th, Pardubice, Czech Republic, 2005, 1, 190-199.
- [17] J. J. Weigand, *Dissertation*, Ludwig Maximilian University Munich, **2005**.
- [18] CrysAlis CCD, Oxford Diffraction Ltd., Version 1.171.27p5 beta (release 01-04-2005 CrysAlis171 .NET).
- [19] CrysAlis RED, Oxford Diffraction Ltd., Version 1.171.27p5 beta (release 01-04-2005 CrysAlis171 .NET).
- [20] A. Altomare, G. Cascarano, C. Giacovazzo, A. Guagliardi, SIR-92, A program for crystal structure solution, *J. Appl. Cryst.* **1993**, 26, 343.
- [21] G. M. Sheldrick, **1997**, *SHELXL-97*, Program for the Refinement of Crystal Structures. University of Göttingen, Germany.
- [22] L. J. Farrugia, WinGX suite for small molecule single-crystal crystallography, *J. Appl. Cryst.* **1999**, 32, 837-838.
- [23] A. L. Spek, **1999**, Platon, A Multipurpose Crystallographic Tool, Utrecht University, Utrecht, The Netherlands.
- [24] Crystallographic data for the structure(s) have been deposited with the Cambridge Crystallographic Data Centre. Copies of the data can be obtained free of charge on application to The Director, CCDC, 12 Union Road, Cambridge CB2 1EZ, UK (Fax: int.code (1223)336-033; e-mail for inquiry: fileserv@ccdc.cam.ac.uk; e-mail for deposition: deposit-@ccdc.cam.ac.uk).
- [25] G. L. Starova, O. V. Frank-Kamenetskaya, E. F. Shibanova, V. A. Lopyrev, M. G. Voronkov, V. V. Makarskii, *Chem. Heterocyclic Comp.* **1979**, 15(10), 1149-1150.

- [26] M. Bichay, J. W. Fronabarger, R. Gilardi, R. J. Butcher, W. B. Sanborn, M. E. Sitzmann, M. D. Williams, *Tetrahedron Lett.* **2006**, *47*, 6663-6666.
- [27] M. v. Denffer, T. M. Klapotke, G. Kramer, G. Spies, J. M. Welch, G. Heeb, *Propellants, Explos. Pyrotech.* **2005**, *30(3)*, 191-1195.
- [28] J. Bernstein, R. E. Davis, L. Shimoni, N.-L. Chang, *Angew. Chem. Int Ed.* **1995**, *34*, 1555-1573.
- [29] RPluto - Graphical Display of Molecular and Crystal Structures. RPluto, The Cambridge Crystallographic Data Centre. **2004**.
- [30] T. M. Klapotke, C. M. Sabaté, J. Stierstorfer, *Z. Anorg. Allg. Chem.* **2008**, *634*, 1867-1874.
- [31] M. J. Frisch et al., Gaussian 03, Revision B04, Gaussian Inc., Wallingford, CT, **2004**.
- [32] a) J. W. Ochterski, G. A. Petersson, and J. A. Montgomery Jr., *J. Chem. Phys.* **1996**, *104*, 2598; b) J. A. Montgomery Jr., M. J. Frisch, J. W. Ochterski G. A. Petersson, *J. Chem. Phys.* **2000**, *112*, 6532.
- [33] a) L. A. Curtiss, K. Raghavachari, P. C. Redfern, J. A. Pople, *J. Chem. Phys.* **1997**, *106(3)*, 1063; b) E. F. C. Byrd, B. M. Rice, *J. Phys. Chem. A* **2006**, *110(3)*, 1005–1013; c) B. M. Rice, S. V. Pai, J. Hare, *Comb. Flame* **1999**, *118(3)*, 445–458.
- [34] <http://webbook.nist.gov/chemistry/>
- [35] a) M. S. Westwell, M. S. Searle, D. J. Wales, D. H. Williams, *J. Am. Chem. Soc.* **1995**, *117*, 5013-5015; b) F. Trouton, *Philos. Mag.* **1884**, *18*, 54–57.
- [36] a) H. D. B. Jenkins, H. K. Roobottom, J. Passmore, L. Glasser, *Inorg. Chem.* **1999**, *38(16)*, 3609–3620; b) H. D. B. Jenkins, D. Tudela, L. Glasser, *Inorg. Chem.* **2002**, *41(9)*, 2364–2367.
- [37] a) M. Sućeska, EXPLO5.3 program, Zagreb, Croatia, **2009**; b) M. Sućeska, EXPLO5.4 program, Zagreb, Croatia, **2010**.
- [38] a) M. Sućeska, *Materials Science Forum*, **2004**, 465-466, 325–330; b) M. Sućeska, *Propellants, Explos., Pyrotech.* **1991**, *16*, 197–202; c) M. Sućeska, *Propellants, Explos., Pyrotech.* **1999**, *24*, 280–285; d) M. L. Hobbs, M. R. Baer, *Proc. of the 10th Symp. (International) on Detonation*, ONR 33395-12, Boston, MA, July 12–16, 1993, p. 409.
- [39] Calculation of oxygen balance: Ω (%) = $(wO - 2xC - 1/2yH - 2zS)1600/M$. (w: number of oxygen atoms, x: number of carbon atoms, y: number of hydrogen atoms, z: number of sulfur atoms, M: molecular weight).
- [40] J. Köhler, R. Meyer, in „Explosivstoffe“ 9th edn., Wiley-VCH, Weinheim, **1998**.
- [41] NATO standardization agreement (STANAG) on explosives, impact sensitivity tests, no. 4489, 1st ed., Sept. 17, **1999**.
- [42] NATO standardization agreement (STANAG) on explosive, friction sensitivity tests, no. 4487, 1st ed., Aug. 22, **2002**.
- [43] NATO standardization agreement (STANAG) on explosive, electrostatic discharge sensitivity tests, no. 4490, 1st ed., Feb. 19, **2001**.
- [44] WIWEB-Standardarbeitsanweisung 4-5.1.02, Ermittlung der Explosionsgefährlichkeit, hier der Schlagempfindlichkeit mit dem Fallhammer, Nov. 8, **2002**.

-
- [45] WIWEB-Standardarbeitsanweisung 4-5.1.03, Ermittlung der Explosionsgefährlichkeit oder der Reibeempfindlichkeit mit dem Reibeapparat, Nov. 8, **2002**.
- [46] <http://www.bam.de>
- [47] Impact: Insensitive > 40 J, less sensitive ≥ 35 J, sensitive ≥ 4 J, very sensitive ≤ 3 J; friction: Insensitive > 360 N, less sensitive = 360 N, sensitive < 360 N a. > 80 N, very sensitive ≤ 80 N, extreme sensitive ≤ 10 N; According to the UN Recommendations on the Transport of Dangerous Goods (+) indicates: not safe for transport.
- [48] a) <http://www.ozm.cz/testing-instruments/small-scaleelectrostatic-discharge-tester.htm>; b) V. Pelikán, OZM research, Czech Republic, private communication.
- [49] a) REICHEL & PARTNER GmbH, <http://www.reichelt-partner.de>; b) Test methods according to the UN Recommendations on the Transport of Dangerous Goods, Manual of Test and Criteria, fourth revised edition, United Nations Publication, New York and Geneva, **2003**, ISBN 92-1-139087-7, Sales No. E.03.VIII.2; 13.4.2 Test 3(a) (ii) BAM Fallhammer.

7. Nitraminoazoles based on ANTA – A comprehensive study of structural and energetic properties

Thomas M. Klapötke, Franz A. Martin and Sandra Wiedbrauk

As submitted to: European Journal of Inorganic Chemistry 2011.

7.1 Introduction

Nitrogen rich heterocycles have been used for the development of new energetic materials over the last decades.^[1] The most prominent examples in this field are the highly used explosives hexahydro-1,3,5-trinitro-1,3,5-triazine (RDX) and octahydro-1,3,5,7-tetranitro-1,3,5,7-tetrazocine (HMX) which discovery promoted the research activities on related compounds.^[1b] The research on these materials is not only focused on a single heterocyclic system but includes all kinds of five membered ring systems with either nitrogen or oxygen as hetero atoms and also six membered heterocyclic ring systems. Many nitrogen rich as well as oxygen rich ionic compounds have been prepared which have been published recently by Shreeve *et al.* as an extensive review.^[2] Heterocyclic systems have been studied in our group over the last couple of years with growing interest.^[3]

The efforts in the synthesis of modern energetic materials starting with triazoles as backbone molecules have been intensified since triazoles, especially 1,2,4-triazoles, show a perfect balance between thermal stability and high positive heats of formation, required for the application as prospective HEDMs. Even though the heats of formation are larger for tetrazoles ($\Delta H_f^0 = + 237.2 \text{ kJ mol}^{-1}$)^[4] as well as 1,2,3-triazoles ($\Delta H_f^0 = + 272 \text{ kJ mol}^{-1}$),^[5] 1,2,4-triazoles ($\Delta H_f^0 = + 109 \text{ kJ mol}^{-1}$)^[6] are better suited for the buildup of energetic materials, since they have less catenated nitrogen atoms, which makes them overall more stable towards outer stimuli. Examples for these kind of molecules are 5-amino-3-nitro-1*H*-1,2,4-triazole (ANTA),^[7] triaminoguanidinium 3,5-dinitro-1,2,4-triazolate,^[8] 3-nitro-5-triazolone (NTO)^[9] or also azo bridged compounds like 5,5'-dinitro-3,3'-azo-1,2,4-triazole (DNAT)^[10] or 5,5'-dinitrimino-3,3'-azo-1,2,4-triazole (DNAAT)^[11] and their corresponding nitrogen rich salts. The thermal stability values for these materials are all remarkably high with decomposition taking place well above 200 °C together with low sensitivity values. *N*-bound nitramines are known for the triazoles series, e.g. 1-

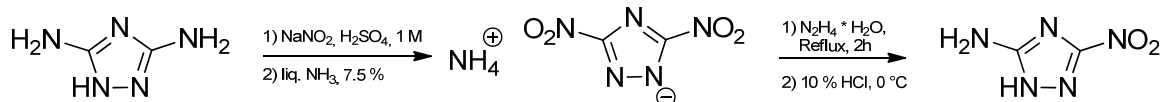
nitramino-1*H*-1,2,3-triazole and 4-nitramino-1*H*-1,2,4-triazole which decompose well below 200 °C, at 105 °C and 179 °C, respectively.^[12] Since *N*-bound nitramines bound to directly linked chains of nitrogen atoms often show low decomposition temperatures and high sensitivities, we took the chance to investigate the characteristics of nitraminoazoles carrying the nitramine group connected to the carbon atoms of 1,2,4-triazoles. To increase the oxygen balance of the molecules, the introduction of a nitro group at the second carbon atom seemed to be a good compromise between stability and performance, since 3,5-bisnitramino-1,2,4-triazole is not known as a neutral compound and its nitrogen rich salts with aminoguanidinium or guanidinium cations decompose at temperatures around 170 °C.^[13] 3-Nitro-5-nitramino-1*H*-1,2,4-triazole was published in literature, but has only been characterized by means of UV absorption and IR spectroscopy and no sensitivity data are presented.^[14]

Hence we present a new synthetic route yielding 3-nitro-5-nitramino-1*H*-1,2,4-triazole in good overall yields compared to the known literature procedure and also focus on the synthesis and full characterization of its 1-methylated derivative, not yet known and described in literature. Additionally, high nitrogen rich mono and double salts of 3-nitro-5-nitramino-1*H*-1,2,4-triazole and 1-methyl-5-nitramino-3-nitro-1,2,4-triazole have been synthesized, fully characterized and examined regarding their potential application as new thermally stable energetic materials.

7.2 Results and Discussion

7.2.1 Synthesis

The synthetic route towards 3-nitro-5-nitramino-1*H*-1,2,4-triazole (**1**) started from 3,5-diamino-1*H*-1,2,4-triazole (DAT). At first, ammonium 3,5-dinitro-1,2,4-triazolate (NH_4^+ DNT⁻) was prepared on a laboratory scale with 65 % yield according to modified literature procedures.^[15] NH_4^+ DNT⁻ was then converted to 3-amino-5-nitro-1*H*-1,2,4-triazole (ANTA) via the route presented earlier by K.-Y. Lee (Los Alamos National Laboratories) by selective reduction of one nitro group with an excess of hydrazine monohydrate and subsequent neutralization with 10 % hydrochloric acid in 94 % yield (Scheme 1).^[16]



Scheme 1: Synthetic pathway towards 3-amino-5-nitro-1H-1,2,4-triazole (ANTA).

Since NH₄⁺ DNT⁻ was also prepared on industrial scale before, a better value of 89 % for the overall yield of ANTA can be achieved than compared to 61 % on the laboratory scale. 3-Nitro-5-nitramino-1H-1,2,4-triazole (**1**) was prepared by the nitration of ANTA using a nitration mixture of concentrated sulfuric acid and 100 % nitric acid in a molar ratio of 3:1 yielding pure **1** in 76 % yield after quenching of the reaction mixture with ice water and subsequent extraction with ethyl acetate. The overall yield of **1**, starting from DAT is 46 % on the laboratory scale, while an increase to 68 % is easily achievable on an industrial scale. (Lit.^[14] yield: 38 %)

Care has to be taken, that the reaction temperature never drops below 0 °C for the nitration of ANTA, otherwise 3-diazo-5-nitro-1,2,4-triazole is formed by the attack of an *in situ* formed NO⁺ cation as a by product in yields of 10 – 40 %. 3-Diazo-5-nitro-1,2,4-triazole was prepared earlier by Russian chemists^[17] and shows an extremely high sensitivity towards friction, impact and, especially, electrostatic discharge (< 15 mJ !). Nevertheless we were able to determine its structural properties. The asymmetric unit of this compound is shown in Figure 1.

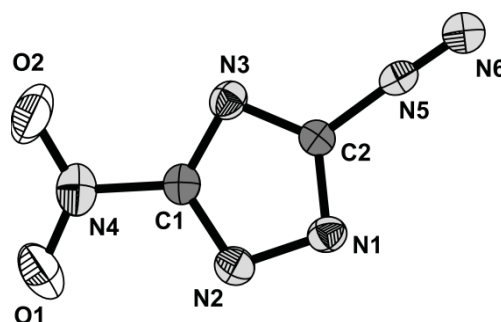
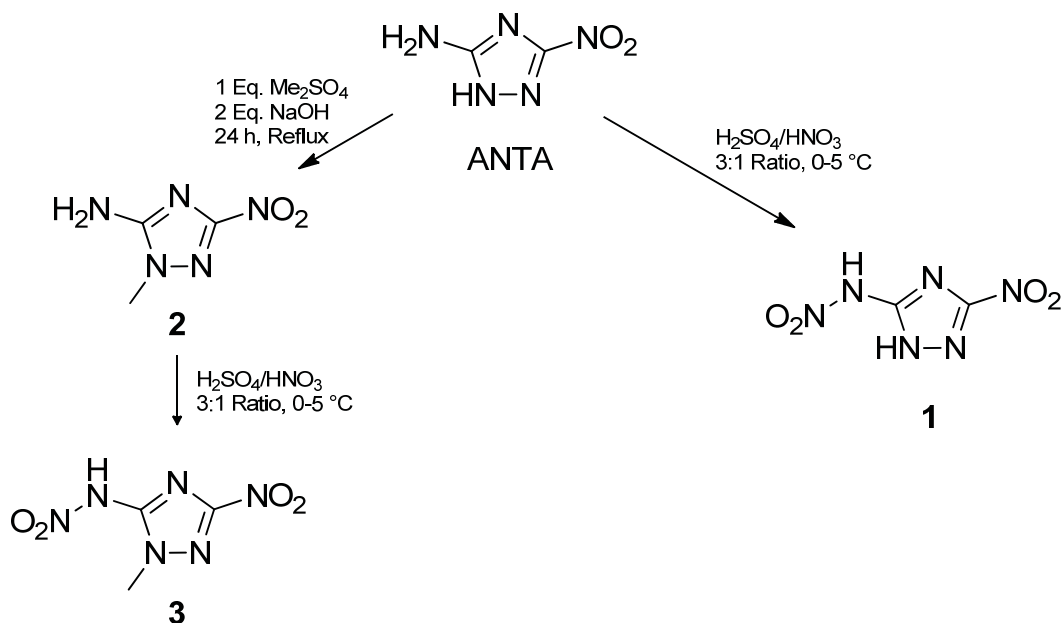


Figure 1: Asymmetric unit of 3-diazo-5-nitro-1,2,4-triazole as formed in the reaction of **1** as a side product.

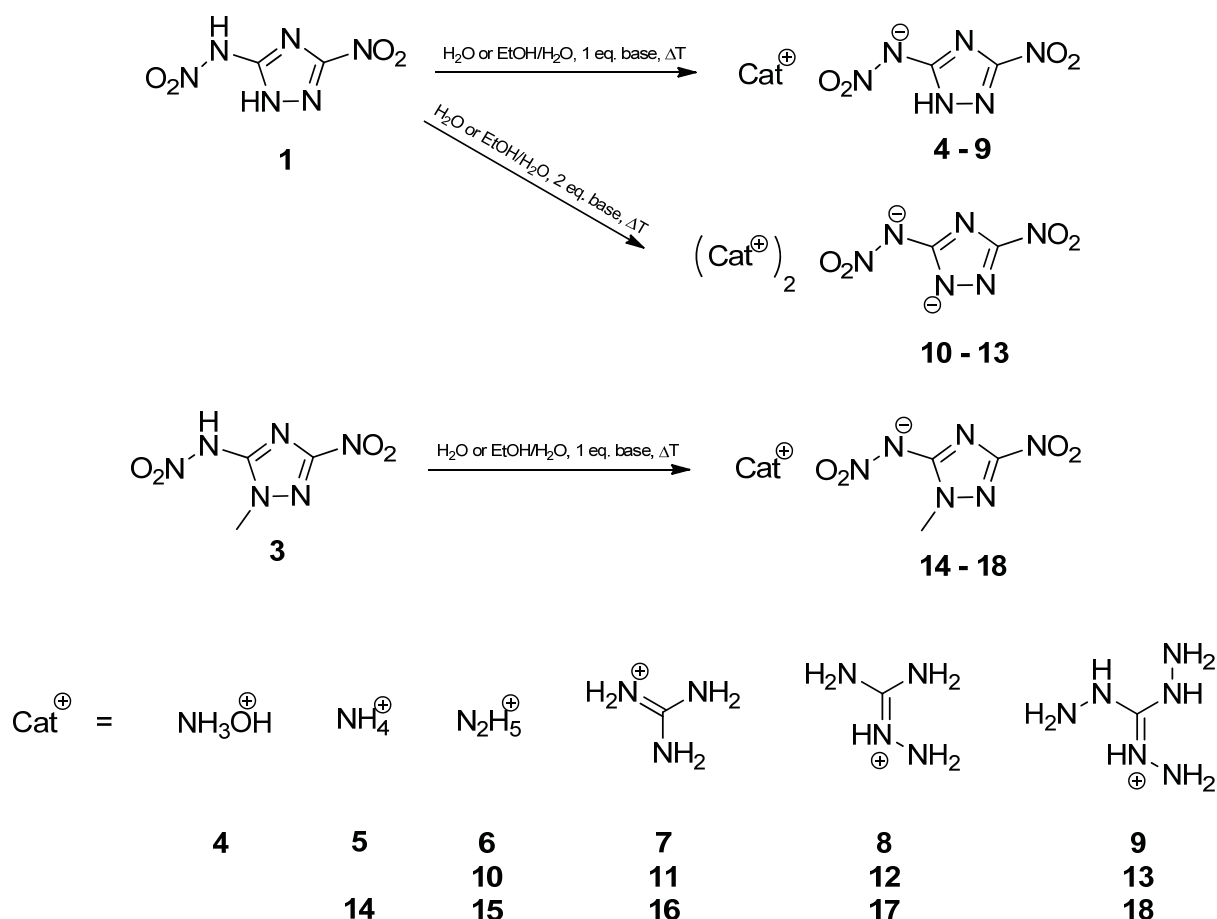
5-Amino-1-methyl-3-nitro-1,2,4-triazole (**2**) was also prepared starting from ANTA using one equivalent of dimethyl sulfate and two equivalents of a 2 M sodium hydroxide solution. Many reaction conditions and ratios have been tested for this reaction, with the 1:2 ratio of dimethyl sulfate and sodium hydroxide serving us best in terms of yield and

also purity.^[18] Compound **2** was nitrated to form 1-methyl-5-nitramino-3-nitro-1,2,4-triazole (**3**) the same reaction conditions applied as for the nitration of compound **1**. The reaction pathways for **1**, **2** and **3** are shown in Scheme 2.



Scheme 2: Reactions pathways for the formation of 3-nitro-5-nitramino-1*H*-1,2,4-triazole (**1**), 5-amino-1-methyl-3-nitro-1,2,4-triazole (**2**) and 1-methyl-5-nitramino-3-nitro-1,2,4-triazole (**3**) starting from ANTA.

The formation of the nitrogen rich salts of **1** and **3** was performed straightforward. Aqueous solutions or, in the case of triaminoguanidine, ethanolic solutions of **1** and **3** were prepared and the corresponding nitrogen rich bases were added in the desired molar ratio, either in 1:1 ratio for the mono salts or in 1:2 ratio for the double salts and reacted at elevated temperature between 65 °C and 90 °C. Not all bases were capable of the formation of the double salts of **1**. While the formation worked well with bis(guanidinium) carbonate, aminoguanidinium bicarbonate and triaminoguanidine, conversion to the double salts was not possible for ammonia and hydroxylamine, even with an excess of the corresponding base. The formation of bis(hydrazinium) 3-nitro-5-nitramino-1*H*-1,2,4-triazolate (**10**) is only favored due to the precipitation from small amounts of water. We were only able to obtain **10** as an amorphous powder precipitating from the reaction mixture. The compound was unstable, always forming the mono hydrazinium salt of **1** when recrystallized from larger amounts of water. The synthetic pathways towards the formation of the nitrogen rich salts are shown in Scheme 3.



Scheme 3: Synthetic pathways towards the formation of nitrogen rich salts of **1** and **2** using the corresponding bases.

7.2.2 Molecular structures

Single crystal X-ray diffraction studies have been undertaken for compounds **1**, **3**, **4 – 7**, **9**, **11**, **12** and **18**. While **1** and **3** have been recrystallized from ethyl acetate as light yellow blocks and colorless plates, respectively, the nitrogen rich salts **4 – 7**, **9**, **11**, **12** and **18** have been recrystallized from ethanolic solutions or water. Selected crystallographic data for all compounds have been compiled in Table S1 (Appendix 12.6). At first, an evaluation of the geometric parameters is undertaken regarding the molecular structure of the neutral compounds **1** and **3** and the corresponding mono and double deprotonated anions, NANTA⁻, NANTA²⁻ and MeNANTA⁻, respectively. The effects of methylation and deprotonation are investigated. Selected bond lengths, bond angles and torsion angles of compounds **1**, **3**, **5 – 7**, **9**, **11**, **12** and **18** are compiled in Table 1. Additionally, the crystal structures and packing schemes of the neutral compounds, 5-nitramino-3-nitro-1*H*-1,2,4-triazole (**1**) and 1-methyl-5-nitramino-3-nitro-1,2,4-triazole (**3**) are discussed in

detail. Only one example for each ionic compound is presented, regarding mono and double deprotonated anions of **1** and the anion of **3**. Since we were able to obtain water free crystal structures of the guanidinium (**7**) and bis(guanidinium) (**11**) salts of **1**, these two compounds are discussed in detail and compared. This is also of interest since only the deprotonation state of the anion changes, but not the cation. During the course of this study we were able to obtain crystal structures of nearly all ionic compounds of **1**, but could only obtain the crystal structure of the triaminoguanidinium salt (**18**) of **3**. Even though different solvents and crystallization methods were used only heavily twinned crystals (**14**, **15**) or crystals too small for measurement (**16**, **17**) were obtained. Hence, finally the crystal structure of triaminoguanidinium 1-methyl-5-nitramino-3-nitro-1,2,4-triazolate (**18**) is discussed as the only example for the ionic compounds of **3**. The hydrogen bonds present in compounds **4** – **6**, **9** and **12**, not discussed in detail, are compiled in Tables S2 – S6 (Appendix 12.6).

No difference is observed for the 1,2,4-triazole system when compared to other heterocyclic ring systems. The bond lengths within the triazole ring in the molecular structure of **1** are all in between the length of formal C–N and N–N single and double bonds (C–N: 1.47 Å, 1.22 Å; N–N: 1.48 Å, 1.20 Å)^[19] with C₁–N₂ (1.319(5) Å) being the shortest and N₁–N₂ (1.365(5) Å) showing the most single bond character. The C₁–N₄ bond shows a length of 1.455(6) Å and is therefore considered a single bond, which also affects the N₂–C₁–N₃ bond angle, which is 117.3(4)°, close to 120° (sp² hybridization of C₁). On the other hand, the N₃–C₂–N₁ bond angle is only 111.6(5)°, hence the C₂–N₅ bond is also very short with only 1.364(6) Å, showing double bond character. The N₅–N₆ bond of the nitramine moiety is in contrast very long, being 1.381(5) Å. The C₂–N₅–N₆ bond angle is also very wide, being 123.7(4)°. The N–O bonds within the compound show double bond character and bond lengths between 1.215(4) Å (N₄–O₂) and 1.233(4) Å (N₆–O₃). The O–N–O bond angles are both bigger than 120° at 126.7(4)° (O₁–N₄–O₂) and 126.1(5)° (O₃–N₆–O₄). The nitramine moiety is only slightly twisted out of plane of the triazole ring at –9.0(7)° (N₁–C₂–N₅–N₆). The whole structure of the nitramine group with unusual bond lengths and angles is a result of the formation of a very strong hydrogen bond N₁–H₁⋯O₃, keeping the nitramine group within the plane of the triazole ring due to the formation of a six membered ring. (Figure 2)

While most of the bond lengths and angles show only slight deviations from the ones observed for **1** in the molecular structure of **3**, the bonding situation of the nitramine has changed dramatically. The bond lengths of C₂–N₅ and N₅–N₆ are turned upside down,

with C₂–N₅ being the longer bond (1.389(3) Å) and N₅–N₆ being the shorter bond (1.363(3) Å) as usually expected for the nitramine moiety.

Table 1: Selected bond lengths[Å], bond angles [°] and torsion angles [°] of compounds **1**, **3**, **5**–**7**, **9**, **11**, **12** and **18**.

	NANTA (1)	NH ₄ ⁺ NANTA ⁻ (5)	N ₂ H ₅ ⁺ NANTA ⁻ (6)	G ⁺ NANTA ⁻ (7)	TAG ⁺ NANTA ⁻ (9)	(G ⁺) ₂ NANTA ²⁻ (11)	(AG ⁺) ₂ NANTA ²⁻ (12)	MeNANTA (3)	TAG ⁺ MeNANTA ⁻ (18)
N1–N2	1.365(5)	1.361(2)	1.362(2)	1.358(3)	1.356(3)	1.361(3)	1.362(2)	1.353(3)	1.358(2)
N2–C1	1.319(5)	1.312(2)	1.313(2)	1.313(3)	1.307(3)	1.322(3)	1.314(2)	1.326(3)	1.311(2)
C1–N3	1.340(5)	1.335(2)	1.334(2)	1.345(3)	1.336(3)	1.341(3)	1.344(2)	1.331(3)	1.343(2)
N3–C2	1.326(6)	1.341(2)	1.342(2)	1.342(3)	1.342(3)	1.345(3)	1.346(2)	1.322(3)	1.346(2)
N1–C2	1.341(5)	1.360(2)	1.351(2)	1.345(3)	1.352(3)	1.359(3)	1.353(2)	1.347(3)	1.364(2)
C1–N4	1.455(6)	1.455(2)	1.449(2)	1.448(4)	1.445(3)	1.433(3)	1.446(2)	1.456(4)	1.446(2)
N4–O1	1.231(4)	1.223(2)	1.225(2)	1.220(2)	1.224(3)	1.234(3)	1.224(2)	1.220(3)	1.236(2)
N4–O2	1.215(4)	1.223(2)	1.218(2)	1.231(3)	1.222(3)	1.230(3)	1.232(2)	1.225(3)	1.223(2)
C2–N5	1.364(6)	1.373(2)	1.369(2)	1.374(3)	1.360(3)	1.395(3)	1.392(2)	1.389(3)	1.361(2)
N5–N6	1.381(5)	1.309(2)	1.314(2)	1.311(3)	1.325(3)	1.292(3)	1.290(2)	1.363(3)	1.325(2)
N6–O3	1.233(4)	1.244(2)	1.247(2)	1.267(3)	1.246(3)	1.263(3)	1.263(2)	1.222(3)	1.257(2)
N6–O4	1.220(4)	1.279(2)	1.265(2)	1.257(3)	1.261(3)	1.288(3)	1.285(2)	1.227(3)	1.250(2)
N1–H1 (CH ₃)	0.77(4)	0.91(2)	0.94(3)	0.82(3)	0.83(3)	--	--	1.451(3)	1.453(2)
N5–H5	0.78(4)	--	--	--	--	--	--	0.89(3)	--
N1–N2–C1	101.3(4)	101.1(1)	100.7(2)	100.3(2)	100.1(2)	103.5(2)	104.0(2)	100.2(2)	100.2(2)
N2–C1–N3	117.3(4)	118.0(1)	118.1(2)	118.1(3)	118.6(2)	117.5(2)	117.4(2)	118.1(3)	119.0(2)
C1–N3–C2	101.0(4)	101.6(1)	101.6(2)	101.0(2)	101.5(2)	99.3(2)	98.9(2)	100.8(2)	101.0(2)
N1–C2–N3	111.6(5)	109.5(1)	109.4(2)	109.6(2)	108.7(2)	113.7(2)	114.1(2)	111.0(2)	109.1(2)
C2–N1–N2	108.8(4)	109.8(1)	110.3(2)	110.9(2)	111.1(2)	106.1(2)	105.6(2)	109.8(2)	110.8(1)
N2–C1–N4	121.2(4)	120.5(1)	120.4(2)	119.0(2)	119.7(2)	120.1(2)	120.1(2)	119.1(3)	119.9(2)
O1–N4–O2	126.7(4)	125.5(1)	125.1(2)	124.9(3)	124.0(2)	122.4(2)	123.6(2)	125.6(3)	124.4(2)
N1–C2–N5	127.4(5)	131.9(1)	132.5(2)	130.4(3)	132.2(3)	114.5(2)	114.1(2)	122.2(3)	115.5(2)
C2–N5–N6	123.7(4)	117.0(1)	116.9(2)	116.0(2)	116.9(2)	119.1(2)	118.9(2)	119.3(2)	116.9(2)
O3–N6–O4	126.1(5)	120.6(1)	120.9(2)	119.2(3)	121.1(2)	119.3(2)	118.8(2)	126.8(3)	120.5(2)
N2–C1–N4–O1	1.1(5)	2.5(2)	1.6(3)	-0.1(5)	-3.0(3)	3.9(4)	3.1(3)	-2.3(4)	5.0(2)
N1–C2–N5–N6	-9.0(7)	2.1(2)	-0.9(3)	3.9(5)	-2.5(4)	-167.3(2)	-178.7(2)	-72.3(3)	-179.9(2)

The $C_2-N_5-N_6$ angle is narrowed to $119.3(2)^\circ$ presenting the perfect angle for a sp^2 hybridized nitrogen atom (N_5). The difference is a result of the introduction of the methyl group in 1 position, preventing the nitramine group oxygen O_3 to form the six membered ring pattern due to the formation of a hydrogen bond. The nitramine group is hence twisted out of plane of the triazole ring by $-72.3(3)^\circ$ ($N_1-C_2-N_5-N_6$).

The deprotonation of the molecules shows different results. While the first deprotonation of **1** shows nearly no deviations within the bond lengths of the triazole ring, the N_5-N_6 bond is shortened by 0.066 \AA (mean value) while the N_6-O_3 and N_6-O_4 bonds are elongated by 0.018 \AA and 0.46 \AA , respectively. The bond angles within the triazole ring and towards the nitro group (N_4) differ also only slightly, while the $N_1-C_2-N_5$ angle is widened by 4.4° (mean value) and at the same time the $C_2-N_5-N_6$ angle is narrowed by 7° (mean value), being now smaller than 120° . The $O_3-N_6-O_4$ angle is also narrowed by 5.7° (mean value), being close to 120° . The nitramine group is now perfectly in the plane of the triazole ring with torsion angles between $-2.5(4)^\circ$ and $3.9(5)^\circ$ for $N_1-C_2-N_5-N_6$.

The second deprotonation step, as observed in **11** and **12**, really affects the structure. As observed before, the bond lengths and angles within the triazole ring and towards the nitro group change only slightly. The biggest change, however, is again observed for the nitramine group. The C_2-N_5 bond is again elongated to app. 1.40 \AA and therefore even closer to the formal single bond (1.47 \AA),^[19] while the N_5-N_6 bond is again shortened to app. 1.29 \AA , being closer to a formal double bond (1.20 \AA). As a counter reaction, both $N-O$ bonds are elongated by app. 0.2 \AA , due to the higher electron density within the system. The mean value for both bond angles, $C_2-N_5-N_6$ and $O_3-N_6-O_4$, is now 119° , nearly perfect for planar sp^2 hybridized atoms. For both compounds **11** and **12**, respectively, a reorientation of the nitramine group is observed, now showing $N_1-C_2-N_5-N_6$ torsion angles of $-167.3(2)^\circ$ and $-178.7(2)^\circ$, a flip of the nitro group by 180° .

Nearly the same pattern is observed for the 1-methyl-5-nitramino-3-nitro-1,2,4-triazolate anion in **18**. While the C_2-N_5 bond is shorter ($1.361(2) \text{ \AA}$), the N_5-N_6 bond is much longer ($1.325(2) \text{ \AA}$). Both $N-O$ bonds are elongated compared to **3** by 0.3 \AA (mean value) and the $O_3-N_6-O_4$ angle is $120.5(2)^\circ$. The nitramine group however shows the same orientation as observed for the double deprotonated anions of **1**, with a $N_1-C_2-N_5-N_6$ torsion angle of $-179.9(2)^\circ$, perfectly in plane with the triazole ring, but pointing away from N_1 .

5-Nitramino-3-nitro-1*H*-1,2,4-triazole (**1**) crystallizes in the monoclinic space group $P2_1$ with a cell volume of $298.38(5) \text{ \AA}^3$ and two molecular moieties in the unit cell. The

calculated density at 173 K is 1.938 g cm^{-3} and hence well above the density of the educt (ANTA, 1.841 g cm^{-3}). The asymmetric unit of **1** together with the atom labels is presented in Figure 2.

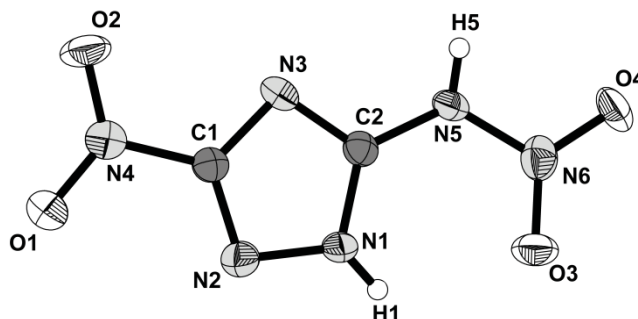


Figure 2: Asymmetric unit of **1**. Thermal ellipsoids are set to 50 % probability.

The strongest hydrogen bond $\text{N}_1\text{-H}_1\cdots\text{O}_3$ keeps, as mentioned before, the nitramine group in plane with the triazole ring. The $\text{D-H}\cdots\text{A}$ is only $118(4)^\circ$ but the $\text{D}\cdots\text{A}$ length is very short with $2.628(6) \text{ \AA}$ and hence we can consider it a mostly electrostatic but moderately strong hydrogen bond. Four individual hydrogen bonds are present building up the crystal structure. Again we have two sets of bifurcated hydrogen bonds with N_1 and N_5 functioning as donor atoms. Two of the bonds are weak with very long $\text{H}\cdots\text{A}$ distance of $2.72(4) \text{ \AA}$ ($\text{N}_1\text{-H}_1\cdots\text{O}_1(\text{i})$) and $2.51(4) \text{ \AA}$ ($\text{N}_5\text{-H}_5\cdots\text{O}_2(\text{ii})$). The two remaining bonds are moderately strong with $\text{D}\cdots\text{A}$ distances $< 3 \text{ \AA}$. The molecules are twisted against one another with angles of 70.64° forming infinite rows, which are then again connected by the next set of hydrogen atoms, forming zigzag layers, presenting the same angle of 70.64° in between (Figure 3).

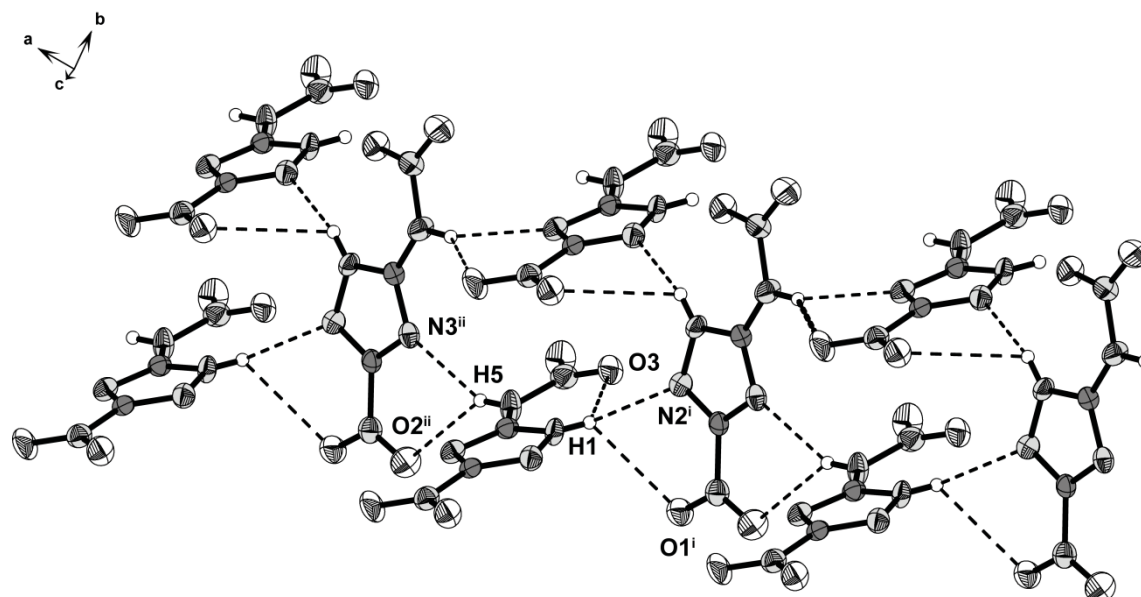


Figure 3: Hydrogen bonding scheme within the crystal structure of **1**, displaying the formation of infinite rows. Thermal ellipsoids are set to 50 % probability. Symmetry Operators: (i) $-x+2, y+1/2, -z+1$; (ii) $-x+1, y+1/2, -z$.

Table 2: Hydrogen bonds present in **1**.

D-H \cdots A	d (D-H) [Å]	d (H \cdots A) [Å]	d (D-H \cdots A) [Å]	\angle (D-H \cdots A) [°]
N1-H1 \cdots O3	0.75(4)	2.19(4)	2.628(6)	118(4)
N1-H1 \cdots N2 ⁱ	0.75(4)	2.31(4)	2.955(5)	144(4)
N1-H1 \cdots O1 ⁱ	0.75(4)	2.72(4)	3.150(6)	117(4)
N5-H5 \cdots N3 ⁱⁱ	0.77(3)	2.27(4)	2.972(5)	151(4)
N5-H5 \cdots O2 ⁱⁱ	0.77(3)	2.51(4)	3.143(5)	140(4)

Symmetry Operators: (i) $-x+2, y+1/2, -z+1$; (ii) $-x+1, y+1/2, -z$.

The layers are oriented along the *b*-axis and stacked above one another. The layers themselves are connected by three short N–O contacts, O₄ \cdots N₆(iii), O₄ \cdots N₅(iii) and O₁ \cdots N₄(iv) (symmetry operators: (iii) $-x, y+1/2, -z+2$; (iv) $-x+1, y-1/2, -z+1$). All three contacts are shorter than the sum of van der Waals radii ($r_w(\text{O}) + r_w(\text{N}) = 3.07 \text{ \AA}$),^[19] with O₄ \cdots N₆(iii) being the shortest (2.929(5) Å) and O₁ \cdots N₄ being the longest (3.065(6) Å). The stacking of the layers is displayed in Figure 4 together with the short contacts between the layers as dotted lines.

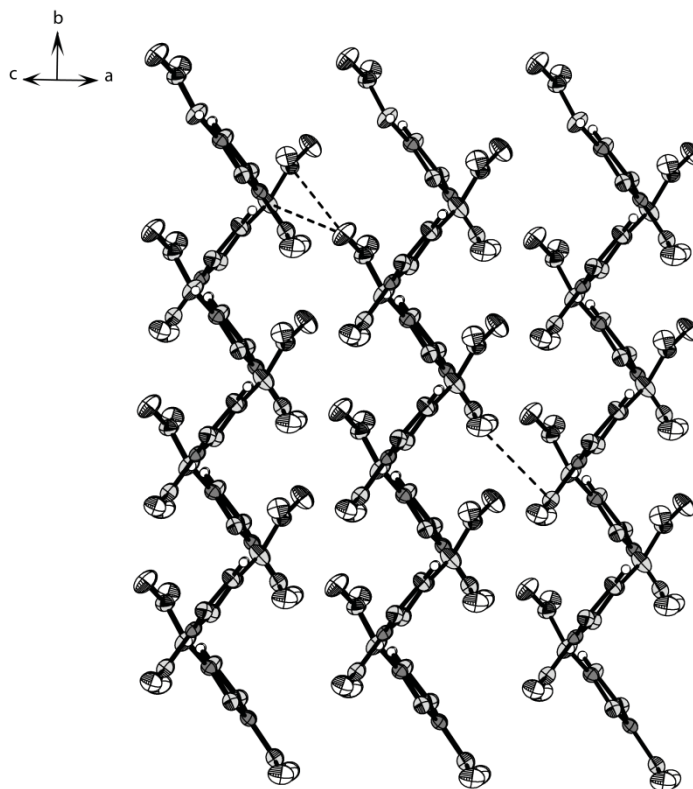


Figure 4: Stacking of the layer formation in the crystal structure of **1** along the *b*-axis. Dotted lines represent short N...O contacts connecting the layers. Thermal ellipsoids are set to 50 % probability.

1-Methyl-5-nitramino-3-nitro-1,2,4-triazole (**3**) crystallizes in the orthorhombic space group $P2_12_12_1$ as colorless plates with a cell volume of $1480.2(2) \text{ \AA}^3$ and eight molecular moieties in the unit cell. The calculated density at 173 K is only 1.688 g cm^{-3} and hence well below the density of the non methylated product. The asymmetric unit consists of two individual molecules of **3**. The asymmetric unit is presented in Figure 5 together with the atom labeling scheme for both individuals.

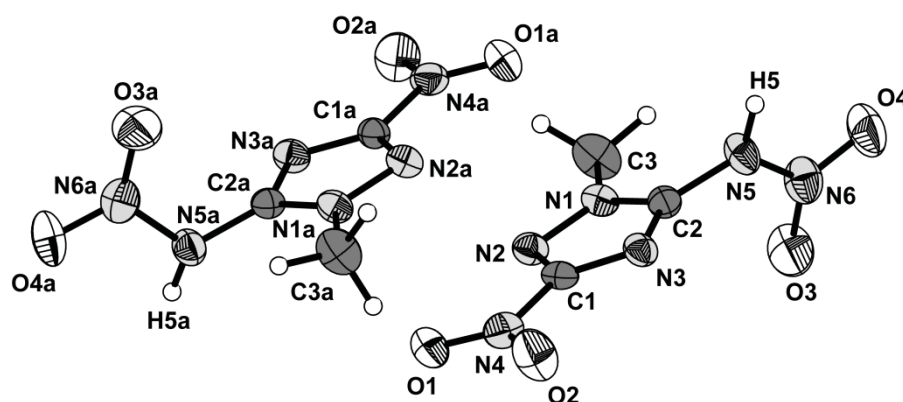


Figure 5: Asymmetric unit of **3**. Thermal ellipsoids are set to 50 % probability.

The crystal structure of **3** consists of infinite rows along the *a*-axis. One infinite row is built up by four hydrogen bonds, again featuring two sets of bifurcated anions using the N₅ and N_{5a} atoms of the two independent molecular moieties as donor atoms. Again, two hydrogen bonds are weak (N₅–H₅⋯O_{2a}(i) and N_{5a}–H_{5a}⋯O₂(ii)) exhibiting very long H⋯A distances of 2.65(3) Å and 2.69(3) Å, respectively. Both hydrogen bonds also show D–H⋯A angles of 116(2)° and are only of electrostatic nature. The other two hydrogen bonds are of moderately strong electrostatic nature and are very directed (170(3)° and 174(3)°). Additionally, two short N–O contacts connect the molecules within the rows, N₃⋯O_{2a}(i) (3.006(3) Å) and N_{3a}⋯O₂(ii) (2.978(3) Å). The hydrogen bonding pattern and the short contacts are shown in Figure 6.

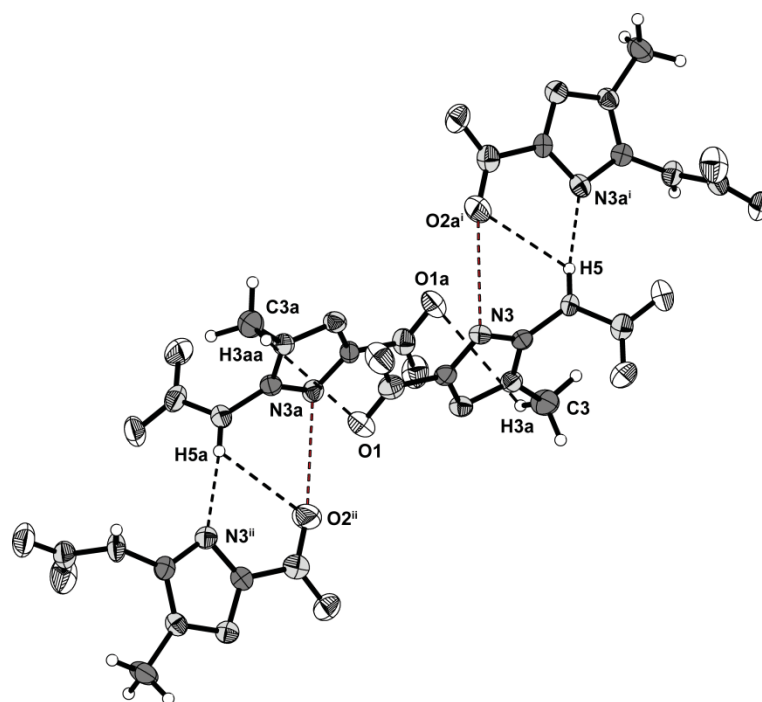


Figure 6: Hydrogen bonding scheme present within the infinite rows in the crystal structure of **3**. Short N⋯O contacts are shown as dotted red lines, additionally. Thermal ellipsoids are set to 50 % probability. Symmetry Operators: (i) $-x+1, y+1/2, -z+1/2$; (ii) $-x, y-1/2, -z+1/2$.

Table 3: Hydrogen bonds present in **3**.

D–H⋯A	d (D–H) [Å]	d (H⋯A) [Å]	d (D–H⋯A) [Å]	< (D–H⋯A) [°]
N5–H5⋯N3a ⁱ	0.89(3)	2.03(3)	2.915(3)	170(3)
N5–H5⋯O2a ⁱ	0.89(3)	2.65(3)	3.144(3)	116(2)
N5a–H5a⋯N3 ⁱⁱ	0.84(3)	2.11(3)	2.944(3)	174(3)
N5a–H5a⋯O2 ⁱⁱ	0.84(3)	2.69(3)	3.153(3)	116(2)
C3–H3a⋯O1a	0.98(3)	3.17(2)	3.524(4)	103(2)
C3a–H3aa⋯O1	0.98(3)	3.03(2)	3.541(4)	114(2)

Symmetry Operators: (i) $-x+1, y+1/2, -z+1/2$; (ii) $-x, y-1/2, -z+1/2$.

The rows are transferred into one another by the symmetry operation $-x, y+1/2, -z+1/2$. They are therefore turned upside down and shifted along the b and c -axis. The rows are connected by two hydrogen bonds involving the methyl group as donor, which is very unusual. $C_3-H_{3a}\cdots O_{1a}$ and $C_{3a}-H_{3aa}\cdots O_1$ are only of weak electrostatic nature, even though the $D\cdots A$ distance is in the range of the sum of van der Waals radii, but the $D-H\cdots A$ angles are very small with $103(2)^\circ$ and $114(2)^\circ$, respectively. The arrangement of the layers is presented in Figure 7.

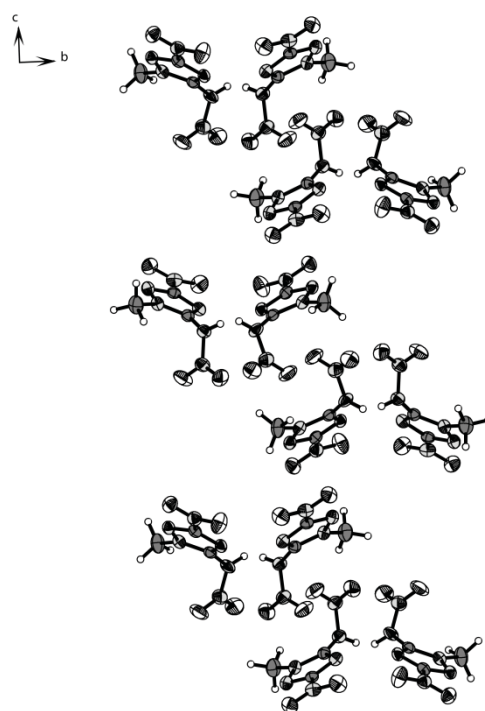


Figure 7: Arrangement of the infinite rows along the c -axis in the crystal structure of **3**. Thermal ellipsoids are set to 50 % probability.

Ammonium 5-nitramino-3-nitro-1*H*-1,2,4-triazolate monohydrate (**5**) crystallizes in the orthorhombic space group $P2_12_12_1$ as orange blocks with a cell volume of $802.17(7) \text{ \AA}^3$ and four molecular moieties in the unit cell. The calculated density at 173 K is 1.732 g cm^{-3} . The asymmetric unit of **5** is presented in Figure 8 together with the atom labeling scheme.

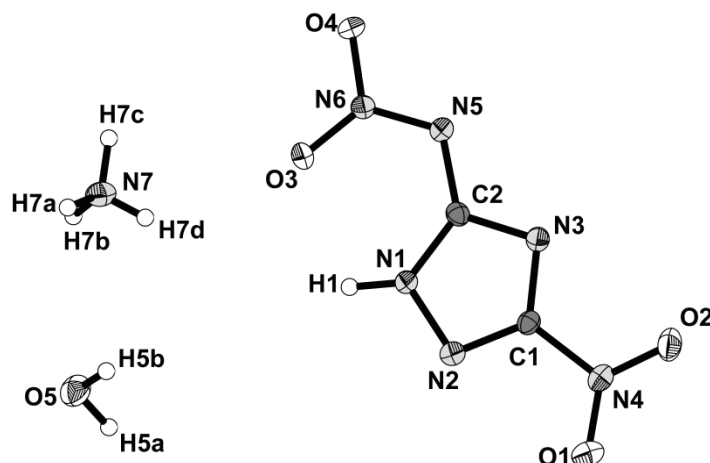


Figure 8: Asymmetric unit of **5**. Thermal ellipsoids are set to 50 % probability.

Hydrazinium 5-nitramino-3-nitro-1*H*-1,2,4-triazolate monohydrate (**6**) crystallizes in the monoclinic space group $P2_1/c$ as colorless plates with a cell volume of $834.06(8) \text{ \AA}^3$ and four molecular moieties in the unit cell. The calculated density at 173 K is 1.785 g cm^{-3} . The asymmetric unit of **6** is presented in Figure 9.

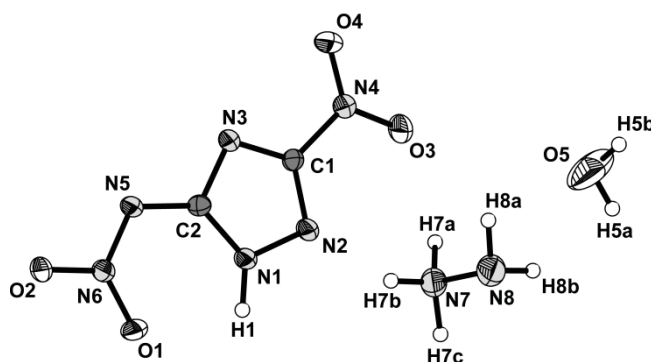


Figure 9: Asymmetric unit of **6**. Thermal ellipsoids are set to 50 % probability.

Guanidinium 5-nitramino-3-nitro-1*H*-1,2,4-triazolate (**7**) crystallizes in the orthorhombic space group $Pna2_1$ as yellow blocks with a cell volume of $896.6(2) \text{ \AA}^3$ and four molecular moieties in the unit cell. The calculated density at 173 K is 1.727 g cm^{-3} . The asymmetric unit of **7** is presented in Figure 10.

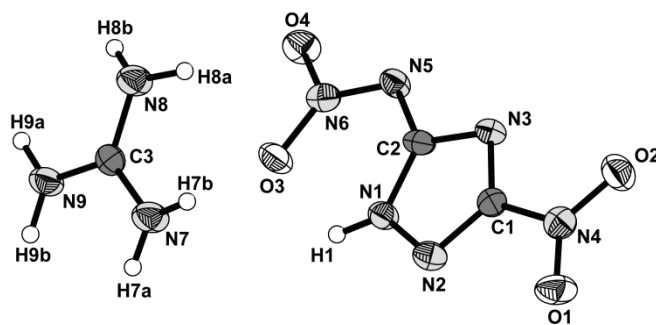


Figure 10: Asymmetric unit of **7**. Thermal ellipsoids are set to 50 % probability.

As observed for the crystal structures of **1** and **3**, **7** is also built up exclusively by hydrogen bonding interactions. In this case, only the $N_1-H_1 \cdots O_3$ hydrogen bond, keeping the nitramine group in plane with the triazole ring shows an $D-H \cdots A$ angle smaller than 130° at 112° , but together with the again very short $D \cdots A$ distance of $2.509(3) \text{ \AA}$ it can be considered a moderately strong hydrogen bond of mostly electrostatic nature.

Rows of guanidinium 5-nitramino-3-nitro-1*H*-1,2,4-triazolate pairs are formed, aided by four hydrogen bonds, which are then coupled to bands by two more hydrogen bonds. The nitrogen atoms of the guanidinium cation function as donor atoms in all six bonds. All six bonds are moderately strong with $H \cdots A$ distances between $2.07(3) \text{ \AA}$ and $2.34(3) \text{ \AA}$ and not only of electrostatic nature, but very directed with $D-H \cdots A$ between $167(2)^\circ$ and $178(3)^\circ$. The hydrogen bonding pattern of the guanidinium cation is shown in Figure 11. Hydrogen bonds $N_9-H_{9b} \cdots N_3(\text{ii})$, $N_7-H_{7a} \cdots O_3(\text{ii})$, $N_7-H_{7b} \cdots O_3$ and $N_8-H_{8a} \cdots O_4$ form the bands, while $N_9-H_{9a} \cdots O_4(\text{iii})$ and $N_8-H_{8b} \cdots N_5(\text{iii})$ connect the rows to bands, enclosing an angle of 105.06° between the rows.

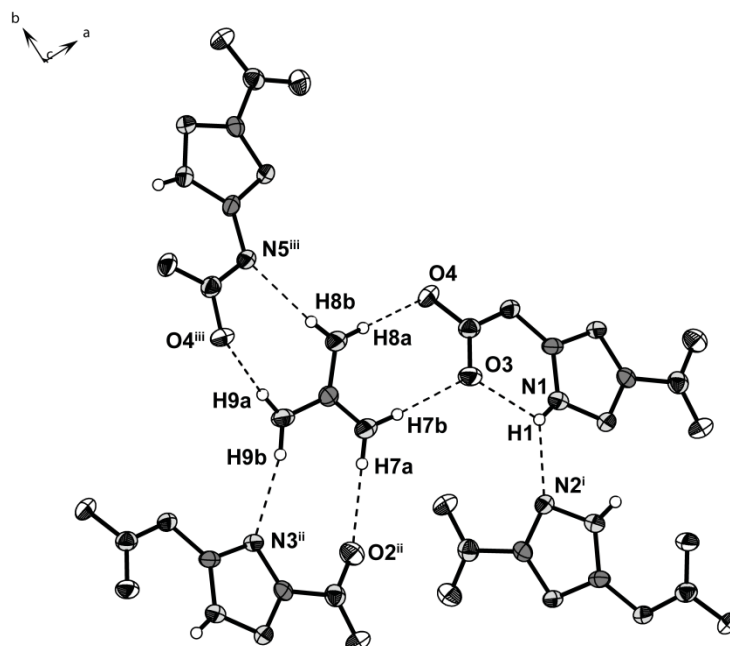


Figure 11: Hydrogen bonding scheme present in **7**. Thermal ellipsoids are set to 50 % probability. Symmetry Operators: (i) $-x+1, -y, z+1/2$; (ii) $x-1, y, z+1$; (iii) $x-1/2, -y+1/2, z+1$.

Table 4: Hydrogen bonds present in **7**.

D-H...A	d (D-H) [Å]	d (H...A) [Å]	d (D-H...A) [Å]	< (D-H...A) [°]
N1-H1...O3	0.82(3)	2.08(3)	2.509(3)	112(2)
N1-H1...N2 ⁱ	0.82(3)	2.27(3)	2.932(3)	138(3)
N7-H7a...O2 ^{ii*}	0.84(3)	2.16(3)	3.001(3)	171(4)
N7-H7b...O3	0.86(3)	2.07(3)	2.924(3)	177(2)
N8-H8a...O4	0.89(3)	2.14(3)	3.035(4)	178(3)
N8-H8b...N5 ⁱⁱⁱ	0.80(3)	2.34(3)	3.130(3)	172(3)
N9-H9a...O4 ⁱⁱⁱ	0.84(3)	2.10(3)	2.934(3)	170(3)
N9-H9b...N3 ⁱⁱ	0.88(2)	2.20(3)	3.057(3)	167(2)

Symmetry Operators: (i) $-x+1, -y, z+1/2$; (ii) $x-1, y, z+1$; (iii) $x-1/2, -y+1/2, z+1$.

The bands are then connected over only one hydrogen bond, N₁-H₁...N₂(i), which can be considered a moderately strong hydrogen bond again. The torsion angle between the two triazole rings, N₂-N₁...N₂(ii)-N₁(ii), is 37.7(2)°, hence the bands are not arranged coplanar to one another. The enclosing angle between the bands, considering also the guanidinium cations and row formation is 73.32°, as shown best in the unit cell representation of **7** in Figure 12.

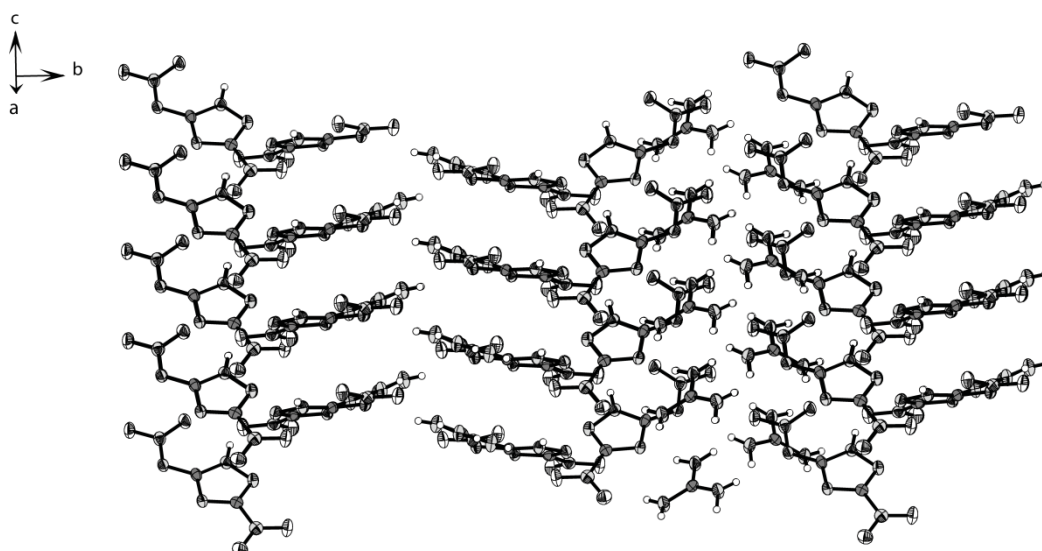


Figure 12: Presentation of the band motives in the crystal structure of **7**. Thermal ellipsoids are set to 50 % probability.

Bis(guanidinium) 5-nitramino-3-nitro-1,2,4-triazolate (**11**) crystallizes also in the orthorhombic space group $Pna2_1$ as yellow plates with a cell volume of $1151.3(2) \text{ \AA}^3$ and four molecular moieties in the unit cell. The calculated density at 173 K is 1.686 g cm^{-3} . The asymmetric unit of **11** is presented in Figure 13.

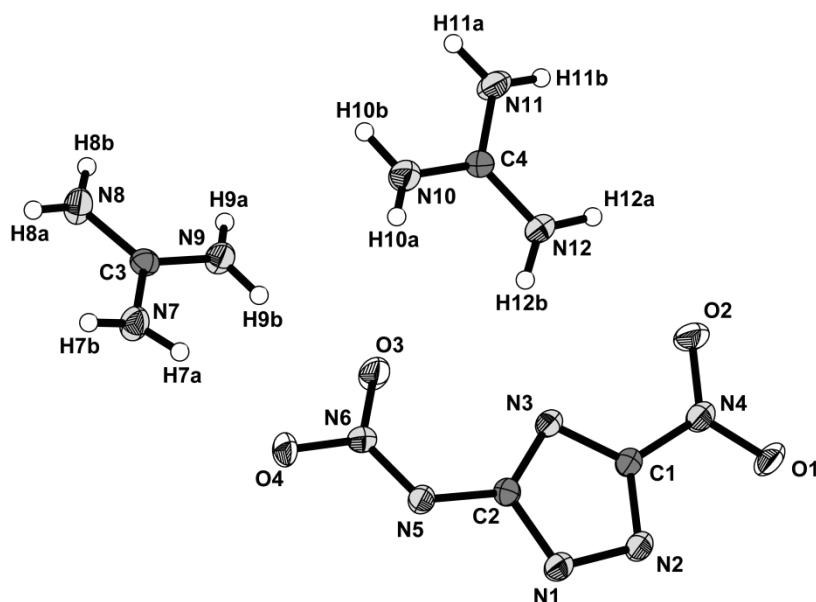


Figure 13: Asymmetric unit of **11**. Thermal ellipsoids are set to 50 % probability.

Both guanidinium compounds crystallize in the same orthorhombic space group $Pna2_1$ with the mono salt having a 0.041 g cm^{-3} higher density. While the structure of **7** consisted of eight hydrogen bonds, sixteen individual hydrogen bonds are observed in the

crystal structure of **11**, forming a very complex three dimensional network. The first guanidinium moiety (N_7, N_8, N_9) forms rows along the c -axis, alternating G^+ and $NANTA^{2-}$ ions over four hydrogen bonds, $N_8-H_{8b} \cdots N_5(ii)$, $N_9-H_{9a} \cdots N_1(ii)$, $N_9-H_{9b} \cdots O_3$ and $N_7-H_{7a} \cdots O_4$ (Figure 14). These rows are connected, forming bands in two directions. First, the connection to a second row, stacked above the one spanned by the first guanidinium moiety along the c -axis, is built up by seven hydrogen bonds with the second guanidinium moiety (N_{10}, N_{11}, N_{12}) as connecting unit (Figure 15). This results in the formation of a two dimensional band coplanar with the bc plane. The participating hydrogen bonds are $N_{10}-H_{10a} \cdots O_3$, $N_{12}-H_{12b} \cdots N_3$, $N_{12}-H_{12a} \cdots O_2$, $N_{11}-H_{11a} \cdots O_1(iii)$, $N_{11}-H_{11a} \cdots N_2(iii)$, $N_{10}-H_{10b} \cdots N_2(iii)$ and $N_{10}-H_{10b} \cdots N_1(iii)$. The second band motive is formed by the connection of the rows (first guanidinium moiety) with a second row in direction of the a -axis by hydrogen bonds $N_{12}-H_{12b} \cdots O_1(iv)$, $N_{11}-H_{11b} \cdots O_1(iv)$ and $N_{11}-H_{11b} \cdots O_2(iv)$. The rows lie coplanar to one another, but the $NANTA^{2-}$ anions are twisted by 24.91° resulting in the arrangement of bands nearly coplanar to the ac plane.

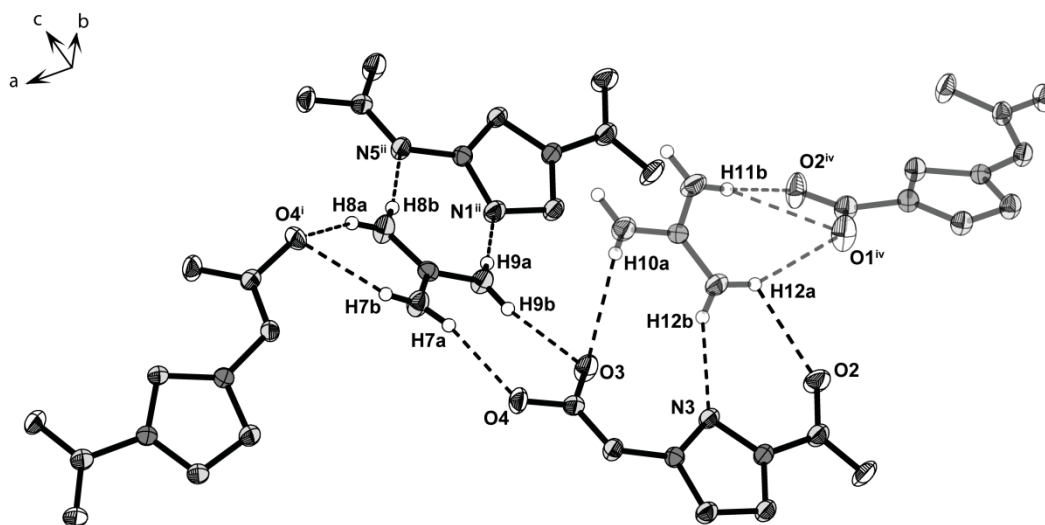


Figure 14: Hydrogen bonding motive as build up by the first guanidinium moiety of **11**. Not all connections are shown for the second guanidinium moiety. Also the second guanidinium moiety and the connections are set transparent for better clarity. Thermal ellipsoids are set to 50 % probability. Symmetry Operators: (i) $-x+1/2, y+1/2, z+1/2$; (ii) $x, y, z+1$.

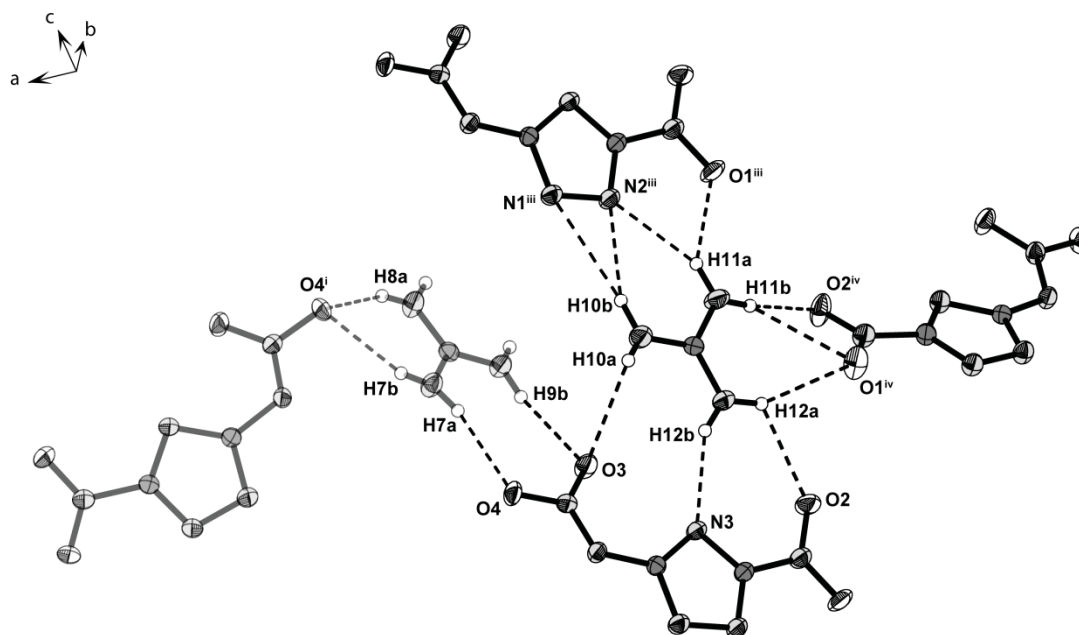


Figure 15: Hydrogen bonding motive as build up by the second guanidinium moiety of **11**. Not all connections are shown for the first guanidinium moiety. Also the first guanidinium moiety and the connections are set transparent for better clarity. Thermal ellipsoids are set to 50 % probability. Symmetry Operators: (iii) $x, y+1, z+1$; (iv) $-x, -y, z+1/2$.

Table 5: Hydrogen bonds present in **11**.

D-H...A	d (D-H) [Å]	d (H...A) [Å]	d (D-H...A) [Å]	< (D-H...A) [°]
N7-H7a...O4	0.82(3)	2.15(4)	2.955(3)	168(3)
N7-H7b...O4 ⁱ	0.84(3)	2.19(3)	2.957(3)	151(3)
N8-H8a...O4 ⁱ	0.84(3)	2.26(3)	3.030(3)	153(3)
N8-H8b...N5 ⁱⁱ	0.82(3)	2.25(3)	3.061(3)	173(3)
N9-H9a...N1 ⁱⁱⁱ	0.83(3)	2.08(3)	2.913(3)	175(3)
N9-H9b...O3	0.82(3)	2.15(3)	2.960(3)	171(3)
N10-H10a...O3	0.72(3)	2.42(3)	2.986(3)	136(3)
N10-H10b...N2 ⁱⁱⁱ	0.88(3)	2.28(3)	3.112(3)	156(2)
N10-H10b...N1 ⁱⁱⁱ	0.88(3)	2.68(4)	3.558(3)	173(2)
N11-H11a...O1 ⁱⁱⁱ	0.87(3)	2.18(3)	2.865(3)	135(2)
N11-H11a...N2 ⁱⁱⁱ	0.87(3)	2.36(3)	3.161(3)	153(2)
N11-H11b...O2 ^{iv}	0.87(3)	2.30(3)	3.153(3)	165(3)
N11-H11b...O1 ^{iv}	0.87(3)	2.55(3)	3.285(3)	142(2)
N12-H12a...O2	0.88(3)	2.35(3)	2.868(3)	118(2)
N12-H12a...O1 ^{iv}	0.88(3)	2.40(3)	3.219(3)	154(3)
N12-H12b...N3	0.83(3)	2.17(3)	2.936(3)	152(2)

Symmetry Operators: (i) $-x+1/2, y+1/2, z+1/2$; (ii) $x, y, z+1$; (iii) $x, y+1, z+1$; (iv) $-x, -y, z+1/2$.

The bands formed nearly coplanar to the ac plane are themselves connected over the first guanidinium moiety (Figure 14, N₇ and N₈) by two moderately strong and directed hydrogen bonds N₇-H_{7b}...O₄(i) and N₈-H_{8a}...O₄(i) (D-H...A angles: 151(3)° and

153(3)°). The bands enclose an angle of 149.29° between themselves. The stacking of the rows and bands together with the connections towards the next band and the resulting angle are presented in Figure 16.

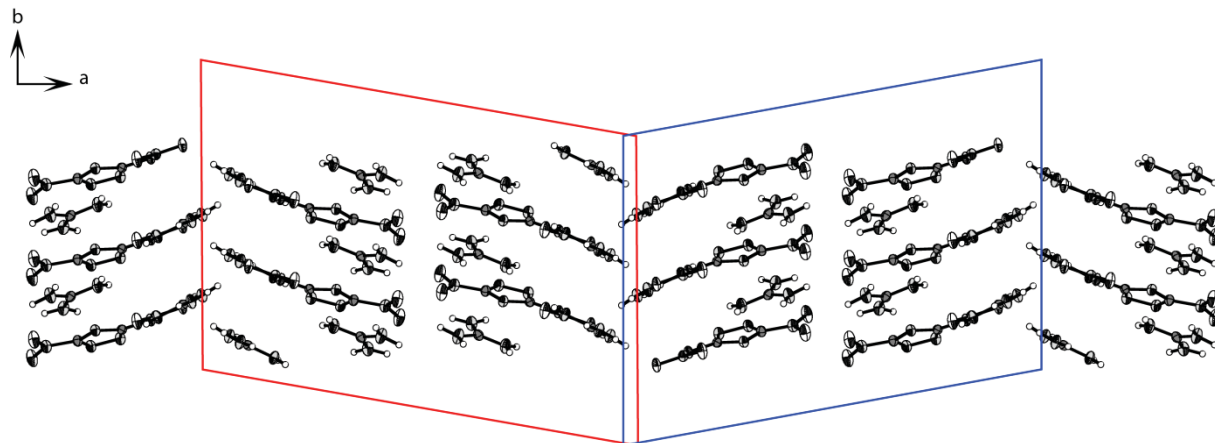


Figure 16: Band motives in the crystal structure of **11** presented coplanar to the *ab* plane, displayed along the *c*-axis. The rhombic prisms (red and blue) represent the arrangement of two bands towards one another at an angle of 149.49°. Thermal ellipsoids are set to 50 % probability.

Triaminoguanidinium 5-nitramino-3-nitro-1*H*-1,2,4-triazolate (**9**) crystallizes in the orthorhombic space group *Pca*2₁ as yellow blocks with a cell volume of 1066.7(2) Å³ and four molecular moieties in the unit cell. The calculated density at 173 K is 1.732 g cm⁻³. The asymmetric unit of **9** is presented in Figure 17.

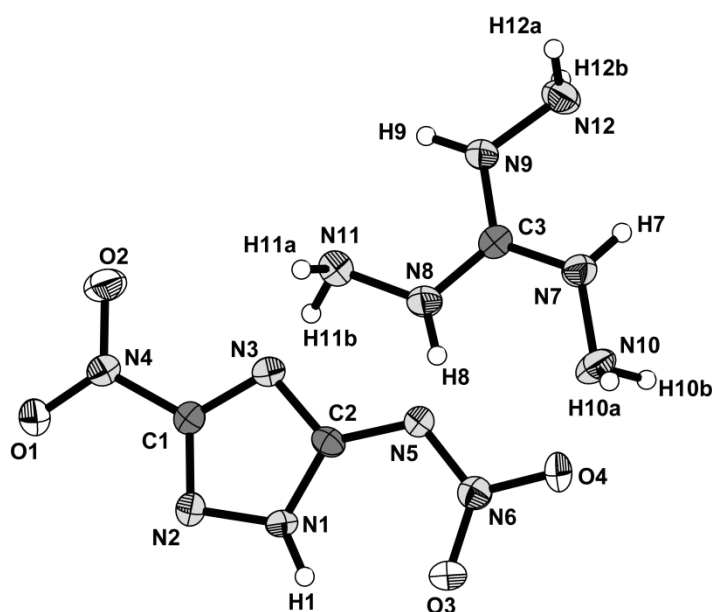


Figure 17: Asymmetric unit of **9**. Thermal ellipsoids are set to 50 % probability.

Triaminoguanidinium 1-methyl-5-nitramino-3-nitro-1,2,4-triazolate (**18**) crystallizes in the triclinic space group $P-1$ as yellow blocks with a cell volume of $583.0(1) \text{ \AA}^3$ and two molecular moieties in the unit cell. The calculated density at 173 K is 1.665 g cm^{-3} . The asymmetric unit of **18** is presented in Figure 18.

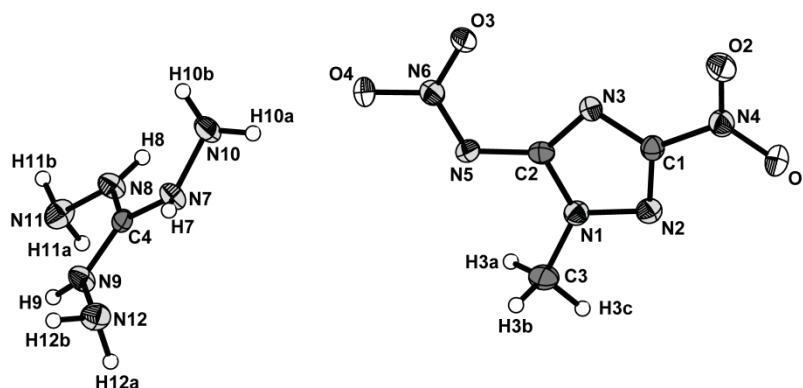


Figure 18: Asymmetric unit of **18**. Thermal ellipsoids are set to 50 % probability.

The structure of **18** is basically built up by hydrogen bonds where all nitrogen atoms of the triaminoguanidinium moiety function as donor atoms. Ten hydrogen bonds are observed, some rather strong and directed, while others are only of electrostatic nature with $D-H \cdots A$ angles smaller than 140° . Nine of these hydrogen bonds connect to the 1-methyl-5-nitramino-3-nitro-1,2,4-triazolate anions using atoms $O_3(ii, v)$, $O_4(1, vii)$, $O_1(iv, viii)$, $N_2(iv)$, $N_3(i)$ and $N_5(iii)$ as acceptor sites. One rather weak hydrogen bond $N_{11} - H_{11b} \cdots N_{12}(vi)$ connects two triaminoguanidinium cations towards one another. The hydrogen bonding pattern of one triaminoguanidinium moiety is displayed in Figure 19, while the hydrogen bonds are compiled in detail in Table 6.

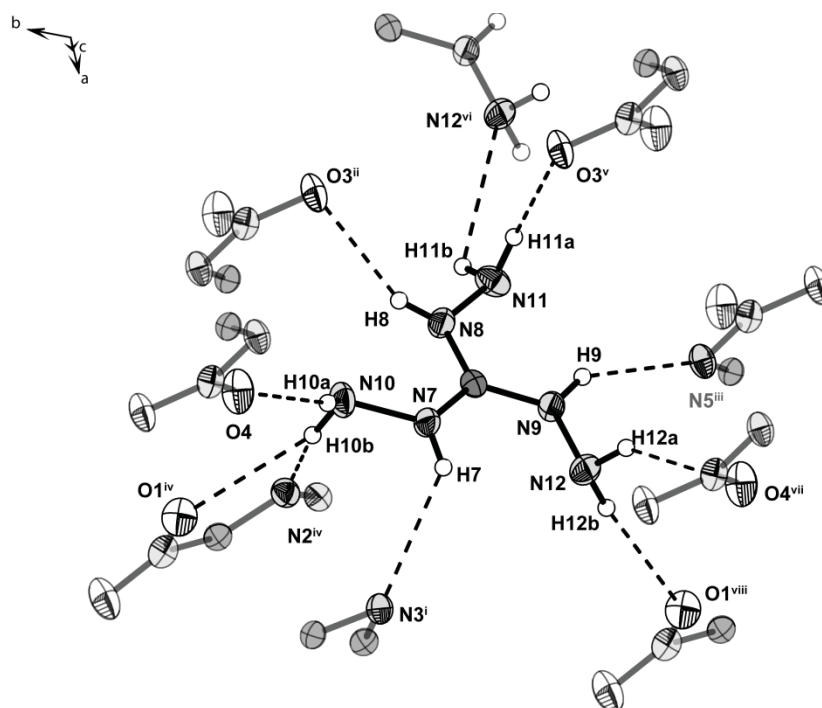


Figure 19: Hydrogen bonds in the surrounding of the triaminoguanidinium cation in compound **18**. Only parts of the acceptor sites are drawn and set transparent, the rest is omitted for clarity. Thermal ellipsoids are set to 50 % probability. Symmetry Operators: (i) $-x+2, -y+1, -z+1$; (ii) $-x+1, -y+1, -z+1$; (iii) $-x+1, -y, -z+1$; (iv) $x, y, z+1$; (v) $x-1, y-1, z$; (vi) $x-1, y, z$; (vii) $x, y-1, z$; (viii) $x, y-1, z+1$.

Table 6: Hydrogen bonds present in **18**.

D-H...A	d (D-H) [Å]	d (H...A) [Å]	d (D-H...A) [Å]	< (D-H...A) [°]
N7-H7...N3 ⁱ	0.81(2)	2.50(2)	3.094(2)	131(2)
N8-H8...O3 ⁱⁱ	0.81(2)	2.21(2)	2.960(2)	154(2)
N9-H9...N5 ⁱⁱⁱ	0.86(2)	2.24(2)	3.015(2)	149(2)
N10-H10a...O4	0.88(2)	2.19(2)	3.001(2)	153(2)
N10-H10b...O1 ^{iv}	0.92(2)	2.56(2)	3.376(2)	149(2)
N10-H10b...N2 ^{iv}	0.92(2)	2.67(2)	3.478(3)	147(2)
N11-H11a...O3 ^v	0.88(2)	2.15(2)	3.009(2)	164(2)
N11-H11b...N12 ^{vi}	0.83(2)	2.67(2)	3.071(2)	112(2)
N12-H12a...O4 ^{vii}	0.88(2)	2.37(2)	3.112(2)	142(2)
N12-H12b...O1 ^{viii}	0.89(2)	2.33(2)	3.204(2)	169(2)

Symmetry Operators: (i) $-x+2, -y+1, -z+1$; (ii) $-x+1, -y+1, -z+1$; (iii) $-x+1, -y, -z+1$; (iv) $x, y, z+1$; (v) $x-1, y-1, z$; (vi) $x-1, y, z$; (vii) $x, y-1, z$; (viii) $x, y-1, z+1$.

Since the nitramino group is located in plane with the triazole ring, planar layers of MeNANTA⁻ anions arranged coplanar to the *bc* plane are observed. The anion layers are connected by layers formed by triaminoguanidinium cations, which are arranged nearly perpendicular to the anion layers. The presentation of the crystal structure along the *a*-axis is displayed in Figure 20.

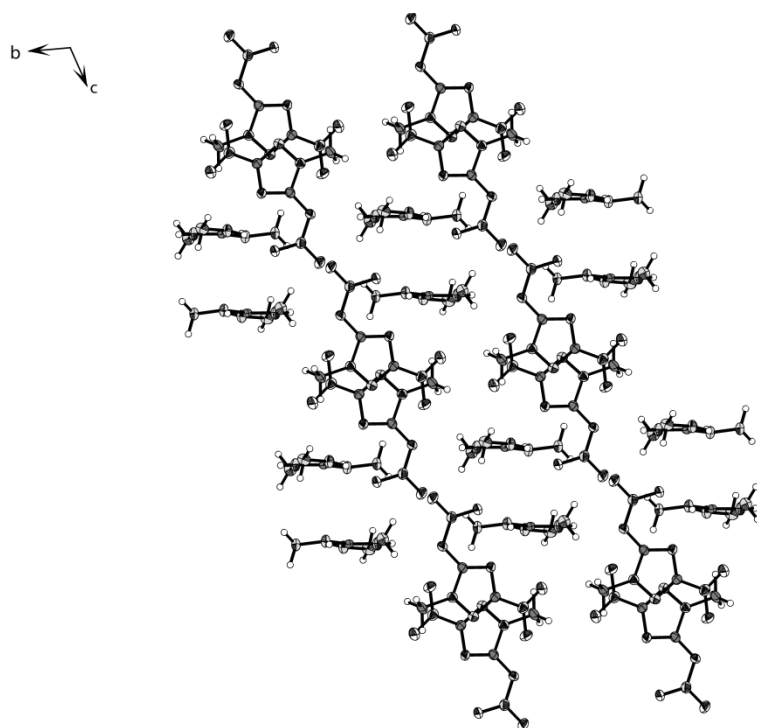


Figure 20: Presentation of the anion and cation layers in the crystal structure of **18**, shown along the a-axis. Thermal ellipsoids are set to 50 % probability.

7.2.3 Spectroscopic Data

Vibrational Spectroscopy

IR and Raman spectra of all compounds have been recorded and the frequencies have been assigned based on literature^[20] and also based on quantum mechanical calculations at the B3LYP/cc-pVDZ^[21] level of theory as implemented in the Gaussian 09W program package.^[22] The calculated frequencies have been fitted according to Witek et al.^[23] with a scaling factor of 0.9704 in order to generate comparable values.

The stretching mode of the N–H bonds is observed at 3175 cm⁻¹ (IR) and 3191 cm⁻¹ (Raman) for **1**, while **2** showed only an absorption in the IR spectra at 3214 cm⁻¹ but no signal in the Raman spectra. The ν_{as} stretching mode of the methyl group of **2** is observed at 3082 cm⁻¹ (IR) and 3038 cm⁻¹ (Raman) while the ν_s stretching mode is observed at 2949 cm⁻¹ (IR) and 2973 cm⁻¹ (Raman). Additionally, the bending deformation mode δ_{as} of the methyl group can also be observed in the IR spectra of **2** at 1375 cm⁻¹ while the δ_s deformation mode of the methyl group is observed at 1439 cm⁻¹ (IR) and 1444 cm⁻¹ (Raman). The nitro groups are observed with both, their symmetric and asymmetric stretching modes. The nitramine NO₂ groups showed absorption bands

and peaks at higher energy for the ν_{as} stretching mode at 1638 cm^{-1} (IR) for **1** and at 1652 cm^{-1} (IR) and 1654 cm^{-1} (Raman) for **2**. The vibrational frequencies for the ν_{as} stretching mode of the nitro group are observed at 1606 cm^{-1} (IR) and 1611 cm^{-1} (Raman) for **1** and at 1606 cm^{-1} (IR) and 1597 cm^{-1} (Raman) for **2**. In addition, the symmetric stretching modes of the nitramine NO_2 group are observed at 1336 cm^{-1} (**1**) and 1309 cm^{-1} (**2**) in the IR spectra and at 1347 cm^{-1} (**1**) and 1320 cm^{-1} (**2**) in the corresponding Raman spectra. The ν_s stretching modes of the nitro group are observed at lower energy at 1311 cm^{-1} (**1**) and 1289 cm^{-1} (**2**) in the IR spectra and at 1316 cm^{-1} (**1**) and 1283 cm^{-1} (**2**) in the Raman spectra. The vibrations of the $\text{C}_1\text{-NO}_2$ bonds are present at 1410 cm^{-1} (**1**) and 1402 cm^{-1} (**2**) in the IR spectra and at 1412 cm^{-1} (**1**) and 1410 cm^{-1} (**2**) in the Raman spectra. The stretching mode of the $\text{C}_2\text{-N}_{\text{Nitramine}}$ bond is observed at higher frequencies at 1558 cm^{-1} (**1**) and 1565 cm^{-1} (**2**) in the IR spectra and at 1572 cm^{-1} (**1**) and 1562 cm^{-1} (**2**) in the corresponding Raman spectra. Since the triazole ring in **1** is nearly chemically equivalent regarding the nitrogen atoms N_1 and N_2 , combined stretching modes of the $\text{C}_1\text{-N}_2$ and $\text{C}_2\text{-N}_1$ bonds are observed. The ν_s stretching mode is observed at 1521 cm^{-1} (IR) and 1525 cm^{-1} (Raman) while the ν_{as} stretching mode is observed at lower energy at 1467 cm^{-1} (IR) and 1470 cm^{-1} (Raman). Due to the methyl group, **2** shows two unique absorptions (lines) for the $\text{C}_1\text{-N}_2$ and $\text{C}_2\text{-N}_1$ bonds, the first being present at 1489 cm^{-1} (IR) and 1496 cm^{-1} (Raman) while the stretching mode of the second bond is observed at 1534 cm^{-1} (IR) and 1524 cm^{-1} (Raman). As for any heterocyclic compound, many combined stretching and deformation as well as torsion modes are observed in the fingerprint region between 1200 cm^{-1} and 600 cm^{-1} .

The nitrogen rich salts of **1** and **2** show absorption bands in the region of $3400 - 3100\text{ cm}^{-1}$ as expected for N-H stretching modes and additionally for the ν_s and ν_{as} stretching vibrations of the amine groups (ammonium, hydrazinium and guanidines). The stretching modes of the C-H bond and the CH_3 group are observed in the region of $2960 - 2850\text{ cm}^{-1}$ in both Raman and IR spectra. The ν_{as} stretching modes of the nitramine NO_2 as well as the nitro group are shifted to higher energy when compared with **1** and **2** and are observed in the region of $1700 - 1658\text{ cm}^{-1}$ and $1630 - 1600\text{ cm}^{-1}$, respectively. The only two exceptions are the ammonium and hydrazinium salts of **1** where the stretching modes are observed at lower energy at 1620 cm^{-1} for the nitramine NO_2 group and at around 1580 cm^{-1} for the nitro group. The ν_s stretching modes for the nitro group and the nitramine NO_2 group are different for the salts of **1** and **2**. While the ν_s (C-NO_2) for the salts of **1**

are observed between 1323 cm^{-1} and 1355 cm^{-1} , the salts of **2** show vibrational frequencies of lower energy between 1302 cm^{-1} and 1277 cm^{-1} . The same is observed for the ν_s (C-N-NO₂) stretching modes. They are observed between 1306 cm^{-1} and 1292 cm^{-1} for **1**, and between 1269 cm^{-1} and 1256 cm^{-1} for **2**. All other stretching modes presented in detail for the neutral compounds are also present in the IR and Raman spectra of the corresponding salts, but are not discussed in detail. The combined stretch and deformation modes as well as torsion modes are also observed between 1200 cm^{-1} and 600 cm^{-1} for the nitrogen rich salts.

Multinuclear NMR spectroscopy

The neutral compounds **1** and **3** differ not too much from the values observed for the starting materials ANTA and MeNANTA (**2**) either in the ¹H or ¹³C{¹H} NMR spectra. While ANTA shows two signals in the ¹H NMR spectra at 12.36 ppm (N_{Tria}H) and 6.79 ppm (-NH₂), only the NH signal of the nitramine group is observed in the spectra of **1** at 6.95 ppm as a broad singlet. The carbon atom connected to the nitro group nearly stays in the same position in the ¹³C NMR spectra at a chemical shift of 160.5 ppm (ANTA, 160.9 ppm) while the newly formed nitramine shifts the signal towards higher field and is observed at 151.7 ppm (ANTA, 157.4 ppm). In addition to the nitro group signal observed at a chemical shift of -23 ppm (ANTA, -23 ppm) in the ¹⁴N NMR spectra a second singlet is observed at -29 ppm representing the nitramine group. The same is observed for **3**. While a certain difference in the ¹H NMR spectra is observed for the hydrogen atom of the nitramine moiety (shift from 7.00 ppm (**2**, NH₂), to 4.64 ppm (**3**)), the signal of the methyl group nearly stays at the position at a chemical shift of 3.77 ppm (3.63 ppm (**2**)). The three carbon atoms show three resonances in the ¹³C{¹H} NMR spectra at chemical shifts of 159.4 ppm (C₁), 151.5 ppm (C₂) and 35.6 ppm (CH₃) (**2**, 158.9 ppm (C₁), 156.4 ppm (C₂), 35.9 ppm (CH₃)), observing the same shift to higher field for the C₂ atom as observed in **1**. The ¹⁴N NMR spectrum showed two resonances at chemical shifts of -22 ppm (N₄) and -27 ppm (N₆) in comparison to only one at -25 ppm for **2**, as expected.

Six well resolved resonances are observed for the six nitrogen atoms contained in both, **1** and **3**, with the aids of proton coupled and decoupled ¹⁵N NMR spectroscopy. For **1**, N₄ is observed in the ¹⁵N NMR spectra at a chemical shift of -26.5 ppm, while N₆ is observed

at -32.3 ppm. N_2 and N_3 are observed at chemical shifts of -101.0 ppm and -163.6 ppm, respectively, while the signals of N_1 and N_5 are so close together at -180.1 ppm and -181.0 ppm, that a correct assignment was impossible. The same pattern is observed for the $^{15}\text{N}\{^1\text{H}\}$ NMR spectra of **1**, where the resonances are located as follows: -26.5 ppm (N_4), -32.4 ppm (N_6), -101.0 ppm (N_2), -163.4 ppm (N_3), -180.0 ppm (N_1/N_5) and -181.2 ppm (N_1/N_5). In **3**, the signal of N_4 is located at a chemical shift of -27.2 ppm and the resonance of N_6 is observed at -29.8 ppm. The resonance of N_2 is observed at -86.7 ppm showing 3J coupling towards the methyl group with a coupling constant of $^3J_{\text{NH}} = 2.16$ Hz. While the signal of N_3 is observed at -146.0 ppm, the N_1 resonance is observed at a chemical shift of -175.3 ppm showing a 2J coupling to the attached methyl group with a coupling constant of $^2J_{\text{NH}} = 2.16$ Hz. Finally, the resonance for N_5 is located at a chemical shift of -191.3 ppm. A very small $^4J_{\text{NH}}$ coupling of only 0.74 Hz is observed for this resonance. The resonances in the $^{15}\text{N}\{^1\text{H}\}$ NMR spectra of **3** show the same pattern as observed for the proton coupled ^{15}N NMR spectra (-27.2 ppm (N_4), -29.8 ppm (N_6), -86.7 ppm (N_2), -145.9 ppm (N_3), -175.3 ppm (N_1), -191.3 ppm (N_5)). The comparison and collection of the ^{15}N and $^{15}\text{N}\{^1\text{H}\}$ NMR spectra of **1** and **3** are shown in Figure 21.

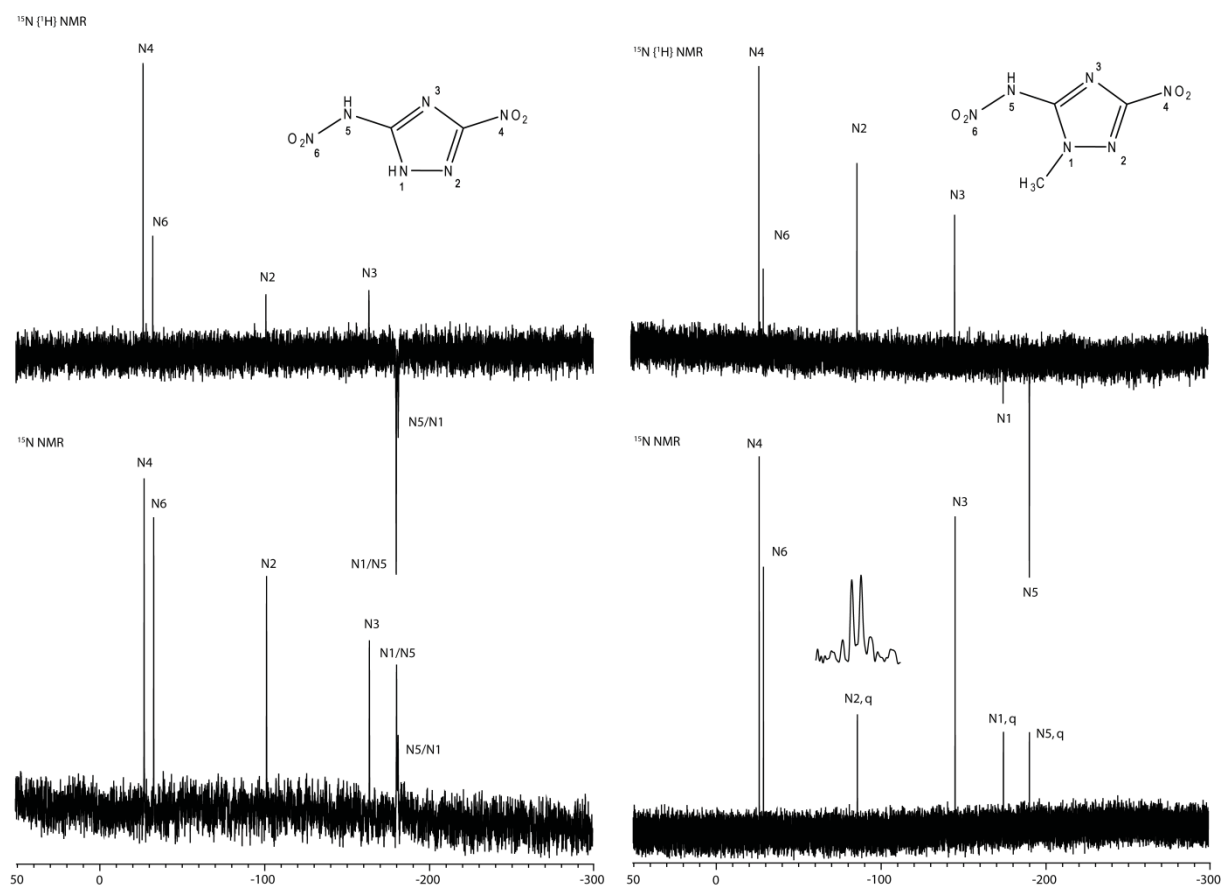


Figure 21: ^{15}N and $^{15}\text{N}\{^1\text{H}\}$ NMR spectra of 5-nitramino-3-nitro-1*H*-1,2,4-triazole (**1**, left) and 4-methyl-5-nitramino-3-nitro-1,2,4-triazole (**3**, right). The x-axis represents the chemical shift δ in ppm.

The mono salts of **1** show the resonance of the hydrogen atom connected to N_1 of the triazole ring in the ^1H NMR spectra at chemical shifts between 13.78 ppm and 13.86 ppm, except for the ammonium salt. The double salts do not show this resonance, since they are double deprotonated. Additionally, the resonances of the cations are observed at chemical shifts of 7.14 ppm (NH_4^+ , **5**), 7.10 ppm (N_2H_5^+ , **6**), 6.91 ppm (G^+ , **7**), 8.53 ppm (-NH-), 7.21 ppm (NH_2), 6.71 ppm (NH_2), and 4.65 ppm (-NH- NH_2 , **8**), 8.55 (-NH-) and 4.56 (NH_2 , **9**), 5.69 (N_2H_5^+ , **10**), 7.26 (G^+ , **11**), 7.60 ppm and 4.67 ppm (AG^+ , **12**) and 7.96 ppm (-NH-) together with 5.70 ppm (NH_2 , **13**). The signals of the triazole carbon atoms are observed for the mono salts in the $^{13}\text{C}\{^1\text{H}\}$ NMR spectra at chemical shifts between 157.9 ppm and 158.0 ppm for C_2 and at exactly 160.8 ppm for C_1 . The signals of the triazole carbon atoms observed for the double salts in the $^{13}\text{C}\{^1\text{H}\}$ NMR spectra are present at chemical shifts between 162.6 ppm and 163.0 ppm for C_2 and between 163.2 ppm and 163.9 ppm for C_1 , except for **10**, where the resonances are observed at chemical shifts of 158.9 ppm (C_2) and 161.1 (C_1). The resonances of the cations are observed at 157.9 ppm (G^+ , **7**), 158.7 ppm (AG^+ , **8**), 159.0 ppm (TAG^+ , **9**), 158.1 ppm (G^+ , **11**), 159.0

ppm (AG^+ , **12**) and at 159.2 ppm (TAG^+ , **13**). The resonances of the nitro and nitramino group nitrogen atoms, N_4 and N_6 , respectively, are observed in the ^{14}N NMR spectra for all ionic compounds of **1** between -14 ppm and -19 ppm for N_4 and between -20 ppm and -23 ppm for N_6 .

The ionic compounds of **3** show on the one hand the resonance of the methyl group at chemical shifts between 3.59 ppm and 3.62 ppm in the ^1H NMR spectra, while the signals of the cations on the other hand are observed at chemical shifts of 7.14 ppm (NH_4^+ , **14**), 7.10 ppm (N_2H_5^+ , **15**), 6.97 ppm (G^+ , **16**), 8.61 ppm ($-\text{NH}-$), 7.26 ppm (NH_2), 6.78 ppm (NH_2) and 4.67 ppm ($-\text{NH}-\text{NH}_2$, **17**) and at 8.55 ($-\text{NH}-$) and 4.45 ppm (NH_2 , **18**). The $^{13}\text{C}\{^1\text{H}\}$ NMR spectra showed resonances at chemical shifts between 159.2 ppm and 161.9 ppm for the C_1 carbon atom of the triazole moiety and between 156.9 ppm and 157.0 ppm for the C_2 carbon atom. The methyl group showed a signal at chemical shifts between 35.0 ppm and 35.1 ppm for all ionic species of **3**. The nitro group nitrogen atom N_4 showed a chemical shift of exactly -15 ppm for ionic compounds **14** – **18** in the ^{14}N NMR spectra, while the signal of the nitramine groups are observed at exactly -25 ppm. For the two triaminoguanidinium mono salts **9** and **18**, proton coupled and decoupled ^{15}N NMR spectra have been recorded additionally as examples for the ionic compounds. The signals have been assigned in comparison with the literature and also based a theoretical calculations of the NMR spectra at the MPW1PW91/cc-pVDZ level of theory. The ^{15}N NMR spectra of **9** shows eight well resolved resonances, as expected. The N_4 resonance is observed at a chemical shift of -15.1 ppm, while the signal of the nitramine nitrogen atom N_6 is observed at -23.7 ppm. Resonances of the N_2 , N_5 , N_3 and N_1 atoms are observed at chemical shifts of -105.3 ppm, -143.1 ppm, -163.8 ppm and -184.7 ppm, respectively. The two resonances of the nitrogen atoms of the triaminoguanidinium cation are observed at chemical shifts of -289.7 ppm ($\text{C}-\text{NH}-\text{NH}_2$), showing a N–H coupling with a coupling constant of $^1J_{\text{NH}} = 102.4$ Hz and at -330.1 ppm ($\text{C}-\text{NH}-\text{NH}_2$). The same pattern is observed in the $^{15}\text{N}\{^1\text{H}\}$ NMR spectra. Signals are observed at chemical shifts of -15.2 ppm (N_4), -23.7 ppm (N_6), -105.4 ppm (N_2), -143.4 ppm (N_5), -163.9 ppm (N_3), -184.8 ppm (N_1), -289.7 ppm ($\text{C}-\text{NH}-\text{NH}_2$, TAG^+) and -330.2 ppm ($\text{C}-\text{NH}-\text{NH}_2$, TAG^+).

As for **9**, eight resonances are also observed for **18** in the proton coupled ^{15}N NMR spectra. The resonances of the N_4 and N_6 atoms are observed at chemical shifts of -15.4 ppm and -24.9 ppm, respectively. The signal of the N_2 nitrogen atom is observed at -96.5 ppm displaying an N–H coupling towards the methyl group showing a coupling constant

of $^3J_{\text{NH}} = 2.02$ Hz. The resonances of the N_5 and N_3 atoms are observed at chemical shifts of -151.5 ppm and -157.1 ppm, respectively. The N_1 nitrogen atoms shows a signal at -188.5 ppm which also displays a coupling towards the hydrogen atoms of the methyl group with a coupling constant of $^2J_{\text{NH}} = 2.09$ Hz. The two remaining resonances belong to the triaminoguanidinium cation at chemical shifts of -289.7 ppm (C-NH-NH₂) showing a doublet with a coupling constant of $^1J_{\text{NH}} = 102.35$ Hz and -330.2 ppm (C-NH-NH₂) showing a triplet with a coupling constant of $^1J_{\text{NH}} = 72.51$ Hz. The pattern observed in the proton decoupled ^{15}N NMR spectra is nearly identical, except the resonance for the N_5 atom is not observed. Resonances are observed at chemical shifts of -15.3 ppm (N_4), -24.8 ppm (N_6), -96.4 ppm (N_2), -157.1 ppm (N_3), -188.7 ppm (N_1 -CH₃), -289.7 ppm (C-NH-NH₂, TAG⁺) and -330.2 ppm (C-NH-NH₂, TAG⁺). The comparison and collection of the ^{15}N and $^{15}\text{N}\{^1\text{H}\}$ NMR spectra of **9** and **18** are presented in Figure 22.

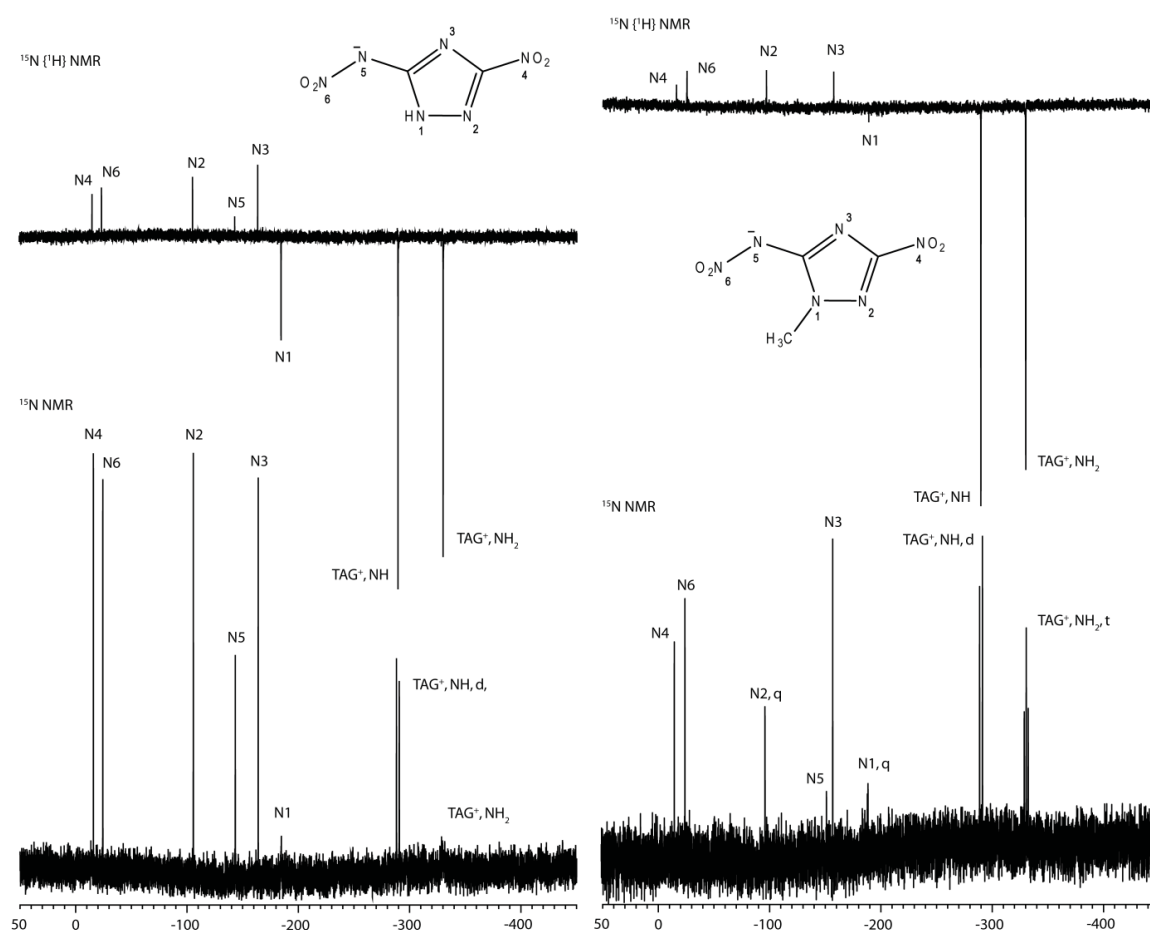


Figure 22: ^{15}N and $^{15}\text{N}\{^1\text{H}\}$ NMR spectra of triaminoguanidinium 5-nitramino-3-nitro-1H-1,2,4-triazolate (**9**, left) and triaminoguanidinium 4-methyl-5-nitramino-3-nitro-1,2,4-triazolate (**18**, right). The x-axis represents the chemical shift δ in ppm.

7.2.4 Mass Spectrometry

Mass spectra were recorded using the FAB+ and FAB- techniques for all ionic compounds in glycerin matrix. The anion of **1** (NANTA⁻) was always observed at m/z 173.0, even for the double deprotonated compounds, while the anion of **3** (MeNANTA⁻) was always observed at m/z 187.0 in the FAB- spectra. The corresponding cations are observed at m/z 18.0 (**5**, **14**), m/z 33.1 (**6**, **10**, **15**), m/z 34.0 (**4**), m/z 60.1 (**7**, **11**, **16**), m/z 75.1 (**8**, **12**, **17**) and m/z 105.13 (**9**, **13**, **18**). The neutral compounds **1**, **2** and **3** are observed using the DEI+ method at m/z 174.0 [M^+], m/z 143.07 [M^+] and m/z 188.1 [M^+], respectively.

7.2.5 Theoretical Calculations, Performance Characteristics and Stabilities

All calculations regarding energies of formation were carried out using the Gaussian G09W Version 7.0 program package.^[22] Since very detailed descriptions of the calculation process have been published earlier^[11, 24] and can be found in specialized books,^[1b] only a short summary of computational methods will be given. The enthalpies (H) and Gibbs free energies (G) were calculated using the complete basis set method (CBS) of Petersson *et al.* in order to obtain very accurate energies. In this contribution, we used the modified CBS-4M method with M referring to the use of minimal population localization, which is a re-parameterized version of the original CBS-4 computational method and also includes additional empirical calculations.^[25]

The enthalpies of formation for the gas phase species were computed according to the atomization energy method, using NIST^[26] values as standardized values for the atoms standard heats of formation ($\Delta_f H^0$) according to equation 1.^[27]

$$\Delta_f H^0_{(g, \text{Molecule}, 298)} = H_{(\text{Molecule})} - \sum H^0_{(\text{Atoms})} + \sum \Delta_f H^0_{(\text{Atoms}, \text{NIST})} \quad (1)$$

The solid state enthalpy of formation for neutral compounds is estimated from the computational results using TROUTONS rule,^[28] where T_m was taken equal to the decomposition temperatures.

$$\Delta H_m = \Delta_f H^0_{(g, \text{Molecule}, 298)} - \Delta H_{\text{sub}} = \Delta_f H^0_{(g, \text{Molecule}, 298)} - (188 [\text{J mol}^{-1} \text{K}^{-1}] * T_m)$$

The solid state enthalpies of formation for the ionic compounds are derived from the calculation of the corresponding lattice energies (U_L) and lattice enthalpies (H_L), calculated from the corresponding molecular volumes,^[29] by the equations provided by Jenkins et al.^[30]

The derived molar standard enthalpies of formation for the solid state (ΔH_m) were used to calculate the solid state energies of formation (ΔU_m) according to equation three, with Δn being the change of moles of gaseous components.^[1b]

$$\Delta U_m = \Delta H_m - \Delta nRT \quad (3)$$

The calculated standard energies of formation were used to perform predictions of the detonation parameters with the program package EXPLO5, Version 5.04.^[31] The program is based on the chemical equilibrium, steady state model of detonation. It uses Becker-Kistiakowsky-Wilsons equation of state (BKW EOS) for gaseous detonation products together with Cowan-Ficketts equation of state for solid carbon.^[32] The calculation of the equilibrium composition of the detonation products is performed by applying modified White, Johnson and Dantzig's free energy minimization technique. The program was designed to enable calculations of detonation parameter at the Chapman-Jouguet point. The BKW equation as implemented in the EXPLO5 program was used with the BKW-G set of parameters (α , β , κ , θ) as stated below the equation, with X_i being the mol fraction of the i -th gaseous detonation product while k_i is the molar co-volume of the i -th gaseous detonation product.^[31-32]

$$pV / RT = 1 + xe^{\beta x} \quad \text{with} \quad x = (\kappa \sum X_i k_i) / [V(T + \theta)]^\alpha$$

$$\alpha = 0.5, \beta = 0.096, \kappa = 17.56, \theta = 4950$$

The results of the detonation runs, together with the calculated energies of formation and the corresponding sensitivities are compiled in Table 7.

Table 7: Physico-chemical properties of compounds **1**, **3**, **5** – **7**, **9** and **11** – **18** in comparison with hexogen (RDX).

	1	3	5	6	7	9	11	RDX*
Formula	C ₂ H ₂ N ₆ O ₄	C ₃ H ₄ N ₆ O ₄	C ₂ H ₅ N ₇ O ₄	C ₃ H ₇ N ₉ O ₄	C ₃ H ₈ N ₁₀ O ₄	C ₃ H ₁₀ N ₁₂ O ₄	C ₄ H ₁₂ N ₁₂ O ₄	C ₃ H ₆ N ₆ O ₆
Molecular Mass [g mol ⁻¹]	174.08	188.11	191.11	233.16	248.17	278.2	292.23	222.12
Impact sensitivity [J] ^a	1	8	23°	35°	25	6	40	7
Friction sensitivity [N] ^b	54	144	288°	360°	360	128	360	120
ESD-test [J]	< 0.25	0.44	0.4°	0.8°	0.5	0.4	0.8	--
<i>N</i> [%] ^c	48.3	44.7	51.3	54.1	56.4	60.4	57.5	37.8
<i>Q</i> [%] ^d	-9.2	-34.0	-20.9	-37.7	-38.7	-40.3		-21.6
<i>T</i> _{dec.} [°C] ^e	135	108	203	220	194	181	225	204
<i>ρ</i> [g cm ⁻³] ^f	1.938	1.688	1.75 ⁿ	1.727	1.73 ⁿ	1.732	1.686	1.80
$\Delta_f H_m^\circ$ [kJ mol ⁻¹] ^g	189	167	105	87	195	418	27	70
$\Delta_f U^\circ$ [kJ kg ⁻¹] ^h	1084	888	548	372	786	1503	93	417
EXPLOS values: V5.04								
$-\Delta_E U^\circ$ [kJ kg ⁻¹] ⁱ	5728	5370	5138	4356	4617	5041	3571	6125
<i>T</i> _E [K] ^j	4425	3966	3758	3229	3319	3437	2625	4236
<i>p</i> _{C-J} [kbar] ^k	385	273	306	267	282	306	238	349
<i>V</i> _{Det.} [m s ⁻¹] ^l	8982	8085	8487	8149	8349	8680	7906	8748
Gas vol. [L kg ⁻¹] ^m	699	713	787	791	808	832	819	739

Table 7: continued.

	12	13	14	15	16	17	18	RDX[*]
Formula	C ₄ H ₁₄ N ₁₄ O ₄	C ₄ H ₁₈ N ₁₈ O ₄	C ₃ H ₇ N ₇ O ₄	C ₃ H ₈ N ₈ O ₄	C ₄ H ₉ N ₉ O ₄	C ₄ H ₁₀ N ₁₀ O ₄	C ₄ H ₁₂ N ₁₂ O ₄	C ₃ H ₆ N ₆ O ₆
Molecular Mass [g mol ⁻¹]	322.26	382.33	205.14	220.16	247.18	262.20	292.23	222.12
Impact sensitivity [J] ^a	> 40	20	32	25°	> 40	> 40	12.5	120
Friction sensitivity [N] ^b	360	192	360	288°	360	360	216	7
ESD–test [J]	0.6	0.4	0.5	0.15°	0.8	0.5	0.4	--
<i>N</i> [%] ^c	60.9	66.2	47.8	50.9	51.0	53.4	57.5	37.8
<i>Ω</i> [%] ^d	-54.6	-54.4	-42.9	-43.6	-55.0	-54.9	-54.7	-21.6
<i>T</i> _{dec.} [°C] ^e	175	149	179	181	195	198	189	204
<i>ρ</i> [g cm ⁻³] ^f	1.7 ⁿ	1.7 ⁿ	1.7 ⁿ	1.7 ⁿ	1.65 ⁿ	1.65 ⁿ	1.665	1.80
$\Delta_f H_m^\circ$ [kJ mol ⁻¹] ^g	268	771	131	285	107	214	435	70
$\Delta_f U^\circ$ [kJ kg ⁻¹] ^h	830	2016	636	1296	432	817	1490	417
EXPLO5 values:								
V5.04								
$-\Delta_E U^\circ$ [kJ kg ⁻¹] ⁱ	4065	4877	5147	5595	4353	4569	4950	6125
<i>T</i> _E [K] ^j	2841	3126	3553	3717	3084	3153	3266	4236
<i>p</i> _{C-J} [kbar] ^k	268	307	279	298	237	249	275	349
<i>V</i> _{Det.} [m s ⁻¹] ^l	8311	8834	8324	8583	7881	8057	8413	8748
Gas vol. [L kg ⁻¹] ^m	836	862	790	809	785	798	820	739

[a] BAM drop hammer; [b] BAM friction tester; [c] Nitrogen content; [d] Oxygen balance^[40]; [e] Temperature of decomposition by DSC ($\beta = 5$ °C, Onset values); [f] X-ray structure; [g] Molar enthalpy of formation; [h] Energy of formation; [i] Energy of Explosion; [j] Explosion temperature; [k] Detonation pressure; [l] Detonation velocity; [m] Assuming only gaseous products; * values based on Ref. ^[33] and the EXPLO5.4 database ^[n] Density values of **12** and **13** estimated in relation to **1**; Densities of the water free versions of **5** and **6** are estimated based on **7** and **9**; Densities of **14**, **15**, **16** and **17** are estimated in relation to TAG MeNANTA, and compared with trends in the row of NANTA salts; ^[o] values for monohydrates.

While both neutral nitrimino compounds **1** and **3** display low decomposition temperatures with 135 °C and 108 °C, respectively, all of their corresponding salts exhibit much higher decomposition temperatures. The mono deprotonated salts of **1** present decomposition temperatures between 181 °C for the triaminoguanidinium salt (**9**) and 220 °C for the guanidinium salt (**7**). Only the bis guanidinium salt of **1** (**11**) exceeds the dec. temperature of the mono salt with 225 °C, while for the bis(hydrazinium) (**10**), bis(aminoguanidinium) (**12**) and bis(triaminoguanidinium) (**13**) salts lower temperatures

are observed. Hence we can state, that the double deprotonation of **1** does not yield higher stability in terms of heat but that those materials exhibit much lower sensitivities towards impact and friction. Compound **13** for example more than triples the impact sensitivity value to 20 J (6 J (**9**)) and also shows higher values for the friction sensitivity at 192 N (128 N (**9**)). Compounds **11** and **13** are both insensitive regarding impact and friction (IS: > 40 J; FS: > 360 N) while **7** and **8** display much lower values for the impact sensitivity (IS: 25 J (**7**), 35 J (**6***H₂O)). The higher stability against physical stress can be explained with the higher electron density within the heterocyclic ring systems, reducing the electron withdrawing effect of the two nitro groups observed by the elongation of the N–O bonds in the molecular structures. Selected DSC plots of the NANTA salts are presented in Figure 23.

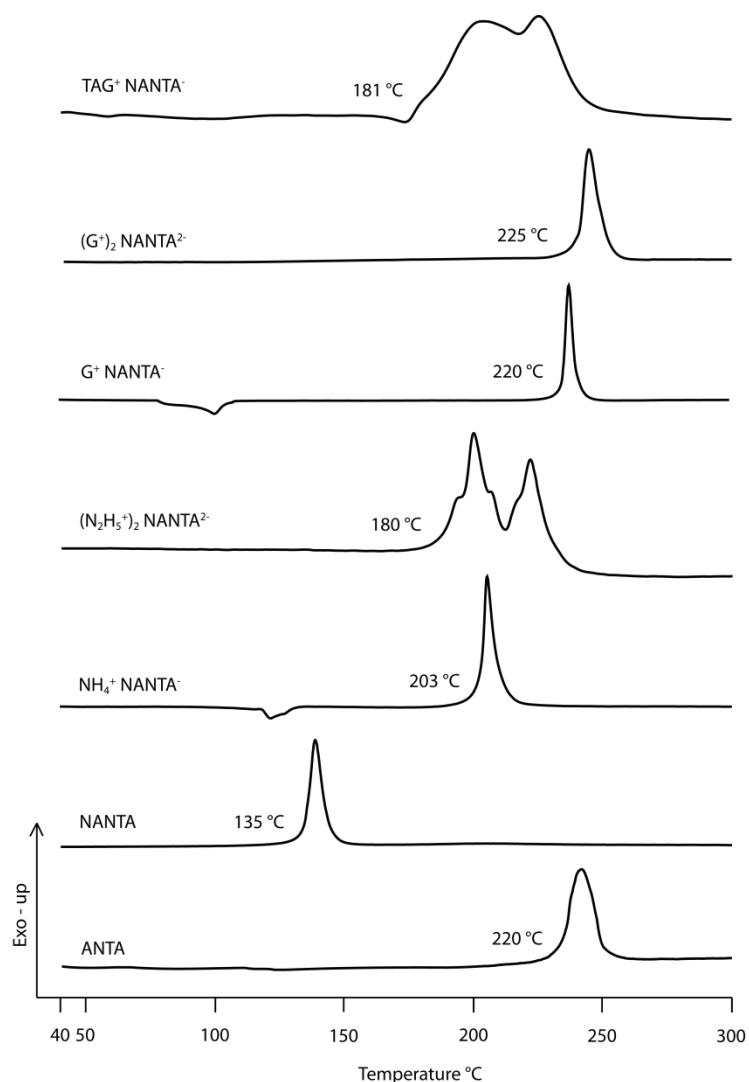


Figure 23: DSC plots of ANTA, NANTA (**1**), NH₄⁺ NANTA⁻ (**5**), G⁺ NANTA⁻ (**7**), TAG⁺ NANTA⁻ (**9**), (N₂H₅⁺)₂ NANTA²⁻ (**10**) and (G⁺)₂ NANTA²⁻ (**11**). DSC plots have been recorded with a heating rate of 5 °C min⁻¹.

As mentioned above, 5-nitramino-3-nitro-1-methyl-1,2,4-triazole (**3**) decomposes at only 108 °C, even though the educt used, 3-nitro-1-methyl-1,2,4-triazole, starts to decompose at 294 °C. The salts show a very homogeneous distribution, the lowest decomposition temperature being 179 °C for the ammonium salt (**14**) and the highest being 198 °C for the aminoguanidinium salt (**17**). The DSC plots of selected compounds are compiled in Figure 24.

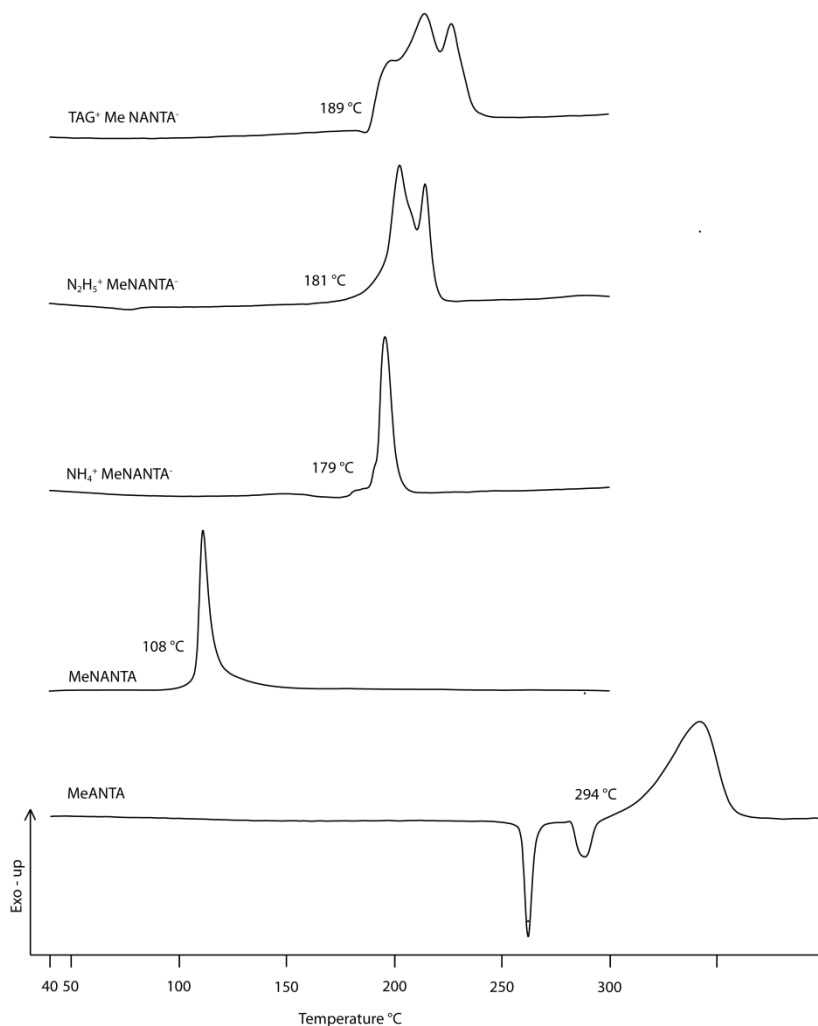


Figure 24: DSC plots of MeANTA, MeNANTA (**3**), NH₄⁺ MeNANTA⁻ (**14**), N₂H₅⁺ MeNANTA⁻ (**15**) and TAG⁺ MeNANTA⁻ (**18**). DSC plots have been recorded with a heating rate of 5 °C min⁻¹.

While **1** is very sensitive towards impact and friction (IS: 1 J; FS: 54 N), **3** shows much lower sensitivity (IS: 8 J; FS: 144 N). These differences also affect the sensitivity values of most of the salts. The sensitivities of the MeNANTA salts are always higher for the mono deprotonated salts, an effect of the +I effect of the methyl group in 1 position. For example, the values for the triaminoguanidinium salts are nearly doubled for both impact

and friction sensitivity when compared to **9** (IS/FS: 6 J/ 128 N (**9**); 12.5 J/ 216 N (**18**)). Guanidinium, aminoguanidinium and ammonium salts of **1** and **3** are sensitive by definition, displaying impact sensitivities > 20 J and friction sensitivities of more than 288 N. The impact sensitivities for the salts of **3** are always found at higher values.

Since the focus of this study was the evaluation of potential replacements for RDX as a secondary explosive, only three compounds show suitable values regarding the detonation parameters, sensitivities and thermal stability. The best compound for the replacement of RDX would be the double salt of NANTA with triaminoguanidinium as the cation if only the performance values and sensitivities are taken into account ($v_{\text{det}} = 8834 \text{ m s}^{-1}$; $p_{\text{C-J}} = 307 \text{ kbar}$; IS 20 J; FS: 192 N). But its decomposition temperature of only $149 \text{ }^\circ\text{C}$ takes **13** out of the equation. While **9** displays the best performance with a detonation velocity of $v_{\text{det}} = 8680 \text{ m s}^{-1}$, a detonation pressure of $p_{\text{C-J}} = 306 \text{ kbar}$ and a decomposition temperature of $181 \text{ }^\circ\text{C}$, the sensitivity values are slightly too high with a friction sensitivity of 128 N and a impact sensitivity of 6 J. Hydrazinium 5-nitramino-3-nitro-1-methyl-1,2,4-triazolate (**15**) shows the same decomposition temperature as **9**, but much higher values for friction and impact sensitivity (IS: 25 J; FS, 288 N) even though measured as a monohydrate. The performance characteristics are only slightly worse, with a detonation velocity of $v_{\text{det}} = 8583 \text{ m s}^{-1}$ and a detonation pressure of $p_{\text{C-J}} = 298 \text{ kbar}$. Even though **18** displays lower performance values ($v_{\text{det}} = 8413 \text{ m s}^{-1}$, $p_{\text{C-J}} = 275 \text{ kbar}$) than **9** and **15**, it displays good sensitivity values with friction sensitivity being 216 N and the impact sensitivity being 12.5 J. Compound **18** shows the highest decomposition temperature of the three compounds at $189 \text{ }^\circ\text{C}$. Even though all compounds are not able to perform better than RDX by calculations they can probably find use in certain applications for civilian use, but not primarily for military applications.

7.3 Conclusion

The starting material ANTA has been synthesized by literature known procedures and was methylated with dimethyl sulfate in good yields resulting in the formation of 5-amino-1-methyl-3-nitro-1,2,4-triazole (**2**). Both compounds have been nitrated using standard nitration techniques in very good yields (**1**: 76 %, **3**: 85 %). The neutral compounds have been fully characterized by means of vibrational and multinuclear NMR spectroscopy, mass spectrometry, dynamic scanning calorimetry and single crystal X-ray diffraction measurements. Additionally, the heats of formation have been calculated with

quantum chemical methods (CBS-4M) and the detonation parameters have been calculated using the experimentally determined densities derived from single crystal X-ray diffraction measurements with the EXPLO5.04 program package. The sensitivities against friction, impact and electrostatic discharge have been determined by standard BAM measurements. Both compounds exhibit low thermal stabilities of 135 °C (**1**) and 108 °C (**3**). The sensitivities differ very much: While **1** is very sensitive towards friction (54 N) and impact (1 J), **3** exhibits reasonable sensitivities of 8 J (impact) and 144 N (friction). Since the density is decreased by 0.25 g cm⁻³ from **1** to **3** together with the heat of formation (ΔH_f^0 : 189 kJ mol⁻¹ (**1**); ΔH_f^0 : 167 kJ mol⁻¹ (**3**)), the detonation velocities exhibit values well above RDX for **1** (v_{det} : 8982 m s⁻¹; $P_{\text{C-J}}$: 385 kbar) but well below RDX for **3** (v_{det} : 8085 m s⁻¹; $P_{\text{C-J}}$: 273 kbar).

Mono and double salts have been synthesized from **1** using nitrogen rich cations, while only the mono salts of these cations have been synthesized for **3**. All reactions were carried out using the free bases or the corresponding carbonates. All energetic, ionic compounds (**5** – **18**), have been characterized with the same techniques as described for the neutral compounds. Crystal structures have only been obtained from selected compounds, as crystallization of the compounds was partially very difficult. Detonation parameters have been calculated for selected compounds, using heats of formation and the densities derived from single crystal X-ray diffraction measurements. Densities have been estimated based on similar compounds if the single crystal X-ray densities were not applicable. The properties of mono and double salts have been intensively studied, exhibiting overall lower thermal stabilities than the mono salts, but also much lower sensitivities towards shock and friction. Performance wise, they exhibit lower values than the mono salts, except for the bis(triaminoguanidinium) salt (**13**) which exhibits higher detonation values than **9** (v_{det} : 8834 m s⁻¹ (**13**); $P_{\text{C-J}}$: 307 kbar (**13**)) but the decomposition temperatures is much lower with only 149 °C in the case of **13**. The best compounds from an application standpoint are the mono salts of the triaminoguanidinium cation (**9** and **18**) and the hydrazinium salt of **3** (**15**). All of these compounds exhibit decomposition temperatures of above 180 °C and performance values right in the range of RDX or only slightly below. They could find application, since they are easy to obtain, safe to handle and show performance characteristics in the range of modern secondary explosives.

7.4 Experimental Part

Caution: Although all presented nitraminoazoles are rather stable against outer stimuli, proper safety precautions should be taken, when handling the dry materials. All derivatives of ANTA are energetic materials and especially **1** tends to explode under the influence of heat, impact or friction. Lab personnel and the equipment should be properly grounded and protective equipment like earthed shoes, leather coat, Kevlar[®] gloves and face shield is recommended.

General. All chemical reagents and solvents were obtained from Sigma-Aldrich Inc. or Acros Organics (analytical grade) and were used as supplied without further purification. ¹H, ¹³C{¹H}, ¹⁴N{¹H}, ¹⁵N{¹H} and ¹⁵N NMR spectra were recorded on a JEOL Eclipse 400 instrument in DMSO-*d*₆ at or near 25 °C. The chemical shifts are given relative to tetramethylsilane (¹H, ¹³C) or nitro methane (¹⁴N, ¹⁵N) as external standards and coupling constants are given in Hertz (Hz). Infrared (IR) spectra were recorded on a Perkin-Elmer Spectrum BX FT-IR instrument equipped with an ATR unit at 25 °C. Transmittance values are qualitatively described as “very strong” (vs), “strong” (s), “medium” (m), “weak” (w) and “very weak” (vw). RAMAN spectra were recorded on a Bruker RAM II spectrometer equipped with a Nd:YAG laser operating at 1064 nm and a reflection angle of 180°. The intensities are reported as percentages of the most intense peak and are given in parentheses. Elemental analyses (CHNO) were performed with a Netzsch Simultaneous Thermal Analyzer STA 429. Melting and decomposition points were determined by differential scanning calorimetry (Linseis PT 10 DSC, calibrated with standard pure indium and zinc). Measurements were performed at a heating rate of 5 °C min⁻¹ in closed aluminum sample pans with a 1 μm hole in the top for gas release to avoid an unsafe increase in pressure under a nitrogen flow of 20 mL min⁻¹ with an empty identical aluminum sample pan as a reference. The mass spectra were recorded with DEI, DCI and FAB methods on a JEOL MStation JMS 700 mass spectrometer.

For initial safety testing, the impact and friction sensitivities as well as the electrostatic sensitivities were determined. The impact sensitivity tests were carried out according to STANAG 4489,^[34] modified according to WIWEB instruction 4-5.1.02^[35] using a BAM^[36] drop hammer. The friction sensitivity tests were carried out according to STANAG 4487^[37] and modified according to WIWEB instruction 4-5.1.03^[38] using the BAM friction tester. The electrostatic sensitivity tests were accomplished according to

STANAG 4490^[39] using an electric spark testing device ESD 2010EN (OZM Research) operating with the “Winspark 1.15 software package”.^[40]

Crystallographic measurements. The single crystal X-ray diffraction data of ANTA, 3-diazo-5-nitro-1,2,4-triazole, **1**, **3**, **4** – **7**, **9**, **11** – **12** and **18** were collected using an Oxford Xcalibur3 diffractometer equipped with a Spellman generator (voltage 50 kV, current 40 mA) and a KappaCCD detector. The data collection was undertaken using the CRYCALIS CCD software^[41] while the data reduction was performed with the CRYCALIS RED software.^[42] The structures were solved with SIR-92^[43] or SHELXS-97^[44] and refined with SHELXL-97^[45] implemented in the program package WinGX^[46] and finally checked using PLATON.^[47] Further information regarding the crystal-structure determination have been deposited with the Cambridge Crystallographic Data Centre^[48] as supplementary publication Nos. 824140 (3-diazo-5-nitro-1,2,4-triazole), 824138 (**1**), 824139 (**3**), 824141 (**4**), 824142 (**5**), 824147 (**6**), 824145 (**7**), 824144 (**9**), 824146 (**11**), 824143 (**12**) and 824148 (**18**).

5-Nitramino-3-nitro-1*H*-1,2,4-triazole (**1**)

5-Amino-3-nitro-1*H*-1,2,4-triazole (5 mmol, 0.735 g) was dissolved in 5.85 mL concentrated H₂SO₄ at 0 °C. 100% nitric acid (1.3 mL) was added dropwise within 10 minutes. The reaction mixture was left stirring at 0 °C for 30 minutes and was then brought to ambient temperature and stirred for an additional 3 hours. The reaction mixture was quenched with 100 ml of ice water and the resulting solution extracted three times with 100 mL of ethyl acetate each. The organic phases were combined, dried over magnesium sulfate and the solvent volume was reduced to app. 20 mL and left for crystallization, yielding 0.66 g (76%) pure 5-nitramino-3-nitro-1*H*-1,2,4-triazole. Crystals suitable for X-ray diffraction measurements were obtained by recrystallization from ethyl acetate.

T_{dec.}: 135 °C (5 °C min⁻¹); ¹H NMR (DMSO-*d*₆, 25 °C) δ (ppm) = 6.95 (s, br); ¹³C{¹H} NMR (DMSO-*d*₆, 25 °C) δ (ppm) = 160.5 (C-NO₂), 151.7 (C-N-NO₂); ¹⁴N NMR (DMSO-*d*₆, 25 °C) δ (ppm) = -23 (-NO₂), -29 (-N-NO₂); ¹⁵N NMR (DMSO-*d*₆, 25 °C) δ (ppm) = -26.5 (-NO₂, N₄), -32.3 (-N-NO₂, N₆), -101.0 (N₂), -163.6 (N₃), -180.1 (N₁/N₅), -181.0 (N₁/N₅); ¹⁵N{¹H} NMR (DMSO-*d*₆, 25 °C) δ (ppm) = -26.5 (-NO₂, N₄), -32.4 (-N-NO₂, N₆), -101.0 (N₂), -163.4 (N₃), -180.0 (N₁/N₅), -181.2 (N₁/N₅); IR (ATR, 25 °C,

cm^{-1} ν = 3175 (s, br), 2961 (w), 2923 (m), 1638 (m), 1607 (m), 1558 (s), 1543 (m), 1521 (s), 1468 (m), 1410 (m), 1336 (m), 1312 (s), 1266 (vs), 1154 (m), 1077 (m), 998 (m), 835 (s), 752 (w), 695 (m); RAMAN (Nd:YAG, 1064 nm, cm^{-1}) ν = 3190 (2), 2262 (8), 1611 (15), 1572 (38), 1543 (53), 1525 (89), 1469 (32), 1412 (100), 1346 (9), 1316 (24), 1264 (11), 1159 (48), 1078 (17), 1031 (31), 1003 (15), 837 (7), 575 (2), 423 (3), 363 (9), 247 (4); m/z : (DEI+): 18.0 (20), 28.0 (78), 30.0 (90), 38.0 (17), 42.0 (12), 43.0 (15), 44.0 (90), 46.0 (100), 53.7 (49), 55.0 (14), 76.2 (29), 128.0 (32), 129.0 (21), 140.0 (21), 174.0 (8, $[\text{M}^+]$); EA ($\text{C}_2\text{H}_2\text{N}_6\text{O}_4$) calcd.: C, 13.80; H, 1.16; N, 48.28; found: C, 47.03; H, 1.03; N, 47.03; Sensitivities (anhydrous) (grain size: 100–500 μm): IS: 1 J ; FS: 54 N ; ESD: < 250 mJ.

5-Amino-1-methyl-3-nitro-1,2,4-triazole (2)

5-Amino-3-nitro-1*H*-1,2,4-triazole monohydrate (50 mmol, 7.35 g) was dissolved in 2 M sodium hydroxide solution (100 mmol, 50 mL). Dimethyl sulfate (50 mmol, 4.75 mL) was added dropwise afterwards and the reaction mixture was stirred under reflux conditions overnight. After cooling the suspension to 0 °C, the orange precipitate was filtered off, washed with water and air dried to yield 3.54 g (50 %) of elemental analysis pure 5-amino-1-methyl-3-nitro-1,2,4-triazole.

T_{melt} : 259 °C, 282 °C (DSC, T_{onset} , 5 °C min^{-1}); $T_{\text{dec.}}$: 294 °C (DSC, 5 °C min^{-1}), 319 °C (DSC, T_{onset} , 5 °C min^{-1}); ^1H NMR ([d_6]-DMSO, 25 °C) δ 7.00 (s, 2H, $-\text{NH}_2$), 3.63 (s, 3H, $-\text{CH}_3$); $^{13}\text{C}\{^1\text{H}\}$ NMR (DMSO- d_6 , 25 °C) δ (ppm) = 158.9, 156.4, 35.9; ^{14}N NMR (DMSO- d_6 , 25 °C) δ (ppm) = -25 ($-\text{NO}_2$); IR (ATR, 25 °C, cm^{-1}) ν = 3423 (s), 3286 (w), 3229 (w), 3170 (m), 3034 (w), 1648 (s), 1580 (m), 1501 (vs), 1465 (w), 1446 (w), 1406 (m), 1312 (s), 1256 (m), 1244 (m), 1090 (w), 1037 (w), 1026 (w), 862 (m), 790 (w), 725 (w), 676 (w), 625 (w); RAMAN (Nd:YAG, 1064 nm, cm^{-1}) ν = 3424 (1), 3165 (1), 3035 (2), 3002 (1), 2961 (6), 2808 (1), 1653 (5), 1571 (7), 1516 (7), 1455 (5), 1406 (100), 1316 (23), 1254 (25), 1096 (1), 1040 (15), 1027 (10), 796 (10), 671 (2), 601 (1), 429 (5), 310 (5), 126 (4), 100 (19); EA: ($\text{C}_3\text{H}_5\text{N}_5\text{O}_2$) calc: C, 25.18; H, 3.52; N, 48.94; found: C, 25.46; H, 3.50; N, 48.58; Sensitivities (anhydrous) (grain size: 100 – 500 μm): IS: > 40 J; FS: > 360 N.

1-Methyl-5-nitramino-3-nitro-1,2,4-triazole (**3**)

Concentrated sulfuric acid (3.51 mL, 64.5 mmol) was added to 5-amino-1-methyl-3-nitro-1,2,4-triazole (0.43 g, 3 mmol). The resulting solution was cooled to 0-3 °C and 100 % nitric acid (0.86 mL, 20.6 mmol) was added dropwise. The solution was stirred for 30 min at 0-3 °C followed by 2 hours at ambient temperature and was then quenched with ice-water (60 g). It was then extracted with ethyl acetate (3 x 50 mL) and the combined organic phases were dried over magnesium sulfate. The solvent was removed by rotary evaporation until about 5 mL were left. After crystallization 1-methyl-5-nitramino-3-nitro-1,2,4-triazole was obtained as yellow crystalline plates in a yield of 85 % (0.48 g)

$T_{\text{dec.}}$: 108 °C (DSC, Onset, 5 °C min⁻¹); ¹H NMR (DMSO-*d*₆, 25 °C): δ (ppm) = 4.64 (br. s, 1H, C-NH-NO₂), 3.77 (s, 3H, CH₃); ¹³C NMR (DMSO-*d*₆, 25 °C): δ (ppm) = 159.4 (C-NO₂), 151.5 (C-NH-NO₂), 35.6 (s, CH₃); ¹⁴N NMR (DMSO-*d*₆, 25 °C): δ (ppm) = -22 (-NO₂, N₄), -27 (-N-NO₂, N₆); ¹⁵N NMR (DMSO-*d*₆, 25 °C) δ (ppm) = -27.2 (-NO₂, N₄), -29.8 (-N-NO₂, N₆), -86.7 (q, ³J_{NH} = 2.16 Hz, N₂), -146.0 (N₃), -175.3 (q, ²J_{NH} = 2.04 Hz, N₁), -191.1 (q, ⁴J_{NH} = 0.74 Hz, N₅); ¹⁵N{¹H} NMR (DMSO-*d*₆, 25 °C) δ (ppm) = -27.2 (-NO₂, N₄), -29.8 (-N-NO₂, N₆), -86.7 (N₂), -145.9 (N₃), -175.3 (N₁), -191.3 (N₅); IR (ATR, 25 °C, cm⁻¹) ν = 3426 (w), 3214 (m), 3082 (s), 2949 (s), 2761 (m), 1606 (vs), 1565 (m), 1534 (s), 1490 (s), 1439 (w), 1402 (m), 1376 (w), 1309 (vs), 1286 (s), 1221 (m), 1034 (vw), 1000 (w), 899 (m), 770 (w), 760 (w), 707 (m), 678 (w), 652 (m); RAMAN (Nd:YAG, 1064 nm, cm⁻¹) ν = 3039 (8), 2974 (47), 1598 (9), 1562 (32), 1524 (33), 1496 (87), 1444 (62), 1410 (99), 1320 (28), 1284 (76), 1036 (34), 1002 (13), 902 (7), 837 (5), 795 (6), 771 (13), 708 (12), 504 (6), 437 (11), 400 (11), 372 (12), 295 (9), 257 (12), 190 (15), 104 (97); EA (C₃H₄N₆O₄) calcd.: C, 19.16; H, 2.14; N, 44.68; found: C, 19.82; H, 2.17; N, 44.45; m/z (DCI+): 189.06 [M+H]⁺; Sensitivities (anhydrous) (grain size: 100–500 μ m): IS: 8 J; FS: 144 N; ESD: 440 mJ.

Hydroxylammonium 5-nitramino-3-nitro-1*H*-1,2,4-triazolate (**4**)

5-Nitramino-3-nitro-1*H*-1,2,4-triazole (2 mmol, 0.348 g) was dissolved in 2 mL water and hydroxylamine solution (2 mmol, 0.12 mL) was added dropwise while stirring was continued. The resulting solution was heated to 90 °C for an additional 15 minutes and left cooling down to ambient temperature. Yellow crystals of hydroxylammonium 5-

nitramino-3-nitro-1*H*-1,2,4-triazolate monohydrate, suitable for X-ray diffraction analysis, deposited overnight with a yield of 85 % (0.38 g).

T: 124 °C (-H₂O, DSC, Onset, 5 °C min⁻¹); T_{dec.}: 164 °C (DSC, Onset, 5 °C min⁻¹); ¹H NMR (DMSO-*d*₆, 25 °C) δ (ppm) = 10.57 (s, br), 7.22 (s, br); ¹³C{¹H} NMR (DMSO-*d*₆, 25 °C) δ (ppm) = 160.8, 157.9; ¹⁴N NMR (DMSO-*d*₆, 25 °C) δ (ppm) = -14 (-NO₂), -23 (-N-NO₂); IR (ATR, 25 °C, cm⁻¹) ν = 3090 (s), 2899 (s), 2712 (m), 1628 (w), 1568 (m), 1536 (m), 1490 (s), 1451 (m), 1423 (s), 1377 (m), 1338 (m), 1292 (vs), 1271 (vs), 1243 (s), 1191 (m), 1148 (m), 1098 (m), 1084 (m), 1026 (w), 1000 (m), 876 (w), 860 (w), 836 (m), 773 (w), 725 (m); *m/z*: (FAB+): 34.0 [NH₃OH⁺]; *m/z*: (FAB-): 173.0 [C₂HN₆O₄⁻]; EA (C₂H₅N₇O₅*2/3 H₂O) calcd.: C, 10.96; H, 2.91; N, 44.75; found: C, 11.29; H, 3.09; N, 44.61; Sensitivities (anhydrous) (grain size: 100–500 μm): IS: 7 J; FS: 120 N; ESD: 300 mJ.

Ammonium 5-nitramino-3-nitro-1*H*-1,2,4-triazolate (5)

5-Nitramino-3-nitro-1*H*-1,2,4-triazole (2 mmol, 0.348 g) was dissolved in 2 mL water and 6.25 % ammonia solution (2 mmol, 0.6 mL) was added dropwise while stirring was continued. A clear red solution developed immediately and was stored overnight at ambient temperature without further stirring. Orange crystals of ammonium 5-nitramino-3-nitro-1*H*-1,2,4-triazolate monohydrate, suitable for X-ray diffraction analysis, deposited overnight in nearly quantitative yield (98 %, 0.41 g).

T: 117 °C (-H₂O, DSC, Onset, 5 °C min⁻¹); T_{dec.}: 203 °C (5 °C min⁻¹); ¹H NMR (DMSO-*d*₆, 25 °C) δ (ppm) = 7.14 (s, br, 4H, NH₄⁺); ¹³C{¹H} NMR (DMSO-*d*₆, 25 °C) δ (ppm) = 160.8 (C-NO₂), 157.9 (C-N-NO₂); ¹⁴N NMR (DMSO-*d*₆, 25 °C) δ (ppm) = -14 (-NO₂), -22 (-N-NO₂); IR (ATR, 25 °C, cm⁻¹) ν = 3264 (m), 3185 (s), 3076 (m), 2899 (m), 1693 (w), 1572 (w), 1535 (m), 1489 (m), 1446 (m), 1423 (s), 1406 (m), 1378 (s), 1340 (m), 1292 (vs), 1245 (s), 1148 (m), 1084 (s), 1024 (w), 988 (m), 894 (w), 859 (w), 837 (w), 742 (w), 727 (m), 638 (w); RAMAN (Nd:YAG, 1064 nm, cm⁻¹) ν = 1535 (20), 1489 (100), 1422 (69), 1380 (21), 1297 (16), 1274 (4), 1151 (27), 1089 (3), 1026 (11), 990 (24), 863 (4), 838 (3), 774 (3), 745 (7), 401 (5), 365 (4), 259 (10), 167 (14), 126 (38), 90 (34), 75 (33); *m/z*: (FAB+): 18.0 [NH₄⁺]; *m/z*: (FAB-): 173.0 [C₂HN₆O₄⁻]; EA (C₂H₅N₇O₄*H₂O) calcd.: C, 11.49; H, 3.37; N, 46.89; found: C, 11.93; H, 3.21; N, 46.70; Sensitivities (monohydrate) (grain size: < 100 μm): IS: 23 J; FS: 288 N; ESD: 0.4 J.

Hydrazinium 5-nitramino-3-nitro-1*H*-1,2,4-triazolate (**6**)

Obtained by recrystallization of **10**.

T: 73.3 °C (DSC, $-\text{H}_2\text{O}$, 5 °C min⁻¹), 192.7 °C (DSC, Onset, 5 °C min⁻¹); ¹H NMR (DMSO-*d*₆, 25 °C) δ (ppm) = 13.86 (N_{Tri}H), 7.10 (s, br, 5H; N₂H₅⁺); ¹³C{¹H} NMR (DMSO-*d*₆, 25 °C) δ (ppm) = 160.8 (C-NO₂), 157.9 (C-N-NO₂); ¹⁴N NMR (DMSO-*d*₆, 25 °C) δ (ppm) = -15 (-NO₂), -23 (-N-NO₂), -359 (N₂H₅⁺).

Bis(hydrazinium) 5-nitramino-3-nitro-1,2,4-triazolate (**10**)

5-Nitramino-3-nitro-1*H*-1,2,4-triazole (2 mmol, 0.348 g) was dissolved in 2 mL water and hydrazine monohydrate (98 %, 0.49 mL, 10 mmol) was added while stirring. The product precipitated immediately, was filtered off, washed with small portions of water and diethyl ether to yield 0.35 g (73 %) of **10** as an amorphous brownish powder. Recrystallization of the product from water, ethanol, methanol and mixtures yielded only amorphous product, not suitable for X-ray diffraction measurements. Recrystallization attempts from water yielded crystals of the mono hydrazinium salt of 5-nitramino-3-nitro-1*H*-1,2,4-triazole.

T_{dec.}: 180 °C, (DSC, 5 °C min⁻¹), 187 °C (DSC, Onset, 5 °C min⁻¹); ¹H NMR (DMSO-*d*₆, 25 °C) δ (ppm) = 5.69 (s, br, 10H; N₂H₅⁺); ¹³C{¹H} NMR (DMSO-*d*₆, 25 °C) δ (ppm) = 161.1 (C-NO₂), 158.9 (C-N-NO₂); ¹⁴N NMR (DMSO-*d*₆, 25 °C) δ (ppm) = -15 (-NO₂), -23 (-N-NO₂), -333 (v br, N₂H₅⁺); IR (ATR, 25 °C, cm⁻¹) ν = 3368 (m), 3296 (m), 2967 (m), 2832 (s), 2709 (s), 2636 (s), 1623 (w), 1582 (w), 1500 (m), 1476 (s), 1435 (vs), 1390 (m), 1355 (vs), 1295 (s), 1112 (s), 1098 (s), 1080 (s), 1037 (m), 1012 (m), 972 (m), 955 (m), 886 (w), 834 (w), 755 (w), 746 (w), 654 (w); RAMAN (Nd:YAG, 1064 nm, cm⁻¹) ν = 3304 (5), 2825 (4), 1478 (22), 1439 (100), 1393 (30), 1346 (32), 1304 (27), 1130 (93), 1083 (38), 1014 (40), 972 (6), 888 (15), 836 (14), 748 (6), 408 (6), 306 (8), 223 (8), 150 (18), 123 (13), 85 (24); *m/z*: (FAB+): 33.1 [N₂H₅⁺]; *m/z*: (FAB-): 172.9 [CHN₆O₄⁻]; EA (C₂H₁₀N₁₀O₄) calcd.: C, 10.09; H, 4.23; N, 58.81; found: C, 10.72; H, 3.99; N, 58.58.

Guanidinium 5-nitramino-3-nitro-1*H*-1,2,4-triazolate (**7**)

5-Nitramino-3-nitro-1*H*-1,2,4-triazole (2 mmol, 0.348 g) was dissolved in 25 mL water, heated to 40 °C and bis(guanidinium)carbonate (1 mmol, 0.180 g) was added in small portions. Gas release occurred immediately and a bright orange solution formed. After heating was continued at 65-70 °C for another half hour, the solution was left standing without stirring until ambient temperature was reached. The solvent was completely evaporated leaving 0.43 g (92 %) of a bright yellow/orange solid. Crystals suitable for X-ray diffraction analysis were obtained from an ethanolic solution (water:ethanol = 4:1).

T: 80–105 °C (–H₂O, DSC, 5 °C min⁻¹); T_{dec.}: 220 °C (5 °C min⁻¹); ¹H NMR (DMSO-*d*₆, 25 °C) δ (ppm) = 13.84 (s, 1H, N_{Tri}-H), 6.91 (s, 6H, G⁺); ¹³C{¹H} NMR (DMSO-*d*₆, 25 °C) δ (ppm) = 160.8 (C-NO₂), 157.9 (G⁺), 157.8 (C-N-NO₂); ¹⁴N NMR (DMSO-*d*₆, 25 °C) δ (ppm) = –15 (–NO₂), –23 (–N-NO₂), –304 (v br, G⁺); IR (ATR, 25 °C, cm⁻¹) ν = 3532 (m), 3355 (vs), 3240 (m), 3166 (vs), 1662 (s), 1628 (m), 1579 (w), 1549 (w), 1529 (m), 1488 (s), 1425 (w), 1394 (m), 1365 (m), 1336 (m), 1306 (s), 1245 (m), 1159 (w), 1118 (w), 1078 (m), 1024 (w), 1000 (m), 860 (w), 839 (w), 774 (w), 749 (w), 721 (w); RAMAN (Nd:YAG, 1064 nm, cm⁻¹) ν = 3240 (2), 1557 (4), 1523 (11), 1491 (100), 1424 (27), 1401 (16), 1365 (10), 1296 (7), 1246 (3), 1162 (16), 1027 (12), 1000 (26), 861 (2), 843 (3), 753 (6), 541 (3), 445 (3), 391 (3), 361 (4), 270 (7), 197 (5); *m/z*: (FAB⁺): 60.1 [CH₆N₃⁺]; *m/z*: (FAB[–]): 172.9 [C₂HN₆O₄[–]]; EA (C₃H₇N₉O₄*H₂O) calcd.: C, 14.35; H, 3.61; N, 50.19; found: C, 14.91; H, 3.39; N, 50.16; Sensitivities (monohydrate) (grain size: < 100 μm): IS: 35 J; FS: 360 N; ESD: 0.8 J.

Bis(guanidinium) 5-nitramino-3-nitro-1,2,4-triazolate (**11**)

5-Nitramino-3-nitro-1*H*-1,2,4-triazole (2 mmol, 0.348 g) was dissolved in 50 mL water, heated to 40 °C and bis(guanidinium)carbonate (2 mmol, 0.360 g) was added in small portions. Gas release occurred immediately and a bright red solution formed. After heating was continued at 65-70 °C for an hour, the solution was left standing without stirring until ambient temperature was reached. The solvent was completely evaporated leaving 0.55 g (94 %) of a bright red solid. Crystals suitable for X-ray diffraction analysis were obtained from water.

$T_{\text{dec.}}$: 225 °C (DSC, 5 °C min⁻¹), 240 °C (DSC, Onset, 5 °C min⁻¹); ¹H NMR (DMSO-*d*₆, 25 °C) δ (ppm) = 7.26 (s, 12H, G⁺); ¹³C{¹H} NMR (DMSO-*d*₆, 25 °C) δ (ppm) = 163.9, 162.8, 158.1 (G⁺); ¹⁴N NMR (DMSO-*d*₆, 25 °C) δ (ppm) = -19, -20; IR (ATR, 25 °C, cm⁻¹) ν = 3456 (m), 3406 (m), 3349 (m), 3148 (m), 1665 (m), 1635 (s), 1467 (s), 1427 (s), 1393 (w), 1375 (s), 1328 (vs), 1295 (s), 1276 (s), 1156 (w), 1094 (m), 1049 (s), 1027 (m), 1005 (m), 860 (m), 836 (w), 741 (m), 657 (w); RAMAN (Nd:YAG, 1064 nm, cm⁻¹) ν = 3402 (1), 3191 (1), 1506 (4), 1462 (7), 1420 (69), 1378 (21), 1320 (49), 1298 (71), 1053 (100), 1013 (24), 835 (27), 744 (3), 589 (1), 531 (8), 443 (12), 409 (2), 273 (5), 199 (11); m/z : (FAB⁺): 60.1 [CH₆N₃⁺]; m/z : (FAB⁻): 173.0 [C₂HN₆O₄⁻]; EA (C₄H₁₂N₁₂O₄) calcd.: C, 16.44; H, 4.14; N, 57.52; found: C, 16.33; H, 3.99; N, 56.83; Sensitivities (anhydrous) (grain size: < 100 μ m): IS: 40 J; FS: 360 N; ESD: 0.8 J.

Aminoguanidinium 5-nitramino-3-nitro-1*H*-1,2,4-triazolate (**8**)

5-Nitramino-3-nitro-1*H*-1,2,4-triazole (3 mmol, 0.522 g) was dissolved in 50 mL water, heated to 40 °C and aminoguanidinium bicarbonate (3 mmol, 0.405 g) was added in small portions. The solution turned red immediately and stirring was continued at 65 °C until no more gas release was observed. The solvent was evaporated until dryness leaving aminoguanidinium 5-nitramino-3-nitro-1*H*-1,2,4-triazolate as an orange powder in 81 % yield (0.60 g).

$T_{\text{dec.}}$: 194 °C (DSC, 5 °C min⁻¹), 207 °C (DSC, Onset, 5 °C min⁻¹); ¹H NMR (DMSO-*d*₆, 25 °C) δ (ppm) = 13.80 (s, 1H, N_{Triaz}H), 8.53 (s, 1H, C-NH-NH₂), 7.21 (s, 2H, C-NH₂), 6.71 (s, 2H, C-NH₂), 4.65 (s, 2H, C-NH-NH₂); ¹³C{¹H} NMR (DMSO-*d*₆, 25 °C) δ (ppm) = 160.8 (C-NO₂), 158.7 (AG⁺), 157.9 (C-N-NO₂); ¹⁴N NMR (DMSO-*d*₆, 25 °C) δ (ppm) = -14 (-NO₂), -23 (-N-NO₂); IR (ATR, 25 °C, cm⁻¹) ν = 3425 (w), 3365 (m), 3321 (m), 3176 (m), 1663 (s), 1607 (w), 1540 (s), 1488 (s), 1422 (w), 1400 (m), 1367 (m), 1334 (s), 1306 (vs), 1240 (m), 1199 (m), 1141 (m), 1079 (s), 1017 (w), 1008 (w), 944 (m), 862 (w), 835 (m), 776 (w), 746 (w), 721 (w), 665 (w); RAMAN (Nd:YAG, 1064 nm, cm⁻¹) ν = 3365 (1), 3300 (1), 1679 (3), 1564 (5), 1527 (18), 1488 (100), 1426 (19), 1407 (29), 1371 (6), 1341 (3), 1300 (3), 1245 (2), 1146 (15), 1087 (2), 1008 (48), 970 (3), 864 (4), 839 (3), 754 (11), 616 (2), 509 (5), 441 (2), 385 (2), 365 (6), 263 (10), 227 (2); m/z : (FAB⁺): 75.1 [CH₇N₄⁺]; m/z : (FAB⁻): 173.0 [C₂HN₆O₄⁻]; EA (C₃H₈N₁₀O₂) calcd.: C, 14.52; H,

3.25; N, 56.44; found: C, 14.82; H, 3.06; N, 55.92; Sensitivities (anhydrous) (grain size: 100-500 μm): IS: 25 J; FS: 360 N; ESD: 0.5 J.

Bis(aminoguanidinium) 5-nitramino-3-nitro-1,2,4-triazolate (**12**)

5-Nitramino-3-nitro-1*H*-1,2,4-triazole (2 mmol, 0.348 g) was dissolved in 50 mL water, heated to 40 °C and aminoguanidinium bicarbonate (4 mmol, 0.544 g) was added in small portions. The solution turned red immediately and stirring was continued at 65 °C until no more gas release was observed. The solvent was evaporated until dryness leaving bis(aminoguanidinium) 5-nitramino-3-nitro-1,2,4-triazolate as an orange powder in 85 % yield (0.49 g). Crystals suitable for X-ray diffraction measurements were obtained by recrystallization from water.

T: 80 °C ($-\text{H}_2\text{O}$, DSC, 5 °C min^{-1}); T_{melt} : 175 °C (DSC, Onset, 5 °C min^{-1}); $T_{\text{dec.}}$: 193 °C (DSC, Onset, 5 °C min^{-1}); ^1H NMR (DMSO- d_6 , 25 °C) δ (ppm) = 7.60 (s, br), 4.67 (s, br); $^{13}\text{C}\{^1\text{H}\}$ NMR (DMSO- d_6 , 25 °C) δ (ppm) = 163.2, 162.6, 159.0 (AG $^+$); ^{14}N NMR (DMSO- d_6 , 25 °C) δ (ppm) = -19; IR (ATR, 25 °C, cm^{-1}) ν = 3429 (m), 3325 (m), 3167 (m), 1660 (vs), 1550 (w), 1542 (w), 1520 (w), 1473 (s), 1433 (s), 1399 (m), 1364 (s), 1336 (s), 1290 (s), 1286 (s), 1207 (m), 1199 (m), 1142 (w), 1106 (m), 1075 (m), 1029 (m), 1005 (m), 945 (m), 928 (m), 886 (w), 862 (w), 832 (w), 814 (w), 777 (w), 763 (w), 747 (m), 733 (w); RAMAN (Nd:YAG, 1064 nm, cm^{-1}) ν = 3331 (1), 3240 (1), 1526 (2), 1488 (5), 1435 (99), 1402 (12), 1366 (18), 1329 (18), 1300 (15), 1281 (12), 1118 (100), 1075 (27), 1010 (12), 971 (4), 889 (4), 833 (2), 745 (1), 630 (1), 507 (2), 423 (1); m/z : (FAB $^+$): 75.1 [CH_7N_4^+]; m/z : (FAB $^-$): 173.0 [$\text{C}_2\text{HN}_6\text{O}_4^-$]; EA ($\text{C}_4\text{H}_{14}\text{N}_{14}\text{O}_4 \cdot \text{H}_2\text{O}$) calcd.: C, 14.12; H, 4.74; N, 57.63; found: C, 14.46; H, 4.39; N, 57.01; Sensitivities (monohydrate) (grain size: 100–500 μm): IS: > 40 J; FS: 360 N; ESD: 0.6 J.

Triaminoguanidinium 5-nitramino-3-nitro-1*H*-1,2,4-triazolate (**9**)

5-Nitramino-3-nitro-1*H*-1,2,4-triazole (3 mmol, 0.522 g) was dissolved in 60 mL boiling ethanol. Triaminoguanidine (2.95 mmol, 0.310 g) was added portionwise to the solution under a nitrogen stream. With continued heating, water was added to the solution in small portions, until complete dissolution of the solid material was observed. After cooling to ambient temperature, the solvent was reduced to 1/3 of its original volume and left

standing for crystallization. Pure triaminoguanidinium 5-nitramino-3-nitro-1*H*-1,2,4-triazolate was obtained as orange crystals, which were filtered off and washed thoroughly with diethyl ether to yield 0.750 g (89 %).

T_{melt} : 164 °C (DSC, 5 °C min⁻¹); $T_{\text{dec.}}$: 181 °C (DSC, Onset, 5 °C min⁻¹); ¹H NMR (DMSO-*d*₆, 25 °C) δ (ppm) = 13.78 (s, 1H, N_{Tri}H), 8.55 (s, 3H, C-NH-NH₂), 4.56 (s, 6H, C-NH-NH₂); ¹³C{¹H} NMR (DMSO-*d*₆, 25 °C) δ (ppm) = 160.8 (C-NO₂), 159.0 (TAG⁺), 158.0 (C-N-NO₂); ¹⁴N NMR (DMSO-*d*₆, 25 °C) δ (ppm) = -14 (-NO₂), -23 (-N-NO₂); ¹⁵N NMR (DMSO-*d*₆, 25 °C) δ (ppm) = -15.2 (-NO₂, N₄), -23.7 (-N-NO₂, N₆), -105.3 (N₂), -143.1 (N₅), -163.8 (N₃), -184.7 (N₁), -289.7 (d, ¹J_{NH} = 102.4 Hz, C-NH-NH₂, TAG⁺), -330.1 (C-NH-NH₂, TAG⁺); ¹⁵N{¹H} NMR (DMSO-*d*₆, 25 °C) δ (ppm) = -15.2 (-NO₂, N₄), -23.7 (-N-NO₂, N₆), -105.4 (N₂), -143.4 (N₅), -163.9 (N₃), -184.8 (N₁), -289.7 (C-NH-NH₂, TAG⁺), -330.2 (C-NH-NH₂, TAG⁺); IR (ATR, 25 °C, cm⁻¹) ν = 3344 (m), 3319 (m), 3259 (m), 1699 (m), 1680 (s), 1600 (w), 1555 (m), 1523 (s), 1488 (s), 1404 (s), 1354 (m), 1328 (m), 1289 (vs), 1236 (s), 1151 (m), 1130 (s), 1077 (m), 1010 (m), 1001 (m), 977 (s), 933 (m), 857 (m), 837 (m), 775 (w), 745 (w), 705 (s); RAMAN (Nd:YAG, 1064 nm, cm⁻¹) ν = 3347 (3), 3319 (3), 3242 (4), 1682 (3), 1555 (8), 1524 (23), 1490 (100), 1409 (43), 1356 (11), 1333 (9), 1237 (4), 1151 (32), 1078 (8), 1002 (74), 886 (6), 859 (6), 840 (6), 756 (9), 639 (2), 521 (3), 443 (3), 411 (2); m/z : (FAB⁺): 105.1 [CH₆N₆⁺]; m/z : (FAB⁻): 173.0 [C₂HN₆O₄⁻]; EA (C₃H₁₀N₁₂O₄) calcd.: C, 12.95; H, 3.62; N, 60.42; found: C, 13.19; H, 3.43; N, 58.76; Sensitivities (anhydrous) (grain size: 100–500 μ m): IS: 6 J; FS: 128 N; ESD: 0.4 J.

Bis(triaminoguanidinium) 5-nitramino-3-nitro-1,2,4-triazolate (**13**)

5-Nitramino-3-nitro-1*H*-1,2,4-triazole (2 mmol, 0.348 g) was dissolved in 60 mL boiling ethanol. Triaminoguanidine (3.9 mmol, 0.406 g) was added portionwise to the solution under a nitrogen stream. With continued heating, water was added to the solution in small portions, until complete dissolution of the solid material was observed. After cooling to ambient temperature, the solvent was reduced to 1/3 of its original volume and left standing for crystallization over night. Pure bis(triaminoguanidinium) 5-nitramino-3-nitro-1,2,4-triazolate was obtained as a red microcrystalline mass, which was filtered off and washed thoroughly with diethyl ether to yield 0.635 g (84 %).

$T_{\text{dec.}}$: 149 °C (DSC, 5 °C min⁻¹); ¹H NMR (DMSO-*d*₆, 25 °C) δ (ppm) = 7.96 (s), 5.70 (s); ¹³C{¹H} NMR (DMSO-*d*₆, 25 °C) δ (ppm) = 163.7, 163.0, 159.2 (TAG⁺); ¹⁴N NMR (DMSO-*d*₆, 25 °C) δ (ppm) = -15; IR (ATR, 25 °C, cm⁻¹) ν = 3320 (m), 3270 (m), 3178 (m), 1682 (s), 1625 (w), 1611 (w), 1556 (w), 1522 (w), 1491 (w), 1470 (m), 1433 (s), 1404 (m), 1359 (s), 1347 (s), 1290 (vs), 1276 (s), 1197 (w), 1131 (s), 1094 (s), 1076 (m), 1029 (m), 999 (s), 977 (s), 964 (s), 877 (w), 857 (w), 838 (w), 828 (w), 748 (w), 708 (w), 659 (w); RAMAN (Nd:YAG, 1064 nm, cm⁻¹) ν = 3324 (3), 3240 (3), 1682 (4), 1473 (32), 1432 (100), 1402 (31), 1369 (32), 1323 (30), 1292 (21), 1278 (16), 1150 (6), 1098 (94), 1076 (96), 1059 (44), 1006 (42), 881 (20), 830 (26), 751 (7), 659 (2), 523 (2), 427 (10); m/z : (FAB+): 105.1 [CH₉N₆⁺]; m/z : (FAB-): 173.0 [C₂HN₆O₄⁻]; EA (C₄H₁₈N₁₈O₄) calcd.: C, 12.57; H, 4.75; N, 65.95; found: C, 13.56; H, 4.48; N, 64.28; Sensitivities (anhydrous) (grain size: < 100 μ m): IS: 20 J; FS: 192 N; ESD: 0.4 J.

Ammonium 1-methyl-5-nitramino-3-nitro-1,2,4-triazolate (**14**)

1-Methyl-5-nitramino-3-nitro-1,2,4-triazole (2 mmol, 0.376 g) was dissolved in 15 mL water and a 6.25 % ammonia solution (0.6 mL, 2 mmol) was added. A clear red solution developed immediately. The solvent was evaporated completely yielding 0.32 g (85 %) of ammonium 1-methyl-5-nitramino-3-nitro-1,2,4-triazolate as an orange powder.

$T_{\text{dec.}}$: 179 °C (DSC, 5 °C min⁻¹), 192 °C (DSC, Onset, 5 °C min⁻¹); ¹H NMR (DMSO-*d*₆, 25 °C) δ (ppm) = 7.14 (s, NH₄⁺), 3.62 (s, -CH₃) ; ¹³C{¹H} NMR (DMSO-*d*₆, 25 °C) δ (ppm) = 159.2, 157.0, 35.1 (-CH₃); ¹⁴N NMR (DMSO-*d*₆, 25 °C) δ (ppm) = -15 (-NO₂), -25 (-N-NO₂), -359 (NH₄⁺); IR (ATR, 25 °C, cm⁻¹) ν = 3183 (m), 3032 (m), 2853 (w), 1551 (m), 1486 (s), 1429 (s), 1402 (s), 1364 (m), 1267 (vs), 1199 (s), 1050 (m), 1020 (m), 922 (m), 878 (w), 829 (m), 804 (w), 774 (w), 753 (w), 726 (m), 701 (m); RAMAN (Nd:YAG, 1064 nm, cm⁻¹) ν = 2958 (7), 2859 (9), 1490 (100), 1406 (62), 1308 (25), 1265 (49), 1211 (12), 1033 (51), 925 (2), 832 (2), 755 (8), 704 (9), 440 (5), 383 (3), 298 (8), 240 (2); m/z : (FAB+): 18.1 [NH₄⁺]; m/z : (FAB-): 187.0 [C₃H₃N₆O₄⁻]; EA (C₃H₇N₇O₄) calcd.: C, 17.57; H, 3.44; N, 47.80; found: C, 18.07; H, 3.35; N, 45.90; Sensitivities (anhydrous) (grain size: 100–500 μ m): IS: 32 J; FS: 360 N; ESD: 0.5 J.

Hydrazinium 1-methyl-5-nitramino-3-nitro-1,2,4-triazolate (**15**)

1-Methyl-5-nitramino-3-nitro-1,2,4-triazole (2 mmol, 0.376 g) was dissolved in 15 mL water and hydrazine monohydrate (0.1 mL, 2 mmol) was added dropwise. A clear red solution developed immediately. The solvent was evaporated completely yielding 0.40 g (91 %) of hydrazinium 1-methyl-5-nitramino-3-nitro-1,2,4-triazolate as a bright orange powder.

$T_{\text{dec.}}$: 181 °C (DSC, 5 °C min⁻¹), 195 °C (DSC, Onset, 5 °C min⁻¹); ¹H NMR (DMSO-*d*₆, 25 °C) δ (ppm) = 7.09 (s, br, N₂H₅⁺), 3.62 (s, -CH₃); ¹³C{¹H} NMR (DMSO-*d*₆, 25 °C) δ (ppm) = 159.2, 157.0, 35.1 (-CH₃); ¹⁴N NMR (DMSO-*d*₆, 25 °C) δ (ppm) = -15 (-NO₂), -25 (-N-NO₂), -358 (N₂H₄⁺); IR (ATR, 25 °C, cm⁻¹) ν = 3429 (w), 3358 (m), 3280 (m), 2948 (w), 1677 (m), 1619 (w), 1541 (m), 1506 (m), 1484 (s), 1432 (m), 1406 (m), 1354 (w), 1277 (vs), 1259 (s), 1196 (m), 1134 (m), 1052 (w), 1021 (m), 967 (m), 924 (m), 904 (w), 878 (w), 830 (m), 805 (w), 774 (w), 754 (w), 726 (w), 713 (w), 701 (w); RAMAN (Nd:YAG, 1064 nm, cm⁻¹) ν = 3295 (1), 2967 (7), 161 (2), 1561 (14), 1493 (100), 1458 (13), 1406 (41), 1394 (37), 1341 (11), 1309 (31), 1263 (54), 1207 (12), 1114 (2), 1092 (2), 1034 (36), 969 (6), 918 (1), 832 (2), 755 (8), 729 (3), 703 (16), 521 (2), 438 (4), 399 (2), 376 (2), 306 (11), 232 (5); m/z : (FAB⁺): 33.0 [N₂H₅⁺]; m/z : (FAB⁻): 187.0 [C₃H₃N₆O₄⁻]; EA (C₃H₈N₈O₄*2 H₂O) calcd.: C, 14.07; H, 4.72; N, 43.74; found: C, 13.83; H, 3.68; N, 43.82; Sensitivities (* 1 ½ H₂O) (grain size: 100–500 µm): IS: 25 J; FS: 288 N; ESD: 0.15 J.

Guanidinium 1-methyl-5-nitramino-3-nitro-1,2,4-triazolate (**16**)

1-Methyl-5-nitramino-3-nitro-1,2,4-triazole (2 mmol, 0.376 g) was dissolved in 15 mL water and bis(guanidinium) carbonate (1 mmol, 0.180 g) was added in one portion. The solution was heated to 65 °C for 30 minutes until no more gas evolution was visible. The solvent was evaporated completely afterwards yielding 0.42 g (85 %) of guanidinium 1-methyl-5-nitramino-3-nitro-1,2,4-triazolate as a red microcrystalline powder.

$T_{\text{melt.}}$: 195 °C (DSC, 5 °C min⁻¹); $T_{\text{dec.}}$: 210 °C (DSC, Onset, 5 °C min⁻¹); ¹H NMR (DMSO-*d*₆, 25 °C) δ (ppm) = 6.97 (s, G⁺), 3.62 (s, -CH₃); ¹³C{¹H} NMR (DMSO-*d*₆, 25 °C) δ (ppm) = 159.3, 157.9 (G⁺), 156.9, 35.1 (-CH₃); ¹⁴N NMR (DMSO-*d*₆, 25 °C) δ (ppm) = -15 (-NO₂), -24 (-N-NO₂), -344 (br, G⁺); IR (ATR, 25 °C, cm⁻¹) ν = 3423 (m),

3353 (m), 3250 (m), 3191 (m), 1658 (s), 1548 (s), 1503 (m), 1484 (s), 1438 (m), 1388 (m), 1360 (m), 1308 (vs), 1267 (s), 1205 (w), 1092 (m), 1048 (w), 1024 (m), 925 (m), 830 (m), 808 (w), 773 (w), 750 (w), 726 (w), 702 (w); RAMAN (Nd:YAG, 1064 nm, cm^{-1}) $\nu = 2960$ (7), 1548 (7), 1509 (18), 1480 (100), 1438 (15), 1401 (38), 1304 (23), 1270 (25), 1208 (6), 1032 (34), 1010 (18), 976 (2), 928 (1), 832 (2), 766 (3), 751 (7), 703 (6), 529 (3), 438 (3), 383 (2), 301 (6), 255 (2); m/z : (FAB+): 60.1 [CH_6N_3^+]; m/z : (FAB-): 187.0 [$\text{C}_3\text{H}_3\text{N}_6\text{O}_4^-$]; EA ($\text{C}_4\text{H}_9\text{N}_9\text{O}_4$) calcd.: C, 19.44; H, 3.67; N, 51.00; found: C, 19.77; H, 3.49; N, 50.12; Sensitivities (anhydrous) (grain size: $< 100 \mu\text{m}$): IS: > 40 J; FS: 360 N; ESD: 0.8 J.

Aminoguanidinium 1-methyl-5-nitramino-3-nitro-1,2,4-triazolate (17)

1-Methyl-5-nitramino-3-nitro-1,2,4-triazole (2 mmol, 0.376 g) was dissolved in 15 mL water and aminoguanidinium bicarbonate (2 mmol, 0.272 g) was added in one portion. The solution was heated to $65 \text{ }^\circ\text{C}$ for 30 minutes until no more gas evolution was visible. The solvent was evaporated completely afterwards yielding 0.44 g (85 %) of aminoguanidinium 1-methyl-5-nitramino-3-nitro-1,2,4-triazolate as a red microcrystalline powder.

T_{melt} : $140 \text{ }^\circ\text{C}$ (DSC, $5 \text{ }^\circ\text{C min}^{-1}$); T_{dec} : $198 \text{ }^\circ\text{C}$ (DSC, $5 \text{ }^\circ\text{C min}^{-1}$), $217 \text{ }^\circ\text{C}$ (DSC, Onset, $5 \text{ }^\circ\text{C min}^{-1}$); $^1\text{H NMR}$ (DMSO- d_6 , $25 \text{ }^\circ\text{C}$) δ (ppm) = 8.61 (s, 1H, C-NH-NH₂), 7.26 (s, 2H, C-NH₂), 6.78 (s, 2H, C-NH₂), 4.67 (s, 2H, C-NH-NH₂), 3.62 (s, 3H, -CH₃); $^{13}\text{C}\{^1\text{H}\}$ NMR (DMSO- d_6 , $25 \text{ }^\circ\text{C}$) δ (ppm) = 159.3, 158.7 (AG⁺), 157.0, 35.1 (-CH₃); $^{14}\text{N NMR}$ (DMSO- d_6 , $25 \text{ }^\circ\text{C}$) δ (ppm) = -15 (-NO₂), -24 (-N-NO₂); IR (ATR, $25 \text{ }^\circ\text{C}$, cm^{-1}) $\nu = 3345$ (w), 3263 (m), 3168 (m), 1724 (vw), 1669 (s), 1609 (vw), 1548 (m), 1508 (m), 1483 (s), 1438 (m), 1394 (m), 1366 (m), 1325 (s), 1300 (vs), 1205 (m), 1110 (w), 1096 (w), 1051 (w), 1023 (m), 985 (m), 959 (m), 923 ((m), 829 (m), 770 (w), 726 (w), 704 (w); RAMAN (Nd:YAG, 1064 nm, cm^{-1}) $\nu = 3352$ (1), 3284 (1), 2958 (3), 1485 (100), 1437 (24), 1422 (30), 1402 (37), 1301 (22), 1269 (34), 1210 (9), 1032 (35), 965 (6), 752 (5), 707 (9), 614 (2), 496 (2), 441 (3), 383 (2), 304 (8), 236 (2); m/z : (FAB+): 75.1 [CH_7N_4^+]; m/z : (FAB-): 187.0 [$\text{C}_3\text{H}_3\text{N}_6\text{O}_4^-$]; EA ($\text{C}_4\text{H}_{10}\text{N}_{10}\text{O}_4$) calcd.: C, 18.32; H, 3.84; N, 53.42; found: C, 18.94; H, 3.64; N, 53.42; Sensitivities (anhydrous) (grain size: $100\text{--}500 \mu\text{m}$): IS: > 40 J; FS: 360 N; ESD: 0.5 J.

Triaminoguanidinium 1-methyl-5-nitramino-3-nitro-1,2,4-triazolate (**18**)

1-Methyl-5-nitramino-3-nitro-1,2,4-triazole (1.5 mmol, 0.282 g) was suspended in 60 mL boiling ethanol. Triaminoguanidine (1.45 mmol, 0.148 g) was added portionwise to the solution under a nitrogen stream. With continued heating, water was added to the solution in small portions, until complete dissolution of the solid material was observed. After cooling to ambient temperature, the solvent was reduced to 1/3 of its original volume and left standing for crystallization. Pure triaminoguanidinium 1-methyl-5-nitramino-3-nitro-1,2,4-triazolate was obtained as orange crystals, which were filtered off and washed thoroughly with diethyl ether to yield 0.38 g (90 %).

T_{melt} : 183 °C (DSC, 5 °C min⁻¹); $T_{\text{dec.}}$: 189 °C (DSC, Onset, 5 °C min⁻¹); ¹H NMR (DMSO-*d*₆, 25 °C) δ (ppm) = 8.55 (s, 3H, C-NH-NH₂), 4.45 (s, 6H, C-NH-NH₂), 3.59 (s, 3H, -CH₃); ¹³C{¹H} NMR (DMSO-*d*₆, 25 °C) δ (ppm) = 161.9, 159.0 (TAG⁺), 157.0, 35.0 (-CH₃); ¹⁴N NMR (DMSO-*d*₆, 25 °C) δ (ppm) = -15 (-NO₂), -24 (-N-NO₂); ¹⁵N NMR (DMSO-*d*₆, 25 °C) δ (ppm) = -15.4 (C-NO₂, N₄), -24.9 (C-N-NO₂, N₆), -96.5 (q, ³*J*_{NH} = 2.02 Hz, N₂), -151.5 (N₅), -157.1 (N₃), -188.5 (q, ²*J*_{NH} = 2.09 Hz, N₁-CH₃), -289.7 (d, ¹*J*_{NH} = 102.35 Hz, C-NH-NH₂, TAG⁺), -330.2 (t, ¹*J*_{NH} = 72.51 Hz, C-NH-NH₂, TAG⁺); ¹⁵N{¹H} NMR (DMSO-*d*₆, 25 °C) δ (ppm) = -15.3 (C-NO₂, N₄), -24.8 (C-N-NO₂, N₆), -96.4 (N₂), -157.1 (N₃), -188.7 (N₁-CH₃), -289.7 (C-NH-NH₂, TAG⁺), -330.2 (C-NH-NH₂, TAG⁺); IR (ATR, 25 °C, cm⁻¹) ν = 3429 (vw), 3358 (w), 3277 (m), 2952 (vw), 1677 (m), 1619 (w), 1541 (m), 1504 (m), 1484 (s), 1432 (m), 1405 (m), 1352 (w), 1277 (vs), 1259 (s), 1197 (s), 1134 (m), 1052 (w), 1021 (m), 968 (m), 924 (m), 904 (w), 878 (w), 830 (m), 805 (w), 774 (w), 754 (vw), 736 (w), 725 (w), 700 (w), 679 (vw); RAMAN (Nd:YAG, 1064 nm, cm⁻¹) ν = 3359 (3), 3287 (4), 3237 (2), 2957 (5), 1680 (2), 1514 (72), 1484 (100), 1416 (72), 1399 (75), 1303 (29), 1261 (82), 1206 (22), 1176 (5), 1136 (3), 1054 (18), 1031 (72), 927 (4), 82 (3), 829 (2), 755 (12), 706 (15), 640 (2), 524 (1), 442 (6), 419 (5), 378 (4), 342 (2), 296 (8), 260 (4), 229 (4); *m/z*: (FAB⁺): 105.0 [CH₉N₆⁺]; *m/z*: (FAB⁻): 187.0 [C₃H₃N₆O₄⁻]; EA (C₄H₁₂N₁₂O₄) calcd.: C, 16.44; H, 4.14; N, 57.52; found: C, 17.62; H, 3.92; N, 56.38; Sensitivities (anhydrous) (grain size: 100–500 μ m): IS: 12.5 J; FS: 216 N; ESD: 400 mJ.

7.5 References

- [1] a) T. M. Klapötke, in *High Energy Density Materials* (Ed.: T. M. Klapötke), Springer, Heidelberg, **2007**, pp. 84-122; b) T. M. Klapötke, *Chemie der hochenergetischen Materialien*, 1 ed., Walter de Gruyter, Berlin, New York, **2009**.
- [2] a) R. P. Singh, R. D. Verma, D. T. Meshri, J. n. M. Shreeve, *Angew. Chem.* **2006**, *118*, 3664-3682; *Angew. Chem. Int. Ed.* **2006**, *45*, 3584-3601.
- [3] a) J. C. Galvez-Ruiz, G. Holl, K. Karaghiosoff, T. M. Klapötke, K. Löhnwitz, P. Mayer, H. Nöth, K. Polborn, C. J. Rohbogner, M. Suter, J. J. Weigand, *Inorg. Chem.* **2005**, *44*, 4237-4253; b) A. Hammerl, Ludwig-Maximilians-University (Munich), **2001**; c) A. Hammerl, G. Holl, T. M. Klapotke, P. Mayer, H. Noth, H. Piotrowski, M. Warchhold, *Eur. J. Inorg. Chem.* **2002**, 834-845; d) T. M. Klapoetke, C. M. Sabate, *Chem. Mater.* **2008**, *20*, 1750-1763; e) T. M. Klapoetke, C. M. Sabate, *New J. Chem.* **2009**, *33*, 1605-1617; f) T. M. Klapoetke, J. Stierstorfer, A. U. Wallek, *Chem. Mater.* **2008**, *20*, 4519-4530; g) T. M. Klapötke, C. M. Sabate, J. M. Welch, *Z. Anorg. Allg. Chem.* **2008**, *634*, 857-866.
- [4] V. A. Ostrovskii, M. S. Pevzner, T. P. Kofman, I. V. Tselinskii, *Targets Heterocyclic System* **1999**, *3*, 467-526.
- [5] J. B. Pedley, *Vol. 1*, Thermodynamic Research College, College Station, **1994**.
- [6] P. Jiminez, M. V. Roux, C. J. Turrión, *Chemical Thermodynamics* **1989**, *21*, 759-764.
- [7] K. Y. Lee, C. B. Storm, M. A. Hiskey, M. D. Coburn, *J. Energ. Mater.* **1991**, *9*, 415-428.
- [8] K.-Y. Lee, M. M. Stinecipher, *Vol. US525672*, US, **1993**.
- [9] a) S. L. Collignon, R. E. Farncomb, K. L. Wagaman, *Statutory Invent. Regist.* **1990**, *US 861 H 19901208*; b) J. Schmidt, H. Gehlen, *Z. Chem.* **1965**, *5*, 304.
- [10] a) D. E. Chavez, B. C. Tappan, B. A. Mason, D. Parrish, *Propell. Explos. Pyrot.* **2009**, *34*, 475-479; b) D. L. Naud, M. A. Hiskey, H. H. Harry, *J. Energ. Mater.* **2003**, *21*, 57-62.
- [11] A. Dippold, Thomas M. Klapötke, Franz A. Martin, *Z. Anorg. Allg. Chem.* **2011**, *637*, in press.
- [12] a) A. R. Katritzky, J. W. Mitchell, *J. Chem. Soc. - Perkin Transactions 1* **1973**, 2624-2626; b) T. P. Kofman, G. Y. Kartseva, M. B. Shcherbinin, *Russ. J. Org. Chem.* **2002**, *38*, 1343-1350.
- [13] E. L. Metelkina, *Russ. J. Org. Chem.* **2004**, *40*, 543-550.
- [14] M. S. Pevzner, N. V. Gladkova, T. A. Kravchenko, *Russ. J. Org. Chem.* **1996**, *32*, 1186-1189.
- [15] a) L. I. Bagal, M. S. Pevzner, A. N. Frolov, N. I. Sheludyakova, *Khimiya Geterotsiklicheskikh Soedinenii* **1970**, 259-264; b) K. Y. Lee, D. G. Ott, (United States Dept. of Energy, USA). Application: US, **1980**, p. 5 pp; c) K. Y. Lee, D. G. Ott, M. M. Stinecipher, *Industrial & Engineering Chemistry Process Design and Development* **1981**, *20*, 358-360.

- [16] K. Y. Lee, C. B. Storm, M. A. Hiskey, M. D. Coburn, *J. Energ. Mat.* **1991**, *9*, 415-428.
- [17] S. D. Stepanov, M. S. Pevzner, Y. V. Serov, T. P. Temchenko, *Russ. J. Org. Chem.* **1989**, *25*, 1819-1826.
- [18] T. P. Kofman, M. S. Pevzner, T. A. K. L. N. Zhukova, G. M. Frolova, *Russ. J. Org. Chem.* **1980**, *16*, 375-378.
- [19] A. F. Holleman, E. Wiberg, *Lehrbuch der anorganischen Chemie*, de Gruyter, 101st Ed., New York, **1995**.
- [20] M. Hesse, Herbert, Meier, B. Zeh, *Spektroskopische Methoden in der Organischen Chemie*, 6 ed., Georg Thieme Verlag, Stuttgart, New York, **2002**.
- [21] a) T. H. Dunning, *J. Chem. Phys.* **1989**, *90*, 1007; b) C. Lee, W. Yang, R. G. Parr, *Phys. Rev. B* **1988**, *7*, 785; c) A. D. Becke, *J. Chem. Phys.* **1993**, *98*, 5648.
- [22] *Gaussian 09W, Version 7.0*, M. J. Frisch, G. W. Trucks, H. B. Schlegel, G. E. Scuseria, M. A. Robb, J. R. Cheeseman, G. Scalmani, V. Barone, B. Mennucci, G. A. Petersson, H. Nakatsuji, M. Caricato, X. Li, H. P. Hratchian, A. F. Izmaylov, J. Bloino, G. Zheng, J. L. Sonnenberg, M. Hada, M. Ehara, K. Toyota, R. Fukuda, J. Hasegawa, M. Ishida, T. Nakajima, Y. Honda, O. Kitao, H. Nakai, T. Vreven, J. A. Montgomery, Jr., J. E. Peralta, F. Ogliaro, M. Bearpark, J. J. Heyd, E. Brothers, K. N. Kudin, V. N. Staroverov, R. Kobayashi, J. Normand, K. Raghavachari, A. Rendell, J. C. Burant, S. S. Iyengar, J. Tomasi, M. Cossi, N. Rega, J. M. Millam, M. Klene, J. E. Knox, J. B. Cross, V. Bakken, C. Adamo, J. Jaramillo, R. Gomperts, R. E. Stratmann, O. Yazyev, A. J. Austin, R. Cammi, C. Pomelli, J. W. Ochterski, R. L. Martin, K. Morokuma, V. G. Zakrzewski, G. A. Voth, P. Salvador, J. J. Dannenberg, S. Dapprich, A. D. Daniels, Ö. Farkas, J. B. Foresman, J. V. Ortiz, J. Cioslowski, and D. J. Fox, *Gaussian, Inc., Wallingford CT*, 2009.
- [23] H. A. Witek, M. Keiji, *J. Comp. Chem. THEOCHEM* **2004**, *25*, 1858-1864.
- [24] T. Altenburg, T. M. Klapötke, A. Penger, J. Stierstorfer, *Z. Anorg. Allg. Chem.* **2010**, *636*, 463-471.
- [25] a) J. W. Ochterski, G. A. Petersson, J. A. Montgomery Jr., *J. Chem. Phys.* **1996**, *104*, 2598; b) J. A. Montgomery, M. J. Frisch, J. W. Ochterski, G. A. Petersson, *J. Chem. Phys.* **2000**, *112*, 6532.
- [26] P. J. Lindstrom, W. G. Mallard, *NIST Chemistry Webbook, NIST Standard Reference 69, June 2005, National Institute of Standards and Technology, Gaithersburg MD, 20899* (<http://webbook.nist.gov>).
- [27] a) E. F. C. Byrd, B. M. Rice, *J. Phys. Chem. A* **2006**, *110*, 1005-1013; b) L. A. Curtiss, K. Raghavachari, P. C. Redfern, J. A. Pople, *J. Chem. Phys.* **1997**, *106*, 1063-1079; c) B. M. Rice, S. V. Pai, J. Hare, *Combust. Flame* **1999**, *118*, 445-458.
- [28] a) F. Trouton, *Philos. Mag.* **1884**, *18*, 54-57; b) M. S. Westwell, M. S. Searle, D. J. Wales, D. H. Williams, *J. Am. Chem. Soc.* **1995**, *117*, 5013-5015.
- [29] *Back-calculated from $V(\text{TAG}^+\text{Cl}^-)$ and the molecular volume of the chloride anion taken from Ref (Jenkins, Inorg Chem); Volume of the energetic anion has been derived from the TAG^+ structure; all other volumes have been backcalculated*

using the corresponding volume of the energetic anion from single crystal measurements.

- [30] a) H. D. B. Jenkins, H. K. Roobottom, J. Passmore, L. Glasser, *Inorg. Chem.* **1999**, *38*, 3609-3620; b) H. D. B. Jenkins, D. Tudela, L. Glasser, *Inorg. Chem.* **2002**, *41*, 2364-2367.
- [31] M. Sućeska, *EXPLO5.4 program, Zagreb, Croatia, 2010*.
- [32] a) M. Sućeska, *Propell. Explos. Pyrot.* **1991**, *16*, 197-202; b) M. Sućeska, *Propell. Explos. Pyrot.* **1999**, *24*, 280-285; c) M. Sućeska, *Materials Science Forum* **2004**, 465-466, 325-330.
- [33] J. Köhler, R. Meyer, *Explosivstoffe, Vol. 9th edition*, Wiley-VCH, Weinheim, **1998**.
- [34] *NATO standardization agreement (STANAG) on explosives, no. 4489, 1st ed., Sept. 17, 1999*.
- [35] *WIWEB-Standardarbeitsanweisung 4-5.1.02, Ermittlung der Explosionsgefährlichkeit, hier: der Schlagempfindlichkeit mit dem Fallhammer, Nov. 08, 2002*.
- [36] <http://www.bam.de>.
- [37] *NATO standardization agreement (STANAG) on explosives, friction tests, no.4487, 1st ed., Aug. 22, 2002*.
- [38] *WIWEB-Standardarbeitsanweisung 4-5.1.03, Ermittlung der Explosionsgefährlichkeit, hier: der Reibempfindlichkeit mit dem Reibeapparat, Nov. 08, 2002*.
- [39] *NATO standardization agreement (STANAG) on explosives, electrostatic discharge sensitivity tests, no.4490, 1st ed., Feb. 19, 2001*.
- [40] <http://www.ozm.cz/en/sensitivity-tests/esd-2008a-small-scale-electrostatic-spark-sensitivity-test/>.
- [41] *CrysAlis CCD, Oxford Diffraction Ltd., Version 1.171.27p5 beta (release 01-04-2005 CrysAlis171.NET)*.
- [42] *CrysAlis RED, Oxford Diffraction Ltd., Version 1.171.27p5 beta (release 01-04-2005 CrysAlis171.NET)*.
- [43] A. Altomare, G. Cascarano, C. Giacovazzo, A. Guagliardi, *J. Appl. Cryst.* **1993**, *26*, 343-350.
- [44] G. M. Sheldrick, *SHELXS-97, Crystal Structure Solution, Version 97-1; Institut Anorg. Chemie, University of Göttingen, Germany, 1990*.
- [45] G. M. Sheldrick, *SHELXL-97, Program for the Refinement of Crystal Structures. University of Göttingen, Germany, 1997*.
- [46] L. Farrugia, *J. Appl. Cryst.* **1999**, *32*, 837-838.
- [47] A. L. Spek, *Platon, A Multipurpose Crystallographic Tool, Utrecht University, Utrecht, The Netherlands, 1999*.
- [48] *Crystallographic data for the structure(s) have been deposited with the Cambridge Crystallographic Data Centre. Copies of the data can be obtained free of charge on application to The Director, CCDC, 12 Union Road, Cambridge CB2 1EZ, UK (Fax: int.code (1223)336-033; e-mail for inquiry: fileserv@ccdc.cam.ac.uk; e-mail for deposition: deposit-@ccdc.cam.ac.uk).*

8. 5-Nitramino-3-tetrazol-1-yl-1*H*-1,2,4-triazole – Synthesis and complete characterization of a novel energetic material

Thomas M. Klapötke and Franz A. Martin

Unpublished results.

8.1 Introduction

The chemistry of 1,2,4-triazoles and especially 3,5-diamino-1*H*-1,2,4-triazole and 5-amino-1*H*-1,2,4-triazole and their corresponding nitrated products has been investigated for the last couple of decades.^[1] Temperature stable and also well performing compounds like triaminoguanidinium 3,5-dinitro-1,2,4-triazole^[1f] or 5-nitramino-1*H*-1,2,4-triazole^[1g] have been synthesized, showing decomposition temperatures above 200 °C. Another class of compounds was found to work well as either gas generators or blowing agents, 1,5-bistetrazoles.^[2] Gaponik *et al.* established 1,5-bistetrazole in 1985^[3] showing a decomposition temperature of only 122 °C, while the corresponding ammonium salt shows a remarkable decomposition temperature of 220 °C.^[2, 4] Since better stabilities can be derived from 1,2,4-triazole derivatives, we thought about the possibility to combine these two systems. The exchange of one nitrogen atom in the heterocyclic system with the isolobal C-*R* (*R* = H, NH₂) group should increase the thermal stabilities as well as the sensitivity values.

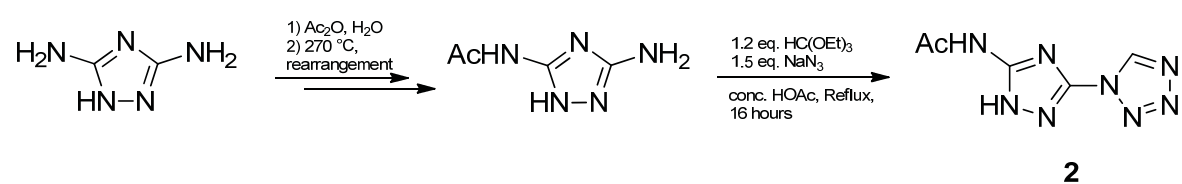
As a result, we describe the synthetic route towards three novel tetrazolyltriazoles, namely 3-tetrazol-1-yl-1*H*-1,2,4-triazole (**1**), 5-amino-3-tetrazol-1-yl-1*H*-1,2,4-triazole (**3**) and the corresponding 5-nitramino-3-tetrazol-1-yl-1*H*-1,2,4-triazole (**4**). Compounds **1** and **3** have also been investigated by theoretical calculations as high nitrogen rich ingredients for gun propellants, developing a lower temperature of combustion and less carbon oxides. The results of these calculations will be presented as well. In addition nitrogen rich salts of **4** have been synthesized and completely characterized in order to investigate the thermal behavior and the sensitivities of the ionic species.

8.2 Results and Discussion

8.2.1 Synthesis

3-Tetrazol-1-yl-1*H*-1,2,4-triazole (**1**) was synthesized according to known literature procedures by the reaction with triethyl orthoformate and sodium azide,^[3] followed by acidic workup and extraction of the reaction residue with hot ethanol. **1** was synthesized as a white powder in 37 % yield.

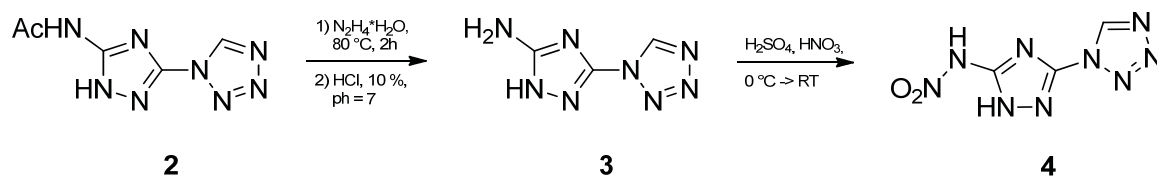
Our efforts to synthesize 5-amino-3-tetrazol-1-yl-1*H*-1,2,4-triazole (**3**) directly from 3,5-diamino-1*H*-1,2,4-triazole (DAT) were not successful due to the reactivity of the two chemically equivalent amine substituents. The reaction, performed as described for **1**, yielded **3** as the main product, but also 5-*N*-ethoxymethylamino-3-tetrazol-1-yl-1*H*-1,2,4-triazole, the second amine group being attacked by triethyl orthoformate. Nevertheless, the second ring closure reaction, yielding 3,5-bis(tetrazol-1-yl)-1*H*-1,2,4-triazole, was not observed. The solution was the selective protection of one amine group using the acetyl protecting group, as described in literature.^[5] Acetic anhydride was used, introducing the acetyl group at the heterocyclic ring in 1 position, while the rearrangement to the 5 position, forming the desired 5-acetamido-3-amino-1*H*-1,2,4-triazole, was performed at 270 °C in decaline. Using the before mentioned compound as starting material, the selective conversion forming 5-acetamido-3-(tetrazol-1-yl)-1*H*-1,2,4-triazole (**2**) was undertaken as described in literature with triethyl orthoformate, sodium azide and acetic acid. (Scheme 1)



Scheme 1: Reaction pathway showing the conversion of DAT to 5-acetamido-3-(tetrazol-1-yl)-1*H*-1,2,4-triazole (**2**).

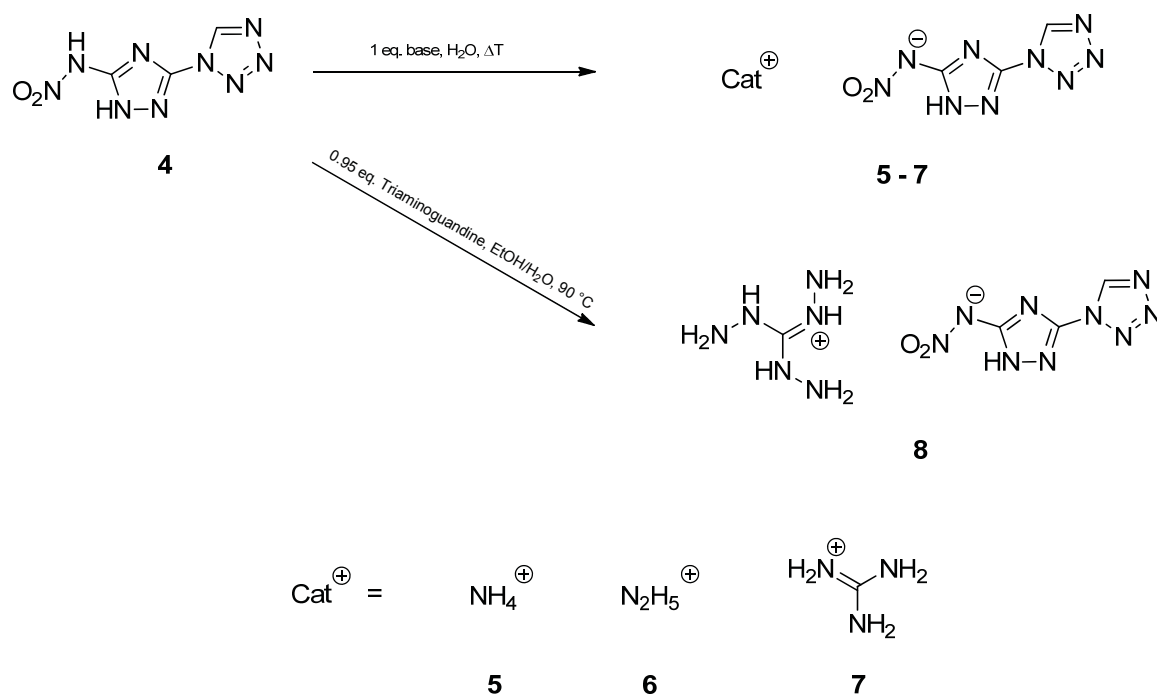
The protecting group was removed afterwards with hydrazine monohydrate yielding **3** as a white powder in 59 % yield. The conversion to the corresponding nitramine was undertaken using a nitration mixture of 98 % concentrated sulfuric acid with 100 % nitric acid in a molar ratio of 3:1 and an eight fold excess of nitric acid. 5-Nitramino-3-

(tetrazol-1-yl)-1*H*-1,2,4-triazole (**4**) was obtained as a yellow crystalline material after extraction of the quenched reaction mixture with ethyl acetate in 59 % yield. (Scheme 2)



Scheme 2: Complete reaction pathway forming 5-nitramino-3-(tetrazol-1-yl)-1*H*-1,2,4-triazole (**4**) from 5-acetamido-3-(tetrazol-1-yl)-1*H*-1,2,4-triazole (**2**) in two steps.

The corresponding salts of **4** with nitrogen rich cations such as ammonium and triaminoguanidinium were synthesized straightforward by the addition of the corresponding bases or carbonates to an aqueous solution of **4** in water or ethanol in the case of triaminoguanidine. All reactions were carried out at an elevated temperature to guarantee complete conversion of **4**. The reaction scheme and numbering of the ionic compounds is presented in Scheme 3.



Scheme 3: Conversion of **4** to its nitrogen rich salts using ammonia, hydrazine, guanidinium carbonate and triaminoguanidine.

8.2.2 Spectroscopic Data

Vibrational spectroscopy

IR and Raman spectra of all compounds have been recorded and the frequencies have been assigned based on literature.^[6] Additionally, the vibrational frequencies of **4** have been calculated at the B3LYP/cc-pVDZ^[7] level of theory as implemented in the Gaussian 09W program package.^[8] The calculated frequencies have been fitted according to Witek et al.^[9] with a scaling factor of 0.9704.

The conversion of 1-acetyl-3,5-diamino-1,2,4-triazole to 5-acetamido-3-amino-1*H*-1,2,4-triazole can easily be monitored by the shift of the C=O double bond vibration in both IR and Raman spectra. While the educt shows a C=O valence stretch at 1710 cm⁻¹, it is shifted towards lower energy in the product and is observed at 1683 cm⁻¹. 5-Acetamido-3-(tetrazol-1-yl)-1*H*-1,2,4-triazole (**2**) shows N–H stretching mode and ν_s and ν_{as} stretching modes of the –NH₂ group, respectively, in the region of 3325 – 3110 cm⁻¹ in both, IR and Raman spectra. The very strong absorption of the C=O double bond is observed at 1690 cm⁻¹ (1700 cm⁻¹, Raman). Stretching and bending vibrations of the tetrazole substituent are observed in the region of 1100 – 980 cm⁻¹ (1014 cm⁻¹, 1068 cm⁻¹ and 1090 cm⁻¹, IR; 1018 cm⁻¹, 1093 cm⁻¹, Raman). Additionally, ν_s and ν_{as} stretching modes of the methyl group are observed between 2950 cm⁻¹ and 2850 cm⁻¹ while the δ_s stretching mode of the methyl group is observed at 1359 cm⁻¹ (IR) and 1362 cm⁻¹ (Raman). The frequencies in the region of 1560 – 1100 cm⁻¹ represent symmetric and asymmetric valence stretching modes of the C–N and N–N bonds of the triazole ring system and the stretching modes of the C–N bonds, C₁–N_{acet} and C₂–N_{tet}. After deprotection of the acetyl protecting group with hydrazine, the ν and δ stretching modes of the acetyl group are no longer present as is the C=O vibration in the spectra of **3**. ν_{as} and ν_s stretching modes of the newly formed NH₂ group as well as ν (N–H) are observed in the region of 3383 – 3110 cm⁻¹ in the IR spectra (3158 cm⁻¹, 3117 cm⁻¹, Raman). Only small differences are observed for the remaining vibrations, belonging to the triazole and tetrazole moieties, respectively.

The nitrated 5-nitramino-3-(tetrazol-1-yl)-1*H*-1,2,4-triazole (**4**) shows two unique ν (N–H) stretching modes in the IR spectra at 3235 cm⁻¹ and 3129 cm⁻¹. The C–H valence stretching mode is observed as a broad peak at 3072 cm⁻¹ in the Raman spectra as well as

at 3085 cm^{-1} in the IR spectra. The ν_{as} stretching mode of the *N*-bound NO_2 group can be observed as a very intense band at 1691 cm^{-1} in the IR spectra and at 1693 cm^{-1} in the Raman spectra. The ν_{s} (NO_2) is observed at 1315 cm^{-1} (IR) and at 1320 cm^{-1} (Raman). Due to the heterocyclic system, many combined stretch and deformation modes are present, favoring the tetrazole moiety in the region of $1400 - 900\text{ cm}^{-1}$ and the triazole moiety in the region of $1600 - 1400\text{ cm}^{-1}$. At 1589 cm^{-1} (IR) and 1584 cm^{-1} (Raman), respectively, a combined mode, consisting of the δ_{s} $\text{C}_1\text{-N}_3\text{-C}_2$ and the two valence stretching modes towards the triazole substituents, ν ($\text{C}_2\text{-N}_{\text{nitramine}}$) and ν ($\text{C}_1\text{-N}_{\text{tet}}$), is present. The combination of the stretching modes ν ($\text{C}_1\text{-N}_2$) and ν ($\text{C}_2\text{-N}_3$), together forming a ν_{as} stretching mode, is observed at 1569 cm^{-1} in the IR spectra. The combination of three valence stretching modes, two from the triazole ring, ν ($\text{C}_2\text{-N}_1$) and ν ($\text{C}_2\text{-N}_3$), and one from the tetrazole ring, ν ($\text{C}_3\text{-N}_7$) are observed in both Raman and IR spectra at 1515 cm^{-1} and 1494 cm^{-1} , respectively. Bending and rocking deformation modes and out of plane/ in plane vibrations of the molecular backbone are observed below 900 cm^{-1} .

The nitrogen rich salts of **4** show absorption bands in the region of $3320 - 3100\text{ cm}^{-1}$ as expected for N-H stretching modes and additionally for the ν_{s} and ν_{as} vibrational modes of the NH_2 groups (ammonium, hydrazinium and guanidines). The stretching modes of the C-H bond are observed between $2960 - 2800\text{ cm}^{-1}$ in both, Raman and IR spectra. The ν_{as} stretching modes of the NO_2 group are only slightly shifted to lower energy when compared to **4** and are observed in the region of $1694 - 1657\text{ cm}^{-1}$. The ν_{s} stretching modes of the NO_2 group are in the same region than the neutral compound between 1338 cm^{-1} and 1317 cm^{-1} in both, IR and Raman spectra. The combined stretch and deformation as well as torsion modes representing the molecular backbone are also observed as for the neutral compound but are not discussed in detail, since no calculations have been performed for each compound, leaving only doubtful assignments for the combined stretching modes.

Multinuclear NMR spectroscopy

The ^1H NMR spectra of **1** shows three resonances for the $\text{N}_1\text{-H}$, $\text{C}_{\text{tet}}\text{-H}$ and $\text{C}_{\text{Tria}}\text{-H}$ at chemical shifts of 14.95 ppm, 10.09 ppm and 8.86 ppm, respectively. The ^{13}C NMR spectrum also presents three resonances at 153.0 ppm (C_1), 146.3 ppm (C_2) and 142.6

ppm (C_3), respectively. Since the backbone, the 3-tetrazol-1-yl-1,2,4-triazole stays basically the same for all compounds (**2** – **8**) presented in this study, almost the same chemical shifts are expected for the tetrazole moiety (hydrogen and carbon shifts) as well as the carbon atom of the triazole moiety connected to the tetrazole. Hence the hydrogen atom located at the tetrazole is observed in the ^1H NMR spectra at chemical shifts between 9.73 ppm and 10.03 ppm while the carbon atom of the tetrazole moiety shows resonances between 142.6 ppm and 143.7 ppm. The C_1 carbon atom of the triazole moiety is observed at chemical shifts between 149.2 ppm and 150.1 ppm.

Nearly the same chemical shift is observed for the C_2 carbon atom in **2** as for the C_1 carbon atom at chemical shifts of 149.7 ppm and 149.2 ppm, respectively. The signals for the acetyl protecting group, the carbonyl and the methyl group, are observed at chemical shifts of 165.5 ppm and 22.8 ppm, respectively. After the deprotection with hydrazine, these signals are no longer observed, but due to the deshielding of the C_2 atom, the signal is shifted to lower field, being present at 157.5 ppm in the ^{13}C NMR spectra of **3** instead of 149.7 ppm in **2**. The newly formed amine group is observed at a chemical shift of 6.62 ppm, while the $\text{N}_1\text{-H}$ hydrogen atom is observed at 12.60 ppm and is therefore shifted 2 ppm towards higher field in comparison with **2** in the ^1H NMR spectra. One signal at –141 ppm is observed in the ^{14}N NMR spectra of **3**, which is assigned to the N_3 nitrogen atom of the triazole moiety from comparison with other 1,2,4-triazole compounds.^[10]

The resonance of the C_2 carbon atom in **4** is shifted 5.5 ppm towards higher field due to the nitration of the amine group and is found at 152.0 ppm in the ^{13}C NMR spectra, while the signal of the hydrogen atom located at the N_8 atom at the nitramine group is observed at 8.06 ppm in the ^1H NMR spectra. Three signals could be assigned in the ^{14}N NMR of **4**. The N_9 atom (NO_2) is assigned the resonance at –15 ppm, while the resonances at –137 ppm and –147 ppm are potentially assigned to the N_4 and N_3 atoms.

All ionic compounds of **4**, except **6**, show the $\text{N}_1\text{-H}$ resonance in the ^1H NMR spectra at chemical shifts between 13.40 ppm and 13.47 ppm. The resonances of the C_2 carbon atoms are found at 158.0 ppm and 157.9 ppm, respectively, in the ^{13}C NMR spectra of compounds **5** – **8**. Additionally the signals of the cations are observed in both the ^1H and ^{13}C NMR spectra and are assigned in the experimental part. The signals of the NO_2 group nitrogen atoms are observed in the ^{14}N NMR spectra of **5** – **8** at a chemical shift of –15 ppm, while the signal of the N_3 atom is observed between –138 ppm and –142 ppm.

Even though no clear ^{15}N NMR spectrum of the neutral nitramino compound **4** was recordable due to solubility problems, fortunately enough a proton decoupled spectra of **8**

was recorded. A possible assignment of the resonances of the nitrogen atoms has been carried out using theoretical calculation carried out at the MPW1PW91/cc-pVDZ level of theory as implemented in the Gaussian 09W program package^[8] and the known literature.^[6] The spectra showed eleven well resolved resonances, as expected for this compound, two belonging to the triaminoguanidinium cation and nine to the 5-nitramino-3-(tetrazol-1-yl)-1*H*-1,2,4-triazolate anion. The two signals of the triaminoguanidinium cation are assigned at -289.1 ppm and -329.5 ppm. It gets rather difficult with the assignment of the signals of the anion. The signal of the N₉ (NO₂) atom is assigned to the chemical shift of -15 ppm as found also in the ¹⁴N NMR spectra. The resonance at $+11.8$ ppm is assigned to the N₆ atom of the tetrazole moiety, known for shifts towards higher field in the literature.^[11] From the calculations, the N₅ and N₇ atoms cannot be clearly distinguished but are assigned to the signals either at -16.7 ppm or -18.7 ppm. The N₂, N₄ and N₃ atoms can be assigned according to the calculations and from comparison with other triazolate salts^[10] to the resonances at chemical shifts of -52.1 ppm, -124.0 ppm and -144.1 ppm. The N₈ atom of the nitramine group is observed at a chemical shift of 167.2 , while the N₁ atom of the triazole moiety is finally assigned to the resonance at -190.4 ppm. The ¹⁵N NMR spectra with assignments is presented in Figure 1.

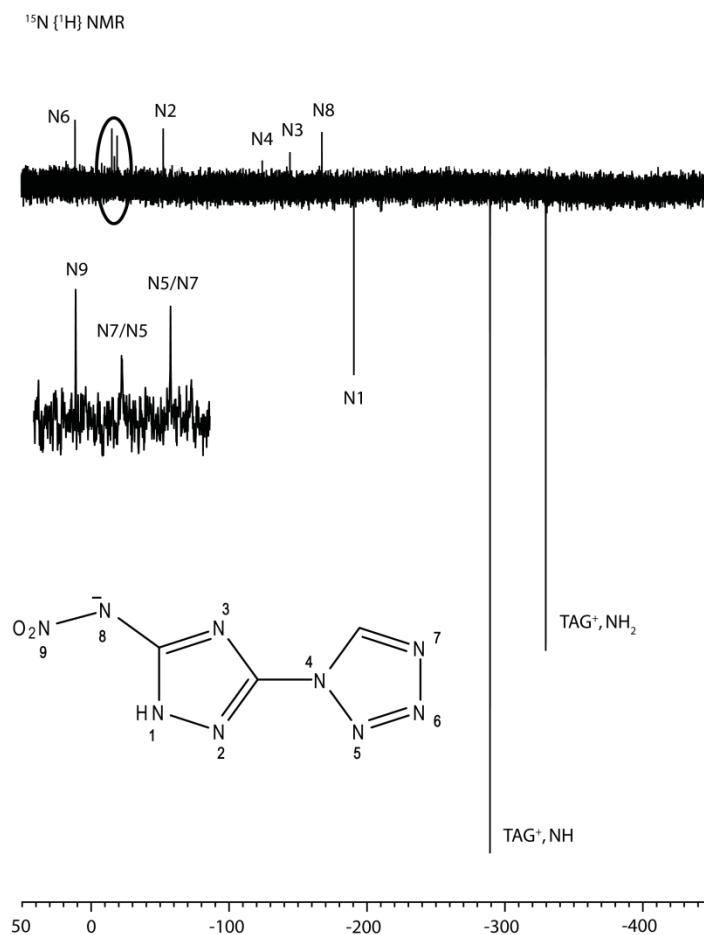


Figure 1: Proton decoupled $^{15}\text{N}\{^1\text{H}\}$ NMR spectra of triaminoguanidinium 5-nitramino-3-(tetrazol-1-yl)-1H-1,2,4-triazolate (**8**) together with possible assignments. The x-axis represents the chemical shift δ in ppm.

8.2.3 Crystal Structures

Crystal structures of **1**, **3** and **4** have been measured and their structures will be discussed in detail. **1** was recrystallized from ethanol as colorless blocks and **3** was recrystallized from an ethanolic solution as colorless plates, while the nitrated product **4** was recrystallized from ethyl acetate as light yellow blocks. While all bond lengths and angles within the tetrazolyltriazole backbone are pretty much the same for **1**, **3** and **4**, the arrangement of the molecules in the crystal structures is unique for each compound. Hence we will focus on the structure of the substituent in 5 position of the triazole ring and the resulting structural changes and the discussion of the crystal packing. Selected crystallographic data for all compounds have been compiled in Table S1 (Appendix 12.7). Even though different solvents, solvent mixtures and diffusion experiments as well

as temperature controlled crystallization techniques were used, no crystals suitable for X-ray crystallographic measurements were obtained from the ionic compounds of **4**, **5** – **8**.

3-Tetrazol-1-yl-1*H*-1,2,4-triazole (**1**) crystallizes in the orthorhombic space group *Pnma* as colorless blocks with a cell volume of 547.3(1) Å³ and four molecular moieties in the unit cell. The calculated density at 173 K is 1.664 g cm⁻³. The asymmetric unit of **1** is presented in Figure 2 together with the atom labeling scheme.

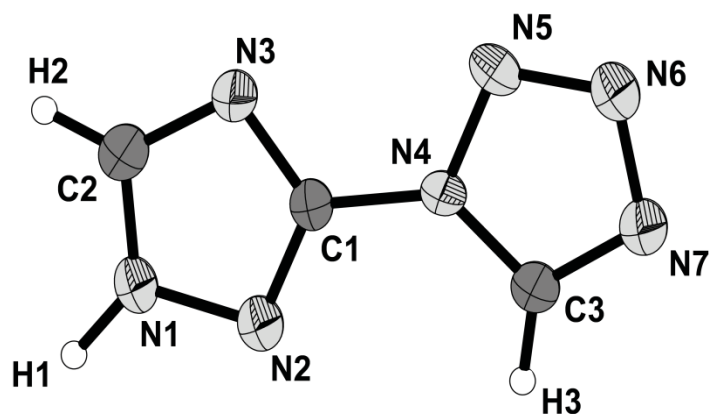


Figure 2: Asymmetric unit of **1**. Thermal ellipsoids are set to 50 % probability. Selected bond lengths (Å): N1–C2 1.312(3), N1–N2 1.365(3), N1–H1 0.97(3), N2–C1 1.306(3), N3–C2 1.320(3), N3–C1 1.332(3), N4–C3 1.329(3), N4–N5 1.354(3), N4–C1 1.413(3), N5–N6 1.290(3), N6–N7 1.360(3), N7–C3 1.311(3), C2–H2 0.93(3), C3–H3 0.94(3); Selected bond angles (°): C2–N1–N2 110.3(2), N2–N1–H1 118.3(15), C1–N2–N1 100.1(2), C2–N3–C1 101.1(2), C3–N4–N5 108.5(2), C3–N4–C1 131.1(2), N5–N4–C1 120.4(2), N6–N5–N4 106.06(18), N5–N6–N7 110.7(2), C3–N7–N6 106.0(2), N2–C1–N3 117.6(2), N2–C1–N4 120.9(2), N3–C1–N4 121.5(2), N1–C2–N3 110.9(3), N1–C2–H2 120.5(17), N7–C3–N4 108.7(2), N4–C3–H3 124.3(15); Selected torsion angles (°): planar.

Due to the complete planarity of the molecule, the packing of the structure is easily described. Infinite rows of **1** are formed by two hydrogen bonds N₁–H₁⋯N₇(i) and N₁–H₁⋯N₆(i) along the *a*-axis. The one dimensional rows are connected by two other moderately strong hydrogen bonds with C₂ and C₃ function as donor atoms, C₂–H₂⋯N₆(ii) and C₃–H₃⋯N₃(iii). The formed layers are oriented coplanar to the *ac* plane, as shown in Figure 3.

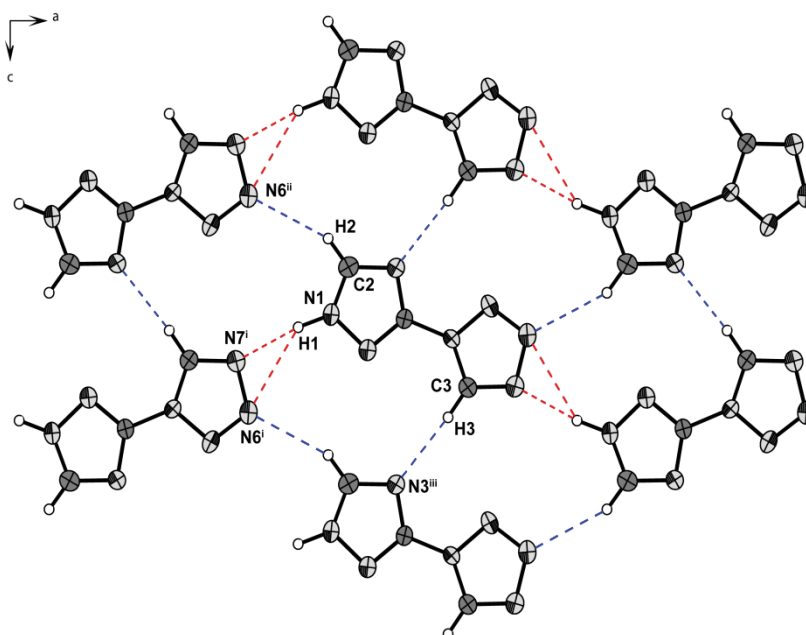


Figure 3: Hydrogen bonding scheme within the layers of **1**. Red dotted lines present the connection of the infinite rows, while the blue dotted lines represent the connection in between. Thermal ellipsoids are set to 50 % probability. Symmetry Operators: (i) $x+1/2, y, -z+3/2$; (ii) $x+1/2, -y+1/2, -z+1/2$; (iii) $x, y, z+1$.

Table 1: Hydrogen bonds present in **18**.

D–H···A	d (D–H) [Å]	d (H···A) [Å]	d (D–H···A) [Å]	< (D–H···A) [°]
N1–H1···N7 ⁱ	0.97(3)	1.94(3)	2.909(3)	173(2)
N1–H1···N6 ⁱ	0.97(3)	2.59(3)	3.409(3)	142(2)
C2–H2···N6 ⁱⁱ	0.93(3)	2.47(3)	3.333(4)	154(2)
C3–H3···N3 ⁱⁱⁱ	0.94(3)	2.26(3)	3.198(4)	176(2)

Symmetry Operators: (i) $x+1/2, y, -z+3/2$; (ii) $x+1/2, -y+1/2, -z+1/2$; (iii) $x, y, z+1$.

The layers show a staggered conformation along the *b*-axis, are completely planar and the distance between the layers is 3.165 Å. The cell is presented along the *c*-axis in Figure 4.

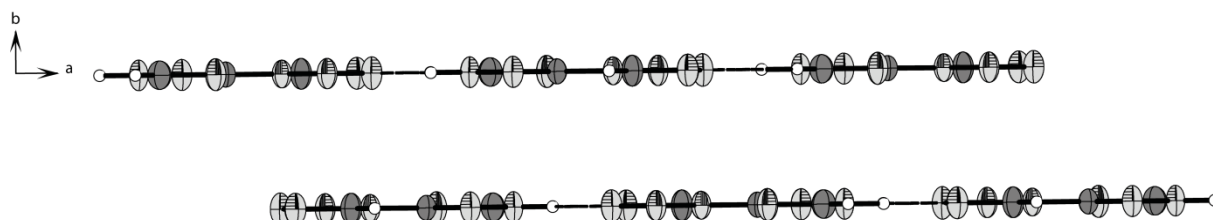


Figure 4: Staggered layers of **1**, coplanar to the *ac* plane and displayed along the *c*-axis. Thermal ellipsoids are set to 50 % probability.

5-Amino-3-tetrazol-1-yl-1*H*-1,2,4-triazole (**3**) crystallizes in the monoclinic space group *Pn* as colorless plates with a cell volume of 298.18(5) Å³ and two molecular moieties in the unit cell. The calculated density at 173 K is 1.695 g cm⁻³. The asymmetric unit of **3** is presented in Figure 5 together with the atom labeling scheme.

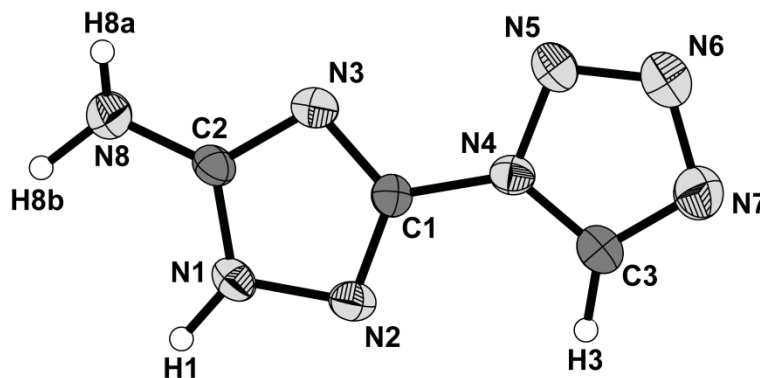


Figure 5: Asymmetric unit of **3**. Thermal ellipsoids are set to 50 % probability. Selected bond lengths (Å): N1–C2 1.332(4), N1–N2 1.391(4), N1–H1 0.91(4), N2–C1 1.299(4), N3–C2 1.342(4), N3–C1 1.345(4), N8–C2 1.340(5), N8–H8a 0.80(5), N8–H8b 0.99(4), N4–C3 1.323(5), N4–N5 1.344(4), N4–C1 1.412(4), N5–N6 1.291(4), N6–N7 1.361(5), N7–C3 1.314(5), C3–H3 0.95(4); Selected bond angles (°): C2–N1–N2 110.0(3), N2–N1–H1 121(2), C1–N2–N1 100.5(3), C2–N3–C1 101.7(3), C2–N8–H8a 117(3), C2–N8–H8b 117(2), H8a–N8–H8b 119(4), C3–N4–N5 108.9(3), N5–N4–C1 121.6(2), N6–N5–N4 105.4(3), N5–N6–N7 111.9(3), C3–N7–N6 104.4(3), N2–C1–N3 117.9(3), N2–C1–N4 120.5(3), N1–C2–N8 125.0(3), N1–C2–N3 110.0(3), N7–C3–H3 130(2), N4–C3–H3 120(2); Selected torsion angles (°): C2–N1–N2–C1 –0.2(3), C3–N4–N5–N6 –0.1(4), C1–N4–N5–N6 –179.5(3), N4–N5–N6–N7 0.2(4), N5–N6–N7–C3 –0.2(4), N1–N2–C1–N3 –0.2(4), C2–N3–C1–N2 0.5(4), C3–N4–C1–N2 4.2(5), N5–N4–C1–N2 –176.6(3), N5–N4–C1–N3 4.0(4), N2–N1–C2–N8 178.0(4), N6–N7–C3–N4 0.1(4), N5–N4–C3–N7 0.0(4).

The amine group in 5 position shows a nearly planar arrangement, indicating a sp² hybridization on the nitrogen atom. The C₂–N₈ bond length is short, being only 1.340(5) Å and hence in between the lengths of formal C–N single and double bonds (1.47 Å, 1.22 Å).^[12] The bond lengths of the tetrazol-1-yl-triazole backbone are also in this range, indicating a delocalized π-electron system. Even though the C₁–N₄ bond is much longer (1.412(4) Å) and has much more single bond character, the delocalization should include both heterocyclic rings, as also observed for azo coupled triazoles.^[13]

As observed for **1**, the structure of **3** also consists of infinite rows, connected by only one hydrogen bond, N₈–H₈⋯N₇(iii). The hydrogen bond is mostly of electrostatic nature, not directed with an D–H⋯A angle of only 110(3)° and hence only a weak interaction with a H⋯A distance of 2.64(4) Å. The rows are opposed to one another by 180° and enclose an angle of 35.45°. They are connected by three moderately strong hydrogen bonds, N₁–H₁⋯N₃(i), N₈–H_{8a}⋯N₂(ii) and N₈–H_{8b}⋯N₅(i). The hydrogen bonding motive for one

asymmetric unit is shown in Figure 6, while the packing within the cell is presented along the *c*-axis in Figure 7.

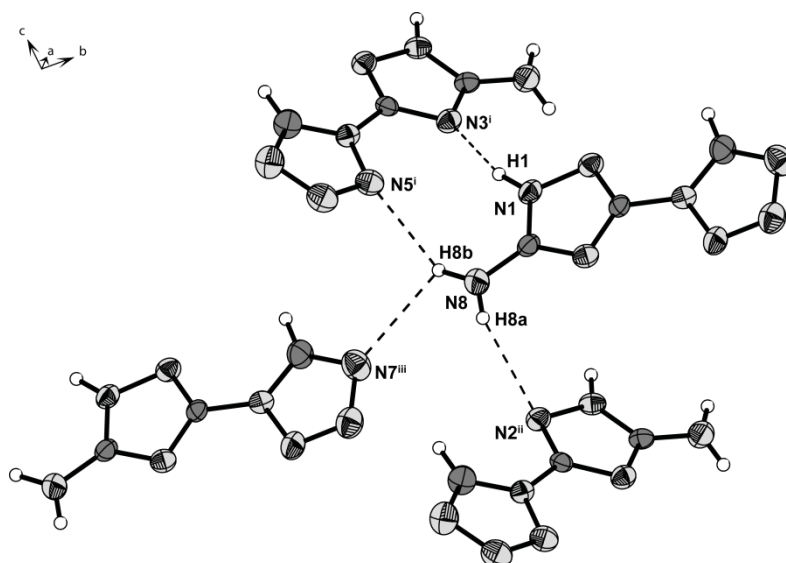


Figure 6: Hydrogen bonding motive, displayed for the asymmetric unit of **3**. Thermal ellipsoids are set to 50 % probability. Symmetry Operators: (i) $x-1/2, -y, z+1/2$; (ii) $x-1/2, -y, z-1/2$; (iii) $x-1, y-1, z$.

Table 2: Hydrogen bonds present in **3**.

D-H...A	d (D-H) [Å]	d (H...A) [Å]	d (D-H...A) [Å]	< (D-H...A) [°]
N1-H1...N3 ⁱ	0.91(4)	2.04(4)	2.929(4)	165(3)
N8-H8a...N2 ⁱⁱ	0.80(5)	2.44(5)	3.161(4)	151(4)
N8-H8b...N5 ⁱ	0.99(4)	2.37(4)	3.197(4)	141(3)
N8-H8b...N7 ⁱⁱⁱ	0.99(4)	2.64(4)	3.125(5)	110(3)

Symmetry Operators: (i) $x-1/2, -y, z+1/2$; (ii) $x-1/2, -y, z-1/2$; (iii) $x-1, y-1, z$.

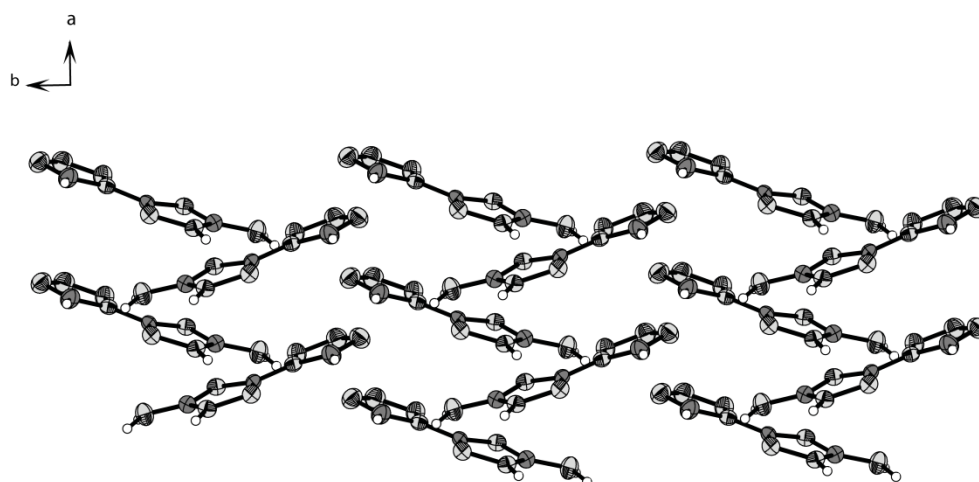


Figure 7: Presentation of the crystal packing and the arrangement of the rows coplanar to the *ab* plane in **3**. Thermal ellipsoids are set to 50 % probability.

5-Nitramino-3-tetrazol-1-yl-1*H*-1,2,4-triazole (**4**) crystallizes in the orthorhombic space group *Pna*2₁ as light yellow blocks with a cell volume of 1447.5(3) Å³ and eight molecular moieties in the unit cell. The calculated density at 173 K is, as expected, much higher than the density of the amino compound, being 1.809 g cm⁻³. The asymmetric unit of **1** consists of two independent molecular units of **4** and is presented in Figure 8.

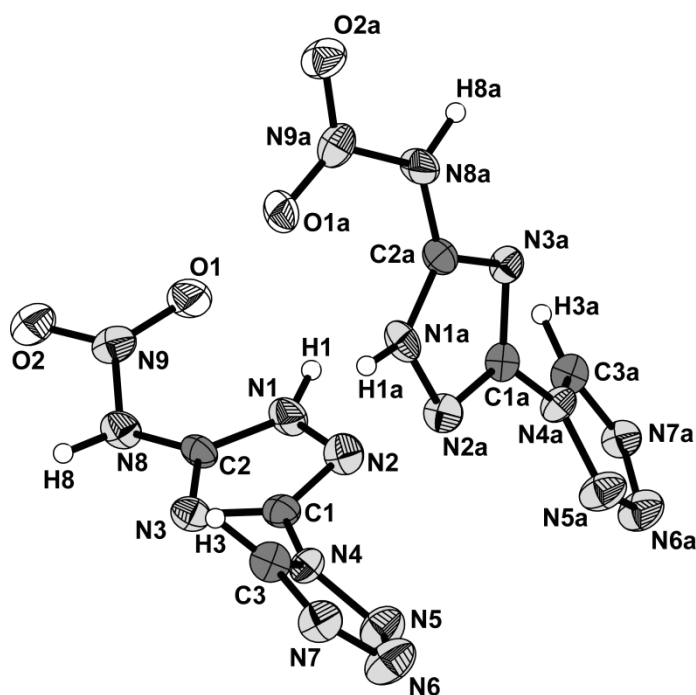


Figure 8: Asymmetric unit of **4**. Thermal ellipsoids are set to 50 % probability. Selected bond lengths (Å): O1–N9 1.229(4), O2–N9 1.225(4), N1–C2 1.315(5), N1–N2 1.362(4), N1–H1 0.85(2), N2–C1 1.302(5), N3–C2 1.336(5), N3–C1 1.349(5), N4–C3 1.344(5), N4–N5 1.356(4), N4–C1 1.418(5), N5–N6 1.292(4), N6–N7 1.371(5), N7–C3 1.305(5), N8–C2 1.371(5), N8–N9 1.378(4), N8–H8 0.88(4), C3–H3 0.99(2), O1a–N9a 1.219(4), O2a–N9a 1.234(4), N1a–C2a 1.313(5), N1a–N2a 1.375(4), N1a–H1a 0.82(2), N2a–C1a 1.303(5), N3a–C2a 1.335(5), N3a–C1a 1.356(5), N4a–C3a 1.341(5), N4a–N5a 1.354(4), N4a–C1a 1.412(5), N5a–N6a 1.293(4), N6a–N7a 1.363(4), N7a–C3a 1.315(4), N8a–N9a 1.354(4), N8a–C2a 1.371(5), N8a–H8a 0.92(4), C3a–H3a 0.99(2); Selected bond angles (°): C2–N1–N2 110.2(3), C2–N1–H1 130(3), N2–N1–H1 119(3), C1–N2–N1 100.9(3), C2–N3–C1 100.5(4), C3–N4–N5 108.7(4), C3–N4–C1 129.8(4), N5–N4–C1 121.3(3), N6–N5–N4 106.1(3), N5–N6–N7 110.4(4), C3–N7–N6 106.6(4), C2–N8–N9 122.6(3), C2–N8–H8 119(3), N9–N8–H8 112(3), O2–N9–O1 126.9(4), O2–N9–N8 115.8(4), O1–N9–N8 117.3(4), N2–C1–N3 117.3(4), N2–C1–N4 121.5(4), N3–C1–N4 121.1(4), N1–C2–N3 111.0(4), N1–C2–N8 128.4(4), N3–C2–N8 120.6(4), N7–C3–N4 108.2(4), N7–C3–H3 132(2), N4–C3–H3 120(2), C2a–N1a–N2a 110.2(3), C2a–N1a–H1a 140(3), N2a–N1a–H1a 109(3), C1a–N2a–N1a 100.4(3), C2a–N3a–C1a 100.1(3), C3a–N4a–N5a 108.9(3), C3a–N4a–C1a 128.5(3), N5a–N4a–C1a 122.3(3), N6a–N5a–N4a 105.4(3), N5a–N6a–N7a 111.6(3), C3a–N7a–N6a 105.5(3), N9a–N8a–C2a 123.4(4), N9a–N8a–H8a 114(2), C2a–N8a–H8a 122(2), O1a–N9a–O2a 125.8(3), O1a–N9a–N8a 118.8(4), O2a–N9a–N8a 115.4(4), N2a–C1a–N3a 117.8(4), N2a–C1a–N4a 121.8(4), N3a–C1a–N4a 120.3(4), N1a–C2a–N3a 111.5(4), N1a–C2a–N8a 129.1(4), N3a–C2a–N8a 119.4(4), N7a–C3a–N4a 108.5(4), N7a–C3a–H3a 126(2), N4a–C3a–H3a 126(2); Selected torsion angles (°): C2–N8–N9–O2 –164.1(4), C2–N8–N9–O1 17.3(5), C1–N3–C2–N8 –178.7(3), N9–N8–C2–N1 –23.2(6), N9–N8–C2–N3 156.2(4), C2a–N8a–N9a–O1a 7.8(6), C2a–N8a–N9a–O2a –171.4(4), N2a–N1a–C2a–N8a 179.4(4), C1a–N3a–C2a–N8a –178.7(4), N9a–N8a–C2a–N1a –20.1(7), N9a–N8a–C2a–N3a 159.4(4).

As seen for **1** and **3**, the molecular backbone shows a delocalized π -electron system with all bond lengths being in between formal single and double bonds. The C_1-N_4 bond is again the longest one (1.418(5) Å), as observed for **1** and **3**. The nitramine moiety shows the same behavior as observed and discussed in detail for 5-nitramino-3-nitro-1*H*-1,2,4-triazole (Chapter 7). The structure consists of eight hydrogen bonds, two of which are intramolecular ($N_1-H_1\cdots O_1$ and $N_{1a}-H_{1a}\cdots O_{1a}$) keeping the nitramine group in plane with the triazole ring. Helical rows are formed by the second independent molecule (*a* nomenclature, molecule 2) of the asymmetric unit by one strong, and directed hydrogen bond ($N_{1a}-H_{1a}\cdots N_{7a}$ (iii), $< 174(4)^\circ$), the $D\cdots A$ distance being much shorter than the sum of van der Waals radii ($r_w(N) + r_w(N) = 3.10$ Å) at 2.889(5) Å. Molecule 2 of the asymmetric unit is connected over one hydrogen bonds $N_8-H_8\cdots N_{3a}$ (iv) to the first independent molecule (molecule 1) of the asymmetric unit (forming an eight membered planar ring system, due to symmetry operation). Molecule 1 connects over three hydrogen bonds to two molecules (*a* nomenclature) all using the N_1 nitrogen atom as donor atom. $N_1-H_1\cdots O_{2a}$ (i) and $N_1-H_1\cdots O_{1a}$ (i) connect to the first molecule, while $N_1-H_1\cdots N_{6a}$ (ii) connects to the second molecule. Hence the rows are only formed by molecule 2 of the asymmetric unit, it is obvious that molecule 1 functions as a connector between the rows (Symmetry Operators: (i) $-x+1/2, y+1/2, z+1/2$; (ii) $x, y-1, z$; (iv) $x-1/2, -y+1/2, z$; (v) $x+1/2, -y+1/2, z$). The hydrogen bonding scheme for the asymmetric unit is hence displayed in Figure 9, while the coordination of molecule 1, showing the connection of rows is presented in Figure 10.

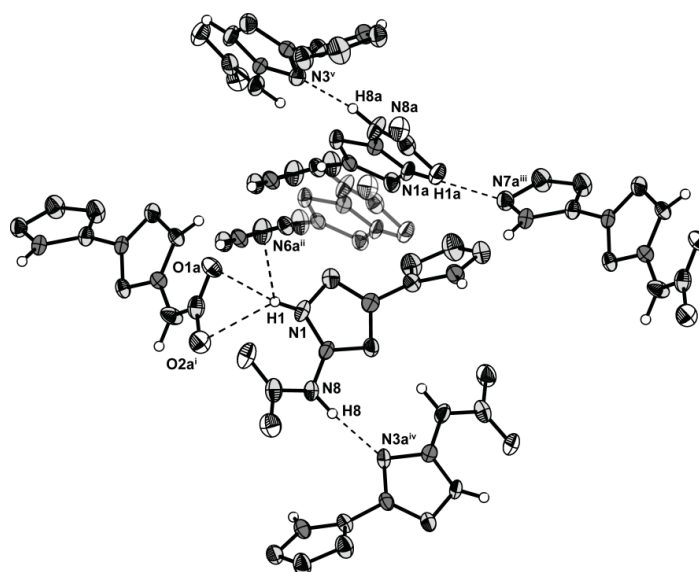


Figure 9: Hydrogen bonding motive for the asymmetric unit of **4**. Thermal ellipsoids are set to 50% probability. Symmetry Operators: (i) $-x+1/2, y+1/2, z+1/2$; (ii) $x, y-1, z$; (iii) $-x+1/2, y-1/2, z-1/2$; (iv) $x-1/2, -y+1/2, z$; (v) $x+1/2, -y+1/2, z$.

Table 3: Hydrogen bonds present in **4**.

D–H⋯A	d (D–H) [Å]	d (H⋯A) [Å]	d (D–H⋯A) [Å]	< (D–H⋯A) [°]
N1–H1⋯O1	0.86(3)	2.25(3)	2.666(4)	109(3)
N1a–H1a⋯O1a	0.82(3)	2.49(3)	2.698(4)	95(2)
N1–H1⋯O1a ⁱ	0.85(2)	2.59(3)	3.116(4)	121(3)
N1–H1⋯N6a ⁱⁱ	0.85(2)	2.60(4)	3.154(5)	124(3)
N1–H1⋯O2a ⁱ	0.85(2)	2.61(4)	3.096(4)	117(3)
N1a–H1a⋯N7a ⁱⁱⁱ	0.82(2)	2.07(3)	2.889(5)	174(4)
N8–H8⋯N3a ^{iv}	0.89(4)	1.94(4)	2.817(5)	173(4)
N8a–H8a⋯N3 ^v	0.92(4)	1.86(4)	2.768(5)	169(4)

Symmetry Operators: (i) $-x+1/2, y+1/2, z+1/2$; (ii) $x, y-1, z$; (iii) $-x+1/2, y-1/2, z-1/2$; (iv) $x-1/2, -y+1/2, z$; (v) $x+1/2, -y+1/2, z$.

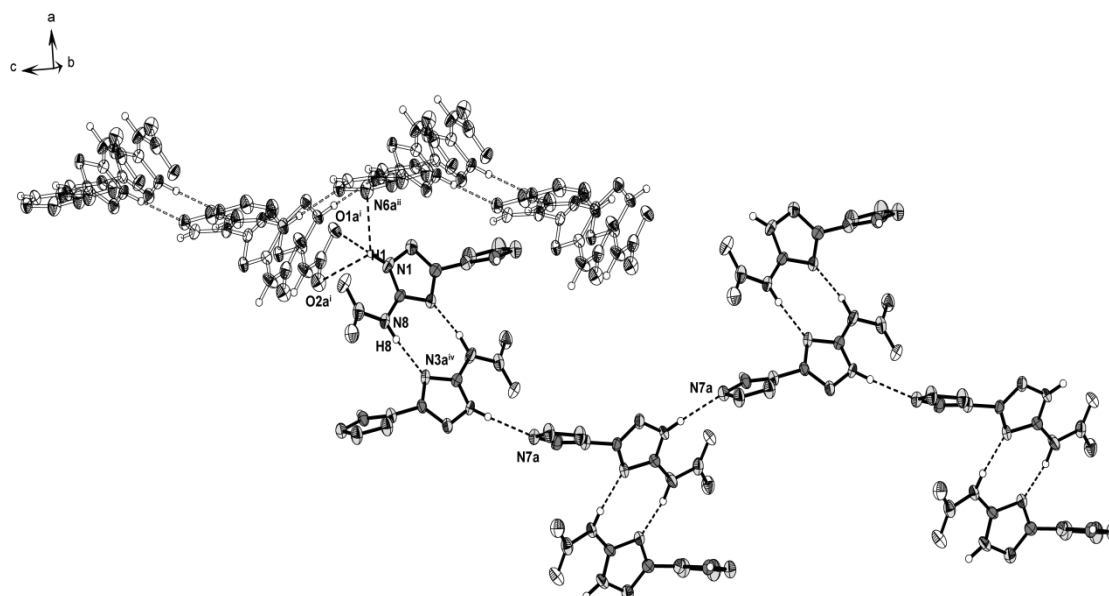


Figure 10: Connection of the rows formed by molecule 2 (*a* nomenclature) over molecule 1 (normal nomenclature). The rows are set transparent partially for better clarity. Symmetry Operators: (i) $-x+1/2, y+1/2, z+1/2$; (ii) $x, y-1, z$; (iii) $-x+1/2, y-1/2, z-1/2$; (iv) $x-1/2, -y+1/2, z$; (v) $x+1/2, -y+1/2, z$.

8.2.4 Sensitivities and Thermal Stabilities

The decomposition temperature of the neutral amine compound **3** is 229 °C and therefore it seemed very promising for the further synthetic efforts towards the nitramine compound. As expected for such kind of material a drop in decomposition temperature was observed for **4**, showing only 91 °C. Since normally the formation of an anion again increases the thermal stability, nitrogen rich cations of **4** have been prepared, displaying decomposition temperatures between 119 °C (NH₄⁺) and 155 °C (G⁺). These values are much too low for the possible application of these materials as energetic materials.

Regardless of these low numbers, sensitivity tests have been performed for compounds **4** and **6 – 8**.

The sensitivities values of **4** (anhydrous) are in the normal range for nitramine compounds being 5 J for impact and 60 N for friction sensitivity. These values have been increased a lot by the formation of high nitrogen rich salts due to the higher electron density within the heterocyclic ring system. The values for **6** and **7** which have only been measured as the monohydrates show impact values of < 12J (**6**) and < 40 J (**7**) and friction sensitivity values of < 192 N (**6**) and < 360 N (**7**). The sensitivities exhibit a large increase in stability, especially for the guanidinium salt (**7**), but it also has to be taken into account that the values are measured for monohydrates. Measurements of the sensitivity values for **8** as an anhydrous compound showed the friction sensitivity to be < 144 N and impact to be < 3 J, just a slight decrease in impact sensitivity when compared to **4**. Since the triaminoguanidinium compounds normally exhibit the highest performance values the prepared compounds seem to be unsuitable for the use as potential energetic materials.

If we take a closer look at the performance data of the neutral compound **4** calculated with the EXPLO 5 (version 5.04) program package,^[14] we obtain a quite high energy of explosion and a good velocity of detonation at 8549 m s⁻¹. But even this isn't high enough if we take the low decomposition temperature into account. Hence only the salt formation could have produced a possible candidate for evaluation, but there also, the decomposition temperatures are the exclusion criterion. The formation of salts normally consumes 200 – 300 m s⁻¹ in detonation velocity which wouldn't also be enough to play in the highest echelons after all.

Table 4: Sensitivity values and calculated detonation parameters of **4**.

Compound	IS (J)	FS (N)	ρ (g cm ⁻³)	ΔH_f^0 (s) (kJ mol ⁻¹)	Q_v (kJ kg ⁻¹)	P_{c-j} (kbar)	V_{det} (m s ⁻¹)
4	5	60	1.809	560	-5101	311	8549

IS: Impact sensitivity; FS: Friction sensitivity; ΔH_f^0 : Heat of formation; Q_v : Heat of explosion; P_{c-j} : Detonation pressure at the Chapman-Jouguet point; V_{det} : Detonation velocity.

The formation of double salts has not been undertaken till now, but as for the 5-nitramino-3-nitro-1,2,4-triazole (Chapter 7) this could yield compounds of higher stability and should be carried out in further studies.

8.3 Conclusion

3-Tetrazol-1-yl-1*H*-1,2,4-triazole (**1**) and 5-amino-3-tetrazol-1-yl-1*H*-1,2,4-triazole (**3**) have been synthesized in very good yields by the literature known route of Gaponik.^[3] Compound **3** was synthesized using acetyl protected 3,5-diamino-1*H*-1,2,4-triazole as the starting material, reacting only one amine group selectively, followed by deprotection with hydrazine. **3** was nitrated afterwards yielding **4** (5-nitramino-3-(tetrazol-1-yl)-1*H*-1,2,4-triazole) in reasonable yields. All three neutral compounds have been characterized fully by means of vibrational and multinuclear NMR spectroscopy as well as mass spectrometry. The decomposition temperatures of **1**, **3** and **4** have been recorded to be 229 °C for **1** and **3**, while the nitrated compound decomposes at a very low temperature of 91 °C. Compounds **1** and **3** exhibit low sensitivities towards shock and friction and have also been investigated as propellants or additives in propellant mixtures (formulations with ADN), but the specific impulses (I_{sp}) of both compounds did not reach the values of azotetrazolate salts. Compound **4** on the other hand shows very high sensitivities of 5 J against impact and 60 N against friction, but reasonable good performance values (v_{det} : 8549 m s⁻¹; P_{C-J} : 311 kbar).

As observed for other compounds, the formation of ionic salts increases both, thermal stability and sensitivity values. Nitrogen rich energetic and ionic compounds of **4** have been synthesized by the addition of the free bases or carbonates, ammonia, hydrazine, guanidinium carbonate and triaminoguanidine. The thermal decomposition points are all observed between 136 °C (**7**, guanidinium) and 155 °C (**6**, hydrazinium). Due to the low decomposition points and the performance values expected to be lower than **4**, no intensive theoretical study of the detonation parameters and heats of formation has been performed, since these materials unfortunately lack of power and especially stability for the use in explosive applications. Nevertheless, all ionic compounds have been fully characterized using Raman, IR and multinuclear NMR spectroscopy. The sensitivity values of all compounds have been determined for safety reasons and found to be well above the values of the neutral compound. Due to twinning problems, no crystal structure of the ionic compounds is presented, while crystal structures of the neutral compounds have been extensively studied and discussed.

8.4 Experimental Part

General. All chemical reagents and solvents were obtained from Sigma-Aldrich Inc. or Acros Organics (analytical grade) and were used as supplied without further purification. ^1H , $^{13}\text{C}\{^1\text{H}\}$, $^{14}\text{N}\{^1\text{H}\}$ and ^{15}N NMR spectra were recorded on a JEOL Eclipse 400 instrument in DMSO- d_6 or CDCl_3 at or near 25 °C. The chemical shifts are given relative to tetramethylsilane (^1H , ^{13}C) or nitromethane (^{14}N , ^{15}N) as external standards and coupling constants are given in Hertz (Hz). Infrared (IR) spectra were recorded on a Perkin-Elmer Spectrum BX FT-IR instrument equipped with an ATR unit at 25 °C. Transmittance values are qualitatively described as “very strong” (vs), “strong” (s), “medium” (m), “weak” (w) and “very weak” (vw). RAMAN spectra were recorded on a Bruker RAM II spectrometer equipped with a Nd:YAG laser operating at 1064 nm and a reflection angle of 180°. The intensities are reported as percentages of the most intense peak and are given in parentheses. Elemental analyses (CHNO) were performed with a Netzsch Simultaneous Thermal Analyzer STA 429. Melting and decomposition points were determined by differential scanning calorimetry (Linseis PT 10 DSC, calibrated with standard pure indium and zinc). Measurements were performed at a heating rate of 5 °C min⁻¹ in closed aluminum sample pans with a 1 µm hole in the top for gas release to avoid an unsafe increase in pressure under a nitrogen flow of 20 mL min⁻¹ with an empty identical aluminum sample pan as a reference.

For initial safety testing, the impact and friction sensitivities as well as the electrostatic sensitivities were determined. The impact sensitivity tests were carried out according to STANAG 4489,^[15] modified according to WIWEB instruction 4-5.1.02^[16] using a BAM^[17] drop hammer. The friction sensitivity tests were carried out according to STANAG 4487^[18] and modified according to WIWEB instruction 4-5.1.03^[19] using the BAM friction tester. The electrostatic sensitivity tests were accomplished according to STANAG 4490^[20] using an electric spark testing device ESD 2010EN (OZM Research) operating with the “Winspark 1.15 software package”.^[21]

Crystallographic measurements. The single crystal X-ray diffraction data of **1**, **3** and **4** were collected using an Oxford Xcalibur3 diffractometer equipped with a Spellman generator (voltage 50 kV, current 40 mA) and a KappaCCD detector. The data collection was undertaken using the CRYCALIS CCD software^[22] while the data reduction was performed with the CRYCALIS RED software.^[23] The structures were solved with SHELXS-

97^[24] and refined with SHELXL-97^[25] implemented in the program package WinGX^[26] and finally checked using PLATON.^[27]

3-Tetrazol-1-yl-1*H*-1,2,4-triazole (**1**)

3-Amino-1*H*-1,2,4-triazole (12 mmol, 1 g) was suspended in triethyl orthoformate (18 mmol, 2.69 g, 2.99 mL) and sodium azide (14.4 mmol, 0.936 g) was added. The suspension was heated up to 100 °C and 6 mL acetic acid was added dropwise while stirring vigorously. The suspension was then refluxed for three hours and allowed to cool down to ambient temperature. Afterwards concentrated HCl (14.4 mmol) was added to the suspension and stirred for 20 minutes. The suspension was filtrated and the residue was extracted thrice with 50 mL ethanol each. The organic phases were combined and the solvent was evaporated to yield 0.6 g (37%) 3-tetrazol-1-yl-1*H*-1,2,4-triazole as a white powder. Crystals suitable for X-ray measurements were derived from recrystallization with water/ethanol (1:9).

m.p. with dec. 229 °C (DSC, T_{onset} , 5 °C min⁻¹); ¹H NMR (DMSO-*d*₆, 25 °C) δ (ppm) = 14.95 (s br, 1H, N-H), 10.09 (s, 1H, C-H), 8.86 (s, 1H, C-H); ¹³C NMR (DMSO-*d*₆, 25 °C) δ (ppm) = 153.0, 146.3, 143.7; ¹⁴N NMR (DMSO-*d*₆, 25 °C) δ (ppm) = --; IR (ATR, 25 °C, cm⁻¹) ν = 3113 (m), 3040 (m), 2986 (m), 2913 (m), 1695 (w), 1643 (w), 1550 (s), 1529 (s), 1487 (s), 1459 (m), 1390 (m), 1374 (w), 1326 (w), 1317 (w), 1284 (s), 1271 (s), 1203 (m), 1185 (m), 1123 (m), 1094 (s), 1047 (w), 1015 (m), 978 (s), 958 (m), 921 (w), 876 (vw), 27 (ms), 731 (s), 713 (w), 660 (m); RAMAN (Nd:YAG, 1064 nm, cm⁻¹) ν = 3137 (32), 3048 (21), 2937 (10), 2917 (10), 2858 (11), 1603 (11), 1552 (78), 1532 (100), 1490 (12), 1460 (41), 1390 (33), 1285 (49), 1203 (17), 1186 (16), 1096 (27), 1084 (14) 1019 (65), 979 (24), 737 (11), 661 (10), 489 (20), 436 (47), 373 (36); Sensitivities (anhydrous) (grain size < 100 μ m): IS: > 15 J; IS: > 240 N.

1-Acteyl-3,5-diamino-1,2,4-triazole

3,5-Diamino-1*H*-1,2,4-triazole (36 g, 364 mmol) was suspended in 130 mL water and acetic anhydride (40.8 mL, 431.6 mmol) was added dropwise under stirring. After further stirring for one hour the precipitate was filtered off, washed with 600 mL water and dried on air. 1-Acteyl-3,5-diamino-1,2,4-triazole was obtained as a white powder in 98 % yield.

^1H NMR (DMSO- d_6 , 25 °C) δ (ppm) = 7.35 (s, 2H, NH_2), 5.63 (s, 2H, NH_2), 2.33 (s, 3H, CH_3); $^{13}\text{C}\{^1\text{H}\}$ NMR (DMSO- d_6 , 25 °C) δ (ppm) = 170.5 (C=O), 162.2 ($\text{C}^1\text{-NH}_2$), 157.0 (s, $\text{C}^2\text{-NH}_2$), 23.56 ($-\text{CH}_3$); IR (ATR, 25 °C, cm^{-1}) ν = 3416 (m), 3390 (vs), 3298 (m), 3225 (m), 3178 (s), 3133 (s), 3018 (m), 1710 (vs), 1641 (vs), 1569 (s), 1449 (m), 1393 (s), 1366 (vs), 1337 (s), 1178 (m), 1135 (m), 1117 (m), 1066 (m), 1044 (m), 973 (w), 839 (w), 758 (w), 732 (vw), 700 (w), 669 (w), 653 (w); RAMAN (Nd:YAG, 1064 nm, cm^{-1}) ν = 3415 (8), 3406 (9), 3221 (17), 3186 (16), 3136 (15), 3125 (15), 3023 (53), 2990 (25), 2935 (100), 1712 (91), 1642 (37), 1568 (40), 1550 (22), 1460 (8), 1426 (19), 1397 (35), 1376 (33), 1341 (36), 1182 (30), 1118 (21), 1077 (4), 1037 (33), 972 (17), 840 (20), 771 (7), 669 (38), 589 (12), 578 (14), 446 (37), 400 (12), 345 (28), 225 (14); m/z : (DEI+): 43.06 (28), 99.09 (100), 141.1 (22) [M^+].

5-Acetamido-3-amino-1*H*-1,2,4-triazole

1-Acetyl-3,5-diamino-1,2,4-triazole (25 g, 177.3 mmol) was suspended in 250 mL decahydro-naphthalene and refluxed at 270 °C for 6 h. After cooling to ambient temperature, the precipitate was filtered off, washed with isohexane (400 mL) and diethyl ether (600 mL) yielding 99 % (24.75 g) 5-acetamido-3-amino-1*H*-1,2,4-triazole as a white powder.

^1H NMR (DMSO- d_6 , 25 °C) δ (ppm) = 12.93 (br. s, 1H, N_{TriazH}), 9.72 (br. s, 1H, NH-CO), 5.11 (br. s, 2H, NH_2), 2.00 (s, 3H, CH_3); $^{13}\text{C}\{^1\text{H}\}$ NMR (DMSO- d_6 , 25 °C) δ (ppm) = 168.5 (C=O), 22.2 ($-\text{CH}_3$); IR (ATR, 25 °C, cm^{-1}) ν = 3423 (m), 3251 (vs), 3116 (m), 3024 (m), 2956 (m), 2874 (m), 2827 (m), 1683 (vs), 1597 (vs), 1583 (vs), 1452 (s), 1380 (w), 1361 (m), 1296 (s), 1269 (m), 1081 (s), 1024 (m), 1006 (m), 832 (w), 818 (m), 760 (vw), 714 (m), 687 (m); RAMAN (Nd:YAG, 1064 nm, cm^{-1}) ν = 3321 (3), 3252 (6), 3222 (3), 2934 (43), 1684 (100), 1648 (14), 1586 (61), 1537 (11), 1457 (14), 1366 (28), 1297 (7), 1261 (9), 1155 (4), 1085 (48), 1027 (46), 971 (28), 819 (11), 739 (13), 693 (5), 591 (40), 494 (13), 364 (14), 324 (27), 183 (26), 128 (135); EA ($\text{C}_4\text{H}_7\text{N}_5\text{O}$) calcd.: C, 34.04; H, 5.00; N, 49.62; found: C, 34.11; H, 4.86; N, 49.12.

5-Acetamido-3-(tetrazol-1-yl)-1*H*-1,2,4-triazole (**2**)

Sodium azide (5.85 g, 90 mmol) and triethyl orthoformate (18.71 mL, 113 mmol) were added to 5-acetamido-3-amino-1*H*-1,2,4-triazole (10.57 g, 75 mmol). 100 mL acetic acid was added dropwise to the mixture with vigorous stirring at 70 °C. After complete addition, the mixture was refluxed at 120 °C for 18 hours, cooled to ambient temperature and acidified with concentrated hydrochloric acid (8.5 mL). The suspension was further stirred for one hour and the solvent was removed completely by rotary evaporation. 100 mL toluene was added to the residue, stirred and also removed by rotary evaporation to remove traces of acetic acid. The dry residue was suspended in 50 mL water and the precipitate was filtered off afterwards. 5-Acetamido-3-(tetrazol-1-yl)-1*H*-1,2,4-triazole was obtained as a white powder in 79 % (11.51 g) yield.

$T_{\text{dec.}}$: 216 °C (DSC, 5 °C min⁻¹), 239 °C (DSC, Onset, 5 °C min⁻¹); ¹H NMR (DMSO-*d*₆, 25 °C) δ (ppm) = 14.05 (s, 1H, N_{Tria}H), 11.93 (s, 1H, NH-CO), 10.03 (s, 1H, C_{Tet}H), 2.03 (s, 3H, -CH₃); ¹³C {¹H} NMR (DMSO-*d*₆, 25 °C) δ (ppm) = 169.5 (s, CO), 149.7 (C_{Tria}), 149.2 (C_{Tria}), 142.8 (C_{Tet}), 22.8 (s, -CH₃); IR (ATR, 25 °C, cm⁻¹) ν = 3323 (m), 3241 (s), 3110 (s), 1690 (s), 1590 (s), 1558 (s), 1530 (m), 1492 (s), 1448 (m), 1424 (m), 1390 (w), 1372 (w), 1359(w), 1324 (w), 1264 (m), 1248 (s), 1188 (m), 1160 (m), 1090 (m), 1068 (m), 1043 (w), 1014 (m), 1002 (w), 978 (m), 962 (w), 905 (w), 792 (m), 736 (m), 712 (w), 689 (w), 656 (m), 617 (m); RAMAN (Nd:YAG, 1064 nm, cm⁻¹) ν = 3320 (1), 3251 (1), 3110 (4), 2939 (8), 1700 (23), 1563 (100), 1529 (12), 1494 (9), 1447 (10), 1389 (2), 1362 (2), 1326 (1), 1251 (17), 1191 (2), 1161 (3), 1093 (5), 1018 (25), 967 (6), 806 (3), 689 (3), 621 (3), 509 (2), 410 (4), 301 (6), 202 (5); EA (C₅H₆N₈O · 1/6 H₂O) calcd.: C, 30.46; H, 3.24; N, 56.83; found: C, 30.76; H, 3.02; N, 56.70.

5-Amino-3-(tetrazol-1-yl)-1*H*-1,2,4-triazole (**3**)

Hydrazine monohydrate (2.74 mL, 56.4 mmol) was added to 5-Acetamido-3-(tetrazol-1-yl)-1*H*-1,2,4-triazole (2.74 g, 14.1 mmol) and refluxed at 90 °C for 3 hours with vigorous stirring. After cooling to ambient temperature, addition of 2 mL water and adjusting to pH 6 with app. 10 % hydrochloric acid, the product was filtered off and washed with cold water (100 mL). 5-Amino-3-(tetrazol-1-yl)-1*H*-1,2,4-triazole was synthesized as a white powder with up to 59 % yield.

$T_{\text{dec.}}$: 229 °C (DSC, 5 °C min⁻¹), 237 °C (DSC, Onset, 5 °C min⁻¹); ¹H NMR (DMSO-*d*₆, 25 °C) δ (ppm) = 12.60 (s, br, 1H, N_{Tria}-H), 9.88 (s, 1H, -H_{Tet}), 6.62 (s, 2H, -NH₂); ¹³C{¹H} NMR (DMSO-*d*₆, 25 °C) δ (ppm) = 157.5 (C_{Tria}-NH₂), 150.0 (C_{Tria}-N_{Tet}), 142.6 (C_{Tet}); ¹⁴N NMR (DMSO-*d*₆, 25 °C): δ (ppm) = -141; IR (ATR, 25 °C, cm⁻¹) ν = 3383 (m), 3358 (m), 3310 (m), 3262 (m), 3167 (s), 3116 (s), 2968 (w), 2811 (vw), 2773 (vw), 1652 (s), 1600 (w), 1567 (m), 1517 (s), 1458 (w), 1447 (w), 1336 (w), 1328 (w), 1272 (m), 1188 (w), 1164 (w), 1103 (m), 1094 (m), 1080 (w), 1052 (w), 1016 (vw), 984 (m), 962 (w), 882 (w), 762 (w), 734 (w), 715 (w), 705 (vw), 631 (w); RAMAN (Nd:YAG, 1064 nm, cm⁻¹) ν = 3158 (12), 3117 (24), 1654 (36), 1598 (27), 1562 (100), 1526 (79), 1459 (40), 1420 (28), 1338 (7), 1272 (100), 1195 (3), 1173 (6), 1095 (37), 1055 (20), 1025 (95), 980 (6), 755 (27), 531 (25), 415 (48), 371 (51), 282 (39); EA: (C₃N₈H₄ · 1/3 H₂O) calcd.: C, 22.79; H, 2.97; N, 70.87; found: C, 22.74; H, 2.91; N, 70.41; m/z: (DCI+): 153.11 [M+H⁺].

5-Nitramino-3-(tetrazol-1-yl)-1*H*-1,2,4-triazole (**4**)

Concentrated sulfuric acid (4.6 mL, 84.6 mmol) was added to 5-amino-3-(tetrazol-1-yl)-1*H*-1,2,4-triazole (0.61 g, 4 mmol). After complete dissolution of 5-amino-3-(tetrazol-1-yl)-1*H*-1,2,4-triazole the reaction mixture was cooled to 0-3 °C and 100 % nitric acid (1.28 mL, 30.7 mmol) was slowly added maintaining the temperature below 5 °C. The mixture was stirred 30 minutes at 0 °C and 2 hours at ambient temperature afterwards. It was then quenched with ice/water (30 g /30 mL) and extracted three times with 50 mL ethyl acetate. The combined ethyl acetate phases were dried over MgSO₄ and the solvent removed by rotary evaporation until about 5 mL were left. After crystallization overnight 5-nitramino-3-(tetrazol-1-yl)-1*H*-1,2,4-triazole was obtained in 58 % (0.46 g) yield as an orange microcrystalline powder.

$T_{\text{dec.}}$: 91 °C (DSC, 5 °C min⁻¹), 118 °C (DSC, Onset, 5 °C min⁻¹), 149 °C (DSC, Onset, 5 °C min⁻¹); ¹H NMR (CD₃OD, 25 °C) δ (ppm)= 9.73 (s, 1H, H_{Tet}), 8.06 (s, 1H, -NH-NO₂); ¹³C{¹H} NMR (CD₃OD, 25 °C) δ (ppm)= 152.0 (C-NH-NO₂), 149.6 (C-N_{Tet}), 143.5 (C_{Tet}); ¹⁴N NMR (CD₃OD, 25 °C) δ (ppm)= -15 (NH-NO₂), -39, -136, -147, -369; IR (ATR, 25 °C, cm⁻¹) ν = 3235 (s), 3129 (s), 3129 (s), 3085 (s), 2921 (m), 2852 (m), 2793 (m), 2157 (w), 1723 (w), 1691 (s), 1618 (w), 1592 (w), 1569 (m), 1512 (w), 1494 (m), 1418 (m), 1375 (m), 1312 (vs), 1260 (s), 1224 (s), 1186 (m), 1145 (m), 1085 (m),

1050 (w), 1036 (m), 999 (m), 982 (w), 942 (w), 802 (w), 774 (w), 764 (w), 717 (w), 681 (w), 650 (w); RAMAN (Nd:YAG, 1064 nm, cm^{-1}) $\nu =$ 3071 (2), 1693 (1), 1584 (100), 1515 (7), 1466 (13), 1445 (4), 1384 (1), 1320 (4), 1265 (12), 1195 (2), 1148 (4), 1090 (12), 1050 (5), 1013 (14), 991 (38), 844 (6), 754 (10), 726 (2), 673 (2), 503 (3), 411 (3), 318 (7), 232 (7); EA ($\text{C}_3\text{H}_3\text{N}_9\text{O}_2 \cdot 2 \text{H}_2\text{O}$) calcd.: C, 16.88; H, 3.25; N, 52.10; found: C, 16.13; H, 2.50; N, 51.70; m/z (FAB+): 198.1 $[\text{M}+\text{H}^+]$; m/z (FAB-): 196.0 $[\text{M}-\text{H}]$; Sensitivities (anhydrous) (grain size: 100-500 μm): IS: 5 J; FS: 60 N; ESD: 400 mJ.

Ammonium 5-nitramino-3-(tetrazol-1-yl)-1*H*-1,2,4-triazolate (**5**)

5-Nitramino-3-(tetrazol-1-yl)-1*H*-1,2,4-triazole (2 mmol, 0.395 g) was dissolved in 20 mL water and a 6.25 % ammonia solution (0.6 mL, 2 mmol) was added dropwise. A clear red solution developed immediately which was heated to 65 °C for 30 minutes. The volume of the reaction mixture was concentrated to 1/2 of its original volume and left standing for crystallization. Yellow crystals developed overnight yielding 0.39 g (85 %) of ammonium 5-nitramino-3-(tetrazol-1-yl)-1*H*-1,2,4-triazolate as the monohydrate.

T: 119 °C ($-\text{H}_2\text{O}$, DSC, 5 °C min^{-1}); $T_{\text{dec.}}$: 143 °C (DSC, 5 °C min^{-1}); ^1H NMR (DMSO- d_6 , 25 °C) δ (ppm) = 13.40 (s, br, 1H, $\text{N}_{\text{Tria}}\text{H}$), 9.99 (s, 1H, $\text{C}_{\text{Tet}}\text{H}$), 7.14 (s, br, 4H, NH_4^+); $^{13}\text{C}\{^1\text{H}\}$ NMR (DMSO- d_6 , 25 °C) δ (ppm) = 158.0 (C-N- NO_2), 150.1 (C-N $_{\text{Tet}}$), 142.8 (C $_{\text{Tet}}$); ^{14}N NMR (DMSO- d_6 , 25 °C) δ (ppm) = -4, -15 (N- NO_2), -142, -359 (NH_4^+); IR (ATR, 25 °C, cm^{-1}) $\nu =$ 3436 (m), 3151 (s), 3060 (s), 2879 (m), 2143 (w), 1687 (w), 1650 (w), 1563 (m), 1531 (w), 1484 (m), 1435 (m), 1411 (m), 1390 (m), 1375 (m), 1311 (m), 1266 (m), 1177 (w), 1158 (w), 1116 (w), 1076 (w), 1001 (w), 982 (w), 956 (w), 878 (w), 857 (w), 825 (w), 774 (w), 724 (w), 685 (w), 647 (w); RAMAN (Nd:YAG, 1064 nm, cm^{-1}) $\nu =$ 3152 (3), 3135 (3), 1701 (2), 1567 (100), 1540 (38), 1479 (27), 1441 (6), 1412 (7), 1390 (6), 1372 (7), 1261 (11), 1179 (4), 1167 (3), 1118 (3), 1098 (6), 1081 (5), 1049 (3), 1015 (43), 1004 (19), 957 (2), 861 (5), 754 (7), 423 (5), 312 (4); m/z : (FAB+): 18.1 $[\text{NH}_4^+]$; m/z : (FAB-): 196.0 $[\text{C}_3\text{H}_2\text{N}_9\text{O}_2]$; EA ($\text{C}_3\text{H}_6\text{N}_{10}\text{O}_2 \cdot \text{H}_2\text{O}$) calcd.: C, 15.52; H, 3.47; N, 60.33; found: C, 16.10; H, 3.30; N, 59.91.

Hydrazinium 5-nitramino-3-(tetrazol-1-yl)-1*H*-1,2,4-triazolate (6)

5-Nitramino-3-(tetrazol-1-yl)-1*H*-1,2,4-triazole (2 mmol, 0.395 g) was dissolved in 20 mL water and hydrazine monohydrate (0.1 mL, 2 mmol) was added dropwise. A clear red solution developed immediately and was heated to 65 °C for 30 minutes. The solvent was evaporated completely yielding 0.42 g (92 %) of hydrazinium 5-nitramino-3-(tetrazol-1-yl)-1*H*-1,2,4-triazolate as a bright orange powder.

$T_{\text{dec.}}$: 155 °C (DSC, 5 °C min⁻¹); ¹H NMR (DMSO-*d*₆, 25 °C) δ (ppm) = 9.96 (s, 1H, C_{Tet}H), 7.75 (s, br, 5H, N₂H₅⁺); ¹³C{¹H} NMR (DMSO-*d*₆, 25 °C) δ (ppm) = 158.0 (C-N-NO₂), 150.1 (C-N_{Tet}), 142.7 (C_{Tet}); ¹⁴N NMR (DMSO-*d*₆, 25 °C) δ (ppm) = -4, -15 (-N-NO₂), -138, -331 (br, N₂H₅⁺); IR (ATR, 25 °C, cm⁻¹) ν = 3303 (m), 3098 (m), 2635 (m), 2146 (w), 1694 (w), 1619 (w), 1598 (m), 1567 (m), 1528 (m), 1482 (m), 1442 (m), 1392 (m), 1317 (vs), 1274 (s), 1244 (s), 1166 (w), 1098 (s), 1074 (s), 1021 (m), 999 (m), 970 (m), 916 (vw), 854 (w), 825 (w), 788 (w), 767 (w), 734 (w), 713 (W), 684 (w), 658 (w); RAMAN (Nd:YAG, 1064 nm, cm⁻¹) ν = 3103 (2), 1640 (3), 1568 (100)m 1531 (49), 1487 (26), 1443 (7), 1403 (7), 1364 (8), 1277 (5), 1248 (6), 1198 (6), 1170 (2), 1134 (4), 1107 (6), 1047 (6), 1024 (30), 1002 (23), 973 (5), 856 (4), 760 (6), 689 (2), 659 (1), 429 (3), 419 (4), 321 (5), 266 (4); m/z : (FAB⁺): 33.0 [N₂H₅⁺]; m/z : (FAB⁻): 196.0 [C₃H₂N₉O₂⁻]; EA (C₃H₇N₁₁O₂ · H₂O) calcd.: C, 14.52; H, 4.05; N, 62.08; found: C, 14.93; H, 3.55; N, 61.34; Sensitivities (monohydrate) (grain size: 100–500 μ m): IS: < 12 J; FS: < 192 N; ESD: 100 mJ.

Guanidinium 5-nitramino-3-(tetrazol-1-yl)-1*H*-1,2,4-triazolate (7)

5-Nitramino-3-(tetrazol-1-yl)-1*H*-1,2,4-triazole (2 mmol, 0.395 g) was dissolved in 30 mL water and bis(guanidinium) carbonate (1 mmol, 0.180 g) was added in one portion. The solution was heated to 65 °C for 30 minutes till no more gas evolution was visible. The solvent was evaporated completely afterwards yielding 0.39 g (76 %) of guanidinium 5-nitramino-3-(tetrazol-1-yl)-1*H*-1,2,4-triazolate as a red powder.

$T_{\text{dec.}}$: 136 °C (DSC, Onset, 5 °C min⁻¹), 184 °C (DSC, 5 °C min⁻¹); ¹H NMR (DMSO-*d*₆, 25 °C) δ (ppm) = 13.47 (s, br, 1H, N_{Tri}H), 9.96 (s, 1H, C_{Tet}H), 6.96 (s, 6H, CH₆N₃⁺); ¹³C{¹H} NMR (DMSO-*d*₆, 25 °C) δ (ppm) = 157.9 (CH₆N₃⁺), 157.9 (C-N-NO₂), 150.1 (C-N_{Tet}), 142.7 (C_{Tet}); ¹⁴N NMR (DMSO-*d*₆, 25 °C) δ (ppm) = -4, -15 (-N-NO₂), -138;

IR (ATR, 25 °C, cm^{-1}) $\nu = 3347$ (m), 3263 (m), 3186 (s), 2143 (w), 1657 (s), 1582 (w), 1562 (m), 1538 (w), 1484 (m), 1444 (m), 1395 (m), 1324 (vs), 1276 (m), 1258 (s), 1184 (m), 1098 (m), 1084 (s), 1029 (w), 1009 (w), 984 (w), 971 (w), 880 (vw), 862 (w), 818 (vw), 791 (vw), 770 (vw), 740 (w), 711 (vw); RAMAN (Nd:YAG, 1064 nm, cm^{-1}) $\nu = 3148$ (3), 1657 (2), 1564 (100), 1538 (60), 1486 (25), 1443 (11), 1402 (9), 1378 (7), 1357 (6), 1259 (12), 1169 (3), 1110 (7), 1086 (5), 1055 (16), 1029 (36), 1007 (33), 975 (3), 865 (5), 751 (10), 689 (2), 542 (5), 503 (1), 425 (5), 319 (6), 237 (8); m/z : (FAB+): 60.1 [CH_6N_3^+]; m/z : (FAB-): 255.8 [M^-]; EA ($\text{C}_4\text{H}_8\text{N}_{12}\text{O}_2 \cdot \text{H}_2\text{O}$) calcd.: C, 17.52; H, 3.68; N, 61.30; found: C, 17.78; H, 3.42; N, 59.40; Sensitivities (monohydrate) (grain size: < 100 μm): IS: < 40 J; FS: < 360 N; ESD: 0.6 J.

Triaminoguanidinium 5-nitramino-3-(tetrazol-1-yl)-1*H*-1,2,4-triazolate (**8**)

5-Nitramino-3-(tetrazol-1-yl)-1*H*-1,2,4-triazole (2 mmol, 0.395 g) was dissolved in 50 mL boiling ethanol. Triaminoguanidine (1.9 mmol, 0.198 g) was added portionwise to the solution under a nitrogen stream. With continued heating, water was added to the solution in small portions, until complete dissolution of the solid material was observed. After cooling to ambient temperature, the solvent was reduced to 1/3 of its original volume and left standing for crystallization. Pure triaminoguanidinium 5-nitramino-3-(tetrazol-1-yl)-1*H*-1,2,4-triazolate was obtained as a orange crystalline solid, yielding 0.53 g (93 %).

T_{dec} : 149 °C (DSC, 5 °C min^{-1}), 169 °C (DSC, Onset, 5 °C min^{-1}); ^1H NMR (DMSO- d_6 , 25 °C) δ (ppm) = 13.40 (s, br, 1H, $\text{N}_{\text{Tri}H}$), 9.96 (s, 1H, $\text{C}_{\text{Tet}H}$), 8.56 (s, 3H, TAG^+ , C-NH-NH₂), 4.46 (s, 6H, TAG^+ , C-NH-NH₂); $^{13}\text{C}\{^1\text{H}\}$ NMR (DMSO- d_6 , 25 °C) δ (ppm) = 159.0 (CH_9N_6^+), 158.0 (C-N-NO₂), 150.1 (C-N_{Tet}), 142.7 (C_{Tet}); ^{14}N NMR (DMSO- d_6 , 25 °C) δ (ppm) = -4, -15 (-N-NO₂), -142; $^{15}\text{N}\{^1\text{H}\}$ NMR (DMSO- d_6 , 25 °C) δ (ppm) = 11.8 (N₆), -14.9 (-NO₂, N₉), -16.7 (N₇/N₅), -18.7 (N₅/N₇), -52.1 (N₂), -124.0 (N₄), -144.1 (N₃), -167.2 (N₈), -190.4 (N₁), -289.1 (TAG^+ , C-NH-NH₂), -329.5 (TAG^+ , C-NH-NH₂); IR (ATR, 25 °C, cm^{-1}) $\nu = 3313$ (m), 3196 (m), 3056 (m), 1740 (w), 1724 (w), 1680 (s), 1661 (m), 1609 (m), 1542 (m), 1592 (m), 1478 (m), 1421 (m), 1399 (m), 1367 (m), 1343 (s), 1319 (vs), 1261 (s), 1187 (m), 1130 (m), 1086 (m), 1019 (w), 1007 (w), 975 (m), 963 (m), 920 (m), 876 (w), 771 (vw), 732 (m); RAMAN (Nd:YAG, 1064 nm, cm^{-1}) $\nu = 3278$ (3), 3156 (3), 1662 (2), 1553 (100), 1502 (24), 1451 (8), 1426 (4), 1376 (5), 1339 (3), 1291 (2), 1263 (12), 1188 (2), 1166 (3), 1088 (8), 1048 (2), 1009 (46), 977 (5),

869 (5), 755 (8), 684 (2), 638 (2), 502 (3), 422 (5)m 401 (4), 328 (4), 313 (3), 226 (5); m/z : (FAB+): 105.1 [CH_9N_6^+]; m/z : (FAB-): 196.0 [$\text{C}_3\text{H}_2\text{N}_9\text{O}_2^-$]; EA ($\text{C}_4\text{H}_{11}\text{N}_{15}\text{O}_2 \cdot \text{H}_2\text{O}$) calcd.: C, 15.05; H, 4.10; N, 65.81; found: C, 17.47; H, 3.63; N, 65.26; Sensitivities (anhydrous) (grain size: < 100 μm): IS: < 3 J; FS: 144 N; ESD: 300 mJ.

8.5 References

- [1] a) T. Abe, G.-H. Tao, Y.-H. Joo, Y. Huang, B. Twamley, J. M. Shreeve, *Angew. Chem.* **2008**, *120*, 7195-7198; b) K. Y. Lee, D. G. Ott, (United States Dept. of Energy, USA). Application: US, **1980**, p. 5 pp; c) K. Y. Lee, D. G. Ott, M. M. Stinecipher, *Industrial & Engineering Chemistry Process Design and Development* **1981**, *20*, 358-360; d) K. Y. Lee, C. B. Storm, M. A. Hiskey, M. D. Coburn, *J. Energ. Mater.* **1991**, *9*, 415-428; e) E. L. Metelkina, *Russ. J. Org. Chem.* **2004**, *40*, 543-550; f) K.-Y. Lee, M. M. Stinecipher, *Vol. US525672*, US, **1993**; g) M. S. Pevzner, T. N. Kulibabina, N. A. Povarova, L. V. Kilina, *Khimiya Geterotsiklicheskikh Soedinenii* **1979**, 1132-1135.
- [2] A. Onishi, H. Tanaka, K. Shimamoto, *Vol. US6300498*, **2001**.
- [3] P. N. Gaponik, V. P. Karavai, *Chem. Het. Comp.* **1985**, *11*, 1521-1524.
- [4] T. M. Klapötke, J. Stierstorfer, in *New Trends in Research of Energetic Materials, Vol. Pt. 1* (Eds.: J. Ottis, J. Pachman), Pardubice, **2008**, pp. 278-298.
- [5] a) M. S. Pevzner, N. V. Gladkova, T. A. Kravchenko, *Russ. J. Org. Chem.* **1996**, *32*, 1186-1189; b) B. G. van den Bos, *Recl. Trav. Chim. Pays-Bas Belg.* **1960**, *79*, 836-842.
- [6] M. Hesse, Herbert, Meier, B. Zeh, *Spektroskopische Methoden in der Organischen Chemie*, 6 ed., Georg Thieme Verlag, Stuttgart, New York, **2002**.
- [7] a) T. H. Dunning, *J. Chem. Phys.* **1989**, *90*, 1007; b) C. Lee, W. Yang, R. G. Parr, *Phys. Rev. B* **1988**, *7*, 785; c) A. D. Becke, *J. Chem. Phys.* **1993**, *98*, 5648.
- [8] *Gaussian 09W, Version 7.0*, M. J. Frisch, G. W. Trucks, H. B. Schlegel, G. E. Scuseria, M. A. Robb, J. R. Cheeseman, G. Scalmani, V. Barone, B. Mennucci, G. A. Petersson, H. Nakatsuji, M. Caricato, X. Li, H. P. Hratchian, A. F. Izmaylov, J. Bloino, G. Zheng, J. L. Sonnenberg, M. Hada, M. Ehara, K. Toyota, R. Fukuda, J. Hasegawa, M. Ishida, T. Nakajima, Y. Honda, O. Kitao, H. Nakai, T. Vreven, J. A. Montgomery, Jr., J. E. Peralta, F. Ogliaro, M. Bearpark, J. J. Heyd, E. Brothers, K. N. Kudin, V. N. Staroverov, R. Kobayashi, J. Normand, K. Raghavachari, A. Rendell, J. C. Burant, S. S. Iyengar, J. Tomasi, M. Cossi, N. Rega, J. M. Millam, M. Klene, J. E. Knox, J. B. Cross, V. Bakken, C. Adamo, J. Jaramillo, R. Gomperts, R. E. Stratmann, O. Yazyev, A. J. Austin, R. Cammi, C. Pomelli, J. W. Ochterski, R. L. Martin, K. Morokuma, V. G. Zakrzewski, G. A. Voth, P. Salvador, J. J. Dannenberg, S. Dapprich, A. D. Daniels, Ö. Farkas, J. B. Foresman, J. V. Ortiz, J. Cioslowski, and D. J. Fox, *Gaussian, Inc., Wallingford CT*, 2009.
- [9] H. A. Witek, M. Keiji, *J. Comp. Chem. THEOCHEM* **2004**, *25*, 1858-1864.
- [10] T. M. Klapötke, F. A. Martin, S. Wiedbrauk, *submitted* **2011**.

- [11] R. N. Butler, in *Comprehensive Hetrocyclic Chemistry*, Vol. 5, 1 ed. (Ed.: A. R. Katritzky), Pergamon Press Ltd., Oxford, **1984**.
- [12] A. F. Holleman, E. Wiberg, *Lehrbuch der anorganischen Chemie*, 101st Ed., de Gruyter, New York, **1995**.
- [13] a) D. E. Chavez, B. C. Tappan, B. A. Mason, D. Parrish, *Propell. Explos. Pyrot.* **2009**, 34, 475-479; b) A. Dippold, Thomas M. Klapötke, Franz A. Martin, *Z. Anorg. Allg. Chem.* **2011**, 637, in press.
- [14] a) M. Suceska, *Propell. Explos. Pyrot.* **1999**, 24, 280-285; b) M. Sućeska, *EXPLO5.4 program*, Zagreb, Croatia, **2010**.
- [15] *NATO standardization agreement (STANAG) on explosives*, no. 4489, 1st ed., Sept. 17, **1999**.
- [16] *WIWEB-Standardarbeitsanweisung 4-5.1.02, Ermittlung der Explosionsgefährlichkeit, hier: der Schlagempfindlichkeit mit dem Fallhammer*, Nov. 08, **2002**.
- [17] <http://www.bam.de>.
- [18] *NATO standardization agreement (STANAG) on explosives, friction tests*, no.4487, 1st ed., Aug. 22, **2002**.
- [19] *WIWEB-Standardarbeitsanweisung 4-5.1.03, Ermittlung der Explosionsgefährlichkeit, hier: der Reibempfindlichkeit mit dem Reibeapparat*, Nov. 08, **2002**.
- [20] *NATO standardization agreement (STANAG) on explosives, electrostatic discharge sensitivity tests*, no.4490, 1st ed., Feb. 19, **2001**.
- [21] <http://www.ozm.cz/en/sensitivity-tests/esd-2008a-small-scale-electrostatic-spark-sensitivity-test/>.
- [22] *CrysAlis CCD*, Oxford Diffraction Ltd., Version 1.171.27p5 beta (release 01-04-2005 CrysAlis171.NET).
- [23] *CrysAlis RED*, Oxford Diffraction Ltd., Version 1.171.27p5 beta (release 01-04-2005 CrysAlis171.NET).
- [24] G. M. Sheldrick, *SHELXS-97, Crystal Structure Solutuion, Version 97-1; Institut Anorg. Chemie, University of Göttingen, Germany*, **1990**.
- [25] G. M. Sheldrick, *SHELXL-97, Program for the Refinement of Crystal Structures. University of Göttingen, Germany*, **1997**.
- [26] L. Farrugia, *J. Appl. Cryst.* **1999**, 32, 837-838.
- [27] A. L. Spek, *Platon, A Multipurpose Crystallographic Tool*, Utrecht University, Utrecht, The Netherlands, **1999**.

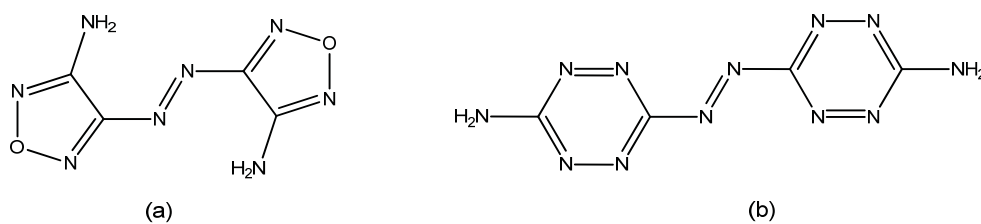
9. Synthesis and characterization of bis(triaminoguanidinium) 5,5'-dinitrimino-3,3'-azo-1H-1,2,4-triazole – A novel insensitive energetic material

Alexander Dippold, Thomas M. Klapötke and Franz A. Martin

As published in: Zeitschrift für Anorganische und Allgemeine Chemie, 2011, 637, DOI: 10.1002/zaac.201100102.

9.1 Introduction

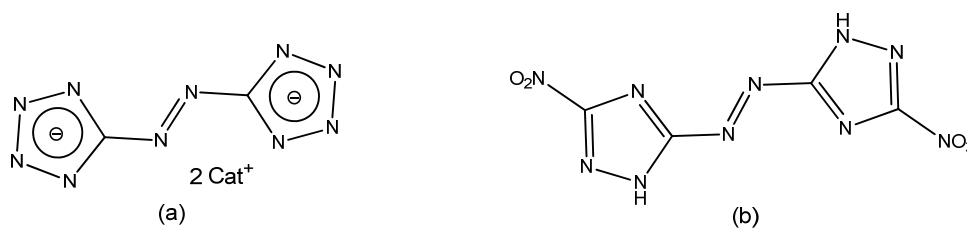
In recent years, the synthesis of energetic, heterocyclic compounds has attracted an increasing amount of interest, since heterocycles generally offer a higher heat of formation, density and oxygen balance than their carbocyclic analogues.^[1] In combination with the advances of a high nitrogen content such as the high average two electron bond energy associated with the nitrogen-nitrogen triple bond^[2], those compounds are of great interest for investigations. The current widely used nitro-explosives TNT, RDX or HMX per se as well as their transformation products are toxic due to the presence of nitro (-NO₂), nitroso (-NO) or nitrito (-ONO) groups either in the explosives itself or its degradation products.^[3] The development of new energetic materials therefore focuses – besides high performance and stability – on environmentally friendly compounds. Nitrogen-rich compounds mainly generate environmentally friendly molecular nitrogen as end-product of propulsion or explosion, therefore they continue to be the focus of energetic materials research across the globe.^[4] A prominent family of compounds regarding the properties mentioned above are azole-based energetic materials, because they are generally highly endothermic compounds with relatively high densities and a high nitrogen content.^[5] Since modern high energy density materials (HEDM) mostly derive their energy of ring or cage strain as well as of a high heat of formation, a lot of research has been done on explosives containing the azo-functionality. Several heterocyclic compounds like 4,4'-diamino-3,3'-azofurazan (a) and 3,3'-azobis(6-amino-1,2,4,5-tetrazine) (b) have been reported in literature so far (Figure 1).^[6]



Scheme 1: Formula structures of some heterocyclic compounds containing the azo-functionality.

The combination of a high nitrogen content with a high heat of formation led to the development of azole-based compounds containing the azo-functionality. The recently reported 5,5'-azotetrazolate anion (Figure 2) is such an energetic compound with a very high nitrogen content and therefore suitable for the synthesis of energetic materials. There has been increased interest in the synthesis of energetic salts based on the 5,5'-azotetrazolate anion, since the neutral compound decomposes at room temperature.^[7] Many 5,5'-azotetrazolate salts have found practical application in combination with nitrogen-rich bases (e.g. guanidinium, triaminoguanidinium, hydrazinium) as propellants,^[8] in gas generators for airbags as well as in fire extinguishing systems.^[9] Heavy metal salts have been used as initiators^[10] and derivatives of 5,5'-azotetrazole are utilized as additives in solid rocket propellants.^[11]

Since triazole derivatives often tend to be thermally and kinetically more stable than their tetrazole analogous, research in this field of azo-bridged azoles shows great promise for energetic materials. For example, 5,5'-dinitro-3,3'-azo-1*H*-1,2,4-triazole and its nitrogen-rich salts have been in the focus as potential insensitive high nitrogen compounds and propellant burn rate modifiers.^[12]



Scheme 2: Formula structures of the 5,5'-azotetrazolate anion (a) and 3,3'-dinitro-5,5'-azo-1*H*-1,2,4-triazole (b).

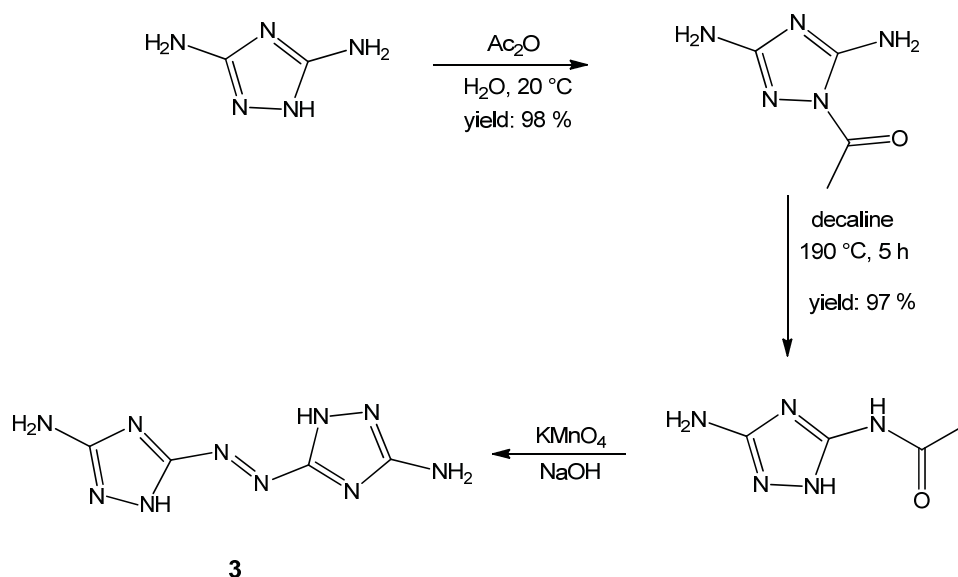
The literature known 5,5'-dinitro-3,3'-azo-1*H*-1,2,4-triazole was first synthesized at Los Alamos National Laboratories by Naud and coworkers in 2003.^[13] Since this molecule and selected nitrogen-rich salts like the triaminoguanidinium compound reveal a high stability and attractive explosive properties,^[14] our goal was the preparation of the

corresponding nitrimino-compound as the introduction of this group is known to better the performance characteristics.

9.2 Results and Discussion

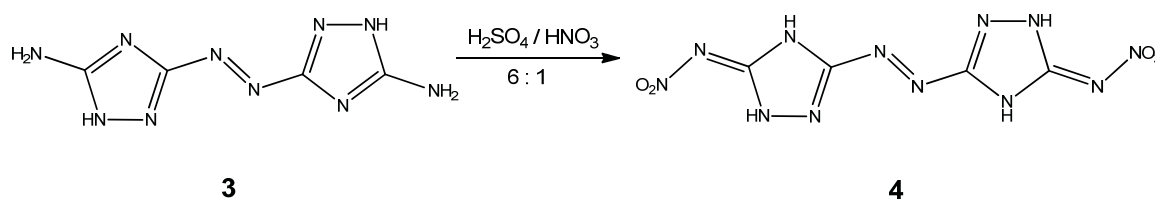
9.2.1 Synthesis

The starting material used for nitration, 5,5'-diamino-3,3'-azo-1*H*-1,2,4-triazole (**3**), is not yet known in literature, since it is not accessible using 3,5-diamino-1*H*-1,2,4-triazole as a starting material. The formation of the azo-bridge apparently only works with a unique amino group in the molecule, which necessitates the protection of one amino group first. The acetyl protecting group is suitable due to the fact that it is stable even in concentrated acids/bases at room temperature and the amine is not deprotected until using elevated temperatures. Theoretically, acylation of 3,5-diamino-1*H*-1,2,4-triazole can proceed both at the heterocyclic nitrogen atoms and at the two amino groups.^[15] The treatment of 3,5-diamino-1*H*-1,2,4-triazole with acetic anhydride in water provides 1-acetyl-diaminotriazole (**1**) in yields of about 98 %. The desired 5-acetylaminotriazole (**2**) is obtained in nearly quantitative yields via thermal isomerization by heating a suspension of **1** in decaline (Scheme 3) as it is described by Pevzner *et al.*^[16]



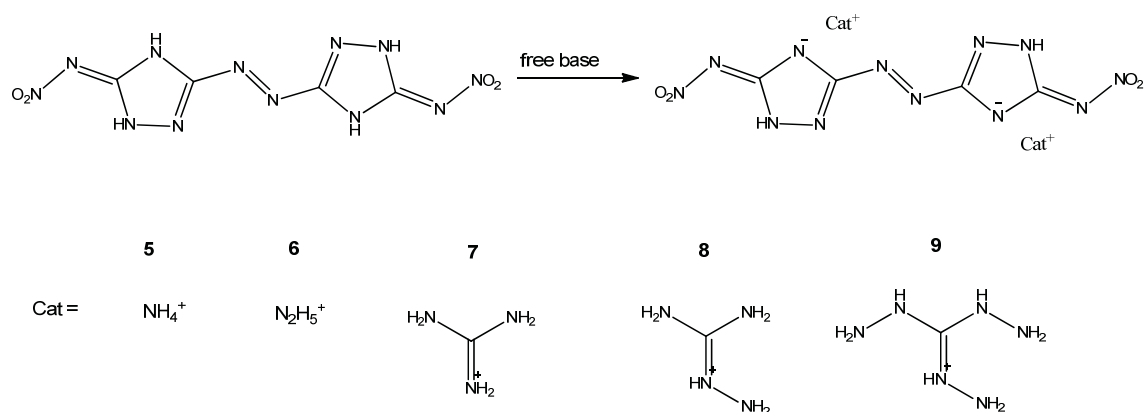
Scheme 3: Reaction pathway towards 5,5'-amino-3,3'-azo-1*H*-1,2,4-triazole starting from 3,5-diamino-1*H*-1,2,4-triazole.

As shown in Scheme 3, the synthesis of 5,5'-diamino-3,3'-azo-1*H*-1,2,4-triazole (**3**) (DAAT) was performed with a stoichiometric amount of potassium permanganate which was added at 0 °C. After removal of the ice bath, the mixture was allowed to warm to room temperature. Subsequent heating to 100 °C for 3 hours completes the formation of the azo-bridge, transforms the remaining permanganate to manganese(IV)-oxide and leads to a complete deprotection of both amine groups. After the removal of the generated manganese oxide by filtration, acidifying the solution to pH 7 leads to the precipitation of compound **3** as an orange solid. Drying at 110 °C over night provides DAAT as elemental analysis pure orange powder. The synthesis of the novel 5,5'-dinitrimino-3,3'-azo-1*H*-1,2,4-triazole (**4**) was accomplished in good yields via nitration of 5,5'-diamino-3,3'-azo-1*H*-1,2,4-triazole (**3**) as it is described for 3-amino-1*H*-1,2,4-triazole by Licht *et. al*^[17] using a volume ratio H₂SO₄/HNO₃ of 6 : 1 and two equivalents of nitric acid per amino group (Scheme 4).



Scheme 4: Synthesis of 5,5'-dinitrimino-3,3'-azo-1*H*-1,2,4-triazole (**4**) via nitration of **3**.

DNAAT immediately precipitates as a yellow solid while pouring the nitration mixture on ice and can easily be isolated by filtration. After drying at 60 °C, the desired elemental analysis pure nitrimino compound (**4**) was obtained in yields of about 80%. The synthesis of the nitrogen-rich salts (**5–9**) was accomplished as shown in Scheme 5 by adding two equivalents of an organic base (ammonia, hydrazine, guanidine, aminoguanidine, triaminoguanidine) to a suspension of the neutral compound in water.



Scheme 5: Synthesis of nitrogen-rich salts (5 – 9) of DNAAT.

The energetic salts of the di-anion DNAAT²⁻ were obtained in good yields as yellow powder while storing the mixture at 5 °C over night. All energetic compounds were fully characterized by IR and Raman as well as multinuclear NMR spectroscopy, mass spectrometry and differential scanning calorimetry. Selected compounds were additionally characterized by low temperature single crystal X-ray spectroscopy.

9.2.2 NMR Spectroscopy

Due to the low solubility of compounds **2** and **3** in common NMR-solvents (but good solubility in bases), NMR spectroscopy was performed in D₂O adding a stoichiometric amount of sodium hydroxide. The NMR signals given in Table 1 correspond to the sodium salts of **2a** and **3a** and present as well the neutral compounds **1** and **2** in [d₆]-DMSO.

Table 1: NMR signals of compounds **1**, **2**, **2a** and **3a**.

compound	¹ H NMR	¹³ C{ ¹ H} NMR			
	CH ₃	C=O	C-NH ₂	C-NHAc ^(a)	CH ₃
1	2.33	170.5	162.2, 157.0		23.6
2	1.99	169.8	161.6	156.4	22.9
2a	2.03	174.1	162.5	154.1	22.7
3a	–	–	165.0	170.0	–

(a) C-azo in the case of **3a**

In the case of compound **2** (**2a**), two different NMR signals for the triazole carbon atoms could be obtained due to the rearrangement of the acetyl protecting group. The NMR signals of the two carbon atoms of compound **3a** can be found at 170.0 and 165.0 in the ^{13}C NMR spectra. The signals of the acetyl protecting group at 2.03 (^1H NMR) and 22.7 (^{13}C NMR) could not be obtained anymore, indicating full deprotection of the amine groups. The signals in the NMR spectra for compounds **4–9** were recorded in $[\text{d}_6]\text{-DMSO}$ and are compiled in Table 2. The neutral compound (**4**) shows two signals for the different carbon atoms at 159.7 and 153.8 ppm, the nitrimino group is visible at -19 ppm in the ^{14}N NMR-spectra. As expected in the case of compounds **5–9**, all NMR signals are nearly identical. The single proton localized at the triazole ring appears at chemical shifts between 13.5–13.6 ppm in the ^1H NMR spectra, while the signals of the two triazole carbon atoms can be found in the range between 166.9–167.7 ppm and 157.7–158.3 ppm. The nitrimino group is identified by a broad signal at around -15 ppm in the ^{14}N NMR spectra.

Table 2: NMR signals of compounds **4–9**.

compound	DNAAT ²⁻			cation	
	^1H	$^{13}\text{C}\{^1\text{H}\}$	$^{14}\text{N}\{^1\text{H}\}$	^1H	$^{14}\text{N}\{^1\text{H}\}$
4	/	159.7, 153.8	-19	/	/
5	13.58	167.7, 158.3	-14	7.23	-359
6	13.51	166.9, 157.8	-16	7.28	-359
					$^{13}\text{C}\{^1\text{H}\}$
7	13.53	167.1, 157.9	-14	7.03	157.7
8	13.61	167.0, 157.7	-15	7.89, 4.71	158.9
9	13.48	167.3, 157.8	-14	8.59, 4.49	159.0

9.2.3 Vibrational Spectroscopy

The isomerization reaction can easily be monitored by IR spectroscopy and is indicated by the shift of the C=O band from 1709 cm^{-1} (**1**) to 1683 cm^{-1} (**2**).

The complete deprotection of the amine groups during the synthesis of **3** can easily be monitored by the missing C=O vibration band at around 1700 cm^{-1} as well as the missing C-H valence vibrations at $2800\text{--}3100\text{ cm}^{-1}$ in the IR and Raman spectra. The latter is

dominated by the absorption of the azo-moiety at 1348 cm^{-1} ,^[7c, 18] the infrared spectrum by the deformation mode of the amino groups at 1624 cm^{-1} .

The Raman spectra of **4** is dominated by the vibration of the azo-moiety at 1436 cm^{-1} , the absorption of the amino groups in the infrared spectrum at 1624 cm^{-1} has disappeared. The N-NO₂ groups result in a strong absorption at $1620\text{--}1560\text{ cm}^{-1}$ ($\nu_{\text{asym}}(\text{NO}_2)$) and $1300\text{--}1240\text{ cm}^{-1}$ ($\nu_{\text{sym}}(\text{NO}_2)$).

The symmetric and N=O valence vibrations of all nitrogen-rich salts (**5–9**) can be found at 1530 cm^{-1} ($\nu_{\text{sym}}(\text{NO}_2)$) and 1335 cm^{-1} ($\nu_{\text{asym}}(\text{NO}_2)$) in the IR spectrum, accompanied by the fundamental frequencies of the triazole ring in the range of $1300\text{--}1500\text{ cm}^{-1}$.^[19] The N-H stretch modes of the amine group of the cations appear in the range of 3350 cm^{-1} to 3100 cm^{-1} and the -NH₂ deformation vibration at $1630\text{--}1680\text{ cm}^{-1}$. The very intense band of the azo-moiety at 1463 cm^{-1} in the Raman spectrum shows only a marginal shift in comparison to the neutral compound (**4**).

9.2.4 Structural Characterization

The single crystal X-ray diffraction data of **4**, **5** and **9** were collected using an Oxford Xcalibur3 diffractometer equipped with a Spellman generator (voltage 50 kV, current 40 mA) and a KappaCCD detector. The data collection was undertaken using the CRYALIS CCD software^[20] while the data reduction was performed with the CRYALIS RED software.^[21] The structures were solved with SIR-92^[22] or SHELXS-97^[23] and refined with SHELXL-97^[24] implemented in the program package WinGX^[25] and finally checked using PLATON.^[26] Further information regarding the crystal-structure determination have been deposited with the Cambridge Crystallographic Data Centre^[27] as supplementary publication Nos. 807480 (**4***DMSO), 807481 (**4***THF), 807482 (**5**) and 807483 (**9**). Crystallographic data and parameters as well as the crystal morphology have been compiled in Table 1.

Table 3: Crystallographic data and parameters.

	4*DMSO	4*THF	5*DMSO	9
Formula	C ₄ H ₄ N ₁₂ O ₄ * 4 DMSO	C ₄ H ₄ N ₁₂ O ₄ * 4 THF	C ₄ H ₁₀ N ₁₄ O ₄ * 2 DMSO	C ₆ H ₂₄ N ₂₄ O ₆
FW [g mol ⁻¹]	596.70	572.6	474.52	528.49
Crystal system	monoclinic	monoclinic	triclinic	monoclinic
Space Group	<i>P2₁/c</i>	<i>P2₁/n</i>	<i>P-1</i>	<i>P2₁/c</i>
Color / Habit	yellow plate	yellow rod	yellow plate	yellow rod
Size [mm]	0.13x0.12x0.03	0.55x0.08x0.05	0.14x0.05x0.05	0.22x0.08x0.02
<i>a</i> [Å]	17.2749(6)	5.9430(6)	7.7810(9)	9.7903(11)
<i>b</i> [Å]	15.8671(8)	15.3647(17)	8.2010(9)	3.6340(5)
<i>c</i> [Å]	9.7594(4)	15.2456(16)	9.0610(10)	29.233(4)
α [°]	90	90	86.453(9)	90
β [°]	100.068(4)	96.237(10)	81.497(9)	96.424(11)
γ [°]	90	90	68.331(10)	90
<i>V</i> [Å ³]	2633.88(19)	1383.9(3)	531.42(10)	1033.5(2)
<i>Z</i>	4	2	1	2
ρ_{calc} [g cm ⁻³]	1.505	1.374	1.483	1.698
μ [mm ⁻¹]	0.422	0.108	0.308	0.145
<i>F</i> (000)	1248	608	248	552
$\lambda_{\text{MoK}\alpha}$ [Å]	0.71073	0.71073	0.71073	0.71073
<i>T</i> [K]	173	173	173	173
<i>R</i> _{int}	0.055	0.045	0.038	0.033
<i>R</i> ₁ , <i>wR</i> ₂ (<i>I</i> > σ <i>I</i> ₀)	0.0386; 0.0440	0.058; 0.143	0.0406; 0.0549	0.0510; 0.1275
<i>R</i> ₁ , <i>wR</i> ₂ (all data)	0.1190; 0.0509	0.132; 0.161	0.0999; 0.0611	0.0881; 0.1381
<i>S</i>	0.663	0.856	0.742	0.899
CCDC	807480	807481	807482	807483

The crystallization of azo-bridged triazole compounds is very difficult due to the completely planar configuration of the molecules and a lack of possibilities for hydrogen bonding. We were finally able to crystallize **4** from DMSO and also THF, but were not able to record a crystal structure of the neutral compound without incorporated solvent molecules. The same problem occurred with the ionic compounds. Only the ammonium salt (**5**) and the triaminoguanidinium salt (**9**) could be crystallized after a number of tries with different solvents and crystallization conditions. While **5** could only be crystallized with incorporated solvent molecules (DMSO), **9** crystallized with two molecules of crystal water per formula unit. Due to this circumstances, the structures of **4*DMSO**, **4*THF** and **5*DMSO** will not be discussed in detail since no results can be drawn from the discussion of the structure, thus only selected parameters and the asymmetric units of the compounds will be presented. The structure of the title compound **9** will be discussed in detail.

The DMSO adduct of 5,5'-dinitrimino-3,3'-azo-1*H*-1,2,4-triazole (**4**) crystallizes in the monoclinic space group *P2₁/c* with 4 molecular moieties in the unit cell, while the THF

adduct crystallizes in the monoclinic spacegroup $P2_1/n$ with only two molecular moieties in the unit cell. Pycnometer measurements of **4** stated a density of 1.85 g cm^{-3} , while the densities derived from the crystallographic measurements are very low with 1.505 g cm^{-3} for **4***DMSO and 1.374 g cm^{-3} for **4***THF, respectively, owed to the solvent incorporation. The asymmetric units for both adducts are displayed in Figure 1 and Figure 2 together with the numbering scheme and selected bond distances and angles.

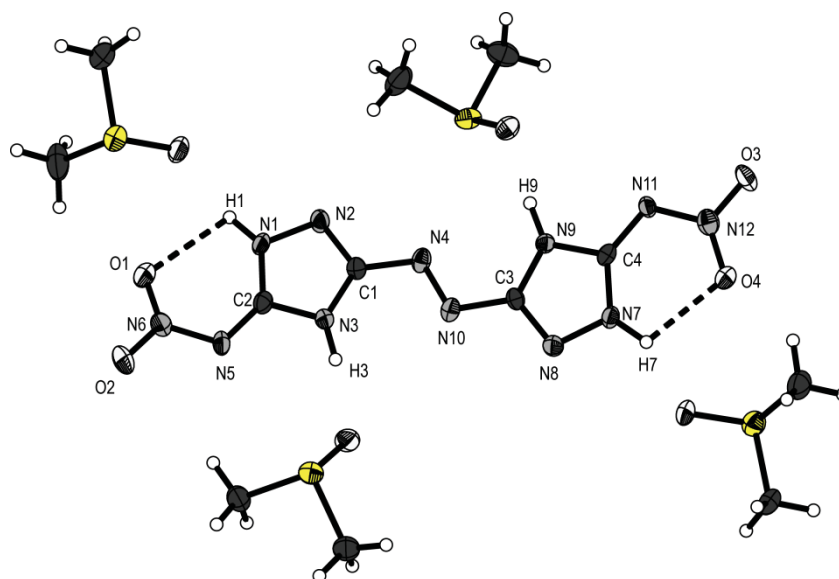


Figure 1: Molecular moiety of **4***DMSO. Thermal ellipsoids represent the 50% probability level. Selected bond lengths (Å): O1–N6 1.243(3), O2–N6 1.242(3), N1–C2 1.340(3), N1–N2 1.370(3), N1–H1 0.90(2), N2–C1 1.307(3), N3–C2 1.352(3), N3–C1 1.355(3), N3–H3 0.913(16), N4–N10 1.280(3), N4–C1 1.397(3), N5–C2 1.341(3), N5–N6 1.343(3); selected bond angles (°): C2–N1–N2 111.9(2), C2–N1–H1 132.8(16), N2–N1–H1 115.2(16), C1–N2–N1 103.1(2), C2–N3–C1 106.3(2), C2–N3–H3 119.7(15), C1–N3–H3 133.8(16), N10–N4–C1 111.8(2), C2–N5–N6 115.7(2), O2–N6–O1 122.0(2), O2–N6–N5 115.7(3), O1–N6–N5 122.3(3), C4–N7–N8 112.46(19), C4–N7–H7 128.8(15), N2–C1–N3 112.9(2), N2–C1–N4 119.3(3), N3–C1–N4 127.4(2), N1–C2–N5 135.9(2), N1–C2–N3 105.8(2), N5–C2–N3 118.2(3).

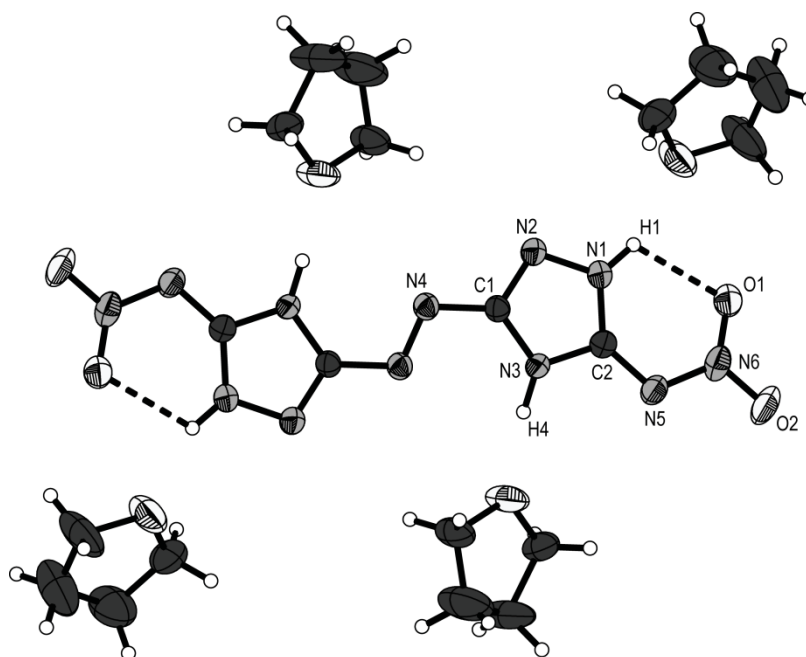


Figure 2: Molecular moiety of **4*THF**. Thermal ellipsoids represent the 50% probability level. Selected bond lengths (Å): C4–C3 1.406(5), C4–C5 1.424(6), N6–O1 1.244(3), N1–C2 1.356(4), N1–N2 1.368(3), N1–H1 0.88(3), N2–C1 1.308(3), N5–C2 1.339(4), N5–N6 1.356(3), N4–N4 1.272(4), N4–C1 1.392(3), N3–C2 1.346(3), N3–C1 1.368(4), N3–H4 0.94(3), N6–O2 1.239(3); selected bond angles (°): C2–N1–N2 111.8(3), C2–N1–H1 129(2), N2–N1–H1 119(2), C1–N2–N1 103.6(2), C2–N5–N6 115.6(3), N4–N4–C1 112.2(3), C2–N3–C1 106.8(2), C2–N3–H4 125(2), C1–N3–H4 128(2), O2–N6–O1 121.5(3), O2–N6–N5 116.0(3), O1–N6–N5 122.4(2), N5–C2–N3 119.8(3), N5–C2–N1 134.8(3), N3–C2–N1 105.5(3), N2–C1–N3 112.3(2), N2–C1–N4 120.8(2), N3–C1–N4 127.0(2).

The DNAAT molecule is nearly planar in both structures, indicating the presence of a delocalized π -electron system, as anticipated for these compounds. Bond lengths and angles are also as expected for this kind of compounds.^[28] The bond length of the azo moiety is in the same range as for the azotetrazole compounds investigated by Hammerl^[7c, 29] while the nitraminogroups also exhibit regular geometrical parameters. The interesting aspect of both structures is the presence of moderately strong intramolecular hydrogen bonds. N1 and N7 are utilized as donor atoms with O1 and O4 function as acceptor atoms respectively for **4*DMSO**, while N1 and O1 build up the hydrogen bond for **4*THF**. Even though, the D–H \cdots A angles are pretty small with 102.15(16) $^\circ$ (N1–H1 \cdots O1, **4*DMSO**), 105.8(1) $^\circ$ (N7–H7 \cdots O4, **4*DMSO**) and 108.21(23) $^\circ$ (N1–H1 \cdots O1, **4*THF**), the D–A distances are very small, ranging between 2.587(1) Å (N1–O1, **4*THF**) and 2.606(4) Å (N1–O1, **4*DMSO**). The hydrogen bonds are considered to be of electrostatic nature rather than being directed.^[30] The build up of a six membered ring between the nitrimino group and the triazole ring, is making the backbone of the molecule more stable, which is also indicated by the very high thermal

stabilities, unusual for this class of compounds. In addition the hydrogen atom can only be deprotonated with the use of earth alkaline bases, not with the bases used to form the di-anion. Further, the incorporated solvent molecules take their space due to the formation of hydrogen bonds with each of the four N–H hydrogen atoms. Thus both structures show the mutual number of solvent molecules surrounding each DNAAT molecule.

Bis(ammonium) 5,5'-dinitrimino-3,3'-azo-1*H*-1,2,4-triazolate (**5***DMSO) crystallizes in the triclinic space group *P*-1, formally with only one molecular moiety occupying the unit cell. The density is as expected very low with only 1.483 g cm⁻³ due to the formation of the DMSO adduct. One molecular moiety together with selected bond length and angles is presented in Figure 3.

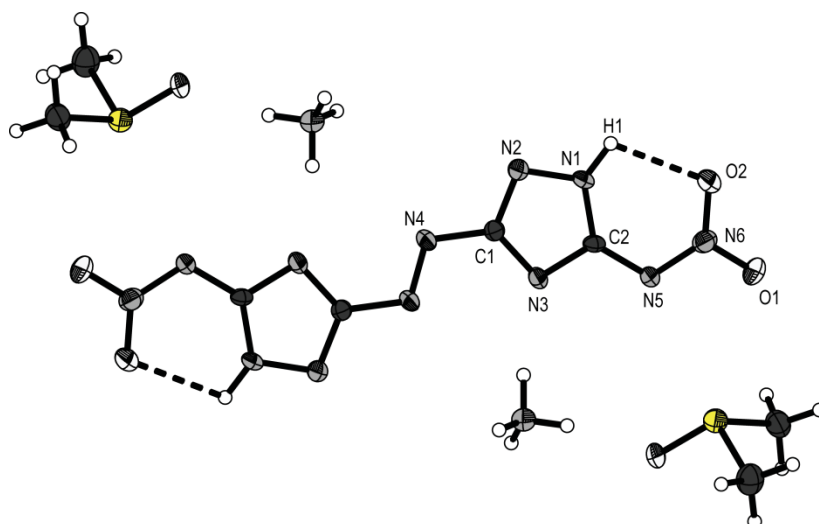


Figure 3: Molecular moiety of **5**. Thermal ellipsoids represent the 50% probability level. Selected bond lengths (Å): O1–N6 1.270(2), O2–N6 1.260(2), N1–C2 1.345(3), N1–N2 1.368(2), N1–H1 0.917(15), N2–C1 1.327(3), N3–C2 1.335(3), N3–C1 1.356(3), N4–N4 1.278(3), N4–C1 1.413(3), N5–N6 1.322(2), N5–C2 1.381(3); selected bond angles (°): C2–N1–N2 110.46(19), C2–N1–H1 133.0(14), N2–N1–H1 116.5(14), C1–N2–N1 101.00(19), C2–N3–C1 102.0(2), N4–N4–C1 112.0(2), N6–N5–C2 116.8(2), O2–N6–O1 120.4(2), O2–N6–N5 123.6(2), O1–N6–N5 116.1(2), N2–C1–N3 116.5(2), N2–C1–N4 117.4(2), N3–C1–N4 126.2(2), N3–C2–N1 110.1(2), N3–C2–N5 117.9(2), N1–C2–N5 132.0(2).

The di-anion is completely planar within the ionic structures with only very slight deviations. The N1–H1···O2 hydrogen bond builds up the six membered ring again, as seen for the neutral compound, keeping the nitriminogroup perfectly in plane with the triazole ring. Since the thermal decomposition temperature differs only by 3 °C when compared with **4** (209 °C (**4**) compared to 212 °C (**5**)) the formation of this stable configuration seems to have an very important impact on the stability of these

compounds. The structure itself is build up from four moderately stable hydrogen bonds, all four of them involving the ammonium cation. An illustration of the surrounding of one ammonium cation is presented in Figure 4, while the parameters of the hydrogen bonds are compiled in Table 4.

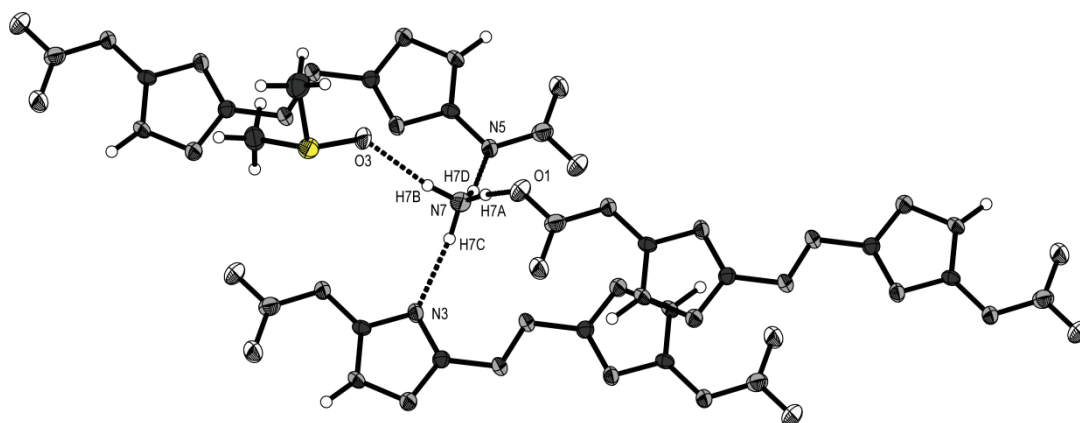


Figure 4: Chemical surrounding of the ammonium cation in **5**, displaying the hydrogen bonds. Thermal ellipsoids represent the 50% probability level.

Table 4: Hydrogen bonds present in the crystal structure of **5**. Since the N–H bonds of the ammonium ion had to be set as restraint, no standard deviation is presented.

D–H···A	Dist D–H [Å]	Dist. H···A [Å]	Dist. D···A [Å]	< D–H···A [°]
N1 – H1···O3 ⁱ	0.917(15)	1.937(18)	2.786(3)	153.0(19)
N7 – H7a···O1 ⁱⁱ	0.96	2.00	2.929(2)	163.8
N7 – H7b···O3	0.92	1.91	2.811(2)	167.1
N7 – H7c···N3	0.92	1.98	2.872(3)	164.3
N7 – H7d···N5 ⁱⁱⁱ	0.93	2.05	2.951(3)	164.8

Symmetry operators: (i) $x, y-1, z$; (ii) $x+1, y, z$; (iii) $-x+1, -y+1, -z$.

The dihydrate of the bis(triaminoguanidinium) 5,5'-dinitrimino-3,3'-azo-1*H*-1,2,4-triazolate (**9**) crystallizes in the monoclinic space group $P2_1/c$ with two formula units in the unit cell. The density is in the same range as other guanidinium salts of nitrimino-compounds with 1.698 g cm^{-3} . The density is also in good agreement with the experimentally determined density of the anhydrous compound being 1.72 g cm^{-3} (pycnometer measurement). The molecular moiety of **9**, as well as the numbering scheme and selected bond lengths and angles are presented in Figure 5.

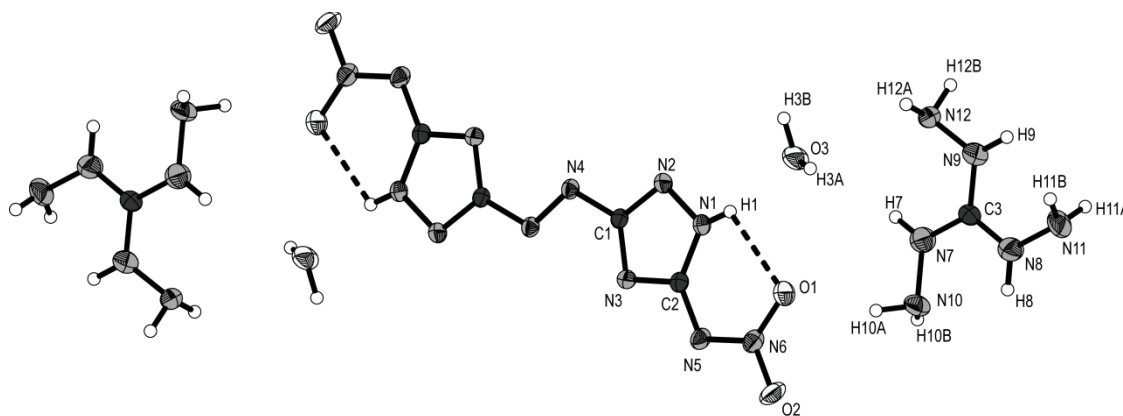


Figure 5: Molecular moiety of **9**. Thermal ellipsoids represent the 50% probability level. Selected bond lengths (Å): O1–N6 1.264(3), O2–N6 1.255(3), N1–N2 1.351(3), N1–C2 1.354(3), N1–H1 0.77(3), N2–C1 1.323(3), N3–C2 1.336(3), N3–C1 1.344(3), N4–N4 1.277(4), N4–C1 1.407(3), N5–N6 1.310(3), N5–C2 1.368(3), N7–C3 1.313(3), N7–N10 1.431(3), N8–C3 1.316(4), N8–N11 1.406(3), N9–C3 1.331(4), N9–N12 1.419(3); selected bond angles (°): N2–N1–C2 110.2(2), N2–N1–H1 116(3), C2–N1–H1 134(3), C1–N2–N1 101.8(2), C2–N3–C1 102.5(2), N4–N4–C1 111.9(3), N6–N5–C2 117.7(2), O2–N6–O1 120.8(2), O2–N6–N5 116.9(2), O1–N6–N5 122.2(2), N2–C1–N3 116.2(2), N2–C1–N4 116.7(2), N3–C1–N4 127.1(2), N3–C2–N1 109.4(2), N3–C2–N5 118.2(2), N1–C2–N5 132.4(2), C3–N7–N10 118.3(2), C3–N8–N11 121.9(3), C3–N9–N12 119.0(2).

As seen in the structure of **5**, the DNAAT²⁻ anion is completely planar. The structural motive of two six membered rings, stabilizing the nitrimino groups is also evident in this structure. The donor acceptor distance is in the same range as for **4** and **5** with 2.579(9) Å and with the D–H···A angle of 106.22(31)° of strong electrostatic nature. The complete structure is build up by a strong hydrogen network including 15 non-equivalent hydrogen bonds. All hydrogen bonds are compiled in Table 5 below.

Table 5: Hydrogen bonds present in the crystal structure of **9**. H7, H8 and H9 had to be set restraint, thus no standard deviations are given for the D–H and H–A distances as well as for the D–H–A angles.

Atoms D–H···A	Dist. D–H [Å]	Dist. H···A [Å]	Dist. D···A [Å]	< D–H···A [°]
N1 – H1···O1	0.770(4)	2.256(37)	2.579(9)	106.2(9)
N1 – H1···O3	0.77(3)	1.98(4)	2.733(3)	165(4)
N7 – H7···O1 ⁱ	0.88	2.34	2.995(3)	130.9
N8 – H8···O2 ⁱⁱ	0.88	2.18	2.954(3)	146.3
N9 – H9···N5 ⁱⁱⁱ	0.88	2.37	3.186(3)	153.7
N10 – H10a···O1	0.96(4)	2.14(4)	3.075(4)	163(3)
N10 – H10b···N10 ⁱⁱ	0.83(4)	2.52(4)	3.198(4)	140(3)
N10 – H10b···O2 ⁱ	0.83(4)	2.57(4)	3.126(3)	125(3)
N11 – H11a···N11 ^{iv}	0.827(19)	2.63(3)	3.142(5)	121(3)
N11 – H11a···O2 ⁱⁱⁱ	0.827(19)	2.54(3)	3.147(3)	131(3)
N11 – H11b···N5 ^v	0.82(4)	2.37(4)	3.176(4)	168(3)
N12 – H12a···N4 ^{vi}	0.82(4)	2.46(4)	3.189(3)	148(3)
N12 – H12b···N3 ⁱⁱⁱ	0.87(4)	2.20(4)	3.000(3)	154(3)
N12 – H12···O3	0.82(4)	2.71(3)	3.197(9)	119.6(3)
O3 – H3a···N12 ^{vii}	0.73(4)	2.31(4)	3.000(3)	159(4)
O3 – H3b···N2 ^{vi}	0.91(4)	2.04(4)	2.922(3)	163(4)

Symmetry operators: (i) $x, y+1, z$; (ii) $-x+1, y+1/2, -z+1/2$; (iii) $x-1, y+1, z$; (iv) $-x, y+1/2, -z+1/2$; (v) $x-1, y, z$; (vi) $-x+1, -y+1, -z$; (vii) $x, y-1, z$.

The structure consists of coplanar bands, build up from DNAAT²⁻ anions, water molecules and triaminoguanidinium cations located approximately 1 Å below and above the layer spanned up by DNAAT²⁻ anions. The water molecules are located between the DNAAT²⁻ molecules forming strong and directed hydrogen bonds with the triazole rings, namely N1–H1···O3 and O3–H3b···N2^{vi}. These hydrogen bonds are well below the sum of van der Waals radii ($r_w(\text{N}) + r_w(\text{O}) = 3.10 \text{ \AA}$).^[31] The third hydrogen bond is formed by the water molecule as donor, while N12^{vii} functions as the donor. Again, the D–A distance is much shorter than the sum of van der Waals radii and the D–H···A angle is 159° which again indicates a rather directed than only electrostatic interaction. The only weak hydrogen bond build up by the H₂O is N12–H12a···O3, with a donor acceptor distance of 3.197(9) Å and therefore longer than the sum of van der Waals radii and an D–H···A angle of only 119.6(3)°. All other hydrogen bonds formed are using the nitrogen atoms of the triaminoguanidinium cation as donor atoms. The two hydrogen bonds utilizing nitrogen atoms of the DNAAT²⁻ anion as acceptors all show D···A distances smaller than the sum of van der Waals radii ($r_w(\text{N}) + r_w(\text{N}) = 3.2 \text{ \AA}$) at 3.186 Å (N9 –

H9 \cdots N5ⁱⁱⁱ) and 3.000 Å (O3 – H3a \cdots N12^{vii}), respectively. The corresponding D–H \cdots A angles (around 150°) indicate the bonds being moderately strong but mostly of electrostatic nature. The three hydrogen bonds using oxygen atoms as acceptors are moderately strong with D \cdots A distances between 2.954 and 3.147 Å and with D–H \cdots A angles between 125° and 131° they are rather of electrostatic nature. The complete hydrogen bonding scheme within the bands is presented in Figure 6.

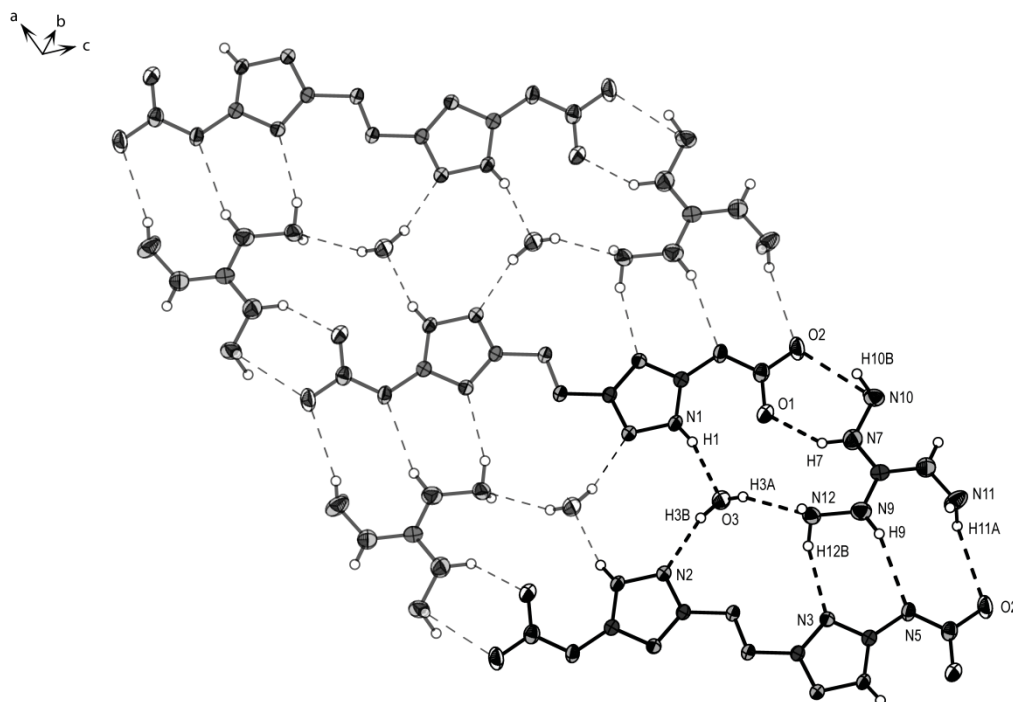


Figure 6: Hydrogen bonding scheme within the band structures of **9**. Thermal ellipsoids represent the 50% probability level.

The distance between the bands is 3.280 Å, while they are stacked along the *b*-axis. The bands are connected via hydrogen bonds formed between the triaminoguanidinium cations and interactions from the triaminoguanidinium cation with the nitramino groups, to form zig-zag layers presenting an angle of 133.99° between the individual bands. The hydrogen bonds involved are namely N11–H11a \cdots N11^{iv} and N10–H10b \cdots N10ⁱⁱ, only involving the triaminoguanidinium cations, while N8–H8 \cdots O2ⁱⁱ presents the interaction between the NH group of the triaminoguanidinium cation in one layer with the nitriminogroup of the DNAAT²⁻ anion in the tilted layer. The layer scheme of the structure is displayed in Figure 7 along the along the *a*-axis.

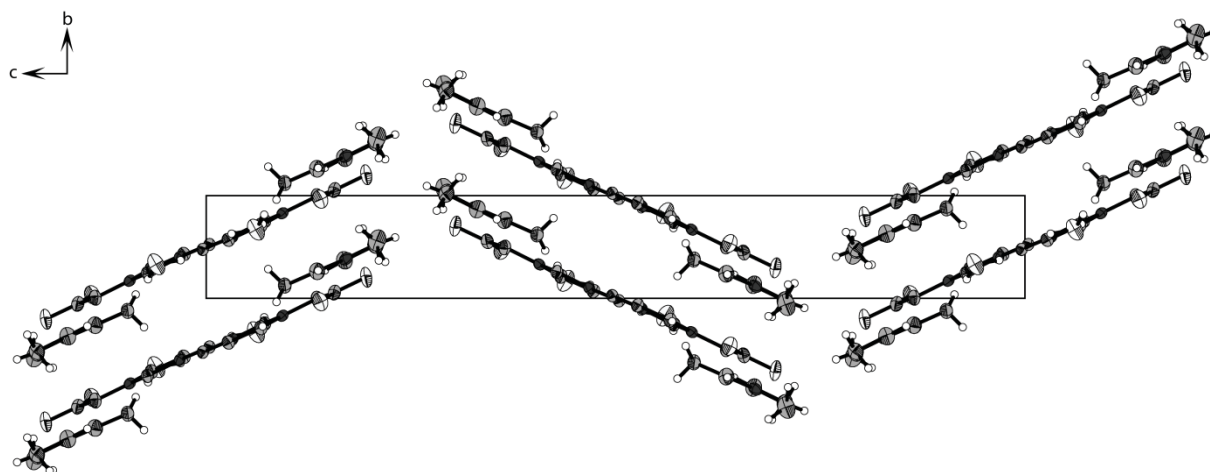


Figure 7: Layer structure of **9**, showing the connectivity of the individual bands along the a-axis. Thermal ellipsoids represent the 50% probability level.

The angle between the bands is due to the connectivity over hydrogen bonds formed by the triaminoguanidinium cations. The $\text{N10-H10b}\cdots\text{N10}^{\text{ii}}$ and $\text{N11-H11a}\cdots\text{N11}^{\text{iv}}$ hydrogen bonds are rather long with $\text{D}\cdots\text{A}$ distances of 3.142 and 3.198 Å, respectively, but shorter than the sum of van der Waals radii. $\text{D-H}\cdots\text{A}$ angles of only 121° and 140° , respectively, indicate mostly electrostatic interactions. Since the donor atoms are the two amine groups, the angle between the bands is given. The third band connecting hydrogen bond $\text{N8-H8}\cdots\text{O2}^{\text{ii}}$ is short rather short with a $\text{D}\cdots\text{A}$ distance of 2.954 Å. The bond is mainly of electrostatic nature, but also directed with a $\text{D-H}\cdots\text{A}$ angle of 146.43° . The surrounding of one triaminoguanidinium cation is displayed in Figure 8, presenting the complete three dimensional hydrogen bonding network. Three moderately strong hydrogen bonds connect the bands towards the next layer, namely $\text{N11-H11b}\cdots\text{N5}^{\text{v}}$, $\text{N12-H12a}\cdots\text{N4}^{\text{vi}}$ and $\text{N10-H10a}\cdots\text{O1}$.

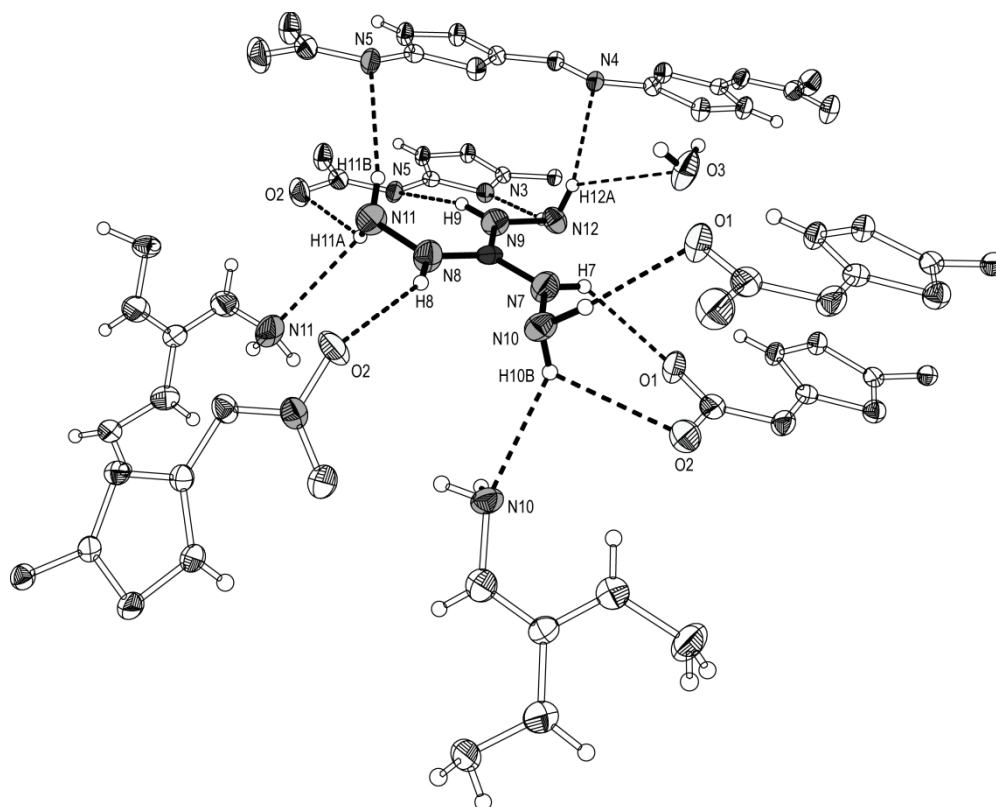


Figure 8: Surrounding of one triaminoguanidinium cation in **9**, showing the connectivity of the structural motive. Non participating atoms are set transparent, molecules are partially omitted for better clarity. Thermal ellipsoids represent the 50% probability level.

9.2.5 Theoretical Calculations

Due to the highly energetic character of **4–9**, bomb calorimetric measurements could only be performed with small amounts, consequently doubtful combustion energies were obtained. Therefore an extensive computational study was accomplished for **4–9**, which is presented in the following section. All calculations were carried out using the Gaussian G03W (revision B.03) program package.^[32] The enthalpies (H) and free energies (G) were calculated using the complete basis set (CBS) method of Petersson and coworkers in order to obtain very accurate energies. The CBS models use the known asymptotic convergence of pair natural orbital expressions to extrapolate from calculations using a finite basis set to the estimated complete basis set limit. CBS-4 begins with a HF/3-21G(d) geometry optimization; the zero point energy is computed at the same level. It then uses a large basis set SCF calculation as a base energy, and a MP2/6-31+G calculation with a CBS extrapolation to correct the energy through second order. A

MP4(SDQ)/6-31+(d,p) calculation is used to approximate higher order contributions. In this study we applied the modified CBS-4M method (**M** referring to the use of Minimal Population localization) which is a re-parametrized version of the original CBS-4 method and also includes some additional empirical corrections.^[33] The enthalpies of the gas-phase species **M** were computed according to the atomization energy method (eq. 1) (Tables 6–8).^[34]

$$\Delta_f H^\circ(\text{g, M, 298}) = H_{(\text{Molecule, 298})} - \sum H^\circ_{(\text{Atoms, 298})} + \sum \Delta_f H^\circ_{(\text{Atoms, 298})} \quad (1)$$

Table 6: Results obtained from theoretical calculations at the CBS-4M level of theory.

	point group	$-H^{298}$ / a.u.	<i>NIMAG</i>
DNAAT	C_1	1111.064789	0
DNAAT²⁻	C_s	1110.009835	0
A⁺	T_d	56.796608	0
Hy⁺	C_s	112.030523	0
G⁺	C_1	205.453192	0
AG⁺	C_1	260.701802	0
TAG⁺	C_3	371.197775	0
H		0.500991	0
C		37.786156	0
N		54.522462	0
O		74.991202	0
Cl		459.674576	0

Table 7: Literature values for atomic $\Delta_f H^\circ_{298}$ / kcal mol⁻¹

	NIST ^[35]
H	52.1
C	171.3
N	113.0
O	59.6
Cl	29.0

Table 8: Enthalpies of the gas-phase species **M**.

M	M	$\Delta_f H^\circ(\text{g,M})$ / kcal mol ⁻¹
DNAAT	C ₄ H ₄ N ₁₂ O ₄	743.6
DNAAT²⁻	C ₄ H ₂ N ₁₂ O ₄ ²⁻	446.5
A	NH ₄ ⁺	151.9
Hy	N ₂ H ₅ ⁺	184.9
G	CH ₆ N ₃ ⁺	136.6
AG	CH ₇ N ₄ ⁺	160.4
DAG	CH ₈ N ₅ ⁺	184.5
TAG	CH ₇ N ₄ ⁺	208.8

The solid state energy of formation (Table 10) of **DNAAT** was calculated by subtracting the gas-phase enthalpy with the heat of sublimation ($22.5 \text{ kcal mol}^{-1}$) obtained by the TROUTON'S rule ($\Delta H_{\text{sub}} = 188 \cdot T_m$) ($T_m=204 \text{ }^\circ\text{C}$).^[36] In the case of the salts, the lattice energy (U_L) and lattice enthalpy (ΔH_L) were calculated from the corresponding molecular volumes (Table 9) according to the equations provided by Jenkins *et al.*^[37] With the calculated lattice enthalpy (Table 9) the gas-phase enthalpy of formation (Table 8) was converted into the solid state (standard conditions) enthalpy of formation. These molar standard enthalpies of formation (ΔH_m) were used to calculate the molar solid state energies of formation (ΔU_m) according to equation 2 (Table 7).

$$\Delta U_m = \Delta H_m - \Delta n RT \quad (2)$$

(Δn being the change of moles of gaseous components)

Table 9: Lattice energies and lattice enthalpies.

	V_M / nm^3	$U_L / \text{kJ mol}^{-1}$	$\Delta H_L / \text{kJ mol}^{-1}$	$\Delta H_L / \text{kcal mol}^{-1}$
(NH₄)₂DNAAT (5)	298	1306.1	1317.0	314.5
(N₂H₅)₂DNAAT (6)	312	1283.5	1294.4	309.2
(G)₂DNAAT (7)	388	1181.0	1191.9	284.7
(AG)₂DNAAT (8)	464	1102.3	1113.2	265.9
(TAG)₂DNAAT (9)	472	1095.0	1105.9	264.1

Table 10: Solid state energies of formation ($\Delta_f U^\circ$)

	$\Delta_f H^\circ(\text{s}) / \text{kcal mol}^{-1}$	$\Delta_f H^\circ(\text{s}) / \text{kJ mol}^{-1}$	Δn	$\Delta_f U^\circ(\text{s}) / \text{kJ mol}^{-1}$	$M / \text{g mol}^{-1}$	$\Delta_f U^\circ(\text{s}) / \text{kJ kg}^{-1}$
DNAAT (4)	154.7	647.7	10	672.5	248.2	2366.3
(NH₄)₂DNAAT (5)	95.8	401.2	14	435.9	318.3	1369.6
(N₂H₅)₂DNAAT (6)	167.3	700.4	16	740.1	348.32	2124.6
(G)₂DNAAT (7)	95.2	398.4	18	443.0	402.4	1101.0
(AG)₂DNAAT (8)	161.6	676.5	20	726.1	432.42	1679.2
(TAG)₂DNAAT (9)	260.1	1089.2	24	1148.7	492.50	2332.3

9.2.6 Detonation Parameters and Thermal Properties

The calculation of the detonation parameters was performed with the program package EXPLO5 (version 5.03 and 5.04).^[38] The program is based on the chemical equilibrium, steady-state model of detonation. It uses the Becker-Kistiakowsky-Wilson's equation of state (BKW EOS) for gaseous detonation products and Cowan-Fickett's equation of state

for solid carbon. The calculation of the equilibrium composition of the detonation products is done by applying modified White, Johnson and Dantzig's free energy minimization technique. The program is designed to enable the calculation of detonation parameters at the CJ point. The BKW equation in the following form was used with the BKWN set of parameters (α , β , κ , θ) as stated below the equations and X_i being the mol fraction of i -th gaseous product, k_i is the molar covolume of the i -th gaseous product^[39]:

$$pV/RT = 1 + xe^{\beta x} \qquad x = (\kappa \sum X_i k_i) / [V(T + \theta)]^\alpha$$

$$\alpha = 0.5, \beta = 0.176, \kappa = 14.71, \theta = 6620. \quad (5.03)$$

$$\alpha = 0.5, \beta = 0.096, \kappa = 17.56, \theta = 4950. \quad (5.04)$$

The detonation parameters calculated with the EXPLO5 versions V5.03 and V5.04 using the experimentally determined densities (X-ray) are summarized in Table 11.

The neutral compound **4** already shows a remarkably high thermal stability of 209 °C, but a quite high sensitivity towards friction and impact. Since salts of energetic compound tend to be more stable as the neutral compound, the nitrogen-rich salts of DNAAT are expected to show an improved stability. The decomposition temperatures of the compounds **5–9** are in the range of the neutral compound, those of the ammonium and guanidium as well as the triaminoguanidinium salt are even higher and appear in the range from 212 °C up to 261 °C. The ammonium and the hydrazinium salts show two decomposition points in the DSC with the first decomposition starting at 212 °C and 154 °C, respectively. As expected, the sensitivity values of all nitrogen-rich salts are considerably higher in comparison to the neutral compound. Nearly all compounds are insensitive towards friction, impact and electrostatic discharge, only the hydrazinium salt is slightly sensitive towards impact (10 J) and the triaminoguanidinium salt towards friction (160 N).

Table 11: Physico-chemical properties of **4 – 9** in comparison with hexogen (**RDX**).

	DNAAT (4)	(NH₄)₂ DNAAT (5)	(N₂H₅)₂ DNAAT (6)	(G)₂ DNAAT (7)	(AG)₂ DNAAT (8)	(TAG)₂ DNAAT (9)	RDX*
Formula	C ₄ H ₄ N ₁₂ O ₄	C ₄ H ₁₀ N ₁₄ O ₄	C ₄ H ₁₂ N ₁₆ O ₄	C ₆ H ₁₄ N ₁₈ O ₄	C ₆ H ₁₆ N ₂₀ O ₄	C ₆ H ₂₀ N ₂₄ O ₄	C ₃ H ₆ N ₆ O ₇
Molecular Mass [g mol ⁻¹]	284.16	318.21	348.12	402.14	432.17	492.38	222.12
Impact sensitivity [J] ^a	2	> 40	10	> 40	> 40	> 40	7
Friction sensitivity [N] ^b	20	> 360	> 360	> 360	> 360	160	120
ESD–test [J]	0.1	0.15	0.05	0.35	0.2	0.2	--
<i>N</i> [%] ^c	59.15	61.62	64.35	62.67	64.80	68.27	37.8
<i>Ω</i> [%] ^d		-45.25	-45.94	-59.65	-59.21	-58.48	-21.6
<i>T</i> _{dec.} [°C] ^e	209	212, 257	154, 228	261	177	219	
<i>ρ</i> [g cm ⁻³] ^f	1.85	1.70	1.70	1.70	1.70	1.70	1.80
$\Delta_f H_m^\circ$ [kJ mol ⁻¹] ^g	647.7	401.2	700.4	398.4	676.5	1089.2	70
$\Delta_f U^\circ$ [kJ kg ⁻¹] ^h	2366.3	1369.6	2124.6	1101.0	1679.2	2332.3	417
EXPLO5 values: V5.03 (V5.04)							
$-\Delta_E U^\circ$ [kJ kg ⁻¹] ⁱ	5268 (5339)	4473 (4461)	5055 (5026)	3731 (3690)	4202 (4147)	4681 (4602)	6038 (6125)
<i>T</i> _E [K] ^j	4237 (4089)	3362 (3234)	3583 (3475)	2855 (2732)	3048 (2944)	3213 (3087)	4368 (4236)
<i>p</i> _{C-J} [kbar] ^k	337 (298)	259 (267)	290 (294)	242 (241)	267 (262)	300 (290)	341 (349)
<i>V</i> _{Det.} [m s ⁻¹] ^l	8784 (8723)	8156 (8229)	8609 (8575)	8034 (7944)	8391 (8244)	8890 (8596)	8906 (8748)
Gas vol. [L kg ⁻¹] ^m	732 (708)	809 (798)	832 (816)	801 (781)	820 (797)	852 (822)	793 (739)

^[a] BAM drophammer, grain size (75–150 μm); ^[b] BAM friction tester, grain size (75–150 μm); ^[c] Nitrogen content; ^[d] Oxygen balance^[40]; ^[e] Temperature of decomposition by DSC ($\beta = 5$ °C, Onset values); ^[f] X-ray structure, Pycnometer for DNAAT; ^[g] Molar enthalpy of formation; ^[h] Energy of formation; ^[i] Energy of Explosion; ^[j] Explosion temperature; ^[k] Detonation pressure; ^[l] Detonation velocity; ^[m] Assuming only gaseous products; * values based on Ref. ^[41] and the EXPLO5 database; n.d.: not determined.

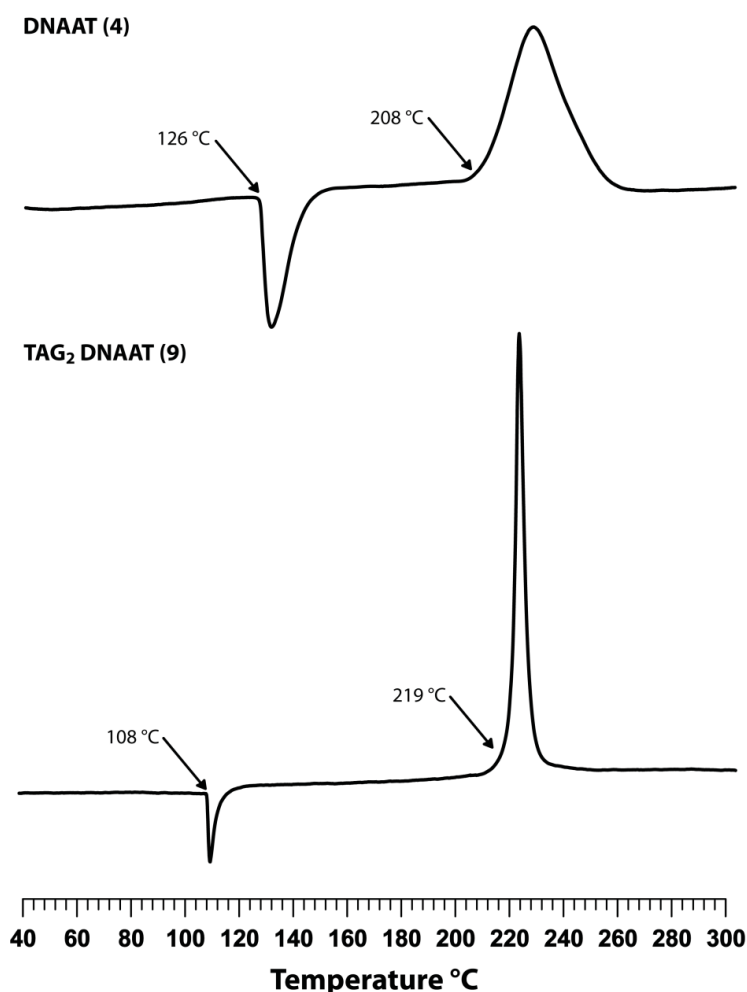


Figure 9: Dynamic scanning calorimetry (DSC) curves for the neutral nitrimino compound **4** and the bis(triaminoguanidinium) salt of **4** (**9**), recorded at a heating rate of 5 °C min⁻¹.

The nitrogen rich salts of DNAAT all exhibit positive heats and energies of formation. The detonation velocities were calculated in the range of 7944 m s⁻¹ (**7**) to 8596 m s⁻¹ (**9**). The best performance was calculated for the triaminoguanidinium salt (**9**) with a detonation velocity of 8596 m s⁻¹, which is only slightly lower than the performance of RDX. With the excellent sensitivity values for friction (160 N), impact (<40 J) and ESD (0.2 J) in addition to the remarkable high temperature of decomposition (219 °C) and a very low solubility in water (2.5 g L⁻¹, 25 °C), the triaminoguanidinium salt (**9**) seems to be the best choice in terms of performance and sensitivity and makes this compound suitable as a potential new high explosive. Additionally, the DSC curves of the 5,5'-dinitrimino-3,3'-azo-1*H*-1,2,4-triazole (**4**) and the corresponding bis(triaminoguanidinium) salt (**9**) are displayed in Figure 9.

Since 3,5-diamino-1*H*-1,2,4-triazole was used previously as a starting material resulting in 3,3'-dinitro-5,5'-azo-1,2,4-triazole (DNAT) and its triaminoguanidinium salt,^[13,14] we

want to put the results obtained for these compounds into relation to the advances we were able to make. DNAT, synthesized by Naud et al. as mentioned in the introduction, shows a much lower sensitivity towards impact and friction with 12.5 J and 250 N, respectively, while the density is in the same region as observed for DNAAT (**4**) (1.85 g cm^{-3}). DNAT as a neutral compound is therefore much more stable regarding outer stimuli, but shows lower performance characteristics than DNAAT with a detonation velocity of 8500 m s^{-1} (**4**: 8723 m s^{-1}). Hence we were able to increase the performance of the molecule with the exchange of the nitro group with the nitrimino group, but the sensitivity values are much too high which prohibits the use as an energetic material (other than for primary explosives). This relation changes, when comparing the triaminoguanidinium salts of DNAT and DNAAT. In this case TAG₂ DNAAT (**9**) is exceeding the properties of TAG₂ DNAT in every respect: the decomposition temperature of **9** is higher ($219 \text{ }^\circ\text{C}$ compared to $202 \text{ }^\circ\text{C}$) together with the sensitivity values being much better in respect to the impact sensitivity (DNAT: 9.3 J, **9**: > 40J) and close to equal with respect to the friction sensitivity (DNAT: 157 N, **9**: 160 N). The performance characteristics of **9** cannot be compared directly, since they have been calculated at different densities, but we can state an overall increase in performance. At a density of 1.58 g cm^{-3} TAG₂ DNAT shows a detonation velocity of 8200 m s^{-1} and a detonation pressure at the Chapman-Jouguet point of 230 kbar while **9** exhibits a detonation pressure of 8596 m s^{-1} paired with a detonation pressure of 290 kbar at a density of 1.70 g cm^{-3} .

9.3 Conclusions

From this combined experimental and theoretical study the following conclusions have been drawn:

The application of the very straightforward and efficient acetyl protection of 3,5-diamino-1*H*-1,2,4-triazole allows selective reactions of the remaining free amino group and establishes a basis to a multitude of potential new energetic compounds that are now accessible. The synthesis of 5,5'-diamino-3,3'-azo-1*H*-1,2,4-triazole (**3**) by reaction of 5-acetylamino-3-amino-1*H*-1,2,4-triazole (**2**) with potassium permanganate is described. **3** acts as starting material for other new high energetic materials, since several modifications of the amine groups are possible. The subsequent nitration of **3** leads to the formation of 5,5'-dinitrimino-3,3'-azo-1*H*-1,2,4-triazole (**4**), which was fully

characterized in terms of sensitivity and energetic properties as well as by single crystal X-ray diffraction. The molecule reveals promising energetic properties but quite high sensitivities towards friction (20 N), impact (2 J) and electrostatic discharge (0.1 J). Therefore, nitrogen rich salts were synthesized by reaction with high-nitrogen bases (ammonia, hydrazine, guanidine, aminoguanidine, triaminoguanidine). All salts were fully characterized by NMR-, IR- and Raman spectroscopy. Special attention was turned on the thermal stabilities and sensitivities values. The triaminoguanidinium salt (**9**) exhibits a remarkable high temperature of decomposition (219 °C) and detonation velocity (8596 m s⁻¹) and therefore turned out to be the most promising compound in terms of performance and stability. The performance characteristics of **9** exceed the ones of TAG₂ DNAT, which served as a reference molecule, especially when comparing the detonation pressure and sensitivity values.

9.4 Experimental Part

Caution: Although all 3,5-diamino-1*H*-1,2,4-triazole derivatives reported in this publication are rather stable against friction, impact and electric discharge, proper safety precautions should be taken when handling primary nitramines. The derivatives are energetic materials and tend to explode under certain conditions, especially under physical stress. Laboratories and personnel should be properly grounded, and safety equipment such as Kevlar gloves, leather coats, face shields and ear plugs are recommended.

General. All chemical reagents, except 3,5-diamino-1,2,4-1*H*-triazole and solvents were obtained from Sigma-Aldrich Inc. or Acros Organics (analytical grade) and were used as supplied. 3,5-diamino-1,2,4-1*H*-triazole was obtained from ABCR. ¹H, ¹³C{¹H}, and ¹⁴N NMR spectra were recorded on a JEOL Eclipse 400 instrument in DMSO-*d*₆ at or near 25 °C. The chemical shifts are given relative to tetramethylsilane (¹H, ¹³C) or nitromethane (¹⁴N) as external standards and coupling constants are given in Hertz (Hz). Infrared (IR) spectra were recorded on a Perkin-Elmer Spectrum BX FT-IR instrument equipped with an ATR unit at 25 °C. Transmittance values are qualitatively described as “very strong” (vs), “strong” (s), “medium” (m) and “weak” (w). Raman spectra were recorded on a Bruker RAM II spectrometer equipped with a Nd:YAG laser (1064 nm) and a reflection

angle of 180°. The intensities are reported as percentages of the most intense peak and are given in parentheses. Elemental analyses were performed with a Netzsch Simultaneous Thermal Analyzer STA 429. Melting points were determined by differential scanning calorimetry (Setaram DSC141 instrument, calibrated with standard pure indium and zinc). Measurements were performed at a heating rate of 5 °C/min in closed aluminum sample pans with a 1 µm hole in the top for gas release under a nitrogen flow of 20 mL/min with an empty identical aluminum sample pan as a reference.

For initial safety testing, the impact and friction sensitivities as well as the electrostatic sensitivities were determined. The impact sensitivity tests were carried out according to STANAG 4489^[42], modified according to instruction^[43] using a BAM^[44] drophammer. The friction sensitivity tests were carried out according to STANAG 4487^[45] and modified according to instruction^[46] using the BAM friction tester. The electrostatic sensitivity tests were accomplished according to STANAG 4490^[47] using an electric spark testing device ESD 2010EN (OZM Research) operating with the “Winspark 1.15 software package”.

1-Acetyl-3,5-diamino-1,2,4-triazole (**1**)

According to literature,^[16] acetic anhydride (40.8 mL, 1.2 eq.) was added dropwise under vigorous stirring to a solution of 3,5-diamino-1,2,4-triazole (36.0 g, 0.36 mol) in 130 mL water at room temperature. After stirring for 1 h, the precipitate was filtered off, washed with water and dried at room temperature to yield **1** as a colorless powder (48.3 g, 0.34 mol, 95% 1-acetyl-3,5-diamino-1*H*-1,2,4-triazole).

¹H NMR ([*d*6]-DMSO, 25 °C): δ 7.35 (s, 2H, NH₂), 5.64 (s, 2H, NH₂), 2.33 (s, 3H, CH₃); ¹³C NMR ([*d*6]-DMSO, 25 °C): δ 170.5 (C=O), 162.2, 157.0, 23.6 (CH₃); IR (ATR, 25 °C, cm⁻¹): 3414(m), 3388(vs), 3295(m), 3127(s), 1709(s), 1640(vs), 1568(s), 1448(m), 1393(s), 1365(vs), 1336(s), 1178(m), 1116(m), 1066(m), 1043(m), 973(m), 839(w), 757(w), 699(w), 669(w); RAMAN (200 mW, 25 °C, cm⁻¹): 3418(4), 3403(5), 3220(10), 3183(9), 3132(9), 3022(35), 2989(16), 2934(68), 1711(100), 1641(40), 1568(44), 1549(25), 1459(9), 1425(21), 1396(41), 1375(39), 1340(43), 1182(37), 1155(80), 1118(25), 1037(42), 972(21), 840(25), 767(8), 719(11), 668(49), 590(15), 577(17), 445(50), 399(15), 385(15), 345(39), 245(13), 224(18).

3-Acetylamino-5-amino-1*H*-1,2,4-triazole (2)

A mixture of 1-acetyl-3,5-diamino-1,2,4-triazole (1) (10.0 g, 70.9 mmol) and 100 mL decaline was refluxed without stirring at 187–190 °C for 6 h. The solid was filtered off, washed with petrol ether (100 mL) and diethyl ether (100 mL) and dried in air to yield **2** as a colorless powder (9.6 g, 68.0 mmol, 96 %).

¹H NMR (D₂O, NaOH, 25 °C): δ 2.03 (s, 3H, CH₃); ¹³C NMR ([D₂O, NaOH, 25 °C): δ 174.1 (C=O), 162.5 (C-NH₂), 154.1 (C-NHAc), 22.7 (CH₃); IR (ATR, 25 °C, cm⁻¹): 3426(m), 3251(s), 1682(vs), 1597(vs), 1581(vs), 1451(s), 1295(m), 1269(m), 1080(m), 1026(w), 1010(w), 816(w), 714(m); RAMAN (200 mW, 25 °C, cm⁻¹): 3243(5), 2933(39), 1684(100), 1647(12), 1586(52), 1537(11), 1456(13), 1366(24), 1296(10), 1261(8), 1084(47), 1027(45), 970(28), 818(11), 793(12), 694(4), 590(38), 493(12), 363(12), 324(24). Elemental analysis: (C₄ H₇ N₅ O₁): calc: C 34.04, H 5.00, N 49.62; found: C 34.11, H 4.86, N 49.12.

5,5'-Diamino-3,3'-azo-1*H*-1,2,4-triazole (3)

Potassium permanganate (2/3 eq., 1.54 g, 9.7 mmol) was added over a period of 10 minutes to a solution of 3-acetylamino-5-amino-1*H*-1,2,4-triazole (**2**, 2.0 g, 14.2 mmol) in sodium hydroxide (32 %, 15 mL) at 0 °C. The mixture was allowed to warm to room temperature and subsequently refluxed for 3 h after addition of sodium hydroxide (5 mL, 2M). The generated manganese oxide was removed by filtration and the filtrate acidified with concentrated hydrochloric acid to pH = 6. The precipitate was filtered off and 5,5'-diamino-3,3'-azotriazole (**3**) was obtained as an orange solid (0.93 g, 4.8 mmol, 68%).

¹³C NMR (D₂O, NaOH): δ 170.2 (C-N=N), 165.3 (C-NH₂); IR (ATR, 25 °C, cm⁻¹): 3452(s), 3351(s), 2677(m), 1624(vs), 1490(m), 1465(m), 1413(w), 1349(m), 1142(m), 1102(m), 1051(m), 880(w), 799(w), 759(w), 708(vw), 676(vw); RAMAN (200 mW, 25 °C, cm⁻¹): 3349(1), 1658(2), 1520(4), 1448(42), 1388(24), 1347(100), 1139(35), 1103(7), 1056(9), 927(2), 912(3). Elemental analysis: (C₄ H₁₀ N₁₀ O₂, dihydrate): calc: C 20.87, H 4.38, N 60.85; found: C 21.58, H 3.85, N 59.05;

5,5'-Dinitrimino-3,3'-azo-1*H*-1,2,4-triazole (**4**)

5,5'-diamino-3,3'-azotriazole (0.35 g, 1.8 mmol) was dissolved in sulfuric acid (conc., 1.75 mL) and nitric acid (conc., 0.30 mL, 7.2 mmol) was added at 0 °C. After stirring at 0 °C for 30 minutes, the mixture was allowed to warm to room temperature, stirred for 1 h and poured on ice (10 g). The precipitate was filtered off, washed with water and dried at 60 °C to obtain **4** as a yellow solid.

DSC (Onset, 5 °C min⁻¹): T_{Dec.}: 209 °C; ¹³C{¹H} NMR ([*d6*]-DMSO, 25 °C): δ 159.7 (C-N=N), 153.8 (C-N-NO₂); ¹⁴N NMR ([*d6*]-DMSO, 25 °C): δ -19 (NO₂); IR (ATR, 25 °C, cm⁻¹): 3066(s), 1695 (w), 1586(vs), 1542(m), 1522(s), 1493(m), 1436(m), 1273(s), 1238(s), 1139(m), 1075(m), 1039(m), 979(m), 845(w), 770(w), 721(w); RAMAN (200 mW, 25 °C, cm⁻¹): 1538(16), 1493(10), 1436(100), 1354(11), 1307(16), 1145(21), 1091(7), 994(11), 905(4), 847(3), 754(2); Elemental analysis: (C₄ H₄ N₁₂ O₄): calc: C 16.91, H 1.42, N 59.15; found: C 18.27, H 1.83, N 58.25; Sensitivities (grain size: 100–500 μm): FS: 20 N, IS: 2 J, ESD: 0.1 J.

General synthesis of nitrogen-rich salts of DNAAT

The free nitrogen-rich base (2 eq., 22.8 mmol) was added to a suspension of 5,5'-dinitrimino-3,3'-azo-1*H*-1,2,4-bistriazole (**4**, 3.24 g, 11.4 mmol) in 75 mL water at 60 °C. After cooling to 5 °C, the precipitate was filtered off, washed with cold water and dried at 60 °C to yield the corresponding nitrogen-rich salt of 5,5'-dinitrimino-3,3'-azo-1*H*-1,2,4-triazole (**5–9**) as a yellow solid.

(NH₄)₂DNAAT (**5**)

yield: 50%; DSC (onset, 5 °C min⁻¹): T_{Dec.}: 212 °C; ¹H NMR ([*d6*]-DMSO, 25 °C): δ 13.58 (s, 2H, N_{ring}-H), 7.23 (NH₄⁺); ¹³C NMR ([*d6*]-DMSO, 25 °C): δ 167.7 (C-N=N), 158.3 (C-N-NO₂); ¹⁴N NMR ([*d6*]-DMSO, 25 °C): δ -14 (-NO₂), -359 (NH₄⁺); IR (ATR, 25 °C, cm⁻¹): 3171(s), 1692(w), 1641(w), 1594(m), 1530(s), 1474(s), 1432(s), 1380(s), 1316(vs), 1168(m), 1078(s), 1035(w), 1004(m), 861(w), 770(m), 733(w), 698(w); RAMAN (200 mW, 25 °C, cm⁻¹): 1544(25), 1466(100), 1403(53), 1352(84), 1167(30), 1099(17), 1044(8), 1002(41), 924(12), 860(8), 748(6), 397(7); Sensitivities (grain size: 100–500 μm): FS: >360 N, IS: >40 J, ESD: 0.15 J.

(N₂H₅)₂DNAAT (6)

yield: 54%; DSC (onset, 5 °C min⁻¹): T_{Dec.}: 154 °C; ¹H NMR ([d6]-DMSO, 25 °C): δ 13.51 (s, 2H, N_{ring}-H), 7.28 (N₂H₅⁺); ¹³C NMR ([d6]-DMSO, 25 °C): δ 166.9 (C-N=N), 157.8 (C-N-NO₂); ¹⁴N NMR ([d6]-DMSO, 25 °C): δ -16 (-NO₂), -359 (N₂H₅⁺); IR (ATR, 25 °C, cm⁻¹): 3103(s), 1631(m), 1528(s), 1472(m), 1426(s), 1385(m), 1315(vs), 1260(s), 1168(m), 1080(s), 996(m), 859(w), 769(w), 732(vw), 705(w); RAMAN (200 mW, 25 °C, cm⁻¹): 1541(9), 1461(100), 1403(36), 1353(54), 1258(3), 1162(19), 1100(10), 1000(20), 924(7), 859(4), 747(2), 399(2); Sensitivities (grain size: 100–500 μm): FS: >360 N, IS: 10 J, ESD: 0.05 J.

G₂DNAAT (7)

yield: 73%; DSC (onset, 5 °C min⁻¹): T_{Dec.}: 261 °C; ¹H NMR ([d6]-DMSO, 25 °C): δ 13.53 (s, 2H, N_{ring}-H), 7.03 (s, G⁺); ¹³C NMR ([d6]-DMSO, 25 °C): δ 167.1 (C-N=N), 157.9 (C-N-NO₂), 157.7 (G⁺); ¹⁴N NMR ([d6]-DMSO, 25 °C): δ -14 (-NO₂); IR (ATR, 25 °C, cm⁻¹): 3336(m), 3241(m), 3167(m), 2790(w), 1680(m), 1635(s), 1532(m), 1471(m), 1436(m), 1391(m), 1368(m), 1339(vs), 1255(m), 1162(m), 1085(s), 1011(m), 864(w), 770(m), 726(w), 690(w); RAMAN (200 mW, 25 °C, cm⁻¹): 1536(14), 1462(100), 1402(23), 1363(56), 1156(18), 1097(14), 1012(24), 917(8), 862(5), 402(5); Elemental analysis: (C₆ H₁₄ N₁₈ O₄): calc: C 17.91, H 3.51, N 62.67; found: C 18.49, H 3.59, N 62.12; Sensitivities (grain size: 100–500 μm): FS: >360 N, IS: >40 J, ESD: 0.35 J.

AG₂DNAAT (8)

yield: 87%; DSC (onset, 5 °C min⁻¹): T_{Dec.}: 177 °C; ¹H NMR ([d6]-DMSO, 25 °C): δ 13.61 (s, 2H, N_{ring}-H), 7.89 (s, AG⁺), 7.12 (s, AG⁺), 4.71 (s, AG⁺); ¹³C NMR ([d6]-DMSO, 25 °C): δ 167.0 (C-N=N), 157.7 (C-N-NO₂), 158.9 (AG⁺); ¹⁴N NMR ([d6]-DMSO, 25 °C): δ -15 (-NO₂); IR (ATR, 25 °C, cm⁻¹): 3435(m), 3341(m), 3252(vs), 3183(s), 2888(w), 1685(vs), 1668(vs), 1530(s), 1475(m), 1436(m), 1386(m), 1346(vs), 1257(m), 1164(w), 1086(s), 1009(m), 864(w), 770(m), 730(w), 692(w); RAMAN (200 mW, 25 °C, cm⁻¹): 1534(16), 1488(12), 1463(100), 1409(22), 1367(51), 1156(20), 1096(12), 1041(5), 1008(29), 918(9), 861(5), 746(4), 403(5); Elemental analysis: (C₆ H₁₆ N₂₀ O₄): calc.: C 16.67, H 3.73, N 64.80; found: C 16.87, H 3.73, N 61.97; Sensitivities (grain size: 100–500 μm): FS: >360 N, IS: >40 J, ESD: 0.20 J.

TAG₂DNAAT (9)

yield: 85%; DSC (onset, 5 °C min⁻¹): T_{Dec.}: 219 °C; ¹H NMR ([d6]-DMSO, 25 °C): δ 13.48 (s, 2H, N_{ring}-H), 8.59 (s, TAG⁺), 4.49 (s, TAG⁺); ¹³C NMR ([d6]-DMSO, 25 °C): δ 167.3 (C-N=N), 157.8 (C-N-NO₂), 159.0 (TAG⁺); ¹⁴N NMR ([d6]-DMSO, 25 °C): δ -14 (-NO₂); IR (ATR, 25 °C, cm⁻¹): 3252(s), 1682(s), 1526(s), 1466(m), 1435(s), 1315(vs), 1250(m), 1133(m), 1073(s), 1003(m), 857(w), 771(w), 728(w), 656(w); RAMAN (200 mW, 25 °C, cm⁻¹): 1534(16), 1488(12), 1463(100), 1409(22), 1367(51), 1156(20), 1096(12), 1041(5), 1008(29), 918(9), 861(5), 746(4), 403(5); Elemental analysis: (C₆ H₂₀ N₂₄ O₄); calc.: C 14.64, H 4.09, N 68.27; found: C 15.22, H 4.37, N 66.73; Sensitivities: (grain size: 100–500 μm): FS: 160 N, IS: >40 J, ESD: 0.20 J.

9.5 References

- [1] P. F. Pagoria, G. S. Lee, A. R. Mitchell, R. D. Schmidt, *Thermochim. Acta* **2002**, *384*, 187-204.
- [2] T. M. Klapötke, in *Structure and bonding* (Ed.: D. M. P. Mingos), Springer-Verlag, Berlin Heidelberg **2007**.
- [3] D. Fournier, A. Halasz, J. Spain, R. J. Spanggord, J. C. Bottaro, J. Hawari, *Appl. Environ. Microb.* **2004**, *70*, 1123-1128.
- [4] a) T. M. Klapoetke, J. Stierstorfer, A. U. Wallek, *Chem.Mat.* **2008**, *20*, 4519-4530; b) T. M. Klapoetke, C. M. Sabate, *Chem.Mat.s* **2008**, *20*, 3629-3637; c) S. Yang, S. Xu, H. Huang, W. Zhang, X. Zhang, *Huaxue Jinzhan* **2008**, *20*, 526-537; d) D. E. Chavez, M. A. Hiskey, D. L. Naud, *Propell. Explo. Pyrot.* **2004**, *29*, 209-215; e) Y. Huang, H. Gao, B. Twamley, J. n. M. Shreeve, *Eur. J. Inorg. Chem.* **2008**, 2560-2568.
- [5] C. M. Sabate, T. M. Klapoetke, *New Trends in Research of Energetic Materials, Proceedings of the Seminar, 12th, Pardubice, Czech Republic, Apr. 1-3, 2009* **2009**, 172-194.
- [6] a) D. E. Chavez, M. A. Hiskey, R. D. Gilardi, *Angew. Chem. Int. Ed.* **2000**, *39*, 1791-1793; b) D. Chavez, L. Hill, M. Hiskey, S. Kinkead, *J. Energ. Mat.* **2000**, *18*, 219-236.
- [7] a) T. M. Klapoetke, C. M. Sabate, *New J. Chem.* **2009**, *33*, 1605-1617; b) T. M. Klapoetke, C. M. Sabate, *Chem. Mat.* **2008**, *20*, 1750-1763; c) A. Hammerl, G. Holl, T. M. Klapoetke, P. Mayer, H. Noth, H. Piotrowski, M. Warchhold, *Eur.J. Inorg. Chem.* **2002**, 834-845.
- [8] a) B. C. Tappan, A. N. Ali, S. F. Son, T. B. Brill, *Propell. Explo. Pyrot.* **2006**, *31*, 163-168; b) R. Sivabalan, M. B. Talawar, N. Senthilkumar, B. Kavitha, S. N. Asthana, *J. Therm. Anal. Calorim.* **2004**, *78*, 781-792.

- [9] M. A. Hiskey, N. Goldman, J. R. Stine, *J. Energ. Mat.* **1998**, *16*, 119-127.
- [10] a) M. M. Chaudhri, *J. Mater. Sci. Lett.* **1984**, *3*, 565-568; b) D. J. Whelan, R. J. Spear, R. W. Read, *Thermochim. Acta* **1984**, *80*, 149-163; c) G. O. Reddy, A. K. Chatterjee, *Thermochim. Acta* **1983**, *66*, 231-244; d) M. M. Chaudhri, *Nature (London, United Kingdom)* **1976**, *263*, 121-122.
- [11] M. M. Williams, W. S. McEwan, R. A. Henry, *J. Phys. Chem.* **1957**, *61*, 261-267.
- [12] D. E. Chavez, B. C. Tappan, 8-ISICP, Los Alamos National laboratory, **2009**.
- [13] D. L. Naud, M. A. Hiskey, H. H. Harry, *J. Energ. Mat.* **2003**, *21*, 57-62.
- [14] D. E. Chavez, B. C. Tappan, B. A. Mason, D. Parrish, *Propell. Explo. Pyrot.* **2009**, *34*, 475-479.
- [15] B. G. van den Bos, *Recueil des Travaux Chimiques des Pays-Bas et de la Belgique* **1960**, *79*, 836-842.
- [16] M. S. Pevzner, N. V. Gladkova, T. A. Kravchenko, *Zh. Org. Khim.* **1996**, *32*, 1230-1233.
- [17] H.-H. Licht, H. Ritter, *J. Energ. Mat.* **1994**, *12*, 223-235.
- [18] N. Biswas, S. Umopathy, *J. Phys. Chem. A* **2000**, *104*, 2734-2745.
- [19] F. Billes, H. Endredi, G. Keresztury, *Theochem* **2000**, *530*, 183-200.
- [20] *CrysAlis CCD*, Oxford Diffraction Ltd., Version 1.171.27p5 beta (release 01-04-2005 *CrysAlis171.NET*).
- [21] *CrysAlis RED*, Oxford Diffraction Ltd., Version 1.171.27p5 beta (release 01-04-2005 *CrysAlis171.NET*).
- [22] A. Altomare, G. Cascarano, C. Giacovazzo, A. Guagliardi, *J. Appl. Cryst.* **1993**, *26*, 343-350.
- [23] G. M. Sheldrick, *SHELXS-97, Crystal Structure Solution, Version 97-1; Institut Anorg. Chemie, University of Göttingen, Germany, 1990*.
- [24] G. M. Sheldrick, *SHELXL-97, Program for the Refinement of Crystal Structures. University of Göttingen, Germany, 1997*.
- [25] L. Farrugia, *J. Appl. Cryst.* **1999**, *32*, 837-838.
- [26] A. L. Spek, *Platon, A Multipurpose Crystallographic Tool, Utrecht University, Utrecht, The Netherlands, 1999*.
- [27] *Crystallographic data for the structure(s) have been deposited with the Cambridge Crystallographic Data Centre. Copies of the data can be obtained free of charge on application to The Director, CCDC, 12 Union Road, Cambridge CB2 1EZ, UK (Fax: int.code (1223)336-033; e-mail for inquiry: fileserv@ccdc.cam.ac.uk; e-mail for deposition: deposit-@ccdc.cam.ac.uk).*
- [28] F. H. Allen, O. Kennard, D. G. Watson, L. Brammer, A. G. Orpen, R. Taylor, *J. Chem. Soc. Perk. T. 2 (1972-1999)* **1987**, S1-S19.
- [29] A. Hammerl, Ludwig-Maximilians-University (Munich), **2001**.
- [30] G. A. Jeffrey, *An Introduction to Hydrogen Bonding*, Oxford University Press, Oxford **1997**.
- [31] A. F. Holleman, E. Wiberg, *Lehrbuch der anorganischen Chemie*, 101st Ed., de Gruyter, New York, **1995**.
- [32] M. J. F. e. al., *Gaussian 03, Revision B04, Gaussian Inc., Wallingford, CT, 2004*.

- [33] a) J. W. Ochterski, G. A. Petersson, J. A. Montgomery Jr., *J. Chem. Phys.* **1996**, *104*, 2598-2619; b) J. A. Montgomery Jr., M. J. Frisch, J. W. Ochterski, G. A. Petersson, *J. Chem. Phys.* **2000**, *112*, 6532-6542.
- [34] a) L. A. Curtiss, K. Raghavachari, P. C. Redfern, J. A. Pople, *J. Chem. Phys.* **1997**, *106*, 1063-1079; b) E. F. C. Byrd, B. M. Rice, *J. Phys. Chem. A* **2006**, *110*, 1005-1013; c) B. M. Rice, S. V. Pai, J. Hare, *Combust. Flame* **1999**, *118*, 445-458.
- [35] <http://webbook.nist.gov/chemistry>
- [36] a) M. S. Westwell, M. S. Searle, D. J. Wales, D. H. Williams, *J. Am. Chem. Soc.* **1995**, *117*, 5013-5015; b) F. Trouton, *Philos. Mag.* **1884**, *18*, 54-57.
- [37] a) H. D. B. Jenkins, H. K. Roobottom, J. Passmore, L. Glasser, *Inorg. Chem.* **1999**, *38*, 3609-3620; b) H. D. B. Jenkins, D. Tudela, L. Glasser, *Inorg. Chem.* **2002**, *41*, 2364-2367.
- [38] a) M. Sućeska, *EXPLO5.4 program, Zagreb, Croatia, 2010*; b) M. Sućeska, *EXPLO5.3 program, Zagreb, Croatia, 2009*.
- [39] a) M. Sućeska, *Mater. Sci. Forum* **2004**, 465-466, 325-330; b) M. Sućeska, *Propell. Explos. Pyrot.* **1991**, *16*, 197-202; c) M. Sućeska, *Propell. Explos. Pyrot.* **1999**, *24*, 280-285; d) M. L. Hobbs, M. R. Baer, in *Proc. of the 10th Symp. (International) on Detonation*, ONR 33395-12, Boston, MA, **July 12-16, 1993**, p. 409.
- [40] *Calculation of oxygen balance: Ω (%) = $(wO - 2xC - 1/2yH - 2zS)1600/M$. (w : number of oxygen atoms, x : number of carbon atoms, y : number of hydrogen atoms, z : number of sulfur atoms, M : molecular weight).*
- [41] J. Köhler, R. Meyer, *Explosivstoffe, Vol. 9th edition*, Wiley-VCH, Weinheim, **1998**.
- [42] i. t. NATO standardization agreement (STANAG) on explosives, no.4489, 1st ed., Sept. 17, **1999**.
- [43] *WIWEB-Standardarbeitsanweisung 4-5.1.02, Ermittlung der Explosionsgefährlichkeit, hier: der Schlagempfindlichkeit mit dem Fallhammer, Nov. 08, 2002.*
- [44] <http://www.bam.de>.
- [45] *NATO standardization agreement (STANAG) on explosives, friction tests, no.4487, 1st ed., Aug. 22, 2002.*
- [46] *WIWEB-Standardarbeitsanweisung 4-5.1.03, Ermittlung der Explosionsgefährlichkeit, hier: der Reibempfindlichkeit mit dem Reibeapparat, Nov. 08, 2002.*
- [47] *NATO standardization agreement (STANAG) on explosives, electrostatic discharge sensitivity tests, no.4490, 1st ed., Feb. 19, 2001.*

10. Nitrated derivatives of 1,3-bis(5-amino-1*H*-1,2,4-triazol-3-yl)-triazene.

Thomas M. Klapötke and Franz A. Martin

Unpublished results

10.1 Introduction

The chemistry of heterocyclic ring systems has not only been focused on the synthesis of monomers carrying energetic groups like for example 5-nitraminotetrazole^[1] or 3,5-dinitro-1*H*-1,2,4-triazole^[2] but also focused on the investigation of bridged systems, connected by azo, triazene, or tetrazene groups. Sodium 5,5'-azotetrazolate has been synthesized first by Thiele^[3] and various nitrogen rich salts have been reinvestigated later as gas generators, additives for fire extinguishing systems and burn rate modifiers.^[4] Azo-bridged compounds have also drawn attention to the synthesis of polyazido compounds using azotriazine as the backbone to obtain high nitrogen containing compounds including the highly energetic azide substituent but with lower sensitivities towards outer stimuli.^[5] Starting from ANTA, Naud and coworkers reported on the synthesis of 5,5'-dinitro-3,3'-azo-1*H*-1,2,4-triazole (DNAT),^[6] while Chavez *et. al* turned it into the triaminoguanidinium salt later in 2009.^[7] Based on their findings, we developed a novel synthesis route for the formation of 5,5'-dinitrimino-3,3'-azo-1*H*-1,2,4-triazole (DNAAT) and were able to convert DNAAT into its triaminoguanidinium salt, exhibiting thermal stabilities of over 210 °C paired with very low sensitivities and performance values in the range of RDX.^[8]

These findings encouraged us to put more effort into the synthesis and investigation of bridged 1,2,4-triazole derivatives. Since tetrazole derivatives bridged by the triazene moiety showed remarkable thermal stability, for example bis(1-methyltetrazol-5-yl)triazene or bis(2-methyltetrazol-5-yl)triazene starting decomposition at around 185 °C,^[9] but lacked of stability against impact, we thought about the possibility of bridging 1,2,4-triazoles via a triazene moiety. Our hopes focused on the exchange of the isolobal C-R ($R = \text{NH}_2$) group with one nitrogen atom stabilizing the system in order to obtain higher decomposition temperatures.

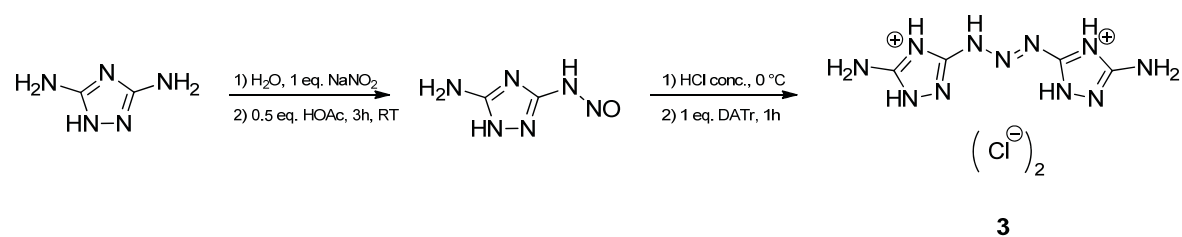
In this contribution we focus on the development of a safe and high yield synthetic pathway for 1,3-bis-(5-amino-1*H*-1,2,4-triazol-3-yl)triazene (BATTH, **2**) as starting

material. The main topic of this contribution presents the synthesis and characterization of two novel triazene compounds, 1,3-bis-(5-nitro-1*H*-1,2,4-triazol-3-yl)triazene (DNBATTH, **5**) and 1,3-bis-(5-nitramino-1*H*-1,2,4-triazol-3-yl)triazene (DNIBATTH, **6**). The focus will not only be directed on the synthesis of these compounds but also on the evaluation of their properties regarding sensitivities and thermal stability and therefore their feasibility for application in energetic compositions.

10.2 Results and Discussion

10.2.1 Synthesis

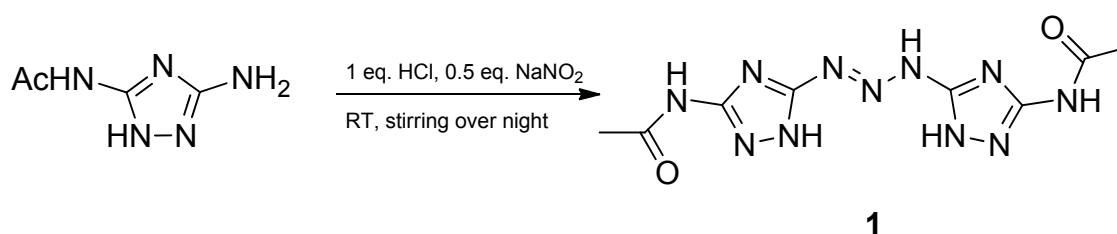
The preparation of 1,3-bis-(5-amino-1*H*-1,2,4-triazol-3-yl)triazene was known for nearly 50 years, but it has never found use except for the preparation of copper(II) and palladium(II) complexes.^[10] The preparation started with 3,5-diamino-1*H*-1,2,4-triazole (DAT), which was then converted to its mononitroso derivative with sodium nitrite and acetic acid,^[11] and afterwards auto coupled with a second 3,5-diamino-1*H*-1,2,4-triazole molecule in concentrated hydrochloric acid, yielding 1,3-bis-(5-amino-1*H*-1,2,4-triazol-3-yl)triazene dihydrochloride as the main product.^[12] The formation of the neutral compound was performed by neutralization with potassium hydroxide, but never worked sufficiently. The overall yield of the reaction described in literature is about 37% for the formation of the dihydrochloride salt of BATTH (**3**). The reaction scheme is shown in Scheme 1.



Scheme 1: Reaction pathway for the synthesis of BATTH * 2 HCl (**3**) by known literature procedures.

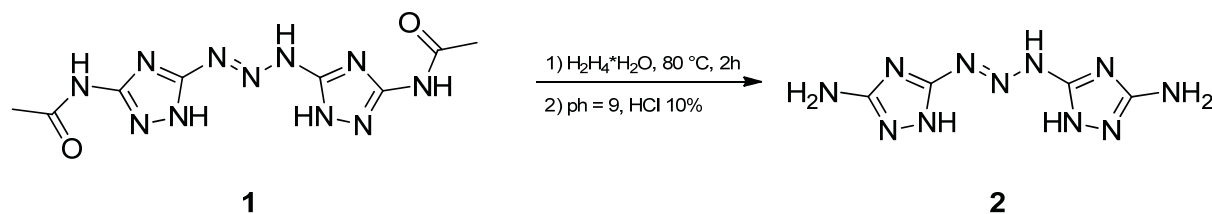
Since the known synthesis route has very low yield and it is difficult to obtain the neutral compound by neutralization, a different route for the formation of **2** was developed. DAT cannot be coupled directly with sodium nitrite and hydrochloric acid, since it carries two chemically equivalent amine groups, resulting in the formation of a polymeric compound. Therefore one amine group has to be protected at first, to enable a selective attack at one

single amine group. The acetyl protection group was chosen since it is very inexpensive, easy to introduce and also easy to cleave after the coupling reaction. One inexpensive and convenient method for the selective protection of the amine group in N5 position is described in literature and starts with the protection of the N1 position with acetic anhydride followed by a thermal rearrangement to the N5 position in decaline at 270 °C.^[13] The yield of the reaction is nearly quantitative (98 %) and the synthesized 5-acetamido-1*H*-1,2,4-triazole can be used without further purification. The coupling reaction was carried out with half an equivalent of sodium nitrite and one equivalent of hydrochloric acid in water, yielding 1,3-bis-[3-(5-acetamido-1*H*-1,2,4-triazolyl)]-triazene (AcetBATTH, **1**) as a bright yellow solid in 81 % yield. (Scheme 2)



Scheme 2: Formation of 1,3-bis-[3-(5-acetamido-1*H*-1,2,4-triazolyl)]-triazene (**1**), prepared from acetyl protected DAT.

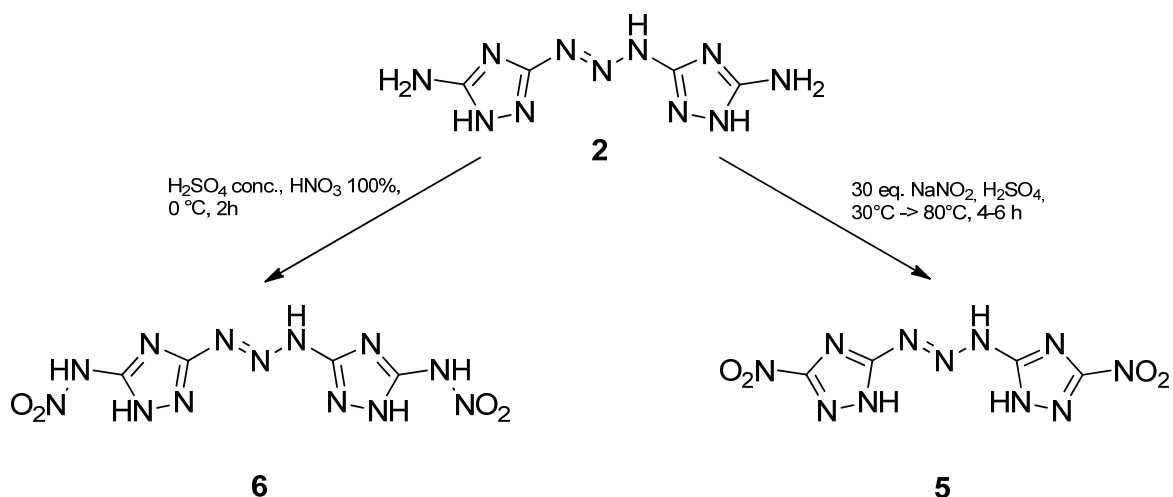
The deprotection of **1** caused some problems at first since the compound has a very bad solubility in aqueous systems and therefore deprotection in acidic or alkaline media failed, either with hydrochloric acid or liquid ammonia, even at elevated temperatures, always recovering **1**. Using hydrazine monohydrate as deprotection reagent finally yielded the desired neutral compound **2** since it is much more reactive than liquid ammonia.^[14] In order to increase the conversion rate, the reaction was held for two hours at an elevated temperature of 80 °C forming a bright red solution. After cooling down to 0 °C and neutralization to a pH value of 9, BATTH (**2**) was isolated as a white powder in 81 % yield. (Scheme 3)



Scheme 3: Deprotection of 1,3-bis-[3-(5-acetamido-1*H*-1,2,4-triazolyl)]-triazene (**1**) with hydrazine monohydrate yielding 1,3-bis-[3-(5-amino-1*H*-1,2,4-triazolyl)]-triazene (**2**).

The complete conversion rate and therefore the overall yield of the newly developed synthetic route for the formation of **2** is 64 % and hence nearly doubles the reaction yields described in literature.^[12a]

The main goal with this contribution is the formation of nitrated derivatives of BATTH (**2**). The formation of 1,3-bis-[3-(5-nitramino-1*H*-1,2,4-triazolyl)]-triazene (DNIBATTH, **6**) was achieved by nitration of **2** with a mixture of concentrated sulfuric acid and 100 % nitric acid in a molar ratio of 7:1 and a five time excess of nitric acid. After quenching of the reaction mixture, **6** was isolated as a bright yellow powder by filtration and air dried with yields up to 57 %. Direct nitration of **1** did not yield the desired product. 1,3-Bis-[3-(5-nitro-1*H*-1,2,4-triazolyl)]-triazene (DNBATTH, **5**) was synthesized only in small yields of 24 %. The direct coupling of 3-amino-5-nitro-1*H*-1,2,4-triazole (ANTA) was favored at first, but failed with either sodium nitrite or amyl nitrite, mainly due to the electron withdrawing character of the nitro group paired with the bad solubility of ANTA in water and alcoholic solutions. Hence the reaction route for the formation of 3,5-dinitro-1*H*-1,2,4-triazole was used,^[15] where **2** had to be dissolved in 20 % sulfuric acid, which was hardly possible. Many attempts with different reaction conditions and molar ratios of sodium nitrite and sulfuric acid as well as the change of the acid did not yield any usable result. We finally figured out the proper reaction conditions to be a 30 fold excess of sodium nitrite, and the addition of the suspension of **2** in 20 % sulfuric acid taking place at 30 °C. The reaction was heated up slowly and held at an elevated temperature (80 °C) for at least four hours, till no more gas evolution was visible. The formation of polymeric side products could not be avoided completely. Extraction of the reaction mixture with ethyl acetate after filtration and subsequent evaporation of the solvent yielded **5** as a yellow powder. (Scheme 4)



Scheme 4: Reaction pathways towards the formation of 1,3-bis-[3-(5-nitramino-1*H*-1,2,4-triazolyl)]-triazene (**6**) and 1,3-bis-[3-(5-nitro-1*H*-1,2,4-triazolyl)]-triazene (**5**).

The synthesis of nitrogen rich salts of **6** was attempted for the guanidinium and triaminoguanidinium salt, but only the bis(guanidinium) salt (**7**) could be synthesized as an amorphous brown powder, soluble in hot water and ethanol, but crystallization of the compound was impossible. Therefore, additional pycnometer measurements have been performed to determine the density of **7** to be 1.65 g cm^{-3} .

The formation of the dinitramide salt of **2** was also not successful. In order to synthesize the bis(dinitramide) salt of **2**, we first started with the synthesis of 1,3-bis-[3-(5-amino-1*H*-1,2,4-triazolyl)]-triazene $\cdot 2 \text{ HClO}_4$ (**4**) as starting material for a metathesis reaction. Compound **4** was synthesized by complete dissolution of **2** in an excess of 45 % perchloric acid at elevated temperature and subsequent removal of the solvent. Potassium dinitramide was prepared according to literature known procedures. Since **4** was not soluble in water or water/ethanol mixtures, even at elevated temperatures, we were not able to undertake the metathesis reaction of **4** with potassium dinitramide in solution. All attempts to perform the reaction in different solvents or in suspension were not successful. Silver chloride was removed from the attempt of reacting 1,3-bis-(5-amino-1*H*-1,2,4-triazol-3-yl)triazene dihydrochloride in a metathesis reaction with silver dinitramide, but the desired dinitramide salt could not be identified from the reaction. Instead of the dinitramide salt neutral BATTH (**2**) was recovered from the reaction mixture indicating HDN (dinitraminic acid) being a too weak base in order to protonate BATTH, which is consistent with the behavior of **2** against very strong acids like perchloric and hydrochloric acid.

10.2.2 Vibrational and NMR Spectroscopy

IR and Raman spectra of all compounds have been recorded and the frequencies have been assigned based on literature.^[16] In order to be able to assign the stretching modes to the correct frequencies, compounds **5** and **6** have been calculated at the B3LYP/cc-pVDZ^[17] level of theory as implemented in the Gaussian 09W program package.^[18] The calculated frequencies have been fitted according to Witek et al.^[19] with a scaling factor of 0.9704.

As already mentioned in Chapter 7, the conversion of 1-acety-3,5-diamino-1,2,4-triazole to 5-acetamido-1*H*-1,2,4-triazole is monitored by the shift of the stretching mode of the carbonyl group from 1710 cm⁻¹ to 1683 cm⁻¹. After the coupling reaction towards the formation of the triazene moiety the stretching vibration of the carbonyl group shifts from 1683 cm⁻¹ to 1687 cm⁻¹. The C–H stretching modes and ν_s and ν_{as} modes of the methyl group are observed at 2879 cm⁻¹ and 2827 cm⁻¹ in the IR spectra of **1**. Together with the line at 1477 cm⁻¹ (maximum intensity) in the Raman spectra, specifying the N=N double bond of the triazene bridge, the successful coupling of two 5-acetamido-1*H*-1,2,4-triazole molecules forming **1** can be stated. After the deprotection of **1** with hydrazine hydrate, no stretching modes of either methyl or the carbonyl groups are evident. The ν_s and ν_{as} modes of the NH₂ groups are observed in the IR spectra of **2** at 3213 cm⁻¹ and 3034 cm⁻¹. The stretch of the N=N double bond in the triazene bridge is observed as a weak absorption band at 1475 cm⁻¹ in the IR spectra and as the peak of maximum intensity at 1438 cm⁻¹ in the Raman spectra. The stretching modes of the N=N double bond are also observed for the dihydrochloride and the dihydroperchlorate salts of **2** at 1486 cm⁻¹ (IR) and 1489 cm⁻¹ (Raman) and at 1485 cm⁻¹ (IR) and 1491 (Raman), respectively.

ν (N–H) stretching modes are observed for either the hydrogen atoms located on the triazole rings or the hydrogen atom located on the triazene bridge in the IR spectra of **5** at 3466 cm⁻¹ and 3370 cm⁻¹, respectively. The ν_{as} stretching mode of the NO₂ group is observed only in the IR spectra as a broad absorption band at 1561 cm⁻¹. The ν_s stretching mode of the NO₂ is present in both, IR and Raman spectra at 1307 cm⁻¹ and 1313 cm⁻¹, respectively. The δ_s in plane deformation mode of the two NO₂ groups can be observed in the IR spectra at 837 cm⁻¹. The stretching modes of the C–NO₂ bonds are observed at 1368 cm⁻¹ (IR) and 1380 cm⁻¹ (Raman), while the stretching mode of the C–NH_{triazene} is present at 1495 cm⁻¹ (IR) and 1507 cm⁻¹ (Raman). The most intense line in the Raman

spectra is assigned to the N=N double bond of the triazene bridge at 1481 cm^{-1} , as shown for **1** and **2** before.

The most intense line in the Raman spectra of **6** is also assigned to the N=N double bond of the triazene bridge at 1478 cm^{-1} . The ν (=N–NH–) stretching mode, displaying the single bond of the triazene bridge, is assigned to the absorption band at 1219 cm^{-1} in the IR spectra. The stretching modes of the five N–H bonds in **6** are observed only in the IR spectrum in the region of $3412 - 3130\text{ cm}^{-1}$ as a broad absorption band. The ν_{as} and ν_{s} modes of the NO₂ group are present in the IR spectra at 1589 cm^{-1} (ν_{as}) and 1305 cm^{-1} (ν_{s}) while only the ν_{s} mode is observed in the Raman spectra at 1311 cm^{-1} . A combined mode, consisting of ν (C_{tria}–NH_{triazene}), ν (C_{tria}–NH_{nitramine}) and additionally two N–C–N in plane bending deformation modes within the same triazole ring, can be assigned to be present at 1558 cm^{-1} in the IR spectra and 1555 cm^{-1} in the Raman spectra. Due to the large molecular backbone with catenated C=N and N=N double bonds many more combined deformation and stretching modes are present between 1200 cm^{-1} and 600 cm^{-1} in both, IR and Raman spectra.

The bis(guanidinium) salt of **6** shows the same pattern of stretching modes in both IR and Raman spectra. The signature triazene valence stretching mode is observed at 1483 cm^{-1} (IR) and as the line with highest intensity at 1485 cm^{-1} in the Raman spectra. NH₂ and N–H stretching modes are only present in the IR spectrum in the region of $3424 - 3180\text{ cm}^{-1}$. The ν_{as} and ν_{s} stretching modes of the NO₂ groups are also only present in the IR spectra at 1657 cm^{-1} and 1308 cm^{-1} , respectively. Only a few combined stretching modes are observable between 1550 cm^{-1} and 900 cm^{-1} in the IR spectra.

Determination of the derived compounds by NMR spectroscopy is very hard, due to some issues. At first, the non nitrated compounds show a very bad solubility in common solvents and hence the solutions prepared for NMR spectroscopy were not of high molarity. A second difficulty results from the large C–N backbone system hence the protons are not localized and the exchange rate in the solvents used was too slow, resulting in very broad resonances, especially in the ¹H NMR spectra. Third, the quaternary carbon atoms of the triazole rings, together with the triazene bridge are very hard to excite and many scans must be performed in order to observe at least a small signal. Some of the resonances are hence not assignable. For compound **1** signals are observed at 12.92 ppm and 11.47 ppm representing the N_{tria}–H hydrogen atoms as broad signals, while the methyl group of the acetyl protecting group showed a well resolved

signal at a chemical shift of 2.09 ppm in the ^1H NMR spectra. The resonances of the methyl group as well as the carbonyl group are observed at chemical shifts of 23.4 ppm and 169.6 ppm, respectively, while only one signal is observed belonging to the triazole ring carbon atoms at 149.1 ppm (probably C–Acetyl). When deprotected, as it is the case for **2**, only one carbon signal at a chemical shift of 156.7 ppm assignable to the C–NH₂ atom is observed, which is reasonable when compared with 5-amino-3-tetrazol-1-yl-1,2,4-triazole (Chapter 10). The two salts of **2**, the dihydrochloride (**3**) and the dihydroperchlorate (**4**) salt showed two resonances in the ^{13}C NMR spectra each, at 157.0 ppm and 151.0 ppm for **3** and at 154.0 ppm and 153.2 ppm for **4**. The resonances at lower field are assigned to the C–NH₂ carbon atoms, obvious for **3**, while the assignment for **4** is not that simple due to the small difference in the chemical shift. While only a very broad singlet at 6.27 ppm is observed for **3**, resonances are observed for **4** at 13.08 ppm, 7.13 ppm and 4.67 ppm in the ^1H NMR spectra. For compounds **1** – **4**, no signals are observed in the ^{14}N NMR spectra.

Compound **5** shows a single resonance in the ^1H NMR spectra at 8.85 ppm, which could belong to the hydrogen atom located at the triazene bridge,^[9a] while **6** shows three resonances at chemical shifts of 14.15 ppm (N_{tria}–H), 9.73 ppm (N_{triazene}–H) and 4.06 ppm (C–NH–NO₂). While the C–NO₂ carbon atom shows a resonance at 160.5 ppm for **5**, the signal of the nitramine NO₂ group is observed at higher field at 151.7 ppm in the ^{13}C NMR spectra. The signals of the second triazole carbon atoms are not observed for both compounds. The signals of the NO₂ groups are observed at chemical shifts of -21 ppm (**5**) and -17 ppm (**6**) in the ^{14}N NMR spectra. Additionally, the signal of the nitrogen atoms in 4 position (N₃, N₁₀) of the triazole rings is observed for **5** at -143 ppm. The bis(guanidinium) salt of **6** shows only two signals in the ^1H NMR and ^{13}C NMR spectra, respectively, at chemical shifts of 12.78 ppm (N_{tria}–H) and 7.38 ppm (G⁺) for the ^1H NMR and at 157.9 ppm (G⁺) and 156.3 ppm (C–N⁻–NO₂) in the ^{13}C NMR. The NO₂ group of the nitramine moiety in **7** is observed in the ^{14}N NMR spectra at -19 ppm. Due to the already mentioned bad solubility of all compounds, even the ionic ones, it was not possible to record ^{15}N NMR spectra in order to shed light on the chemical shifts of the nitrogen atoms, and hence to get more detailed and also reliable informations about the compounds structures.

10.2.3 Molecular Structures

The crystallization of neutral molecules with a large C–N backbone is not that easy, as experienced before with 5,5'-dinitramino-3,3'-azo-1,2,4-triazole and its ionic derivatives.^[8] For the triazene compounds presented in this study, it gets even worse. Neither the acetyl protected (**1**) nor the amine compound BATTH (**2**) could be crystallized from any solvent. The same occurred for 1,3-bis-[3-(5-nitramino-1*H*-1,2,4-triazolyl)]-triazene (**6**). Numerous attempts with water, alcoholic mixtures, DMF, DMSO or ethyl acetate at different temperatures as well as diffusion controlled crystallization with volatile solvents like diethyl ether always yielded **1**, **2** and **6** as amorphous powders. The ionic compounds **3** and **4** could be crystallized from the corresponding half concentrated acids, chloric and perchloric acid, respectively, due the incorporation of water molecules in the crystal structures and therefore the ability to form hydrogen bonded networks. 1,3-Bis-[3-(5-nitro-1*H*-1,2,4-triazolyl)]-triazene (**5**) could be crystallized from water after slow evaporation of the solvent over several days. The molecular structures of **3** – **5** are discussed shortly, focusing on the hydrogen bonding networks in all three compounds. A compilation of the crystallographic data of **3** – **5** can be found in Table S1 (Appendix 12.9).

1,3-Bis-[3-(5-amino-1*H*-1,2,4-triazolyl)]-triazene dihydrochloride (**3**) crystallizes as the monohydrate in the shape of colorless blocks in the monoclinic space group $P2_1/n$ with a cell volume of 1215.4(1) Å³ and four molecular moieties in the unit cell. The density of the compound is 1.640 g cm⁻³ and therefore a little bit higher than the non bridged 3,5-diamino-1,2,4-triazolium chloride hemihydrates (1.584 g cm⁻¹).^[20] The asymmetric unit of **3** is presented in Figure 1. All bond lengths and angles are as expected for the molecular moiety of **3**, with the N₆–N₇ bond being the shortest at 1.272(2) Å, and hence in the range of a formal double bond. The two triazole rings are nearly in plane (torsion angle 3.36°) with one another and hence indicate a big delocalized π -system for the backbone.

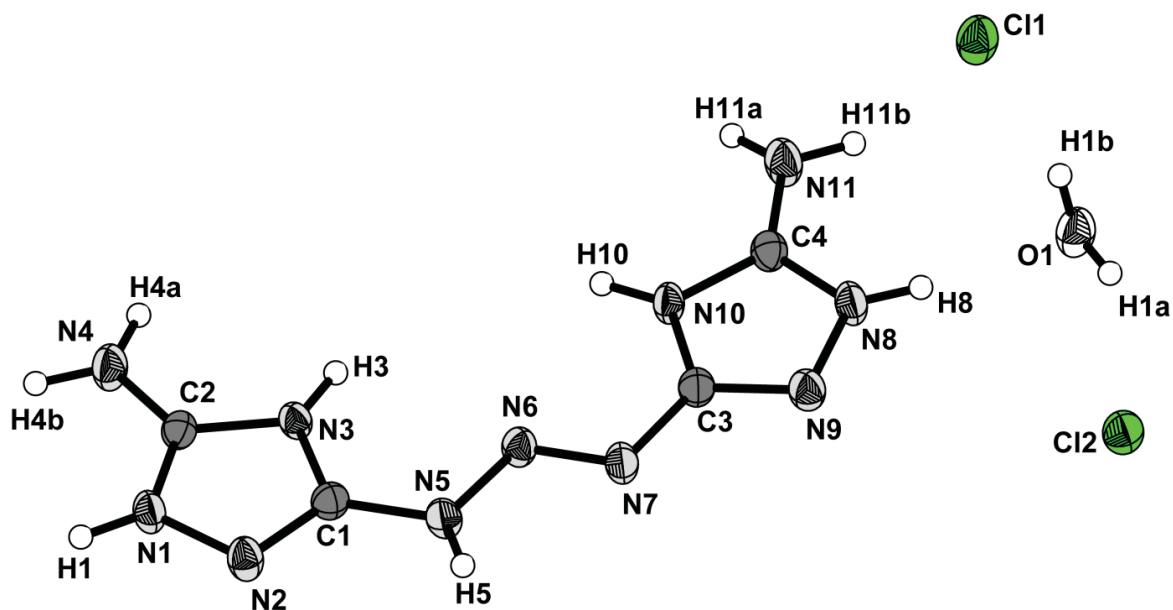


Figure 1: Asymmetric unit of **3**, thermal ellipsoids representing the 50 % probability level.

An extensive hydrogen bonded network is built up in nearly planar layers, arranged coplanar to the *bc* plane. Eleven individual hydrogen bonds are present within the layers, none of them exceeding the sum of van der Waals radii^[21] and therefore considered strong hydrogen bonds. Bifurcated hydrogen bonds are found with N₄ as the donor, N₄–H_{4b}⋯Cl₁(iii) being not only of electrostatic nature, but rather directed with a N₄–H_{4b}⋯Cl₁(iii) angle of 162°, while N₄–H_{4b}⋯N₇(ii) is more of electrostatic nature with a N₄–H_{4b}⋯N₇(ii) angle of only 108°. Cl₁ is also participating in two additional hydrogen bonds, N₅–H₅⋯Cl₁(iv) and N₁₁–H_{11a}⋯Cl₁(v), with both bonds being directed (169° and 149° for D–H⋯A angle) and below the sum of van der Waals radii at D–A distances of 3.144(2) Å and 3.242(2) Å, respectively. Cl₂ is located directly between the two triazole rings, connected with two hydrogen bonds, N₃–H₃⋯Cl₂(ii) and N₁₀–H₁₀⋯Cl₂(ii), both directed with angles of 174° and 179°, respectively and well below the sum of van der Waals radii ($r_w(\text{N}) + r_w(\text{Cl}) = 3.31 \text{ \AA}$)^[21] at 3.120(2) Å and 3.069(2) Å, respectively. The BATTH moieties are connected directly with nitrogen atoms working as both, donor and acceptor atoms, as found for N₄–H_{4a}⋯N₉(ii), N₄–H_{4b}⋯N₇(ii) and N₁₁–H_{11b}⋯N₂(vi). The water molecule is incorporated in hydrogen bonds using nitrogen atoms as donor atoms, N₁–H₁⋯O₁(i) and N₈–H₈⋯O₁, while it functions a donor itself for hydrogen bonds towards Cl₁ and Cl₂. All hydrogen bonds are compiled in detail in Table 1, while the hydrogen bonding scheme coplanar to the *bc* plane is presented in Figure 2.

Only one hydrogen bond connects the layer with one another, $O_1-H_{1b}\cdots Cl_1$ being well below the sum of van der Waals radii ($r_w(N) + r_w(Cl) = 3.31 \text{ \AA}$)^[21] with a donor acceptor distance of $3.077(2) \text{ \AA}$ and an $D-H\cdots A$ angle of 166° . The distance between the layers is 3.284 \AA and the stacking of the layers along the a -axis is shown in Figure 3.

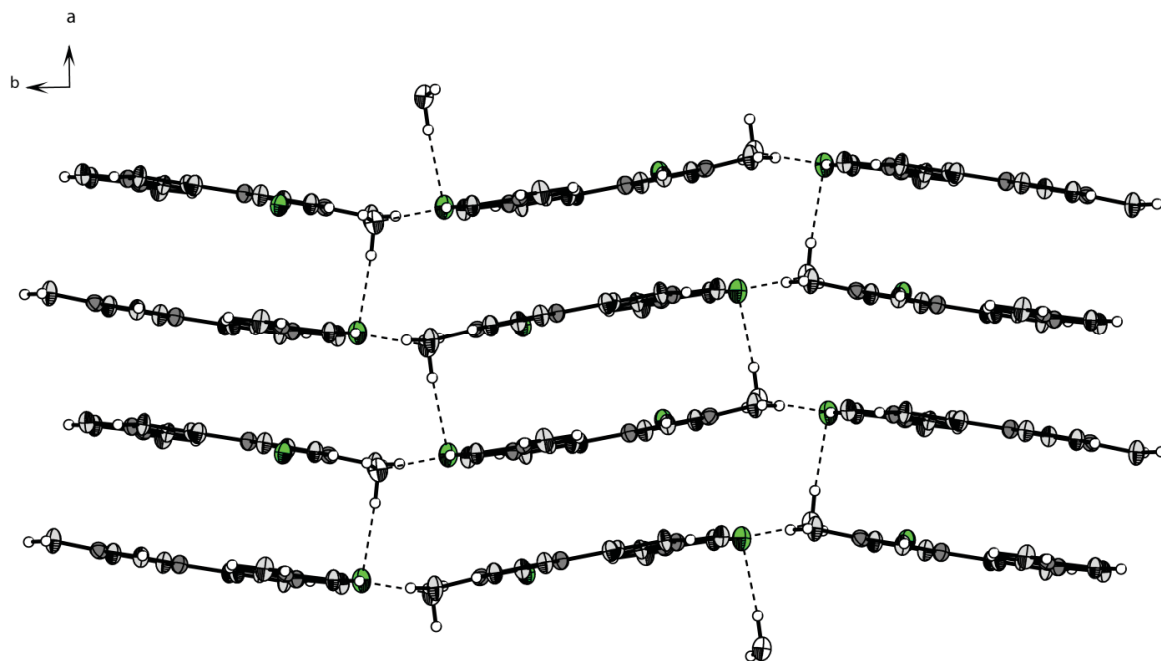


Figure 3: Layers of **3** stacked along the a -axis, connected by $O_1-H_{1b}\cdots Cl_1$ hydrogen bonds. Thermal ellipsoids represent the 50 % probability level.

1,3-Bis-[3-(5-amino-1*H*-1,2,4-triazolyl)]-triazene dihydroperchlorate (**4**) crystallizes also as the monohydrate in the shape of colorless blocks in the monoclinic space group $P2_1/n$ with a cell volume of $1467.4(1) \text{ \AA}^3$ and four molecular moieties in the unit cell. The density of the compound is 1.938 g cm^{-3} , being again a little bit higher than the non bridged 3,5-diamino-1,2,4-triazolium perchlorate (1.848 g cm^{-3}).^[20] The asymmetric unit of **4** is presented in Figure 4.

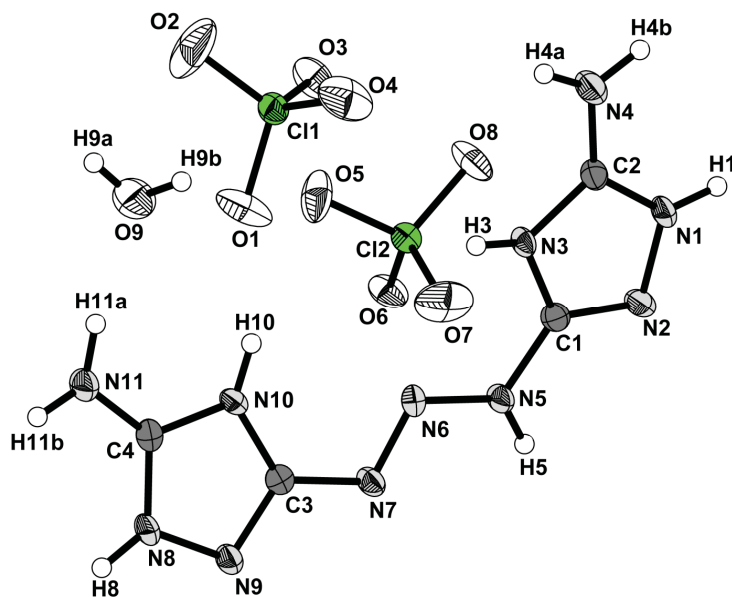


Figure 4: Asymmetric unit of **4**, thermal ellipsoids representing the 50 % probability level.

The structure of **4** consists of rows of BATTH^{2+} cations, held together by mainly three hydrogen bonds, two of them having nitrogen atoms as both, donor and acceptor atoms, $\text{N}_4\text{-H}_{4a}\cdots\text{N}_7(\text{vi})$, $\text{N}_4\text{-H}_{4b}\cdots\text{N}_9(\text{vi})$ and one with nitrogen as the donor atom and oxygen as the acceptor atom ($\text{N}_{11}\text{-H}_{11a}\cdots\text{O}_9$). The rows themselves are connected by six hydrogen bonds using the oxygen atoms of the perchlorate anions as acceptor atoms and are opposed to one another by 180° . Three of these hydrogen bonds, $\text{N}_8\text{-H}_8\cdots\text{O}_3(\text{i})$, $\text{N}_{11}\text{-H}_{11b}\cdots\text{O}_3(\text{i})$ and $\text{N}_9\text{-H}_9\cdots\text{O}_2(\text{viii})$ are moderately strong and show $\text{D}\cdots\text{A}$ distances well below the sum of van der Waals radii ($r_w(\text{O}) + r_w(\text{N}) = 3.07 \text{ \AA}$)^[21] at $2.776(3) \text{ \AA}$, $2.976(3) \text{ \AA}$ and $2.854(3) \text{ \AA}$, respectively. The $\text{D-H}\cdots\text{A}$ angles are between 138° and 145° . The three other hydrogen bonds, $\text{N}_1\text{-H}_1\cdots\text{O}_5(\text{v})$, $\text{N}_1\text{-H}_1\cdots\text{O}_1(\text{iv})$ and $\text{N}_4\text{-H}_{4b}\cdots\text{O}_5(\text{v})$ are right at or slightly higher than the sum of van der Waals radii at $\text{D}\cdots\text{A}$ distances of $3.052(3) \text{ \AA}$, $3.044(3) \text{ \AA}$ and $3.164(3) \text{ \AA}$ and show $\text{D-H}\cdots\text{A}$ angles between 129° and 136° . They are hence more of electrostatic nature and much weaker than the before mentioned ones. The hydrogen bonding pattern of **4** is shown in Figure 5.

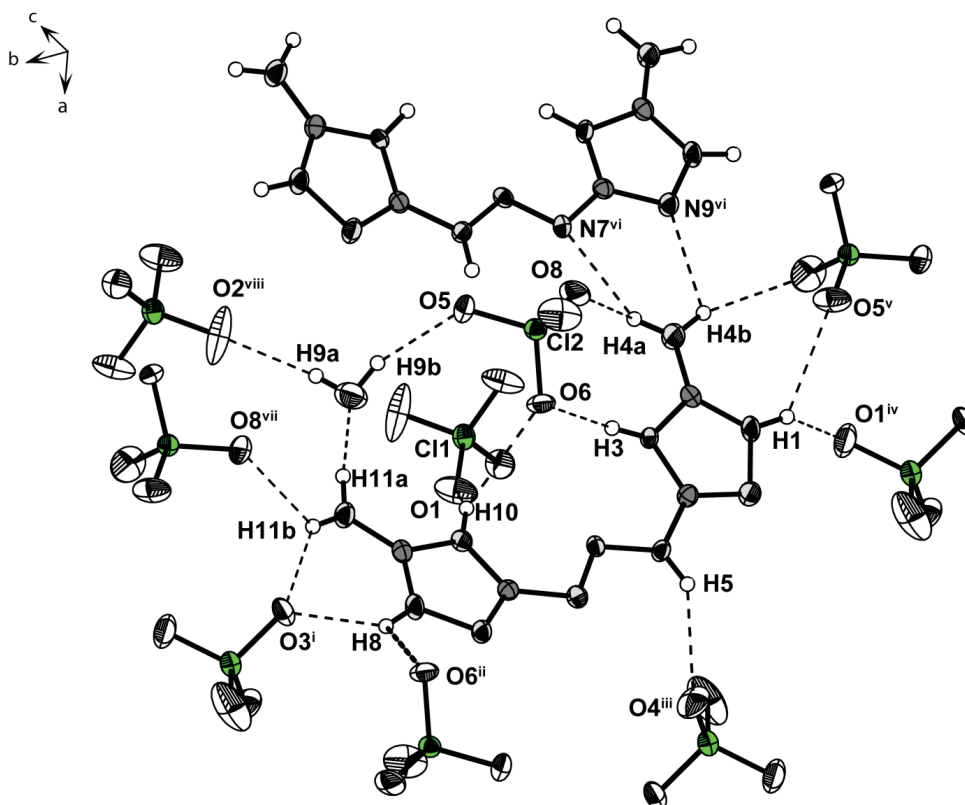


Figure 5: Hydrogen bonding scheme in the crystal structure of **4**, showing all present hydrogen bonds surrounding an asymmetric unit. Thermal ellipsoids represent the 50% probability level. Symmetry Operators: (i) $-x+3/2, y+1/2, -z+1/2$; (ii) $-x+1, -y+1, -z$; (iii) $x+1/2, -y+1/2, z-1/2$; (iv) $-x+3/2, y-1/2, -z+1/2$; (v) $-x+1/2, y-1/2, -z+1/2$; (vi) $x-1/2, -y+1/2, z+1/2$; (vii) $-x+1/2, y+1/2, -z+1/2$; (viii) $-x+1, -y+1, -z+1$.

Since perchlorate anions are not planar but three dimensional anions, they are not placed within the layers, and hence lie below (Cl_1) and above (Cl_2) the layers spanned by the BATTH^{2+} rows. The before mentioned six hydrogen bonds are formed with oxygen atoms placed within or near the layers, while all other hydrogen bonds formed by the perchlorate anions connect the bands to one another. Nearly all of the remaining hydrogen bonds show $\text{D}\cdots\text{A}$ distances below the sum of van der Waals radii with only one hydrogen bond, $\text{N}_4\text{-H}_{4a}\cdots\text{O}_8$, showing a longer $\text{D}\cdots\text{A}$ distance at 3.195(3) Å. All hydrogen bonds are compiled in Table 2, while the stacking of the layers is shown perpendicular to the ac plane with the perchlorate anions situated between the layers in Figure 6.

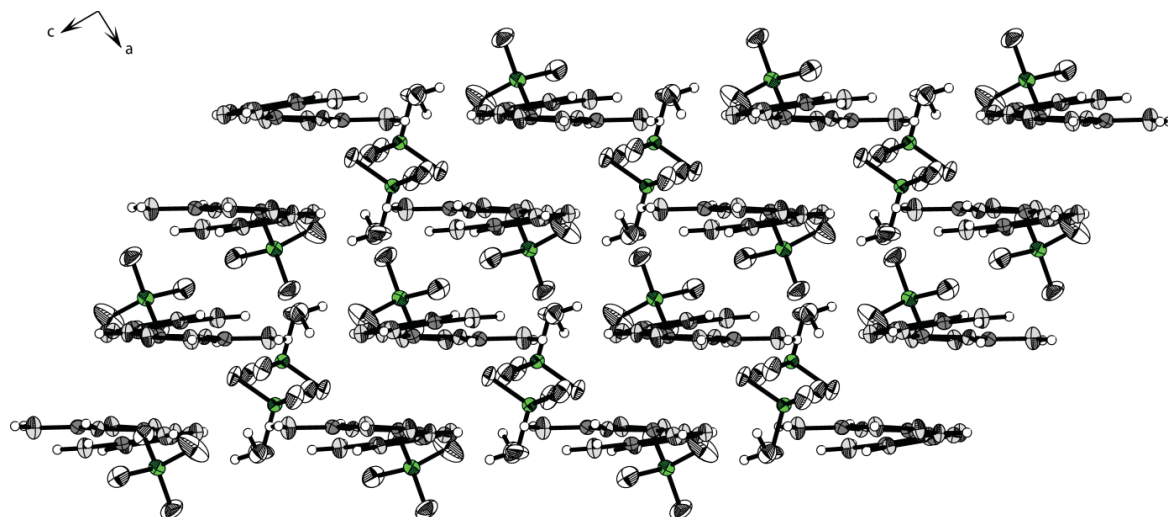


Figure 6: Layers of **4** shown perpendicular to the *ac* plane with perchlorate anions connecting the layers. Thermal ellipsoids represent the 50 % probability level.

Table 2: Hydrogen bonds present in the crystal structure of **4**.

D–H···A	d (D–H) [Å]	d (H · A) [Å]	d (D–H · A) [Å]	<(D–H···A) [°]
N3–H3···O6	0.84(2)	2.10(2)	2.901(3)	160(3)
N10–H10···O1	0.84(2)	2.19(2)	2.878(3)	140(2)
N10–H10···O6	0.84(2)	2.51(2)	3.051(3)	123(2)
N8–H8···O3 ⁱ	0.84(2)	2.10(2)	2.776(3)	138(3)
N8–H8···O6 ⁱⁱ	0.84(2)	2.53(3)	3.042(3)	120(2)
N5–H5···O4 ⁱⁱⁱ	0.84(2)	2.29(2)	2.979(3)	140(3)
N1–H1···O1 ^{iv}	0.85(2)	2.35(2)	3.044(3)	139(2)
N1–H1···O5 ^v	0.85(2)	2.45(2)	3.052(3)	129(2)
N4–H4a···N7 ^{vi}	0.84(2)	2.37(2)	3.055(3)	138(2)
N4–H4a···O8	0.84(2)	2.57(2)	3.195(3)	132(2)
N11–H11b···O3 ⁱ	0.84(2)	2.28(2)	2.976(3)	141(3)
N11–H11b···O8 ^{vii}	0.84(2)	2.47(2)	3.058(3)	128(2)
N4–H4b···N9 ^{vi}	0.85(2)	2.45(3)	2.971(3)	120(2)
N4–H4b···O5 ^v	0.85(2)	2.50(2)	3.164(3)	136(2)
N11–H11a···O9	0.89(2)	1.87(2)	2.749(3)	173(3)
O9–H9a···O2 ^{viii}	0.80(2)	2.16(3)	2.854(3)	145(5)
O9–H9b···O5	0.82(2)	2.11(2)	2.887(3)	157(4)

Symmetry Operators: (i) $-x+3/2, y+1/2, -z+1/2$; (ii) $-x+1, -y+1, -z$; (iii) $x+1/2, -y+1/2, z-1/2$; (iv) $-x+3/2, y-1/2, -z+1/2$; (v) $-x+1/2, y-1/2, -z+1/2$; (vi) $x-1/2, -y+1/2, z+1/2$; (vii) $-x+1/2, y+1/2, -z+1/2$; (viii) $-x+1, -y+1, -z+1$.

1,3-Bis-[3-(5-nitro-1*H*-1,2,4-triazolyl)]-triazene (**5**) crystallizes in the monoclinic space group $P2_1/c$ as the monohydrate in the shape of yellow blocks presenting four molecular moieties in the unit cell at a cell volume of 1159.6(1) Å³. Compound **5** crystallizes with a density of 1.748 g cm⁻³, being in the range of other nitro substituted derivatives of 1,2,4-

triazoles, for example 5-amino-3-nitro-1*H*-1,2,4-triazole displaying a density of 1.841 g cm⁻³ (water free) and 1.682 g cm⁻³ for the monohydrate, respectively. The asymmetric unit of **5** is presented in Figure 7.

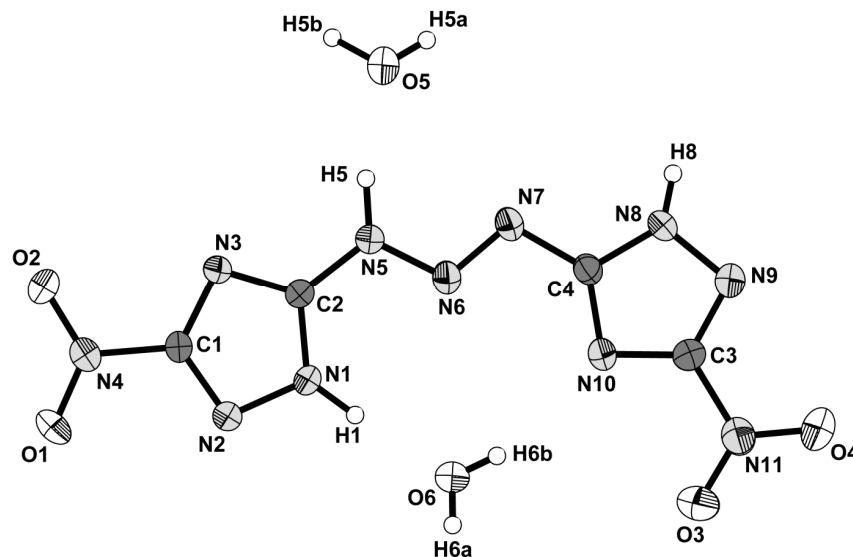


Figure 7: Asymmetric unit of **5**, thermal ellipsoids representing the 50 % probability level.

The hydrogen bonded network in **5** is only two dimensional, building up layers of DNBATTH molecules partially involving the crystal water molecules. Only two hydrogen bonds in this system are slightly longer than the sum of van der Waals radii ($r_w(\text{O}) + r_w(\text{N}) = 3.07 \text{ \AA}$; $r_w(\text{N}) + r_w(\text{N}) = 3.10 \text{ \AA}$)^[21] for the D···A distances at 3.221(2) Å, N₈–H₈···O₂(i) and at 3.138(2) Å for O₅–H_{5b}···O₄(ii). Both donor atoms of the hydrogen bonds, N₈ and O₅ show bifurcated hydrogen bonds to two acceptor atoms, explaining the slightly elongated distance and the smaller D–H···A angles of 131° and 140°, respectively. The two other parts of the bifurcated hydrogen bonds, N₈–H₈···N₃(i) and O₅–H_{5b}···N₉(ii), show much shorter D···A distances of 2.952(2) Å and 2.891(2) Å, respectively. The D–H···A angles are also closer to 180° being 158° and 144°, respectively. All hydrogen bonds within the layers are presented in Figure 8. The compilation of the all hydrogen bonds in this structure is displayed in Table 3.

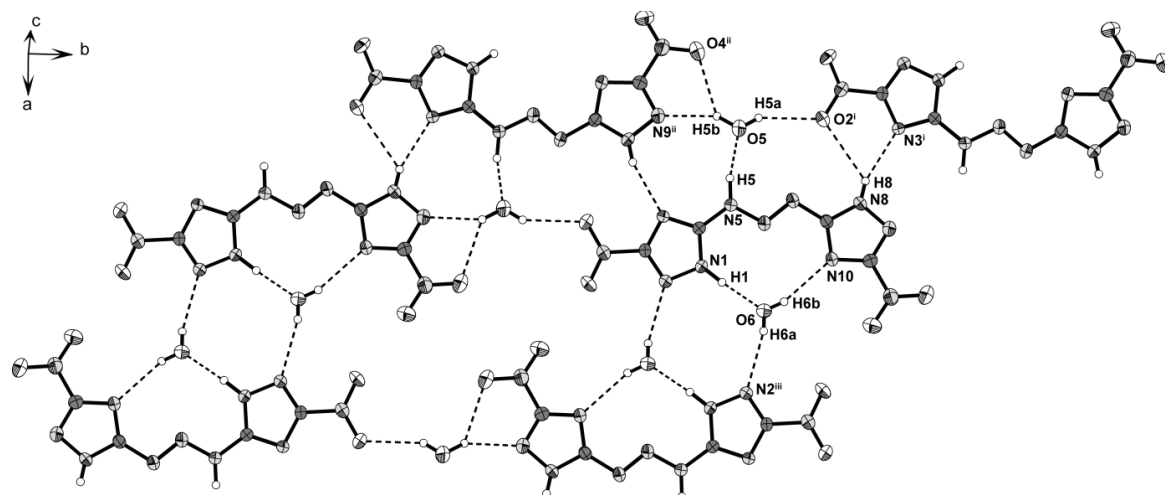


Figure 8: Hydrogen bonding scheme in **5** within the layers. Thermal ellipsoids represent the 50 % probability level. Symmetry Operators: (i) $-x+1, y+1/2, -z+3/2$; (ii) $-x+1, y-1/2, -z+3/2$; (iii) $-x+2, -y, -z+1$.

Table 3: Hydrogen bonds present in the crystal structure of **5**.

D–H⋯A	d (D–H) [Å]	d (H⋯A) [Å]	d (D–H⋯A) [Å]	< (D–H⋯A) [°]
N1–H1⋯O6	0.98(2)	1.70(2)	2.683(2)	176(2)
N5–H5⋯O5	1.02(2)	1.68(2)	2.683(2)	168(2)
N8–H8⋯N3 ⁱ	0.82(2)	2.18(2)	2.952(2)	158(2)
N8–H8⋯O2 ⁱ	0.82(2)	2.63(2)	3.221(2)	131(2)
O5–H5a⋯O2 ⁱ	0.82(2)	2.22(2)	2.950(2)	150(2)
O5–H5b⋯N9 ⁱⁱ	0.86(2)	2.15(2)	2.891(2)	144(2)
O5–H5b⋯O4 ⁱⁱ	0.86(2)	2.43(2)	3.138(2)	140(2)
O6–H6a⋯N2 ⁱⁱⁱ	0.79(2)	2.23(2)	2.945(2)	152(3)
O6–H6b⋯N10	0.80(2)	2.25(2)	2.992(2)	154(2)

Symmetry Operators: (i) $-x+1, y+1/2, -z+3/2$; (ii) $-x+1, y-1/2, -z+3/2$; (iii) $-x+2, -y, -z+1$.

The layers themselves are, as mentioned before, not connected by hydrogen bonds but held together by two short nitrogen/oxygen interactions formed by one of the NO₂ groups (N₂). The contacts are not very strong, but right at the sum of van der Waals radii^[21] at distances of 3.056(6) Å (O₁⋯N₄) and 3.144(6) Å (N₄⋯O₂). The symmetry operator generating these two contacts is $x, -y-1/2, z-1/2$ for the layer underneath and $x, -y-1/2, z+0.5$ for the layer above. As one can see from these operators, the layers are stacked along the *c*-axis. The gap between the layers was measured to be 3.201 Å. The shorts N/O contacts between the layers are shown in Figure 9, while the stacking of the layers is presented in Figure 10.

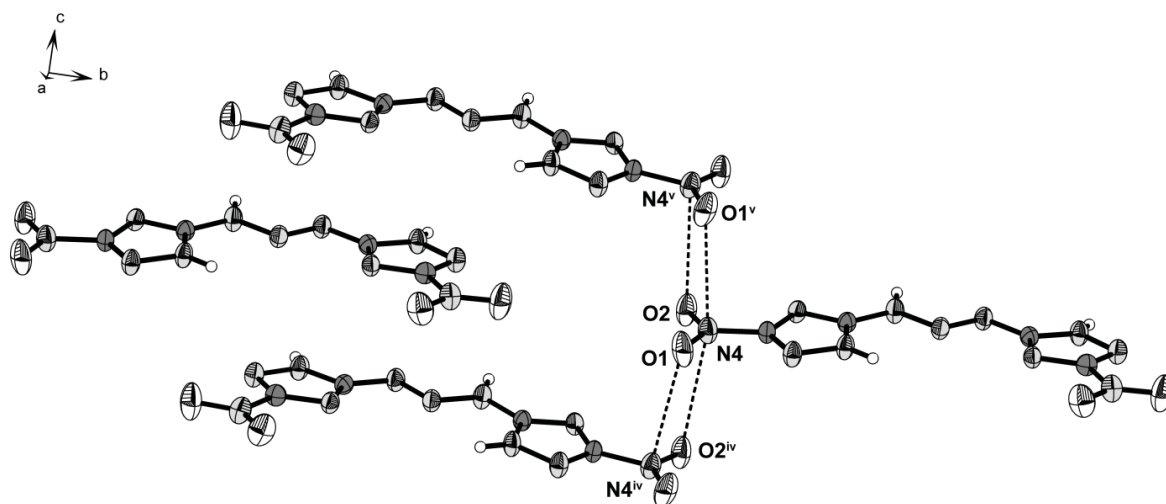


Figure 9: Short N/O contacts connecting the layers of **5**. Thermal ellipsoids represent the 50 % probability level. Symmetry operators: $(iv) x, -y-1/2, z-1/2$; $(v) x, -y-1/2, z+0.5$.

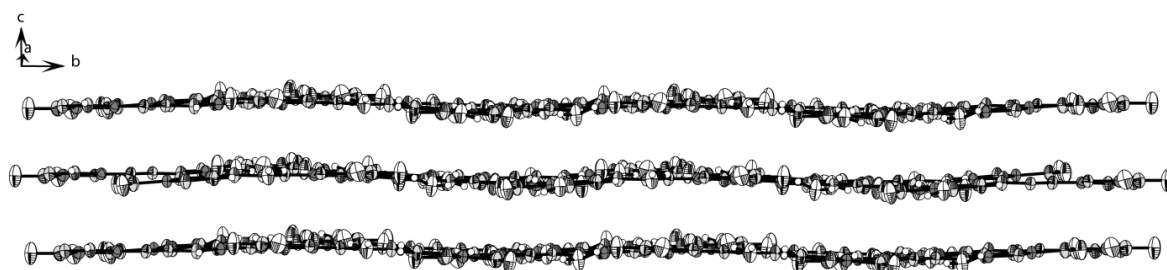


Figure 10: Layers of **5** stacked along the c -axis. Thermal ellipsoids represent the 50 % probability level.

10.2.4 Physical Properties.

Our goal with the synthesis of the triazene bridged 1,2,4-triazoles, carrying either nitro or nitramino substituents, was a gain in thermal stability as well as in sensitivity values. The neutral BATTH (**2**) showed some promising signs with the thermal stability only slightly lower than the one of 5,5'-diamino-3,3'-azo-1*H*-1,2,4-triazole at 177 °C. But as observed for non bridged triazoles like 5-nitramino-3-nitro-1*H*-1,2,4-triazole,^[22] the thermal stabilities dropped to a lower level on nitration of **2** or the exchange of the amine with nitro substituents. The decomposition temperature of **5** (DNBATTH) is only 136 °C while the one of **6** (DNIBATTH) is even lower at 123 °C and hence more than 80 °C below the 5,5'-dinitramino-3,3'-azo-1*H*-1,2,4-triazole,^[8] our benchmark molecule. Even the double deprotonation of **6** with guanidine, usually exhibiting the highest thermal stability values, failed. The decomposition temperature could only be increased to 147 °C. Even though **7** displays very low sensitivities with 35 J for impact and 360 N for friction sensitivity, the

much too low thermal stabilities makes these class of compounds not useful for application by any means. Hence no theoretical calculations of the detonation parameters have been performed for these compounds.

10.3 Conclusion

A novel synthetic route for BATTH has been developed by utilizing the acetyl protected 3,5-diamino-1*H*-1,2,4-triazole as the starting material. The four step reaction process yields BATTH in yields of 64 % and hence nearly doubles the literature known synthesis route. Subsequent exchange of the amine groups with sodium nitrite in sulfuric acid yielded **5** in small yields of only 24 % due to solubility problems of BATTH. Compound **6** was synthesized by applying standard nitration procedures using concentrated sulfuric and 100 % nitric acid in 57 % yield. The corresponding bis(guanidinium) salt of **6** was synthesized by deprotonating **6** with guanidinium carbonate at elevated temperatures. Neither the energetic salts of **2** (nitrate and dinitramide salts) nor the nitrogen rich triaminoguanidinium salt of **6** could be prepared. All described compounds have been fully characterized by means of vibrational and multinuclear NMR spectroscopy. Single crystal X-ray diffraction measurements could only be performed of **3**, **4** and **5** due to solubility problems. Additionally, the thermal stabilities of all compounds and the sensitivity values of **2**, **5**, **6** and **7** have been determined. Although the compounds show remarkable stability against outer stimuli, they are not stable against thermal stress, decomposing at 123 °C (**6**), 136 °C (**5**) and 147 °C (**7**). Since much better thermal stabilities have been measured for the azo bridged compounds presented in Chapter 9 together with low sensitivities, a thoroughly investigation of the detonation parameters by theoretical calculations has been omitted.

10.4 Experimental Part

General. All chemical reagents and solvents were obtained from Sigma-Aldrich Inc. or Acros Organics (analytical grade) and were used as supplied without further purification. ^1H , $^{13}\text{C}\{^1\text{H}\}$, and $^{14}\text{N}\{^1\text{H}\}$ NMR spectra were recorded on a JEOL Eclipse 400 instrument in DMSO- d_6 at or near 25 °C. The chemical shifts are given relative to tetramethylsilane (^1H , ^{13}C) or nitro methane (^{14}N) as external standards and coupling constants are given in Hertz (Hz). Infrared (IR) spectra were recorded on a Perkin-Elmer Spectrum BX FT-IR

instrument equipped with an ATR unit at 25 °C. Transmittance values are qualitatively described as “very strong” (vs), “strong” (s), “medium” (m), “weak” (w) and “very weak” (vw). RAMAN spectra were recorded on a Bruker RAM II spectrometer equipped with a Nd:YAG laser operating at 1064 nm and a reflection angle of 180°. The intensities are reported as percentages of the most intense peak and are given in parentheses. Elemental analyses (CHNO) were performed with a Netzsch Simultaneous Thermal Analyzer STA 429. Melting and decomposition points were determined by differential scanning calorimetry (Linseis PT 10 DSC, calibrated with standard pure indium and zinc). Measurements were performed at a heating rate of 5 °C min⁻¹ in closed aluminum sample pans with a 1 µm hole in the top for gas release to avoid an unsafe increase in pressure under a nitrogen flow of 20 mL min⁻¹ with an empty identical aluminum sample pan as a reference.

For initial safety testing, the impact and friction sensitivities as well as the electrostatic sensitivities were determined. The impact sensitivity tests were carried out according to STANAG 4489,^[23] modified according to WIWEB instruction 4-5.1.02^[24] using a BAM^[25] drop hammer. The friction sensitivity tests were carried out according to STANAG 4487^[26] and modified according to WIWEB instruction 4-5.1.03^[27] using the BAM friction tester. The electrostatic sensitivity tests were accomplished according to STANAG 4490^[28] using an electric spark testing device ESD 2010EN (OZM Research) operating with the “Winspark 1.15 software package”.^[29]

Crystallographic measurements. The single crystal X-ray diffraction data of **3 – 5** were collected using an Oxford Xcalibur3 diffractometer equipped with a Spellman generator (voltage 50 kV, current 40 mA) and a KappaCCD detector. The data collection was undertaken using the CRYVALIS CCD software^[30] while the data reduction was performed with the CRYVALIS RED software.^[31] The structures were solved with SHELXS-97^[32] and refined with SHELXL-97^[33] implemented in the program package WinGX^[34] and finally checked using PLATON.^[35]

1-Acetyl-3,5-diamino-1,2,4-triazole

3,5-Diamino-1*H*-1,2,4-triazole (36 g, 364 mmol) was suspended in 130 mL water and acetic anhydride (40.8 mL, 431.6 mmol) was added dropwise under stirring. After further stirring for one hour the precipitate was filtered off, washed with 600 mL water and dried

on air. 1-Acetyl-3,5-diamino-1,2,4-triazole was obtained as a white powder with 98 % yield.

^1H NMR (DMSO- d_6 , 25 °C) δ (ppm) = 7.35 (s, 2H, NH_2), 5.63 (s, 2H, NH_2), 2.33 (s, 3H, CH_3); $^{13}\text{C}\{^1\text{H}\}$ NMR (DMSO- d_6 , 25 °C) δ (ppm) = 170.5 (C=O), 162.2 ($\text{C}^1\text{-NH}_2$), 157.0 (s, $\text{C}^2\text{-NH}_2$), 23.56 ($-\text{CH}_3$); IR (ATR, 25 °C, cm^{-1}) ν = 3416 (m), 3390 (vs), 3298 (m), 3225 (m), 3178 (s), 3133 (s), 3018 (m), 1710 (vs), 1641 (vs), 1569 (s), 1449 (m), 1393 (s), 1366 (vs), 1337 (s), 1178 (m), 1135 (m), 1117 (m), 1066 (m), 1044 (m), 973 (w), 839 (w), 758 (w), 732 (vw), 700 (w), 669 (w), 653 (w); RAMAN (Nd:YAG, 1064 nm, cm^{-1}) ν = 3415 (8), 3406 (9), 3221 (17), 3186 (16), 3136 (15), 3125 (15), 3023 (53), 2990 (25), 2935 (100), 1712 (91), 1642 (37), 1568 (40), 1550 (22), 1460 (8), 1426 (19), 1397 (35), 1376 (33), 1341 (36), 1182 (30), 1118 (21), 1077 (4), 1037 (33), 972 (17), 840 (20), 771 (7), 669 (38), 589 (12), 578 (14), 446 (37), 400 (12), 345 (28), 225 (14); m/z : (DEI+): 43.06 (28), 99.09 (100), 141.1 (22) [M^+].

5-Acetamido-3-amino-1*H*-1,2,4-triazole

1-Acetyl-3,5-diamino-1,2,4-triazole (25 g, 177.3 mmol) was suspended in 250 mL decahydro-naphthalene and refluxed at 270 °C for 6 h. After cooling to ambient temperature, the precipitate was filtered off, washed with isohexane (400 mL) and diethyl ether (600 mL) yielding 99 % (24.75 g) 5-acetamido-3-amino-1*H*-1,2,4-triazole as a white powder.

^1H NMR (DMSO- d_6 , 25 °C) δ (ppm) = 12.93 (br. s, 1H, N_{TriazH}), 9.72 (br. s, 1H, NH-CO), 5.11 (br. s, 2H, NH_2), 2.00 (s, 3H, CH_3); $^{13}\text{C}\{^1\text{H}\}$ NMR (DMSO- d_6 , 25 °C) δ (ppm) = 168.5 (C=O), 22.2 ($-\text{CH}_3$); IR (ATR, 25 °C, cm^{-1}) ν = 3423 (m), 3251 (vs), 3116 (m), 3024 (m), 2956 (m), 2874 (m), 2827 (m), 1683 (vs), 1597 (vs), 1583 (vs), 1452 (s), 1380 (w), 1361 (m), 1296 (s), 1269 (m), 1081 (s), 1024 (m), 1006 (m), 832 (w), 818 (m), 760 (vw), 714 (m), 687 (m); RAMAN (Nd:YAG, 1064 nm, cm^{-1}) ν = 3321 (3), 3252 (6), 3222 (3), 2934 (43), 1684 (100), 1648 (14), 1586 (61), 1537 (11), 1457 (14), 1366 (28), 1297 (7), 1261 (9), 1155 (4), 1085 (48), 1027 (46), 971 (28), 819 (11), 739 (13), 693 (5), 591 (40), 494 (13), 364 (14), 324 (27), 183 (26), 128 (135); EA ($\text{C}_4\text{H}_7\text{N}_5\text{O}$) calcd.: C, 34.04; H, 5.00; N, 49.62; found: C, 34.11; H, 4.86; N, 49.12.

1,3-Bis-[3-(5-acetamido-1*H*-1,2,4-triazolyl)]-triazene (AcetBATTH, **1**)

5-Acetamido-3-amino-1*H*-1,2,4-triazole (3.19 mmol, 0.45 g) was suspended in 2 mL water and cooled to 0°C with stirring. After adding concentrated hydrochloric acid (0.25 mL, 1 eq) a white slurry formed which was diluted with 13 mL water. A solution of sodium nitrite (1.59 mmol, 0.11 g, 0.5 eq.) in 5 mL water was added dropwise. A yellow reaction mixture formed which was stirred at ambient temperature overnight. After 24 hours the reaction mixture was filtered off, washed with water (2 x 50 mL) and 100 mL diethyl ether and dried on air. A yellow solid was obtained yielding 0.41 g (78%) of pure 1,3-bis-[3-(5-acetamido-1*H*-1,2,4-triazolyl)]-triazene.

The reaction described was scaled up to 71 mmol (10 g) of 5-acetamido-3-amino-1*H*-1,2,4-triazole yielding 9.45 g (81%) of pure 1,3-bis-[3-(5-acetamido-1*H*-1,2,4-triazolyl)]-triazene.

T_{dec.}: 189 °C (DSC, Onset, 5 °C min⁻¹); ¹H NMR (DMSO-*d*₆, 25 °C) δ (ppm) = 12.92 (s, 1H), 11.47 (s, 1H), 2.09 (s, 6H, -CH₃); ¹³C{¹H} NMR (DMSO-*d*₆, 25 °C) δ (ppm) = 169.6 (C=O), 149.1, 23.4 (-CH₃); IR (ATR, 25 °C, cm⁻¹) ν = 3380 (m), 3206 (s), 3028 (s), 2879 (m), 2827 (m), 1687 (m) 1579 (m), 1532 (s), 1411 (m), 1354 (m), 1248 (m), 1210 (m), 1150 (m), 1150 (m), 1073 (w), 1003 (w), 812 (w), 747 (w), 698 (w); RAMAN (Nd:YAG, 1064 nm, cm⁻¹) ν = 3238 (1), 2936 (4), 1702 (7), 1596 (28), 1551 (8), 1477 (100), 1424 (3), 1379 (4), 1361 (10), 1269 (1), 1205 (3), 1157 (4), 1080 (6), 965 (3), 926 (2), 804 (1), 748 (2), 707 (1), 651 (1), 597 (2), 502 (5), 447 (2), 330 (1), 270 (1), 243 (1); EA (C₈H₁₁ N₁₁ O₂ · 2 H₂O) (329.1): calcd.: C, 29.18; H, 4.59; N, 46.79; O, 19.44; found: C, 29.56, H, 4.37, N, 46.49.

1,3-Bis-[3-(5-amino-1*H*-1,2,4-triazolyl)]-triazene (BATTH, **2**)

AcetBATTH (1.51 mmol, 0.5 g) was suspended in 3 mL hydrazine hydrate. The resulting red suspension was stirred and heated to 80°C under reflux conditions. After a few minutes an orange slurry formed which developed into a clear orange solution with proceeded heating. The reaction solution was stirred at this elevated temperature for 2 hours and was afterwards cooled down to ambient temperature. The chilled mixture was diluted with 3 mL water and the pH value was adjusted to 9 with 10 % hydrochloric acid.

A yellow precipitate formed, which was filtered off and washed extensively with water. The product was dried at 60 °C to yield 0.30 g (81 %) BATTH as the dihydrate.

$T_{\text{dec.}}$: 177 °C (DSC, Onset, 5 °C min⁻¹); ¹H NMR (DMSO-*d*₆, 25 °C) δ (ppm) = 8.35 (s, br, 1H), 6.16 (s, 4H, -NH₂); ¹³C{¹H} NMR (DMSO-*d*₆, 25 °C) δ (ppm) = 156.7; IR (ATR, 25 °C, cm⁻¹) ν = 3213 (m), 3034 (m), 2939 (m), 1693 (m), 1586 (m), 1541 (s), 1475 (w), 1415 (m), 1360 (m), 1333 (w), 1254 (m), 1213 (m), 1158 (m), 1076 (w), 1007 (w), 956 (vw), 811 (w), 750 (w), 699 (w), 647 (w), 595 (w); RAMAN (Nd:YAG, 1064 nm, cm⁻¹) ν = 2990 (1), 1656 (3), 1581 (24), 1525 (44), 1454 (12), 1438 (100), 1378 (80), 1289 (2), 1122 (10), 1101 (3), 1040 (5), 964 (3), 928 (8), 805 (2), 762 (2), 517 (5), 426 (5), 367 (3), 304 (3), 282 (3), 282 (4); m/z (DCI+): 210.1 [M+H⁺]; EA (C₄H₇N₁₁ · H₂O) calcd.: C, 21.15; H, 3.99; N, 67.82; O, 7.04 ; found: C, 21.72; H, 3.76; N, 68.32; Sensitivities (anhydrous) (grain size: < 100 μ m): IS: 10 J; FS: 360 N; ESD: 80 mJ.

1,3-Bis-[3-(5-amino-1*H*-1,2,4-triazolyl)]-triazene dihydrochloride dihydrate (**3**)

5-Amino-3-nitrosamino-1*H*-1,2,4-triazole (0.5 g, 3.9 mmol) was dissolved in concentrated hydrochloric acid (12.5 mL) and cooled to 0 °C. To the stirred solution, 3,5-diamino-1*H*-1,2,4-triazole (386 mg, 1eq), dissolved in 12.5 mL water, was added dropwise and stirring continued for one hour. An orange precipitate formed, which was isolated by filtration. From the mother liquor a second fraction of product was isolated as light yellow crystals, suitable for X-ray diffraction measurements. Overall yield: 0.39 g, 1.22 mmol, 31%.

$T_{\text{dec.}}$: 176 °C (DSC, Onset, 5 °C min⁻¹); ¹H-NMR (DMSO-*d*₆, 25 °C): δ (ppm) = 6.27 (s, v br., -NH₂); ¹³C{¹H} NMR (DMSO-*d*₆, 25 °C): δ (ppm) = 157.0, 151.0; IR (ATR, 25 °C, cm⁻¹) ν = 3318 (m), 3278 (m), 3213 (s), 3143 (s), 2997 (m), 2694 (s), 2625 (s), 2512 (s), 1697 (m), 1678 (m), 1641 (s), 1589 (m), 1486 (s), 1419 (m), 1388 (m), 1343 (m), 1295 (w), 1243 (s), 1131 (m), 1112 (m), 1032 (m), 1012 (m), 903 (m), 796 (w), 728 (w), 713 (m), 681 (m); Raman (Nd:YAG, 1064 nm, 25 °C, cm⁻¹) ν = 3156 (1), 1703 (7), 1680 (6), 1647 (65), 1581 (71), 1547 (7), 1511 (4), 1489 (100), 1425 (26), 1353 (2), 1327 (11), 1296 (35), 1131 (19), 1116 (6), 1063 (8), 133 (2), 1015 (3), 906 (10), 798 (4), 741 (8), 529 (5), 439 (1), 227 (2), 368 (3), 337 (2), 300 (3), 272 (9); m/z (FAB+): 210.3 (5) [M+H⁺]; EA: (C₄H₉Cl₂N₁₁ · 2 H₂O) calcd.: C, 15.10; H, 4.12; N, 48.43; found: C, 15.31; H, 4.01; N, 48.00.

1,3-Bis-[3-(5-amino-1*H*-1,2,4-triazolyl)]-triazene dihydroperchlorate dihydrate (**4**)

2 (1 mmol, 0.209 g) was dissolved in half concentrated perchloric acid at 50 °C, stirred for 30 minutes and cooled down to ambient temperature afterwards. After 30 minutes a white precipitate began to form. After 24 hours the precipitate was filtered off, rejected and the mother liquor left standing on air. Crystals suitable for X-ray diffraction studies deposited after two days. Yield: 240 mg, 0.74 mmol, 74%.

¹H NMR (DMSO-*d*₆, 25 °C) δ (ppm) 13.08 (s, 2H, NH), 7.13 (s, 1H), 4.67 (s, 4H, -NH₂); ¹³C{¹H} NMR (DMSO-*d*₆, 25 °C) δ (ppm) 154.0, 153.2; IR (ATR, 25 °C, cm⁻¹) ν = 3436 (w), 3399 (w), 3300 (m), 3269 (w), 3184 (m), 3086 (m), 3048 (m), 2962 (w), 1686 (s), 1653 (s), 1604 (w), 1584 (vw), 1542 (vw), 1518 (vw), 1482 (s), 1444 (w), 1412 (w), 1367 (vw), 1247 (m), 1138 (s), 1110 (s), 1096 (s), 1042 (s), 1011 (s), 933 (m), 919 (m), 898 (m), 793 (vw), 746 (w), 718 (w), 698 (w); RAMAN (Nd:YAG, 1064 nm, cm⁻¹) ν = 3135 (1), 1703 (3), 1658 (52), 1587 (80), 1540 (3), 1491 (100), 1461 (4), 1412 (6), 1317 (8), 1294 (22), 1128 (9), 1109 (3), 1049 (6), 1010 (2), 939 (12), 903 (7), 798 (2), 743 (4), 336 (2), 518 (6), 464 (1), 431 (2), 360 (4), 333 (2), 289 (3), 256 (4); *m/z*: (FAB+): 210.1 [C₄H₈N₁₁⁺]; (FAB-): 407.9 [C₄H₈N₁₁Cl₂O₈⁻], 99.0 [ClO₄⁻]; EA (C₄H₉N₁₁Cl₂O₈ · 2 H₂O) calc.: C, 11.22; H, 2.59; N, 35.99; found: C, 11.44; H, 2.33; N, 36.04.

1,3-Bis-[3-(5-nitro-1*H*-1,2,4-triazolyl)]-triazene (DNBATTH, **5**)

BATTH (4.02 mmol, 1 g) was suspended in 20 % sulfuric acid (5.06 mL, 3 eq.) and the suspension added dropwise to a solution of sodium nitrite (120.6 mmol, 8.32 g, 30 eq.) in 50 mL water at 30 °C. After complete addition, the reaction mixture was heated to 80 °C and kept at this temperature for 4 hours. The chilled red suspension was then filtrated (polymeric byproduct: 150 mg) and the resulting clear, yellow filtrate was extracted with ethyl acetate (3 x 200 mL). The combined organic phases were dried over magnesium sulfate and concentrated via rotary evaporation. The resulting residue was recrystallized from water, yielding 0.27 g (24 %) yellow crystals, suitable for X-ray diffraction measurements.

T_{dec.}: 136 °C (DSC, Onset, 5 °C min⁻¹); ¹H NMR (DMSO-*d*₆, 25 °C) δ (ppm) = 8.85 (s, 1H); ¹³C{¹H} NMR (DMSO-*d*₆, 25 °C) δ (ppm) = 160.5 (C-NO₂); ¹⁴N NMR (DMSO-*d*₆, 25 °C) δ (ppm) = -21 (-NO₂), -143; IR (ATR, 25 °C, cm⁻¹) ν = 3588 (w), 3466 (m), 3370

(m), 3213 (m), 1699 (w), 1629 (m), 1561 (vs), 1495 (s), 1316 (w), 1369 (m), 1307 (s), 1217 (vw), 1171 (vw), 1089 (vw), 1021 (w), 1005 (vw), 838 (m), 823 (m), 764 (vw), 713 (vw), 649 (w); RAMAN (Nd:YAG, 1064 nm, cm^{-1}) ν = 1623 (32), 1507 (42), 1481 (100), 1433 (68), 1414 (45), 1381 (66), 1313 (22), 1176 (14), 1161 (29), 1076 (8), 1050 (6), 1023 (8), 908 (7), 842 (3), 764 (2), 458 (3), 357 (2), 285 (4); m/z : (DEI+): 169.0 (13) [DNBATTH(CHN_4O_2)⁺]; Sensitivities (anhydrous): IS: nd.; FS: nd.; ESD: nd..

1,3-Bis-[3-(5-nitramino-1*H*-1,2,4-triazolyl)]-triazene (DNIBATTH, **6**)

BATTH (4.08 mmol, 1 g) was added in small portions to 7 mL concentrated sulfuric acid at 0°C. The educt dissolved completely after about 5 minutes. 100 % HNO_3 (0.8 mL) was added dropwise over the course of 10 minutes keeping the temperature of the reaction mixture below 5 °C. After stirring at 0°C for two hours, the green reaction mixture was quenched on 200 mL ice-water. The precipitate was filtered off, washed with 200 mL water and air-dried to yield 0.78 g (57 %) of DNIBATTH as the dihydrate.

T_{dec} : 123 °C (DSC, Onset, 5 min^{-1}); ^1H NMR (DMSO- d_6 , 25 °C) δ (ppm) = 14.15 (s, 2H, N_{TriazH}), 9.73 (s, 1H), 4.06 (s, v br, 2H, NH-NO_2); $^{13}\text{C}\{^1\text{H}\}$ NMR (DMSO- d_6 , 25 °C) δ (ppm) = 151.7 (C- NO_2); ^{14}N NMR (DMSO- d_6 , 25 °C) δ (ppm) = -17 (-N- NO_2); IR (ATR, 25 °C, cm^{-1}) ν = 3416 (br, m), 3131 (br, s), 2232 (m), 2098 (m), 1698 (m), 1641 (m), 1589 (s), 1556 (m), 1448 (m), 1308 (s), 1277 (m), 1220 (vs), 1086 (m), 1047 (w), 987 (w), 905 (w), 845 (w), 770 (m), 722 (m); RAMAN (Nd:YAG, 1064 nm, cm^{-1}) ν = 3014 (1), 2231 (8), 1646 (17), 1582 (4), 1544 (100), 1481 (27), 1302 (1), 1291 (6), 1124 (12), 1080 (3), 998 (21), 912 (3), 854 (7), 779 (2), 755 (5), 523 (3), 482 (1), 450 (1), 241 (1); EA ($\text{C}_4\text{H}_5\text{N}_{13}\text{O}_4 \cdot 1\frac{1}{2} \text{H}_2\text{O}$) calc.: C, 14.73; H, 2.47; N, 55.82; found: C, 16.56; H, 2.56; N, 55.80; Sensitivities (DNIBATTH · $1\frac{1}{2} \text{H}_2\text{O}$) (grain size: < 100 μm): IS: > 40 J; FS: > 192 N; ESD: 70 mJ.

Bis(guanidinium) 1,3-bis-[3-(5-nitramino-1*H*-1,2,4-triazolyl)]-triazenate (**7**)

6 (2 mmol, 0.67 g, dihydrate) was dissolved in 50 mL water and heated to 65 °C with stirring. Guanidinium carbonate (2 mmol, 0.360 g) was added in small portions and gas evolution started immediately. The reaction mixture was stirred until no gas evolution was observed. After cooling to ambient temperature, the solvent was completely

evaporated and the solid residue recrystallized from hot water yielding 0.71 g of **7** as a brownish powder (84%).

$\rho(\text{pyc})$: 1.65 g cm⁻³; T_{dec} : 147 °C, (DSC, 5 °C min⁻¹), 167 °C (DSC, Onset, 5 min⁻¹); ¹H NMR (DMSO-*d*₆, 25 °C) δ (ppm) = 12.78 (s, br, 2H, N_{Tria}H), 7.38 (s, 12 H, CH₆N₃⁺); ¹³C{¹H} NMR (DMSO-*d*₆, 25 °C) δ (ppm) = 157.9 (CH₆N₃⁺), 156.3 (C-N-NO₂); ¹⁴N NMR (DMSO-*d*₆, 25 °C) δ (ppm) = -19 (-N-NO₂); IR (ATR, 25 °C, cm⁻¹) ν = 3425 (m), 3345 (m), 3250 (m), 3180 (m), 1657 (s), 1546 (m), 1500 (m), 1483 (m), 1435 (m), 1389 (m), 1356 (m), 1308 (s), 1267 (s), 1241 (m), 1088 (m), 1050 (w), 1023 (m), 1008 (m), 926 (w), 876 (vw), 830 (w), 807 (w), 771 (w), 749 (w), 725 (vw), 700 (vw); RAMAN (Nd:YAG, 1064 nm, cm⁻¹) ν = 3235 (1), 3063 (1), 1597 (16), 1528 (28), 1485 (100), 1433 (19), 1382 (9), 1163 (4), 1099 (2), 1012 (28), 928 (3), 861 (3), 791 (2), 747 (2), 531 (3); *m/z* (FAB⁺): 60.1 [CH₆N₃⁺]; (FAB⁻): 298.0 [C₄H₄N₁₃O₄⁻]; EA (C₆H₁₅N₁₉O₄ · 2 H₂O) calc.: C, 15.90; H, 4.22; N, 58.70; found: C, 16.82; H, 3.90; N, 59.01; Sensitivities (anhydrous) (grain size: < 100 μm): IS: 35 J; FS: 360 N; ESD: 300 mJ.

10.5 References

- [1] a) J. A. Garrison, R. M. Herbst, *J. Org. Chem.* **1957**, *22*, 278-283; b) R. M. Herbst, J. Garrison, *J. Org. Chem.* **1953**, *18*, 941-945.
- [2] L. I. Bagal, M. S. Pevzner, A. N. Frolov, N. I. Sheludyakova, *Khimiya Geterotsiklicheskih Soedinenii* **1970**, 259-264.
- [3] a) J. Thiele, *Liebigs Ann. Chem.* **1892**, *270*, 54-63; b) J. Thiele, J. T. Marais, *Liebigs Ann. Chem.* **1893**, 273.
- [4] a) T. M. Klapötke, *Chemie der hochenergetischen Materialien*, 1 ed., Walter de Gruyter, Berlin, New York, **2009**; b) T. M. Klapötke, in *High Energy Density Materials* (Ed.: T. M. Klapötke), Springer, Heidelberg, **2007**, pp. 84-122; c) A. Hammerl, G. Holl, T. M. Klapötke, P. Mayer, H. Noth, H. Piotrowski, M. Warchhold, *Eur. J. Inorg. Chem.* **2002**, 834-845; d) T. M. Klapötke, C. M. Sabate, *New J. Chem.* **2009**, *33*, 1605-1617; e) A. Hammerl, Ludwig-Maximilians-University (Munich), **2001**.
- [5] M. H. V. Huynh, M. A. Hiskey, E. L. Hartline, D. P. Montoya, R. Gilardi, *Angew. Chem. Int. Ed.* **2004**, *43*, 4924-4928.
- [6] D. L. Naud, M. A. Hiskey, H. H. Harry, *J. Energ. Mater.* **2003**, *21*, 57-62.
- [7] a) D. E. Chavez, B. C. Tappan, 8-ISICP, Los Alamos National laboratory, **2009**; b) D. E. Chavez, B. C. Tappan, B. A. Mason, D. Parrish, *Propell. Explos. Pyrot.* **2009**, *34*, 475-479; c) J. B. Ledgard, *The preparatory manual of explosives - a laboratory manual*, Paranoid Publications Group, **2003**.

- [8] A. Dippold, Thomas M. Klapötke, Franz A. Martin, *Z. Anorg. Allg. Chem.* **2011**, 637, in press.
- [9] a) T. M. Klapötke, N. K. Minar, J. Stierstorfer, *Polyhedron* **2009**, 28, 13-26; b) T. M. Klapötke, J. Stierstorfer, in *New Trends in Research of Energetic Materials, Vol. Pt. 1* (Eds.: J. Ottis, J. Pachman), Pardubice, **2008**, pp. 278-298.
- [10] V. Hanot, T. Robert, L. v. d. Elst, *Synth. React. Inorg. Met.-Org. Chem.* **1994**, 24, 1911.-1211.
- [11] R. Stolle, K. J. Krauch, *J. Prakt. Chem.* **1913**, 88, 306.
- [12] a) M. Hauser, *J. Org. Chem.* **1964**, 29, 3449-3450; b) M. Hauser, *Vol. US 3,431,251*, **1969**.
- [13] M. S. Pevzner, N. V. Gladkova, T. A. Kravchenko, *Russ. J. Org. Chem.* **1996**, 32, 1186-1189.
- [14] T. W. Green, P. G. M. Wuts, *Protective Groups in Organic Synthesis*, John Wiley & Sons, New York, **1999**.
- [15] a) A. R. Katrizky, G. L. Sommen, A. V. Grovoma, R. M. Witek, P. J. Steel, R. Damavarapu, *Chem. Het. Comp.* **2005**, 41, 111-118; b) K. Y. Lee, D. G. Ott, (United States Dept. of Energy, USA). Application: US, **1980**, p. 5 pp; c) K. Y. Lee, D. G. Ott, M. M. Stinecipher, *Industrial & Engineering Chemistry Process Design and Development* **1981**, 20, 358-360.
- [16] M. Hesse, Herbert, Meier, B. Zeh, *Spektroskopische Methoden in der Organischen Chemie*, 6 ed., Georg Thieme Verlag, Stuttgart, New York, **2002**.
- [17] a) T. H. Dunning, *J. Chem. Phys.* **1989**, 90, 1007; b) C. Lee, W. Yang, R. G. Parr, *Phys. Rev. B* **1988**, 7, 785; c) A. D. Becke, *J. Chem. Phys.* **1993**, 98, 5648.
- [18] *Gaussian 09W, Version 7.0*, M. J. Frisch, G. W. Trucks, H. B. Schlegel, G. E. Scuseria, M. A. Robb, J. R. Cheeseman, G. Scalmani, V. Barone, B. Mennucci, G. A. Petersson, H. Nakatsuji, M. Caricato, X. Li, H. P. Hratchian, A. F. Izmaylov, J. Bloino, G. Zheng, J. L. Sonnenberg, M. Hada, M. Ehara, K. Toyota, R. Fukuda, J. Hasegawa, M. Ishida, T. Nakajima, Y. Honda, O. Kitao, H. Nakai, T. Vreven, J. A. Montgomery, Jr., J. E. Peralta, F. Ogliaro, M. Bearpark, J. J. Heyd, E. Brothers, K. N. Kudin, V. N. Staroverov, R. Kobayashi, J. Normand, K. Raghavachari, A. Rendell, J. C. Burant, S. S. Iyengar, J. Tomasi, M. Cossi, N. Rega, J. M. Millam, M. Klene, J. E. Knox, J. B. Cross, V. Bakken, C. Adamo, J. Jaramillo, R. Gomperts, R. E. Stratmann, O. Yazyev, A. J. Austin, R. Cammi, C. Pomelli, J. W. Ochterski, R. L. Martin, K. Morokuma, V. G. Zakrzewski, G. A. Voth, P. Salvador, J. J. Dannenberg, S. Dapprich, A. D. Daniels, Ö. Farkas, J. B. Foresman, J. V. Ortiz, J. Cioslowski, and D. J. Fox, *Gaussian, Inc., Wallingford CT*, 2009.
- [19] H. A. Witek, M. Keiji, *J. Comp. Chem. THEOCHEM* **2004**, 25, 1858-1864.
- [20] T. M. Klapötke, F. A. Martin, N. Mayr, J. Stierstorfer, *Z. Anorg. Allg. Chem.* **2010**, 636, 2555-2564.
- [21] A. Bondi, *J. Phys. Chem.* **1964**, 68, 441-451.
- [22] T. M. Klapötke, F. A. Martin, S. Wiedbrauk, *submitted* **2011**.
- [23] *NATO standardization agreement (STANAG) on explosives, no. 4489, 1st ed., Sept. 17*, **1999**.

- [24] *WIWEB-Standardarbeitsanweisung 4-5.1.02, Ermittlung der Explosionsgefährlichkeit, hier: der Schlagempfindlichkeit mit dem Fallhammer, Nov. 08, 2002.*
- [25] <http://www.bam.de>.
- [26] *NATO standardization agreement (STANAG) on explosives, friction tests, no.4487, 1st ed., Aug. 22, 2002.*
- [27] *WIWEB-Standardarbeitsanweisung 4-5.1.03, Ermittlung der Explosionsgefährlichkeit, hier: der Reibempfindlichkeit mit dem Reibeapparat, Nov. 08, 2002.*
- [28] *NATO standardization agreement (STANAG) on explosives, electrostatic discharge sensitivity tests, no.4490, 1st ed., Feb. 19, 2001.*
- [29] <http://www.ozm.cz/en/sensitivity-tests/esd-2008a-small-scale-electrostatic-spark-sensitivity-test/>.
- [30] *CrysAlis CCD, Oxford Diffraction Ltd., Version 1.171.27p5 beta (release 01-04-2005 CrysAlis171.NET).*
- [31] *CrysAlis RED, Oxford Diffraction Ltd., Version 1.171.27p5 beta (release 01-04-2005 CrysAlis171.NET).*
- [32] G. M. Sheldrick, *SHELXS-97, Crystal Structure Solution, Version 97-1; Institut Anorg. Chemie, University of Göttingen, Germany, 1990.*
- [33] G. M. Sheldrick, *SHELXL-97, Program for the Refinement of Crystal Structures. University of Göttingen, Germany, 1997.*
- [34] L. Farrugia, *J. Appl. Cryst.* **1999**, 32, 837-838.
- [35] A. L. Spek, *Platon, A Multipurpose Crystallographic Tool, Utrecht University, Utrecht, The Netherlands, 1999.*

11. Summary

In the course of this work, many novel energetic materials as well as families of energetic salts have been developed. In Chapter 2, 4,5-dicyano-2*H*-1,2,3-triazole was synthesized together with the corresponding nitrogen-rich guanidinium salts from cheap starting materials. All compounds have been fully characterized by means of vibrational and multinuclear NMR spectroscopy as well as single crystal X-ray diffraction measurements. Detonation parameters have been calculated for the energetically most promising guanidinium salts with triaminoguanidinium 4,5-dicyano-1,2,3-triazolate being the most promising compound for the use as burn rate modifiers with v_{det} of 7919 m s^{-1} and a volume of gaseous decomposition products of 759 L mol^{-1} .

Chapter 3 – 5 concentrate on the chemistry of 1,5-diaminotetrazole. The synthesis of novel *N*-bound nitramines under mild reaction conditions is described together with the full characterization and the calculation of the corresponding detonation parameters in Chapter 3 for 5-amino-1-nitrimino-4*H*-tetrazole and 5-amino-4-methyl-1-nitriminotetrazole. Both compounds represent structurally very interesting zwitter ionic compounds but show extremely high sensitivities towards all outer stimuli paired with very high performance values. To increase the stability values, nitrogen rich salts of 5-amino-1-nitrimino-4*H*-tetrazole have been synthesized by metathesis reactions in various solvents. The most promising candidates for the use as secondary explosives, ammonium and hydrazinium 5-amino-1-nitriminotetrazolate show very high v_{det} of around 9110 m s^{-1} but are way too sensitive and decompose too early at $107 \text{ }^{\circ}\text{C}$ and $134 \text{ }^{\circ}\text{C}$, respectively. The compound exhibiting the highest thermal stability is the triaminoguanidinium salt at $160 \text{ }^{\circ}\text{C}$, also showing a performance in the range of RDX, but unfortunately it shows sensitivity values way too high. Chapter 4 and 5 deal with a very interesting topic, the formation of novel azidotetrazoles utilizing the 1,5-diaminotetrazole backbone. The introduction of higher amounts of nitrogen was performed by the diazotization of triaminoguanidinium followed by subsequent ring closure reactions. Three unique compounds 5-azido-1-diazidocarbamoyltetrazole, 5-azido-1-(amino-azidocarbamoyl)-tetrazole and finally 1-amino-5-azidotetrazole could be obtained and identified under different reaction conditions. All three compounds are extremely sensitive and tend to explode under certain conditions, sometimes also in solution. Even though our hopes of stabilizing the azide groups by the introduction of an amine group as electron donor and also as a hydrogen bonding donor did not prove to be true, the single crystal X-ray

structures of these materials exhibit very interesting details. Additionally a full spectroscopic characterization of all three compounds was performed and the results were extensively studied also by the utilization of quantum mechanical calculations.

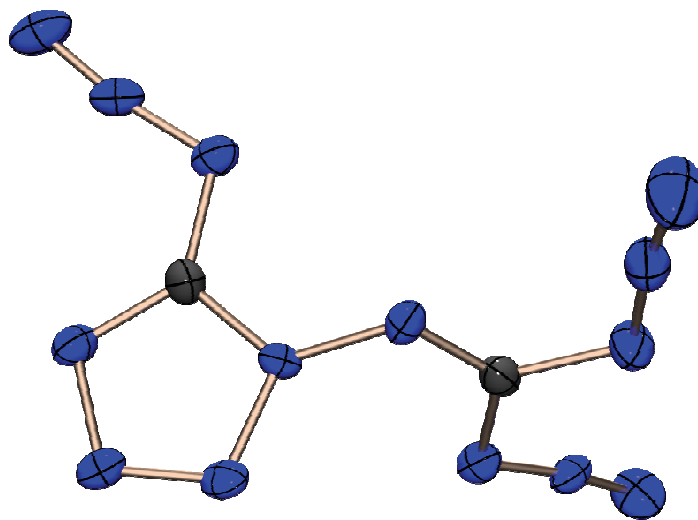


Figure 1: Single crystal X-ray structure of 5-azido-1-diazidocarbamoyltetrazole (asymmetric unit). The structure is exclusively built up from nitrogen/nitrogen interactions, enabling a very dense packing. (Chapter 4). A complete characterization could be obtained, even though the compound is extremely! sensitive.

Chapter 6 – 10 of this thesis use the 3,5-diamino-1*H*-1,2,4-triazole as the backbone compound. While only 3,5-diamino-1*H*-1,2,4-triazole is used as the monocyclic compound in Chapters 6 – 8 with various energetic substituents, directly coupled compounds containing two triazole moieties connected by azo and triazene functionalities are described in Chapter 9 and 10. The before mentioned 3,5-diamino-1*H*-1,2,4-triazole was used as a cation in Chapter 6, where energetic salts have been synthesized by the use of strong acids like nitric and perchloric acid and by the metathesis reaction of 3,5-diamino-1,2,4-triazolium perchlorate with potassium dinitramide. All energetic ionic compounds have been characterized fully by spectroscopic as well as single crystal X-ray diffraction measurements. Additionally, the thermal stabilities and performance characteristics have been studied. The dinitramide salt exhibits the best detonation parameters with v_{det} of 8681 m s⁻¹ and a detonation pressure of 321 kbar, but the decomposition temperature of 164 °C together with the high impact sensitivity of 3 J diminishes the potential applications. Two 1,2,4-triazole derivatives carrying both a nitro and a nitramine group are described in Chapter 7. 5-Nitramino-3-nitro-1*H*-1,2,4-triazole and 1-methyl-5-nitramino-3-nitro-1,2,4-triazole have been synthesized starting from ANTA by subsequent methylation with dimethyl sulfate in the case of the methylated

derivative followed by nitration of the amine group in very good yields. The neutral compounds as well as the prepared energetic ionic salts have been characterized by means of vibrational and multinuclear NMR spectroscopy and by single crystal X-ray diffraction measurements. An extensive theoretical study was performed for mono and double salts of 5-nitramino-3-nitro-1*H*-1,2,4-triazole and salts of 1-methyl-5-nitramino-3-nitro-1,2,4-triazole with high nitrogen rich cations in order to get a good comparison of the energetic properties and an idea of effect of the deprotonation state. Except for the two neutral compounds that decompose at temperatures of 135 °C (5-nitramino-3-nitro-1*H*-1,2,4-triazole) and 108 °C (1-methyl-5-nitramino-3-nitro-1,2,4-triazole), respectively, and bis(triaminoguanidinium) 5-nitramino-3-nitro-1,2,4-triazolate the thermal stabilities of the compounds are all above 180 °C. Since the sensitivities of all compounds are below the values of our benchmark molecule RDX, application of some of these compounds seems possible, since the performance values are close to RDX for the triaminoguanidinium salts as well as for the hydrazinium salts. The exchange of the nitro group with the tetrazole ring moiety as the substituent in 3 position, while the nitramine group remained in 5 position is described in Chapter 8. A new reaction pathway was developed yielding 5-amino-3-tetrazol-1-yl-1*H*-1,2,4-triazole in good yields, exhibiting high thermal stabilities. The subsequent nitration was performed in yields of 58 %. Even though the decomposition temperatures of this compound and its nitrogen rich salts are below 150 °C and hence prohibit these compounds from the application as energetic materials, a complete spectroscopic characterization was performed together with the determination of their physical properties in terms of sensitivity and thermal stability. Single crystal X-ray diffraction measurements have been performed for selected compounds. 5-Amino-3-tetrazol-1-yl-1*H*-1,2,4-triazole and 3-tetrazol-1-yl-1*H*-1,2,4-triazole were also under investigation as burn rate modifiers or propellants, but it turned out, that the specific impulses of both compounds were too low, although they exhibit high nitrogen contents.

The synthesis of dimers built from 3,5-diamino-1*H*-1,2,4-triazole was one extensively studied topic in the course of this thesis. While the connectivity is established over a triazene bridge in Chapter 10, an azo functionality connects two molecules in Chapter 9. Both coupling reaction use the selectively protected 5-acetamido-3-amino-1*H*-1,2,4-triazole in order to control the reaction site. The electron donating effect of the acetyl protecting group enables coupling reactions with very good yields for both compounds. The subsequent nitration procedures, forming the nitrimino compound in the case of the

azo functionality and the nitramino compound in the case of the triazene bridge, work also in good yields for both compounds. While the triazene bridged compounds show low thermal stabilities, but on the other hand low sensitivities against friction and impact, the azo bridged compounds either the neutral compound or the corresponding nitrogen rich salts, show remarkable high decomposition temperatures of well above 200 °C. Since the impact and friction sensitivities for 5,5'-dinitrimino-3,3'-azo-1*H*-1,2,4-triazole are very high with an impact sensitivity of 2 J and an friction sensitivity of 20 N, corresponding nitrogen rich salts have been prepared first in order to decrease the sensitivity and also to increase the thermal stability. Both goals have been achieved for selected salts of 5,5'-dinitrimino-3,3'-azo-1*H*-1,2,4-triazole, showing decomposition temperatures between 212 °C (ammonium) and 261 °C (guanidinium). All impact and friction sensitivities are well above the values of RDX, and hence much less sensitive, while the performance values of the bis(triaminoguanidinium) 5,5'-dinitrimino-3,3'-azo-1*H*-1,2,4-triazolate show promising values very close to RDX.

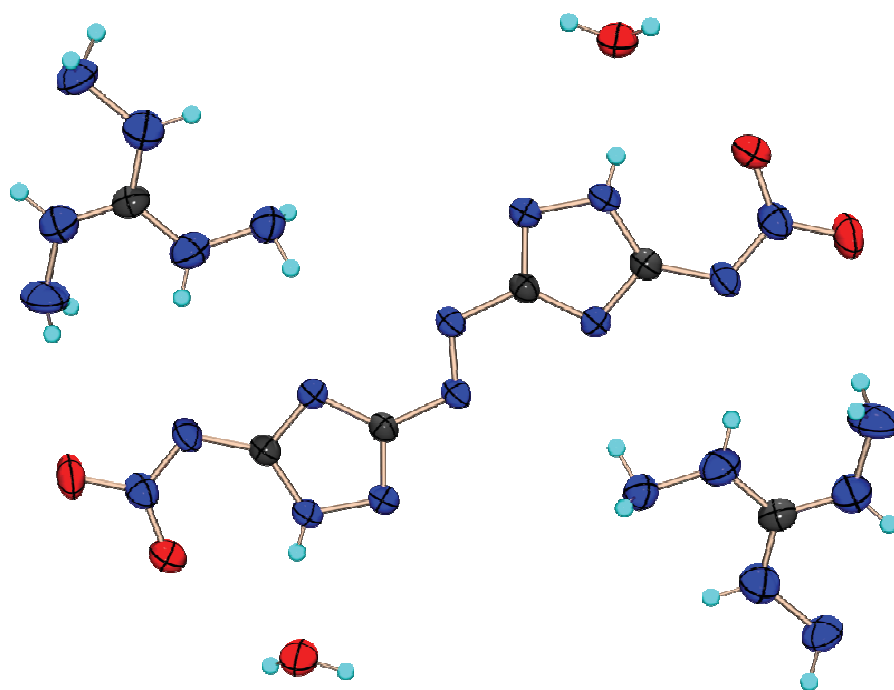


Figure 2: Illustration of bis(triaminoguanidinium) 5,5'-dinitrimino-3,3'-azo-1*H*-1,2,4-triazolate, which shows the best balance between thermal stability (219 °C) and performance values. While the later are in the range of RDX, the sensitivities of the compound are exceptionally low, making it a very promising compound for application.

12 Appendix

12.1 Supplementary Material for Chapter 2

Table S1: Crystallographic data and parameter.

	HDCT (1)	Na ⁺ DCT ⁻ *H ₂ O(2)	NH ₄ ⁺ DCT ⁻ (4) ⁻	G ⁺ DCT ⁻ (5)
Measurement number	--	--	--	ax096
Formula	C ₄ HN ₅	C ₄ H ₂ N ₅ NaO	C ₄ H ₄ N ₆	C ₅ H ₆ N ₈
FW [g mol ⁻¹]	119.08	159.08	136.12	178.16
Crystal system	monoclinic	monoclinic	orthorhombic	monoclinic
Space Group	P2 ₁ /c	P2 ₁ /c	Pnma	Cc
Color / Habit	colorless cubes	colorless plates	colorless cubes	colorless cubes
Size [mm]	0.06x0.055x0.05	0.08x0.06x0.01	0.05x0.04x0.04	0.06x0.04x0.03
<i>a</i> [Å]	6.0162(6)	3.6767(6)	6.5646(13)	12.6000(11)
<i>b</i> [Å]	11.2171(10)	20.469(4)	7.5707(16)	17.1138(15)
<i>c</i> [Å]	7.5625(7)	9.6223(13)	13.303(3)	12.0952(9)
α [°]	90	90	90	90
β [°]	94.214(8)	97.355(13)	90	106.098(7)
γ [°]	90	90	90	90
<i>V</i> [Å ³]	508.97(8)	718.2(2)	661.1(2)	2505.9(4)
<i>Z</i>	4	4	4	12
ρ_{calc} [g cm ⁻³]	1.554	1.470	1.368	1.417
μ [mm ⁻¹]	0.114	0.164	0.100	0.104
<i>F</i> (000)	240	320	280	1104
$\lambda_{\text{MoK}\alpha}$ [Å]	0.71073	0.71073	0.71073	0.71073
<i>T</i> [K]	200	200	200	200
Theta Min-Max [°]	4.53 – 30.06	4.39 – 30.16	4.39 – 30.07	4.45 – 30.08
Dataset h	-8; 8	-5; 5	-9; 7	-17; 15
Dataset k	-15; 15	-28; 24	-10; 10	-23; 24
Dataset l	-10; 10	-11; 13	-18; 18	-17; 15
Reflections collected	6740	4920	4323	8632
Independent reflections	1498	2092	1036	3639
Observed reflections	1239	1476	851	2553
No. parameters	86	100	59	424
<i>R</i> _{int}	0.0223	0.0186	0.0446	0.0443
<i>R</i> ₁ , w <i>R</i> ₂ (I> σ I ₀)	0.0393; 0.1140	0.0354; 0.0955	0.0527; 0.1295	0.0469; 0.1004
<i>R</i> ₁ , w <i>R</i> ₂ (all data)	0.0481; 0.1191	0.0505; 0.1036	0.0696; 0.1422	0.0690; 0.1138
<i>S</i>	1.191	1.014	1.133	0.988
Resd. Dens. [e Å ⁻³]	-0.261; 0.248	-0.192; 0.265	-0.216; 0.290	-0.204; 0.215
Device type	Oxford Xcalibur3 CCD	Oxford Xcalibur3 CCD	Oxford Xcalibur3 CCD	Oxford Xcalibur3 CCD
Solution	SHELXS-97	SHELXS-97	SHELXS-97	SHELXS-97
Refinement	SHELXL-97	SHELXL-97	SHELXL-97	SHELXL-97
Absorption correction	multi-scan	multi-scan	multi-scan	multi-scan
CCDC	702141	702142	702143	702144

Table S1: continued.

	AG ⁺ DCT ⁻ (6)	DAG ⁺ DCT ⁻ (7)	TAG ⁺ DCT ⁻ (8)
Measurement number	ax112	ax110	ax109
Formula	C ₅ H ₇ N ₉	C ₅ H ₈ N ₁₀	C ₅ H ₉ N ₁₁
FW [g mol ⁻¹]	193.20	208.21	223.2
Crystal system	monoclinic	monoclinic	monoclinic
Space Group	Pa	P2 ₁	C2/c
Color / Habit	colorless plates	colorless block	colorless blocks
Size [mm]	0.06x0.05x0.02	0.07x0.05x0.04	0.05x0.04x0.04
<i>a</i> [Å]	7.0921(9)	3.7727(4)	14.0789(14)
<i>b</i> [Å]	7.2893(9)	15.6832(17)	11.5790(11)
<i>c</i> [Å]	8.8671(11)	8.3416(10)	13.5840(14)
α [°]	90	90	90
β [°]	105.141(11)	101.797(10)	115.239(10)
γ [°]	90	90	90
<i>V</i> [Å ³]	442.28(10)	483.13(9)	2003.1(3)
<i>Z</i>	2	2	8
ρ_{calc} [g cm ⁻³]	1.450	1.431	1.480
μ [mm ⁻¹]	0.108	0.107	0.111
<i>F</i> (000)	200	216	927
$\lambda_{\text{MoK}\alpha}$ [Å]	0.71073	0.71073	0.71073
<i>T</i> [K]	200	200	200
Theta Min-Max [°]	4.32 – 30.06	4.63 – 30.70	4.57 – 30.06
Dataset h	-9; 9	-5; 5	-19; 19
Dataset k	-10; 10	-22; 22	-16; 16
Dataset l	-12; 12	-11; 11	-19; 19
Reflections collected	5758	6518	13317
Independent reflections	1298	1465	2928
Observed reflections	1242	1268	2058
No. parameters	155	168	153
<i>R</i> _{int}	0.0349	0.0716	0.0735
<i>R</i> ₁ , <i>wR</i> ₂ (<i>I</i> > σ <i>I</i> ₀)	0.0313; 0.0779	0.0467; 0.0975	0.0817; 0.1325
<i>R</i> ₁ , <i>wR</i> ₂ (all data)	0.0335; 0.0799	0.0571; 0.1036	0.1335; 0.1552
<i>S</i>	1.076	1.074	1.215
Resd. Dens. [e Å ⁻³]	-0.177; 0.133	-0.180; 0.158	-0.222; 0.217
Device type	Oxford Xcalibur3 CCD	Oxford Xcalibur3 CCD	Oxford Xcalibur3 CCD
Solution	SHELXS-97	SHELXS-97	SHELXS-97
Refinement	SHELXL-97	SHELXL-97	SHELXL-97
Absorption correction	multi-scan	multi-scan	multi-scan
CCDC	702145	702146	702147

12.2 Supplementary Material for Chapter 3

Table S1: Crystallographic data and parameter.

	HDATNO ₂ (1)	MeDATNO ₂ (2)	NH ₄ ⁺ DATNO ₂ ⁻ (4)	N ₂ H ₅ ⁺ DATNO ₂ ⁻ (5)
Measurement number	dx188	fx513	fx409	fx418
Formula	CH ₃ N ₇ O ₂	C ₂ H ₅ N ₇ O ₂	CH ₆ N ₈ O ₂	CH ₇ N ₉ O ₂
FW [g mol ⁻¹]	145.08	159.11	162.11	177.13
Crystal system	orthorhombic	monoclinic	monoclinic	monoclinic
Space Group	<i>Pna</i> 2 ₁	<i>P</i> 2 ₁ / <i>n</i>	<i>C</i> 2/ <i>c</i>	<i>P</i> 2 ₁ / <i>c</i>
Color / Habit	colorless block	colorless plates	colorless block	colorless block
Size [mm]	0.32 x 0.26 x 0.19	0.38 x 0.12 x 0.03	0.39 x 0.35 x 0.21	0.48 x 0.43 x 0.39
<i>a</i> [Å]	9.2439(4)	8.8549(13)	25.9575(13)	7.3086(12)
<i>b</i> [Å]	5.5129(2)	5.8149(9)	6.8900(4)	14.265(2)
<i>c</i> [Å]	10.3026(4)	12.8131(18)	14.0178(7)	6.7782(11)
α [°]	90	90	90	90
β [°]	90	102.872(14)	102.123(5)	97.060(14)
γ [°]	90	90	90	90
<i>V</i> [Å ³]	525.03(4)	643.17(16)	2451.1(2)	701.32(19)
<i>Z</i>	4	4	16	4
$\rho_{\text{calc.}}$ [g cm ⁻³]	1.835	1.643	1.757	1.678
μ [mm ⁻¹]	0.164	0.142	0.155	0.147
<i>F</i> (000)	296	328	1344	368
$\lambda_{\text{MoK}\alpha}$ [Å]	0.71073	0.71073	0.71073	0.71073
<i>T</i> [K]	200	173	173	200
Theta Min-Max [°]	3.96 – 26.48	4.23 – 26.49	4.15 – 26.50	4.16 – 26.49
Dataset h	-10; 11	-11; 7	-32; 31	-6; 9
Dataset k	-6; 5	-7; 6	-7; 8	-17; 17
Dataset l	-12; 12	-15; 16	-13; 17	-7; 8
Reflections collected	2613	3299	6321	3565
Independent reflections	573	1332	2528	1451
Observed reflections	518	860	1996	1009
No. parameters	100	109	235	130
<i>R</i> _{int}	0.0190	0.0300	0.0222	0.0321
<i>R</i> ₁ , w <i>R</i> ₂ (<i>I</i> > σ <i>I</i> ₀)	0.0230; 0.0584	0.0343; 0.0802	0.0309; 0.0768	0.0371; 0.0934
<i>R</i> ₁ , w <i>R</i> ₂ (all data)	0.0262; 0.0614	0.0592; 0.0848	0.0408; 0.0795	0.0576; 0.0989
<i>S</i>	1.083	0.881	0.989	0.966
Resd. Dens. [e Å ⁻³]	-0.157; 0.195	-0.189; 0.158	-0.255; 0.212	-0.237; 0.195
Device type	Oxford Xcalibur3 CCD	Oxford Xcalibur3 CCD	Oxford Xcalibur3 CCD	Oxford Xcalibur3 CCD
Solution	SIR-92	SHELXS-97	SHELXS-97	SHELXS-97
Refinement	SHELXL-97	SHELXL-97	SHELXL-97	SHELXL-97
Absorption correction	multi-scan	multi-scan	multi-scan	multi-scan
CCDC	824129	824135	824133	824134

Table S1: continued.

	G ⁺ DATNO ₂ ⁻ (6)	AG ⁺ DATNO ₂ ⁻ (7)	TAG ⁺ DATNO ₂ ⁻ (8)
Measurement number	ex068	dx406	ex343
Formula	C ₂ H ₈ N ₁₀ O ₂	C ₂ H ₉ N ₁₁ O ₂	C ₂ H ₁₁ N ₁₃ O ₂
FW [g mol ⁻¹]	204.15	219.17	249.195
Crystal system	orthorhombic	monoclinic	orthorhombic
Space Group	<i>Pca</i> 2 ₁	<i>P</i> 2 ₁ / <i>c</i>	<i>Pna</i> 2 ₁
Color / Habit	colorless block	colorless plates	colorless rods
Size [mm]	0.40 x 0.28 x 0.10	0.20 x 0.10 x 0.04	0.40 x 0.05 x 0.05
<i>a</i> [Å]	10.3476(5)	9.6343(5)	16.4949(17)
<i>b</i> [Å]	8.4252(6)	7.4589(4)	15.3796(14)
<i>c</i> [Å]	9.6067(5)	13.0404(7)	3.9809(4)
α [°]	90	90	90
β [°]	90	109.681(6)	90
γ [°]	90	90	90
<i>V</i> [Å ³]	837.52(8)	882.36(8)	1009.89(17)
<i>Z</i>	4	4	4
ρ _{calc.} [g cm ⁻³]	1.619	1.650	1.639
μ [mm ⁻¹]	0.138	0.140	0.138
<i>F</i> (000)	424	456	520
λ _{MoKα} [Å]	0.71073	0.71073	0.71073
<i>T</i> [K]	200	200	173
Theta Min-Max [°]	3.94 – 26.50	4.22 – 26.49	4.16 – 26.50
Dataset h	-12; 9	-12; 12	-10; 20
Dataset k	-4; 10	-9; 9	-19; 16
Dataset l	-12; 10	-16; 16	-3; 4
Reflections collected	2095	8820	3948
Independent reflections	919	1829	1182
Observed reflections	723	1178	813
No. parameters	151	163	187
<i>R</i> _{int}	0.0291	0.0408	0.0377
<i>R</i> ₁ , w <i>R</i> ₂ (I > σI ₀)	0.0302; 0.0581	0.0332; 0.0789	0.0311; 0.0466
<i>R</i> ₁ , w <i>R</i> ₂ (all data)	0.0439; 0.0611	0.0627; 0.0956	0.0584; 0.0502
<i>S</i>	0.936	1.009	0.853
Resd. Dens. [e Å ⁻³]	-0.157; 0.140	-0.221; 0.195	-0.153; 0.136
Device type	Oxford Xcalibur3	Oxford Xcalibur3	Oxford Xcalibur3
	CCD	CCD	CCD
Solution	SHELXS-97	SHELXS-97	SHELXS-97
Refinement	SHELXL-97	SHELXL-97	SHELXL-97
Absorption correction	multi-scan	multi-scan	multi-scan
CCDC	824131	824130	824132

Table S2: Hydrogen bonds present in the structure of hydrazinium 5-amino-1-nitriminotetrazolate (5).

D–H⋯A	d (D–H) [Å]	d (H⋯A) [Å]	d (D–H⋯A) [Å]	< (D–H⋯A) [°]
N7–H7a⋯O2 ⁱ	0.95(2)	2.01(2)	2.934(2)	165(2)
N7–H7b⋯O1 ⁱⁱ	0.87(2)	2.24(2)	3.042(2)	152(2)
N8–H8a⋯O2	0.93(2)	2.28(2)	2.961(2)	129(2)
N8–H8a⋯O1 ⁱ	0.93(2)	2.46(2)	3.144(2)	131(1)
N8–H8a⋯N3 ⁱⁱⁱ	0.93(2)	2.53(2)	3.045(2)	115(1)
N8–H8c⋯N4 ⁱⁱ	0.84(2)	2.05(2)	2.886(2)	172(2)
N9–H9a⋯N5 ^{iv}	0.85(2)	2.17(2)	2.981(2)	161(2)
N9–H9b⋯N3 ⁱⁱ	0.87(2)	2.32(2)	3.047(2)	142(2)

Symmetry Operators: (i) $x, -y+1/2, z-1/2$; (ii) $-x+1, -y, -z$; (iii) $-x+1, y+1/2, -z+1/2$; (iv) $x+1, y, z$.

Table S3: Hydrogen bonds present in the structure of guanidinium 5-amino-1-nitriminotetrazolate (6).

D–H⋯A	d (D–H) [Å]	d (H⋯A) [Å]	d (D–H⋯A) [Å]	< (D–H⋯A) [°]
N7–H7a⋯O1 ⁱ	0.94(3)	2.48(3)	3.373(3)	159(2)
N7–H7b⋯O1 ⁱⁱ	0.84(3)	2.14(3)	2.961(3)	167(3)
N8–H8a⋯N2 ⁱⁱⁱ	0.84(3)	2.40(3)	3.192(4)	159(3)
N8–H8b⋯N5 ^{iv}	0.90(3)	2.12(3)	2.990(3)	164(3)
N9–H9a⋯N4 ^v	0.82(3)	2.34(3)	3.085(3)	152(3)
N9–H9b⋯N3 ⁱⁱⁱ	0.90(3)	2.17(3)	3.041(4)	164(2)
N10–H10a⋯O2 ^{iv}	0.91(3)	2.02(3)	2.897(3)	161(2)
N10–H10b⋯N4 ^v	0.80(3)	2.34(3)	3.073(3)	152(3)

Symmetry Operators: (i) $-x+1, -y, z-1/2$; (ii) $-x+3/2, y, z-1/2$; (iii) $x-1/2, -y+1, z$; (iv) $-x+1/2, y, z+1/2$; (v) $-x+3/2, y, z+1/2$.

Table S4: Hydrogen bonds present in the structure of aminoguanidinium 5-amino-1-nitriminotetrazolate (7).

D–H⋯A	d (D–H) [Å]	d (H⋯A) [Å]	d (D–H⋯A) [Å]	< (D–H⋯A) [°]
N7–H7a⋯N2 ⁱ	0.85(2)	2.38(2)	3.126(2)	147(2)
N7–H7b⋯O1 ⁱⁱ	0.92(2)	2.02(2)	2.927(2)	172(2)
N8–H8⋯N5	0.82(2)	2.29(2)	3.096(2)	165(2)
N9–H9a⋯O2 ⁱⁱⁱ	0.84(2)	2.20(2)	2.970(2)	152(2)
N10–H10a⋯O2	0.82(2)	2.15(2)	2.960(2)	166(2)
N10–H10b⋯N3 ^{iv}	0.90(2)	2.09(2)	2.978(2)	170(2)
N10–H10b⋯N4 ^{iv}	0.90(2)	2.62(2)	3.363(2)	140(2)
N11–H11a⋯O1 ^v	0.86(2)	2.47(2)	3.043(2)	125(2)
N11–H11a⋯O2 ^{vi}	0.86(2)	2.57(2)	3.271(2)	139(2)
N11–H11b⋯N4 ^{vii}	0.84(2)	2.39(2)	3.191(2)	160(2)

Symmetry Operators: (i) $-x+1, y-1/2, -z+1/2$; (ii) $x, -y+1/2, z-1/2$; (iii) $-x, y+1/2, -z+1/2$; (iv) $x-1, y, z$; (v) $-x+1, y+1/2, -z+1/2$; (vi) $x, -y+3/2, z-1/2$; (vii) $-x+1, -y+1, -z$.

Table S5: Hydrogen bonds present in the structure of triaminoguanidinium 5-amino-1-nitriminotetrazolate (**8**).

D-H \cdots A	d (D-H) [Å]	d (H \cdots A) [Å]	d (D-H \cdots A) [Å]	< (D-H \cdots A) [°]
N8-H8 \cdots N2 ⁱ	0.83(2)	2.25(3)	3.060(3)	163(2)
N9-H9 \cdots O2 ⁱⁱ	0.85(2)	2.17(2)	2.902(3)	144(2)
N10-H10 \cdots O1 ⁱⁱⁱ	0.91(2)	2.51(2)	3.052(3)	119(2)
N10-H10 \cdots N7 ⁱⁱⁱ	0.91(2)	2.68(2)	3.327(3)	129(2)
N11-H11a \cdots N5 ^{iv}	0.83(2)	2.35(3)	3.025(3)	139(2)
N12-H12a \cdots O2 ^v	0.85(3)	2.52(3)	3.300(3)	152(2)
N12-H12b \cdots N3 ^{vi}	0.84(3)	2.38(3)	3.205(4)	167(2)
N13-H13a \cdots O1	0.84(2)	2.20(3)	3.011(3)	162(2)
N7-H7a \cdots O1 ^{vii}	0.85(3)	2.09(3)	2.943(3)	175(3)
N7-H7b \cdots N4 ^{viii}	0.86(2)	2.11(2)	2.951(3)	167(2)

Symmetry Operators: (i) $x+1/2, -y+1/2, z$; (ii) $-x+1/2, y-1/2, z-1/2$; (iii) $x, y, z-1$; (iv) $x+1/2, -y+1/2, z-1$; (v) $-x+1/2, y-1/2, z-3/2$; (vi) $-x, -y, z-1/2$; (vii) $x, y, z+1$; (viii) $-x, -y, z+1/2$.

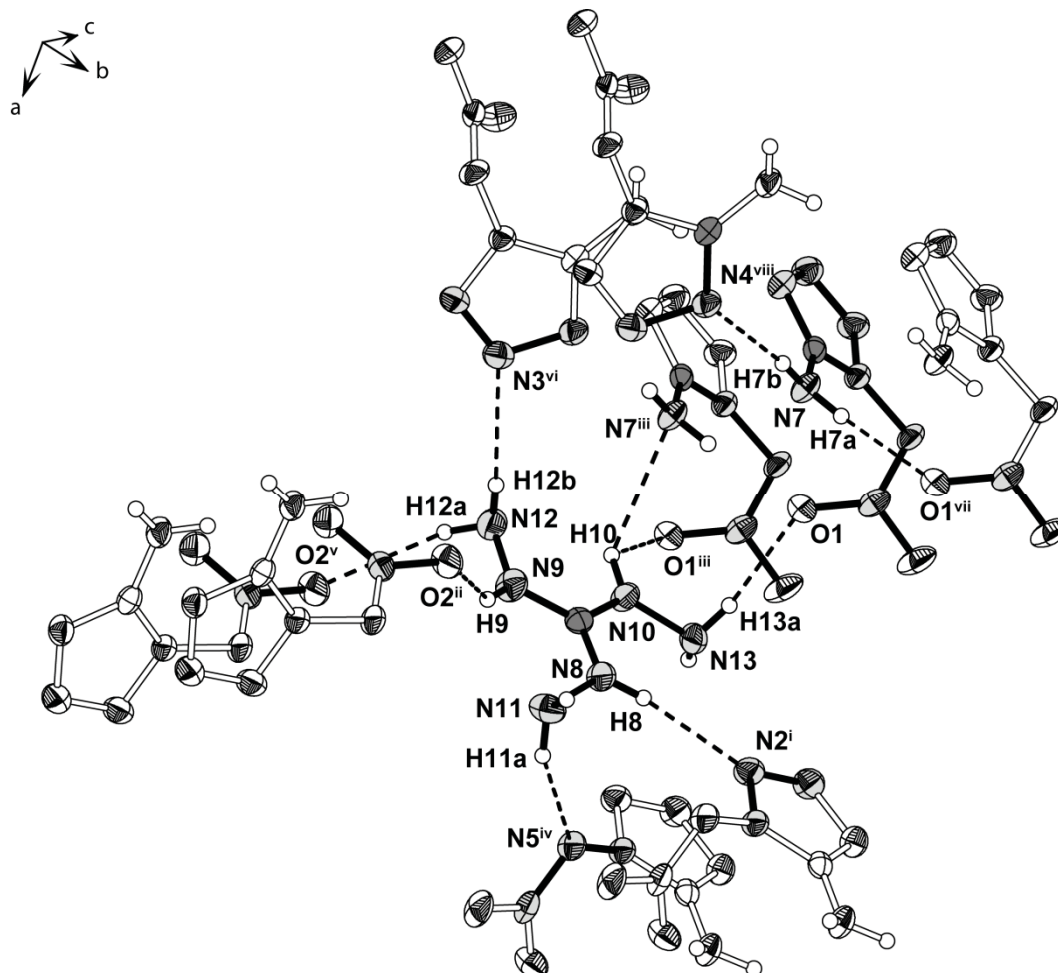


Figure S1: Hydrogen bonding pattern present in the structure of triaminoguanidinium 5-amino-1-nitriminotetrazolate (**8**). Thermal ellipsoids are set to 50 % probability. Symmetry Operators: (i) $x+1/2, -y+1/2, z$; (ii) $-x+1/2, y-1/2, z-1/2$; (iii) $x, y, z-1$; (iv) $x+1/2, -y+1/2, z-1$; (v) $-x+1/2, y-1/2, z-3/2$; (vi) $-x, -y, z-1/2$; (vii) $x, y, z+1$; (viii) $-x, -y, z+1/2$.

12.3 Supplementary Material for Chapter 4

Experimental section:

Caution: The presented compound is extremely!! sensitive towards friction, impact and electric discharge and proper safety precautions must be taken when handling these material. It is a highly energetic material and tends to explode under certain conditions, especially under physical stress. Laboratories and personnel must be properly grounded, and safety equipment such as Kevlar gloves, leather coats, face shields and ear plugs are recommended.

General. All chemical reagents, except triaminoguanidinium chloride, and solvents were obtained from Sigma-Aldrich Inc. or Acros Organics (analytical grade) and were used as supplied. ^1H , ^{13}C , and ^{14}N NMR spectra were recorded on a JEOL Eclipse 400 instrument in DMSO- d_6 or chloroform- d at or near 25 °C. The chemical shifts are given relative to tetramethylsilane (^1H , ^{13}C) or nitro methane (^{14}N) as external standards and coupling constants are given in Hertz (Hz). Infrared (IR) spectra were recorded on a Perkin-Elmer Spectrum BX FT-IR instrument equipped with an ATR unit at 25 °C. Transmittance values are qualitatively described as “very strong” (vs), “strong” (s), “medium” (m) and “weak” (w). Raman spectra were recorded on a Bruker RAM II spectrometer equipped with a Nd:YAG laser (1064 nm) and a reflection angle of 180°. The intensities are reported as percentages of the most intense peak and are given in parentheses. Melting points were determined by differential scanning calorimetry (Linseis PT 10 DSC, calibrated with standard pure indium and zinc). Measurements were performed at a heating rate of 5 °C min⁻¹ in closed aluminium sample pans with a 1 µm hole in the top for gas release under a nitrogen flow of 20 mL min⁻¹ with an empty identical aluminium sample pan as reference. For initial safety testing, the impact and friction sensitivities were determined. The impact sensitivity tests were carried out according to STANAG 4489^[1] modified according to instruction^[2] using a BAM^[3] drop hammer. The friction sensitivity tests were carried out according to STANAG 4487^[4] modified according to instruction^[5] using the BAM friction tester.

Synthesis of 1-diaزيدocarbamoyl-5-azidotetrazole (1)

0.282 g (2 mmol) triaminoguanidinium chloride was dissolved in 30 mL of water and 2 mL 2 M hydrochloric acid were added. The reaction was carried out at 0 °C (ice bath cooling). A solution of 0.278 g (4 mmol) sodium nitrite in 30 mL water was added drop wise over the course of 20 minutes. After complete addition, the mixture was allowed to warm up and stirred for an additional 30 minutes. Exactly one equivalent of a 0.1 M sodium hydroxide solution was added slowly (slightly orange color). Afterwards, the reaction mixture was extracted with 150 mL of diethyl ether which was allowed to evaporate until dryness to yield 0.058 g (26.3 %) as raw product. The raw material was cleaned by short column chromatography using chloroform as solvent yielding 0.036 g of pure **1** (16.4 %).

T_{melt}: 78 °C (DSC, T_{onset}, 5 °C min⁻¹); **T_{dec}**: 124°C (DSC, T_{onset}, 5 °C min⁻¹); **¹³C NMR** ([*d6*]-DMSO, 25°C) δ 148.1, 160.4; **¹⁴N NMR** ([*d6*]-DMSO, 25°C) δ -148 (N_β); **¹⁴N NMR** (CDCl₃, 25°C) δ -145 (br, N_γ), -147 (N_β), -149 (N_β), -305 (br, N_α); **IR** (ATR, 25 °C, cm⁻¹): 3367 (m), 3314 (m), 3231 (m), 3190 (m), 2175 (vs), 2155 (vs), 2133 (vs), 1636 (s), 1578 (s), 1530 (s), 1456 (m), 1414 (s), 1290 (m), 1261 (m), 1213 (s), 1190 (s), 1106 (m), 1087 (m), 984 (w), 936 (w), 855 (w), 786 (w), 720 (w), 698 (w), 682 (w), 646 (w); **Raman**: (200 mW, 25 °C, cm⁻¹): 3196 (12), 2179 (48), 2165 (33), 2133 (25), 1653 (15), 1573 (28), 1534 (100), 1454 (13), 1408 (27), 1386 (12), 1293 (34), 1266 (27), 1216 (18), 1189 (23), 1115 (13), 1092 (38), 936 (22), 857 (30), 598 (29), 522 (35), 395 (27), 297 (37); **MS (DCI+)**: [M+H⁺] 221.1; **impact sensitivity**: < 0.25 J, **friction sensitivity**: < 1 N.

Crystal structure

The single crystal X-ray diffraction data of **1** were collected using an Oxford Xcalibur3 diffractometer with a Spellman generator (voltage 50 kV, current 40 mA) and a KappaCCD detector. The data collection was undertaken using the CRYALIS CCD software^[6] and the data reduction was performed with the CRYALIS RED software.^[7] The structure was solved with SIR-92^[8] and refined with SHELXL-97^[9] implemented in the program package WinGX^[10] and finally checked using PLATON.^[11]

Table 1S: Crystallographic data and parameter of **1**.

	1
Formula	C_2N_{14}
Form. weight [g mol ⁻¹]	220.16
Crystal system	orthorhombic
Space Group	<i>Pbcn</i>
Color / Habit	colorless needles
Size [mm]	0.01 x 0.05 x 0.10
<i>a</i> [Å]	18.1289(1)
<i>b</i> [Å]	8.2128(7)
<i>c</i> [Å]	11.4021(9)
α [°]	90
β [°]	90
γ [°]	90
<i>V</i> [Å ³]	1697.6(2)
<i>Z</i>	8
ρ_{calc} [g cm ⁻³]	1.723
μ [mm ⁻¹]	0.140
F(000)	880
$\lambda_{\text{MoK}\alpha}$ [Å]	0.71073
T [K]	150
Theta Min-Max [°]	3.8, 25.5
Dataset h	-21; 17
Dataset k	-8; 9
Dataset l	-13; 13
Reflections collected	6862
Independent reflections	1563
R_{int}	0.142
Observed reflections	763
No. parameters	145
R_1 (obs)	0.0673
wR_2 (all data)	0.1177
<i>S</i>	1.08
Resd. Dens. [e Å ⁻³]	-0.46, 0.36
Device type	Oxford Xcalibur3 CCD
Solution	SIR-92
Refinement	SHELXL-97
Absorption correction	multi-scan
CCDC	693485

Table 2S: Selected bond lengths, bond angles and torsion angles of **1**.

Bond lengths (Å)			
N1–C1	1.344(5)	N9–C2	1.388(5)
N1–N2	1.351(4)	N2–N3	1.298(4)
N1–N8	1.403(4)	N6–N7	1.121(5)
N4–C1	1.313(5)	N6–N5	1.263(5)
N4–N3	1.377(4)	N12–N13	1.279(5)
N10–N11	1.119(5)	N12–C2	1.395(5)
N10–N9	1.265(5)	N5–C1	1.384(5)
N8–C2	1.288(5)	N14–N13	1.121(5)
Bond angles (°)			
C1–N1–N2	108.0(3)	N6–N5–C1	112.0(4)
C1–N1–N8	126.2(3)	N2–N3–N4	111.4(3)
N2–N1–N8	123.3(3)	N14–N13–N12	173.2(4)
C1–N4–N3	104.5(3)	N8–C2–N9	124.6(4)
N11–N10–N9	171.0(4)	N8–C2–N12	120.4(4)
C2–N8–N1	113.8(3)	N9–C2–N12	115.0(4)
N10–N9–C2	114.5(3)	N4–C1–N1	109.9(4)
N3–N2–N1	106.1(3)	N4–C1–N5	130.4(4)
N7–N6–N5	172.4(5)	N1–C1–N5	119.7(4)
N13–N12–C2	111.1(4)		
Torsion angles (°)			
C1–N1–N8–C2	-123.8(5)	N13–N12–C2–N8	2.9(6)
N2–N1–N8–C2	76.3(5)	N13–N12–C2–N9	-175.9(4)
C1–N1–N2–N3	2.1(5)	N3–N4–C1–N1	1.5(5)
N8–N1–N2–N3	165.1(3)	N3–N4–C1–N5	-179.1(4)
N1–N2–N3–N4	-1.2(5)	N2–N1–C1–N4	-2.3(5)
C1–N4–N3–N2	-0.2(5)	N8–N1–C1–N4	-164.7(4)
N1–N8–C2–N9	-2.2(6)	N2–N1–C1–N5	178.3(4)
N1–N8–C2–N12	179.1(4)	N8–N1–C1–N5	15.9(7)
N10–N9–C2–N8	162.5(4)	N6–N5–C1–N4	4.2(7)
N10–N9–C2–N12	-18.8(5)	N6–N5–C1–N1	-176.5(4)

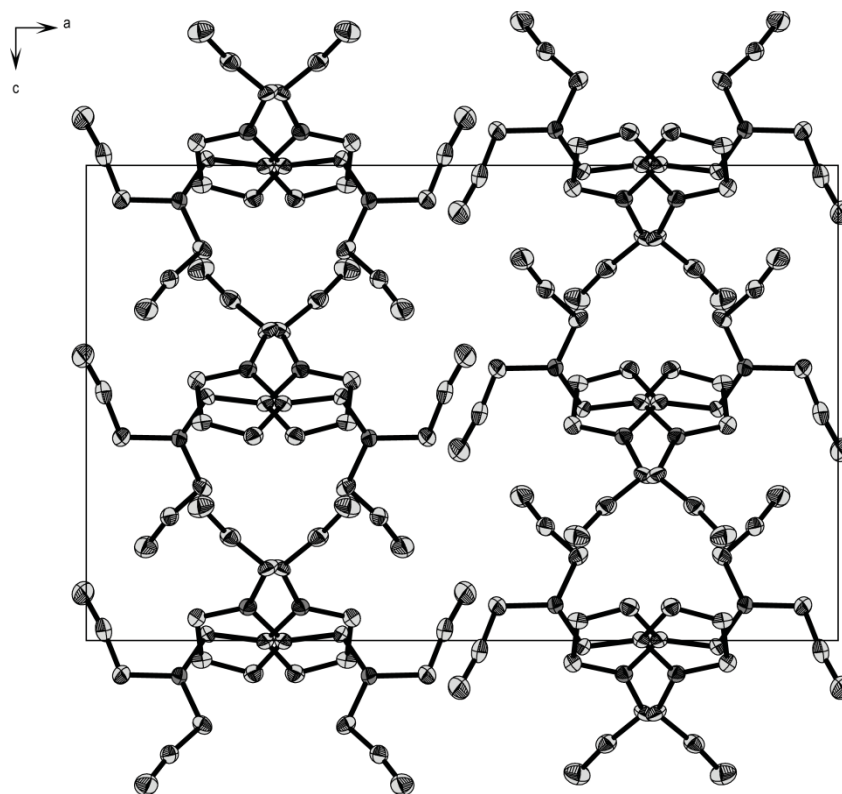


Figure 1S: Ortep representation of the unit cell content of **1** along the *b*-axis. Thermal ellipsoids represent the 50 % probability level.

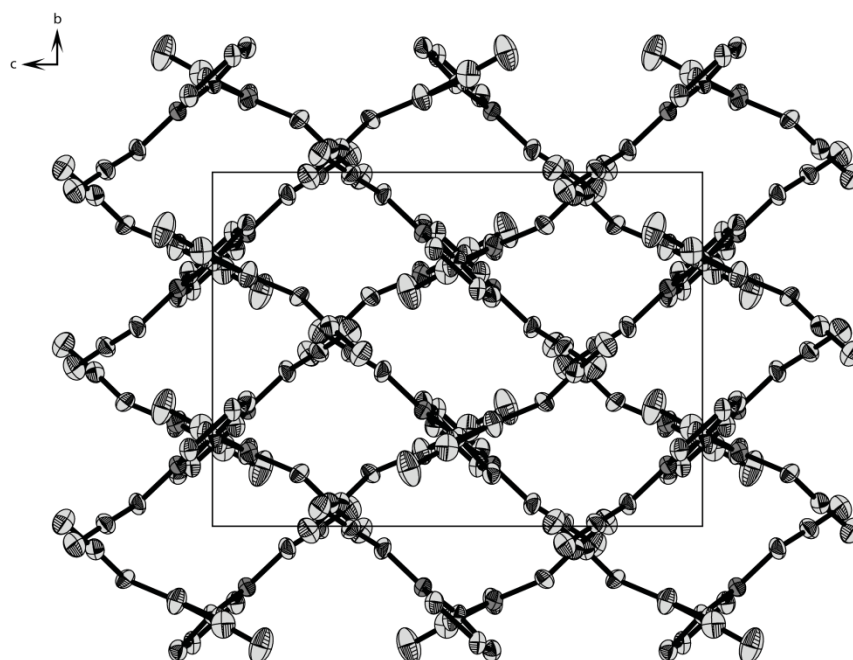


Figure 2S: Ortep representation of the unit cell content of **1** along the *a*-axis. Thermal ellipsoids represent the 50 % probability level.

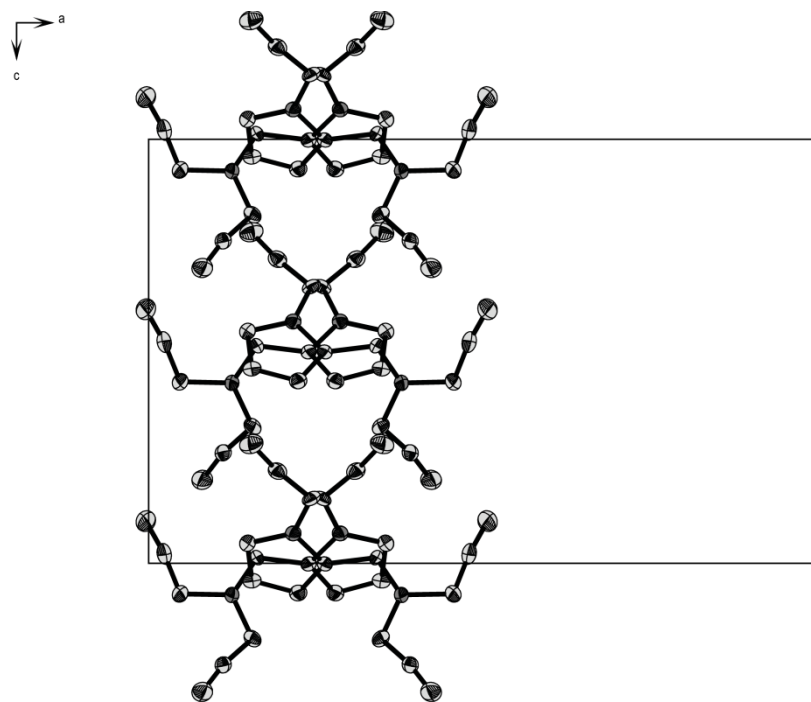


Figure 3S: Ortep representation of only one stack of chains of **1** along the *b*-axis. Thermal ellipsoids represent the 50 % probability level.

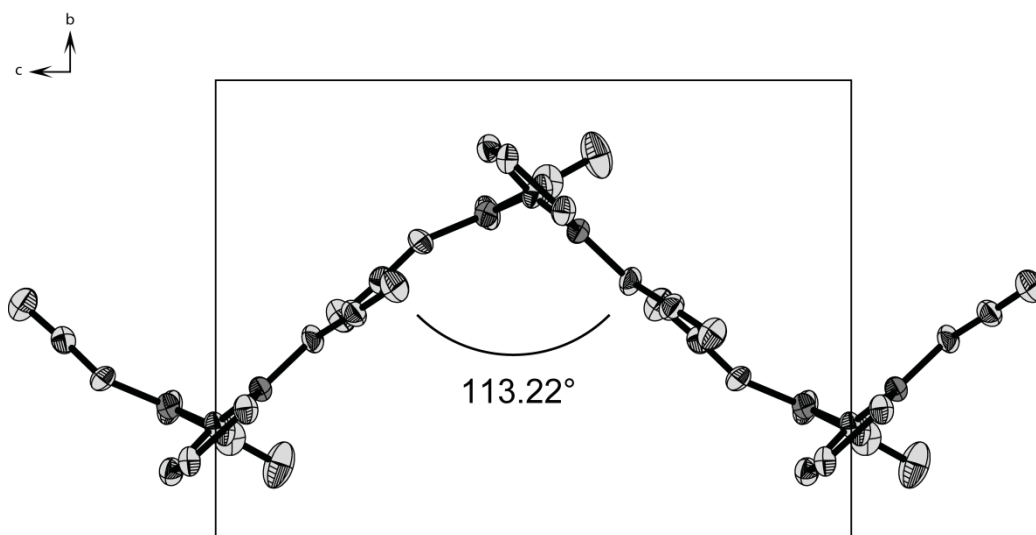


Figure 4S: Ortep representation of one independent chain along the *a*-axis. Thermal ellipsoids represent the 50 % probability level.

Calculations

Geometry optimization as well as frequency and electrostatic potential calculations have been performed at the B3LYP/cc-pVDZ level of theory using the program package Gaussian G09W, Rev A1.^[12,13]

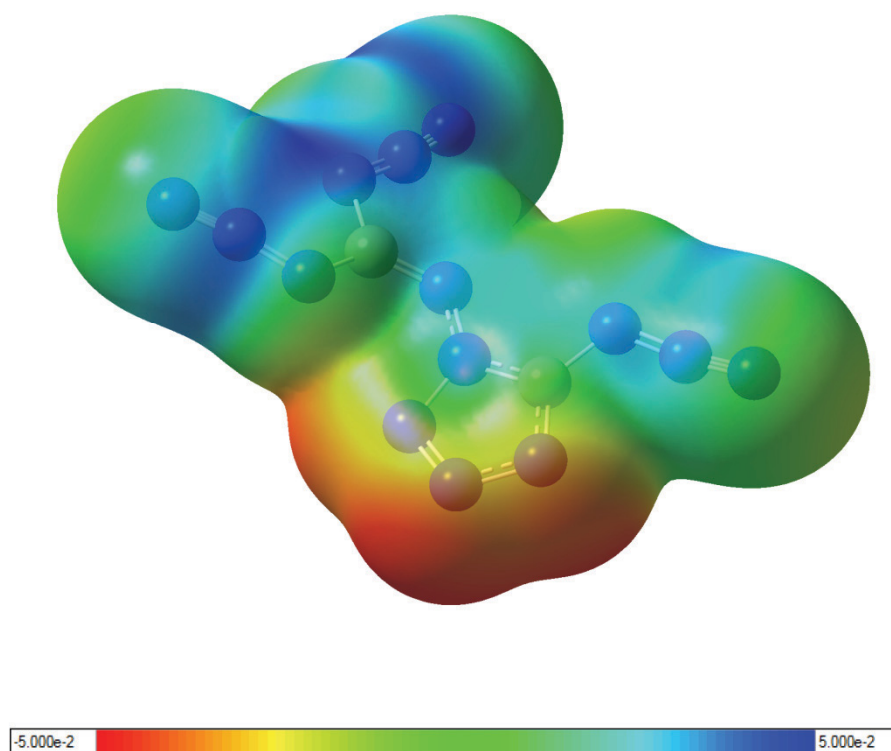


Figure 5S: Electrostatic potential plot of **1**, calculated at the B3LYP/cc-pVDZ level of theory using the program package Gaussian G09W together with GaussView 5 for illustration purposes.^[12,13] The electrostatic potential of **1** for the 0.001 electron/bohr³ isosurface is illustrated with the color range from -0.05 to 0.05 hartrees, with blue denoting extreme electron deficient regions and red denoting electron rich regions.

Table 3S: Infrared frequencies and intensities derived from calculations at the B3LYP/cc-pVDZ level of theory. The frequencies have been fitted according to Witek et al. with a scaling factor of 0.9704.^[14]

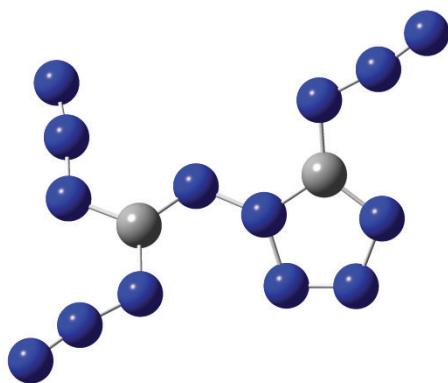
IR Frequencies	IR Frequencies (fitted)	IR Intensities
2308	2240	437.96
2301	2233	208.18
2293	2225	1280.74
1670	1621	375.29
1580	1533	503.74
1481	1437	158.58
1398	1357	641.13
1371	1330	22.22
1338	1298	31.79
1307	1268	186.96
1240	1203	6.71
1184	1149	23.69
1115	1082	21.02
1079	1047	152.94
1005	975	2.46
947	919	27.32
823	799	6.28
775	752	20.02
726	705	14.23
698	677	1.60
683	663	0.77
656	636	9.75
644	625	13.86
572	555	0.71
557	540	7.36
539	523	15.92
501	486	3.42
443	430	4.90
398	386	3.55
361	350	4.36
294	285	0.58
241	234	0.11
191	185	0.77
154	149	0.81
143	139	0.88

The stretching modes at 2308 cm⁻¹, 2301 cm⁻¹ and 2293 cm⁻¹ all present stretching modes of the N₃ group. From the motions of the modes, we can state, that at each wave number one of the azide groups is clearly favored in the movement. For 2308 cm⁻¹ one of the C(N₃)₂ azide groups shows a stronger movement than the other two azide groups, while the opposite is the case for the second azide group of the C(N₃)₂ group at 2293 cm⁻¹. The

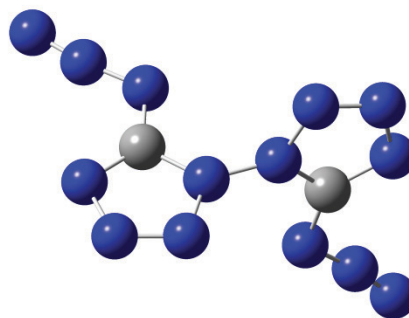
stretching mode at 2301 cm^{-1} shows a very strong movement for the tetrazole connected azide group with the other two azide groups moving less.

Calculations on Isomers of C_2N_{14} carried out at the B3LYP/cc-pVDZ level of theory

	Isomer A	Isomer B
point group	C_1	C_2
$-E / \text{a.u.}$	842.499666	842.498176
$zpe / \text{kcal mol}^{-1}$	48.6	49.6
<i>NIMAG</i>	0	0
$E_{\text{rel.}} / \text{kcal mol}^{-1}$	0.0	+ 0.9
$E_{\text{rel.}}^{\text{zpe corrected}} / \text{kcal mol}^{-1}$	0.0	+ 1.9



A



B

Since the isolated yields of compound A were always very low (16.4%), on recommendation by one of the referees of this paper we also calculated and looked for the isomer B containing two tetrazole rings. Although isomer B lies only approximately 2 kcal mol^{-1} above the experimentally isolated isomer A, we were neither able to detect isomer B from the reaction mixture, nor find any evidence for it.

References:

- [1] NATO standardization agreement (STANAG) on explosives, impact sensitivity tests, no. 4489, 1st ed., Sept. 17, **1999**.
- [2] WIWEB-Standardarbeitsanweisung 4-5.1.02, Ermittlung der Explosionsgefährlichkeit, hier der Schlagempfindlichkeit mit dem Fallhammer, Nov. 8, **2002**.
- [3] <http://www.bam.de>
- [4] NATO standardization agreement (STANAG) on explosive, friction sensitivity tests, no. 4487, 1st ed., Aug. 22, **2002**.
- [5] WIWEB-Standardarbeitsanweisung 4-5.1.03, Ermittlung der Explosionsgefährlichkeit oder der Reibeempfindlichkeit mit dem Reibeapparat, Nov. 8, **2002**.
- [6] CrysAlis CCD, Oxford Diffraction Ltd., Version 1.171.27p5 beta (release 01-04-2005 CrysAlis171 .NET).
- [7] CrysAlis RED, Oxford Diffraction Ltd., Version 1.171.27p5 beta (release 01-04-2005 CrysAlis171 .NET).
- [8] A. Altomare, G. Cascarano, C. Giacovazzo, A. Guagliardi, SIR-92, A program for crystal structure solution, *J. Appl. Cryst.* **1993**, 26, 343.
- [9] G. M. Sheldrick, **1997**, *SHELXL-97*, Program for the Refinement of Crystal Structures. University of Göttingen, Germany.
- [10] L. J. Farrugia, WinGX suite for small molecule single-crystal crystallography, *J. Appl. Cryst.* **1999**, 32, 837-838.
- [11] A. L. Spek, **1999**, Platon, A Multipurpose Crystallographic Tool, Utrecht University, Utrecht, The Netherlands.
- [12] A. D. Becke, *J. Chem. Phys.* **1993**, 98, 5648.
- [13] Gaussian 09 (Revision **A.1**): M. J. Frisch, G. W. Trucks, H. B. Schlegel, G. E. Scuseria, M. A. Robb, J. R. Cheeseman, G. Scalmani, V. Barone, B. Mennucci, G. A. Petersson, H. Nakatsuji, M. Caricato, X. Li, H. P. Hratchian, A. F. Izmaylov, J. Bloino, G. Zheng, J. L. Sonnenberg, M. Hada, M. Ehara, K. Toyota, R. Fukuda, J. Hasegawa, M. Ishida, T. Nakajima, Y. Honda, O. Kitao, H. Nakai, T. Vreven, J. A. Montgomery, Jr., J. E. Peralta, F. Ogliaro, M. Bearpark, J. J. Heyd, E. Brothers, K. N. Kudin, V. N. Staroverov, R. Kobayashi, J. Normand, K. Raghavachari, A. Rendell, J. C. Burant, S. S. Iyengar, J. Tomasi, M. Cossi, N. Rega, J. M. Millam, M. Klene, J. E. Knox, J. B. Cross, V. Bakken, C. Adamo, J. Jaramillo, R. Gomperts, R. E. Stratmann, O. Yazyev, A. J. Austin, R. Cammi, C. Pomelli, J. W. Ochterski, R. L. Martin, K. Morokuma, V. G. Zakrzewski, G. A. Voth, P. Salvador, J. J. Dannenberg, S. Dapprich, A. D. Daniels, Ö. Farkas, J. B. Foresman, J. V. Ortiz, J. Cioslowski, and D. J. Fox, Gaussian, Inc., Wallingford CT, 2009.
- [14] H. A. Witek, M. Keiji, *J. Comp. Chem. THEOCHEM* **2004**, 25, 1858–1864.

12.4 Supplementary Material for Chapter 5

Table S1: Selected RAMAN and IR frequencies for **1** (1-amino-5-azidotetrazole) presented with the frequencies calculated at the B3LYP/cc-pVDZ level of theory and their possible assignment.

IR	RAMAN	Selected Calc. Frequencies (fitted)	Possible assignment
3332, 3228	--, 3205	3426	ν_s NH ₂
3152	3154	3347	ν_{as} NH ₂
2150	2156	2234	ν N _{3(Tet)}
1639	1648	1640	δ_s NH ₂
1532	1536	1536	ν C ₁ =N ₄ + δ_s NH ₂
1472	1476	1465	ν_{as} N ₁ -C ₁ =N ₄
1302	1308	1334	ν N ₂ =N ₃
1272	1272	1287	ν C ₁ =N ₄ + ν N ₂ =N ₃
1191	1200	1213	ν_{as} N ₈ -N ₁ -N ₂ + ν N ₅ =N ₆
1117	1105	1099	ν_{as} (N ₁ -N ₂ + N ₃ -N ₄)
1079	1076	1063	ν_s (N ₁ -N ₂ + N ₃ -N ₄)
992	--	989	τ NH ₂ + deformation tetrazole ring
930	--	906	τ NH ₂

Table S2: Selected RAMAN and IR frequencies for **2** (5-azido-1-diazidocarbamoyltetrazole) presented with the frequencies calculated at the B3LYP/cc-pVDZ level of theory and their possible assignment.

IR	RAMAN	Selected Calc. Frequencies (fitted)	Possible assignment
2175	2179	2240	ν N ₃ (N ₁₂ =N ₁₃ =N ₁₄)
2155	2165	2233	ν N ₃ (Tetrazole)
2133	2133	2225	ν N ₃ (N ₉ =N ₁₀ =N ₁₁)
1578	1573	1621	ν C ₂ =N ₈
1530	1534	1533	ν C ₁ -N ₅
1456	1454	1437	ν_{as} N ₁ -C ₁ =N ₄
1414	1408	1356	ν_{as} N ₉ -C ₂ -N ₁₂
1291	1293	1329	ν N ₂ =N ₃
1261	1266	1267	ν_s (C ₁ =N ₄ + N ₂ =N ₃) + ν (N ₅ =N ₆ + N ₉ =N ₁₀ + N ₁₂ =N ₁₃)
1114	1105	1082	ν N ₃ -N ₄
1092	1087	1046	ν N ₁ -N ₂

Table S3: Selected RAMAN and IR frequencies for **3** (1-(amino-azidocarbamoyl)-5-azidotetrazole) presented with the frequencies calculated at the B3LYP/cc-pVDZ level of theory and their possible assignment.

IR	RAMAN	Selected Calc. Frequencies (fitted)	Possible assignment
--	--	3580	ν_{as} NH ₂
3278	--	3376	ν_s NH ₂
2164	2170	2240	ν N ₃
2152	2157	2229	ν N _{3(Tet)}
1584	1586	1666	ν C ₂ =N ₈
1522	1534	1539	ν C ₁ -N ₅
--	1526	1505	δ_s NH ₂
1448	1451	1441	ν_{as} N ₁ -C ₁ =N ₄
1329	1331	1321	ν N ₂ =N ₃ + ν N ₅ =N ₆
1287	1288	1255	ν_s (C ₁ =N ₄ + N ₂ =N ₃) + ν (N ₅ =N ₆ + N ₉ =N ₁₀)
1105	1108	1109	ν N ₃ -N ₄
1084	1086	1073	ν N ₁ -N ₂

Table S4: Crystallographic data and parameter.

	C₂N₁₄ (2)	C₂H₂N₁₂ (3)	CH₂N₈ (1)
Formula	C ₂ N ₁₄	C ₂ H ₂ N ₁₂	CH ₂ N ₈ *H ₂ O
FW [g mol ⁻¹]	220.16	194.12	144.10
Crystal system	orthorhombic	triclinic	monoclinic
Space Group	<i>Pbcn</i>	<i>P</i> -1	<i>P2</i> ₁
Color / Habit	colorless needles	colorless rods	light yellow block
Size [mm]	0.01 x 0.05 x 0.10	0.12 x 0.08 x 0.07	0.43 x 0.18 x 0.05
<i>a</i> [Å]	18.1289(1)	7.2321(3)	4.7942(3)
<i>b</i> [Å]	8.2128(7)	7.2828(4)	8.0012(5)
<i>c</i> [Å]	11.4021(9)	7.8104(5)	7.7650(6)
α [°]	90	108.408(5)	90
β [°]	90	98.467(4)	99.566(7)
γ [°]	90	91.593(4)	90
<i>V</i> [Å ³]	1697.6(2)	384.86(4)	293.72(3)
<i>Z</i>	8	2	2
ρ_{calc} [g cm ⁻³]	1.723	1.675	1.629
μ [mm ⁻¹]	0.140	0.135	0.138
<i>F</i> (000)	880	196	148
$\lambda_{\text{MoK}\alpha}$ [Å]	0.71073	0.71073	0.71073
<i>T</i> [K]	150	100	173
Theta Min-Max [°]	3.74 – 25.50	3.93 – 30.12	4.31 – 26.50
Dataset h	-21; 17	-10; 10	-6; 5
Dataset k	-8; 9	-10; 10	-9; 10
Dataset l	-13; 13	-10; 10	-4; 9
Reflections collected	6862	5862	1588
Independent reflections	1563	2238	651
Observed reflections	763	1765	581
No. parameters	145	122	103
<i>R</i> _{int}	0.1423	0.0198	0.0197
<i>R</i> ₁ , w <i>R</i> ₂ (<i>I</i> > σ <i>I</i> ₀)	0.0673; 0.0847	0.0307; 0.0774	0.0239; 0.0502
<i>R</i> ₁ , w <i>R</i> ₂ (all data)	0.1660; 0.1177	0.0433; 0.0827	0.0289; 0.0513
<i>S</i>	1.084	1.075	0.971
Resd. Dens. [e Å ⁻³]	-0.461; 0.360	-0.360; 0.277	-0.106; 0.144
Device type	Oxford Xcalibur3	Oxford Xcalibur3	Oxford Xcalibur3
	CCD	CCD	CCD
Solution	SIR-92	SIR-92	SHELXS-97
Refinement	SHELXL-97	SHELXL-97	SHELXL-97
Absorption correction	multi-scan	multi-scan	multi-scan
CCDC	693485	693484	795273

12.5 Supplementary Material for Chapter 6

Table S1: Crystallographic data and parameter.

	DATr (1)	DATr ⁺ Cl ⁻ (2)	DATr ⁺ NO ₃ ⁻ (3)
Formula	C ₂ H ₅ N ₅	C ₄ H ₁₄ N ₁₀ Cl ₂ O	C ₂ H ₆ N ₆ O ₃
FW [g mol ⁻¹]	99.11	289.15	162.13
Crystal system	monoclinic	monoclinic	monoclinic
Space Group	<i>P2₁/c</i> (No. 14)	<i>P2₁/n</i> (No. 14)	<i>P2₁/c</i> (No. 14)
Color / Habit	colorless rods	colorless plates	colorless rods
Size [mm]	0.13 x 0.14 x 0.16	0.05 x 0.17 x 0.18	0.13 x 0.15 x 0.30
<i>a</i> [Å]	10.6366(6)	6.0570(5)	9.5615(7)
<i>b</i> [Å]	4.3042(2)	24.662(2)	9.1082(6)
<i>c</i> [Å]	10.8114(6)	8.1341(6)	7.4390(6)
α [°]	90	90	90
β [°]	118.784(7)	93.516(7)	96.362(8)
γ [°]	90	90	90
<i>V</i> [Å ³]	433.81(5)	1212.78(16)	643.86(8)
<i>Z</i>	4	4	4
$\rho_{\text{calc.}}$ [g cm ⁻³]	1.518	1.584	1.673
μ [mm ⁻¹]	0.114	0.541	0.150
<i>F</i> (000)	208	600	336
$\lambda_{\text{MoK}\alpha}$ [Å]	0.71073	0.71073	0.71073
<i>T</i> [K]	200	200	200
Theta Min-Max [°]	3.8 – 26.0	4.2 – 26.0	4.3 – 26.0
Dataset h	-12; 13	-7; 4	-11; 11
Dataset k	-5; 5	-30; 26	-11; 7
Dataset l	-13; 8	-9; 10	-9; 9
Reflections collected	2134	4625	3272
Independent reflections	852	2375	1264
Observed reflections	677	1518	1264
No. parameters	84	106	124
<i>R</i> _{int}	0.019	0.038	0.033
<i>R</i> ₁ (<i>I</i> > σ <i>I</i> ₀)	0.0315	0.0350	0.0276
<i>wR</i> ₂ (all data)	0.0862	0.0623	0.0639
<i>S</i>	1.04	0.82	0.92
Resd. Dens. [e Å ⁻³]	-0.22, 0.14	-0.29, 0.31	-0.16, 0.15
Device type	Oxford Xcalibur3 CCD	Oxford Xcalibur3 CCD	Oxford Xcalibur3 CCD
Solution	SIR-92	SIR-92	SIR-92
Refinement	SHELXL-97	SHELXL-97	SHELXL-97
Absorption correction	multi-scan	multi-scan	multi-scan
CCDC	784960	784963	784962

Table S1: continued.

	DATr ⁺ ClO ₄ ⁻ (4)	DATr ⁺ DN ⁻ (5)
Formula	C ₂ H ₆ N ₅ ClO ₄	C ₂ H ₆ N ₈ O ₄
FW [g mol ⁻¹]	199.57	206.15
Crystal system	triclinic	monoclinic
Space Group	<i>P</i> -1 (No. 2)	<i>P</i> 2 ₁ / <i>n</i> (No. 14)
Color / Habit	colorless prism	colorless rods
Size [mm]	0.14 x 0.17 x 0.18	0.12 x 0.14 x 0.20
<i>a</i> [Å]	5.3035(5)	13.0772(7)
<i>b</i> [Å]	7.6267(7)	17.4883(5)
<i>c</i> [Å]	9.2813(8)	14.1722(5)
α [°]	74.399(8)	90
β [°]	84.825(7)	107.678(4)
γ [°]	83.683(8)	90
<i>V</i> [Å ³]	358.67(6)	3088.1(2)
<i>Z</i>	2	16
ρ_{calc} [g cm ⁻³]	1.848	1.774
μ [mm ⁻¹]	0.520	0.162
<i>F</i> (000)	204	1696
$\lambda_{\text{MoK}\alpha}$ [Å]	0.71073	0.71073
<i>T</i> [K]	200	200
Theta Min-Max [°]	3.9 – 26.0	3.7 – 26.0
Dataset h	-6; 6	-16; 16
Dataset k	-9; 9	-21; 21
Dataset l	-11; 11	-17; 17
Reflections collected	3539	30659
Independent reflections	1419	6040
Observed reflections	1011	4065
No. parameters	133	602
<i>R</i> _{int}	0.023	0.026
<i>R</i> ₁ (<i>I</i> > σ <i>I</i> ₀)	0.0327	0.0319
<i>wR</i> ₂ (all data)	0.0885	0.0984
<i>S</i>	1.00	1.03
Resd. Dens. [e Å ⁻³]	-0.28, 0.27	-0.31, 0.40
Device type	Oxford Xcalibur3 CCD	Oxford Xcalibur3 CCD
Solution	SIR-92	SIR-92
Refinement	SHELXL-97	SHELXL-97
Absorption correction	multi-scan	multi-scan
CCDC	784959	784961

12.6 Supplementary Material for Chapter 7

Table S1: Crystallographic data and parameter for NANTA, MeNANTA and the corresponding salts.

	ANTA	NANTA (1)	AzoNTA	MeNANTA (3)
Measurement #	ex121	fx385	fx433	fx419
Formula	C ₂ H ₃ N ₅ O ₂	C ₂ H ₂ N ₆ O ₄	C ₂ N ₆ O ₂	C ₃ H ₄ N ₆ O ₄
FW [g mol ⁻¹]	129.09	174.08	140.06	188.10
Crystal system	monoclinic	monoclinic	monoclinic	orthorhombic
Space Group	C2/c	P2 ₁	P2 ₁ /c	P2 ₁ 2 ₁ 2 ₁
Color / Habit	colorless plate	light yellow plate	colorless plate	colorless plate
Size [mm]	0.21 x 0.14 x 0.03	0.31 x 0.28 x 0.02	0.22 x 0.21 x 0.05	0.28 x 0.15 x 0.04
<i>a</i> [Å]	14.109(5)	6.8663(7)	7.9129(7)	7.5559(5)
<i>b</i> [Å]	4.841(5)	5.3554(5)	8.1679(8)	10.1845(6)
<i>c</i> [Å]	14.199(5)	8.3117(7)	8.0907(8)	19.2349(12)
α [°]	90	90	90	90
β [°]	106.148(5)	102.513(8)	98.709(9)	90
γ [°]	90	90	90	90
<i>V</i> [Å ³]	931.6(11)	298.38(5)	516.89(9)	1480.18(16)
<i>Z</i>	8	2	4	8
ρ_{calc} [g cm ⁻³]	1.841	1.938	1.799	1.688
μ [mm ⁻¹]	0.161	0.182	0.159	0.154
<i>F</i> (000)	528	176	280	768
$\lambda_{\text{MoK}\alpha}$ [Å]	0.71073	0.71073	0.71073	0.71073
<i>T</i> [K]	200	173	173	173
Theta Min-Max [°]	4.47 – 26.45	4.34 – 26.43	4.64 – 26.48	4.14 – 26.49
Dataset h	-17; 17	-8; 8	-8; 9	-9; 8
Dataset k	-6; 6	-6; 2	-10; 10	-12; 11
Dataset l	-17; 15	-10; 10	-10; 8	-16; 24
Reflections collected	2820	1576	2690	8014
Independent reflections	955	677	1068	1770
Observed reflections	623	392	642	1067
No. parameters	94	117	91	243
<i>R</i> _{int}	0.0385	0.0623	0.0368	0.0550
<i>R</i> ₁ , w <i>R</i> ₂ (I> σ I ₀)	0.0315; 0.0563	0.0374; 0.0320	0.0357; 0.0657	0.0299; 0.0453
<i>R</i> ₁ , w <i>R</i> ₂ (all data)	0.0617; 0.0598	0.0830; 0.0362	0.0699; 0.0709	0.0659; 0.0490
<i>S</i>	0.844	0.777	0.822	0.788
Resd. Dens. [e Å ⁻³]	-0.214; 0.172	-0.202; 0.239	-0.190; 0.160	-0.134; 0.144
Device type	Oxford Xcalibur3 CCD	Oxford Xcalibur3 CCD	Oxford Xcalibur3 CCD	Oxford Xcalibur3 CCD
Solution	SIR-92	SHELXS-97	SHELXS-97	SHELXS-97
Refinement	SHELXL-97	SHELXL-97	SHELXL-97	SHELXL-97
Absorption correction	multi-scan	multi-scan	multi-scan	multi-scan
CCDC	--	824138	824140	824139

Table S1: continued.

	$\text{NH}_4^+ \text{NANTA}^- \cdot \text{H}_2\text{O}$ (5)	$\text{NH}_3\text{OH}^+ \text{NANTA}^- \cdot \text{H}_2\text{O}$ (4)	$\text{N}_2\text{H}_5^+ \text{NANTA}^- \cdot \text{H}_2\text{O}$ (6)	$\text{G}^+ \text{NANTA}$ (7)
Measurement number	fx462	fx453	gx093	gx054
Formula	$\text{C}_2\text{H}_7\text{N}_7\text{O}_5$	$\text{C}_2\text{H}_7\text{N}_7\text{O}_6$	$\text{C}_2\text{H}_8\text{N}_8\text{O}_5$	$\text{C}_3\text{H}_7\text{N}_9\text{O}_4$
FW [g mol ⁻¹]	209.12	225.12	224.14	233.15
Crystal system	orthorhombic	orthorhombic	monoclinic	orthorhombic
Space Group	P2 ₁ 2 ₁ 2 ₁	P2 ₁ 2 ₁ 2 ₁	P2 ₁ /c	Pna2 ₁
Color / Habit	orange block	yellow rod	colorless plate	yellow block
Size [mm]	0.49 x 0.21 x 0.15	0.50 x 0.21 x 0.18	0.45 x 0.16 x 0.03	0.42 x 0.13 x 0.11
<i>a</i> [Å]	4.5463(2)	4.5724(3)	3.6175(2)	9.9341(11)
<i>b</i> [Å]	9.2334(5)	9.5186(6)	9.6176(6)	24.361(2)
<i>c</i> [Å]	19.1095(10)	19.6674(13)	24.0045(13)	3.7050(4)
α [°]	90	90	90	90
β [°]	90	90	92.930(5)	90
γ [°]	90	90	90	90
<i>V</i> [Å ³]	802.17(7)	855.98(10)	834.06(8)	896.63(16)
<i>Z</i>	4	4	4	4
ρ_{calc} [g cm ⁻³]	1.732	1.75	1.785	1.727
μ [mm ⁻¹]	0.163	0.168	0.167	0.154
<i>F</i> (000)	432	464	464	480
$\lambda_{\text{MoK}\alpha}$ [Å]	0.71073	0.71073	0.71073	0.71073
<i>T</i> [K]	173	173	173	173
Theta Min-Max [°]	4.41 – 29.98	4.14 – 26.49	4.24 – 26.50	4.43 – 26.48
Dataset h	-6; 6	-5; 5	-3; 4	-12; 10
Dataset k	-12; 6	-11; 7	-12; 6	-28; 30
Dataset l	-26; 23	-23; 24	-29; 30	-2; 4
Reflections collected	5590	4650	4356	2075
Independent reflections	1394	1071	1725	1077
Observed reflections	1231	882	1216	714
No. parameters	148	157	161	166
<i>R</i> _{int}	0.0237	0.0366	0.0296	0.0281
<i>R</i> ₁ , w <i>R</i> ₂ (I > σ I ₀)	0.0264; 0.0635	0.0263; 0.0538	0.0405; 0.0929	0.0325; 0.0578
<i>R</i> ₁ , w <i>R</i> ₂ (all data)	0.0327; 0.0652	0.0354; 0.0552	0.0659; 0.0996	0.0610; 0.0621
<i>S</i>	1.031	0.965	1.005	0.868
Resd. Dens. [e Å ⁻³]	-0.199; 0.241	-0.185; 0.174	-0.293; 0.214	-0.202; 0.176
Device type	Oxford Xcalibur3 CCD	Oxford Xcalibur3 CCD	Oxford Xcalibur3 CCD	Oxford Xcalibur3 CCD
Solution	SHELXS-97	SHELXS-97	SHELXS-97	SHELXS-97
Refinement	SHELXL-97	SHELXL-97	SHELXL-97	SHELXL-97
Absorption correction	multi-scan	multi-scan	multi-scan	multi-scan
CCDC	824142	824141	824147	824145

Table S1: continued.

	(G ⁺) ₂ NANTA ²⁻ (11)	(AG ⁺) ₂ NANTA ²⁻ * H ₂ O (12)	TAG ⁺ NANTA (9) ⁻	TAG ⁺ MeNANTA ⁻ (18)
Measurement number	gx055	fx490	fx511	gx098
Formula	C ₄ H ₁₂ N ₁₂ O ₄	C ₄ H ₁₆ N ₁₄ O ₅	C ₃ H ₁₀ N ₁₂ O ₄	C ₄ H ₁₂ N ₁₂ O ₄
FW [g mol ⁻¹]	292.22	340.26	278.19	292.22
Crystal system	orthorhombic	monoclinic	orthorhombic	triclinic
Space Group	Pna2 ₁	P2 ₁ /n	Pca2 ₁	P-1
Color / Habit	yellow plate	orange block	yellow block	yellow
Size [mm]	0.24 x 0.23 x 0.11	0.28 x 0.10 x 0.10	0.50 x 0.30 x 0.13	block
<i>a</i> [Å]	36.123(4)	6.8700(8)	21.624(3)	6.9627(10)
<i>b</i> [Å]	3.5763(5)	11.8507(12)	4.2575(5)	8.3194(8)
<i>c</i> [Å]	8.9117(10)	17.1600(19)	11.5870(16)	11.3713(15)
α [°]	90	90	90	103.130(10)
β [°]	90	90.463(10)	90	104.061(12)
γ [°]	90	90	90	105.959(10)
<i>V</i> [Å ³]	1151.3(2)	1397.0(3)	1066.7(2)	583.01(13)
<i>Z</i>	4	4	4	2
ρ _{calc.} [g cm ⁻³]	1.686	1.618	1.732	1.665
μ [mm ⁻¹]	0.145	0.141	0.152	0.144
<i>F</i> (000)	608	712	576	304
λ _{MoKα} [Å]	0.71073	0.71073	0.71073	0.71073
<i>T</i> [K]	173	173	173	173
Theta Min-Max [°]	4.51 – 26.49	4.16 – 26.49	4.79 – 26.49	4.17 – 26.50
Dataset h	-45; 45	-7; 8	-27; 25	-8; 8
Dataset k	-4; 4	-14; 13	-5; 2	-10; 10
Dataset l	-6; 11	-21; 14	-8; 14	-10; 14
Reflections collected	5740	7440	2842	3214
Independent reflections	1272	2891	1166	2408
Observed reflections	1071	1470	959	1538
No. parameters	217	256	202	209
<i>R</i> _{int}	0.0422	0.0506	0.0244	0.0234
<i>R</i> ₁ , w <i>R</i> ₂ (I > σI ₀)	0.0285; 0.0571	0.0367; 0.0584	0.276; 0.0543	0.0396; 0.0683
<i>R</i> ₁ , w <i>R</i> ₂ (all data)	0.0369; 0.0591	0.0949; 0.0666	0.0385; 0.0568	0.0703; 0.0737
<i>S</i>	0.933	0.779	0.971	0.870
Resd. Dens. [e Å ⁻³]	-0.166; 0.150	-0.186; 0.185	-0.184; 0.151	-0.244; 0.202
Device type	Oxford Xcalibur3 CCD	Oxford Xcalibur3 CCD	Oxford Xcalibur3 CCD	Oxford Xcalibur3 CCD
Solution	SHELXS-97	SHELXS-97	SHELXS-97	SHELXS-97
Refinement	SHELXL-97	SHELXL-97	SHELXL-97	SHELXL-97
Absorption correction	multi-scan	multi-scan	multi-scan	multi-scan
CCDC	824146	824143	824144	824148

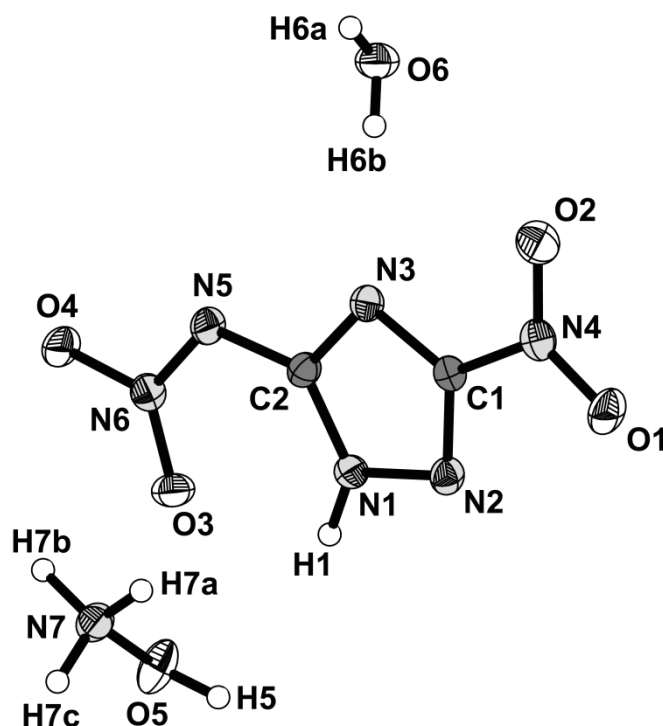


Figure S1: Asymmetric unit of hydroxylammonium 5-nitramino-3-nitro-1*H*-1,2,4-triazolate (**4**). Thermal ellipsoids present the 50 % probability level.

Table S2: Hydrogen bonds present in the structure of hydroxylammonium 5-nitramino-3-nitro-1*H*-1,2,4-triazolate (**4**).

D–H···A	d(D–H) [Å]	d(H···A) [Å]	d(D–H···A) [Å]	<(D–H···A) [°]
N1–H1···O3	0.89(2)	2.22(2)	2.605(2)	106(1)
N1–H1···O4 ⁱ	0.89(2)	1.90(2)	2.781(2)	171(2)
O5–H5···N5 ⁱⁱ	0.91(3)	1.83(3)	2.729(2)	171(3)
O5–H5···O4 ⁱⁱ	0.91(3)	2.60(3)	3.103(2)	116(2)
O5–H5···N6 ⁱⁱ	0.91(3)	2.62(3)	3.397(3)	143(2)
N7–H7a···O4 ⁱⁱ	0.91(3)	2.10(3)	2.884(2)	144(2)
N7–H7a···O3 ⁱⁱⁱ	0.91(3)	2.48(2)	3.112(3)	127(2)
N7–H7b···N2 ^{iv}	0.96(2)	2.06(3)	3.017(3)	178(2)
N7–H7c···O6 ^v	0.94(3)	1.89(3)	2.786(3)	158(2)
O6–H6a···O6 ^{vi}	0.74(3)	2.08(3)	2.819(2)	176(3)
O6–H6b···N3	0.79(3)	2.12(3)	2.903(2)	171(3)

Symmetry Operators: (i) $-x, y-1/2, -z+1/2$; (ii) $-x+1, y-1/2, -z+1/2$; (iii) $x+1, y, z$; (iv) $-x+1, y+1/2, -z+1/2$; (v) $-x+3/2, -y+1, z+1/2$; (vi) $x+1/2, -y+3/2, -z$.

Table S3: Hydrogen bonds present in the structure of ammonium 5-nitramino-3-nitro-1*H*-1,2,4-triazolate (5).

D–H⋯A	d (D–H) [Å]	d (H⋯A) [Å]	d (D–H⋯A) [Å]	< (D–H⋯A) [°]
N1–H1⋯O3	0.91(2)	2.22(2)	2.610(2)	105(2)
N1–H1⋯O4 ⁱ	0.91(2)	1.89(2)	2.780(2)	167(2)
N7–H7a⋯O5 ⁱⁱ	0.90(2)	1.93(2)	2.812(2)	167(2)
N7–H7b⋯O4 ⁱⁱⁱ	0.98(2)	2.11(2)	3.064(2)	165(2)
N7–H7c⋯N2 ^{iv}	0.90(2)	2.13(2)	3.029(2)	178(2)
N7–H7c⋯O1 ^{iv}	0.90(2)	2.56(2)	3.023(2)	113(2)
N7–H7d⋯O4 ⁱ	0.80(2)	2.14(2)	2.911(2)	160(2)
O5–H5a⋯N3 ^v	0.87(2)	2.02(2)	2.890(2)	175(2)
O5–H5b⋯O5 ^{vi*}	0.81(2)	1.98(2)	2.783(1)	174(3)

Symmetry Operators: (i) $-x+1, y-1/2, -z+1/2$; (ii) $x+1/2, -y+1/2, -z$; (iii) $-x+2, y-1/2, -z+1/2$; (iv) $-x+1, y+1/2, -z+1/2$; (v) $-x, y-1/2, -z+1/2$; (vi) $x-1/2, -y+1/2, -z$.

Table S4: Hydrogen bonds present in the structure of hydrazinium 5-nitramino-3-nitro-1*H*-1,2,4-triazolate (6).

D–H⋯A	d (D–H) [Å]	d (H⋯A) [Å]	d (D–H⋯A) [Å]	< (D–H⋯A) [°]
N1–H1⋯O3	0.94(4)	2.20(3)	2.603(3)	105(2)
N1–H1⋯O4 ⁱ	0.94(3)	1.86(3)	2.791(2)	168(3)
N7–H7a⋯N8 ⁱⁱ	1.10(4)	1.73(4)	2.833(3)	178(3)
N7–H7b⋯N2	0.93(4)	2.17(4)	3.039(3)	155(3)
N7–H7c⋯O4 ⁱⁱⁱ	0.99(4)	1.95(4)	2.894(2)	159(3)
N7–H7c⋯N5 ⁱⁱⁱ	0.99(4)	2.65(3)	3.189(3)	114(2)
N8–H8a⋯O1	0.94(4)	2.35(4)	3.100(3)	136(3)
N8–H8a⋯O2 ^{iv}	0.94(4)	2.39(4)	3.198(2)	144(3)
N8–H8b⋯O5 ^v	0.90(4)	2.32(3)	2.862(3)	118(3)
N8–H8b⋯N5 ⁱⁱⁱ	0.90(4)	2.46(4)	3.071(3)	126(3)
O5–H5a⋯N3 ⁱⁱⁱ	0.83(4)	2.06(5)	2.896(3)	176(4)

Symmetry Operators: (i) $-x, y+1/2, -z+1/2$; (ii) $x+1, y, z$; (iii) $x, y+1, z$; (iv) $-x+1, -y+1, -z$; (v) $x-1, y, z$.

Table S5: Hydrogen bonds present in the structure of triaminoguanidinium 5-nitramino-3-nitro-1*H*-1,2,4-triazolate (**9**).

D–H···A	d (D–H) [Å]	d (H···A) [Å]	d (D–H···A) [Å]	< (D–H···A) [°]
N7–H7···O2 ⁱ	0.83(3)	2.37(3)	2.982(3)	131(2)
N8–H8···O4 ⁱⁱ	0.82(3)	2.38(3)	3.099(3)	147(2)
N9–H9···O4 ⁱⁱⁱ	0.87(3)	2.15(3)	2.964(3)	155(2)
N10–H10a···O4	0.84(3)	2.60(3)	3.339(3)	146(2)
N10–H10b···N3 ^{iv}	0.88(3)	2.47(3)	3.322(4)	163(2)
N11–H11a···N3	0.88(3)	2.56(3)	3.292(3)	141(2)
N11–H11b···N5 ⁱⁱ	0.85(3)	2.26(3)	3.005(3)	146(2)
N12–H12a···O3 ^v	0.85(3)	2.22(3)	3.051(3)	165(2)
N12–H12b···N2 ^{vi}	0.85(3)	2.45(3)	3.281(3)	166(2)
N1–H1···O3	0.83(3)	2.12(3)	2.581(3)	114(2)
N1–H1···O1 ^{vii}	0.83(3)	2.22(3)	2.996(3)	155(3)

Symmetry Operators: (i) $-x+1/2, y+1, z-1/2$; (ii) $x, y-1, z$; (iii) $-x+1/2, y-1, z+1/2$; (iv) $-x+1/2, y, z-1/2$; (v) $-x+1/2, y, z+1/2$; (vi) $x-1/2, -y, z$; (vii) $-x+1, -y, z-1/2$.

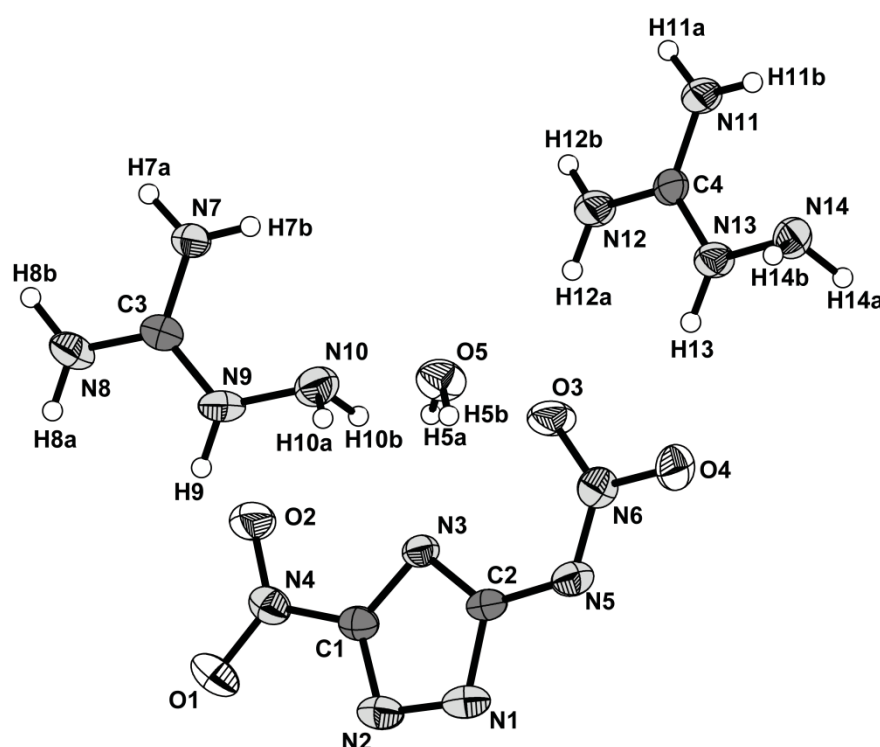
**Figure S2:** Asymmetric unit of bis(aminoguanidinium) 5-nitramino-3-nitro-1,2,4-triazolate (**12**). Thermal ellipsoids represent the 50 % probability level.

Table S6: Hydrogen bonds present in the structure of bis(aminoguanidinium) 5-nitramino-3-nitro-1,2,4-triazolate (**12**).

D–H⋯A	d (D–H) [Å]	d (H⋯A) [Å]	d (D–H⋯A) [Å]	< (D–H⋯A) [°]
N7–H7a⋯O2 ⁱ	0.88(2)	2.34(2)	3.003(2)	132(2)
N7–H7a⋯O5 ⁱ	0.88(2)	2.36(2)	3.094(2)	141(2)
N7–H7b⋯N14 ⁱⁱ	0.87(2)	2.34(2)	3.097(2)	145(2)
N8–H8a⋯N1 ⁱⁱⁱ	0.86(2)	2.39(2)	3.141(2)	146(2)
N8–H8a⋯N5 ⁱⁱⁱ	0.86(2)	2.41(2)	3.206(2)	154(2)
N8–H8b⋯O5 ^{iv}	0.93(2)	1.93(2)	2.816(3)	158(2)
N9–H9⋯O4 ⁱⁱⁱ	0.88(2)	2.32(2)	3.126(2)	152(2)
N9–H9⋯N5 ⁱⁱⁱ	0.88(2)	2.37(2)	3.165(2)	150(2)
N10–H10a⋯O1 ^v	0.88(2)	2.41(2)	3.079(2)	133(2)
N10–H10a⋯O5 ^{vi}	0.88(2)	2.42(2)	3.167(2)	142(2)
N10–H10b⋯N3	0.88(2)	2.42(2)	3.240(2)	155(2)
N11–H11a⋯N2 ^{vii}	0.86(2)	2.08(2)	2.906(2)	161(2)
N11–H11b⋯N10 ⁱⁱ	0.93(2)	2.32(2)	3.096(3)	140(2)
N12–H12a⋯O3	0.90(2)	2.06(2)	2.932(2)	163(2)
N12–H12b⋯N1 ^{vii}	0.81(2)	2.49(2)	3.288(2)	167(2)
N12–H12b⋯N2 ^{vii}	0.81(2)	2.52(2)	3.203(2)	142(2)
N13–H13⋯O4	0.91(2)	1.99(2)	2.879(2)	165(2)
N13–H13⋯O3	0.91(2)	2.58(2)	3.313(2)	138(2)
N13–H13⋯N6	0.91(2)	2.66(2)	3.542(2)	165(2)
N14–H14a⋯O2 ^{viii}	0.90(2)	2.50(2)	3.114(2)	126(2)
N14–H14b⋯N1 ^v	0.92(2)	2.31(2)	3.184(2)	159(2)
O5–H5a⋯O4 ^{ix}	0.85(2)	1.99(2)	2.837(2)	173(2)
O5–H5b⋯N3	0.83(2)	2.14(2)	2.886(2)	150(2)
O5–H5b⋯O3	0.83(2)	2.31(2)	2.969(2)	136(2)

Symmetry Operators: (i) $-x+1, -y, -z$; (ii) $-x+1, -y+1, -z$; (iii) $-x+1/2, y-1/2, -z+1/2$; (iv) $-x+1, -y, -z$; (v) $-x+1/2, y+1/2, -z+1/2$; (vi) $x-1, y, z$; (vii) $x+1/2, -y+1/2, z-1/2$; (viii) $x, y+1, z$; (ix) $-x+3/2, y-1/2, -z+1/2$.

12.7 Supplementary Material for Chapter 8

Table S1: Crystallographic data and parameter.

	TzTr (1)	ATzTr (3)	NO ₂ TzTr (4)
Measurement number	fx001	ex496	fx401
Formula	C ₃ H ₃ N ₇	C ₃ H ₄ N ₈	C ₃ H ₃ N ₉ O ₂
FW [g mol ⁻¹]	137.12	152.14	197.12
Crystal system	orthorhombic	monoclinic	orthorhombic
Space Group	Pnma	Pn	Pna2 ₁
Color / Habit	colorless block	colorless plate	light yellow block
Size [mm]	0.22 x 0.09 x 0.04	0.18 x 0.14 x 0.06	0.36 x 0.14 x 0.08
<i>a</i> [Å]	15.5490(15)	3.6270(4)	17.0917(19)
<i>b</i> [Å]	6.3300(10)	9.2390(10)	5.6431(6)
<i>c</i> [Å]	5.5610(5)	8.9640(9)	15.0077(14)
α [°]	90	90	90
β [°]	90	96.948(10)	90
γ [°]	90	90	90
<i>V</i> [Å ³]	547.34(11)	298.18(5)	1447.5(3)
<i>Z</i>	4	2	8
ρ_{calc} [g cm ⁻³]	1.664	1.695	1.809
μ [mm ⁻¹]	0.127	0.130	0.154
<i>F</i> (000)	280	156	800
$\lambda_{\text{MoK}\alpha}$ [Å]	0.71073	0.71073	0.71073
<i>T</i> [K]	173	173	173
Theta Min-Max [°]	4.15 – 26.50	4.41 – 26.50	4.33 – 26.50
Dataset h	-19; 19	-4; 3	-21; 21
Dataset k	-7; 7	-10; 11	-6; 7
Dataset l	-4; 6	-10; 11	-18; 18
Reflections collected	2659	1863	7124
Independent reflections	613	631	1551
Observed reflections	370	474	923
No. parameters	67	112	272
<i>R</i> _{int}	0.0563	0.0377	0.0856
<i>R</i> ₁ , w <i>R</i> ₂ (<i>I</i> > σ <i>I</i> ₀)	0.0398; 0.0768	0.0359; 0.0649	0.0348; 0.0469
<i>R</i> ₁ , w <i>R</i> ₂ (all data)	0.0826; 0.0846	0.0530; 0.0687	0.0741; 0.0522
<i>S</i>	0.882	0.881	0.783
Resd. Dens. [e Å ⁻³]	-0.157; 0.203	-0.178; 0.180	-0.174; 0.181
Device type	Oxford Xcalibur3 CCD	Oxford Xcalibur3 CCD	Oxford Xcalibur3 CCD
Solution	SHELXS-97	SHELXS-97	SHELXS-97
Refinement	SHELXL-97	SHELXL-97	SHELXL-97
Absorption correction	multi-scan	multi-scan	multi-scan
CCDC	--	--	--

12.8 Supplementary Material for Chapter 9

Table S1: Crystallographic data and parameter.

	4*DMSO	4*THF	5*DMSO	9
Measurement number	fx153	fx179	fx198	gx091
Formula	C ₄ H ₄ N ₁₂ O ₄ * 4 DMSO	C ₄ H ₄ N ₁₂ O ₄ * 4 THF	C ₄ H ₁₀ N ₁₄ O ₄ * 2 DMSO	C ₆ H ₂₄ N ₂₄ O ₆
FW [g mol ⁻¹]	596.70	572.6	474.52	528.49
Crystal system	monoclinic	monoclinic	triclinic	monoclinic
Space Group	<i>P</i> 2 ₁ / <i>c</i>	<i>P</i> 2 ₁ / <i>n</i>	<i>P</i> -1	<i>P</i> 2 ₁ / <i>c</i>
Color / Habit	Yellow plate	Yellow rod	Yellow plate	Yellow rod
Size [mm]	0.13x0.12x0.03	0.55x0.08x0.05	0.14x0.05x0.05	0.22x0.08x0.02
<i>a</i> [Å]	17.2749(6)	5.9430(6)	7.7810(9)	9.7903(11)
<i>b</i> [Å]	15.8671(8)	15.3647(17)	8.2010(9)	3.6340(5)
<i>c</i> [Å]	9.7594(4)	15.2456(16)	9.0610(10)	29.233(4)
α [°]	90	90	86.453(9)	90
β [°]	100.068(4)	96.237(10)	81.497(9)	96.424(11)
γ [°]	90	90	68.331(10)	90
<i>V</i> [Å ³]	2633.88(19)	1383.9(3)	531.42(10)	1033.5(2)
<i>Z</i>	4	2	1	2
ρ _{calc.} [g cm ⁻³]	1.505	1.374	1.483	1.698
μ [mm ⁻¹]	0.422	0.108	0.308	0.145
<i>F</i> (000)	1248	608	248	552
λ _{MoKα} [Å]	0.71073	0.71073	0.71073	0.71073
<i>T</i> [K]	173	173	173	173
Theta Min-Max [°]	4.2 – 28.80	4.2 – 26.50	4.55 – 26.50	4.15 – 26.50
Dataset h	-20; 22	-7; 7	-6; 9	-12; 12
Dataset k	-19; 18	-17; 19	-6; 10	-3; 4
Dataset l	-7; 13	-8; 19	-8; 11	-36; 36
Reflections collected	12529	6392	3720	4163
Independent reflections	5979	2827	2179	2129
Observed reflections	2609	1284	1122	1272
No. parameters	437	205	141	190
<i>R</i> _{int}	0.055	0.045	0.038	0.033
<i>R</i> ₁ , w <i>R</i> ₂ (I>σI ₀)	0.0386; 0.0440	0.058; 0.143	0.0406; 0.0549	0.0510; 0.1275
<i>R</i> ₁ , w <i>R</i> ₂ (all data)	0.1190; 0.0509	0.132; 0.161	0.0999; 0.0611	0.0881; 0.1381
<i>S</i>	0.663	0.856	0.742	0.899
Resd. Dens. [e Å ⁻³]	-0.375, 0.312	-0.313, 0.282	-0.241; 0.245	-0.217; 0.693
Device type	Oxford	Oxford	Oxford	Oxford
	Xcalibur3 CCD	Xcalibur3 CCD	Xcalibur3 CCD	Xcalibur3 CCD
Solution	SIR-92	SHELXS-97	SHELXS-97	SHELXS-97
Refinement	SHELXL-97	SHELXL-97	SHELXL-97	SHELXL-97
Absorption correction	multi-scan	multi-scan	multi-scan	multi-scan
CCDC	807480	807481	807482	807483

12.9 Supplementary Material for Chapter 10

Table S1: Crystallographic data and parameter.

	BATTH ²⁺ (Cl) ₂ * H ₂ O (3)	BATTH ²⁺ (ClO ₄) ₂ * H ₂ O (4)	DNBATTH * H ₂ O (5)
Measurement number	fx240	fx328	fx397
Formula	C ₄ H ₁₁ Cl ₂ N ₁₁ O	C ₄ H ₁₁ Cl ₂ N ₁₁ O ₉	C ₄ H ₇ N ₁₁ O ₆
FW [g mol ⁻¹]	300.14	428.14	305.21
Crystal system	monoclinic	monoclinic	monoclinic
Space Group	P2 ₁ /n	P2 ₁ /n	P2 ₁ /c
Color / Habit	colorless block	colorless block	yellow block
Size [mm]	0.42 x 0.38 x 0.20	0.40 x 0.40 x 0.15	0.48 x 0.29 x 0.24
<i>a</i> [Å]	6.8987(4)	7.5004(3)	10.4731(5)
<i>b</i> [Å]	20.2357(8)	15.6027(5)	16.3457(7)
<i>c</i> [Å]	9.1130(4)	12.5461(5)	6.9104(5)
α [°]	90	90	90
β [°]	107.179(5)	91.871(4)	101.414(6)
γ [°]	90	90	90
<i>V</i> [Å ³]	1215.42(10)	1467.44(10)	1159.60(11)
<i>Z</i>	4	4	4
ρ_{calc} [g cm ⁻³]	1.640	1.938	1.748
μ [mm ⁻¹]	0.545	0.523	0.159
<i>F</i> (000)	616	872	624
$\lambda_{\text{MoK}\alpha}$ [Å]	0.71073	0.71073	0.71073
<i>T</i> [K]	173	173	173
Theta Min-Max [°]	4.32 – 26.50	4.24 – 26.50	4.11 – 25.49
Dataset h	-8; 8	-8, 9	-12; 12
Dataset k	-25; 24	-11; 19	-19; 19
Dataset l	-4; 11	-8; 15	-5; 8
Reflections collected	4967	5823	5678
Independent reflections	2511	3020	2154
Observed reflections	1768	2119	1221
No. parameters	196	280	142
<i>R</i> _{int}	0.0274	0.0272	0.0434
<i>R</i> ₁ , w <i>R</i> ₂ (I > σ I ₀)	0.0342; 0.0745	0.0385; 0.0906	0.0367; 0.0746
<i>R</i> ₁ , w <i>R</i> ₂ (all data)	0.0566; 0.0788	0.0592; 0.0955	0.0765; 0.0811
<i>S</i>	0.908	0.992	0.820
Resd. Dens. [e Å ⁻³]	-0.234; 0.261	-0.511; 0.602	-0.185; 0.229
Device type	Oxford Xcalibur3 CCD	Oxford Xcalibur3 CCD	Oxford Xcalibur3 CCD
Solution	SHELXS-97	SHELXS-97	SHELXS-97
Refinement	SHELXL-97	SHELXL-97	SHELXL-97
Absorption correction	multi-scan	multi-scan	multi-scan
CCDC	--	--	--

12.10 List of Abbreviations

Å	Angström (10^{-10} m)
AcetTzTr	5-Acetamido-3-(tetrazol-1-yl)-1 <i>H</i> -1,2,4-triazole
ADN	Ammonium dinitramide
AG	Aminoguanidinium cation
ANTA	5-Amino-3-nitro-1 <i>H</i> -1,2,4-triazole
AP	Ammonium perchlorate
ATR	Attenuated total reflection
ATzTr	5-Amino-3-(tetrazol-1-yl)-1 <i>H</i> -1,2,4-triazole
BATTH	1,3-Bis-[3-(5-amino-1 <i>H</i> -1,2,4-triazolyl)]-triazene
d	doublet
δ	Chemical shift
DAAT	5,5'-Diamino-3,3'-azo-1 <i>H</i> -1,2,4-triazole
DAT	1,5-Diaminotetrazole
DATNO ₂	5-Amino-1-nitriminotetrazolate
DATr	3,5-Diamino-1 <i>H</i> -1,2,4-triazole
DCI	Desorption chemical ionization (MS)
DCT	4,5-Dicyano-1,2,3-triazolate anion
dec.	Decomposition
DEI	Desorption electron impact (MS)
DN	Dinitramide anion
DNAAT	5,5'-Dinitrimino-3,3'-azo-1 <i>H</i> -1,2,4-triazole
DNBATTH	1,3-Bis-[3-(5-nitro-1 <i>H</i> -1,2,4-triazolyl)]-triazene
DNIBATTH	1,3-Bis-[3-(5-nitramino-1 <i>H</i> -1,2,4-triazolyl)]-triazene
DSC	Differential Scanning Calorimetry
EI	Electron impact (MS)
FAB	Fast atom bombardment (MS)
FW	Formula weight
G	Guanidinium cation
HDATNO ₂	5-Amino-1-nitrimino-4 <i>H</i> -tetrazole
HDCT	4,5-Dicyano-2 <i>H</i> -1,2,3-triazole
Hz	Hertz
IR	Infrared
J	Coupling constant (NMR); Joule (Sensitivity)
KDN	Potassium dinitramide
m	medium (IR); multiplett (NMR)
<i>m/z</i>	mass per charge (MS)
MeANTA	5-Amino-1-methyl-3-nitro-1,2,4-triazole
MeDAT	1-Amino-5-imino-4-methyltetrazole
MeDATNO ₂	1-Nitrimino-5-amino-4-methyltetrazole
MeNANTA	5-Nitramino-1-methyl-3-nitro-1 <i>H</i> -1,2,4-triazole

MeNO ₂	Nitromethane
MS	Mass spectrometry
N	Newton
NANTA	5-Nitramino-3-nitro-1 <i>H</i> -1,2,4-triazole
NMR	Nuclear Magnetic Resonance
NO ₂ TzTr	5-Nitramino-3-(tetrazol-1-yl)-1 <i>H</i> -1,2,4-triazole
<i>P</i> _{C-J}	Detonation pressure at the Chapman-Jouguet point
ppm	parts per million (NMR)
q	quartet
ρ	Density (g cm ⁻³)
RDX	1,3,5-Trinitro-1,3,5-triazinane
<i>r</i> _w	van der Waals radii
<i>S</i>	Goodness of Fit
s	strong (IR); singlet (NMR)
STANAG	Standardization agreement
t	triplet
T	Temperature
<i>T</i> _{ex}	Temperature of explosion
TAG	Triaminoguanidinium cation
TLC	Thin layer chromatography
TMS	Tetramethylsilyl
TzTr	3-Tetrazol-1-yl-1 <i>H</i> -1,2,4-triazole
vs	very strong (IR)
Ω	Oxygen balance
w	weak (IR)
Z	Number of asymmetric units in unit cell

13. Curriculum vitae

Personal Details:

Name	Franz Albert Martin
Date of birth	19. December 1980
Place of birth	Würzburg
Citizenship	German
Marital status	married

Education:

- 04/2008 – 08/2011 PhD thesis in inorganic molecular chemistry in the group of Prof. Dr. Thomas M. Klapötke at the department of chemistry, Ludwig Maximilian University of Munich.
Topic: “Novel Energetic Materials based on 1,5-Diaminotetrazole and 3,5-Diamino-1*H*-1,2,4-triazole”
- 02/2007 – 09/2007 Diploma thesis in inorganic molecular chemistry in the group of Prof. Dr. Thomas M. Klapötke at the department of chemistry, Ludwig Maximilian University of Munich.
Topic: “Reinvestigation of Diaminotetrazole, energetic salts and synthetic ways towards 1,1'-Diamino-5,5'-azotetrazole”
- 10/2001 – 01/2007 Ludwig Maximilian University (LMU) of Munich, diploma studies in chemistry, degree: diploma chemist.
- 10/2000 – 09/2001 Technical University (TU) of Munich, diploma studies in engineering.
- 09/1990 – 06/1999 Secondary school education, Röntgen Gymnasium Würzburg, degree: Abitur.
- 09/1986 – 07/1990 Primary school education, Oskar Popp Grundschule, Kist

Bibliography:

1. F. Martin, H. Zipse, "Charge distribution in the water molecule – A comparison of methods", *J. Comp. Chem.* **2005**, 26(1), 97-105.
2. M.-J. Crawford, K. Karaghiosoff, T. M. Klapötke, F. A. Martin, "Synthesis and characterization of 4,5-dicyano-2H-1,2,3-triazole and its sodium, ammonium and guanidinium salts", *Inorg. Chem.* **2009**, 48(4), 1731-1743.
3. T. M. Klapötke, F. A. Martin, S. Sproll, J. Stierstorfer, "Azidotetrazoles - Promising energetic materials or a waste of time?", *New Trends in Research of Energetic Materials, Pardubice, Czech Republic, Proceedings of the 12th Seminar 2009, Pt. 1*, 327-340.
4. M.-J. Crawford, A. Ellern, K. Karaghiosoff, F. A. Martin, P. Mayer, "First actinide complexes of the nitrogen-containing ligands dinitramide ($N(NO_2)_2^-$), 4,5-dicyano-1,2,3-triazolate ($C_4N_5^-$) and dicyanamide ($N(CN)_2^-$)", *Inorg. Chem.* **2010**, 49(6), 2674-2683.
5. N. Fischer, T. M. Klapötke, F. A. Martin, J. Stierstorfer, "Energetic materials based on 1-amino-3-nitroguanidine", *NTREM, Proceedings of the 13th Seminar 2010, Pt. 1*, 113-129.
6. T. M. Klapötke, F. A. Martin, N. Mayr, J. Stierstorfer, "Synthesis and characterization of 3,5-diamino-1,2,4-triazolium dinitramide", *Z. Anorg. Allg. Chem.* **2010**, 636(15), 2555-2564.
7. M.-J. Crawford, T. M. Klapötke, F. A. Martin, M. Rusan, C. M. Sabate, "Energetic salts of the binary 5-cyanotetrazolate anion ($[C_2N_5]^-$) with protonated nitrogen bases", *Chem. Eur. J.* **2011**, 17(5), 1683-1695.
8. T. M. Klapötke, F. A. Martin, J. Stierstorfer, " C_2N_{14} – A new energetic and highly sensitive binary CN azidotetrazole", *Angew. Chem. Int. Ed.* **2011**, 50(18), 4227-4229; *Angew. Chem.* **2011**, 123, 4313-4316.
9. A. Dippold, T. M. Klapötke, F. A. Martin, "Synthesis and characterization of bis(triaminoguanidinium) 5,5'-dinitrimino-3,3'-azo-1H-1,2,4-triazole – A novel insensitive energetic material", *Z. Anorg. Allg. Chem.* **2011**, 637, DOI: 10.1002/zaac.201100102.
10. M. I. Eremets, J. Evers, M. Göbel, T. M. Klapötke, B. Krumm, F. A. Martin, S. Medvedyev, G. Oehlinger, F. X. Steemann, I. Troyan, "Molecular structure of

- hydrazoic acid with hydrogen bonded tetramers in nearly planar layers*", *J. Am. Chem. Soc.*, **2011**, DOI: 10.1021/ja2027053.
11. T. M. Klapötke, F. A. Martin, J. Stierstorfer, "*N-bound primary nitramines based on 1,5-diaminotetrazole*", *Chem. Eur. J.*, **2011**, accepted.
 12. T. M. Klapötke, B. Krumm, F. A. Martin, J. Stierstorfer, "*Novel azidotetrazoles – structurally interesting and extremely sensitive*", *Chem. Asian J.*, **2011**, accepted.
 13. T. M. Klapötke, F. A. Martin, S. Wiedbrauk, „*Nitraminoazoles based on ANTA – A comprehensive study of structural and energetic properties*", *Eur. J. Inorg. Chem.*, **2011**, submitted.

Conference contributions:

1. M.-J. Crawford, A. Ellern, K. Karaghiosoff, F. A. Martin, P. Mayer, "*First actinide complexes of the nitrogen-containing ligands dinitramide ($N(NO_2)_2^-$), 4,5-dicyano-1,2,3-triazolate ($C_4N_5^-$) and dicyanamide ($N(CN)_2^-$)*", *Inorg. Chem.* **2010**, 49(6), 2674-2683.
2. M.-J. Crawford, K. Karaghiosoff, T. M. Klapötke, F. A. Martin, "*Novel nitrogen rich salts based on 4,5-dicyano-1,2,3-triazole*", *New Trends in Research of Energetic Materials, NTREM, Proceedings of the 12th Seminar 2009*, Pt. 2, 741-761.
3. Alexander Dippold, Thomas M. Klapötke, Franz A. Martin, "*Synthesis and energetic properties of 5,5'-dinitrimino-3,3'-azo-1H-1,2,4-bistriazole and its nitrogen rich salts*", *New Trends in Research of Energetic Materials, NTREM, Proceedings of the 14th Seminar 2011*, Pt. 2, 561-578.
4. Alexander Dippold, Michael Feller, Thomas M. Klapötke, Franz A. Martin, "*Synthesis and energetic properties of novel nitramino- and nitrimino azoles and corresponding nitrogen rich salts*", *New Trends in Research of Energetic Materials, NTREM, Proceedings of the 14th Seminar 2011*, Pt. 2, 579-592.